

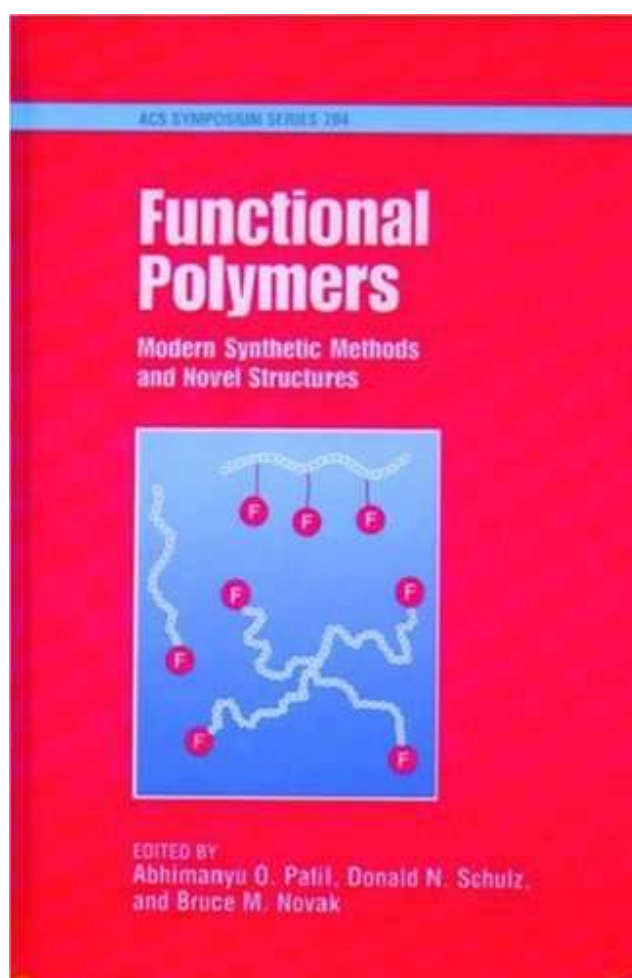
Functional Polymers: Modern Synthetic Methods and Novel Structures

Editors: Patil, A.O.¹, Schulz, D.N.¹, & Novak, B.M.²

¹Exxon Research and Engineering Company

²University of Massachusetts

Sponsoring Divisions: Division of Polymeric Materials: Science and Engineering



ACS Symposium Series Volume 704

Copyright © 1998 American Chemical Society

ISBN13: 9780841235779

eISBN: 9780841216860

DOI: 10.1021/bk-1998-0704

Functional Polymers

Modern Synthetic Methods and Novel Structures

Abhimanyu O. Patil, EDITOR

Exxon Research and Engineering Company

Donald N. Schulz, EDITOR

Exxon Research and Engineering Company

Bruce M. Novak, EDITOR

University of Massachusetts

Developed from a symposium sponsored by the Division
of Polymeric Materials: Science and Engineering,
at the 213th National Meeting
of the American Chemical Society,
San Francisco, California,
April 13–17, 1997



Functional polymers : modern synthetic methods and novel



Library of Congress Cataloging-in-Publication Data

Functional polymers : modern synthetic methods and novel structures /
Abhimanyu O. Patil, editor, Donald N. Schulz, editor, Bruce M. Novak,
editor.

p. cm.—(ACS symposium series, ISSN 0097-6156; 704)

“Developed from a symposium sponsored by the Division of Polymeric
Materials: Science and Engineering at the 213th National Meeting of the
American Chemical Society, San Francisco, California, April 13–17, 1997.”

Includes bibliographical references and indexes.

ISBN 0-8412-3577-5

1. Polymerization—Congresses. 2. Polymers—Congresses.

I. Patil, Abhimanyu O., 1952– . II. Schulz, Donald N., 1943– . III. Novak,
Bruce M., 1955– . IV. American Chemical Society. Division of Polymeric
Materials: Science and Engineering. V. American Chemical Society. Meeting
(213rd : 1997 : San Francisco, Calif.) VI. Series.

QD281.P6F77 1998
547'.7—dc21

98-21508
CIP

The paper used in this publication meets the minimum requirements of American National Standard for Information Sciences—Permanence of Paper for Printed Library Materials, ANSI Z39.48-1984.

Copyright © 1998 American Chemical Society

Distributed by Oxford University Press

All Rights Reserved. Reprographic copying beyond that permitted by Sections 107 or 108 of the U.S. Copyright Act is allowed for internal use only, provided that a per-chapter fee of \$20.00 plus \$0.25 per page is paid to the Copyright Clearance Center, Inc., 222 Rosewood Drive, Danvers, MA 01923, USA. Replication or reproduction for sale of pages in this book is permitted only under license from ACS. Direct these and other permissions requests to ACS Copyright Office, Publications Division, 1155 16th Street, N.W., Washington, DC 20036.

The citation of trade names and/or names of manufacturers in this publication is not to be construed as an endorsement or as approval by ACS of the commercial products or services referenced herein; nor should the mere reference herein to any drawing, specification, chemical process, or other data be regarded as a license or as a conveyance of any right or permission to the holder, reader, or any other person or corporation, to manufacture, reproduce, use, or sell any patented invention or copyrighted work that may in any way be related thereto. Registered names, trademarks, etc., used in this publication, even without specific indication thereof, are not to be considered unprotected by law.

PRINTED IN THE UNITED STATES OF AMERICA
American Chemical Society
Library
1155 16th St., N.W.

Table of Contents

Copyright, Advisory Board, Foreword		i-vii
Patil, A.O., Schulz, D.N. & Novak, B.M.	Preface	xiii-xiv
Schulz, D.N. & Patil, A.O.	Functional Polymers: An Overview	1-14

DIRECT POLYMERIZATION

Synthesis of Functional Polymers by Atom Transfer Radical Polymerization Krzysztof Matyjaszewski, Veerle Coessens, Yoshiki Nakagawa, Jianhui Xia, Jian Qiu, Scott Gaynor, Simion Coca, and Christina Jasieczek		16-27
Functional Polymers: Random Copolymers by Stable Free Radical Polymerization Paula J. MacLeod, Gordon K. Hamer, Pushpamma Lukose, and Michael K. Georges		28-37
Use of Protecting Groups in Polymerization D.N. Schulz, S. Datta, and R.M. Waymouth		38-57
Novel, Protected Functionalized Initiators for Anionic Polymerizations Douglas E. Sutton and James A. Schwindeman		58-70
Anionic Synthesis of Hydroxyl-Functionalized Polymers Using Protected, Functionalized Alkylolithium and Isoprenyllithium Initiators Roderic P. Quirk, Sung H. Jang, Kwansoo Han, Huimin Yang, Brad Rix, and Youngjoon Lee		71-84
Anionic Synthesis of Macromonomer Carrying Amino Group Using Diphenylethylene Derivative Jungahn Kim, Jae Cheol Cho, Keon Hyeong Kim, Kwang Ung Kim, Won Ho Jo, and R.P. Quirk		85-95
Functionalized Polymers with Dimethylamine and Sulfozwitterionic End-Groups: Synthesis, Dilute Solution, and Bulk Properties Nikos Hadjichristidis, Marinos Pitsikalis, and Stergios Pispas		96-120
Novel Functional Copolymers by Combination of Living Carbocationic and Anionic Polymerizations Jesper Feldthusen, Bela Ivan, and Axel H.E. Muller		121-34
Synthesis and Characterization of α -Hydroxyl- ω -Methoxycarbonyl and α -Hydroxyl- ω -Carboxyl Asymmetric Telechelic Polyisobutylenes Balint Koroskenyi and Rudolf Faust		135-48
Organo Rare Earth Metal Initiated Living Polymerizations of Polar and Nonpolar Monomers Hajime Yasuda, Eiji Ihara, Yuu Nitto, T. Takehi, Masakazu Morimoto, and Mitsufumi Nodono		149-62

New Reactive Polyolefins Containing p-Methylstyrene; Ranging from Semicrystalline Thermoplastics to Amorphous Elastomers H.L. Lu and T.C. Chung	163-81
--	--------

POST POLYMERIZATION

A Novel Reactive Functionalization of Polyolefin Elastomers: Direct Functionalization of Poly(isobutylene-co-p-methylstyrene) by a Friedel-Crafts Acylation Reaction A.O. Patil	184-98
--	--------

New Options via Chemical Modifications of Polyolefins: Part 1. Synthesis and Properties of Novel Phosphonium Ionomers From Poly(Isobutylene-co-4-Bromomethylstyrene) P. Arjunan, H-C. Wang, and J.A. Olkusz	199-216
--	---------

NOVEL APPROACHES AND/OR STRUCTURES

Multifunctional Supramolecular Materials Gregory N. Tew and S.I. Stupp	218-26
---	--------

Weil-Defined Smectic C* Side Chain Liquid Crystalline Polymers Wen-Yue Zheng, Thomas Epps, David Wall, and Paula Hammond	227-47
---	--------

Design of Assemblies of Functionalized Nanoscopic Gridlike Coordination Arrays Ulrich S. Schubert, Jean-Marie Lehn, J. Hassmann, C.Y. Hahn, N. Hallschmid, and P. Muller	248-60
---	--------

Functional Polyphosphazenes Harry R. Allcock	261-75
---	--------

Synthesis of Biodegradable Copolymers with Pendant Hydrophilic Functional Groups S. Jin and K.E. Gonsalves	276-85
---	--------

Photoinitiated Ring-Opening Polymerization of Epoxidized Polyisoprene C. Decker and T. Hoang Ngoc	286-302
--	---------

Synthesis of Cyclic Carbonate Functional Polymers Dean C. Webster and Allen L. Crain	303-20
---	--------

Functionalized Polydiacetylenes with Polar, Hydrogen Bonding and Metal-Containing Groups I. H. Jenkins, W.E. Lindsell, C. Murray, P.N. Preston, and T.A.J. Woodman	321-29
---	--------

INDEXES

Author Index	333
Subject Index	335-47

Advisory Board

ACS Symposium Series

Mary E. Castellion
ChemEdit Company

Arthur B. Ellis
University of Wisconsin at Madison

Jeffrey S. Gaffney
Argonne National Laboratory

Gunda I. Georg
University of Kansas

Lawrence P. Klemann
Nabisco Foods Group

Richard N. Loepky
University of Missouri

Cynthia A. Maryanoff
R. W. Johnson Pharmaceutical
Research Institute

Roger A. Minear
University of Illinois
at Urbana-Champaign

Omkaram Nalamasu
AT&T Bell Laboratories

Kinam Park
Purdue University

Katherine R. Porter
Duke University

Douglas A. Smith
The DAS Group, Inc.

Martin R. Tant
Eastman Chemical Co.

Michael D. Taylor
Parke-Davis Pharmaceutical
Research

Leroy B. Townsend
University of Michigan

William C. Walker
DuPont Company

Foreword

THE ACS SYMPOSIUM SERIES was first published in 1974 to provide a mechanism for publishing symposia quickly in book form. The purpose of the series is to publish timely, comprehensive books developed from ACS sponsored symposia based on current scientific research. Occasionally, books are developed from symposia sponsored by other organizations when the topic is of keen interest to the chemistry audience.

Before agreeing to publish a book, the proposed table of contents is reviewed for appropriate and comprehensive coverage and for interest to the audience. Some papers may be excluded in order to better focus the book; others may be added to provide comprehensiveness. When appropriate, overview or introductory chapters are added. Drafts of chapters are peer-reviewed prior to final acceptance or rejection, and manuscripts are prepared in camera-ready format.

As a rule, only original research papers and original review papers are included in the volumes. Verbatim reproductions of previously published papers are not accepted.

ACS BOOKS DEPARTMENT

Preface

Functional polymers impact many aspects of polymer science and technology. These macromolecules contain functional groups that have polarity or reactivity differences from backbone chains. Such polymers often show unusual or improved properties by virtue of enhancement in phase separation, reactivity, or associations.

Functional polymers are and will continue to be in demand because they expand the property and application range of their nonfunctional counterparts. Today most functional polymers are tailored for specific properties and therefore specialty applications. However, polymers are being driven more and more toward higher value/performance analogs. Consequently, the expectation is that there will be increasing penetration of functional polymers into commodity markets. Yet, one of the primary factors slowing the growth of functional polymers has been the relative complexity and cost of their preparation. The synthesis of functional polymers is often made difficult because of chemical and/or phase incompatibilities or antagonisms.

There are very few books on the market today dealing with functional polymers. Moreover, such books focus mainly on functional polymers for specialty applications. Nevertheless, there has been tremendous progress in recent years in synthesizing functional polymers. In addition, there have been several national and international symposiums discussing such developments. Yet there are no books discussing such advances. This volume aims to fill this void.

The book contains 22 chapters, logically organized into an overview chapter with three other subsections: Part one: The synthesis of functional polymers by direct methods, such as anionic, cationic, free radical and coordination polymerization. Part two: The synthesis of functional polymers by post-polymerization functionalization. Part three: Novel approaches and structures. Special emphasis is given to more modern techniques that allow for controlled and directed functionalization via “living” polymerization.

Acknowledgments

We wish to thank all of the authors for their cooperation and for their high quality chapters. We also gratefully acknowledge the secretarial support of Pat Ko

cian. Finally, we thank Anne Wilson, the Acquisitions Editor at the ACS Books Department, who kept us on task in a firm but patient manner.

ABHIMANYU O. PATIL
Corporate Research Laboratory
Exxon Research and Engineering Company
Route 22 East
Annandale, NJ 08801

DONALD N. SCHULZ
Corporate Research Laboratory
Exxon Research and Engineering Company
Route 22 East
Annandale, NJ 08801

BRUCE M. NOVAK
Department of Polymer Science and Engineering
University of Massachusetts
Amherst, MA 01003

Chapter 1

Functional Polymers: An Overview

D. N. Schulz and Abhimanyu O. Patil

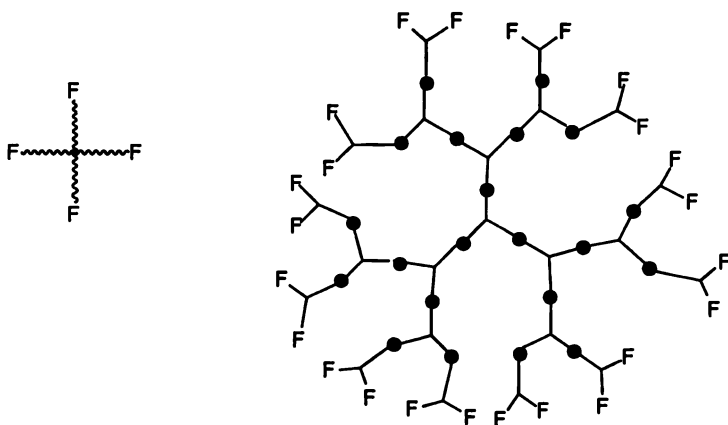
Corporate Research Laboratory, Exxon Research and Engineering Company,
Route 22 East, Clinton Township, Annandale, NJ 08801

This chapter surveys the synthesis of functional polymers by direct methods, such as anionic, cationic, free radical and coordination polymerization, as well as post-polymerization functionalization of chains in the bulk or on the surface. Special emphasis is given to more modern techniques that allow for controlled and directed functionalization via “living” polymerization. Moreover, an introduction to typical applications of functional polymers is presented.

Functional polymers are macromolecules that have unique properties or uses.^{1,2} The properties of such materials are often determined by the presence of chemical functional groups that are dissimilar to those of the backbone chains. Examples are polar or ionic functional groups on hydrocarbon backbones or hydrophobic groups on polar polymer chains. Chemical heterogeneity on the polymer chains can lead to enhanced reactivity, phase separation, or association. The ability of functional polymers to form self-assemblies or supramolecular structures is a further incentive. When the formation or dissociation of the self-assemblies is triggered by chemical or physical stimuli so called “smart” materials can result.³

Most functional polymers are based on simple linear backbones. These can be chain-end (telechelic), in-chain, block or graft structures. However, there has also been interest in functional polymers with special topologies or architectures.⁴ These include 3-dimensional polymers, such as stars, hyperbranched polymers,^{5,7,8} or dendrimers⁹⁻¹¹ (treelike structures) (Scheme 1)

This chapter surveys the synthesis of functional polymers by direct anionic, cationic, free radical and coordination polymerization, as well as the bulk and surface modification of preformed polymer backbones. Moreover, an introduction to typical applications of functional polymers is presented.



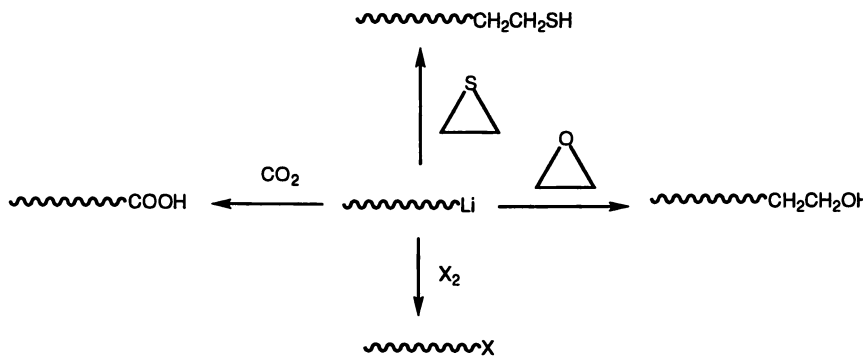
Scheme 1

Functional Polymers by Direct Polymerization

Anionic Polymerization

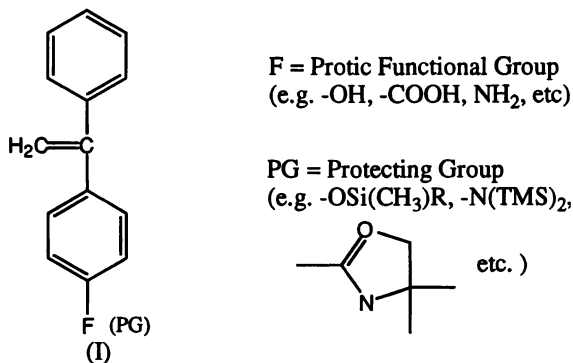
Perhaps the most controlled method for the direct introduction of functionality is by “living” anionic polymerization. Such polymerization proceeds with an absence of chain transfer and termination, leading to polymers with predictable MW’s, narrow MWD’s, defined architectures and a high degree of functional purity. It is not uncommon to prepare linear or star polymers with MWD’s < 1.1 and functional purity > 95%.^{12a}

Both chain-end (telechelic) and in-chain functional polymers can be synthesized by anionic methods. For example, termination of “living” lithiomacromolecules with electrophilic reagents can, in principle, result in a wide variety of telechelic polymers (Scheme 2).^{12b}

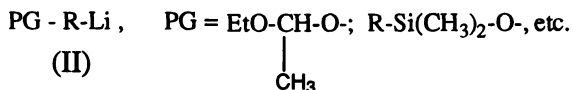


Scheme 2

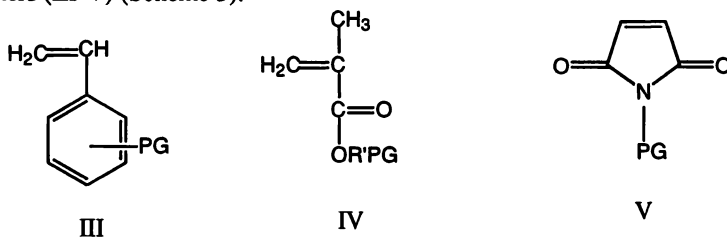
However, these simple termination reactions can be subject to subtle side reactions,^{13,14} which can be an issue if one wants to perform linear chain extension of telechelic polymers.



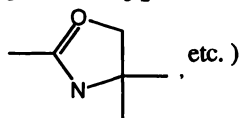
Improved results are obtained by using functional 1,1-diphenylethylenes (I) as terminating agents, especially when the functional groups are suitably protected.^{15,16} Alternatively, the protected functionality can be built into the initiator (II) itself.¹⁷



In-chain functional anionic polymers can be prepared by use of protected functional monomers (III-V) (Scheme 3).¹⁷⁻²¹



PG = Protecting Group
(e.g. -OSi(CH₃)₂R, -N(TMS)₂,

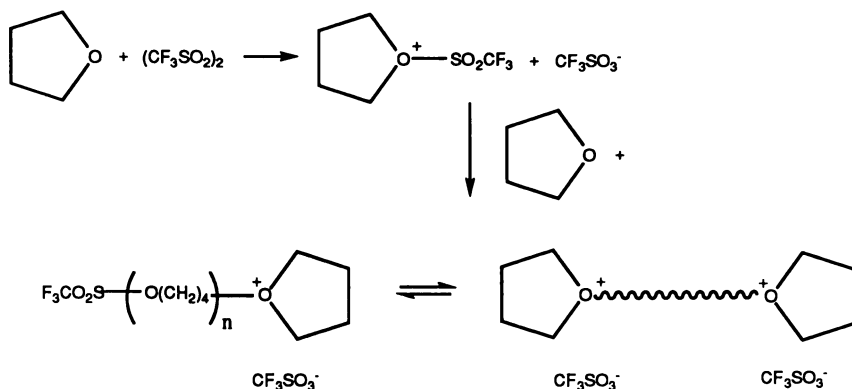


Scheme 3

Suitable deprotection methods yield the corresponding functional anionic polymers.

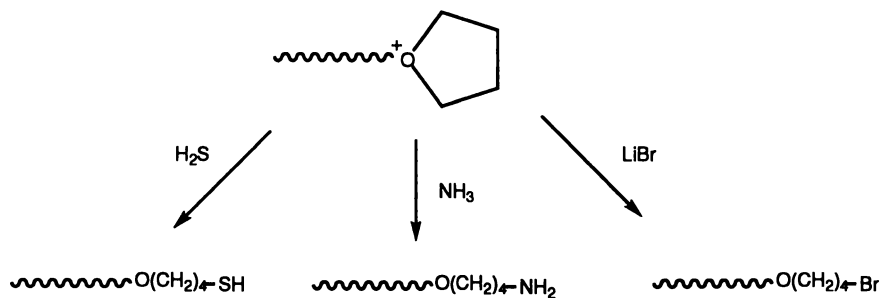
Cationic Polymerization

It was long believed that cationic polymerization was an unsatisfactory route to synthesize well-defined functional polymers because of inter- or intra-molecular transfer or rearrangement. However, in recent years, several monomers have exhibited sufficient control of initiation, propagation and termination to allow the synthesis of functional polymers.^{22a} Tetrahydrofuran (THF) has been cationically polymerized using the difunctional initiator triflic anhydride (Scheme 4).^{22b}



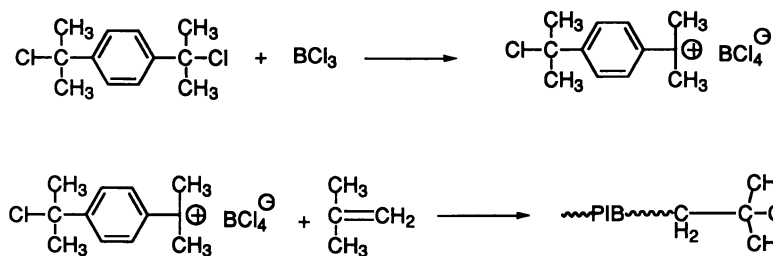
Scheme 4

The “living” polyTHF may then be reacted with a suitable terminating agent to give the desired end-groups, either directly or after prior reaction with a weakly nucleophilic monomer, such as aziridine, to produce a less reactive chain end. Some of these reactions are shown in Scheme 5.²³



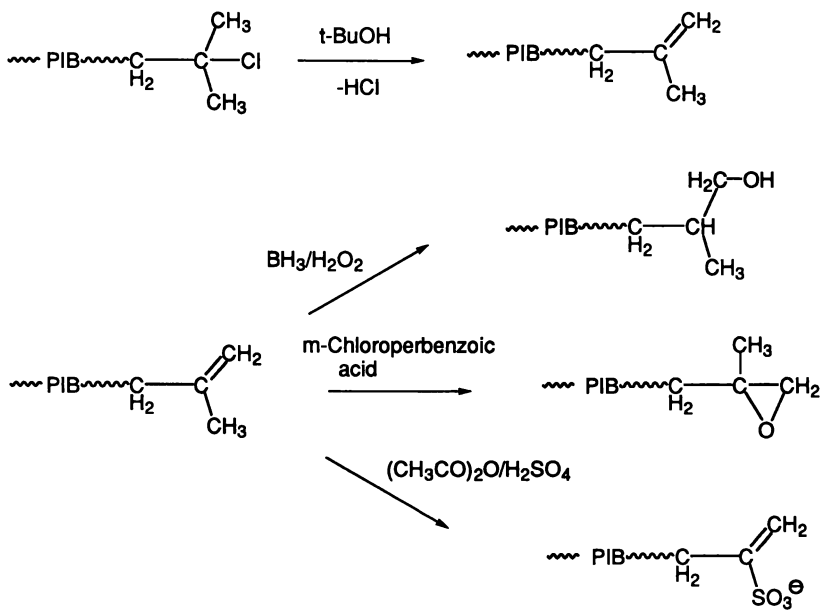
Scheme 5

The INIFER technique has been used for quasi “living” cationic polymerization of isobutylene. Bi- and trifunctional initiators yield telechelics with two or three chlorine end groups (Scheme 6).²⁴



Scheme 6

These functional groups can then be converted to other functional groups by subsequent reaction (Scheme 7).²⁵



Scheme 7

Recently vinyl ether monomers have been cationically polymerized by processes that are close to “living” polymerizations for the preparation of well-controlled polymer structures. In these processes, chain transfer is strongly suppressed or virtually eliminated by use of relatively stable (i.e., less-ionized) propagating species. End-functionalized polymers can be prepared by terminating a living polymerization with suitable functionalized agents. End capping of the HI/I_2 induced vinyl ether polymerization with $\text{Na}^+ \text{~}^-\text{CH}(\text{COOC}_2\text{H}_5)_2$ gives malonate end groups, which can be converted into a $-\text{COOH}$ functional group by hydrolysis.

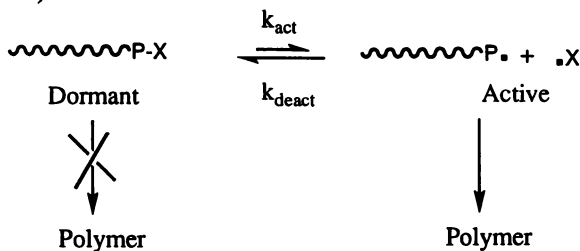
“Living” polymerization has also been observed for isobutylene with *tert*-alcohol/ BCl_3 . Some of the more promising concepts involve the use of proton traps, weak electron donors, such as DMSO, and various Lewis acids. Certain specific functional groups have been introduced by direct end capping of living carbocationic polyisobutylene.²⁶ These functional polymers include macromonomers (oligomers with at least one end group that allows polymerization, for example $-\text{CH}=\text{CH}_2$), telechelics (oligomers with one, two, or even more functional end groups such as $-\text{OH}$, $-\text{COOH}$, $-\text{NH}_2$, $-\text{SH}$ etc.), polymers with pendant functional groups, star-shaped macromolecules, block and graft copolymers (thermoplastic elastomers, amphiphilic blocks).²⁷

Both telechelics and macromonomers are of great interest, owing mainly to their ease of handling. Because of their low molecular weights, they have low melt viscosities and can be processed without solvent. They are also less toxic and have a lower vapor pressure than their corresponding monomers. Such functional polymers can be converted to chain extended polymers, networks, blocks, and graft copolymers upon subsequent reaction.

Free-radical polymerization

Free-radical polymerization has been used for the preparation of a wide variety of lab-scale polymers, as well as a significant quantity of commodities. Free-radical polymerization, until recently, has been the method of choice for the synthesis of many functional polymers because this polymerization method tolerates polar functional groups.^{28a} However, the disadvantages of free-radical polymerization are broad polydispersity and poor control over chain architecture and end groups. These problems are due to the polymerization process being highly affected by termination or transfer, which lead to deactivation or branching of the growing polymer. In free-radical polymerization, if the chain transfer agent is very reactive and the molecular weights of the products formed are consequently very low, the process is referred to as ‘telomerization’. The use of telomers to produce telechelic oligomers has been reviewed.^{28b} More recently, telechelics have been prepared by addition/fragmentation.^{28c-d}

Considerable advances in direct or indirect control of radical polymerization have been accomplished in the past decade.²⁹⁻³⁸ A common key to the control of radical polymerizations seems to involve reversible and rapid formation of a dormant species, with an atom covalently bonded to the reactive radical species. The rapid and reversible interchange equilibrium, in turn decreases the instantaneous concentration of the activated form and thereby suppresses terminal reactions between the growing radical species (Scheme 8).



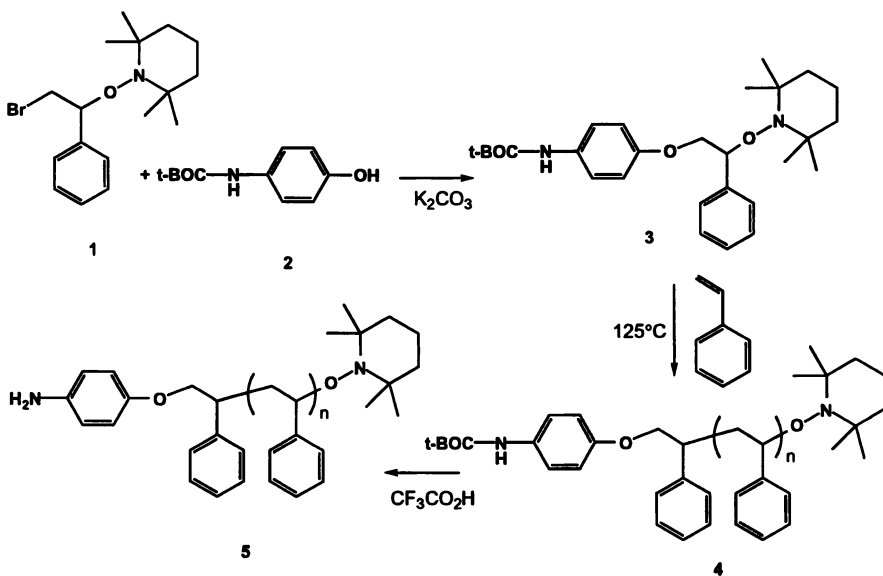
Scheme 8

This ‘living’ polymerization can be used to control molecular weights, polymer architectures and chain ends in a manner similar to the synthetically more demanding

anionic or cationic techniques. A free radical polymerization process (that is easy to perform, is economical, and can be readily performed in bulk or suspension) has a distinct cost advantage. Additionally, unlike these other techniques, which are incapable of incorporating a wide range of functional groups, "living" free radical polymerization is tolerant to numerous reactive functional groups, while still leading to well-defined polymers with low polydispersities.

Stable free radical polymerization (SFRP) employs a combination of a conventional radical initiator, benzoyl peroxide, with 2,2,6,6-tetramethyl-1-piperidinoxyl (TEMPO) as a stable free radical.²⁹⁻³⁰ The concept of using a unimolecular initiator, containing both the initiating radical and the TEMPO 'counter' radical, was introduced to better control molecular weight and chain end functional group (Scheme 9).³²⁻³³ For example, aminophenol protected with *t*-butoxycarbonyl (*t*-BOC) can be coupled with the bromo-substituted TEMPO derivative, 1, to give the functionalized initiator, 3. This initiator can be used to prepared the functional polymer, 5. Furthermore, polyfunctional molecules bearing multiple initiating centers have been synthesized to make three arm star polystyrene.³⁴

Similarly, atom transfer radical polymerization (ATRP) has been used by Matyjaszewski and others for the synthesis of polystyrene and polyacrylates with controlled molecular weights. This process is based on a Cu(I) assisted atom-transfer radical polymerization (ATRP)³⁵⁻³⁶ One of the end groups is defined by the structure of the initiator, whereas the other one contains an alkyl halide, such as chloride or bromide that can be converted to other functional groups. Additionally, the radical intermediates of ATRP are tolerant to many functional groups, which can not be used directly in anionic or cationic processes, such as hydroxyalkyl, epoxy, enabling the direct synthesis of well-defined glycidyl, hydroxyethyl(meth)acrylates and other functional monomers. Percec and Barboiu have prepared polystyrene derivatives with efficient control of chain-end chemistry by the use of functionalized arenesulfonyl chlorides.³⁷



Scheme 9

Sawamoto and coworkers have developed an initiating system based on transition metal complexes that consists of CCl_4 and $\text{RuCl}_2(\text{PPh}_3)_3$, which is also equally effective for 'living' free-radical polymerization processes.³⁸⁻³⁹ Such transition-metal-based systems can afford polymers with controlled architectures, including end-functionalized polymers.

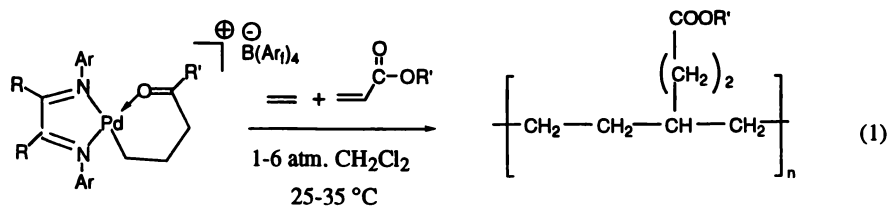
Coordination Polymerization

Coordination polymerization involves the use of transition metal catalysts. Examples are Ziegler-Natta polymerization by Ti/Al systems, metallocene polymerization with Ti, Zr, Hf catalysts, or metathesis polymerization with W, Mo, Re metals. Synthesis of functional polymers by organometallic catalysts are particularly difficult because transition metals are not only killed by protic functionality, they are often poisoned by heteroatoms (e.g. N, O).

Strategies for synthesizing functional polymers by coordination polymerization have followed two directions, i.e. modifying the catalyst or protecting the monomer itself. Modification of the catalyst entails choosing the appropriate metals, ligands, and/or anions.

For examples, late transition metals (e.g. Ni, Pd)⁴⁰⁻⁴³ and lanthanides (e.g. Sm)⁴⁴⁻⁴⁸ tend to be more tolerant of polar functionalities than are early transition metals (e.g. Ti, Zr, Hf). When the transition metal center is chosen further to the right in the periodic table, it becomes softer and contains more d-electrons, thereby favoring complexation with softer bases like olefins rather than harder oxygen containing functional groups.⁴⁹

Brookhart and coworkers⁴¹⁻⁴³ combined late transition metals with sterically bulky ligands and noncoordinating anions to synthesize olefin-acrylate copolymers (Scheme 10). The bulky ligands block associative displacement and thus minimizing chain transfer. Anions like $\text{B}(\text{Ar})_4^-$ promote a more active cationic catalytic species and improve the solubility of these systems. However, the current late transition metal catalysts still don't achieve the activities (productivities) of the conventional Ziegler-Natta or metallocene catalysts for nonfunctional monomers, such as ethylene.



Ar: 2,6-(iPr)₂C₆H₃; 2,6-(CH₃)₂C₆H₃

Ar': 3,5-(CF₃)₂C₆H₃

R': Me; t-Bu; CH₂(CF₂)₆CF₃

Scheme 10

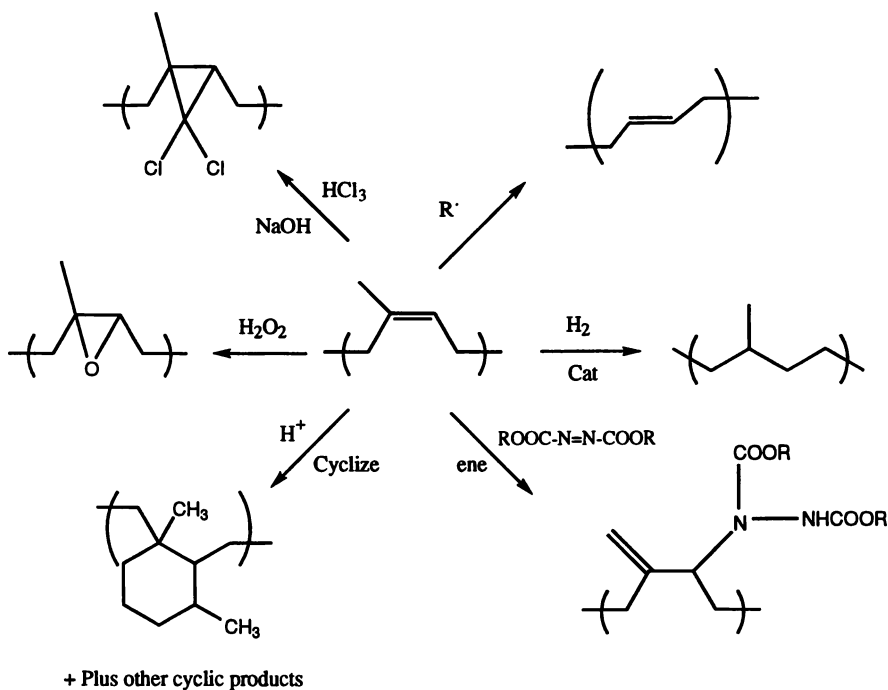
Coordination polymerization of hydroxyl, carboxyl and amino monomers can also be effected by the judicious use of protecting groups. For example, amino and hydroxyl monomers have been protected by silyl ethers and aluminate salts for Ziegler Natta and/or metallocene polymerization and carboxyl monomers have been protected via aluminate salts.¹⁷ Alternatively, organoborane synthons have been used to carry

hydroxyl and other functional groups through Ziegler Natta, metallocene and metathesis polymerizations.⁵⁰

Chemical Modification of Polymers

In principle, any organic reaction that has been applied to small molecules can be applied to chemically modifying (functionalizing) polymers. Chemical modification can be done in bulk, solution or on surfaces of polymers. However, the reactivity of a functional group attached to a polymer chain may or may not be the same as when it is attached to a small molecule. For example, the reactivity of such a group may be controlled or influenced by (a) the type of neighboring groups, (b) the type and conformation of the polymer backbone (c) the morphology and crystallinity of the backbone (d) the solubility/miscibility of reactant and catalyst phases.⁵¹ In addition, reactions on polymers have the added complication of polymer crosslinking or chain cleavage.

Solution reactions of polydienes illustrate the diversity of chemical modifications on polymers (Scheme 11).⁵²⁻⁵³ Such polymers can be isomerized, cyclized, hydrogenated, epoxidized, and reacted with carbenes or enophiles. Most of these transformations increase the T_g 's of the polymers with a consequent change in the physical/mechanical properties of the materials.



Scheme 11

Polyolefins (especially polyethylene, propylene, poly(1-butene), polyisobutylene, and their copolymers) are used in a wide range of applications. These polyolefins incorporate an excellent combination of mechanical, chemical, and electronic properties, as well as processability, recyclability, and low cost.

Nevertheless, the lack of reactive groups limit some of their end uses, particularly where adhesion, dyeability, paintability, printability, or compatibility are needed. Consequently, the chemical modification of polyolefins has been an area of increasing interest as a route to higher value products.⁵⁴

Free-radical grafting is a preferred way to add functionality to polyolefins, e.g. reaction with maleic anhydride. Amine functionalized polymers can be obtained by further derivatization of carboxylic anhydride functionalized polyolefin with amines. Polymeric materials containing amino groups are important because of the chemical versatility of the amino function. Although such procedures are useful, they lack control over molecular weight and functional-group distribution in the polymer.

Surface modification of polymers has also become a vigorous area of polymer research.⁵⁵⁻⁵⁶ Surface functionalization is a means of modifying the surface properties of the polymer without affecting the properties of the bulk phase. For example, surface modification changes the interfacial properties of polymers, such as adhesion,⁵⁷⁻⁵⁸ biocompatibility,⁵⁹⁻⁶⁰ permeability,⁶¹ wettability,⁶²⁻⁶⁴ printability,⁶⁵ weatherability,⁶⁶ or friction.⁶⁷

Just as polydienes and polyolefins have been modified in solution, they have also been surface-modified. For example, polar functional groups have been introduced to syndiotactic 1,2 polybutadiene surfaces by photolytic addition of thiols, as well as treatment with aqueous permanganate. Such surface functionalization leads to changes in wettability, as evidenced by contact angle measurements. Furthermore, the surface functionalization can be reconstructed upon heating.⁶⁸⁻⁶⁹ In turn, polyolefins have been surface modified by oxidation, chlorination, sulfonation, etc.^{56,70}

Applications

Polymer functionalization aims at imparting new properties (e.g. chemical, biophysical, physicochemical or optoelectronic) to materials.² Functional polymers have been developed for a wide range of diverse applications. These include organic catalysis (supported catalysts), medicine (red-blood-cell substitutes), optoelectronics (conducting polymers, magnetic polymers and polymers for nonlinear optics), biomaterials, paints and varnishes, building materials, photographic materials as well as lube and fuel additives. While it is not possible to enumerate all of the applications of functional polymers, some representative examples of functional polymers are listed below.

Polymer supported catalysts have advantages because of the ease of catalyst recovery and the opportunity for simultaneously using otherwise incompatible catalytic systems. Indeed, the immobilization of several catalysts onto a polymer matrix is a unique way of avoiding antagonistic reactions between them, and of allowing reagents to participate in a 'cascade' of reactive processes.⁷¹ For example, polymer-supported catalysts have been used as the Lewis acid catalysts in the carbocationic polymerization of isobutylene.⁷²⁻⁷³ After the reaction, polyisobutylene is obtained by simply filtering the supported catalyst. The reaction cycle can be repeated many times.

Metal containing polymers are useful for a wide range of applications including analysis and catalysis, optical and electronic devices, colorants and coatings, structural composites, ceramics, controlled-released medicaments, and biocides.⁷⁴

Photosensitive polymers can be applied in areas such as printing, electronics, paints, biomaterials, information recording, and UV curing inks. One of the major applications of photosensitive polymers is in the development of resist materials with submicron resolution for semiconductor fabrication. Resist science and technology is an expanding field, and there is an increasing demand for more sensitive photopolymers and exposure equipment.⁷⁵ Thus, the new photosensitive polymers will continue to make significant contributions to electronic and photonics through

improvements of material and related technologies, especially for deep-UV, electron beam, and X-ray lithography and chemical amplification resist systems.

Liquid crystalline polymers offer a range of properties that include ferroelectric behavior that has potential for fast switching devices, piezo- and pyroelectric properties.⁷⁶ The ability of liquid crystalline polymers to improve hardness and impact strength can impact the coating industry. The self-assembling properties of liquid crystalline polymers coupled with the development of new block copolymers containing liquid crystalline units, which can also undergo microphase separation, could also yield new materials with increased strength.

Conducting polymers are polymers having a conjugated backbone structure that is capable of being doped to yield high electronic mobility and electrical conductivity. The delocalised electronic structures of π -conjugated polymers, which are responsible for their unusual electronic properties, tend to yield relatively stiff chains with little flexibility and with relatively strong inter-chain attractive interactions, which make them insoluble and non-processable. Such monomers have been modified to obtain polymers that are soluble in water and organic solvents. Potential applications include solid-state rechargeable batteries, "smart" windows, photo- or electrochromic materials, antistatic coating, sensors, photocells, and electromagnetic screening applications.⁷⁷

Some of these polymers have the ability to be electroluminescent for use in plastic light emitting diodes (LED).⁷⁸⁻⁷⁹ Optical components (including transmitter, receiver, modulator, couplers, multiplexing system, and data links) could be manufactured from specifically tailored functional polymers in the near future.

Functional polymers may be used for different types of chemical sensors, including acoustic wave sensors (bulk acoustic wave, surface acoustic wave, and flexural plate wave sensors), electronic conductance sensors (semiconducting and capacitance sensors), and calorimetric sensors.²

Summary and Outlook

Functional polymers are and will continue to be in demand because they expand the property and application range of their nonfunctional counterparts. Today most functional polymers are tailored for specific properties and therefore specific applications. However, polymers are being driven more and more toward higher value/performance analogs. Consequently, the expectation is that there will be increasing penetration of functional polymers into commodity markets.

One of the primary factors slowing the growth of functional polymers has been the relative complexity and cost of their preparation. The synthesis of functional polymers is often made difficult because of chemical or phase incompatibilities or antagonisms. This chapter surveys the general methods for functional polymer syntheses. It reviews the scope and limitations of functionalization by direct polymerization (e.g. anionic, cationic, free radical and organometallic methods), as well as post-polymerization bulk and surface modification of preformed backbones.

For example, in anionic polymerization, careful selection of solvent, initiator, and temperature are important for successful polymerization. Sensitivity of anionic species toward oxygen and moisture remains an inconvenient factor inherent in anionic polymerization. On the other hand, many novel block copolymers and functional polymers can be prepared by "living" anionic polymerization, providing access to a variety of specialty polymers. The problem of controlled anionic polymerization of highly reactive monomers remains a challenging target in the field of anionic polymerization.

One of the significant developments in "living" cationic polymerization has been the synthesis of telechelics and production of diblock copolymers. PIB based macromonomers are another class of functional precursors. Copolymerization of these

macromonomers with specific monomers holds promise for biomedical applications, such as amphiphilic networks for drug-delivery systems and artificial organs.

The field of 'living' free-radical polymerizations (e.g. ATRP, TEMPO systems) has been growing in recent years. Yet, no "living" radical polymerizations have thus far been reported for α -olefins. Further developments may include the design of functional initiators for living polymerization. Also, ATRP may benefit from the design of homogeneous redox systems that can be easily removed from the polymerization mixture.

The advent of late transition metal catalysts for polymerization promises to expand this method as a route to functional polymers. Late transition metals are definitely more tolerant to functionality. The outstanding question is will they have enough activity for traditional nonfunctional monomers, such as ethylene or propylene. A catalyst that can polymerize both olefins and polars with high activity will be the next breakthrough.

Post-polymerization modification is the most expensive method for preparing functional polymers. It is expensive because it means added steps. However, it is the method of choice when one wants to directly compare structure and reactivity or properties of functional with nonfunctional polymers. The only caveat is that chemical modification of polymers must not introduce adventitious chain scission or crosslinking. The other benefit of post-polymerization modification is that it can be accomplished for bulk polymers, as well as polymer surfaces. For some applications surface modification will be enough to achieve the desired effect.

Literature Cited

- (1) Bergbeiter, B. E.; Martin, C. R. *Functional Polymers*; Plenum Press: New York, 1989
- (2) Arshady, R. *Desk Reference of Functional Polymers: Syntheses and Applications* ACS: Washington DC, 1997.
- (3) Jerome, R.; Vanhoorne, P. *Trends in Polymer Science* **1994**, 2, 382.
- (4) Frechet, J. M. J. *Science* **1994**, 263, 1710.
- (5) Kim, Y. H.; Webster, O. W. *J. Am. Chem. Soc.* **1990**, 112, 4592.
- (6) Hawker, C. J.; Lee, R.; Frechet, J. M. J. *J. Am. Chem. Soc.* **1991**, 113, 4583.
- (7) Malmstrom, E.; Hult, A. *J. Macromol. Sci.-Rev. Macromol. Chem. Phys.* **1997**, C37(3), 555.
- (8) Turner, S. R. *Polymer News*, **1997**, 22(6), 197.
- (9) Tomalia, D. A. *Polym. J.* **1985**, 17, 117.
- (10) Hawker, C. J.; Frechet, J. M. J. *J. Am. Chem. Soc.* **1990**, 112, 7638.
- (11) Chemical & Engineering News, (September 22) **1997**, 75(38), 28.
- (12a) Hsieh, H. L. Quirk, R. P. *Anionic Polymerization*, Marcel Decker, NY 1996.
- (12b) Halasa, A. F.; Schulz, D. N.; Tate, D. P.; Mochal, V. D. in *Advances in Organometallic Chemistry* Stone, F. G. A.; West, R., Eds., Academic Press: New York, 1980, 18, pp 55-97.
- (13) Quirk, R. P. in *Comprehensive Polymer Science*, First Supplement, Agarwal, S. L. and Russo, S., Eds., Pergamon Press, Oxford, U.K., 1992, pp. 83-106.
- (14) Quirk, R. P., Jang, S. H. *Rubber Chem. Tech.* **1996**, 69(3), 444.
- (15) Quirk, R. P. *Rubber Chem. Tech.* **1991**, 64, 658.
- (16) Quirk, R. P.; Lynch, R. *Macromolecules* **1993**, 26, 1206.
- (17) Schulz, D. N.; Datta, S.; Waymouth, R. M. see chapter in this volume.
- (18) Nakahama, S.; Hirao, A. *Progr. Polym. Sci.* **1990**, 15, 299.
- (19) Nakahama, S.; Hirao, A. *Trend. Polym. Sci.* **1994**, 2, 267.
- (20) Hirao, A.; Nakahama, S. *Progr. Polym. Sci.* **1992**, 17, 283.
- (21) Dasgupta, A.; Swaram, S. *J. Macromol. Sci.-Rev. Macromol. Chem. Phys.* **1997**, C37(1), 1.

- (22a) Katyjaszewski, K. *Cationic Polymerization*, Marcel Decker, NY 1996.
- (22b) Smith, S.; Hubin, A. J. *J. Macromol. Sci., Chem.* **1973**, A7, 1399. Smith, S.; Schultz, W. J.; Mewmark, R. A. *ACS Symp. Ser.* **1977**, 59, 13.
- (23) Tezuka, Y.; Goethals, E. J. *Eur. Polym. J.* **1987**, 18, 991.
- (24) Nuyken, O. in *The Polymeric Materials Encyclopedia: Synthesis, Properties and Applications*; Salamone, J. C. Ed; CRC Press, Boca Raton, 1996, 4, 2672.
- (25) Mishra, M. K.; Kennedy, J. P. in *Desk Reference of Functional Polymers: Synthesis and Applications*, R. Arshady, Ed. ACS: Washington, DC 1997, Chapter 1.4, 57-72.
- (26) Kennedy, J. P.; Ivan, B. *Designed Polymers by Carbocationic Macromolecular Engineering: Theory and Practice*, Hanser Publishers: Munich, New York, 1992.
- (27) Kamigaito, M.; Maeda, Y.; Sawamoto, M.; Higashimura, T. *Macromolecules* **1993**, 26, 2670.
- (28a) Moad, G.; Solomon, D. H. *The Chemistry of Free Radical Polymerization*; Elsevier Science inc.: New York, 1995.
- (28b) Boutevin, B.; Pietrasanto, Y. in *Comprehensive Polymer Science* Allen, G. and Bevington, J. C. Eds. Pergamon Press, Oxford, Vol. 3, Ch. 14, 1989.
- (28c) Busfield, W. K.; Jenkin, I. D.; Nakamura, T.; Monteiro, M. J.; Rizzardo, E.; Sayama, S.; Thang, S. H.; Van Le, P.; Zayas-Holdsworth, C. I. *Polym. Adv. Technol.* **1998**, 9, 94.
- (28d) Krstina, J.; Moad, C. L.; Moad, G.; Rizzardo, E.; Berge, C. T.; Fryd, M. *Macromol. Symp.* **1996**, 111, 13.
- (29) Georges, M. K.; Veregin, R. P. N.; Kazmaier, P. M.; Hamer, G. K. *Trends Polym. Sci.* **1994**, 2, 66.
- (30) Georges, M. K.; Veregin, R. P. N.; Kazmaier, P. M.; Hamer, G. K. *Macromolecules* **1993**, 26, 2987.
- (31) Hawker, C. J. *J. Am. Chem. Soc.* **1994**, 116, 11185.
- (32) Hawker, C. J. *Trends Polym. Sci.* **1996**, 4, 183.
- (33) Hawker, C. J. *Macromolecules* **1995**, 28, 2993.
- (34) Hawker, C. J. *Angew. Chem., Int. Ed. Eng.* **1995**, 34, 1456.
- (35) Wang, J. S. and Matyjaszewski, K. *J. Am. Chem. Soc.* **1995**, 117, 5614.
- (36) Wang, J. S. and Matyjaszewski, K. *Macromolecules* **1995**, 28, 7901.
- (37) Percec, V.; Barboiu, B. *Macromolecules* **1995**, 28, 7970.
- (38) Kato, M.; Kamigaito, M.; Sawamoto, M. and Higashimura, T. *Macromolecules* **1995**, 28, 1721.
- (39) Sawamoto, M. and Kamigaito, M. *Trends Polym. Sci.* **1996**, 4, 371.
- (40) Abu-Surrah, A.; Rieger, B. *Ang. Chem. Int. Ed.* **1996**, 35(21) 2475.
- (41) Brookhart, M.; Wagner, M. I. *J. Am. Chem. Soc.* **1994**, 116, 3641.
- (42) Johnson, L. K.; Mecking, S.; Brookhart, M. *J. Am. Chem. Soc.* **1996**, 118, 267. Mecking, S.; Johnson, L. K.; Wang, L.; Brookhart, M. *J. Am. Chem. Soc.* **1998**, 120, 888.
- (43) Brookhart, M.; DeSimone, J. M.; Barborak, J. C.; Rix, F. C.; Tahiliani, M. K.; Wagner, D. *Am. Chem. Soc. Div. Polym. Chem. Polym. Prepr.* **1994**, 35(2), 530.
- (44) Yasuda, H.; Ihara, E. *Adv. Polym. Sci.* **1997**, 133, 53.
- (45) Yasuda, H.; Ihara, E.; Nitto, Y.; Kakedhi, T.; Morimoto, M.; Nodono, M. see chapter in this volume.
- (46) Boffa, L. S.; Novak, B.M. *Macromolecules* **1994**, 27, 6993.
- (47) Boffa, L. S.; Novak, B. M. *Macromolecules* **1997**, 30, 3494.
- (48) Boffa, L. S.; Novak, B. M. *Tetrahedron*, **1997** 53(45), 15367.
- (49) Grubbs, R.H., in *Aqueous Organometallic Chemistry and Catalysis*; Horvath, I. T.; Joo, F., Eds., Kluwer Academic Publishers: Netherlands, 1995, pp 15-22.
- (50) Chung, T. C. in *Polymeric Materials Encyclopedia*; Salamone, J. C., Ed.; CRC Press: Boca Raton, FL, 1996, 4, pp 2681-2691.

- (51) Marechal, E. in *Comprehensive Polymers Science*; Eastmond, G. C.; Ledwith, A.; Russo.; Sigwalt, P., Eds. Pergamon Press: Oxford, U.K. 199 , Vol. 6, pp 1-47.
- (52) Schulz, D. N.; Turner, S. R.; Golub, M. A. *Rubber Chem. Technol.* **1982**, 55, 809.
- (53) Schulz, D. N. in *Handbook of Elastomers*; Bhowmick, A. K.; Stephens, H. L., Eds., Marcel Dekker: New York, 1988, pp 75-100.
- (54) Naqri, K. M.; Choudhary, M. S. *J. Rev. Macromol. Chem. Phys.*, **1996**, C36(3), 601.
- (55) Garbassi, F.; Morra, M.; Occhiello, E. *Polymer Surfaces from Physics to Technology*; John Wiley and Sons: New York, 1994.
- (56) Ward, W. J.; McCarthy, T. J.: in *Encycl. Polym. Sci. Eng.*; Kroschwitz, J. I., Ed.: John Wiley: New York, NY, 1990, 1152.
- (57) Kaczinski, M. B.; Dwight, D. W. *J. Adhesion Sci. Technol.* **1993**, 7, 165.
- (58) Martin-Martinez, J. M.; Fernandez-Garcia, T. C.; Huerta, F.; Orgiles-Barcelo, A. *C. Rubber Chem. Technol.* **1991**, 64, 510.
- (59) Andrade, J. D. in *Surfaces and Interfacial Aspects of Biomedical Polymers*; Andrade, J. D., Ed.; Plenum: New York, 1985, Vol. 1, pp 249-292.
- (60) Feast, W. J.; Munro, H. S., Eds. *Polymer Surfaces and Interfaces*; John Wiley and Sons: New York, 1987.
- (61) Le Roux, J. D.; Paul, D. R.; Arendt, M. F.; Yuan, Y.; Cabasso, I. *J. Membrane Sci.* **1994**, 90,37.
- (62) Costello, C. A.; McCarthy, T. J. *Macromolecules* **1987**, 20(11), 2819.
- (63) Whitesides, G. M.; Ferguson, G. S. *Chemtracts* **1988**, 1, 171.
- (64) Bi, T. G.; Cross, E. M.; Dias, A. J.; Lee, K. W.; Shoichet, Molly S.; McCarthy, T. J. *J. Adhes. Sci, Technol.* **1992**, 6(6), 719.
- (65) Harth, K.; Hibst, H. *Surf. Coatings Technol.* **1993**, 59, 350.
- (66) Jagur-Grodzinski, J. *Prog. Polym. Sci.* **1992**, 17, 361.
- (67) Bu, T. G.; McCarthy, T. J. *Polym. Mat. Sci. Eng.* **1990**, 63, 94.
- (68) Carey, D. H. *The Synthesis, Characterization and Dynamics of Surface-Modified Syndiotactic 1,2-Polybutadiene*; Ph.D. Thesis, Lehigh University, 1995.
- (69) Carey, D. H.; Ferguson, G. S. *Macromolecules* **1994**, 27, 7263.
- (70) Cross, E.; McCarthy, T. J. *Am. Chem. Soc. Div. Polym. Chem. Polym. Prepr.* **1990**, 31(1), 422.
- (71) Jerome, R; Vanhoorne, P. *Trends Polym. Sci.* **1994**, 2, 382.
- (72) Chung, T. C.; Kumar, A. *Polym. Bull.* **1992**, 28, 123.
- (73) Chung, T. C.; Rhubright, D.; Kumar, A. *Polym. Bull.* **1993**, 30, 385.
- (74) Sheats, C. E.; Pittman, C. U.; Zeldin, M.; Currell, B. *Inorganic and Metal-Containing Polymeric Materials*; Plenum: New York 1990.
- (75) Reichmanis, E.; Nalamasu, O. in *The Polymeric Materials Encyclopedia: Synthesis, Properties and Applications*; CRC Press: Boca Raton, 1996, 2, 1170.
- (76) Zentel, R.; Brehmer, M. *The Polymeric Materials Encyclopedia: Synthesis, Properties and Applications*; CRC Press, Boca Raton, 1996, 5, 3655.
- (77) Patil, A. O. *Bulletin of Electrochemistry* **1992**, 8, 509 and references therein.
- (78) Cacialli, F.; Friend, R. H.; Moratti, S. C.; Holmes, A. B. *Synth. Met.* **1994**, 67, 157.
- (79) Friend, R. H.; Bradley, D. D. C.; Townsend, P. D. *J. Phys. D: Appl. Phys.* **1987**, 20, 1367.

Chapter 2

Synthesis of Functional Polymers by Atom Transfer Radical Polymerization

Krzysztof Matyjaszewski, Veerle Coessens, Yoshiki Nakagawa, Jianhui Xia, Jian Qiu, Scott Gaynor, Simion Coca, and Christina Jasieczek

Department of Chemistry, Carnegie Mellon University, 4400 Fifth Avenue, Pittsburgh, PA 15213

Atom Transfer Radical Polymerization (ATRP) provides an efficient way to conduct controlled/'living' radical polymerizations. The resulting polymers have predefined molecular weights and the molecular weight distributions are narrow. In addition, ATRP is particularly suitable for the preparation of well-defined polymers with side and chain-end functional groups. A large variety of monomers were polymerized using numerous halogenated initiators and macroinitiators containing hydroxy, amido, ester, epoxy, cyano, etc. groups. The chain-end halogen groups were converted to other functional groups such as azido and aminogroups.

The importance of radical polymerizations can be ascribed to the large variety of vinyl monomers that can be polymerized and copolymerized and to the undemanding experimental conditions (1). Radical polymerizations require the absence of oxygen but can be carried out in the presence of water and other impurities. In addition, radical polymerizations are tolerant to many functional groups. With atom transfer radical polymerization (ATRP), it is now possible to conduct radical polymerizations in a controlled/'living' fashion (2-4). Structural variables of polymeric chains such as molecular weight, molecular weight distribution (4), copolymer composition (5-6) and terminal functionalities can be controlled (7). Furthermore, a variety of molecular architectures can be prepared such as linear, branched and hyperbranched structures (8).

Mechanism of ATRP

The mechanism of ATRP, outlined in Figure 1, is based on the repetitive addition of a monomer to growing radicals, generated from dormant alkyl halides by a reversible redox process (3-4). The redox process is catalyzed by transition metal compounds, mostly cuprous halides, complexed by suitable ligands such as 2,2'-bipyridine (bpy) or 4,4'-di-(5-nonyl)-2,2'-bipyridine (dNbpy). The control of the polymerization is dependent upon the establishment of an equilibrium between active and dormant species. By maintaining a low, stationary concentration of radicals, the contribution of

bimolecular termination between growing radicals can be suppressed and the result is a 'living' polymerization. Therefore, ATRP leads to excellent control of molecular weight, $DP_n = \Delta[M]/[I]_0$, and low polydispersities, $M_w/M_n < 1.3$.

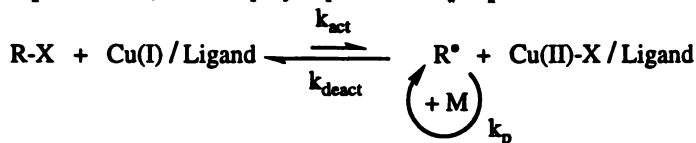


Figure 1 : Mechanism of Atom Transfer Radical Polymerization

In homogeneous systems, the rate of polymerization has been shown to be first order with respect to monomer, initiator and transition metal complexed by two dNBpy ligands (9). The reaction is usually negative first (or fractional) order with respect to the deactivator. The rate of the polymerization can thus be influenced by the monomer concentration, the initiator concentration and the ratio of activator to deactivator.

$$R_p = k_p K_{\text{eq}} [R-X] \frac{[Cu(I)]}{[Cu(II)]} [M]$$

In the context of this paper, preparing functionalized polymers, ATRP has many advantages over other controlled/'living' radical polymerizations. TEMPO-mediated polymerizations can only be used for a limited number of monomers such as styrenes (10-11). Removal of TEMPO from the chain ends is difficult, preparation of functional initiators requires multiple steps. ATRP uses halogen containing initiators which can contain other functional groups and which can be easily purchased/prepared. Also the halogen at the end of the resulting polymer chain can be easily replaced with other functional groups by simple chemical reactions.

An overview of the possibilities of ATRP in order to synthesize functional polymers is shown in Figure 2. The use of different polymers, different functional initiators and the conversion of the halogen end group to other functional end groups will be discussed in the following paragraphs.

Polymers with side functional groups

Contrary to the high reactivity of the active centers in cationic and anionic polymerizations, radical polymerizations are tolerant to many functionalities. It has been possible to polymerize a wide range of functional monomers such as substituted styrenes, functional acrylates and substituted acrylamide.

In Table I, the results of the polymerization of substituted styrenes with electron-withdrawing (p-Cl, p-Br, -CF₃) as well as with electron-donating substituents (p-Me, p-t-Bu) are listed. All of these monomers were polymerized in diphenyl ether or dimethoxybenzene at 110°C using the heterogeneous ATRP catalyst CuX/Bipy (12). In general, most of the monomers polymerized in a controlled manner so that the molecular weights increased linearly with conversion and were in agreement with the theoretical values. Polydispersities were usually low ($M_w/M_n < 1.3$).

In agreement with conventional radical polymerizations, it was observed that electron-withdrawing substituents increased the rate of polymerization (12). The increase was ascribed to the fact that the bond dissociation energy of the carbon-halogen bond was lowered by the presence of the electron-withdrawing substituents on the phenyl ring.



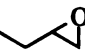
The various acrylates polymerized by ATRP are shown in Table II. Poly(methyl acrylate) was synthesized with molecular weights up to 75,000 with excellent control (13). Molecular weights increased linearly with conversion, the polydispersity at 90% conversion was $M_w/M_n = 1.10$.

Table I. Substituted polystyrenes polymerized by ATRP

R	M_n	M_w/M_n
<i>p</i> -Me	4200	1.38
<i>m</i> -Me	10800	1.17
<i>p</i> -tBu	6600	1.52
<i>p</i> -Br	10100	1.13
<i>p</i> -Cl	13300	1.12
<i>p</i> -F	7100	1.14
<i>p</i> -CF ₃	65500	1.06
<i>m</i> -CF ₃	12400	1.17
<i>p</i> -OAc	5600	1.32
H	11300	1.06
H	55300	1.12

Polymerizations were carried out in diphenylether at 110°C, $[M] = 4.37M$, $[M]_0/[I]_0/[CuBr]_0/[bipy]_0 = 100/1/1/3$.

Table II. Substituted acrylates polymerized with ATRP

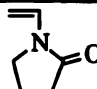
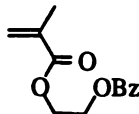
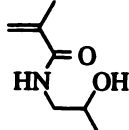
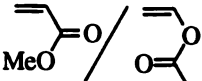
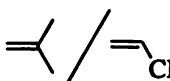
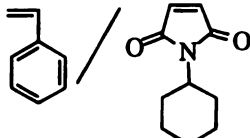
R	Me	<i>n</i> -Bu	<i>t</i> -Bu	<i>i</i> -Bor			
M_n	74700	15930	13200	3720	2810	36000	4320
M_w/M_n	1.10	1.14	1.10	1.15	1.21	1.17	1.23

Poly(*t*-butyl acrylate) and poly(isobornyl acrylate) are interesting polymers because they can be easily converted into poly(acrylic acid). The latter polymer can not be directly prepared by ATRP from acrylic acid, presumably because of reactions between the carboxylic groups and the catalyst. ATRP of *t*-butyl acrylate, as well as of isobornyl acrylate, in bulk led to well-defined polymers with molecular weights controlled by the ratio $\Delta[M]/[I]_0$ and narrow molecular weight distributions (14). In all cases, well-defined homopolymers were obtained starting from vinyl, hydroxyethyl and glycidyl substituted acrylates (15-16). The narrow molecular weight distributions indicated that chain breaking processes were suppressed in the polymerizations.

Other functionalized monomers that were polymerized by ATRP are shown in Table III. Using ATRP, *N*-vinylpyrrolidone and hydroxypropyl methacrylamide were successfully homopolymerized when a cyclam was used as the ligand instead of bipy. Methyl acrylate and vinyl acetate were copolymerized and a random copolymer with narrow molecular weight distribution was obtained. Copolymerization of isobutene and acrylonitrile monomers was also successful to prepare alternating copolymers. An alternating copolymer was also obtained when styrene and *N*-(cyclohexyl)maleimide

were copolymerized. This copolymer displayed a very high T_g (270°C) and may find application as a high temperature polymer.

Table III. Functionalized monomers, homo or copolymerized by ATRP

Monomer	M_n	M_w/M_n
	2000	1.15
	5780	1.28
	21180	1.32
	11140	1.16
	2880	1.46
	4730	1.19

Functional Initiators

In ATRP, the initiator used is an alkyl halide, RX, whose main role is to quantitatively generate growing chains. In the initiation step, the transition metal species abstracts the halogen atom X from the organic halide to form the radical R^* which then reacts with a vinyl monomer to form an active species that further propagates. Inherent in this mechanism is the incorporation of the alkyl group R as the head group of the polymer chain (see Figure 1). An obvious method to prepare end functionalized polymers is the use of a functional initiator. In principle, any alkyl halide with activating substituents on the α -carbon such as aryl, carbonyl or allyl can be used as initiator. This includes not only low molar mass molecules but also macromolecular species which can be used to synthesize block or graft copolymers. Initiators that are not applicable in ATRP are simple alkyl halides such as butyl chloride, and alkyl halides with a thiol or a carboxyl substituent on the α -carbon. Simple alkyl halides prevent a facile generation of initiating radicals because the carbon-halogen bond is too strong. Introduction of an inductive or resonance stabilizing substituent into the R-group reduces the bond dissociation energy of the R-X bond which leads to a higher

initiator efficiency. Thiol and carboxylic acid substituents however, cause side reactions and interfere with the catalyst system resulting in uncontrolled polymerizations.

Table IV presents the results of the ATRP of styrene in bulk using various initiators with attached functional groups (17). After a fixed period of time, the polymerization reactions were stopped and conversion, molecular weight and polydispersity were measured. In nearly all cases, polymers with molecular weights predetermined by the ratio of concentration of reacted monomer to introduced initiator were obtained. The polydispersities were generally low. Only when allyl-2-chloroacetate or α -chloro-acetamide were used as initiators, inefficient initiation was observed, resulting in molecular weights higher than expected and higher polydispersities. The results in Table IV indicate that ATRP proceeds in the presence of various functionalities including cyano, allyl ester, hydroxy, epoxide, lactone and vinyl ester groups. Carboxylic groups as end-chain functionalities can be prepared by using *p*-cyano-benzylbromide or *t*-butyl-2-bromo-propionate as the initiator. After the polymerization, the cyano groups or *t*-butyl groups can be hydrolyzed to give the acids. Polymers with epoxide or allyl groups as head groups can further be used to make graft/block copolymers.

As presented in Table V, similar results were obtained when the functional initiators were used to polymerize methyl acrylate.

For the low molecular weight polystyrenes and poly(methyl acrylates), the end groups were clearly observed in $^1\text{H-NMR}$ spectra. The concentrations of head groups and end groups were equal within $\pm 5\%$ accuracy.

A special class of functional initiators are the difunctional initiators which lead to the formation of telechelic polymers. α , α' -Dibromo-*p*-xylene, for example, was used as an initiator for the ATRP of styrene and butyl acrylate in bulk (17). The polymerizations occurred in a controlled fashion. The α , ω -dibromopolystyrene was converted to the diazido derivative and then reduced to the α , ω -diaminopolystyrene ($M_n=5100$, $M_w=6100$). The latter polymer was reacted with an equimolar amount of terephthaloyl chloride to yield a polystyrene with internal amide functionalities ($M_n=23,000$, $M_w=53,000$).

Macromolecular initiators have also been applied successfully. The left column of Table VI represents several examples of such initiators. Poly(tetrahydrofuran) and poly(norbornene) were used as macroinitiators for ATRP to make block copolymers. α , ω -Dichloro terminated polyisobutene ($M_n=28800$, $M_w/M_n=1.3$) was reacted with styrene, methacrylate and methyl acrylate to form triblock copolymers with soft polyisobutene central segments (18). The polydispersities of the corresponding monomodal triblock copolymers remained low. Other difunctional macroinitiators such as poly(butyl acrylate), polysulfone and polyester were also applied successfully (19). Polysulfone and polyester oligomers were also used to prepare ABA block copolymers of styrene and butyl acrylate (20).

Transformation of halogen chain-ends

As mentioned earlier, one of the chain-end functional groups is defined by the structure of the initiator used, the other is a halide which can be converted to some other functional groups. The halogen end groups were transformed to azide end groups by using azidotrimethylsilane and tetrabutylammonium fluoride (TBAF) (17). TBAF was added or in an equivalent amount or in the presence of one equivalent potassium fluoride in a catalytic amount. When the bromine end group was used, the reaction was carried out at room temperature. Chlorine end groups required the reaction to be performed at 50°C.

Table IV. Functional initiators used in ATRP for the polymerization of styrene at 110°C; $[I]_0/[CuBr]_0/[dNbipy]_0 = 1/1/2$.

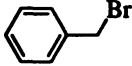
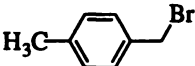
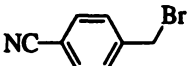
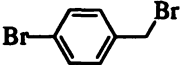
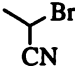
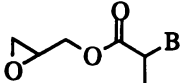
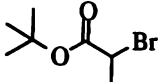
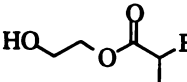
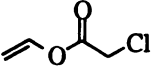
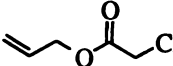
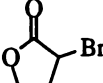
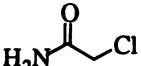
Initiator	Conv. (%)	M_n, Cal	M_n, SEC	M_w/M_n
	53.7	5370	6460	1.10
	51.1	5110	4400	1.17
	47.6	4760	5530	1.10
	47.5	4750	4520	1.16
	48.0	4800	5130	1.09
	61.9	6190	6790	1.12
	41.1	4110	4030	1.17
	48.1	4810	7520	1.10
	94.0	5000	5800	1.12
	14.3	1430	2600	1.77
	40.5	4050	4030	1.17
	12.0	1200	4010	1.51

Table V. Functional initiators used in ATRP for the polymerization of acrylates at 90°C; $[I]_0/[CuBr]_0/[dNbipy]_0 = 0.4/1/2$.

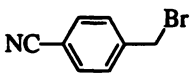
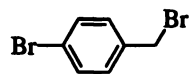

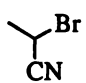
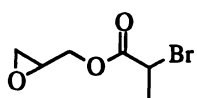
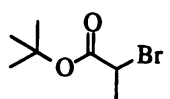
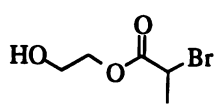
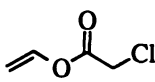
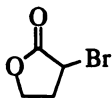
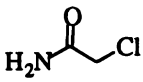
Initiator	Conv. (%)	$M_{n, Cal}$	$M_{n, SEC}$	M_w/M_n
	93.1	3720	4110	1.13
	94.6	3780	4010	1.22
	88.6	3540	6220	1.34
	82.0	3280	3550	1.10
	92.9	3720	4020	1.18
	94.3	3770	3980	1.17
	97.0	3880	4560	1.18
	70.2	280	3260	1.34
	83.3	3330	4120	1.13
	32.2	1290	7220	1.22

Table VI. Macromolecular initiators with one or two functionalities (F) were reacted with a second monomer using ATRP with a blockcopolymer or a triblockcopolymer as result

	Before			2nd Monomer	After	
	M_n	M_w/M_n	F		M_n	M_w/M_n
PolyTHF	15418	1.38	1	styrene	31000	1.46
				MMA	56700	1.21
				MA	28500	1.32
PolyNB	15000	1.09	1	styrene	95000	1.06
				MA	60000	1.07
PolyDCPD	7000	1.24	1	styrene	17000	1.37
				MA	21000	1.47
PolyIB	28800	1.31	2	styrene	48820	1.14
				MMA	33500	1.47
				MA	31810	1.42
				IBA	49500	1.21
PolyBA	96700	1.30	2	styrene	109500	1.47
PolySulfone	4100	1.50	2	styrene	10700	1.10
				BA	15300	1.20
PolyEster	1750	2.50	2	styrene	21000	1.40

THF = tetrahydrofuran, NB= norbornene, DCPD = dicyclopentadiene, IB = isobutene, BA = butylacrylate

Table VII. The methine proton of the end group of pSt in $^1\text{H-NMR}$ spectra

$\text{PSt}-\text{CH}_2-\underset{\text{Ph}}{\text{CH}}-\text{X}$	-Br	$-\text{N}_3$	$-\text{NH}_2$
δ -value of $-\text{CH}-\text{X}$	4.5	3.9	3.4

Pst = polystyrene

An alternative method for this conversion was the treatment of the bromine end groups with sodium azide in DMF at 80°C. Both methods led to complete conversion of the halogen groups which was clearly observed in the $^1\text{H-NMR}$ spectrum for polystyrene (Table VII) (7). The azide end groups were also noticeable in IR-spectra at about 2100 cm^{-1} . For acrylates, the intensity of this peak was used to quantify the amount of azide present.

The azide end groups were further converted into amino groups. For polystyrene, this conversion was obtained using lithium aluminiumhydride. A milder procedure, which was also applicable for the acrylates, was the reaction of the azides with triphenylphosphine with the formation of a phosphoranimine intermediate (the Staudinger reaction), which was then hydrolyzed to give the amino end group (Figure 3). For polystyrene, complete conversion was clearly observed by the $^1\text{H-NMR}$ spectrum (Table VII). The conversion of the bromine into azide, the azide into phosphoranimine and then the phosphoranimine into amine was demonstrated by analysis with MALDI-TOFMS for polystyrene as well as for poly(methyl acrylate). Hereby it was demonstrated that the phosphoranimine intermediate was preferentially ionized by MALDI. When polystyrenes with phosphoranimine respectively with azide end groups were mixed in a 1 to 3 ratio, the peaks with the highest intensity in the MALDI-TOFMS spectrum still corresponded to the polystyrene with phosphoranimine end groups (Series A, Figure 4).

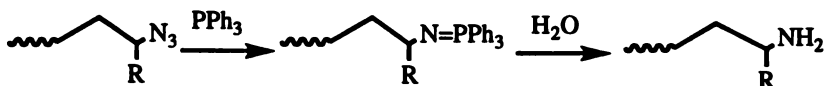


Figure 3 : The transformation of the azide end group into the amino end group

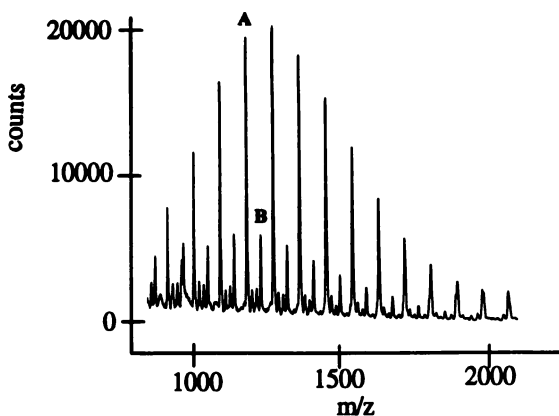


Figure 4 : MALDI-TOFMS spectrum of a mixture of polystyrenes with phosphoranimine (series A) and azide end groups (B), in a 1 to 3 ratio respectively.

Hyperbranched Polymers

The possibility of controlling architecture with ATRP is exemplified in the one-pot synthesis of hyperbranched polymers. These hyperbranched polymers contain n halogen atoms where $n=DP$. The halogen groups can be either activated to reinitiate polymerization or be transformed to other functional groups.

In order to prepare a polar material with low T_g , hyperbranched polyacrylate was synthesized (21). The monomer 2-(2-bromopropionyloxy)ethyl acrylate was homopolymerized in bulk by ATRP to yield a highly branched polyacrylate (Figure 5). The bromine end groups of the branches were completely converted into azide groups using trimethylsilyl azide and *t*-butylammonium fluoride. Upon heating, a crosslinked material was obtained. The crosslinking reaction was observed in the DSC spectrum at 180°C to 210°C (Figure 6).

The hyperbranched polymer with bromine end groups was also used as a macroinitiator for the ATRP of *n*-butyl acrylate. A multi-armed star polymer with a hyperbranched core was obtained with, against linear polystyrene standards, $M_n=110,000$ and $M_w/M_n=2.6$.

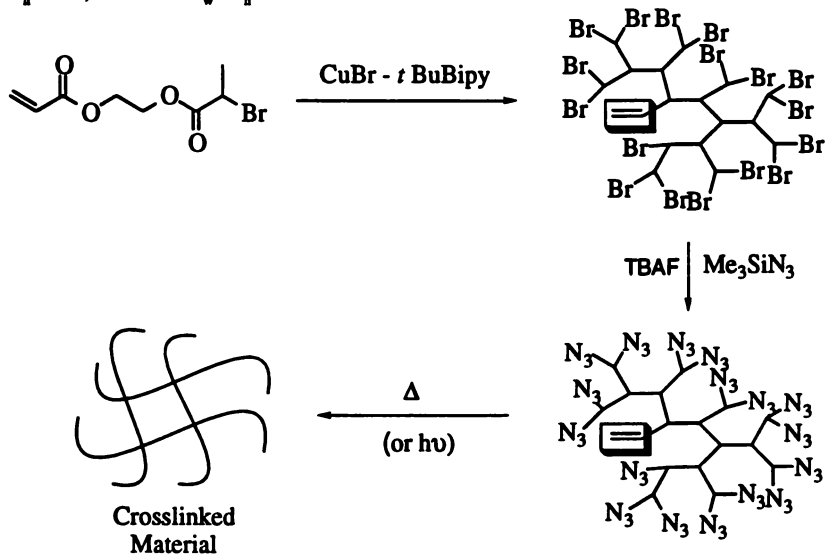


Figure 5: The hyperbranched acrylate

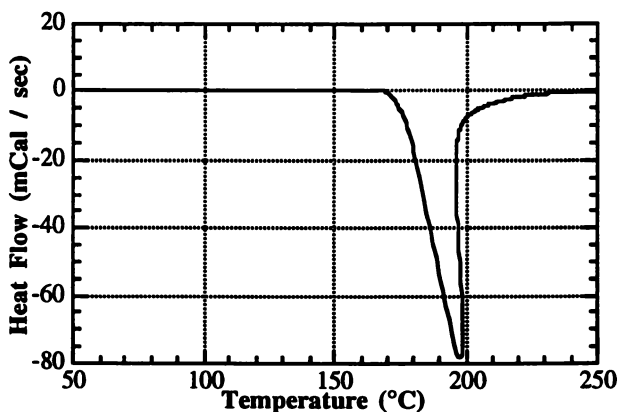


Figure 6: DSC-spectrum of the crosslinked material

Conclusion

ATRP is an excellent method for the preparation of functional polymers. Polymers with molecular weights up to $M_n=100,000$ can be obtained with narrow molecular weight distribution. Many functionalized styrenes, acrylates and other functional monomers were successfully polymerized using a wide range of functional initiators or macroinitiators. Furthermore chain-end halogens can be displaced. Because of all these possibilities, ATRP can find applications in solventless coatings, adhesives, lubricants, surfactants and additives.

Acknowledgments

The support of the industrial members of the ATRP Consortium at CMU and Donors of the Petroleum Research Foundation is gratefully acknowledged.

References

- (1) Moad, G.; Solomon, D.H. *The chemistry of free radical polymerization*; Elsevier Science Inc. : New York, 1995.
- (2) Wang, J.; Matyjaszewski, K. *J. Am. Chem. Soc.* **1995**, *117*, 5614.
- (3) Wang, J.S.; Matyjaszewski, K. *Macromolecules* **1995**, *28*, 7901.
- (4) Patten, T.E.; Xia, J., Abernathy, T., Matyjaszewski, K. *Science* **1996**, *272*, 866.
- (5) Greszta, D.; Matyjaszewski, K; Pakula, T. *ACS Polym. Preprints* **1997**, *(1)*, 709.
- (6) Arehart, S.V.; Greszta, D; Matyjaszewski, K. *ACS Polym. Preprints* **1997**, *38(1)*, 705.
- (7) Nakagawa, Y.; Gaynor, S.G.; Matyjaszewski, K. *ACS Polym. Preprints* **1996**, *37(1)*, 577.
- (8) Gaynor, S.G.; Edelman, S.Z.; Matyjaszewski, K. *Macromolecules* **1996**, *29*, 1079.
- (9) Matyjaszewski, K , Patten, T.E.; Xia, J. *J. Am. Chem. Soc.* **1997**, *119*, 674.
- (10) Georges, M.K.; Veregin, R.P.N.; Kazmaier, P.M. *Macromolecules* **1993**, *26*, 2987.
- (11) Mansky, P.; Liu, Y.; Huang, E.; Russell, T.P.; Hawker, C.J. *Science* **1997**, *275*, 1458.
- (12) Qiu, J.; Matyjaszewski, K. *Macromolecules* **1997**, *30*, 5643.
- (13) Paik, K.; Matyjaszewski, K. *ACS Polym. Preprints* **1996**, *37(2)*, 274.
- (14) Coca, S.; Davis, K; Miller, P; Matyjaszewski, K. *ACS Polym. Preprints* **1997**, *38(1)*, 689.
- (15) Grimaud, T.; Matyjaszewski, K. *Macromolecules* **1997**, *30*, 2216.
- (16) Coca, S.; Matyjaszewski, K. *ACS Polym. Preprints* **1997**, *38(1)*, 691.
- (17) Matyjaszewski, K.; Coca, S.; Nakagawa, Y; Xia J. *Polym. Mat. Sci. Eng.* **1997**, *76*, 147.
- (18) Coca, S.; Matyjaszewski, K. *Macromolecules* **1997**, *30*, 2808.
- (19) Jo, S.M.; Gaynor, S.G., Matyjaszewski, K. *ACS Polym. Preprints* **1996**, *37(2)*, 272.
- (20) Gaynor, S.G.; Matyjaszewski, K. *Macromolecules* **1997**, *30*, 4241.
- (21) Matyjaszewski, K., Gaynor, S.G.; Kulfan, A.; Podwika, M. *Macromolecules* **1997**, *30*, 5192.

Chapter 3

Functional Polymers: Random Copolymers by Stable Free Radical Polymerization

Paula J. MacLeod, Gordon K. Hamer, Pushpamma Lukose, and
Michael K. Georges

Xerox Research Centre of Canada, Mississauga, Ontario L5K 2L1, Canada

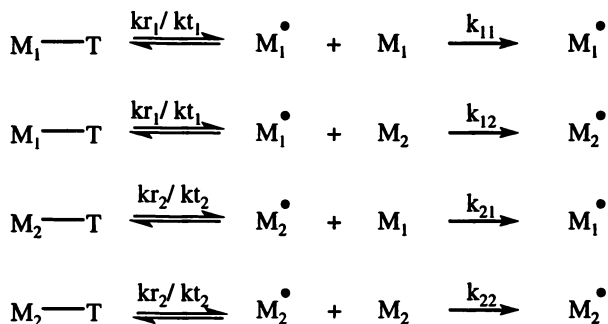
Random copolymers of styrene/isoprene and styrene/acrylonitrile were prepared by the stable free radical polymerization process. The molecular weight of the polymers increased as a function of conversion, as expected for a living radical polymerization. The microstructure of the copolymers and reactivity ratios of the monomers were found to be very similar to what would be obtained for a conventional free radical polymerization. The propagating living radical chain reacts similarly to a conventionally propagating chain.

Over the past few years there has been a tremendous interest in living radical polymerizations. One type of living radical polymerization is stable free radical polymerization, SFRP, where a stable free radical such as TEMPO (2,2,6,6-tetramethylpiperidinoxyl) is used to reversibly cap the growing polymer chain (1,2). SFRP has the advantage over conventional radical polymerization in that the polymers prepared are living and can be used for further polymerization to make blocks or other complex architectures. The polymers prepared by the SFRP process have a narrower molecular weight distribution compared to polymers prepared by conventional radical polymerization; in the case of block copolymers this may be a desirable attribute. This article focuses on the use of the SFRP process to prepare random copolymers.

A question that continually arises when the topic of stable free radical copolymerization is discussed is: what is the composition and microstructure of the copolymers? Scheme 1 shows the four possible propagation reactions for a stable free radical copolymerization based on the terminal model. It is expected that if in the uncapped form, the nitroxide leaves the vicinity of the propagating chain end the copolymer microstructure should not be affected by the presence of nitroxide. Unsuccessful attempts by Sogah and Puts to influence the microstructure of polymers prepared by the SFRP process using chiral nitroxides suggest that the nitroxide does leave the vicinity of the propagating chain end (3). This is in agreement with Fukuda's results, which show that the microstructure of styrene-acrylonitrile (SAN) copolymers

prepared by SFRP from an azeotropic mixture of the monomers is the same as that of SAN copolymers prepared by conventional radical polymerization (4).

If the nitroxide does leave the vicinity of the propagating chain end then the reactivity ratios for the radicals should also be the same as in conventional radical polymerizations. However, if the capping and uncapping rates for the two monomers are different this would lead to different concentrations of the two types of propagating chain ends relative to what would be present in a conventional radical polymerization. To address this issue, stable free radical copolymerizations of styrene-isoprene and styrene-acrylonitrile were studied in detail to compare the low conversion copolymer compositions to those prepared by conventional radical polymerization. The microstructure of the polymers was also examined.



Scheme 1. The four propagation reactions based on the terminal model for random copolymerization by the stable free radical polymerization process.

Experimental

Materials. All reagents were used as received unless otherwise stated. Isoprene, acrylonitrile, benzoyl peroxide (BPO), and TEMPO were purchased from Aldrich. Styrene was obtained from Fluka.

Analysis. Molecular weights and polydispersities were estimated by gel permeation chromatography (GPC) using a Waters/Millipore liquid chromatograph equipped with a Waters/Millipore 510 pump, Ultrastyrigel columns of pore size 10^4 Å, 2×500 Å, and 100 Å, and a Waters model 410 differential refractometer. A flow rate of 1 mL/min was used and samples were prepared in tetrahydrofuran. Polystyrene standards were used for calibration. Molecular weights were determined for samples before they were purified by precipitation into methanol. Conversion measurements were performed on a TA Instruments Thermogravimetric Analyzer 2950 (TGA) under nitrogen at a heating rate of 20°C/min over the temperature range 25-520°C. Percent conversions were calculated by comparing the weight loss due to residual monomer vaporization to that due to polymer decomposition. Gas chromatography (GC) measurements of monomer contents were made using a Hewlett Packard 5890 GC equipped with a Carbowax 20M column and flame ionization detector. Proton NMR spectra of precipitated polymer samples were recorded at ambient temperature on a

Bruker DPX300 spectrometer operating at 300.13 MHz. Samples were dissolved in CDCl_3 (~50 mg/mL) containing 0.03% TMS as an internal chemical shift reference.

Polymerization Reactions. To demonstrate the livingness of SFR styrene/isoprene copolymers, 1.05 g of benzoyl peroxide (BPO) and 0.855 g of 2,2,6,6-tetramethylpiperidinoxyl (TEMPO) were dissolved in 200 mL of styrene and 200 mL of isoprene. The reaction mixture was charged into a 1L Buchi pressure reactor, purged with argon while stirring, and heated to 130°C. Samples were removed periodically by discharging a small amount of the reaction mixture from a valve at the bottom of the reactor. The molecular weight distribution of each polymer sample was obtained by GPC analysis.

To determine the composition of the copolymers a series of polymerizations taken to low conversion (<10%) were performed. The polymerizations were done in a Parr pressure reactor with a total monomer volume of 70 mL. The relative amounts of the two monomers were varied to give mole fractions of isoprene from 0.1-0.9. The reactions were conducted at 125°C under an atmosphere of argon using 0.2 g of BPO and 0.17 g of TEMPO. After a period of 5-30 min (see Table II), the reaction mixture was cooled to room temperature and a sample taken for GPC, TGA and GC measurements; the remainder of the mixture was precipitated into methanol to isolate the polymer for ^1H NMR analysis.

To demonstrate the livingness of styrene-acrylonitrile random copolymerizations, TEMPO (0.084 g) and BPO (0.101 g) were dissolved in 30 mL of styrene and 10 mL of acrylonitrile. The reaction mixture was stirred and purged with argon. The flask was sealed, lowered into a oil bath at 125°C and the mixture allowed to reflux. Periodically the flask was removed from the bath, cooled and a sample withdrawn for GPC analysis. To measure the composition of the copolymers, a series of polymerizations taken to low conversion were done in a Parr pressure reactor. The total moles of monomer were kept constant at 0.55, and the relative amounts of the two monomers were adjusted to vary the mole fraction of acrylonitrile from 0.1-0.9.

Results

Styrene-Isoprene. Styrene and isoprene (53 mol %) were heated neat at 130°C in the presence of BPO and TEMPO in a closed pressure reactor. Samples were taken periodically over a six hour period; the molecular weight distributions of the polymer samples, determined by GPC, are shown in Figure 1. The entire distribution moves to higher molecular weight as a function of time. The molecular weight and conversion data for these samples are given in Table I. After six hours the molecular weight of the polymer was 32.1 kDa and the conversion was 35%. As expected for a living polymerization, M_n increased linearly with conversion.

To examine the composition of the polymers a classical method was used (5). A series of experiments were performed varying the initial mole fraction of isoprene. Polymerizations were carried out to as low a conversion as possible so as not to significantly change the feed from the initial value. The incorporation of isoprene in the polymer was then determined by ^1H NMR spectroscopy, the details of which are discussed below. The percentage of styrene and isoprene remaining in the feed was determined by GC; the results were in good agreement with the NMR measurements

of the styrene/isoprene ratio in the precipitated product. The feed of isoprene (f_i) and the corresponding incorporation of isoprene in the copolymer (F_i) are given in Table II. Other characterization details for the isolated polymers are also given in Table II.

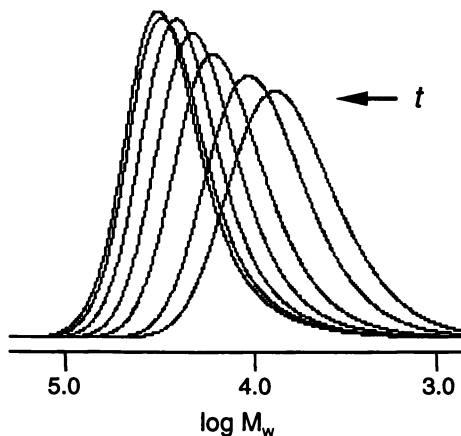


Figure 1. Molecular weight distributions determined by GPC as a function of reaction time (t) for the SFR copolymerization of styrene/isoprene.

Table I. Molecular weight and conversion data corresponding to the GPC curves in Figure 1. The polymerization temperature was 130°C.

<i>Time (h)</i>	<i>M_w (kDa)</i>	<i>Conversion (%)</i>
0.5	8.1	10
1	10.8	14
2	16.3	19
3	21.0	23
4	26.1	28
5	30.3	33
6	32.1	35

A plot of the mole fraction of isoprene in the SFR prepared copolymers as a function of the mole fraction of isoprene in the feed is shown in Figure 2. The data points are the results for the SFRP process initiated with BPO at 125°C in the presence of TEMPO; the curve represents data reported by Wiley and Davis (6) for a conventional styrene/isoprene copolymerization initiated with peroxide at 100°C. The

relationship between isoprene feed and incorporation for the SFRP process is similar to that obtained by conventional radical copolymerization. The data suggest that the mechanism of styrene/isoprene copolymerization by the SFR process is similar to the conventional radical mechanism. This implies that, in the styrene/isoprene/TEMPO system, the TEMPO capping/uncapping reaction has no influence on the copolymer composition.

Table II. Results for the SFR copolymerization of styrene/isoprene at 125°C as a function of the mole fraction of isoprene in the feed, f_I .

f_I	F_I	M_w (Da)	PD	% Conv.	Time (min)
0.1	0.17	5000	1.56	6	30
0.2	0.31	6000	1.70	9	30
0.3	0.42	4800	1.64	5	30
0.4	0.52	6200	1.73	8	25
0.5	0.64	6800	1.82	11	20
0.6	0.75	6100	1.73	9	15
0.7	0.80	5300	1.72	8	19
0.8	0.87	6100	1.73	17	15
0.9	0.91	6100	1.77	21	5

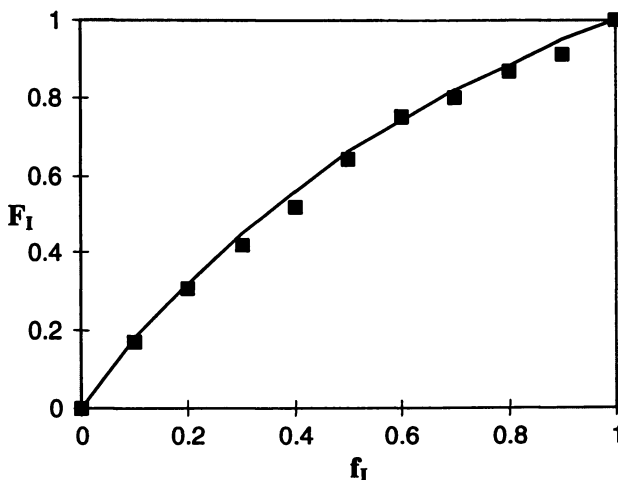


Figure 2. Plot of the incorporation of isoprene in the SFR copolymerization of styrene/isoprene (F_I) versus the feed of isoprene in the reaction mixture (f_I). The squares are the data points from the SFRP reaction; the curve represents data for a conventional radical copolymerization (6).

The series of styrene-isoprene copolymers prepared by the SFRP process were analysed by ^1H NMR spectroscopy to determine copolymer compositions, as discussed above, and to examine the polymer microstructure, specifically end groups and the stereochemistry of isoprene incorporation (*i.e.*, *cis/trans*-1,4; 1,2; 3,4). The 300 MHz ^1H NMR spectrum of a copolymer containing 91 mol% isoprene is shown in Figure 3. In this polymer a majority of the initiator chain ends will consist of benzoyloxy-isoprene units and the living chain ends, of isoprene-TEMPO units. The low molecular weight of the copolymer readily enables end-group analysis by ^1H NMR spectroscopy. The boxed resonances labelled A, B and C (Figure 3) can be attributed to the chain-end units. The aromatic protons of the benzoyloxy group are observed between 7.3–8.2 ppm (A); the small peak at 7.95 ppm may be assigned to the *ortho* protons of benzoyloxy units attached to the minor comonomer, styrene. The two sharp peaks at 1.1 and 1.2 ppm (B) are characteristic of the methyl group resonances of TEMPO bonded to an isoprene unit. The complex group of resonances between 4.1 and 4.5 ppm (C) arises from the methylene (1,4-, 1,2- and 3,4-units) and methine protons (3,4-units) of isoprene attached to benzoyloxy and/or TEMPO chain ends. As the styrene content of the copolymer increases (spectra not shown), the boxed resonances of Figure 3 are progressively replaced by peaks characteristic of benzoyloxy and piperidinyloxy groups bonded to styrene, and the methylene and methine protons of the attached styryl units (see Figure 6 of reference 7). The ratio of benzoyloxy to TEMPO end groups is $\sim 1:1$, which suggests that, as expected for a living polymer system, each polymer chain is initiated with BPO and reversibly capped with TEMPO.

The remaining signals are assigned to the bulk of the copolymer. The peaks at 7.0–7.3 ppm arise from the aromatic protons of the styrene units. The vinylic protons of the various isoprenyl stereoisomers give a complex pattern in the 4.6–5.9 ppm range. Signals between 0.9 and 2.8 ppm are due to the aliphatic protons of styrene and isoprene units as well as the methyl and methylene protons of the terminal TEMPO group.

Although a detailed analysis of the styrene/isoprene copolymer sequence distribution is beyond the scope of this article, certain key features of the isoprene stereochemistry can be identified. For example, the most intense signal in the vinylic region (5.15 ppm) can be attributed to the $-\text{CH}=\text{}$ protons of *cis/trans*-1,4-isoprene units. The small cluster of peaks at 4.6–5.0 ppm has been assigned to $=\text{CH}_2(1,2)$ and $=\text{CH}_2(3,4)$ protons; similarly, the group of peaks at 5.3–5.9 ppm has been assigned to the $-\text{CH}=\text{}$ protons of 1,2-isoprene units (8). Despite this simplification, the ratios of the integrated area of the 1,4 peak to those of the 1,2 and 3,4 resonances clearly show that isoprene is largely incorporated in the copolymer as *cis/trans*-1,4 units. The 1,2 and 3,4 stereoisomers are present in approximately equal (minor) amounts. The *cis/trans* ratio of the 1,4-units can be determined from the intensities of the CH_3 peaks at 1.7 (*cis*) and 1.6 ppm (*trans*), respectively. Making allowance for other overlapping resonances, the measured *cis/trans* ratio is $\sim 2:5$. This distribution of isoprene stereoisomers in SFR styrene/isoprene random copolymers is very similar to the distribution found for analogous copolymers prepared by conventional radical processes (8,9), particularly if the known temperature dependence of 1,3-diene stereoisomer enchainment (10) is considered. Thus it may be concluded that the

presence of the TEMPO chain-capping agent in the SFRP process has no effect on either the reactivity ratios of the comonomers nor the stereochemistry of monomer addition.

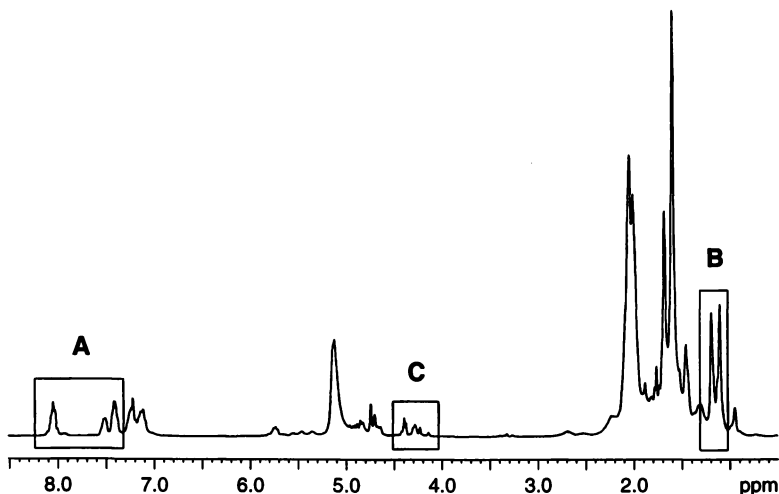


Figure 3. 300 MHz ^1H NMR spectrum of an SFR styrene/isoprene random copolymer containing 91 mol% isoprene. The boxes highlight resonances attributed to end groups (A,B) and isoprene units adjacent to end groups (C).

Styrene-Acrylonitrile. The second random SFR copolymerization studied in detail was that of styrene/acrylonitrile. A copolymerization of neat styrene and acrylonitrile with BPO and TEMPO was performed at 125°C using an azeotropic mixture of the two monomers (76 wt% styrene, 24 wt% acrylonitrile). The reaction mixture was sampled over a period of 8.5 h; GPC traces for the polymer samples are shown in Figure 4. The entire molecular weight distribution moves to higher molecular weight with increasing polymerization time. Molecular weight and conversion data are given in Table III. As for the styrene-isoprene system, M_n increases linearly with conversion, confirming the living nature of the SFR styrene/acrylonitrile copolymerization reaction.

To determine the SAN copolymer composition, the same procedure used for styrene/isoprene was followed. A series of reactions was performed varying the feed of acrylonitrile and measuring the incorporation of acrylonitrile in the copolymer at low conversion by ^1H NMR spectroscopy. All reactions were done in a closed pressure reactor at $115\text{--}120^\circ\text{C}$. The results of these experiments are shown in Table IV. A plot of the incorporation of acrylonitrile in the polymer (F_A) as a function of the acrylonitrile feed (f_A) is shown in Figure 5. The data points are copolymer compositions for the SFR process while the curve represents literature data for a

conventional radical copolymerization of styrene/acrylonitrile at 130°C (11). Since there is excellent agreement between the conventional polymerization and SFRP data, the conventional copolymerization kinetics of styrene/acrylonitrile can also be applied to SAN copolymers synthesized by the SFRP process.

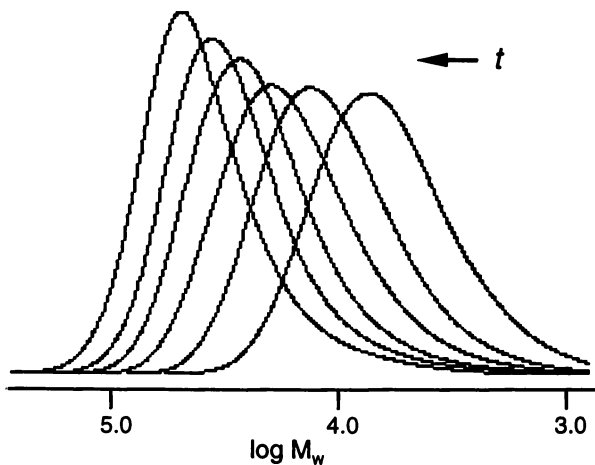


Figure 4. Molecular weight distribution determined by GPC as a function of reaction time (t) for the SFR copolymerization of styrene/acrylonitrile.

Table III. Molecular weight and conversion data corresponding to the GPC curves in Figure 4. The reaction was performed at the azeotropic composition at 125°C.

<i>Time (h)</i>	<i>M_w (kDa)</i>	<i>Conversion (%)</i>
1	7.5	9
2	12.8	19
3	18.9	24
4	26.1	37
5	33.3	54
8.5	44.4	75

Table IV. Results for the SFR random copolymerization of styrene/acrylonitrile as a function of the mole fraction of acrylonitrile in the feed, f_A .

f_A	F_A	M_w (kDa)	PD	% Conv.	Time (min), Temp. (°C)
0.1	0.20	54.8	1.93	2	15, 115
0.2	0.28	73.3	1.92	8	15, 115
0.3	0.34	64.5	1.93	12	15, 115
0.4	0.39	65.4	1.96	3	10, 115
0.5	0.43	74.7	1.85	15	15, 120
0.6	0.46	57.0	1.90	23	5, 120
0.7	0.50	78.5	2.02	22	10, 120
0.8	0.55	58.6	2.02	21	15, 120
0.9	0.64	17.0	1.79	9	15, 120

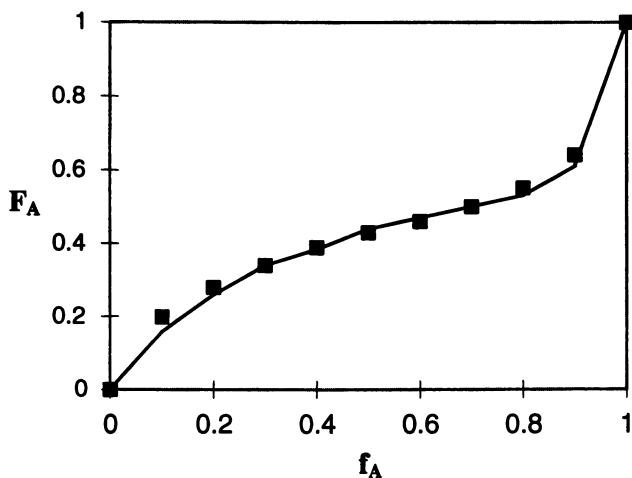


Figure 5. Plot of the the incorporation of acrylonitrile (F_A) in the SFR random copolymerization of styrene/acrylonitrile versus the mole fraction of acrylonitrile in the feed (f_A). The squares are the data points from the SFRP reaction; the curve represents data for a conventional radical polymerization (11).

Conclusions

Random copolymers of styrene/isoprene and styrene/acrylonitrile have been prepared by stable free radical polymerization. By varying the comonomer mole fractions over the range 0.1-0.9 in low conversion SFRP reactions it has been demonstrated that the incorporation of the two monomers in the copolymer is analogous to that found in conventional free radical copolymerizations. The composition and microstructure of random copolymers prepared by SFRP are not significantly different from those of copolymers synthesized conventionally. These two observations support the conclusion that the presence of nitroxide in the SFR process does not influence the monomer reactivity ratios or the stereoselectivity of the propagating radical chain. Rather, the SFR propagation mechanism is essentially the same as that of the conventional free radical copolymerization process.

Literature Cited

- (1) Georges, M.K.; Veregin, R.P.N.; Kazmaier, P.K.; Hamer, G.K. *Macromolecules* **1993**, *26*, 2987.
- (2) Veregin, R.P.N.; Odell, P.G.; Michalak, L.M.; Georges, M.K. *Macromolecules* **1996**, *29*, 2746 and references therein.
- (3) Puts, R.D.; Sogah, D.Y. *Macromolecules* **1996**, *29*, 3323.
- (4) Fukuda, T.; Terauchi, T.; Goro, A.; Tsujii, Y.; Miyamoto, T.; Shimizu, Y. *Macromolecules* **1996**, *29*, 3050.
- (5) Odian, G. *Principles of Polymerization*; 3rd Edition; Wiley-Interscience: New York, NY, 1991; pp 467-472.
- (6) Wiley, R.H.; Davis, B. *J. Polym. Sci. Part A* **1963**, *1*, 2819.
- (7) Georges, M.K.; Veregin, R.P.N.; Kazmaier, P.M.; Hamer, G.K. *Trends Polym. Sci.* **1994**, *2*, 66.
- (8) Pham, Q.-T.; Petiaud, R. *Spectres RMN des Polymères ¹H-¹³C*; Éditions SCM: Paris, **1980**; Vol. 1, pp 126-127 and references therein.
- (9) Crossley, G., Queen's University (Kingston, Ontario, Canada) and Xerox Research Centre of Canada, personal communication of unpublished data, 1997.
- (10) Reference 5, pp 662-663.
- (11) Johnston, N.W. *J. Macromol. Sci., Rev. Macromol. Chem.* **1976**, *C14*, 215.

Chapter 4

Use of Protecting Groups in Polymerization

D. N. Schulz¹, S. Datta², and R. M. Waymouth³

¹Corporate Research Laboratory, Exxon Research and Engineering Company,
Route 22 East, Clinton Township, Annandale, NJ 08801

²Exxon Chemical Company, 5200 Bayway Drive, Baytown, TX 77520

³Department of Chemistry, Stanford University, Stanford, CA 94305

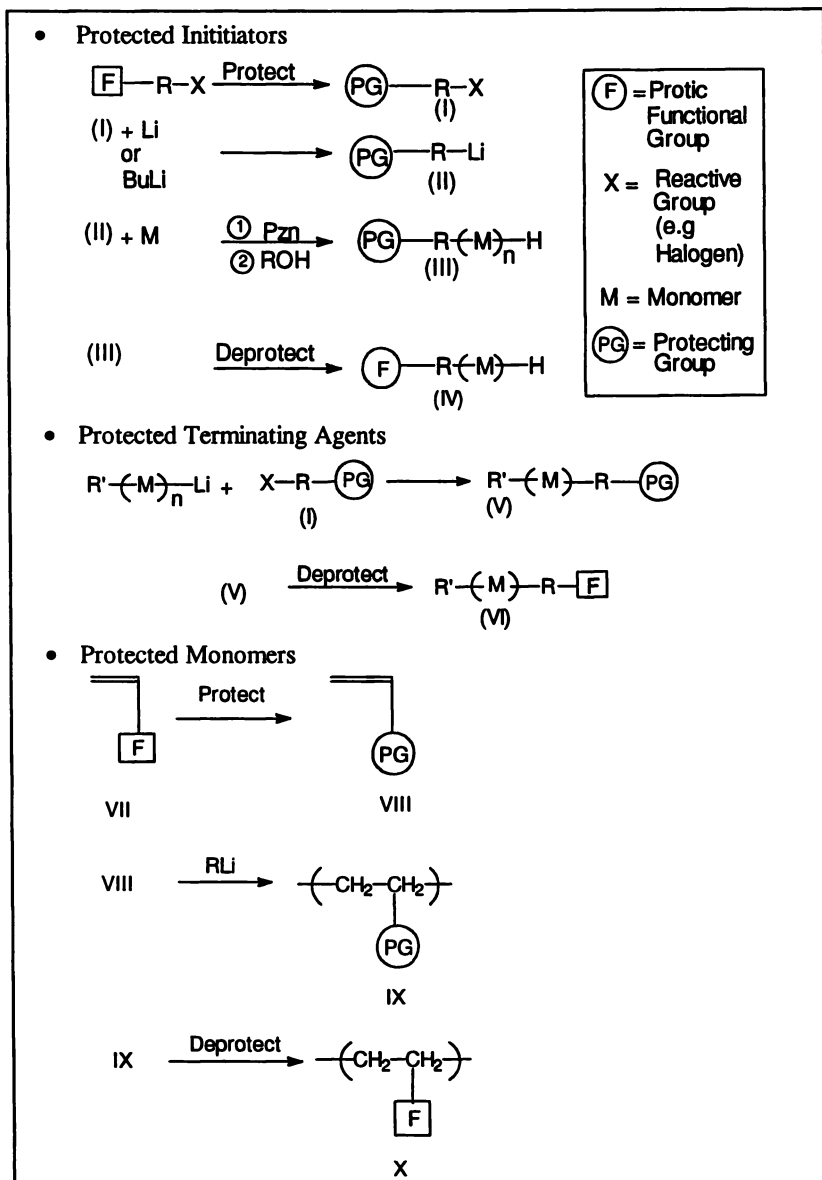
Functional polymers are often difficult to synthesize because of the antagonism or competition of functional groups with the active sites of catalysts or initiators. In addition functional groups can sometimes act as sites for chain transfer or termination. This paper reviews recent advances in the application of protecting groups in anionic, cationic, Ziegler-Natta, metallocene and metathesis polymerization. Such groups have been built into initiators, terminating agents, and monomers. The most versatile and robust protecting groups are the silyl ethers, which have remarkably been applied to all of the above polymerization types. Borane mediated synthesis of functional polymers has also been proven effective for several polymerization methods.

Functional polymers are macromolecules containing functional groups that have polarity or reactivity different from backbone chains. Such polymers often show improved properties by virtue of enhancements in phase separation, reactivity, or interpolymer associations. Alternatively, functional polymers may be viewed as polymers that have a function or use. Unfortunately, functional polymers are often difficult to synthesize because of the antagonism or competition of functional groups with the active sites of catalysts or initiators. In addition, functional groups can sometimes act as sites for chain transfer or termination. Following the lead of peptide chemists, polymer chemists have increasingly used protecting groups during polymerization to mask reactive functionality. This paper reviews recent advances in the application of protecting groups in anionic, cationic, Ziegler-Natta, metallocene and metathesis polymerization.

Protecting Groups In Anionic Polymerization

Protecting groups have been used in several ways for the preparation of functional anionic polymers; e.g. as protected functional initiators, terminating agents, and monomers. Scheme 1 illustrates these methods.

Scheme 1



The first two methods in Scheme 1 (i.e. protected initiators and protected terminating agents) result in end functional polymers. The third method (i.e. protected monomers) yields functional backbone polymers.

The synthesis of functional polymers using protected and other alkyl lithium initiators has been the subject of a recent critical and comprehensive review by Quirk¹. Protecting groups are especially needed for functional groups with active hydrogens; e.g. ROH, RNH₂, R₂NH and RCOOH. In contrast, R₃N, R₂NLi are stable to alkyl lithium compounds and "living" lithium chain ends. A listing of protected functional anionic initiators is given in Table I²⁻²⁰. Although R₂NLi initiators require no additional protection, there have been several recent reports of these interesting initiators as carriers of *tert*-amino functionality²¹⁻²³.

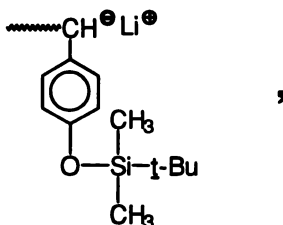
The key science questions to be addressed with protected anionic initiators are: What are the solubility and stability characteristics of the initiators? What is the microstructure of the resulting polymers? Can the protecting groups be removed easily and quantitatively, without concomitant chain crosslinking or scission?

Hydrocarbon solubility is important for diene polymerization, where a high 1,4 polymer microstructure is often desired. Polar solvents have a tendency to decrease the 1,4 content and elevate the 1,2 addition product. Hydrocarbon solubility is less of an issue for styrene or epoxide polymerization. Thus, the hydrocarbon soluble *t*-butyldimethylsilyl (TBDMS) protected initiator (5) (Table I) is recommended for high 1,4 polydienes. Most of the other compounds in Table I can be used with other anionic monomers or where high 1,4 microstructure is not needed.

Rather than carrying the protected functionality along with the initiator, one can build the protected functional group into the terminating agent (Scheme 1). Here issues of hydrocarbon solubility are less of a concern because the polymerization step (that controls polymer microstructure) precedes the termination step. Often similar kinds of protecting groups are used for terminating agents as are used for protected initiators. Table II shows examples of protected anionic terminating agents²⁴⁻³².

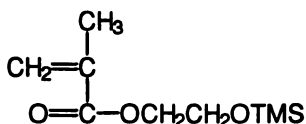
In turn, protected anionic monomers have been thoroughly studied and reviewed by Nakahama³³⁻⁵⁵ and more recently reviewed by Sivaram⁵⁶. Typical examples are shown in Table III. Styrenic, methacrylate and maleimide monomers with protected functionalities have been examined. Since every monomer unit contains a (protected) functionality, concern about protecting group stability and removal are even more of an issue than with protected initiators or terminators. Sometimes, small structural differences can lead to huge differences in stability. For example, the TBDMS protected monomer (15b)(Table III) does not polymerize with Li, Na, or K naphthalenes, oligo(α -methyl styrene)dilithium, or butyllithium to give living TBDMS polymers. However, the TMS monomer (15a) does³⁸. Also, the stability of the protected monomer can depend upon temperature.

Thus, the living protected anion from monomer (15b)



is stable at -78°C for 24 hours but loses 40% of its activity at 30°C in just 0.5 hours³⁸.

Moreover, the trimethylsilyl (TMS) protected monomer (16a) does not polymerize well with $n\text{-BuLi}$ at -78°C .



(16a)

However, it does polymerize with the more bulky and less basic 1,1-diphenylhexyl lithium at -78°C to give quantitative yield of polymer. In general, the more sterically bulky the protecting group, the greater is the stability of the group and the more difficult is its deprotection. Ring protecting groups like the oxazoline protecting groups for carboxyl functionality are also difficult to remove.

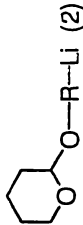
Protecting Groups in Cationic Polymerization

A review of functional polymers by carbocationic polymerization both with and without the use of protecting groups has recently appeared⁵⁷. Protecting groups have also been employed as cationic coinitiators, cationic terminating agents, and cationic polymerizable monomers. Scheme 2 illustrates the use of protected functional cationic coinitiators for vinyl ether polymerization.

Table IV shows examples of protected functional cationic coinitiators for vinyl ether polymerization and the corresponding deprotected polymer end group⁵⁸⁻⁶⁵. Table V lists several protected terminating agents for vinyl ether polymerization^{60,61}. The latter list is short because the vinyl ether chain can be terminated and functionalized with non protected nucleophiles as well⁵⁷.

Living cationic polymerization has been achieved with the hydroxyl and amino protected vinyl ether monomers (Scheme 3)^{58,69,70}. The bulkier *t*-butyldimethylsilyl (TBDMS) containing monomer polymerizes slower than the trimethylsilyl (TMS) substituted monomer. The TMS monomer requires $\text{CH}_3\text{OH}/\text{H}^+$ to remove the

Table I. Protected Functional Anionic Initiators

Protected Initiator	Deprotection Method	Deprotected End-Group	Comments	Refs.
$\text{EtO}-\underset{\text{CH}_3}{\text{CH}}-\text{O}-\text{R}-\text{Li} \quad (1)$	CCl_2COOH in toluene/ H_2O with entrainment of volatile by-products followed by neutralization.	-OH	<ul style="list-style-type: none"> Initiator soluble in benzene, ether; insoluble in hexane. Moderate 1,4 (45-64%) contents in PBD's. 	2,3
 $\text{EtO}-\underset{\text{CH}_3}{\text{CH}}-\text{O}-\text{R}-\text{Li} \quad (2)$	CCl_2COOH in toluene/ H_2O with entrainment of volatile by-products followed by neutralization.	-OH	<ul style="list-style-type: none"> Tetrahydropyranyl ether is more difficult to deprotect than α-ethoxy ether group (above). 	2,3
$\text{EtO}-\underset{\text{CH}_3}{\text{CH}}-\text{O}-\text{R}-\text{O}^{\ominus}\text{K}^{\oplus} \quad (3)$	CCl_2COOH in toluene/ H_2O with entrainment of volatile by-products followed by neutralization.	-OH	<ul style="list-style-type: none"> Initiator used to polymerize epoxides and lactones 	4,5
$\text{i-Bu}-\underset{\text{CH}_3}{\text{CH}}-\text{O}-\text{R}-\overset{\text{Li}}{\text{C}}\text{H}-\text{CH}_3 \quad (4)$	CCl_2COOH in toluene/ H_2O with entrainment of volatile by-products followed by neutralization.	-OH	<ul style="list-style-type: none"> Initiator soluble in hexane; high 1,4 (69-72%) PBD's prepared. 	16
$\text{i-Bu}-\underset{\text{CH}_3}{\text{Si}}(\text{CH}_3)-\text{O}-\text{R}-\text{Li} \quad (5)$	Bu_4NF	-OH	<ul style="list-style-type: none"> Initiator soluble in hexane; high 1,4 (89%) PBD's prepared. 	6-12

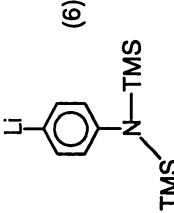
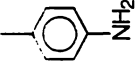
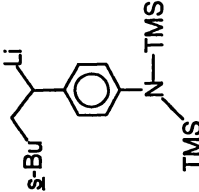
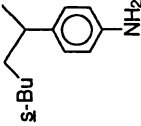
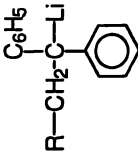
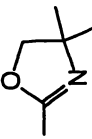
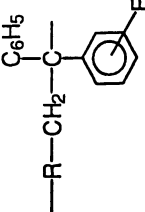
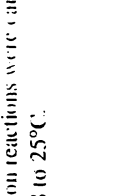
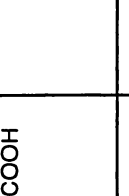

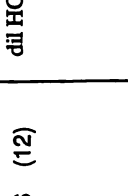
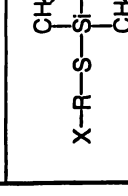
 <p>(6)</p>	<p>TSOH or HCl in refluxing hydrocarbon/H₂O mixtures.</p>		<ul style="list-style-type: none"> Initiator soluble in ether, insoluble in hexane. 	13
 <p>(7)</p>	<p>dil HCl</p>		<ul style="list-style-type: none"> Initiator soluble in nonpolar solvents; initiator used to prepare polydimethylsiloxanes. 	14,15
 <p>(8)</p> <p>PG = ---N(TMS)_2 (a), $\text{---OSi(CH}_3)_2$ (b)</p>  <p>(c)</p>	<p>dil HCl in THF</p>	 <p>F = $\text{---NH}_2, \text{---OH}, \text{---COOH}$</p>	<ul style="list-style-type: none"> Initiators soluble in THF and benzene. Initiators used mainly to prepare polystyrene. 	17-20

Table II. Protected Functional Terminating Agents for Anionic Polymerization

Protected Terminating Agent	Deprotection Method	Reprotected End Group	Comments	Refs.
 <p style="text-align: center;">(9)</p> <p style="text-align: center;">X-R-N</p>	acid catalyst	-NH ₂	<ul style="list-style-type: none"> Termination reactions were carried out at 78 to 25°C. 	24
 <p style="text-align: center;">(10)</p> <p style="text-align: center;">X-R-C</p>	acid catalyst	-COOH		25
 <p style="text-align: center;">(11)</p> <p style="text-align: center;">X-R-O-Si</p>	dil HCl or (Bu) ₄ N ⁺ F ⁻	-OH	<ul style="list-style-type: none"> Termination in heptane had coupling side reaction; termination near quantitative in THF and THF/heptane; deprotection quantitative. 	27,32
 <p style="text-align: center;">(12)</p> <p style="text-align: center;">X-R-O-Si</p>	dil HCl	-OH	<ul style="list-style-type: none"> Termination in heptane had coupling side reaction; termination near quantitative in THF and THF/heptane; deprotection quantitative. 	27
 <p style="text-align: center;">(11)</p> <p style="text-align: center;">X-R-S-Si</p>	dil HCl	-SH	<ul style="list-style-type: none"> Termination quantitative in THF and THF/heptane; deprotection requires care because of possible oxidation of -SH. 	27

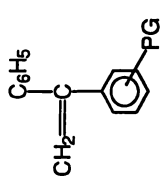
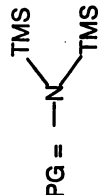
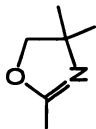
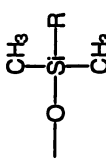
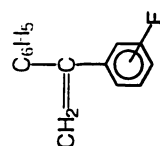
<p>(14)</p>  <p>PG =</p> <p>(a) </p> <p>(b) </p> <p>(c) </p>	dil acid	 <p>F = -NH_2, -OH, -COOH</p>	<p>28:31</p> <p>• Termination reactions were carried out at -78 to 25°C.</p>
--	----------	--	--

Table III. Protected Anionic Monomers


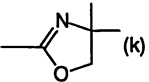
Protected Monomers	Protecting Group (PG)	Functional Group	References
 (15)	$-\text{OTMS}$ (a), $-\text{O}-\text{Si}(\text{CH}_3)_2-\text{t-Bu}$ (b),	$-\text{OH}$	38,39
	$-\text{R}'-\text{OTMS}$ (c), $-\text{R}'-\text{O}-\text{Si}(\text{CH}_3)_2-\text{t-Bu}$ (d)	$-\text{R}'-\text{OH}$	40,41
	$-\text{S}-\text{OTMS}$ (e), $-\text{S}-\text{Si}(\text{CH}_3)_2-\text{t-Bu}$ (f)	$-\text{SH}$	42
	$-\text{R}'-\text{S}-\text{TMS}$ (g), $-\text{R}'-\text{S}-\text{Si}(\text{CH}_3)_2-\text{t-Bu}$ (h)	$-\text{R}'-\text{NH}_2$	
	$-\text{N}(\text{TMS})_2$ (i), $-\text{R}'-\text{N}(\text{TMS})_2$ (j)	$-\text{NH}_2$ $-\text{R}-\text{NH}_2$	43-45
	 (k)	$-\text{COOH}$	48

Table III. Protected Anionic Monomers (Cont'd.)

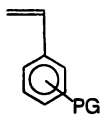
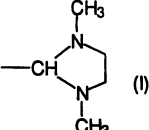
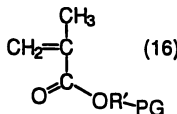
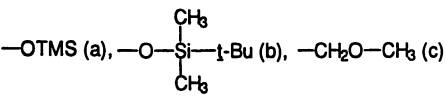
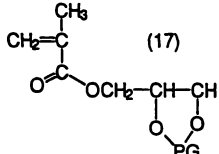
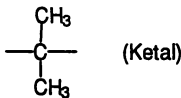
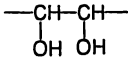
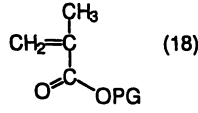
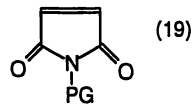
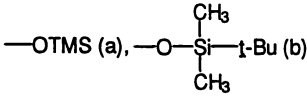
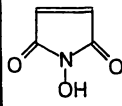
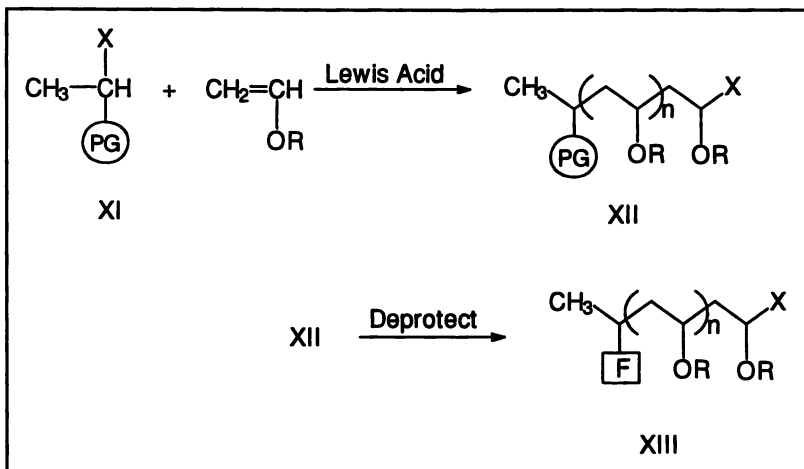
Protected Monomers	Protecting Groups (PG's)	Deprotected Functionalities	Refs
 (15)	 (l)	-CHO	48
	-C≡C-TMS (m)	-C≡C-H	49
 (16)	 (a), (b), (c)	-OH	50, 51
 (17)	 (Ketal)		52
 (18)	-t-Bu	-COOH	53
 (19)	 (a), (b)		54,55

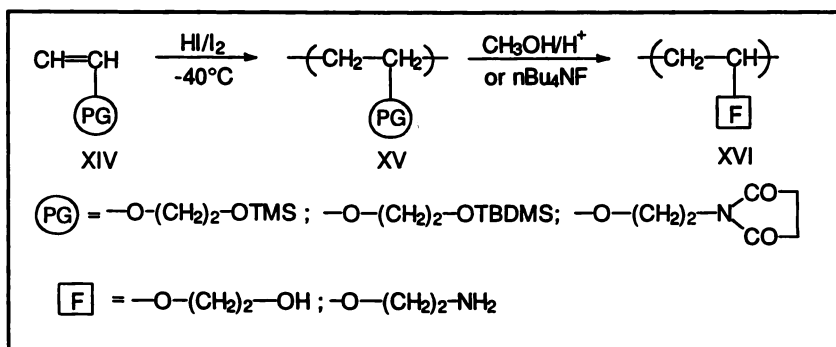
Table IV. Protected Functional Cationic Coinitiators for Vinyl Ether Polymerization

Protected Functional Coinitiators	Deprotected End Group	Refs.
$\begin{array}{c} R_1 \quad X \\ \diagdown \quad / \\ C \\ / \quad \diagdown \\ R_2 \quad O-(CH_2)_2-OCH_2OR \end{array} \quad (20)$	$\begin{array}{c} R_1 \\ \diagdown \quad / \\ C \\ / \quad \diagdown \\ R_2 \quad O-(CH_2)_2-OCH_2OR \end{array}$	58,59
$\begin{array}{c} R_1 \quad X \\ \diagdown \quad / \\ C \\ / \quad \diagdown \\ R_2 \quad CH \begin{array}{l} \diagup \quad COOEt \\ \diagdown \quad COOEt \end{array} \end{array} \quad (21)$	$\begin{array}{c} R_1 \\ \diagdown \quad / \\ C \\ / \quad \diagdown \\ R_2 \quad COOH \end{array}$	58,59
$\begin{array}{c} R_1 \quad X \\ \diagdown \quad / \\ C \\ / \quad \diagdown \\ R_2 \quad O(CH_2)_2-N \begin{array}{l} \diagup \quad CO \\ \diagdown \quad CO \end{array} \begin{array}{c} \text{C}_6\text{H}_4 \end{array} \end{array} \quad (22)$	$\begin{array}{c} R_1 \\ \diagdown \quad / \\ C \\ / \quad \diagdown \\ R_2 \quad O-(CH_2)_2-NH_2 \end{array}$	59-61
$\begin{array}{c} R_1 \quad X \\ \diagdown \quad / \\ C \\ / \quad \diagdown \\ R_2 \quad OTMS \end{array} \quad (23)$	$\begin{array}{c} R_1 \\ \diagdown \quad / \\ C \\ / \quad \diagdown \\ R_2 \quad OH \end{array}$	62-64
$\begin{array}{c} R_1 \quad X \\ \diagdown \quad / \\ C \\ / \quad \diagdown \\ R_2 \quad O-(CH_2)_n-OTMS \end{array} \quad (24)$	$\begin{array}{c} R_1 \\ \diagdown \quad / \\ C \\ / \quad \diagdown \\ R_2 \quad O-(CH_2)_n-OH \end{array}$	65,66

Scheme 2



Scheme 3

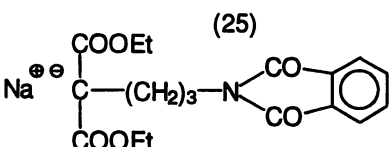
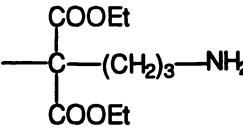
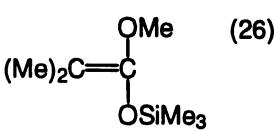
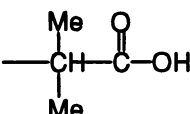


protecting group. The TBDMS monomer uses $n\text{-Bu}_4\text{NF}$ for protection. Cationic substituted monomer. for deprotection. Cationic polymerization of protected alpha methyl styrene and *p*-hydroxystyrene have also been reported^{71,72}.

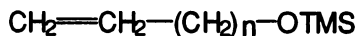
Protecting Groups in Ziegler-Natta Polymerization

The attempts to introduce polar functionality in Ziegler-Natta (Z-N) polymerization have been reviewed in 1979⁷³, 1984⁷⁴ and 1989⁷⁵, and more recently by Kesti⁷⁶. Whereas anionic initiators are killed by protic material, Ziegler-Natta (e.g. Ti, V) catalysts are poisoned by both protons (H) and heteroatoms (e.g. N, O). Silyl groups help mask both; they protect the protons, as well as sterically block and reduce the electron density around the heteroatoms via $p\pi\text{-}d\pi$ overlap. Thus, silyl

Table V. Protected Functional Terminating Agents for Vinyl Ether Polymerization

Protected Terminating Agent	Deprotected End Group	Refs.
 <p>(25)</p>		60
 <p>(26)</p>		61

groups have been used to protect the hydroxyl and amino functionalities in alpha olefin monomers (27) and (28) used in Ziegler-Natta polymerization⁷⁷.

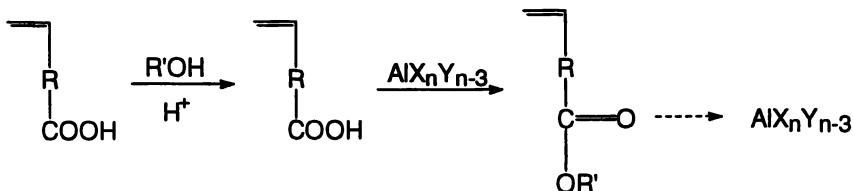


(27)



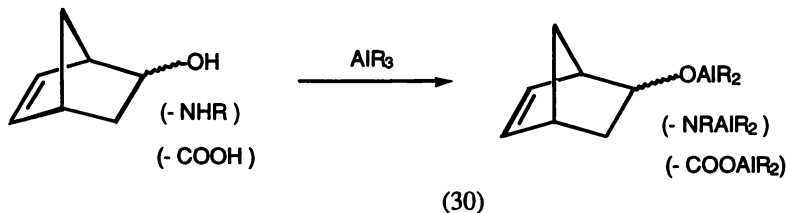
(28)

Carboxyl monomers have been protected in several ways for Z-N polymerization. In one method, the carboxyl functionality is first converted to an ester group and subsequently precomplexed with an aluminum compound to further mute its reactivity with Z-N catalysts⁷³⁻⁹⁰. The precomplexed ester monomer (29) is stable to Z-N conditions and is removed during work-up. Of course, the ester groups can be further hydrolyzed to carboxylic acids or salts, which can associate via hydrogen bonding or ionic interactions.

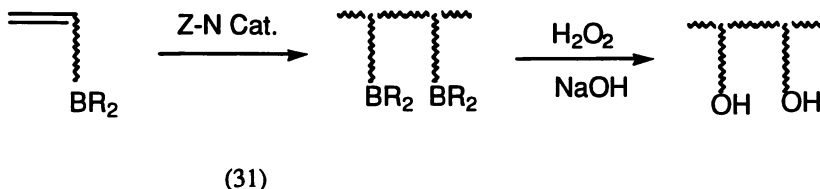


(29)

Alternatively, the acid, amino, or alcohol monomers can be converted to aluminate salts (30) by alkyl aluminum reducing agents. These salts are stable to Z-N catalysts, e.g. vanadium⁹⁰⁻⁹³. Specifically, 5-norbornene-2 carboxylic acid, amine or alcohol is masked by alkyl aluminums, such as (i-Bu)₃Al. Terpolymerization of the masked monomers with ethylene and propylene and work-up leads to functional (-COOH, -OH, -NHR) EPDM rubbers directly.

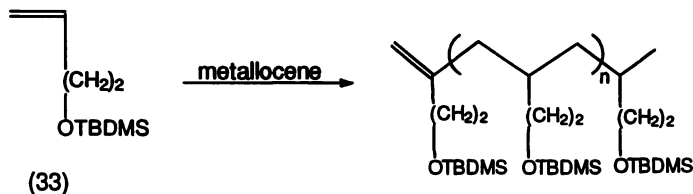
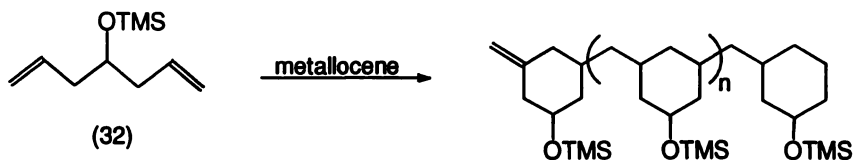


Another method for preparing functional Ziegler-Natta polymers is to use an organoborane mediated synthesis. This method has been extensively studied and reviewed by Chung⁹⁴⁻¹⁰⁰. The success of this technique results from these factors: (a) trialkyl boranes are Lewis acids, which are stable to Z-N catalysts, (b) they are soluble in Z-N (hydrocarbon) solvents, (c) they are remarkably versatile synthons for a variety of functional groups. In this case, borane functional alpha olefin monomers (31) are polymerized to polyboranes which can be hydrolyzed to a variety of functional groups.



Protecting Groups in Metallocene Polymerization

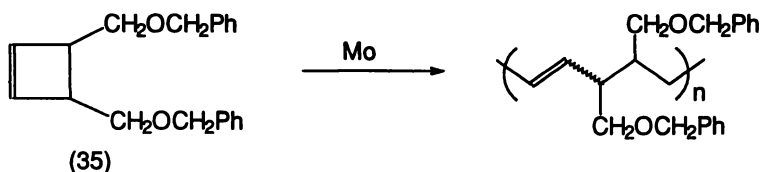
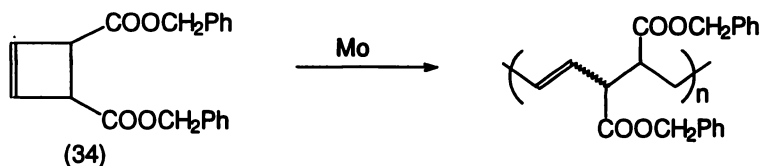
Waymouth¹⁰⁴⁻¹⁰⁶ has polymerized silyl protected alcohols and amines, and non conjugated diene monomers, with cationic Group IV metallocene single site-catalysts. He has found that chiral [(EBTHI)ZrMe]⁺X⁻ catalysts, where EBTHI = ethylene-1,2 bis(η⁵-4,5,6,7-tetrahydro-1-indenyl), are more easily poisoned by silyl ethers than are [Cp₂*ZrMe]⁺X⁻ catalysts. Also [(EBTHI)ZrMe]⁺X⁻ catalysts are inactive for the polymerization of 4-TMSO-1,6 heptadiene but readily polymerize with the more sterically hindered TBDMS protected monomer.



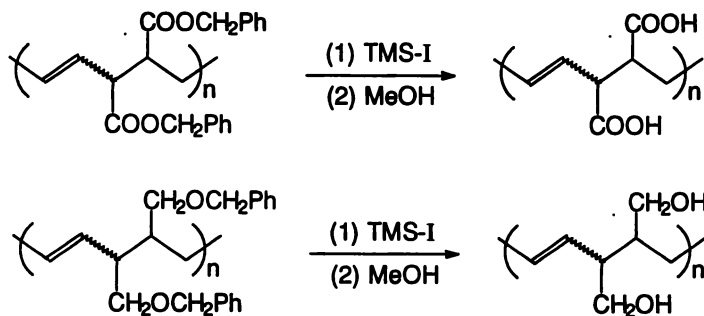
In turn, Chung has used MAO activated Zr metallocene catalysts^{107,108} with borane containing monomers to make functional polymers.

Protecting Groups in Metathesis Polymerization

Group VI or VII metathesis catalysts (e.g. W, Mo, Re) are typically more stable to esters and halogens than are Ziegler-Natta or Group IV metallocene catalysts. Nevertheless, the presence of more reactive functional groups (e.g. ROH, RCOOH) still requires protection. For example, Grubbs⁶⁹, has used a silyl protecting group for the ring opening metathesis polymerization (ROMP)¹⁰⁹ of silyl protected 2-(exo-5-norbornene-2-carboxamido)-2-deoxy-D-gluco-pyranose. Novak¹¹⁰ has conducted ROMP on benzyl ether protected cyclobutenenes (34) (35) to prepare functional polybutadienes using Mo catalysts.



Interestingly, conventional methods for removal of the benzyl protecting groups [e.g. reduction with Na/NH₃(l) or hydrogenolyses] do not work. The benzyl ether protecting groups has to be converted to a silyl group to facilitate removal of the protecting group and generation of the corresponding carboxyl and hydroxyl polybutadienes.



Moreover, Chung^{110,111} has used organoboranes as carriers of the hydroxyl functionality during ROMP of *exo*-B-5-norborn-2-enyl-9-BBN and cyclootenyborane monomer. In addition, telechelic polymers have been prepared by cometathesis of organoborane containing olefins¹¹². More recently¹¹³, the development of ruthenium catalysts, which are highly tolerant of functional groups, has yielded polymers of certain unprotected functional monomers.

Summary and Conclusion

Protecting groups have been advantageously used in anionic, cationic, Ziegler-Natta, metallocene and metathesis polymerizations. Such groups have been built into initiators, terminating agents, and monomers. The most versatile and robust protecting groups are the silyl ethers, which have remarkably been applied to all of the above polymerization types. Borane mediated synthesis of functional polymers has also proven very effective for several polymerization methods.

The use of protecting groups in polymerization is the preferred laboratory method for preparing many functional polymers. Protecting group methods have allowed the synthesis of otherwise difficult to synthesize functional and reactive polymers. Industrial applications are expected to be more in the specialty rather than commodity polymer area because of the costs associated with the protection and deprotection steps. For example, FMC has just announced a new line of protected functional anionic initiators for use in specialty block polymer synthesis. Commodity polymer applications will have to await the development of new catalysts that not only tolerate functionality but also incorporate it in a single step.

Acknowledgments

The authors wish to thank R. Roper and E. Hoel for assistance with literature searches.

Literature Cited

1. Quirk, R. P.; Jang, S. H. *Rubber Chem. Tech.*, **1996**, 69(3), 444.
2. Schulz, D. N.; Halasa, A. F.; Oberster, A. E. *J. Polym. Sci., Polym. Chem. Ed.*, **1974**, 12, 153.
3. Schulz, D. N.; Sanda, J. C.; Willoughby, B. G. In "Anionic Polymerization. Kinetics, Mechanisms, and Synthesis", McGrath, J. E., Ed., ACS Symp. Ser., 166, 1981, 427.
4. Wagener, K.; Wanigatunga, S. *Macromolecules*, **1987**, 20(7), 1717.
5. Wagener, K.; Wanigatunga, S. *ACS Div. of Polym. Chem. Polym. Prepr.*, **1986**, 27(1), 105.
6. Shepherd, N.; Stewart, M. J., U.S. 5,331,058 (July 19, 1994).
7. Shepherd, N.; Stewart, M. J., U.S. 5,362,699 (November 8, 1994).
8. Handlin, D. L.; Jr., Bening, R. C.; Willis, C. L., U.S. 5,376,745 (December 27, 1994).
9. Bening, R. C.; Willis, C. L., U.S. 5,391,663 (February 21, 1995).
10. Bening, R. C.; St. Clair, D. J., U.S. 5,486,568 (January 23, 1996).
11. Sutton, D. E.; Schwindeman, *Polym. Matl. Sci. Eng.*, **1997**, 76.
12. Quirk, R. P. *Polym. Matl. Sci. Eng.*, 1997, 76, (1997)
13. Schulz, D. N.; Halasa, A. F., *J. Polym. Sci. Polym. Chem. Ed.*, **1997**, 15, 2401.
13. Dickstein, W. H.; Lillya, C. P. *Macromolecules*, **1989**, 22, 3882.
14. Dickstein, W. H.; Lillya, C. P. *Macromolecules*, **1989**, 22, 3886.
16. Pyati, M., Ph.D. Thesis, Univ. of Mass., 1996. *Dist Abstr. Int. B*, **1996** 57(2), 1091.
17. Quirk, R. P. In "Comprehensive Polymer Science," First Supplement, S. L. Aggarwal and S. Russo, Eds.; Pergamon Press, Oxford, U.K., 1992, pp. 83-106.
18. Quirk, R. P., U.S. Pat. 4,975,491 (December 4, 1990).
19. Quirk, R. P., U.S. Pat. 5,081,191 (January 14, 1992).
20. Quirk, R. P.; Takizawa, T.; Lizarraga, G.; Zhu, L.-F. *J. Appl. Polym. Symp.*, **1992**, 50, 23.
21. Cheng, T. C. In "Anionic Polymerization, Kinetics, Mechanisms, and Synthesis", McGrath, J. E., Ed.; ACS Symp. Ser., 166, 513.
22. Antkowiak, T. A.; Lawson, D. F.; Koch, R. W.; Stayer, M. L., U.S. 5,153,159 (October 6, 1992); U.S. 5,268,413 (December 7, 1993), U.S. 5,354,822 (October 11, 1994).
23. Lawson, D. F.; Stayer, M. L. Jr.; Morita, K.; Ozawa, Y.; Fujio, R., U.S. 5,329,005 (July 12, 1994).
24. Ueda, K.; Hirao, A.; Nakahama, S. *Macromolecules*, **1990** 23, 939.
25. Hirao, A.; Nagahama, T.; Ishizone, T.; Nakahama, S. *Macromolecules*, **1993**, 26, 2145.
26. Hirao, A.; Hattori, I.; Sasagawa, T.; Yamaguchi, K.; Nakahama, S. *Makromol. Chem. Rapid Commun.*, **1982**, 3, 59.
27. Tohyama, M.; Hirao, A.; Nakahama, S. *Macromol. Chem. Phys.*, **1996**, 197, 3135.

28. Quirk, R.; Zhu, L. F. *Makromol. Chem.*, **1989**, 190(3), 487.
29. Quirk, R. P.; Zhu, L.-F. *British Polym. J.*, 1990, 23, 47.
30. Quirk, R. P. *Rubber Chem. Tech.*, **1991**, 64, 648.
31. Quirk, R. P.; Lynch, T. *Macromolecules*, **1993**, 26, 1206.
32. Peters, M. A.; Belu, A. M.; Linton, R. W.; Dupray, L.; Meyer, T. J.; DeSimone, J. M. *J. Am. Chem. Soc.*, **1995**, 117(12), 3380.
33. Nakahama, S.; Hirao, A.; *Prog. Polym. Sci.*, **1990**, 15, 299.
34. Hirao, A.; Nakahama, S. *Trends in Polym. Sci.*, **1994**, 2(8), 267.
35. Hirao, A.; and Nakahama, S. *Prog. Polym. Sci.*, **1992**, 17, 283.
36. Hirao, A.; Kato, K.; Nakahama S. *Macromolecules*, **1992**, 25, 535.
37. Hirao, A.; Takamaka, K.; Kitamura, K.; Nakahama, S. *Macromolecules*, **1993**, 26, 4995.
38. Hirao, A.; Takenaka, S.; Pakirisamy, K.; Yamaguchi, K.; Nakahama, S.; *Makromol. Chem.*, **1985**, 186, 1157.
39. Hirao, A.; Kitamura, K.; Takenaka, K.; Nakamura, S. *Macromolecules*, **1993**, 26, 4995.
40. Hirao, A.; Takenaka, K.; Yamaguchi, K.; Nakahama, S. *Polymer*, **1987**, 28, 303 (1987).
41. Hirao, A.; Takenaka, K.; Yamaguchi, K.; Nakahama, S.; Yamazaki, N. *Polym. Commun.*, **1983**, 24, 339.
42. Wakabayashi, S.; Hirao, A.; Nakahama, S. *Polym. Prepr. Jap.*, **1987**, 36, 252.
43. Yamaguchi, K.; Hirao, A.; Suzuki, K.; Takenaka, K.; Nakahama, S.; Yamazaki, N. *J. Polym. Sci., Polym. Lett.*, **1983**, 21, 395.
44. Suzuki, K.; Yamaguchi, K.; Hirao, A.; Nakahama, S. *Macromolecules*, **1989**, 22, 2607.
45. Suzuki, K.; Hirao, A.; Nakahama, S. *Makromol. Chem.*, 190, 2893.
46. Ishino, Y.; Hirao, A.; Nakahama, S. *Makromolecules*, **1986**, 19, 2307.
47. Hirao, A.; Ishiro, Y.; Nakahama, S. *Makromolecules*, **1988**, 21, 561.
48. Hirao, A.; Ishino, Y.; Nakahama, S. *Makromol. Chem.*, **1986**, 187, 141.
49. Ishizone, T.; Hirao, A.; Nakahama, S. *Macromolecules*, **1991**, 24(18), 5230.
50. Hirao, A.; Kato, H.; Yamaguchi, K.; Nakahama, S. *Macromolecules*, **1986**, 19, 1294.
51. Mori, H.; Wakisaka, D.; Hirao, A.; Nakahama, S. *Makromol. Chem.*, **1994**, 195(9), 3213.
52. Mori, H.; Hirao, A.; Nakahama, S. *Macromolecules*, **1994**, 27(1), 35.
53. Bugner, D. E *ACS Div. of Polym. Chem. Polym. Prepr.*, **1983**, 27(2), 57.
54. Matsumoto, A.; Oki, Y.; Otsu, T. *Polym. J.*, **1992**, 24, 679.
55. Matsumoto, A.; Oki, Y.; Otsu, T. *Polym. J.*, **1993**, 25, 237.
56. Dasgupta, A.; Sivaram, S. J. *Macromol. Sci.-Rev. Macromol. Chem. Phys.*, **1997**, C(37)1, 1.
57. Deffieux, A. In "Polymeric Materials Encyclopedia", Salomone, J., Ed.; CRC Press, Boca Raton, FL, 1996, Vol. 4, pp. 2641-2653.
58. Shohi, H.; Sawamoto, M.; Higashimira, T. *Polym. Bull.*, **1989**, 21, 357.
59. Sawamoto, M.; Enoki, T.; Higashimura, T. *Macromolecules*, **1987**, 20, 1.

60. Sawamoto, M.; Enoki, T.; Higashimura, T. *Makromol. Chem. Makromol. Symp.*, **1988**, *13/14*, 513.
61. Hashimoto, T.; Sawamoto, M.; Higashimura J. *Polym. Sci. Polym Chem. Ed.*, **1987**, *25*, 1073.
62. Kamigaito, M.; Sawamoto, M.; Higashimura, T. *J. Polym. Sci. Polym. Chem. Ed.*, **1991**, *29*, 1909.
63. Kamigaito, M.; Sawamoto, M.; Higashimura, T. *Makromol. Chem.*, **1993**, *194*, 727.
64. Mairene, D. V. *Polym. Bull*, **1990**, *23*, 185.
65. Haucourt, N.; Goethals, E. J. *Makromol. Chem. Rapid Commun.*, **1992**, *13*, 329.
66. Goethals, E. J.; Haucourt, N.; Peng, L-B. *Makromol. Symp.*, **1994**, *85*, 97.
67. Cramail, H. *Polym. Adv. Technol.*, **1994**, *5*, 568.
68. Verna, A.; Riffle, J. S. *ACS Div. of Polym. Chem. Polym. Prepr.*, **1990**, *31(1)*, 590.
69. Higashimura, T.; Ebara, K.; Aoshima, S. *J. Polym. Sci. Part A: Polym. Chem.*, **1989**, *27(9)*, 2937.
70. Hashimoto, T.; Ibuki, H.; Sawamoto, M.; Higashimura, T. *J. Polym. Sci. Part A: Polym. Chem.*, **1988**, *26(12)*, 3361.
71. Ito, H.; Willson, C. G.; Frechet, J. M.; Farral, M. J.; Eichler, E. *Macromolecules*, **1983**, *16(4)*, 510.
72. Frechet, J. M.; Eichler, E.; Ito, Hiroshi; Willson, C. G. *Polymer*, **1983**, *24(8)*, 995.
73. Boor, J., Jr. "Ziegler-Natta Catalysts and Polymerizations", Academic Press, 1979.
74. Purgett, M. D., Ph.D. Thesis, University of Massachusetts, 1984.
75. Padwa, A. R. *Prog. Polym. Sci.*, **1989**, *14*, 811.
76. Kesti, M., Ph.D. Thesis, Stanford University, 1992.
77. Giannini, U.; Brückner, G.; Pellino, E.; Cassata, A. *J. Polym. Sci. Polym. Lett. Ed.*, **1967**, *5*, 527.
78. Clark, U.S. 3,492,277 (1970).
79. Kitano, K.; Ueno, H., Jap. Pat. Appl. 57-1522767, 57-188996, 57-188997.
80. Schulz, D. N.; Kitano, K.; Burkhardt, T.; Langer, A. W., U.S. 4,518,757 (1985).
81. Schulz, D. N.; Bock, J. *J. Macromol. Sci. Chem.*, **1991**, *A28(11-12)*, 1235.
82. Vogl, O. *J. Macromol. Sci. Chem.*, **1985**, *A22(5-7)*, 541
83. Purgett, M. D.; MacKnight, W. J.; Vogl, O. *Polym. Eng. Sci.*, **1987**, *27*, 1461.
84. Purgett, M. D.; Vogl, O. *J. Polym. Sci., Part A: Polym. Chem.*, **1989**, *26*, 671.
85. Purgett, M. D.; Vogl, O. *J. Polym. Sci., Part. A: Polym. Chem.*, **1989**, *27*, 2051.
86. Collete, J. W.; Ro, R. S.; Sonnenberg, F. M., U.S. 3,884,888 (1975); U.S. 3,901,860 (1975); U.S 4,017,669 (1977).
87. Londoll, L. M.; Breslow, D. S. *J. Polym. Sci. Part A: Polym. Chem.*, **1989**, *27*, 2189.

88. Marie, G.; Lang, A.; Chapelet, G., U.S. 4,139,417 (1979).
89. Hoeschst, F., Fr. Pat. 1,498,009 (1967).
90. Tanaka, K.; Iwata, T.; Sasaki, J., Jap. Pat. 73/37 755 (1973); Jap. Pat 73/37 756 (1973).
91. Datta, S.; Kresge, E. N., U.S. 4,987,200 (1991).
92. Datta, S.; Ver Strate, G.; Kresge, E. N. *ACS Div. of Polym. Chem. Polym. Prepr.*, **1992**, *33(1)*, 899.
93. Datta, S. In “*High Value Polymers*”, Fawcett, A., Ed.; Royal Society of Chemistry, London 1991; Chapter 2.
94. Chung, T. C. In “*Polymeric Materials Encyclopedia*”, Salemone J. C., Ed.; CRC Press, Boca Raton, FL, 1996, Vol 4; pp 2681-2691.
95. Chung, T. C. *Trends in Polym. Sci.*, **1995**, *3(6)*, 191.
96. Chung, T. C.; Schulz, D. N. *Heteroatom Chem.*, **1991**, *2(5)*, 545.
97. Chung, T. C. *ChemTech.*, **1991**, *27*, 496.
98. Chung, T. C. *Macromolecules*, **1988**, *21*, 865.
99. Chung, T. C.; Ramakrishnan, S.; Kim, M. W. *Macromolecules*, **1991**, *24*, 2675.
100. Ramakrishnan, S.; Berluche, E.; Chung, T. C. *Macromolecules*, **1990**, *23*, 318.
101. Chung, T. C.; Rhubright, D. *Macromolecules*, **1991**, *24*, 970.
102. Chung, T. C.; Rhubright, D. *Macromolecules*, **1993**, *26*, 3019.
103. Chung, T. C.; Rhubright, D. *J. Polym. Sci. Pol. Chem. Ed.*, **1993**, *31*, 2729.
104. Kesti, M. R.; Coates, G. W.; Waymouth, R. M. *J. Am. Chem. Soc.*, **1992**, *114*, 9679.
105. Stein, K. M.; Kesti, M. R.; Coates, G. W.; Waymouth, R. *ACS Div. of Polym. Chem. Polym. Prepr.*, **1994**, *35(1)*, 480.
106. Mogstad, A.; Kesti, M. R.; Coates, G. W.; Waymouth, R. M. *ACS Div. of Polym. Chem. Polym. Prepr.*, **1993**, *34(1)*, 211.
107. Chung, T. C.; Lu, H. L.; Li, C. L. *Polym. Intl.*, **1995**, *37(3)*, 197.
108. Chung, T. C.; Lu, H. L.; Janvikul, W., *Polym. Mater. Sci. Eng. Prepr.*, **1995**, *73*, 463.
109. Cassandra, F.; Grubbs, R. H. *Macromolecules*, **1995**, *28(21)*, 7248.
110. Perrott, M. G.; B. M. Novak, *Macromolecules*, **1996**, *29*, 1917.
111. Ramakrishnan, S.; Chung, T. C. *Macromolecules*, **1989**, *22*, 3181.
112. Ramakrishnan, S.; Chung, T. C. *Macromolecules*, **1990**, *23*, 4519.
113. Chung, T. C.; Chasrnawaia, M. *Macromolecules*, **1991**, *24*, 3721.
114. Wu, Z.; Nguyen, S. T.; Grubbs, R. H.; Ziller, J. W. *J. Am. Chem. Soc.*, **1995**, *117(2)*, 5503.

Chapter 5

Novel, Protected Functionalized Initiators for Anionic Polymerizations

Douglas E. Sutton and James A. Schwindeman¹

FMC Lithium Division, P.O. Box 795, Bessemer City, NC 28016

ABSTRACT. A new class of protected hydroxyl containing functionalized initiators were recently disclosed by the Defense Evaluation and Research Agency (DERA). These novel initiators have the general structure: TBS-O-(CH₂)_n-Li. Excellent solubility in hydrocarbon solvents was exhibited by these materials which allowed the preparation of telechelic, high 1,4-microstructure polybutadienes. The two-step synthesis of these functionalized initiators from commercially available raw materials will be presented in detail. The first step involved reaction of an omega-haloalcohol with *t*-butyldimethylsilyl chloride, in the presence of an acid acceptor, to form the precursor. This precursor was then reacted with lithium metal in a hydrocarbon solvent to afford a solution of the functionalized initiator. The thermal stability of these initiators in hydrocarbon solution will also be presented. The application of the precursors and functionalized initiators in anionic polymerization of dienes will be briefly discussed.

The facile preparation of alpha, omega-difunctional (“telechelic”) polymers has long been sought. These polymers have utility in coatings, adhesives, sealants, asphalt modification, and rocket fuel binders.¹ One approach to these types of polymers that has great commercial potential is the employment of a protected functionalized initiator.² Advantages to the employment of protected functional initiators include: each macromolecule contains a functional group and a living anionic species; gelation is avoided upon functionalization of the living polymer anion with electrophilic agents; and a variety of polymer types can be prepared,

¹Corresponding author.

such as telechelic polymers, functionalized block copolymers, and functionalized star polymers, by judicious choice of electrophiles, coupling agents, or co-monomers.³

BACKGROUND

The seminal work of Schulz and co-workers on anionic polymer initiators which contain protected hydroxyl functionality was reported in 1974.⁴ These researchers prepared 2-(6-lithio-*n*-hexyloxy)tetrahydropyran by metal-halogen exchange in diethyl ether, see Figure 1. The lithium chloride co-product was removed by filtration. This initiator was successfully employed in the polymerization of 1,3-butadiene. The resultant functionalized living anion was subsequently functionalized with ethylene oxide or coupled with dimethyldichlorosilane. Mild acid hydrolysis with dichloroacetic acid liberated the telechelic dihydroxy polybutadiene. The polybutadienes produced with this initiator exhibited narrow molecular weight distributions ($M_w/M_n = 1.05-1.08$).

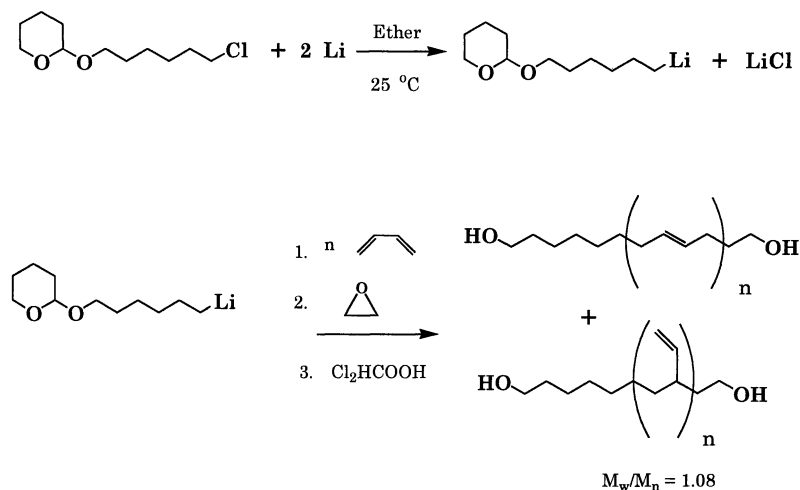
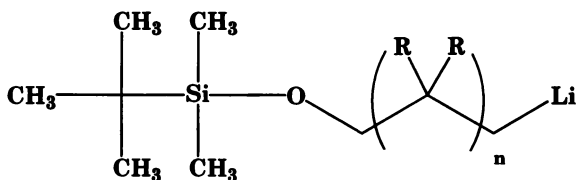


Figure 1

Excellent difunctionality of the resultant polymers was obtained ($f = 2.0 \pm 0.1$). However, since the initiator was synthesized in diethyl ether, the amount of 1,2-microstructure was relatively high (36-54%). The initiator was insoluble in hexane solution, thus the formation of high 1,4 microstructure was impossible. In addition, from a practical perspective, the cleavage of diethyl ether by the alkyl lithium initiator was of concern.⁵

Recently, a group at the Defense Evaluation and Research Agency (DERA) in the U.K. reported the preparation of a group of compounds that were employed as polymerization initiators, omega-(*t*-butyldimethylsilyloxy)-1-alkyllithiums.⁶ In contrast



$$n = 1, 2, 4, 6$$



to the previous report, these functionalized lithium species were prepared in a hydrocarbon solvent. These initiators effectively polymerized 1,3-butadiene, and the resultant living anion could be efficiently functionalized, see Figure 2. The polybutadienes produced from these initiators had narrow molecular distributions ($M_w/M_n = 1.1$) and high 1,4-microstructure (87–91% 1,4). The resultant polymer exhibited high functionality. The *t*-butyldimethylsilyl protecting group was readily removed by treatment of the protected telechelic polymer with tetra-*n*-butylammonium fluoride in tetrahydrofuran.

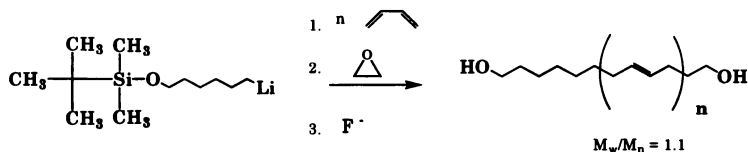
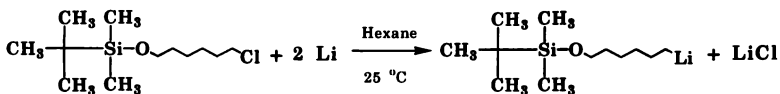


Figure 2

DISCUSSION

FMC has supplied *n*-butyllithium and *s*-butyllithium as initiators for anionic polymerization for over thirty years. The utility of this family of protected functional initiators to prepare telechelic polymers was intriguing. The retrosynthesis of 6-(*t*-butyldimethylsilyloxy)-1-hexyllithium is illustrated in Figure 3. In addition, FMC was basic in

two of the three principle raw materials, lithium metal and *t*-butyldimethylsilyl chloride (TBSCl). FMC is the only fully integrated producer of lithium metal in the world. Furthermore, FMC was the world's largest producer of TBSCl. FMC negotiated exclusive, world-wide rights to this technology from the DERA. FMC then began development efforts to commercialize this new family of omega-(*t*-butyldimethylsilyloxy)-1-alkyllithiums.

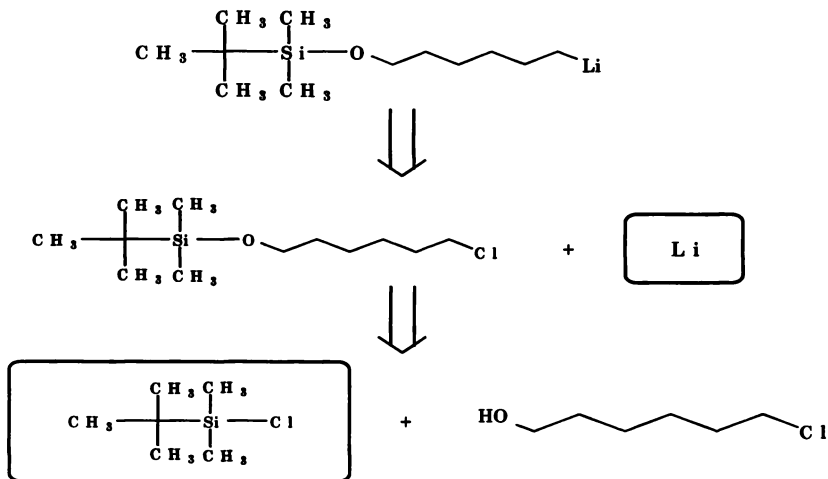


Figure 3

The additional raw materials required to prepare these protected functional initiators are the omega-haloalcohols, such as 6-chloro-1-hexanol. A variety of these halogenated alcohols are available on a commercial scale. A partial listing of these

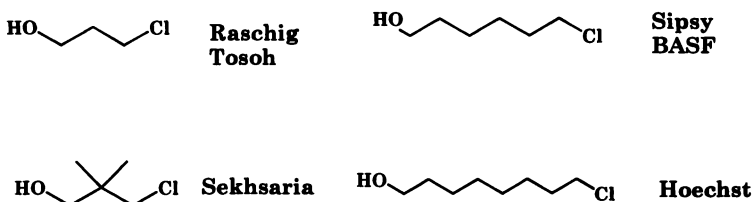


Figure 4

haloalcohols, and their commercial suppliers, are tabulated in Figure 4. These compounds are typically prepared by the mono-chlorination of the corresponding diol.⁷ In addition to this route, the compound 4-chloro-1-butanol was also prepared by the ring opening of tetrahydrofuran with anhydrous hydrogen chloride, see Figure 5.⁸

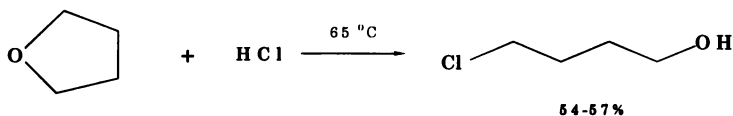


Figure 5

The initial research efforts focused on the preparation of the precursor, the omega-*t*-butyldimethylsilyloxyalkyl halide, from the corresponding haloalcohol and *t*-butyldimethylsilyl chloride. The *t*-butyldimethylsilyl moiety was originally introduced as an alcohol protecting group by Corey.⁹ In this procedure, 1.2 equivalents of *t*-butyldimethylsilyl chloride and 2.5 equivalents of imidazole, as the acid acceptor, were utilized. The solvent employed was *N,N*-dimethylformamide. These reaction conditions afforded the desired product in excellent yield. However, the cost of the excess reagents, their subsequent removal, the utilization of an expensive, hygroscopic solvent, and an aqueous workup were not very practical from a commercial perspective. Since its inception in 1972, a variety of other procedures have been described for the preparation of *t*-butyldimethylsilyl ethers.¹⁰ These procedures typically require solvents that are expensive, difficult to recycle, or environmentally unfriendly. Furthermore, traces of some of these solvents, such as methylene chloride, in the precursor would be incompatible with lithium metal in the subsequent lithiation step.

The silylation of the omega-haloalcohols was therefore initially investigated in a hydrocarbon solvent, as this was the solvent for the subsequent lithium-halogen exchange reaction. It was discovered that the silylation reaction proceeded to completion at ambient temperature in a hydrocarbon solvent.¹¹ Only one equivalent of imidazole was required as the acid acceptor. The *t*-butyldimethylsilyl chloride (one equivalent) was dissolved in the hydrocarbon solvent. One equivalent of imidazole was added to the reaction mixture, which was insoluble. This was followed by addition of the omega-haloalcohol. This reaction was conveniently monitored by gas chromatography (GC) for disappearance of the starting materials. The imidazole hydrochloride by-product was also insoluble in the reaction mixture. At the conclusion of the reaction, this by-product was removed by simple filtration. The imidazole hydrochloride in the filter cake was easy to dry on the filter. This material could then be readily recycled by liberating the free amine from this salt. The filtrate, a hydrocarbon solution of the precursor, could be employed directly in the subsequent lithiation reaction. Alternatively, the filtrate could be concentrated, and the precursor purified by vacuum distillation. The volatiles removed from the precursor at this stage, during the concentration, were composed of essentially pure solvent. This material was easily recycled back into the silylation reaction

without complication. This procedure is illustrated in Figure 6, for the silylation of 3-chloro-1-propanol in cyclohexane.

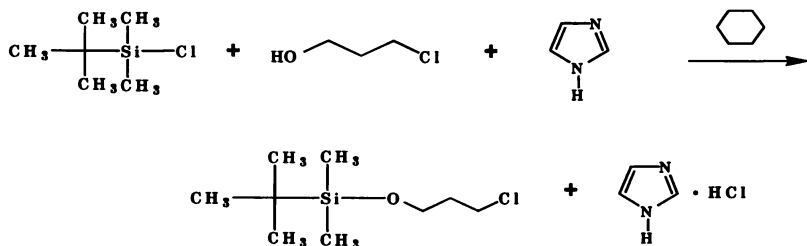


Figure 6

The kinetics of the silylation of 6-chloro-1-hexanol as a function of the acid acceptor was investigated, see Figure 7. These experiments were conducted in cyclohexane solvent

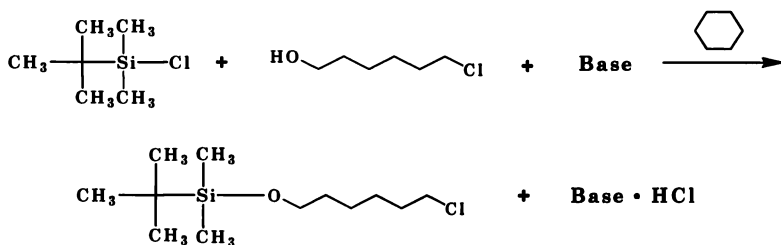


Figure 7

at room temperature. The reactions were monitored by GC analysis for conversion to the silyl ether. The results are compiled in Figure 8. Complete conversion was observed in 30 hours, when imidazole was employed as the acid acceptor. In contrast, triethylamine was relatively ineffective. Even after six days, the starting materials were still observed, by GC analysis. Thus, imidazole, while it was totally insoluble in the reaction mixture, was the most effective acid acceptor in the silylation reaction in hydrocarbon solvent.

Base	Time (hrs.)	Conversion (%)
Imidazole	5	82.2
Imidazole	30	100
Triethylamine	21	53.3
Triethylamine	162	88.0

Figure 8

The generality of these silylation conditions was then briefly explored. A variety of silyl ethers were synthesized from various alcohols and one equivalent of the corresponding trialkylsilyl chloride in hydrocarbon solvent. One equivalent of imidazole was utilized in each experiment. A partial listing of the results are tabulated in Figure 9. The yield and

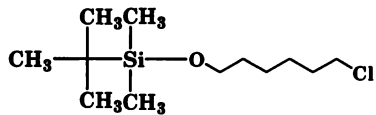
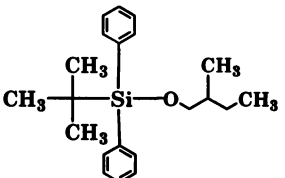
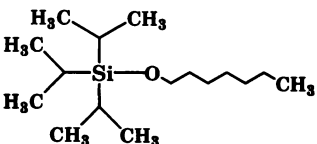
	<u>Yield</u>	<u>Assay</u>
	101.5 %	98.3 %
	101.1 %	96.6 %
	100 %	96.3 %

Figure 9

assay were determined by concentration of the crude filtrate on a rotary evaporator, after removal of the imidazole hydrochloride by filtration. Residual solvent was the principle impurity present in the crude silyl ethers. *T*-Butyldimethylsilyl, *t*-butyldiphenylsilyl, and triisopropylsilyl ethers were readily prepared, in high yield and excellent assay, by this procedure. The newly developed silylation procedure in hydrocarbon solvent required no aqueous workup or chromatography to generate assorted silyl ethers in excellent purity and high yield. The silylation of 4-chloro-1-butanol was problematic, see Figure 10. Cyclization of the halo-alcohol to tetrahydrofuran was observed, under the reaction conditions, in addition to the desired silyl ether. Up to 20% of the starting halo-alcohol was consumed by this reaction manifold. This cyclization phenomenon was not observed in the silylation of other omega-halo-alcohols, such as 3-chloro-1-propanol or 6-chloro-1-hexanol.

After an efficient synthesis of the precursor in hydrocarbon solvent was developed, the lithium/halogen exchange reaction was then scrutinized. The lithiation experiments were typically conducted by slow addition of the precursor to a suspension of lithium dispersion in a

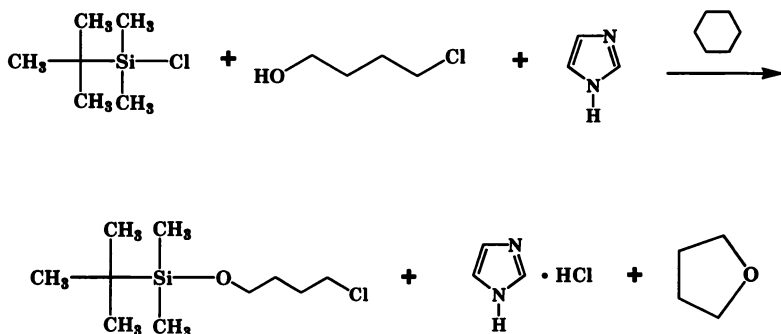


Figure 10

hydrocarbon solvent. The lithium dispersion contained 0.3–0.7 weight percent sodium. This chemistry is illustrated for the preparation of 3-(*t*-butyldimethylsilyloxy)-1-propyllithium in cyclohexane solvent, Figure 11. The by-product, lithium chloride, and any unreacted lithium metal dispersion were removed by filtration through a sintered glass filter. The filter cake was rinsed with fresh solvent to remove the last vestiges of the product. The filtrate was a clear, yellow solution of the protected functional initiator. The impact of various parameters, such as reaction concentration, agitation rate, and reaction temperature on the yield of the protected functionalized initiator were investigated. Minimal yield effects were observed for agitation rate, solvent identity, reaction concentration, and length of the connecting group between the carbon–lithium bond and the *t*-butyldimethylsilyloxy group. The amount of lithium metal employed in the reaction was successfully reduced from the recommended six equivalents⁶ to less than three with no reduction in yield.

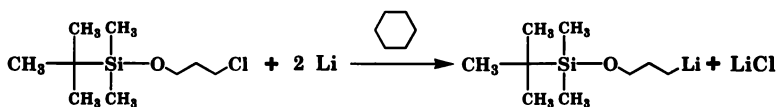


Figure 11

The reaction temperature was found to bear a significant influence on the lithiation yield. The cardinal description of this lithiation in hydrocarbon solvents reported that at temperatures above 40 °C undesirable by-products were observed.⁶ When the lithiation was conducted at 40 °C, with less than the six equivalents of lithium reported in the literature,⁶ the yield fell off substantially. In addition, the yield of the organolithium species was not reproducible at lower temperatures. Recent lithiation experiments conducted in FMC laboratories indicated

that elevated temperature can improve the yield in certain organometallic reactions.¹² Indeed, it was discovered that higher yields of the organolithium species were obtained when the metallation reaction was conducted at temperatures above 40 °C.¹³ The relationship of yield versus the lithiation temperature for 3-(*t*-butyldimethylsilyloxy)-1-chloropropane is plotted in Figure 12. The maximum yield, 92%, was obtained when the lithiation was conducted at 60 °C. Positive or negative deviations from this temperature caused a significant decline in the yield. The filtered product contained only traces of by-products, such as the Wurtz coupling dimer and the olefin, produced by elimination of HCl from the precursor. Thus, the yield and reproducibility of the lithium/halogen exchange of omega-(*t*-butyldimethylsilyloxy)-1-chloroalkanes was notably improved by conducting the reaction at elevated temperatures.

LITHIATION OF 3-(*t*-BUTYLDIMETHYLSILYLOXY)-1-CHLOROPROPANE

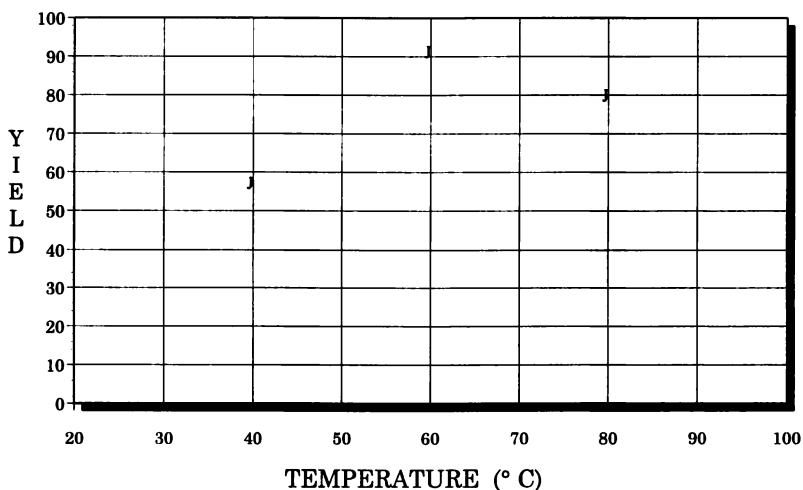


Figure 12

The thermal stability of the hydrocarbon solutions of the protected functional initiators was then explored. The organolithium compounds were found to be fairly soluble in a variety of hydrocarbon solvents, including hexane, cyclohexane, heptane, and toluene. A typical formulation of one of these initiators contained the active organolithium, 15–25 weight percent, and the solvent of choice, 75–85 weight percent. The thermal stability was determined by suspending sample bottles containing the protected functional initiator formulations in constant

temperature baths at 0, 15, and 40 °C. Periodically, a sample was withdrawn and analyzed for total base and active carbon–lithium base by Watson–Eastham titration.¹⁴ The thermal stability of 3-(*t*-butyldimethylsilyloxy)-1-propyllithium in cyclohexane is presented in Figure 13. The samples held at 40 °C exhibited substantial

**THERMAL STABILITY OF 3-(*t*-BUTYLDIMETHYLSILYLOXY)
-1-PROPYLLITHIUM**

TOTAL BASE (wt. %)	ACTIVE BASE (wt. %)	NO. DAYS	TEMP.	% LOSS/ DAY (wt. %)	COMMENTS
13.4	12.9	0	n/a	n/a	START
13.4	12.5	7	40 °C	0.44	CLEAR
13.4	12.1	14	40 °C	0.44	CLEAR
13.8	11.6	21	40 °C	0.48	CLEAR/DARK
13.7	11.0	28	40 °C	0.53	CLEAR/DARK
13.5	12.9	35	15 °C	0.00	CLEAR
13.7	13.0	67	15 °C	-0.01	CLEAR
13.6	12.7	117	0 °C	0.01	CLEAR

Figure 13

decomposition, as evidenced by the loss in active base analysis and the formation of a dark color after 21 days. However, essentially no thermal decomposition was observed in the samples that were maintained at 0 or 15 °C. Even after almost four months at 0 °C, essentially no change was observed in the assay. A similar thermal stability profile was observed for a cyclohexane solution of 6-(*t*-butyldimethylsilyloxy)-1-hexyllithium. The hydrocarbon formulations of omega-(*t*-butyldimethylsilyloxy)-1-alkyllithiums demonstrated excellent thermal stability, when the solutions were maintained at 15 °C or lower.

The pyrophoricity of the various hydrocarbon formulations of omega-(*t*-butyldimethylsilyloxy)-1-alkyllithiums were tested, according to the official Department of Transportation (DOT) protocol.¹⁵ In this test, samples of the solution were placed on indented filter paper. After five minutes, the filter paper was examined for signs of charring. All the formulations tested by this official protocol were classified as NON-Pyrophoric.

In conclusion, FMC has developed a viable, commercial synthesis of a family of omega-(*t*-butyldimethylsilyloxy)-1-alkyllithiums that are valuable anionic initiators. A variety of chain lengths are available between the protected hydroxyl function and the carbon–lithium bond. These hydrocarbon soluble initiators afford very high 1,4-microstructure in the polymerization of polydienes, such as

1,3-butadiene or isoprene. These compounds were all synthesized from commercially available raw materials. The precursors, omega-(*t*-butyldimethylsilyloxy)-1-haloalkanes, were prepared in high yield from the corresponding omega-haloalcohol and one equivalent of *t*-butyldimethylsilyl chloride and imidazole in a hydrocarbon solvent. High yields in the lithium/halogen exchange of these precursors were achieved at elevated reaction temperatures. The formulations of the protected functional initiator in a hydrocarbon solution were thermally stable, when maintained below ambient temperature. In addition, the formulations were all non-pyrophoric. This family of protected functional initiators provides the polymer chemist with a unique set of reagents for the preparation of telechelic polymers and functionalized star polymers with high functionality.

EXPERIMENTAL

Preparation of 3-(*t*-Butyldimethylsilyloxy)-1-Chloropropane

A two liter, three-necked flask was fitted with a mechanical stirrer, a 250 ml. pressure-equalizing addition funnel, and a Claisen adapter fitted with a thermocouple, a reflux condenser, and an argon inlet. This apparatus was dried in an oven overnight at 125 °C, assembled hot, and allowed to cool to room temperature in a stream of argon. The flask was charged with 221.00 grams (1.466 moles, 1.01 equivalents, FMC) of *t*-butyldimethylsilyl chloride, 101.80 grams of imidazole (1.495 moles, 1.03 equivalents, BASF), and 850 grams of cyclohexane. The *t*-butyldimethylsilyl chloride rapidly dissolved in the reaction medium, endothermically. The imidazole remained insoluble. 3-Chloro-1-propanol, 137.27 grams (1.452 mole, 1.00 equivalent, Raschig) was added dropwise via the addition funnel. The reaction temperature climbed 22 °C during the course of the chloroalcohol addition. The total alcohol feed time was 75 minutes. The addition funnel was rinsed with additional cyclohexane (50 grams). After the exotherm had subsided (about one hour), the reaction mixture was heated to 40 °C with a heating mantle controlled by a Thermo-Watch®. A fluffy, white precipitate formed during the reaction. Periodically, the stirrer was halted, and the clear supernatant solution was analyzed by gas chromatography (GC). After four hours at 40 °C, all the starting material had been consumed with the formation of a single, higher boiling compound. The mixture was stirred overnight at 40 °C, let cool to room temperature, then transferred to a medium porosity glass filter funnel. The flask was rinsed with fresh cyclohexane (2 X 250 ml.). The filter cake was reslurried with cyclohexane (2 X 350 ml.). The combined filtrate was concentrated on the rotary evaporator, bath temperature = 30 °C. This afforded a clear, colorless oil, yield = 296.1 grams (97.7%).

GC assay (area percent):

3-(*t*-butyldimethylsilyloxy)-1-chloropropane 95.8 %, cyclohexane 3.15%,
3-chloro-1-propanol 0.05% and unknowns 1.42%.

Preparation of 3-(*t*-Butyldimethylsilyloxy)-1-Propyllithium

A one liter, three-necked, Morton flask was fitted with a mechanical stirrer, a 250 ml. pressure-equalizing addition funnel, and a Claisen adapter fitted with a thermocouple, a reflux condenser, and an argon inlet. This apparatus was dried in an oven overnight at 125 °C, assembled hot, and allowed to cool to room temperature in a stream of argon. Lithium metal dispersion was washed free of mineral oil with hexane (2 X 100 ml.) and pentane (1 X 100 ml.). The resultant lithium dispersion was dried in a stream of argon, weighed (11.70 grams, 1.686 moles, 2.80 equivalents), and transferred to the reaction flask with 500 ml. cyclohexane. The reaction mixture was stirred at 450 RPMs and heated to 65 °C with a heating mantle. The heat source was removed. 3-(*t*-butyldimethylsilyloxy)-1-chloropropane, 139.56 grams of 90% assay (0.602 moles, 1.00 equivalent) was added dropwise via the addition funnel. An exotherm was detected after 12% of the halide feed had been added. A dry ice/hexane cooling bath was applied as necessary to maintain the reaction temperature at 60–65 °C. The total halide feed time was 112 minutes. The reaction temperature fell off rapidly to room temperature at the end of the halide feed. The reaction mixture was stirred for one hour at 450 RPMs and one hour at 300 RPMs, then transferred with argon pressure to a dry sintered glass filter. The lithium chloride muds were reslurried with fresh cyclohexane (2 X 75 ml.). The filtrate was a clear, orange solution, yield = 750 ml., 591.7 grams. Total base = 17.7 wt. %. Active C–Li = 17.1 wt. %. Yield = 93.3 % (based on active analysis). Chloride = 55 ppm.

REFERENCES

1. For a recent review, see *Telechelic Polymers: Synthesis and Applications*; Goethals, E. J., Ed.; CRC Press: Boca Raton, FL, 1989.
2. Quirk R. P.; Jang, S. H.; Kim, J. *Rubber Chem. Technol.* **1996**, *69*, 444.
3. Hsieh, H. L.; Quirk, R. P. *Anionic Polymerization: Principles and Practical Applications*; Marcel Dekker: New York, NY, 1996.
4. Schulz, D. N.; Halasa, A. F.; Oberster, A. E. *J. Polym.Sci., Polym. Chem. Ed.* **1974**, *12*, 153.

5. Wakefield, B. J. *Organolithium Methods*; Academic Press: New York, NY, 1988, pp. 3–8; Wakefield, B. J. *The Chemistry of Organolithium Compounds*; Pergamon Press: Oxford, 1974, pp. 198–203; Bartlett, P. D.; Friedman, S.; Stiles, M. *J. Amer. Chem. Soc.* **1953**, *75*, 1771; Gilman, H.; Haubein, A. H.; Hartzfeld, H. *J. Org. Chem.* **1954**, *19*, 1034; Seyferth, D.; Cohen, H. M. *J. Organometal. Chem.* **1963**, *1*, 15; Gilman, H.; Gaj, B. J. *J. Org. Chem.* **1957**, *22*, 1165; Gilman, H.; McNinch, H. A. *J. Org. Chem.* **1962**, *27*, 1889.
6. (a) Shepherd, N.; M. J. Stewart, (to Secretary of State for Defense in U.K.), UK Patent Application 2,241,239, (August 28, 1991); (b) Shepherd, N.; Stewart, M. J. (to Secretary of State for Defense in U.K.), US 5,331,058 (July 19, 1994); (c) Shepherd, N.; Stewart, M. J. (to Secretary of State for Defense in U.K.), U.S. 5,362,699 (November 8, 1994); (d) Shepherd, N.; Stewart, M. J. (to Secretary of State for Defense in U.K.), U.S. 5,665,829 (September 9, 1997).
7. For example, see Marvel, C. S.; Calvery, H. O. *Org. Syntheses Coll. Vol. I* **1932**, 533 and Campbell, K. N.; Sommers, A. H. *Org. Syntheses Coll. Vol. III* **1955**, 446.
8. Starr, D.; Hixon, R. M. *Org. Syntheses Coll. Vol. II* **1943**, 571.
9. Corey, E. J.; Venkateswarlu, A. *J. Amer. Chem. Soc.* **1972**, *94*, 6190.
10. Greene, T. W.; Wuts, P. G. M. *Protective Groups in Organic Synthesis*, 2nd. Ed., John Wiley & Sons: New York, NY, 1991, pp. 77–80.
11. Schwindeman, J. A. (to FMC Corporation) U. S. 5,493,044 (February 20, 1996).
12. Schwindeman, J. A.; Morrison, R. C.; Dover, B. T.; Engel, J. F.; Kamienski, C. W.; Hall, R. W.; Sutton, D. E. (to FMC Corporation) U. S. 5,332,533 (July 26, 1994).
13. Schwindeman, J. A. (to FMC Corporation) U. S. 5,321,148 (June 14, 1994).
14. Watson, S. C.; Eastham, J. F. *J. Organometal. Chem.* **1967**, *9*, 165.
15. Department of Transportation regulations, 49 CFR 173, Appendix

Chapter 6

Anionic Synthesis of Hydroxyl-Functionalized Polymers Using Protected, Functionalized Alkylolithium and Isoprenyllithium Initiators

Roderic P. Quirk, Sung H. Jang, Kwansoo Han, Huimin Yang, Brad Rix, and Youngjoon Lee

Maurice Morton Institute of Polymer Science, University of Akron,
Akron, OH 44325-3909

Five experimental criteria have been described for the evaluation of protected, functionalized alkylolithium initiators for anionic polymerization. Several alkoxy- and *t*-butyldimethylsiloxy-protected, hydroxyl-functionalized initiators have been evaluated using these criteria for the polymerization of styrene, isoprene and butadiene. All of the initiators satisfied the criteria for diene polymerization, but inefficient initiation and broader molecular weight distributions were observed for styrene polymerization, especially in cyclohexane.

Major advances in the science and technology of polymers have resulted from the preparation and characterization of polymers with well-defined structures (1,2). Living polymerizations are particularly suited for the preparation of these "model" polymers since it is possible to vary and control important structural parameters such as molecular weight, molecular weight distribution, copolymer composition and microstructure, tacticity and chain-end functionality (3,4). Although polymer chain-end groups are often difficult to detect using conventional analytical methods and historically were erroneously believed to be absent in natural polymeric materials (5a), the importance of functional chain-end groups has been demonstrated via useful applications of their chemistry such as ionic association, chain extension, branching or crosslinking with polyfunctional reagents, coupling and linking with reactive groups on other oligomer or polymer chains, and initiation of polymerization of other monomers (6-8).

The methodology of living anionic polymerization, especially alkylolithium-initiated polymerization, is very useful for the preparation of chain-end functionalized polymers with well-defined structures (9,10). Since these living polymerizations generate stable, anionic polymer chain ends ($P^-\text{Li}^+$) when all of the monomer has been consumed, post-polymerization reactions with a variety of electrophilic species can be used to generate a diverse array of chain-end functional groups as shown in eq. 1,



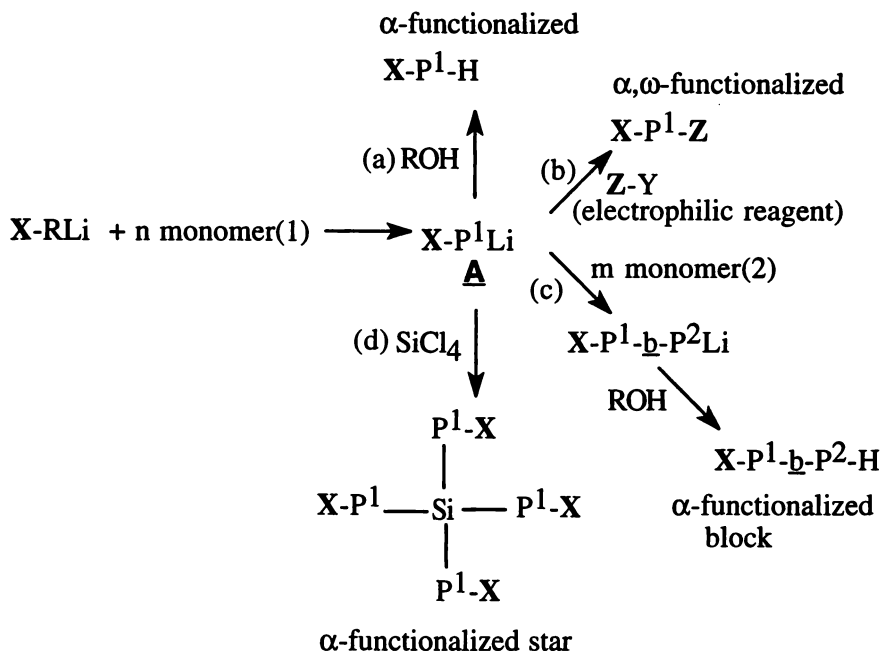
where X-Y is an electrophilic functionalizing agent which introduces functional group X at the terminal (ω) chain end (9,10). The literature is replete with tabular and text descriptions of numerous functionalization reactions of this type with a variety of electrophilic species (2,11-14). Unfortunately, many of these functionalization reactions fail the test of careful scrutiny with respect to optimization of procedures, as well as characterization and purity of the functionalized polymers (10,15). In fact, careful, systematic investigations of several of these post-polymerization functionalization reactions of polymeric carbanions have shown that the functionalization efficiency is often sensitive to the nature of the carbanionic chain end, the mode of addition of reagents, the stoichiometry, the presence or absence of Lewis bases and alkali metal salts, and even the temperature.

Functionalized Alkylolithium Initiators.

An alternative method for the preparation of chain-end functionalized polymers is to use alkylolithium initiators which contain the desired functional groups as shown in Scheme 1, where P represents a polymer chain and -X, -Z are functional end groups (16-18). Because most functional groups of interest (e.g., hydroxyl, carboxyl, amino) are not stable in the presence of either simple or polymeric organolithium reagents, it is generally necessary to use suitable protecting groups in the initiator (19-22). A suitable protecting group is one that is not only stable to the anionic chain ends but is also readily removed upon completion of the polymerization to generate the desired functional group.

There are several unique advantages of using functionalized alkylolithium initiators to prepare chain-end functionalized polymers (16). For living alkylolithium-initiated polymerization, each functionalized initiator molecule will produce one macromolecule with a functional group from the initiator residue at the initiating (α) chain end and with the active carbanionic propagating species at the terminal (ω) chain end (see **A** in Scheme 1) regardless of molecular weight. Advantages relative to functionalization by electrophilic termination are that it is not necessary to be concerned about efficient and rapid mixing of reagents with viscous polymers or with the stability of the chain end that is of concern at the elevated temperature polymerization conditions often employed (9). This methodology of producing α -functionalized living polymers which retain the carbanionic chain end provides the added advantage of the ability to prepare telechelic (α,ω -functionalized) polymers [see (b) in Scheme 1], functionalized block copolymers [see (c) in Scheme 1] and star-branched polymers with functional groups at the initiating ends of each branch [see (d) in Scheme 1] (16).

In this paper, several experimental criteria are enunciated for evaluation of the usefulness of protected, functionalized initiators. Four commercially available organolithium initiators with protected hydroxyl-functional groups are evaluated with respect to these criteria for polymerization of styrene and diene monomers.



Scheme 1. Polymer synthesis with functionalized initiators.

Initiator Criteria.

Several criteria must be satisfied for a functionalized alkyl lithium initiator to be generally useful for preparation of well-defined, α -functionalized polymers:

1. The functionalized alkyl lithium initiator must be soluble in hydrocarbon media. If this criterion is not met, then it will not be possible to prepare polydienes with high 1,4-microstructure (9,23-25).

2. The initiator must efficiently initiate chain-growth polymerization such that all of the initiator is consumed before monomer consumption is complete. Initiator efficiency is essential to prepare polymers with controlled molecular weight. If the initiator is efficient, then the observed number average molecular weight will be in agreement with the value calculated based on the stoichiometry of the polymerization as shown in eq. 2 (3,9).

$$M_n = \frac{\text{g of monomer polymerized}}{\text{moles of RLi initiator}} \quad (2)$$

3. The rate of initiation should be competitive with or faster than the rate of propagation ($R_i \geq R_p$). As delineated by Flory (5b,26), it is possible to obtain a Poisson-like, narrow molecular weight distribution ($M_w/M_n \leq 1.1$), if all of the chains are initiated at approximately the same time and grow for approximately the same time

(no termination and no irreversible chain transfer). Under these conditions the molecular weight distribution will obey the following relationship (eq. 3), where X_w is the weight average degree of polymerization and X_n is the number average degree of

$$X_w/X_n = 1 + \frac{X_n}{(X_n-1)^2} \quad (3)$$

polymerization. When the number average molecular weight is large relative to one ($X_n \gg 1$), eq. 3 reduces to eq. 4.

$$X_w/X_n = 1 + \frac{1}{X_n} \quad (4)$$

4. The functional group or its protected analog should be stable to the anionic polymerization conditions. This insures that the polymerization will remain living using this initiator and that the functional group or its protected analog will survive the polymerization intact.

5. The protected functional group can be easily removed after completion of the polymerization. The utility of a protecting group depends on the facility with which it can be removed to regenerate the desired functional group at the chain end.

Experimental Section

Materials. Cyclohexane, benzene, tetrahydrofuran, ethylene oxide, styrene, isoprene and 1,3-butadiene were purified as described previously (27-30). Protected hydroxyl-functionalized initiators (see Scheme 2) (FMC, Lithium Div.) were used without further purification after double titration analyses (31). All chemicals for deprotection were used as received.

Polymerizations and deprotection. Anionic polymerization of styrene, 1,3-butadiene and isoprene in cyclohexane or benzene with functionalized initiators was carried out at room temperature for 12-24 h in all-glass, sealed reactors using breakseals and standard high-vacuum techniques (32). After polymerization and prior to further functionalization reactions, aliquots of polymeric organolithium compounds were isolated in attached ampoules and terminated with well-degassed methanol. Deprotection of the *t*-butyldimethylsiloxy group was effected by hydrolysis using one equivalent of 37 % aqueous hydrochloric acid (HCl) solution in tetrahydrofuran (THF). The reaction was allowed to continue for 1 h under reflux. After cooling to room temperature, the polymer was isolated by precipitation in methanol and dried under high vacuum. The deprotection reaction was monitored by thin layer chromatography (TLC). The removal of *t*-butoxy group was effected by the treatment of the *t*-butoxy-functionalized polybutadiene with the ion exchange resin (Amberlyst[®] H15, Aldrich) in cyclohexane. Polymer samples mixed with the same weighed amount of powdered Amberlyst[®] were heated in cyclohexane under reflux for 6 h; then the Amberlyst[®] powder was removed by filtration and recycled. The filtered solution

was dried under reduced pressure to remove the solvent and the isolated polymer was dried under high vacuum.

Characterization. Molecular weights and molecular weight distributions of polymer samples were determined using a Waters GPC with a differential refractometer detector at a flow rate of 0.4 mL min^{-1} in THF at $30 \text{ }^\circ\text{C}$ after calibration with standard samples [American Polymer Standards Corp.(PBD) and Polymer Laboratories (PS and PI)]. $^1\text{H-NMR}$ (CDCl_3) and $^{13}\text{C-NMR}$ (CDCl_3) spectra were recorded on a Gemini-2000 spectrometer. The concentration of hydroxyl chain ends in functionalized polybutadienes was determined as described in ASTM E222-94 using acetic anhydride in pyridine (33). Thin layer chromatography (TLC) analysis was carried out on silica gel coated glass plates using toluene/cyclohexane (1/1, vol/vol) as eluent.

DISCUSSION

In the following sections, several protected hydroxyl-functionalized alkyl lithium initiators are evaluated in terms of the criteria described for evaluation of functionalized initiators. The structures of the initiators and a short-hand formula description for each are shown in Scheme 2.

Criterion 1. Initiator solubility. One of the limitations of previously described protected initiators was that they were not soluble in aromatic and aliphatic hydrocarbon media (17,24,25), a requisite for the synthesis of polydienes with high 1,4-microstructure (23). Therefore, it was necessary to prepare and use the initiators in the presence of either polar (ethereal) solvents or Lewis base additives (17,24,25). All of the initiators described herein were soluble in hydrocarbon media such as cyclohexane or toluene. The concentrations and solvents are listed in parenthesis after the abbreviations for each initiator shown in Scheme 2. In order to further promote solubility and to obtain higher concentrations of active initiators, samples of alkoxy-functionalized initiators which had been chain-extended with an average of two moles of isoprene monomer per initiator (see A, B in Scheme 2) were also investigated. It is also important to note that using these initiators, polybutadienes with high 1,4-microstructure are obtained as shown in Figure 1. Thus, using the *t*-butyldimethylsiloxy-functionalized initiator, C, a polybutadiene with 90 % 1,4-microstructure is obtained as determined by peak integration (34,35). This ability to obtain polydienes with high 1,4-microstructure is the result of using a hydrocarbon-soluble alkyl lithium initiator and is an important requisite for a useful initiator for elastomer synthesis (9,16,18).

Criterion 2. Initiator Efficiency. (a) Styrene polymerization. The results for polymerization of styrene are listed in Table 1. The initiator efficiency has been evaluated by comparison of the calculated number average molecular weight (M_n) based on the stoichiometry of the polymerization after complete conversion (see eq. 2) with the observed M_n determined by SEC after calibration with polystyrene standards. The initiator efficiencies for the protected hydroxyl initiators (Samples 8-11, Table 1) were high in the aromatic solvent, benzene. It would be expected that

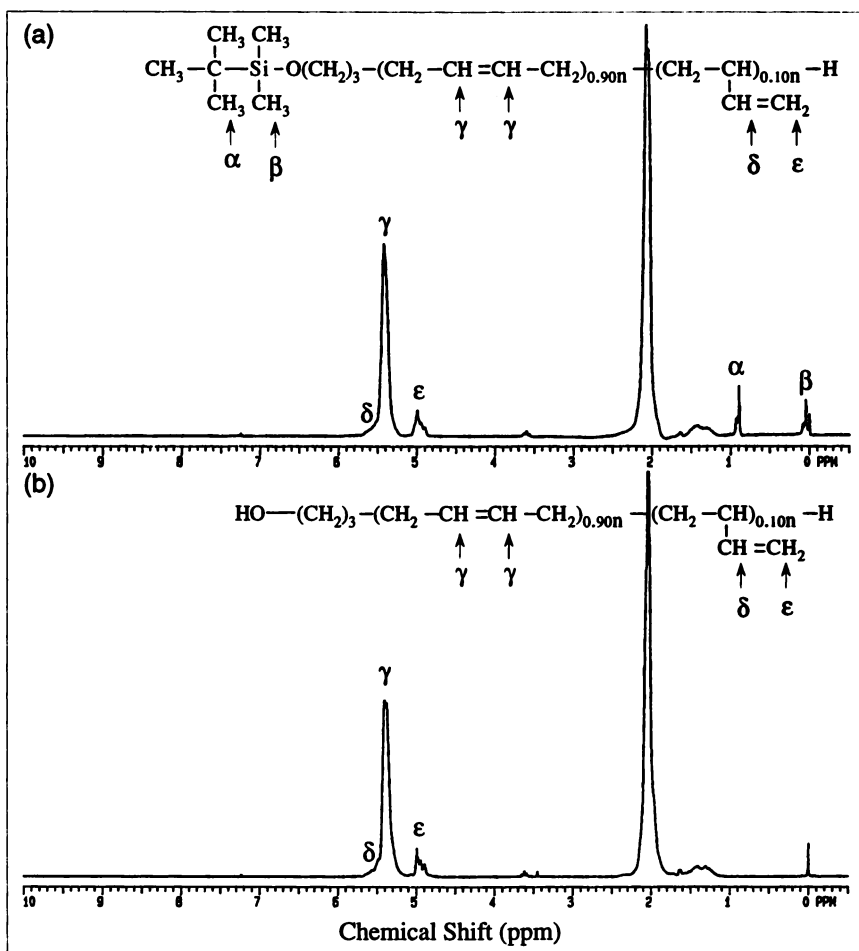


Figure 1. (a) ^1H NMR spectrum of polybutadiene (Sample 1, Table 2) prepared using the *t*-butyldimethylsilyloxypropyllithium initiator (C, Scheme 2). (b) ^1H NMR spectrum of polybutadiene (Sample 1, Table 2) after removal of the *t*-butyldimethylsilyloxy protecting group.

Table 1. Data for polymerization of styrene using protected hydroxyl-functionalized organolithium initiators at 25°C compared with *sec*-butyllithium.

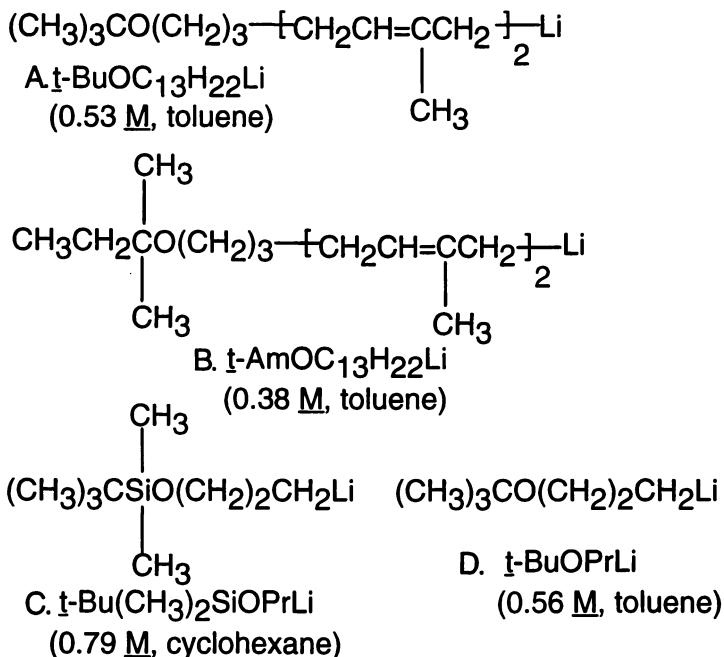
Run	Initiator ^a	Solvent	M _n (g/mol)		M _w /M _n ^c
			calc ^b	obs ^c	
1	<i>sec</i> -C ₄ H ₉ Li	C ₆ H ₁₂	1,500	1,400	1.09
2	<i>sec</i> -C ₄ H ₉ Li	C ₆ H ₁₂	4,000	3,500	1.06
3	<i>t</i> -BuOPrLi	C ₆ H ₁₂	4,000	6,000	1.25
4	<i>t</i> -BuOPrLi	C ₆ H ₁₂	20,000	32,500	1.47
5	<i>t</i> -BuOPrLi ^d	C ₆ H ₁₂	6,000	12,500	1.20
6	<i>t</i> -BuOC ₁₃ H ₂₂ Li	C ₆ H ₁₂	4,000	8,000	1.27
7	<i>t</i> -Bu(CH ₃) ₂ SiOPrLi	C ₆ H ₁₂	7,300	7,200	1.42
8	<i>t</i> -BuOPrLi	C ₆ H ₆	7,000	6,900	1.08
9	<i>t</i> -BuOC ₁₃ H ₂₂ Li	C ₆ H ₆	4,000	4,100	1.17
10	<i>t</i> -AmOC ₁₃ H ₂₂ Li	C ₆ H ₆	3,000	3,100	1.18
11	<i>t</i> -AmOC ₁₃ H ₂₂ Li	C ₆ H ₆	7,000	7,200	1.14
12	<i>t</i> -AmOC ₁₃ H ₂₂ Li	C ₆ H ₆ /THF (95/5;vol/vol)	3,000	3,250	1.05

^aSee Scheme 2 for structures of initiators.

^bBased on g of styrene/moles RLi (see eq 2).

^cMeasured by SEC using polystyrene standards (Polymer Laboratories).

^dInitiation at 58°C for 1 h, followed by 25°C for 12 h.



Scheme 2. Structures, concentrations and solvents for protected, hydroxyl-functionalized organolithium initiators.

analogous results would be obtained for other aromatic solvents such as toluene, ethylbenzene or *t*-butylbenzene. However, the data in Table 1 indicate that the initiator efficiencies for the *t*-butoxy-based initiators in cyclohexane were much less than 100% [as judged by the lack of correspondence between $M_n(\text{calc})$ and $M_n(\text{obs})$] for samples 3-6, i.e. the $M_n(\text{obs})$ results were much higher than the corresponding calculated molecular weights. This result suggests that not all of the initiator molecules were initiating polymer chains in this solvent at room temperature. This effect presumably results from cross-association of the initiator with the growing poly(styryl)lithium chains which renders the residual initiator unreactive. Analogous observations have been reported by Morton and Fetters (32) for the system *t*-butyllithium/styrene in cyclohexane. Even when initiation proceeded at 58 °C for one hour and then at 25°C for 12 hours, the initiator efficiency was low (see Sample 5, Table 1). When THF (5 vol %) was added to the resulting living polymer solution followed by addition of more styrene monomer, a bimodal molecular weight distribution product mixture was obtained (see Figure 2) which is consistent with the presence of residual unreacted initiator after the complete polymerization of the first batch of monomer. The subtle effects of molecular structure on initiator efficiency are indicated by the observation that the *t*-butyldimethylsiloxy-protected initiator (C, Scheme 2) is an efficient initiator even in cyclohexane at room temperature (see Sample 7, Table 1) in contrast to the *t*-butoxy analog (see Samples 3-5, Table 1). It is

anticipated that initiator efficiency for the *t*-butoxy-substituted alkyllithium initiators would be acceptable by effecting initiation at elevated temperatures and/or by using polar promoters such as weak Lewis bases (e.g. Et₃N) or alkali metal salts (e.g. LiOR or KOR).

(b) Diene polymerization. The results for polymerization of butadiene and isoprene in cyclohexane are listed in Table 2 and Table 3, respectively. In contrast to the results for the polymerization of styrene in cyclohexane using these protected initiators, the initiator efficiencies are high for diene polymerizations in cyclohexane at room temperature. Within experimental error (SEC), the observed M_n determined by SEC is in good agreement with the calculated number average molecular weight based on the stoichiometry of the polymerization (see eq. 2). Furthermore, this agreement spans the molecular weight range from 2,000 g/mol to 43,000 g/mol. The ability to obtain high initiator efficiencies even at low molecular weights (2,000-3,000 g/mol) indicates that these are indeed very efficient and useful initiators for diene polymerization in cyclohexane at room temperature.

Criterion 3. Rate of initiation relative to propagation. (a) Styrene

polymerization. In order to obtain narrow molecular weight distribution polymers, the initiator should be sufficiently reactive such that the rate of initiation is competitive with propagation (3,36). For less reactive initiators, Hsieh and McKinney (37) have shown that rather broad molecular weight distributions are obtained even for relatively high molecular weight polymers. As shown by eqs 3,4, a strict test of initiator reactivity can be obtained by determining the ability of the initiator to prepare low molecular weight polymers, i.e. $M_n < 5,000$ g/mol, with narrow molecular weight distributions ($M_w/M_n \leq 1.1$), since it is predicted that the molecular weight distribution will become narrower with increasing molecular weight (5b,26). The data in Table 1 indicate that the protected hydroxyl-functionalized initiators are generally not sufficiently reactive to produce narrow molecular weight distribution polystyrenes at low molecular weights ($M_n < 5,000$ g/mol). However, at higher molecular weights in aromatic solvents (Table 1, Sample 8), or in the presence of added Lewis base, THF (Table 1, Sample 12), narrow molecular weight distribution polymers can be prepared.

(b) Diene polymerization. Narrow molecular weight distribution polymers are obtained for both butadiene (Table 2) and isoprene (Table 3) using all of the protected hydroxyl-functionalized initiators in cyclohexane at 25°C. The SEC curve for Sample 1 in Table 2 is shown in Figure 3. Although the distribution exhibits some asymmetry toward the low molecular weight side, the overall distribution is still narrow ($M_w/M_n = 1.07$). It is important to note that narrow molecular weight distributions are obtained even with calculated molecular weights as low as 2,000-3,000 g/mol (Sample 2 in Table 2; Sample 3 in Table 3). These results attest again to the efficiency, reactivity and usefulness of these initiators for the polymerization of diene monomers to prepare the corresponding α -functionalized polymers.

Criterion 4. Protected functional group is stable with respect to anionic

polymerization conditions. The stability of the alkoxy and *t*-butyldimethylsiloxy protecting groups was directly determined by ¹H NMR analysis. For example, the

Table 2. Data for polymerization of butadiene using protected hydroxyl-functionalized organolithium initiators at 25°C in cyclohexane.

Run	Initiator ^a	M _n (g/mol)		M _w /M _n ^c	% 1,4-enchainment
		calc ^b	obs ^c		
1	<i>t</i> -Bu(CH ₃) ₂ SiOPrLi	4,000	3,700	1.07	90
2	<i>t</i> -Bu(CH ₃) ₂ SiOPrLi	2,000	2,280	1.08	86
3	<i>t</i> -BuOC ₁₃ H ₂₂ Li	4,000	4,400	1.09	81
4	<i>t</i> -BuOC ₁₃ H ₂₂ Li	20,000	20,200	1.07	90
5	<i>t</i> -AmOC ₁₃ H ₂₂ Li	4,000	4,600	1.07	82

^aSee Scheme 2 for structures of initiators.

^bBased on g of butadiene/moles RLi (see eq 2).

^cMeasured by SEC using polybutadiene standards (American Polymer Standards Corp.).

Table 3. Data for polymerization of isoprene using protected hydroxyl-functionalized organolithium initiators at 25°C in cyclohexane.

Run	Initiator ^a	M _n (g/mol)		M _w /M _n ^c	% 1,4-enchainment
		calc ^b	obs ^c		
1	<i>t</i> -BuOC ₁₃ H ₂₂ Li	7,000	6,910	1.08	90
2	<i>t</i> -AmOC ₁₃ H ₂₂ Li	7,000	7,420	1.07	91
3	<i>t</i> -AmOC ₁₃ H ₂₂ Li	3,000	3,150	1.06	87
4	<i>t</i> -Bu(CH ₃) ₂ SiOPrLi	40,000	43,000	1.07	93

^aSee Scheme 2 for structures of initiators.

^bBased on g of isoprene/moles RLi (see eq 2).

^cMeasured by SEC using polyisoprene standards (Polymer Laboratories).

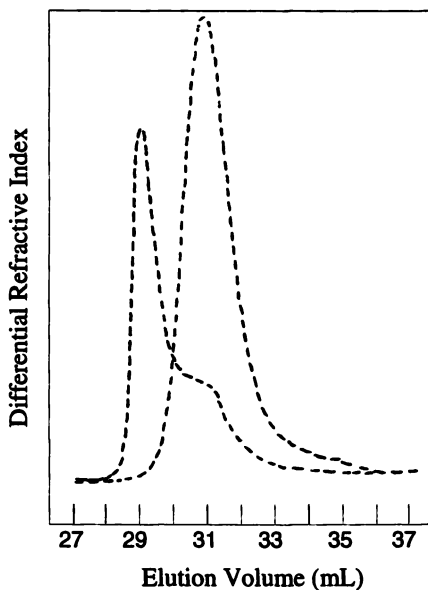


Figure 2. SEC chromatogram of base polystyrene and product of reinitiation after addition of 5 vol % THF and more styrene monomer.

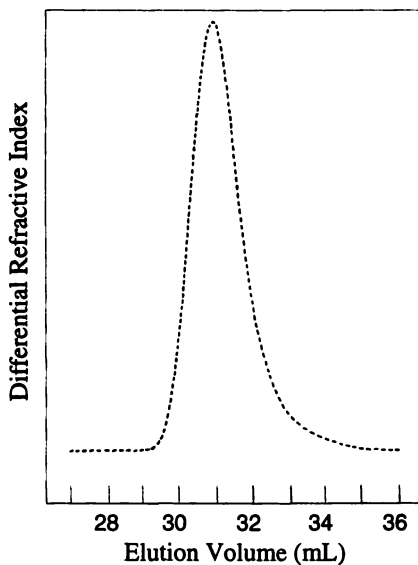


Figure 3. Size exclusion chromatogram of polybutadiene (Sample 1, Table 2) prepared using the *t*-butyldimethylsiloxypropyllithium initiator (C, Scheme 2).

^1H NMR spectrum of the polybutadiene sample 1 in Table 2 is shown in Figure 1 (a). The resonances for $-\text{Si}(\text{CH}_3)_2\text{C}(\text{CH}_3)_3$ and $-\text{Si}(\text{CH}_3)_2\text{C}(\text{CH}_3)_3$ protons are clearly observed at δ 0.05 and 0.90 ppm, respectively. Similarly, for the *t*-butoxy-functional initiators (A, D, Scheme 2), a clean ^1H NMR resonance is observed for the $(\text{CH}_3)_3\text{CO}-$ protons at δ 1.17 ppm. Somewhat indirect evidence for the retention of the protected functional group is the observation that when the living polymers, prepared using the protected hydroxyl-functionalized initiators, are terminated with methanol and then isolated by precipitation into methanol, TLC analysis of the polymers on silica gel plates using hydrocarbon solvents as eluents, the spot corresponding to the polymer moves with the solvent front. This is the same type of elution behavior which is observed for the unfunctionalized polymers. In contrast, after deprotection and removal of the protecting group, the resulting hydroxyl-functionalized polymers exhibit very low R_f values.

Criterion 5. Protected functional group can be easily removed after completion of the polymerization. If all of the first four criteria are satisfied for a given functional initiator, but the protecting group cannot be easily removed after the polymerization has been completed, then the initiator will not be generally useful. The *t*-butyldimethylsiloxy-functional group is readily removed using a variety of reagents. For example, in the seminal patents of Shepherd and Stewart (38), this functional group was easily removed by stirring the α -*t*-butyldimethylsiloxy-functionalized polybutadienes in tetrahydrofuran at room temperature with tetra(*n*-butyl)ammonium fluoride for 2 hours. Handlin, Benning and Willis (39) removed this siloxy protecting group by treatment of a cyclohexane solution of the polymer with methanesulfonic acid in isopropanol with a small amount of water. As described herein, the *t*-butyldimethylsiloxy-functional group can also be removed by stirring a THF solution of the polymer with one equivalent of aqueous HCl and heating under reflux for 1 hour. The protecting group was completely removed after this relatively mild procedure as shown by the ^1H NMR of the resulting polymer in Figure 1(b). The functionality of the resulting α -hydroxyl-functionalized polybutadiene was 1.0 as determined by end-group titration (33).

The *t*-alkoxy protecting group was observed to be more stable to mild acid hydrolysis conditions than the *t*-butyldimethylsiloxy-protecting group. This protecting group was removed by heating the polymer with Amberlyst[®] acid ion exchange resin in cyclohexane under reflux for 6 h. The functionality of the resulting α -hydroxyl-functionalized polybutadiene was 1.0 as determined by end-group titration (33).

Conclusions

The usefulness of *t*-alkoxy- and *t*-butyldimethylsiloxy-functionalized alkylolithium initiators for anionic polymerization have been evaluated using five experimental criteria. All of these criteria must be satisfied for an initiator to be generally useful. These protected hydroxyl-functionalized initiators are all useful for the polymerization of butadiene and styrene monomers. Inefficient initiation of styrene polymerization was observed in cyclohexane, but not in benzene.

Acknowledgements

The authors are grateful to FMC, Lithium Division, for support of this research and for providing samples of functionalized initiators and sec-butyllithium.

References

1. L. J. Fetters and E. L. Thomas in *Material Science & Technology*, Vol. 12, VCH Verlagsgesellschaft, Weinheim, Germany, 1993, p 1.
2. P. Rempp, E. Franta and J.-E. Herz, *Adv. Polym. Sci.*, **86**, 145(1988).
3. R. P. Quirk and B. Lee, *Polym. Int.*, **27**, 359(1992).
4. O. W. Webster, *Science*, **251**, 887(1991).
5. P. J. Flory, *Principles of Polymer Chemistry*, Cornell University Press, Ithaca, New York, 1953, (a) p 4-11; (b) p 338.
6. A. Akelah and A. Moet, *Functionalized Polymers and Their Applications*, Chapman and Hall, New York, 1990.
7. *Telechelic Polymers: Synthesis and Applications*, E. J. Goethals, Ed., CRC Press, Boca Raton, Florida, 1989.
8. R. Jerome, M. Henriouille-Granville, B. Boutevin and J. J. Robin, *Prog. Polym. Sci.*, **16**, 837(1991).
9. H. L. Hsieh and R. P. Quirk, *Anionic Polymerization: Principles and Practical Applications*, Marcel Dekker, New York, 1996.
10. R. P. Quirk in *Comprehensive Polymer Science*, First Supplement, S. L. Aggarwal and S. Russo, Eds., Pergamon Press, Elmsford, New York, 1992, p. 83.
11. M. Morton, *Anionic Polymerization: Principles and Practice*, Academic Press, New York, 1983.
12. L. J. Fetters, *J. Polym. Sci., Polym. Symp.*, **26**, 1(1969).
13. M. Morton and L. J. Fetters, *J. Polym. Sci. Macromol. Rev.*, **2**, 71(1967).
14. S. Bywater, *Prog. Polym. Sci.*, **4**, 27(1974).
15. R. N. Young, R. P. Quirk and L. J. Fetters, *Adv. Polym. Sci.*, **56**, 1(1984).
16. R. P. Quirk, S. H. Jang and J. Kim, *Rubber Chem. Tech., Rubber Rev.*, **69**, 444(1996).
17. D. N. Schulz, J. C. Sanda and B. G. Willoughby in *Anionic Polymerization: Kinetics, Mechanisms and Synthesis*, J. E. McGrath, Ed., *ACS Symposium Series*, **166**, 427(1981).
18. R. P. Quirk and V. M. Monroy in *Kirk-Othmer Encyclopedia of Chemical Technology*, 4th ed., J. I. Kroschwitz, Ed., Wiley, New York, 1995, Vol. 14, p. 461-475.
19. D. N. Schulz, S. Datta and R. M. Waymouth, *Polym. Mater., Sci. Eng.*, **76**, 3(1997).
20. A. Hirao and S. Nakahama, *Prog. Polym. Sci.*, **17**, 283(1992)
21. S. Nakahama and A. Hirao, *Prog. Polym. Sci.*, **15**, 299(1990).
22. T. W. Greene and P. G. M. Wuts, *Protective Groups in Organic Synthesis*, 2nd ed., Wiley-Interscience, New York, 1991.

23. S. Bywater in *Comprehensive Polymer Science, Vol. 3. Chain Polymerization I*, G. C. Eastmond, A. Ledwith, S. Russo and P. Sigwalt, Eds., Pergamon Press, New York, 1989, p. 433.
24. D. N. Schulz, A. F. Halasa and A. E. Oberster, *J. Polym. Sci., Polym. Chem. Ed.*, **12**, 153(1974).
25. D. N. Schulz and A. F. Halasa, *J. Polym. Sci., Polym. Chem. Ed.*, **15**, 2401(1977).
26. P. J. Flory, *J. Am. Chem. Soc.*, **62**, 1561(1940).
27. R. P. Quirk and J.-J. Ma, *Polym. Int.*, **24**, 197(1991).
28. R. P. Quirk and J. Yin, *J. Polym. Sci., Polym. Chem. Ed.*, **30**, 2349(1992).
29. R. P. Quirk and J.-J. Ma, *J. Polym. Sci., Polym. Chem. Ed.*, **26**, 2031(1988).
30. R. P. Quirk and M. Alsamarraie, *Ind. Eng. Chem., Prod. Res. Dev.*, **25**, 381(1986).
31. H. Gilman and F. K. Cartledge, *J. Organomet. Chem.*, **2**, 447(1964).
32. M. Morton and L. J. Fetters, *Rubber Chem. Tech.*, **48**, 359(1975).
33. "Standard Test Methods for Hydroxyl Groups Using Acetic Anhydride Acetylation", *ASTM Standard E222-94*, **1995**, 15.05, 288.
34. J. A. Frankland, H. G. M. Edwards, A. F. Johnson, I. R. Lewis and S. Poshyachinda, *Spectrochim. Acta*, **47A**(11), 1511(1991).
35. H. Sato and Y. Tanaka, *J. Polym. Sci., Polym. Chem. Ed.*, **17**, 3551(1979).
36. J. F. Henderson and M. Szwarc, *J. Polym. Sci., Macromol. Rev.*, **3**, 317(1968).
37. H. L. Hsieh and O. F. McKinney, *Polym. Lett.*, **4**, 843(1966).
38. N. Shepherd and M. J. Stewart (to Secretary of State for Defense in U. K.), U. S. 5,331,058 (July 19, 1994); U.S. 5,362,699 (November 8, 1994).
39. D. L. Handlin, Jr., R. C. Bening and C. L. Willis (to Shell Oil Company), U.S. 5,376,745 (December 27, 1994).

Anionic Synthesis of Macromonomer Carrying Amino Group Using Diphenylethylene Derivative

Jungahn Kim¹, Jae Cheol Cho¹, Keon Hyeong Kim¹, Kwang Ung Kim¹,
Won Ho Jo², and Roderic P. Quirk³

¹Division of Polymer, Korea Institute of Science and Technology, Seoul, Korea
²Department of Fiber and Polymer Science, Seoul National University, Seoul Korea
³The Maurice Morton Institute of Polymer Science, University of Akron,
Akron, OH 44325-3909

Anionic synthesis of macromonomer of 1,1-diphenylethylene-type unit carrying amino group has been performed in a variety of solvents. The product was characterized by a combination of ¹H NMR spectroscopic and size exclusion chromatographic analysis. Based on the UV/Visible spectroscopic analysis, the crossover reaction of *n*-butyllithium (*n*-BuLi) with 1-[4-bis(trimethylsilyl)amino]phenyl]-1-phenylethylene was found to be so slow in benzene, but it was completed in the benzene/THF mixture within 2 h. The synthesis of macromonomer of the 1,1-diphenylethylene-type unit (over 95 %) carrying amine-functional group (maximum 94 %) was successful on the basis of ¹H NMR spectroscopic analysis.

Macromolecular monomers have received a great attention in many fields since the synthetic methodology of the Macromer[®] has been reported in the patent (1) and other literature (2-4). Macromonomer can be defined as polymeric or oligomeric materials carrying some polymerizable functional group at one chain end or at both chain ends (4-6). As a consequence, graft copolymers or network polymers can be produced by post-polymerization or reaction with other reagents (2,3,7). Morphology and physical properties of the graft copolymers are usually dependent of their structural compositions. Thus, the choice of the molecular weights of macromonomers should be carefully considered for the optimization of physical properties of polymers synthesized from a post-reaction using macromonomers. In this respect, the molecular weights of macromonomers should be chosen in the range of 5×10^2 to 2×10^4 g/mol for compromise between copolymerizability and physical property (6).

Macromonomer can be synthesized by a variety of mechanistic reaction types such as free radical transfer (8), anionic polymerization (2,9), cationic polymerization (10), and step-growth polymerization (11). Anionic polymerization provides the best methodology to synthesize a variety of terminally functionalized polymers with well-defined structure and narrow molecular weight distribution (12,13). In order to prepare macromonomers with non-homopolymerizable functional groups such as 1,1-diphenylethylene-type unit using double diphenylethylene derivatives, a new method has been suggested (14-16). It has been well-known that diphenylethylene derivatives as the terminating agents possess a great potential for the preparation of the aromatic functionalized polymers in anionic polymerization (17-19). Diphenylalkyllithium can reinitiate other vinyl monomers or dienes resulting in the formation of polymers with functional groups at the α -position of the polymer backbone (20). In this respect, macromonomers with functional group can be prepared by a combination of anionic polymerization using functional initiator and the chain-end functionalization method. Herein, we report the results for the preparation of new macromonomer carrying aromatic amine group.

Experimental Section

Chemicals. Styrene, benzene, and tetrahydrofuran (THF) were purified as described elsewhere (21). *n*-Butyllithium (*n*-BuLi) as initiator was used without further purification. 1,3-Bis(1-phenylethenyl)-benzene (MDDPE) was prepared using procedures analogous to those reported by Schulz and Hocker (22) and Tung, et al (23). The synthesis of 1-[4-[*N,N*-bis(trimethylsilyl)amino]phenyl]-1-phenylethylene (ADPE) was performed by following the same procedures as reported by Quirk and Lynch (17). 1-(4-Aminophenyl)-1-phenylethylene was first prepared in benzene by the reaction of 4-aminobenzophenone with phosphorus ylide formed by the reaction of methyltriphenylphosphonium iodide with methyl lithium, followed by protecting amine group using methyl lithium and chlorotrimethylsilane. 1-[4-[*N,N*-bis(trimethylsilyl)amino]phenyl]-1-phenylethylene (ADPE) was then purified by column chromatography and distillation under high vacuum, followed by making ampoule in a high vacuum line using a calibrated cylinder.

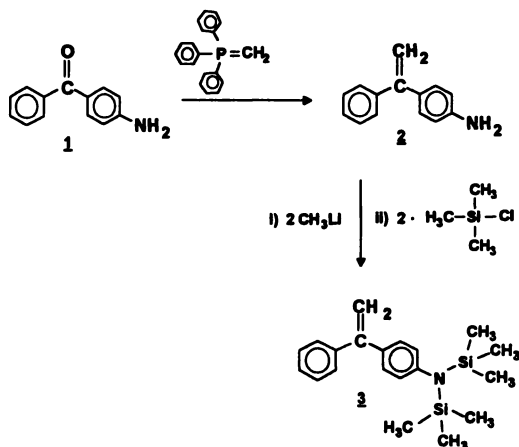
Synthesis of Amine-functionalized Macromonomer. All experiments were carried out in all-glass, sealed reactors using breakseals and standard high vacuum techniques at room temperature (21). Aromatic amine-functionalized initiator was first prepared by the reaction of *n*-butyllithium and ADPE in benzene or benzene/THF ([THF]/[*n*-BuLi] = 20/1, mol/mol). The completion of the reaction of *n*-BuLi with ADPE was determined by the UV/Visible spectroscopic analysis. The relative intensities of the UV/Visible absorption bands at specific wavelength were monitored by adding the initiator into the ADPE/benzene solution, for instance, at $\lambda_{\text{max}} = 455$ nm and 280 nm in benzene/THF mixture and at $\lambda_{\text{max}} = 422$ nm and 280 nm in pure benzene. Styrene was then added to the initiator-containing solution. Anionic polymerization of styrene was carried out at 25 °C for 8 h. An aliquot of the polymer solution was taken for the use as the base polymer, followed by reacting the remaining poly(styryl)lithium with MDDPE ([MDDPE]/[PLi] = 1.5) in benzene/THF mixture ([benzene]/[THF] = 75/25, vol/vol) at room temperature. These reactions were also monitored using the UV/Visible spectroscopic instrument for at least 12 h. The resulting living polymer was quenched with degassed methanol and precipitated several times into excess methanol to remove the unreacted excess MDDPE, followed by filtering and drying in vacuum oven at room temperature for at least 48 h.

Characterization. Size-exclusion chromatographic (SEC) analysis of polymers was performed at a flow rate of 1.0 mL/min in THF at 30 °C using a Waters HPLC component system equipped with five Ultra- μ -styrigel® columns (2 × 10⁵, 10⁴, 10³, 500 Å) after calibration with standard polystyrene samples. ¹H NMR spectra were obtained using a Varian Gemini-200 spectrometer with CDCl₃ as solvent. UV-Visible absorption spectra of the functionalized initiator, living polymer, and macromonomer were obtained using a Hewlett-Packard 8453 diode array spectrophotometer using 0.5 cm UV cell.

Results and Discussion

Synthesis of 1-[4-[*N,N*-bis(trimethylsilyl)amino]phenyl]-1-phenylethylene. 4-Aminobenzophenone is first converted to 1-(4-aminophenyl)-1-phenylethylene by the 'Wittig' reaction using phosphorus ylide. The diphenylethylene derivative still includes active hydrogens which act as reactive impurities in anionic polymerization. Chlorotrimethylsilane effects the protection of the primary amine group after treatment of 2 equivalent of methyl lithium (17). The whole reaction processes are shown in *Scheme 1*. The occurrence of a competitive reaction between the abstraction of the protons on the aromatic amine group and the crossover reaction with the ethylene-unit by methyl lithium in the second step reaction in *Scheme 1* is inevitable irrespectively of the reactivity of simple alkyl lithium showing a dependence on the dissociated state in the reaction medium (13). The pK_a values of the diphenylethylene-unit (estimation for diphenylmethane) and the aromatic amine (estimation for aniline) are 32.2 and 30.6, respectively (24). In our case the protection yield was about 60 mole %. It seems effective for dislylation of the amine using chlorotrimethylsilane in THF

Scheme 1



after the treatment of 1-(4-aminophenyl)-1-phenylethylene with methyl lithium because of its lower reactivity compared to *n*-butyllithium found to be an efficient substance for protecting the amine group of aniline using chlorotrimethylsilane (25). ¹H NMR spectra of the intermediate material (2) and the final product (3) purified are shown in Figure 1. Specifically, in Figure 1(a) the chemical shift at $\delta = 3.8$ ppm corresponds to the protons on the aromatic amine (Ph-NH₂) and the peak at $\delta = 5.4$ ppm is assigned to the protons on the methylene unit (CH₂ = CPh₂). As shown in Figure 1(b), the chemical shift at $\delta = 0.08$ ppm corresponds to the protons of trimethylsilyl group (-N-[Si(CH₃)₃]₂) adjacent to nitrogen atom. The integration of the chemical shifts allowed to confirm the successful synthesis of 1-[4-[N,N-bis(trimethylsilyl)amino]phenyl]-1-phenylethylene.

Synthesis of Macromonomer carrying Amine-functional Group. Macromonomer of 1,1-diphenylethylene-type unit carrying amine-functional group at the chain end can be prepared by following the reaction procedures as shown in Scheme 2. Diphenylalkyllithium with the silyl-protected amine group ([1]), as a functional anionic initiator, is first synthesized from the reaction of *n*-butyllithium with 1-[4-[N,N-bis(trimethylsilyl)amino]phenyl]-1-phenylethylene in benzene or benzene/THF solution ([THF]/[*n*-BuLi] = 20/1, mol/mol). Subsequently, polymerization of styrene at room temperature for at least 8 h allows to produce poly(styryl)lithium ([2]) with amine-functional group. Next, macromonomer of the 1,1-diphenylethylene-type unit ([3]) is produced by adding *meta*-substituted double diphenylethylene (MDDPE)/benzene solution into the poly(styryl)lithium solution in benzene/THF solution ([benzene]/[THF] = 75/25, vol/vol) within 2 h.

It has been well-known that 1,1-diphenylethylene is anionically non-homopolymerizable but copolymerizable with other vinyl monomers (26-28). In addition, it has been reported that the diadduct was negligibly small and monoadduct was exclusively obtained from observation through ¹H NMR and UV/Visible spectroscopic analysis from the reaction of poly(styryl)lithium and 1,4-bis(1-phenylethenyl)benzene (PDDPE) in hydrocarbon with polar additive (29). This indicates that the addition of polar additive suppresses the formation of diadduct even in benzene solution at room temperature.

As shown in Scheme 2, diphenylalkyllithium ([1]) formed from the reaction of ADPE with *n*-butyllithium revealed the absorption maximum at $\lambda_{\text{max}} = 455$ nm in benzene/THF mixture and at $\lambda_{\text{max}} = 422$ nm in pure benzene. Specifically, the cross-over reaction was finished in benzene/THF mixture within at least 2 h, which will be discussed in more detail later. The addition of styrene renders the absorption band at $\lambda_{\text{max}} = 455$ nm disappeared rapidly and simultaneously new absorption

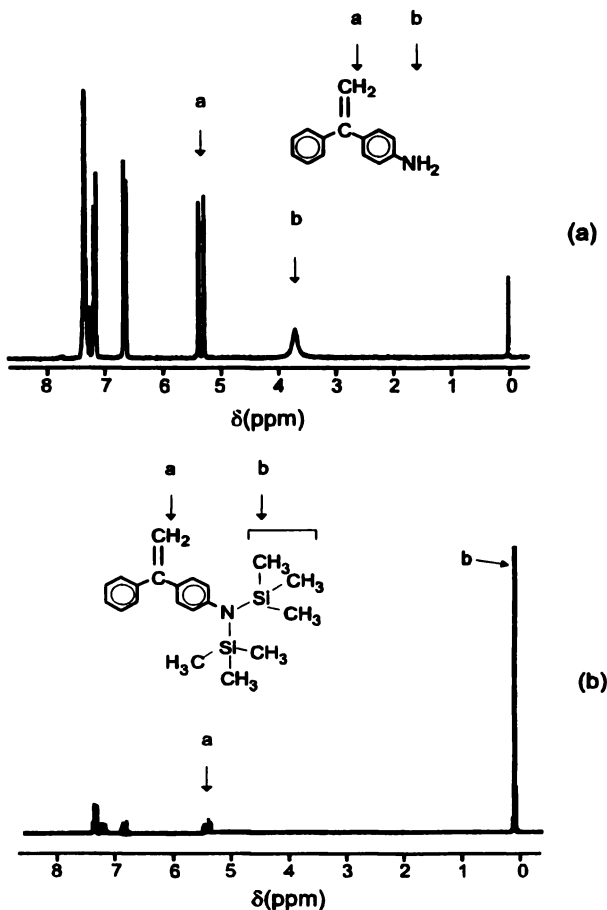
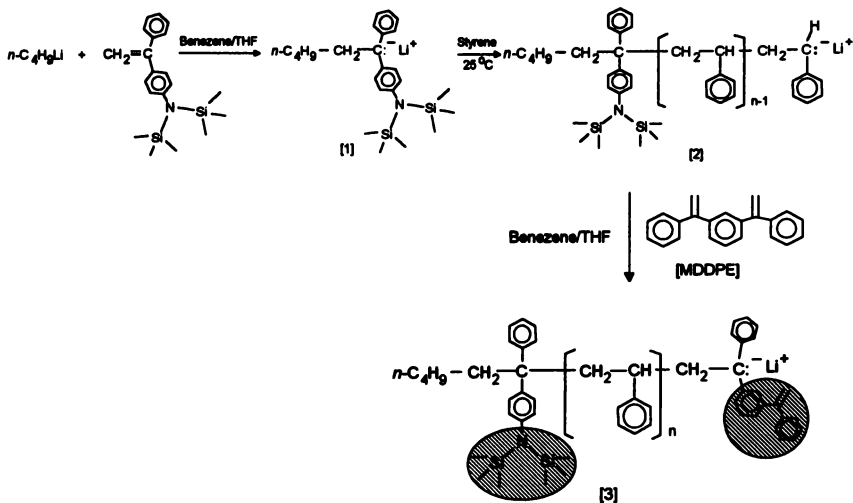


Figure 1. ^1H NMR spectra of 1-(4-aminophenyl)-1-phenylethylene (a) and 1-[4-[N,N-bis(trimethylsilyl)amino]phenyl]-1-phenylethylene (b).

band appeared at $\lambda_{\text{max}} = 344$ nm corresponding to the formation of poly(styryl)lithium in benzene/THF mixture.

The UV/Visible absorption spectra of active species prepared in this experiment are shown in Figure 2. On adding MDDPE, the fast cross-over reaction from styryl anion to MDDPE is observed without homopolymerization of MDDPE with regard to the reappearance of an absorption band at $\lambda_{\text{max}} = 455$ nm and new development of the absorption peak at $\lambda_{\text{max}} = 280$ nm corresponding to the unreacted ethylene unit of the MDDPE without formation of diadduct. From these observations, the initiation rate of diphenylhexyllithium ([1]) can be deduced in benzene/THF solution. Completion of the cross-over reaction from the substituted diphenylalkyllithium ([1]) to poly(styryl)lithium ([2]) can be also determined by comparison of the relative intensity of the absorption peaks at $\lambda_{\text{max}} = 455$ nm and 344 nm, as shown in Figure 3. In this respect, the stoichiometric balance between *n*-BuLi

Scheme 2



and ADPE can be readily controlled by adding *n*-BuLi dropwise to the ADPE/benzene solution until the ratio ($I_{455\text{nm}}/I_{280\text{nm}}$) of the relative peak intensity at $\lambda_{\text{max}} = 455 \text{ nm}$ to at $\lambda_{\text{max}} = 280 \text{ nm}$ is leveled off. The results of kinetic studies provide an information on the relative reaction rates of the above organolithium compounds with other reagents. Surprisingly, the cross-over reaction of *n*-BuLi with ADPE in pure benzene was too slow to complete for a week. The addition of THF was effective to complete the cross-over reaction within 2 h.

Thus, from the plot of the $I_{455\text{nm}}/I_{280\text{nm}}$ against the reaction time, the initial slope is directly related to the rate constant of the cross-over reaction of *n*-BuLi with 1-[4-[*N,N*-bis(trimethylsilyl)-amino]phenyl]-1-phenylethylene (ADPE). The key factor to prepare macromonomer quantitatively is how to synthesize effectively diphenylalkyllithium with amine group (ADPELi). Furthermore, the initiation rate of the functional initiator (ADPELi) to styrene is another important variable. It can be deduced by the slope from the plot of the $I_{344\text{nm}}/I_{455\text{nm}}$ ratio against the reaction time in benzene/THF mixture. From the inflection point in the plot of $I_{455\text{nm}}/I_{344\text{nm}}$ ratio against the reaction time, it was found that the initiation was completed within 5 minutes. In addition, the cross-over reaction of diphenylalkyllithium to poly(isoprenyl)lithium was also found to be completed in the mixture of benzene/THF within 5 minutes from the plot of the $I_{455\text{nm}}/I_{278\text{nm}}$ ratio against the reaction time. It was also found that the cross-over reaction of poly(styryl)lithium to 1,3-bis(1-phenylethenyl)benzene (MDDPE) was so fast in benzene/THF mixture from the observation on the intensity ratio ($I_{455\text{nm}}/I_{344\text{nm}}$) change as shown in Figure 3. The results of these kinetic studies provided a useful information how to control the active species during all reactions. From comparison of ^1H NMR spectra of the amine-functionalized polystyrene and the corresponding macromonomer shown in Figure 4, a successful synthesis of macromonomer carrying amino-functional group can be confirmed. For example, the chemical shift at $\delta = 0.08 \text{ ppm}$ is assigned to the protons on the trimethylsilyl group of the silyl-protected amine group ($-\text{N}[\text{Si}(\text{CH}_3)_3]_2$), as shown in Figure 4(a). The number average molecular weight of the amine-functionalized polymer was 2300 g/mol by size exclusion chromatographic analysis. It was in accord with that by ^1H NMR spectroscopic analysis as shown in Table 1. All functionalized polymers prepared in our experiments are summarized in Table 1.

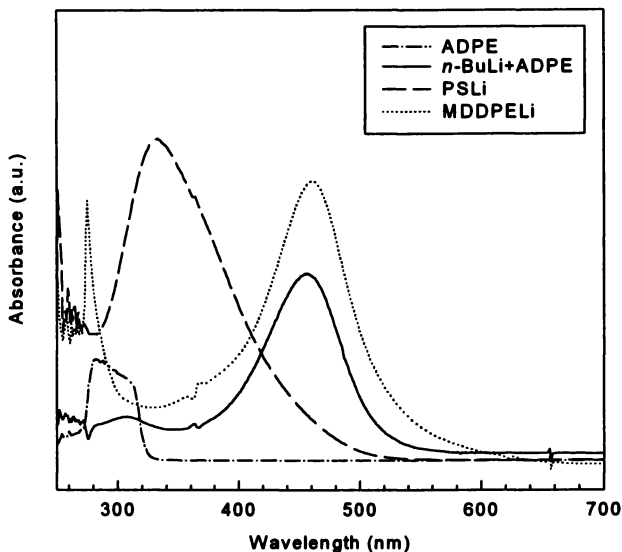


Figure 2. UV/Visible absorption spectra of amine-functionalized initiator, poly(styryl)lithium, and macromonomer in benzene/THF mixture (20/1, v/v).

The chemical shift at $\delta = 5.4$ ppm shown in Figure 4(b) arises from the protons on the methylene group of diphenylethylene-type unit ($CH_2 = CPh_2$) shown in Scheme 2. Simultaneously, from comparison of the chemical shifts at $\delta = 0.08$ ppm in Figures 4(a) and 4(b), it is clear that macromonomer carrying amine-functional group was successfully synthesized.

Comparison of the SECs of the amine-functionalized polystyrene and the corresponding macromonomer inferred that the reaction of MDDPE with poly(styryl)lithium produced mostly monoadduct (below 2 % diadduct) in our experimental condition as shown in Figure 5. As already described, the synthesis of macromonomer was effective in hydrocarbon/THF mixtures with regard to consider the reaction time. The synthesis of macromonomers carrying amine group was meaningless in pure hydrocarbon because the cross-over reaction of *n*-BuLi with ADPE was too slow to be completed. Thus, the unreacted ADPE may allow to copolymerize with styrene under our reaction conditions with regard to the reaction time. This copolymerization may produce diphenylalkyllithium which can not react with MDDPE. This situation makes efficient synthesis of macromonomer of 1,1-diphenylethylene-type difficult. Thus, Poly 1 and Poly 4 in Table 1 were α -amine functionalized polystyrene and polyisoprene excluding the diphenylethylene-type unit. It has been well-known that lithium *sec*-butoxide was effective to control the 1,4-enchainment of polydienes in the crossover reaction of diphenylalkyllithium with dienes in hydrocarbon (30) while polymerization in THF as solvent produced 59 % of 3,4-enchainment microstructure (31). In this respect, anionic synthesis of macromonomer having the polyisoprene backbone should be performed in hydrocarbon to control the microstructure (30). Although lithium *sec*-butoxide employed as an additive was effective to control the microstructure of polydienes, it did not effect to the increase of the reaction rate of *n*-BuLi with ADPE in hydrocarbon. However, in the mixture of benzene/THF,

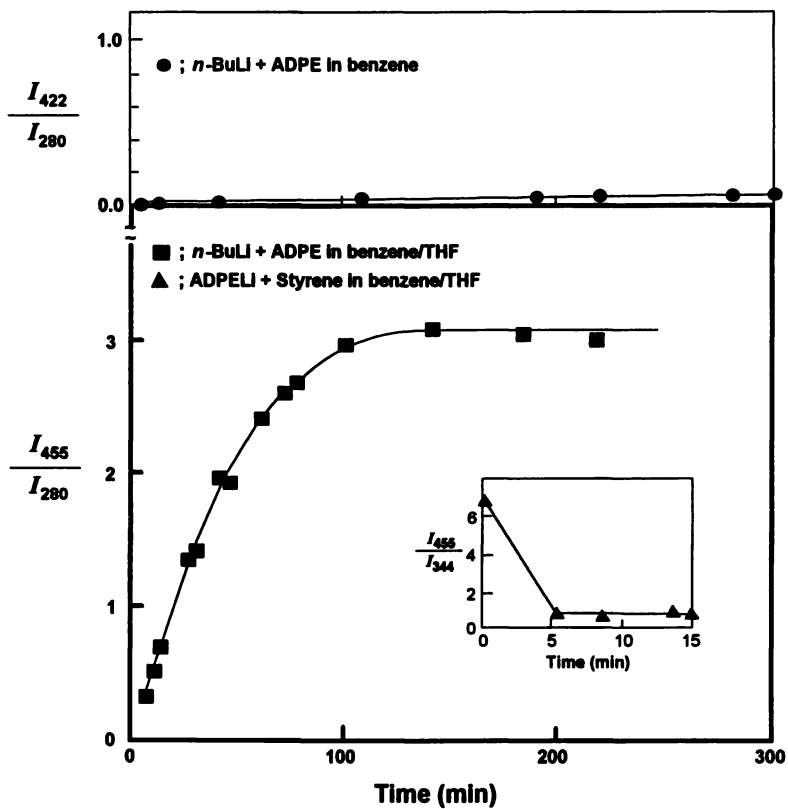


Figure 3. Kinetic studies of organolithium compounds prepared by the reaction of *n*-BuLi with ADPE, styrene, and MDDPE in benzene or benzene/THF mixture ([THF]/[*n*-BuLi] = 20/1).

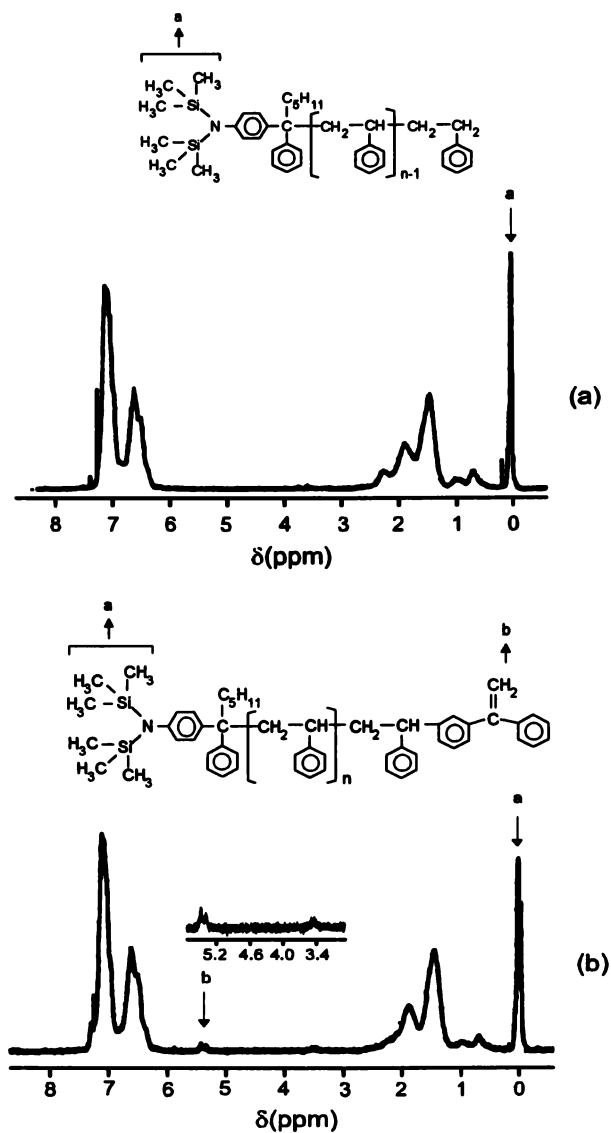


Figure 4. ^1H NMR spectra of amine-functionalized polystyrene (a) and the corresponding macromonomer from the reaction with MDDPE (b) (Poly 2 in Table 1).

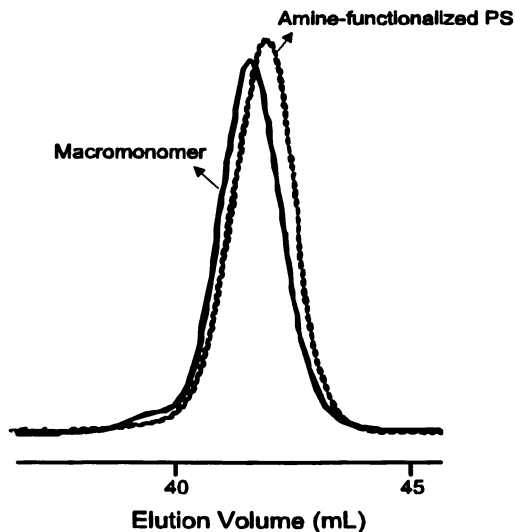


Figure 5. Size exclusion chromatograms of amine-functionalized polystyrene and the corresponding macromonomer (Poly 2 in Table 1).

Table 1. The reaction conditions and the results of the characterization of various macromonomers synthesized at 25°C.

Sample	Solvent	Theoretical (M_n)	Observed (M_n)		Functionality (f) ^{a)}	
			SEC	¹ H NMR	Amine	Ethylene
Poly 1 ^{b)}	Benzene	7,000	6,200	8,900	0.70	0
Poly 2 ^{c)}	Benzene THF	3,000	2,800	3,000	0.93	0.60
Poly 3 ^{c)}	Benzene THF	4,000	3,300	3,800	1.20	1.05
Poly 4 ^{d)}	Benzene	5,000	4,500	21,000	0.21	0
Poly 5 ^{e)}	Benzene THF	5,000	7,300	5,300	1.02	0.94

- a) Amine and ethylene functionality of polymer by ¹H NMR analysis.
 b) α -Aromatic amine functionalized polystyrene.
 c) Macromonomer of 1,1-diphenylethylene-type of polystyrene carrying amino group.
 d) α -Aromatic amine functionalized polyisoprene.
 e) Macromonomer of 1,1-diphenylethylene-type of polyisoprene carrying amino group.

similar kinetic study as shown in Figure 4 provided that polymerization of isoprene using the functionalized initiator revealed a high yield (over 95 %) based on the result of ^1H NMR spectroscopic analysis. It is noteworthy that lithium *sec*-butoxide as additive did not provide any synergistic effect in polymerization of isoprene.

Conclusion

Non-homopolymerizable macromonomer of 1,1-diphenylethylene-type unit carrying amino-functional group was successfully synthesized through the chain end functionalization methodology of living polymers using 1-[4-[N,N-bis(trimethylsilyl)amino]phenyl]-1-phenylethylene (ADPE) and 1,3-bis(1-phenylethenyl)benzene (MDDPE). The crossover reaction of 1-[4-[N,N-bis(trimethylsilyl)amino]phenyl]-1-phenylethylene (ADPE) with *n*-BuLi was completed in benzene/THF within 2 h while it took over a week in pure benzene. The initiation rate of styrene or isoprene by the corresponding diphenylalkyllithium with amine group on phenyl ring was very fast, for instance, it was completed within 5 minutes for the both cases of styrene and isoprene in benzene/THF mixture. The amine and the ethylene unit functionalities were maximum 0.94 and 0.95, respectively.

Acknowledgments

This work has been supported by KIST and The Institute of LG Chemical. The authors would like to acknowledge this support. Especially, the authors gratefully acknowledge the extensive assistance of Drs. Moonseok Chun and Chan Hong Lee who not only provided alkylolithium but also characterized a part of the final products.

Literature Cited

1. Milkovich, R.; Chiang, M. T. *U. S. Pat.* 3,786,116 (1974)
2. Schulz, G. O.; Milkovich, R. *J. Appl. Polym. Sci.* **1982**, *27*, 4773.
3. Rempp, P.; Franta, E.; Masson, P.; Lutz, P. *Prog. Colloid Polym. Sci.* **1986**, *72*, 112.
4. Kawakami, Y. in *Encyclopedia of Polymer Science and Engineering*; Kroschwitz, J. I. Ed.; Wiley-Interscience: New York, 1987; Vol. 9, p.195.
5. Quirk, R. P.; Kim, J. in *Ring-Opening Polymerization. Mechanisms, Catalysis, Structure, Utility*; Brunelle, D. J. Ed.; Hanser Publishers: Munich, 1993; Chap. 9, p.263.
6. Rempp, P.; Franta, F. *Adv. Polym. Sci.* **1984**, *58*, 1.
7. Schulz, G. O.; Milkovich, R. *J. Polym. Sci., Polym. Chem. Ed.* **1984**, *22*, 1633.
8. Gillman, K. F.; Senogles, E. *Polym. Lett.* **1967**, *5*, 477.
9. Milkovich, R. *Polym. Prepr.; Am. Chem. Soc.; Div. Polym. Chem.* **1980**, *21*, 40.
10. Kennedy, J. P.; Lo, C. Y. *Polym. Prepr.; Am. Chem. Soc.; Div. Polym. Chem.* **1982**, *23*, 99.
11. Nitadori, Y.; Tsurata, T. *Makromol. Chem.* **1979**, *180*, 1877.
12. Quirk, R. P. in *Comprehensive Polymer Science*; Aggarwal, S. L.; Russo, S. Eds.; Pergamon: New York, 1992; Vol. 1st Suppl.; p.83.
13. Hsieh, H. L.; Quirk, R. P. *Anionic Polymerization: Principles and Practical Applications*; Marcel Dekker: New York, 1996.
14. Quirk, R. P.; Kim, Y. J. *Polym. Prepr.; Am. Chem. Soc.; Div. Polym. Chem.* **1996**, *37(2)*, 643.
15. Quirk, R. P.; Dixon, H.; Kim, Y. J.; Yoo, T. *Polym. Prepr.; Am. Chem. Soc.; Div. Polym. Chem.* **1996**, *37(2)*, 402.
16. Quirk, R. P.; Yoo, T. *Polym. Bull.* **1993**, *31*, 29.
17. Quirk, R. P.; Lynch, T. *Macromolecules* **1993**, *26*, 1206.
18. Quirk, R. P.; Zhu, L.-F. *Brit. Polym. J.* **1990**, *23*, 47.
19. Quirk, R. P.; Wang, Y. *Polym. Int.* **1993**, *31*, 51.
20. Zhu, L.-F. *Ph. D. Dissertation*, The University of Akron, 1992.
21. Morton, M.; Fetters, L. J. *Rubber Chem. Technol.* **1975**, *48*, 359.
22. Schulz, G. G. H.; Hocker, H. *Makromol. Chem.* **1977**, *178*, 2589.

23. Tung, L. H.; Lo, G. Y.; Beyer, D. E. *U.S. Pat.* 4,172,100 (1979)
24. Bordwell, F. G. *Acc. Chem. Res.* **1988**, *21*, 456.
25. Pratt, J. R.; Massey, W. C.; Pinkerton, F. H.; Thames, S. F. *J. Org. Chem.* **1975**, *40*, 1090.
26. Evans, A. G.; George, D. B. *J. Chem. Soc.* **1961**, 4653.
27. Wakefield, J. *The Chemistry of Organolithium Compounds*; Pergamon: New York, 1974.
28. Yuki, H. *Prog. Polym. Sci. Jpn.* **1972**, *3*, 141.
29. L. H. Tung, L. H.; Lo, G. Y.-S.; Beyer, D. E. *Macromolecules* **1978**, *11*, 616.
30. Quirk, R. P.; Ma, J.-J. *Polym. Int.* **1991**, *24*, 197.
31. Bywater, S.; Worsfold, D. J. *Can. J. Chem.* **1967**, *45*, 1821.

Functionalized Polymers with Dimethylamine and Sulfozwitterionic End-Groups

Synthesis, Dilute Solution, and Bulk Properties

Nikos Hadjichristidis^{1,2}, Marinos Pitsikalis¹, and Stergios Pispas¹

¹University of Athens, Department of Chemistry Panepistimiopolis Zographou, 15771 Athens, Greece

The synthesis of end-functionalized (telechelic or semitelechelic) polymers has been the subject of numerous studies over the last decades due to both the academic and industrial interest developed for these polymers (1-4). The incorporation of end groups is capable to lead to dramatic changes in the dilute solution (5-7) and bulk properties (8,9) of the parent materials giving rise to practically and potentially numerous applications.

A wide variety of methods has been used to prepare end-functionalized polymers including anionic, cationic radical and group transfer polymerizations (10-12). The technique of living anionic polymerization has been proven to be the most efficient method for the synthesis of model end-reactive polymers, due to the absence of any chain termination and chain transfer reactions (13,14). The anionic polymerization offers the possibility to prepare polymers with control of structural variables such as molecular weight, molecular weight distribution, copolymer composition, diene microstructure and tacticity. The living character of the polymerization leads to the synthesis of macromolecules with different architectures (diblock and triblock copolymers, star, graft, cyclic polymers etc.) and to the possibility to perform several post polymerization reactions.

This presentation summarizes results on the synthesis, the dilute solution and bulk properties of dimethylamine and sulfozwitterionic end-functionalized polymers having different architectures (linear homopolymers, diblock and triblock copolymers and star polymers with different number of functional groups).

The Functional Initiator 3-Dimethylaminepropyl-lithium (DMAPLi)

3-Dimethylaminepropyl-lithium (DMAPLi) was used as initiator for the introduction of the dimethylamine group at the end of the polymer chain. DMAPLi was prepared by the reaction of the corresponding chloride (DMAPCl) and Li dispersion according to Stewart et al.(15). The purity of the products was checked by deactivating the living species with methanol (MeOH) under vacuum, using a specific glass apparatus

²Also at the Institute of Electronic Structure and Laser (FORTH), 71110 Heraclion, Crete, Greece

and by analyzing the products by gas chromatography-mass spectroscopy (GC-MS) (16). The desired product, 3-dimethylamine propane was the only low boiling point compound observed at 98% yield. The high boiling point impurities were essentially tertiary amines. In order to reduce the presence of polar impurities the synthesis was carried out in hexane where DMAPLi is insoluble, whereas the byproducts are soluble and thus they can be removed by filtering the hexane solution. The initiator is then dissolved in benzene for subsequent use.

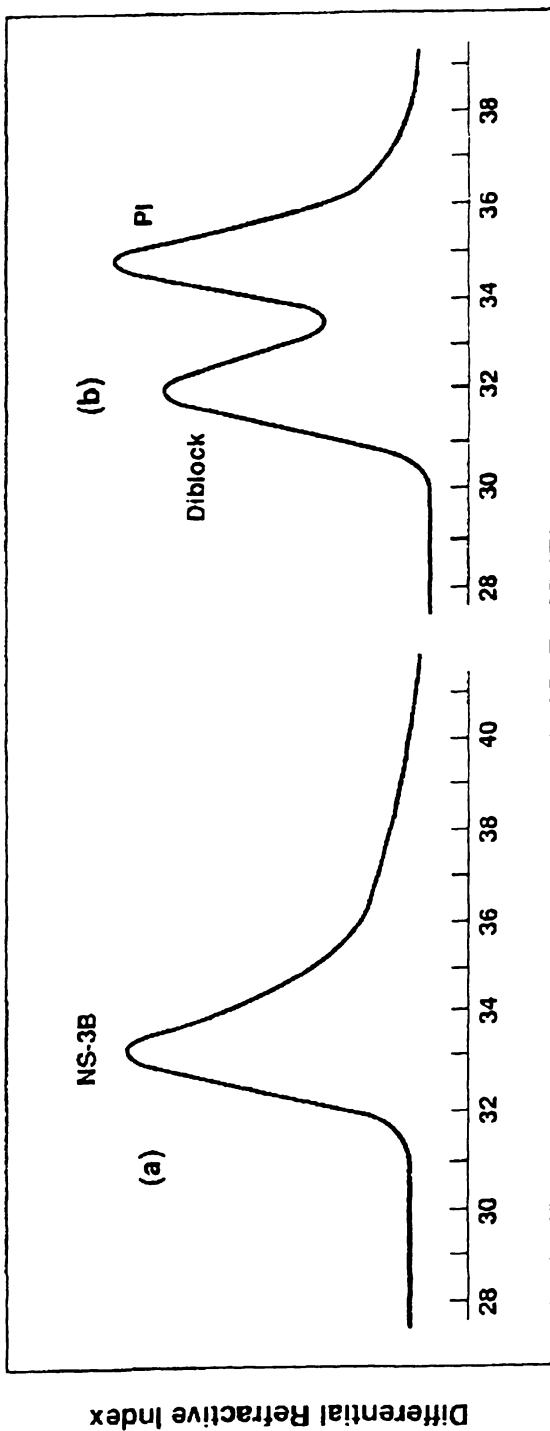
Synthesis and Characterization

Homopolymers. Styrene (St), Isoprene (Is) and butadiene (Bd) were polymerized with DMAPLi. Isoprene was polymerized in benzene at room temperature using purified DMAPLi as initiator (16). The molecular weight distribution is lower than 1.1 in almost all cases, due to the rather slow propagation rate of the polymerization of Is (17). In all cases the stoichiometric molecular weight is in very good agreement with the number average molecular weight, measured by osmometry, meaning that all the initiator is consumed during the initiation reaction. These results indicate that DMAPLi is an efficient initiator for the polymerization of isoprene.

There is no great difference for the polymerization of butadiene (Bd) with DMAPLi compared with *s*-BuLi (16). The stoichiometric molecular weights, M_s are in very close agreement with the number average molecular weights, measured by osmometry and the molecular weight distributions are in the range 1.05-1.07 similar to that obtained with *s*-BuLi polymerizations. The even lower polydispersity indices, I observed for NPBD compared with NPI are explained by the slower propagation rate for the polymerization of Bd, which overshadows the slow initiation rate (18).

The microstructure of the polydienes was investigated using $^1\text{H-NMR}$ spectroscopy. The results clearly show an increase of the vinyl content with decreasing chain length. This behavior is reasonable having in mind the increased initiator concentration, used to prepare lower molecular weight samples and the modifying effect of *t*-amines on polydiene microstructure (19). Nevertheless as the molecular weight approaches the value 10^5 the microstructure becomes indistinguishable from polymers prepared by conventional organolithium initiators.

The slow initiation rate was readily observed during the polymerization of St by the gradual appearance of the orange color (16), which is characteristic of the living polystyryllithium chains. This fact in combination with the very fast propagation rate for the polymerization of St resulted in very broad molecular weight distributions ($I=1.23-1.27$). When $M_s > 12000$ there was a good agreement with the number average molecular weight, M_n , meaning the complete consumption of the initiator. However when $M_s < 9300$ the molecular weights, measured by SEC were much higher than the stoichiometric ones, with the difference being higher as M_s was decreasing. In addition broader molecular weight distributions having long tails at the low molecular weight region were observed. This behavior can be explained by the partial consumption of the initiator, which means that an appreciable amount of the initiator remains unreacted. This was verified by the subsequent addition of Is, which produced polymers having bimodal distribution (figure 1). The lower molecular



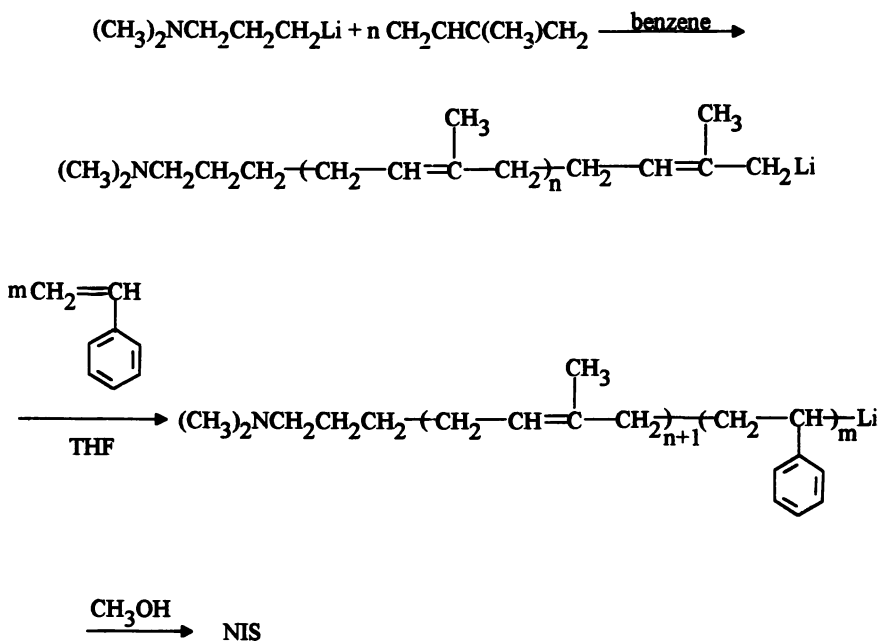
Elution Volume (ml)

1. SEC chromatograms of (a) NS-3B (purified DMAPLi; polymerization in pure benzene) and (b) NS-3B after the addition of isoprene (first peak, diblock formed; second peak, homopolyisoprene formed by reaction of isoprene with unreacted DMAPLi). (Reproduced by permission from reference 16)

weight peak corresponds to NPI homopolymer, produced by the DMAPLi, which remained unreacted during the polymerization of St. The higher molecular weight peak is attributed to the NPS**t**-b-PI block copolymer with the amine group at the PSt chain end, produced by the cross-over reaction of NPS**t**Li with Is.

Addition of THF to the mixture of St and DMAPLi ($[\text{THF}]/[\text{Li}] > 3$) gave polymers with close agreement between M_w and M_n , even for low molecular weights, which means that it promotes the initiation reaction.

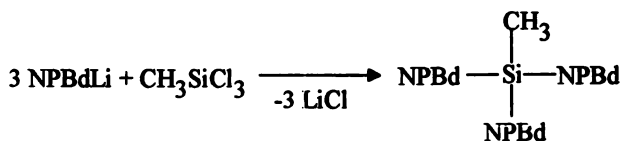
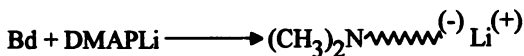
DI- and Triblock Copolymers. Block copolymers of styrene and isoprene having dimethylamine end-groups at the one or the other chain end were prepared using DMAPLi and sequential addition of monomers (20). When Is is polymerized first a small amount of THF is added after the polymerization of the diene is completed to accelerate the crossover reaction with St. The reaction scheme is the following:



Scheme 1

Triblock copolymers, having dimethylamine groups at both chain ends were also prepared by coupling diblock chains with dimethyldichlorosilane, $(\text{CH}_3)_2\text{SiCl}_2$. The products are characterized by compositional and chemical homogeneity and low molecular weight distributions. The samples are designated with the letter N corresponding to the end-amine group, followed by the sequence of blocks starting with the block at which the functional group is attached. The letter F accounts for samples where THF was added before the polymerization of St by DMAPLi to accelerate the initiation reaction.

Mono-, Di- and Tri- ω -Functionalized Three Arm Star Polybutadienes. ω -Functionalized star polymers can be prepared by the reaction of end-functionalized living polymers with suitable chlorosilanes which act as linking agents. Three and twelve arm PI stars (21) and three arm star PBd with all ends functionalized with dimethylamine groups (22) were synthesized following this procedure. An example is given in scheme 2.



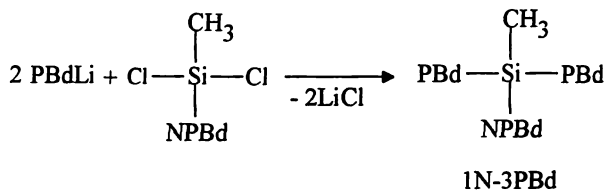
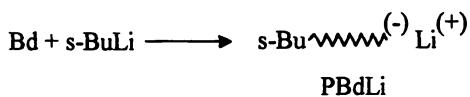
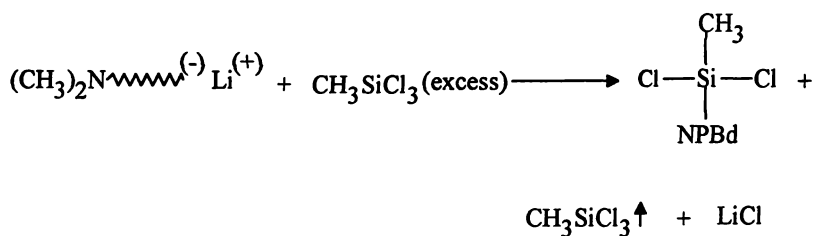
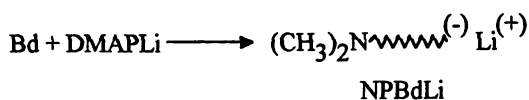
3N-3PBd

Three arm stars PBd with one or two end-amine groups were also prepared using suitable procedures (22). The presence of one or two functional groups is denoted by the symbols 1N- and 2N- respectively, whereas the symbol 3PBd denotes a three arm star PBd. So 1N-3PBd is a three arm star PBd with one end-amine group. The following numbers differentiate samples of the same series. A schematic representation of the reaction sequence used for the synthesis of samples 1N-3PBd is shown in Figure 2.

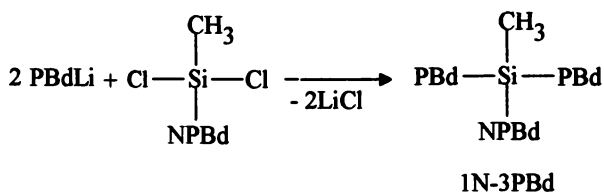
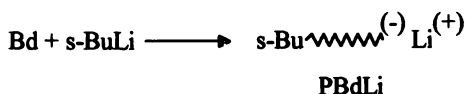
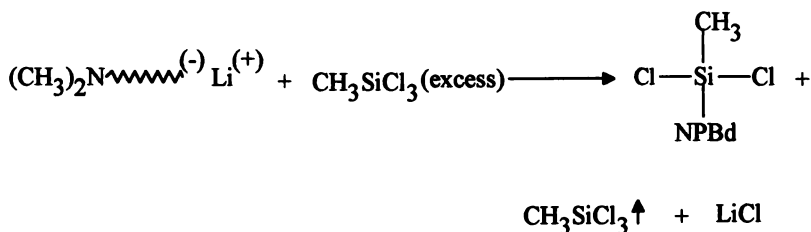
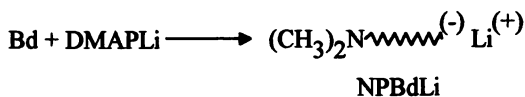
A living end-functionalized PBd chain was prepared in benzene using DMAPLi as initiator. The living polymer solution was added to a large excess of methyltrichlorosilane (Si-Cl/C-Li ~100/1) in order to prepare the methyltrichlorosilane-capped PBd. Excess linking agent was removed under vacuum line conditions. The polymer was repeatedly redissolved and pumped to extract traces of the silane from the bulk polymer. Finally benzene was distilled into the reactor to dissolve the ω -methyltrichlorosilane PBd arm.

The next step involved the synthesis of the unfunctionalized arm, using *s*-BuLi as initiator. A small excess of this living polymer was coupled with the macromolecular linking agent to produce the final product. Termination of the residual active anions with degassed MeOH and subsequent fractionation to remove the excess Pbd arm gave the pure 1N-3PBd star polymer.

A similar procedure is followed for the synthesis of 2N-3PBd stars, starting from the reaction of the living unfunctionalized arm with excess methyltrichlorosilane followed, after the removal of the excess linking agent by the coupling reaction of the



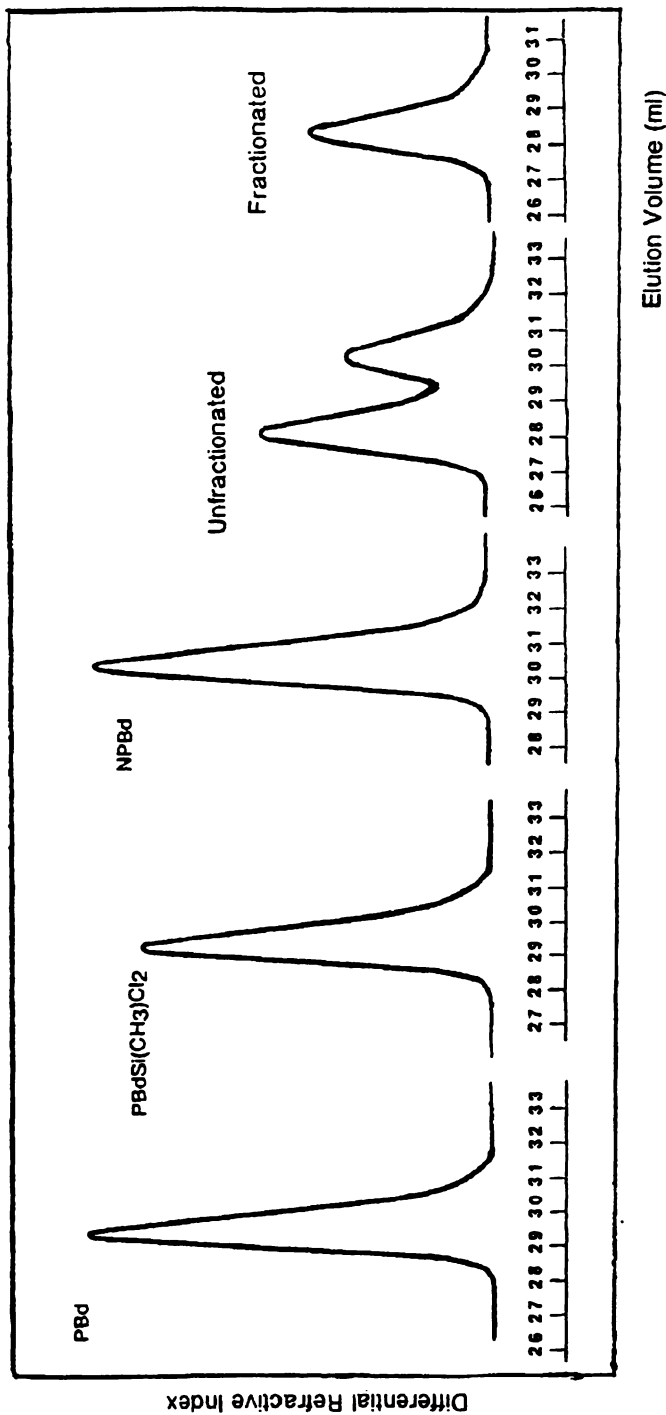
2. Reaction sequence for the synthesis of samples 1N-3PBd.
(Reproduced by permission from reference 22)



dichlorosilane-capped arm with a small excess of the amine-functionalized living arm. All these procedures were monitored by SEC. A representative example is given in figure 3.

In the case of samples with low arm molecular weight ($M_n < 10^4$) it is not easy to control the reaction of the living polymer (B^{\cdot}) with the linking agent towards the reaction of only one of the silane's Si-Cl bonds. So instead of having the desired product $\text{CH}_3\text{SiCl}_2\text{B}$ a mixture of $\text{CH}_3\text{SiCl}_2\text{B}$ and $\text{CH}_3\text{SiClB}_2$ is obtained. In order to prevent the formation of the byproduct the steric hindrance of the living arm B^{\cdot} was increased by reaction with diphenylethylene (DPE). A few drops of THF were added to accelerate the crossover reaction. The coupling reaction was minimized using this procedure giving less than 3 % of the byproduct.

The molecular characteristics of the three-arm stars PBd having one, two or three amine end-groups are given in Table I.



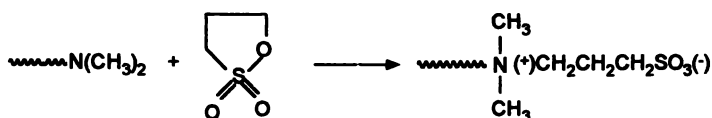
3. SEC chromatograms concerning the synthesis of the 2N-3PBd40 star polymer. (Reproduced by permission from reference 22)

Table I. Molecular characteristics of the three-arm PBd stars with one, two, or three dimethylamino end groups in toluene (MO) and THF (LALLS)

Sample	$M_n \times 10^{-3}$ (PBd arm)	$M_n \times 10^{-3}$ (NPBd arm)	$M_n \times 10^{-3}$ (star)	$M_w \times 10^{-3}$ (star)	I (SEC)	$I = M_w/M_n$	f^a
1N-3PBd8	7.1	9.1	23.8	25.8	1.05	1.08	3.1
1N-3PBd15	14.9	12.6	42.9	47.9	1.05	1.12	3.0
1N-3PBd20	15.7	14.3	46.9	49.8	1.05	1.06	3.1
1N-3PBd30	34.8	34.0	104.9	111.0	1.06	1.07	3.0
1N-3PBd40	45.5	35.6	131.4	149.7	1.06	1.14	3.1
2N-3PBd8	6.3	7.6	21.3	22.5	1.05	1.06	3.0
2N-3PBd15	13.2	14.7	43.4	46.5	1.04	1.07	3.1
2N-3PBd30	22.1	21.9	61.8	62.4	1.06	1.01	2.9
2N-3PBd40	35.0	30.7	89.0	99.0	1.06	1.11	2.8
3N-3PBd15		11.2	31.1	33.7	1.06	1.08	2.8
3N-3PBd25		23.2	62.5	67.4	1.06	1.08	2.7
3N-3PBd40		33.0	91.4	93.1	1.06	1.02	2.8

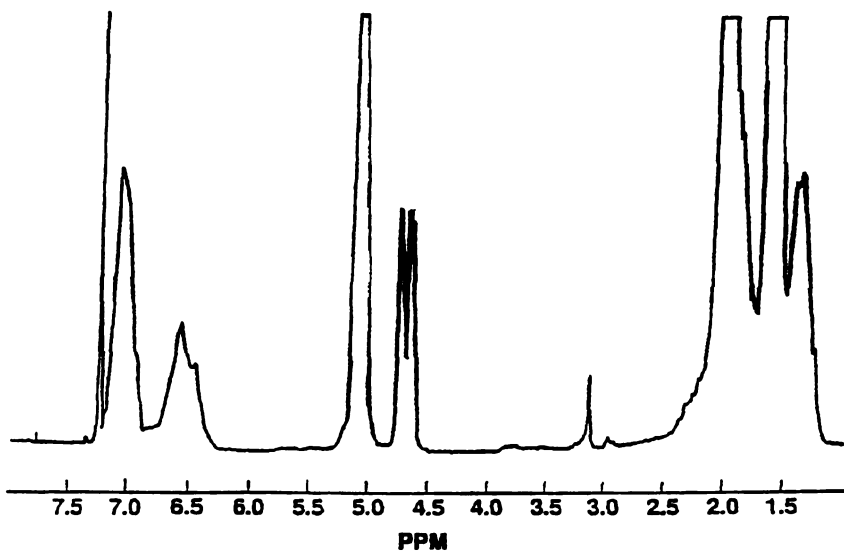
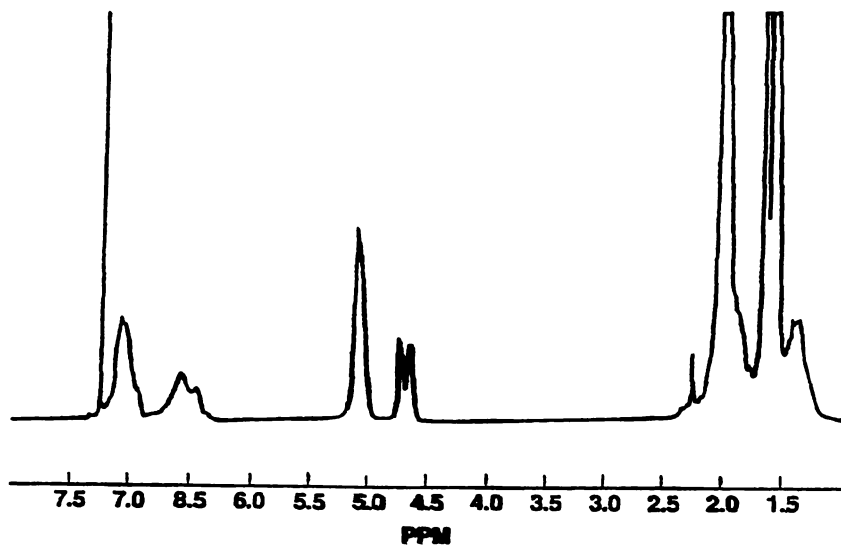
a Functionality, $f = M_n(\text{star})/M_n(\text{average of the arms})$

Post-polymerization Reaction of the Amine-Functionalized Polymers. The amine end groups can be easily transformed to ionic dipoles after the reaction with 1,3-cyclopropane sultone (23,24), illustrated in the following scheme:



The reaction takes place in dilute THF solutions (2-3 w/v %) at 70 °C for several days using an excess of the sultone over the amine groups (sultone/amine = 10/1). For the PBd samples inert atmosphere was used. Under these conditions this post-polymerization reaction is free of side reactions (crosslinking, degradation etc.) as was verified by SEC. Similar peaks with the corresponding amine-capped polymers were observed in CHCl_3 in all cases.

It is difficult to determine the extent of the conversion of the t-amine groups to sulfobetaines due to the low concentration of these groups in the polymer chains. However qualitative results by $^1\text{H-NMR}$ show that the reaction yield is very high (20,25). In the following figure the $^1\text{H-NMR}$ spectra of linear block copolymer NIS-5 and the corresponding zwitterion sample are given. The peak at 2.2 ppm is assigned to the



4. $^1\text{H-NMR}$ spectra of samples NIS-5 (top) and ZwIS-5 (bottom) in CDCl_3 . (Reproduced by permission from reference 20)

methyl protons of the carbons which are attached to the nitrogen atom. This peak is completely disappeared after the reaction with 1,3 cyclopropane sultone and two new peaks at 3.15 and 2.95 ppm are emerged. These peaks are assigned to the methyl protons attached to the positively charged nitrogen atom of the zwitterionic group and to the methylene protons of the carbon which is attached to the sulfur atom respectively (24,26).

Dilute Solution and Bulk Properties

Homopolymers. The dilute solution properties of ω -functionalized linear homopolymers were studied by MO, LALLS viscometry and DLS in various non-polar solvents (21,27,28). The conclusions obtained from this study are the following:

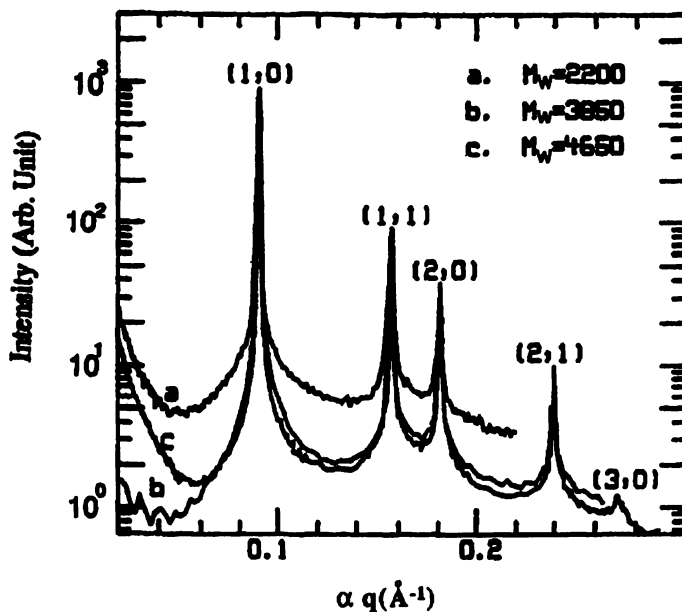
- a. The dimethylamine-capped samples present no evidence of association in non-polar solvents (cyclohexane, CCl_4 , toluene)
- b. The zwitterion-capped samples form large aggregates in these solvents with aggregation numbers increasing with decreasing molecular weight of the parent material. However, aggregation numbers for PS homopolymers are lower than those obtained for polydiene homopolymers probably because of the solvating effect of the phenyl rings on the dipolar groups.
- c. The aggregates are polydisperse as concluded by LALLS, MO and DLS measurements.
- d. The associates behave hydrodynamically as star polymers as evidenced by the increasing k_H values with increasing degree of association and by the good agreement between experimental aggregation numbers and those calculated assuming the star model.
- e. The linear head packing model describes fairly well the structures of the associates. Detailed studies by small angle x-ray scattering (SAXS) were performed on low molecular weight zwitterion-capped polyisoprenes (29). For samples having $14000 < M_w < 28000$ the scattering profiles show that the aggregates form a body-centered cubic lattice with long range order.

Figure 5 shows the corresponding scattering profiles for the lower molecular weight samples ($2200 < M_w < 4650$). The peaks can be indexed on a two dimensional hexagonal lattice of tubes. In other words the aggregates have a tubular structure with the tubes closed packed on a two dimensional hexagonal lattice with crystalline order. The core is formed by the dipoles which are arranged in an antiparallel configuration as shown in figure 6.

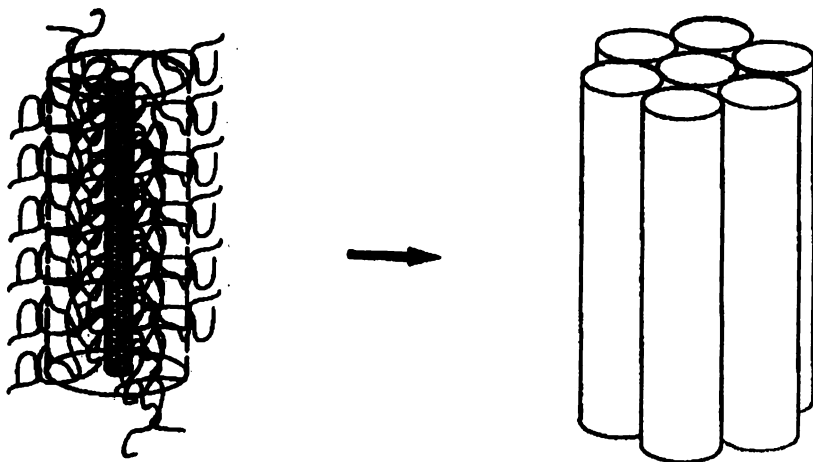
It is characteristic that a very small volume fraction of ionic species (<1 %) is able to promote long range order in contrast to usual block copolymers.

The viscoelastic behavior in the melt state of end-functionalized polyisoprenes was also investigated (30). The results can be compared with predictions based on the star model for the aggregates. It is well known that the viscoelastic properties of star polymers in the melt state depend on arm molecular weight and they are insensitive to their functionality (31).

The amine-capped samples behave more or less as conventional polyisoprenes indicating that only weak association may exist in the melt state. The situation is very



5. X-ray scattering profiles of the samples with molecular weights of 4650, 3850, and 2200. The profiles of the last two samples have been shifted by a factor (α) to make the first peak positions overlap. (Reproduced by permission from reference 29)



6. A schematic representation of the formation of two-dimensional lattices of the close-packed tubular aggregates. (Reproduced by permission from reference 29)

different for the zwitterion-capped polymers with the dynamic moduli broadened and shifted to much lower frequencies. For samples with high base molecular weights the viscoelastic behavior more closely resembles the behavior of conventional star polymers.

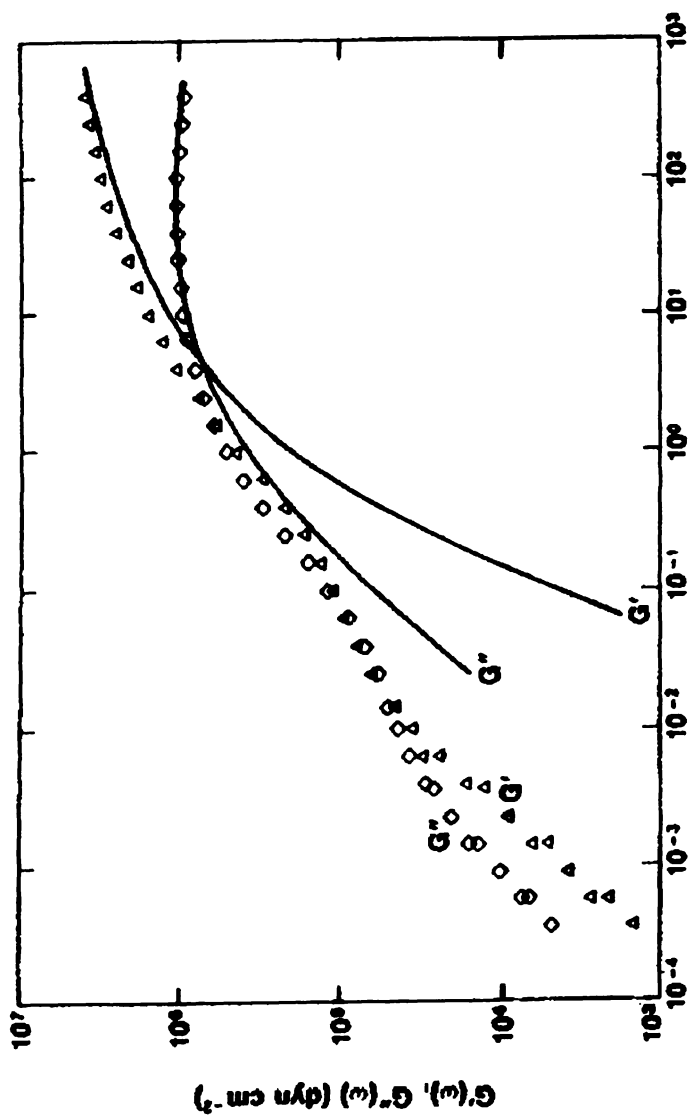
Samples with intermediate and lower molecular weights show a second relaxation regime at very low frequencies. A characteristic example is given in figure 7. It is observed that some resemblance exist between the zwitterion and star polymer only at intermediate and high frequencies.

The viscosities of the zwitterion polymers, specially of low and intermediate molecular weights are much larger than those predicted assuming the star model. Consequently it is reasonable to consider that the aggregates have extended morphologies (lamellae, strings etc.). Only in the case of low aggregation numbers, observed for samples of high base molecular weight the behavior is similar to those of star polymers because the core size is rather small and can be considered as the star's center. The extended structures are delicate in a mechanical sense making it possible to explain the remarkable strain sensitivity observed at low frequencies. It is noted that there is close agreement with the results obtained by melt rheology and SAXS.

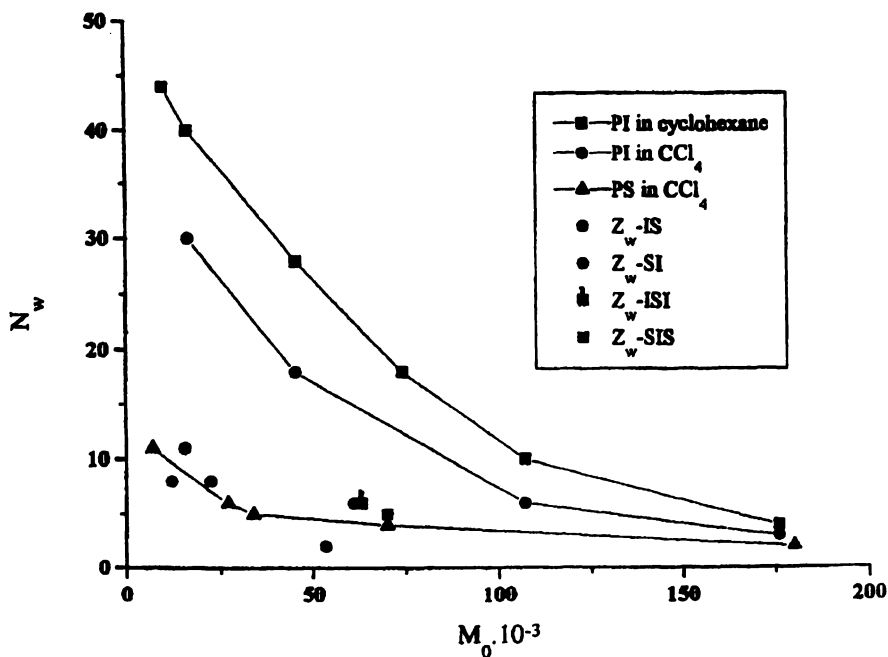
ω -Functionalized Block Copolymers of Styrene and Isoprene. The association behavior of end-functionalized diblock and triblock copolymers of isoprene and styrene was studied in CCl_4 , which is a nonpolar and good solvent for both blocks (20,32). The aggregation numbers, N_w are almost the same whether the zwitterion group is linked at the PI or the PS chain end. Their value depends strongly on the M_w of the base polymer. N_w decreases with increasing molecular weight of the precursor polymer, M_0 . The variation of N_w with M_0 for the case of ZwPI in cyclohexane (21) and CCl_4 (20), PS in CCl_4 (27) di- and triblock copolymers is given in figure 8. The aggregation numbers for ZwPI are lower in CCl_4 than in cyclohexane due to the higher polarizability of the former solvent. Another point to be noticed is that the degrees of association of the copolymers are closer to those determined for the ZwPS samples than the ZwPI samples in CCl_4 . The aromatic rings, due to their high polarizability cause some kind of solvation, thus leading to reduced N_w values. The aggregation numbers are almost the same for the monofunctional and difunctional samples. This is rather surprising, since the difunctional polymers form gels at concentrations lower than c_{gel} ($c_{\text{gel}}=0.5 \text{ c}^*$) and can be seen as evidence of intramolecular association in very dilute solutions.

DLS was used to study the hydrodynamic properties of the end-functionalized copolymers. The zwitterionic polymers have a substantially different behavior than their precursors, due to the formation of aggregates in CCl_4 . The values of the diffusion coefficient at infinite dilution, D_0 are lower, the R_H values higher and the aggregates are polydisperse. The k_D values are negative in most cases, due to the aggregation process and is consistent with the low A_2 values obtained by LALLS.

Viscosity measurements were also performed to complement the DLS data. The $[\eta]$ values for the zwitterionic samples are considerably higher than those for the amine-capped samples and the reduced viscosity vs concentration plots are not always



7. Comparison of dynamic moduli for a four-arm polyisoprene star and a monofunctional zwitterion polyisoprene in the melt state at 25°C. Data for the star ($M_w=4.4 \times 10^5$) are shown by the solid lines; the points are data for a sample with $M_w=4.61 \times 10^4$. Triangles correspond to G' and diamonds to G'' . (Reproduced by permission from reference 30)



8. Dependence of the weight average degree of association, N_w from the base molecular weight, M_0 for various polymer series.

linear. The Huggins plots are concave upwards in some cases and specially for the difunctional samples.

The nonlinear dependance of the reduced viscosity on concentration is an indication that the association number changes by increasing concentration, something which is expected to be more pronounced in the case of the difunctional triblocks.

As in the case of ZwPI samples the stability of the aggregates was studied by adding small amounts of an alcohol, namely 2-methylcyclohexanol (at 1% and 5% content). The association is reduced in the presence of the alcohol, but even at 5% alcohol content there are samples remained aggregated. With increasing alcohol content the aggregation numbers are reducing, the A_2 values are increasing and the k_H values are decreasing.

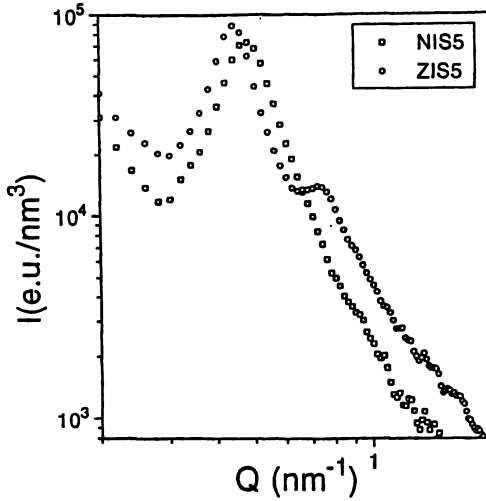
SAXS, rheology and dielectric spectroscopy were used to study the statics and dynamics of the end-functionalized block copolymer (33,34). SAXS profiles from the amine and the corresponding zwitterion-capped samples confirm the existence of ionic aggregation. A characteristic example is given in figure 9. The following features were observed: a) a background originating from density and concentration fluctuations, b) an excess intensity at low Q which is related to heterogeneities with long correlation lengths in the case of ionomers (35), c) the microdomain peak (36) characteristic of the microphase separation process between PI and PS phases and d) the peak related to the polar groups, which was emerged in the case of the zwitterionic sample.

The last three characteristics are temperature dependent with the aggregate peak intensity being much less sensitive to changes of temperature for the specific temperature range used for the experiment. The microdomain peak intensity has a similar temperature dependence for both the amine and the zwitterion-capped copolymers.

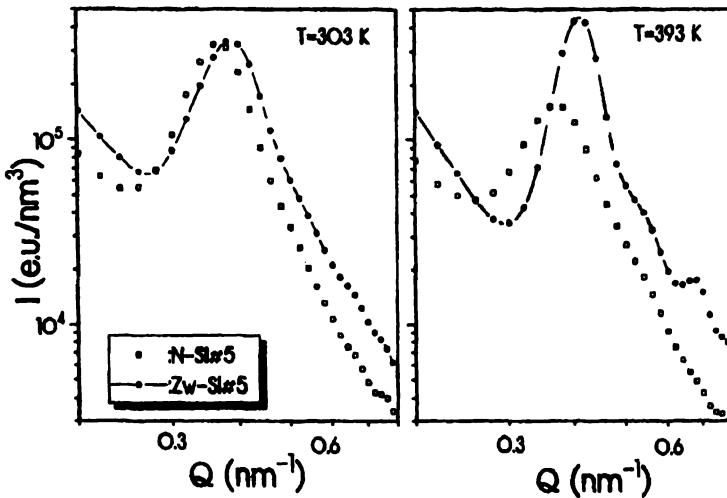
A completely different behavior is observed when the functional group is attached to the PS chain-end, as shown in figure 10. The microdomain peak dominates the scattering pattern in this case. The peak increases in intensity, sharpens and moves to slightly higher Q values with increasing temperature. The absence of any dissolution process clearly indicates that the microdomain structure is stabilized by the ionic aggregates. In the case of ZwSI samples the ionic groups are trapped within the PS phase without being able to aggregate. The increase of temperature increases the mobility of the polar groups leading to the formation of aggregates within the "hard" phase. This is schematically illustrated in figure 11 for both systems, ZwIS and ZwSI. As a consequence the incompatibility of PI and PS is enhanced and a completely different phase behavior is observed. So only by changing the position of the polar group, from the PI to the PS chain-end it is possible to change the phase diagram.

The conclusions derived by SAXS studies were confirmed by rheology. In the case of the zwitterionic copolymers an extension of the rubbery plateau is observed. This behavior is explained considering that the aggregates act as physical crosslinks within the PI phase. Furthermore within the temperature range investigated no sign of an order-disorder transition was observed in agreement with SAXS results, meaning that the cubic microdomain structure is stable up to high temperatures.

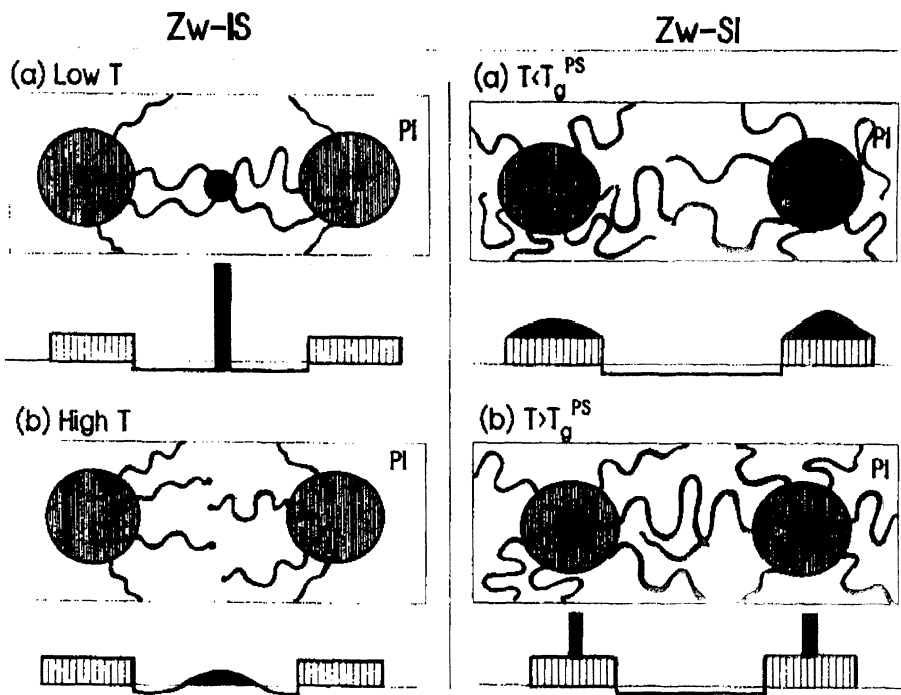
Dielectric spectroscopy also offers the means to verify the conclusions drawn



9. SAXS profiles for two ω -functionalized IS diblock copolymers at $T=303 \text{ K}$. Data have been corrected for the density fluctuations, and the intensities are given in absolute units. (Reproduced by permission from reference 33)



10. Comparison of the SAXS profiles for the dimethylamino- and zwitterion-substituted ω -functionalized copolymers at two temperatures. (Reproduced by permission from reference 33)



11. Schematic illustration of the microstructures in ϕ -functionalized SI block copolymers, showing the Zw-IS (left) and Zw-SI (right) cases at low (upper) and high (lower) temperatures. The corresponding electron density distributions are also shown. (Reproduced by permission from reference 33)

so far through the selective probing of the PI chains. In the case of ZwIS copolymers in addition to the fast segmental and the slow normal mode an intermediate process, with activation parameters which are reminiscent of the segmental process is observed. This intermediate process arises from the regions of the reduced mobility created around the aggregates impeding the motion of the PI chains in their immediate environment. However differential scanning calorimetry, DSC is not so sensitive and the size of these regions very small in order to detect an intermediate Tg value.

The combination of the association process caused by the presence of polar groups in a nonpolar solvent with the micellization procedure, promoted in selective solvents leads to complicated solution behavior. The dilute solution properties of ω -functionalized diblock copolymers having dimethylamine or zwitterion groups at the PS chain-end were studied in *n*-decane a nonpolar selective solvent for the PI blocks (37).

The presence of the polar groups introduces another factor capable to enhance the aggregation numbers for the zwitterionic samples in *n*-decane. Much lower N_w values were observed for the amine-capped copolymers, meaning that the amine groups are not polar enough to enhance the association process. Typical LALLS plots are given in figure 12.

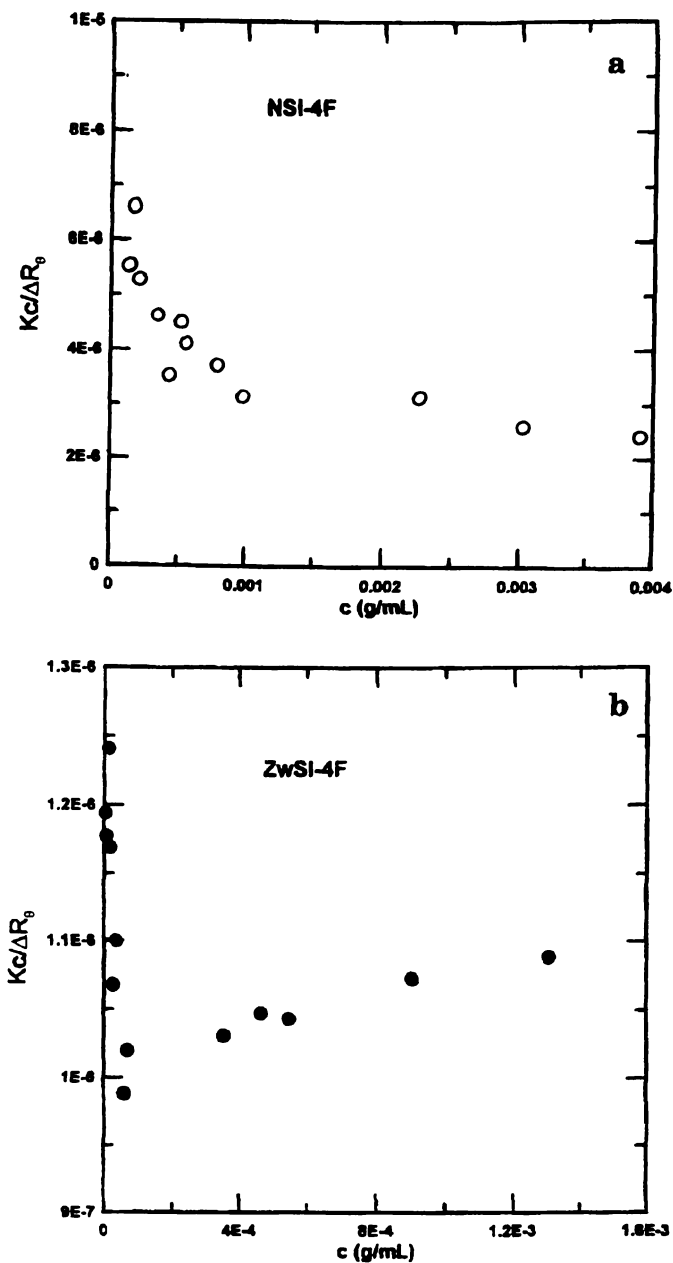
In both cases the plots are curves. For the amine-capped copolymers negative A_2 values are obtained meaning that the equilibrium is not completely shifted towards the micelles.

From DLS measurements negative k_D values were obtained for the amine-capped polymers as expected having in mind the negative A_2 values. For the zwitterionic samples the k_D values were positive meaning that the equilibrium is shifted in favor of the micelles.

Viscometry measurements were also conducted. The Huggins coefficients increase with increasing molecular weight for the amine-capped polymers. This behavior is consisted with a star-like structure. For the zwitterionic samples constant k_H values, around 1.1 were obtained, meaning that rather compact structures exist in solution.

The R_v and R_H values are identical within experimental error for the amine polymers but for the zwitterionic polymers R_H is much higher than R_v . The former result is consistent with star-like structures, whereas the latter can be explained considering the high sensitivity of DLS to large structures and/or to the development of shear forces in the capillary tube able to disrupt the larger aggregates. The fact that the polar core probably has a linear structure with antiparallel placement of the zwitterionic groups is able to support the above assumption, since a break of the association at one point can cause a large reduction of the micelle's size.

Star Shaped Polybutadienes with End-Functional Groups. The amine-capped star polymers provide no evidence of association in cyclohexane, whereas strong association is observed in the case of zwitterionic samples. It is evident that (a) among the different series of polymers the aggregation number decreases with increasing number of functional groups and (b) among the samples with the same



12. $Kc/\Delta R_0$ vs concentration plots are given for (a) sample NSI-4F and (b) sample ZwSI-4F in n-decane at 25°C. (Reproduced by permission from reference 37)

number of polar groups the degree of association decreases with increasing molecular weight of the precursor polymer, due to excluded volume repulsions. These results are given schematically in figure 13.

The multifunctional samples, specially the trifunctional stars form gels even at low concentrations. This result connected with the low aggregation numbers for these samples leads to the conclusion that in very dilute solution intramolecular association dominates and by increasing concentration there is a rather sharp transition from intramolecular to intermolecular association, able to produce stable gels.

The degrees of association of the monofunctional stars are lower than those measured for the linear ω -functionalized PBd, meaning that the star structure prevents the association due to the steric hindrance caused by the unfunctionalized arms.

The hydrodynamic behavior of the functionalized stars was studied by DLS and viscometry (38). The increased values of μ_2/Γ^2 (>0.2) indicate that the aggregates produced by the zwitterionic samples are polydisperse in agreement with the MO and LALLS results. Low k_D values were observed in most cases as a consequence of the decreased second virial coefficients.

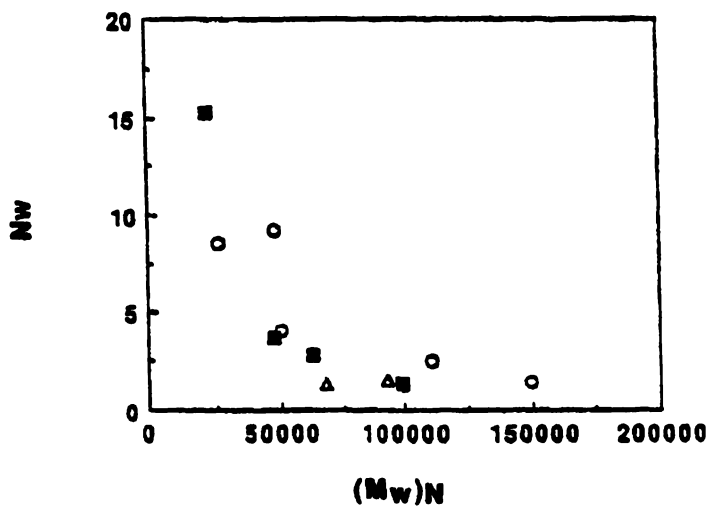
The strongly negative k_D values for the trifunctional stars indicate the existence of strong hydrodynamic interactions between the macromolecular chains eventhough these samples have low aggregation numbers and show only small increases in R_H compared to their precursors. This behavior can be seen as evidence of intramolecular association in very dilute solutions. For the case of difunctional stars the above analysis is not straightforward. It is clear that intermolecular association cannot be ruled out.

For the monofunctional samples there is no possibility of intramolecular association. The star model can be used for these samples considering that the aggregates correspond to star polymers and their precursors to the arms of these stars. Concequently it is possible to calculate the aggregation numbers from DLS measurements, N_{DLS} . The results show that the aggregates formed from the monofunctional samples behave hydrodynamically as star polymers with functionality equal to $2N_w$. It seems that the two unfunctionalized arms anchored at the periphery of the aggregates are responsible for the overall size of the micelles.

The conclusions drawn by DLS are verified by viscometry for the amine-capped polymers. The zwitterionic trifunctional samples have lower intrinsic viscosities than their precursors but the k_H values are extremely high, indicating the presence of strong hydrodynamic interactions. This behavior implies that in very dilute solutions compact structures are formed through intramolecular association. This result is in agreement with LALLS and DLS data.

Comparative examination of R_v and R_H values show that $R_v < R_H$ for the zwitterionic polymers, meaning that the aggregates desassociate to some extent in the capillary tube, due to the shear forces applied therein. It seems that the increased steric repulsions introduced by the unfunctionalized arms lead to the formation of not so strong associates as in the case of linear polymers.

The adsorption behavior of functionalized linear and three arm star PBd was studied by ellipsometry at 20 °C in a mixed solvent of cyclohexane and toluene (50 % by volume) (39). A mixture of cyclohexane and toluene was used. In this mixture



13. Weight-average degree of association, N_w vs base molecular weight $(M_w)N$ of the star polymers: Zw-1N-3PBd (○), Zw-2N-3PBd (■), and Zw-3N-3PBd (△). (Reproduced by permission from reference 22)

association is not detected up to the concentration of 2.0 mg/ml from DLS measurements and the dn/dc values (0.050 ml/g at 589.4 nm at 20.0 °C) provide enough contrast for accurate measurements.

Various parameters of the adsorption behavior of the samples are reported in Table II. The adsorped amount A is increased with decreasing molecular weight for the

TableII. Various parameters of ω -functionalized linear (L) and mono-(1N)-, Di-(2N)-, and tri-(3N)- ω -functionalized polybutadienes.

Sample	A_{plateau} (mg/m ²)	σ (chains/nm ²)	D_{inter} (nm)	D_{over} (nm)	$\delta = D_{\text{inter}}/D_{\text{over}}$
Zw-L-PBd12	2.47+0.01	0.125	2.8	10.5	0.27
Zw-L-PBd20	2.410+.25	0.07	3.8	14.5	0.26
Zw-L-PBd80	1.69+0.18	0.012	9.1	33.3	0.27
Zw-1N-3PBd30	1.77+0.17	0.0096	10.2	25.2	0.4
Zw-2N-3PBd30	1.86+0.06	0.0179	7.5	19.1	0.39
Zw-2N-3PBd40	1.90+0.12	0.0128	8.8	25.2	0.35
Zw-3N-3PBd25	2.14+0.18	0.0191	7.2	19.7	0.37
Zw-3N-3PBd40	2.3+0.2	0.0148	8.2	24.3	0.34

linear samples. The longer the PBd chains adsorped the bigger space they occupy and the stronger the repulsion between them. The ratio $\delta = D_{\text{inter}}/D_{\text{over}}$ of the interchain distance (D_{int}) over the space needed to accomodate a swollen polymer coil in a good solvent in it's unperturbed state on the surface (D_{over}) is much lower than unity. This indicates that the adsorped chains are stretched adopting a brush-like conformation.

In the case of the zwitterionic stars the adsorped amount increases with increasing number of functionalized arms. The grafting density ϕ , defined as $\phi = AN_A/M_w$, where A is the adsorped amount, N_A the Avogadro number and M_w the weight average molecular weight of the star seems to present stronger dependance on the molecular weight than the functionality of the stars. The σ values of the samples Zw-2N-3PBd30 and Zw-3N-3PBd25 are very close indicating that despite the fact that the adsorption energy is high the entropic loss involved in the attachment of the third arm when two arms are already attached may be very high.

The adsorption kinetics, studied by time-resolved ellipsometry show two processes. At the initial stages the adsorption is diffusion controled. At longer times the polymers must penetrate the barrier formed by the initially adsorped chains. It was found that the star polymers penetrate this barrier faster than the linear chains, due to the different conformations adopted by the stars.

Literature Cited

1. Lundberg R.D.; Phillips R.R. *J. Polym. Sci. Polym. Phys. Ed.* **1982**, *20*, 1143
2. Hegedus R.D.; Lenz R.W. *J. Polym. Sci., Part A: Polym. Chem.* **1988**, *26*, 367
3. Hara M.; Wu J. *Multiphase Polymers: Blends and Ionomers*; Utracki L.A.; Weiss

- R.A Eds.; ACS Symposium Series 395; American Chemical Society: Washington, DC, 1988, Chapter 19
4. Nagata N.; Kobatake T.; Watanabe H.; Veda A.; Yoshioka A. *Rubber Chem. Technol.* **1987**, *60*, 837.
 5. Broze G.; Jerome R.; Teyssie P. *Macromolecules* **1981**, *14*, 224
 6. Broze G.; Jerome R.; Teyssie P. *Macromolecules* **1982**, *15*, 1300
 7. Zhou Z.; Chu B.; Wu G.; Peiffer D.G. *Macromolecules* **1993**, *26*, 2968
 8. Fitzgerald J.J.; Weiss R.A. *J. Macromol. Sci., Rev. Macromol. Chem. Phys.* **1988**, *C28*, 1
 9. Mauritz K. A. *J. Macromol. Sci., Rev. Macromol. Chem. Phys.* **1988**, *C28*, 65
 10. Lenz R.W. *Organic Chemistry of Synthetic High Polymers* Interscience, New York, 1967
 11. Kennedy J.P. *Rubber Chem. Technol. Reviews* **1983**, *56*, 639
 12. Sogah D.Y.; Webster O.N. *J. Polym. Sci. Polym. Lett. Ed.* **1983**, *21*, 927
 13. Young R.N.; Quirk R.P.; Fetters L.J. *Adv. Polym. Sci.* **1984**, *56*, 1
 14. Bywater S. Anionic Polymerization in *Encyclopedia of Polymer Science and Engineering* Vol. 2
 15. Stewart M.J.; Shepherd N.; Service D.M. *Br. Polym. J.* **1990**, *22*, 319
 16. Pispas S.; Pitsikalis M.; Hadjichristidis N.; Dardani P.; Morandi F. *Polymer* **1995**, *36*, 3005
 17. Morton M. Anionic Polymerization. Principles and Practice Academic Press, New York, 1983.
 18. Johnson A.F.; Worsfold D.J. *J. Polym. Sci.* **1965**, *3*, 449
 19. Tobolsky A.V.; Rogers C.E. *J. Polym. Sci.* **1959**, *40*, 73
 20. Pispas S.; Hadjichristidis N. *Macromolecules* **1994**, *27*, 1891
 21. Davidson N.S.; Fetters L.J.; Funk W.G.; Graessley W.W.; Hadjichristidis N. *Macromolecules* **1988**, *21*, 112
 22. Pitsikalis M.; Hadjichristidis N. *Macromolecules* **1995**, *28*, 3904
 23. Bahr U.; Weiden H.; Rinkler H.-A.; Nische G. *Makromol. Chem.* **1972**, 161
 24. Monroy Soto V.M.; Galin J.C. *Polymer* **1984**, *25*, 121
 25. Pitsikalis M. Ph. D. Thesis University of Athens, 1994
 26. Schulz D.N.; Peiffer D.G.; Agarwal P.K.; Larabee J.; Kaladas J.J.; Soni L.; Handwerker B.; Garner R.T. *Polymer* **1986**, *27*, 1734
 27. Borlenghi A.; Pitsikalis M.; Pispas S.; Hadjichristidis N. *Macromol. Chem. Phys.* **1995**, *196*, 4025
 28. Pitsikalis M.; Siakali-Kioulafa E.; Hadjichristidis N. *J. Polym. Sci., Part B: Polym. Phys. Ed.* **1996**, *34*, 249
 29. Shen Y.; Safinya C.R.; Fetters L.J.; Adam M.; Witten T.; Hadjichristidis N. *Phys. Rev.* **1991**, *43*, 1886
 30. Fetters L.J.; Graessley W.W.; Hadjichristidis N.; Kiss A.D.; Pearson D.S.; Younhouse L.B. *Macromolecules* **1988**, *21*, 1644
 31. Pearson D.S.; Helfand E. *Macromolecules* **1984**, *17*, 888
 32. Pispas S.; Hadjichristidis N.; Mays J.W. *Macromolecules* **1994**, *27*, 6307
 33. Floudas G.; Fytas G.; Pispas S.; Hadjichristidis N.; Pakula T.; Khokhlov A.R. *Macromolecules* **1995**, *28*, 5109

34. Floudas G.; Fytas G.; Pispas S.; Hadjichristidis N.; Pakula T.; Khokhlov A.R. *Macromol. Symp.* **1996**, *106*, 137
35. Chu B.; Wang J.; Li Y.; Peiffer D. *Macromolecules* **1992**, *25*, 4229
36. de Gennes P.-G. *Scaling Concepts of Polymer Physics*, Cornell University Press, Ithaca, New York **1979**
37. Pispas S.; Allorio S.; Hadjichristidis N.; Mays J.W. *Macromolecules* **1996**, *29*, 2903
38. Pitsikalis M.; Hadjichristidis N.; Mays J.W. *Macromolecules* **1996**, *29*, 179
39. Siqueira D.F.; Pitsikalis M.; Hadjichristidis N.; Stamm M. *Langmuir* **1996**, *12*, 1631

Chapter 9

Novel Functional Copolymers by Combination of Living Carbocationic and Anionic Polymerizations

Jesper Feldthusen, Bela Iván¹, and Axel H. E. Müller²

Institut für Physikalische Chemie, Universität Mainz, Germany

A new synthetic route for the preparation of polyisobutylene (PIB) based block copolymers was developed by combining living carbocationic and anionic polymerizations. Living PIB chains were quantitatively end-capped with 1,1-diphenylethylene (DPE) leading to 1,1-diphenyl-1-methoxy (DPOMe) and/or 2,2-diphenylvinyl (DPV) termini. This end-capping process is very sensitive to temperature, and retroaddition of DPE occurs in an equilibrium reaction above about -70 °C. Both the DPOMe and DPV terminated PIBs, and the mixtures of the two endgroups were quantitatively metalated with K/Na alloy, Cs metal and Li dispersion in THF at room temperature. ¹H NMR studies of the corresponding model compounds, 3,3,5,5-tetramethyl-1,1-diphenylhex-1-ene (DPV) and 1-methoxy-3,3,5,5-tetramethyl-1,1-diphenylhexane (MDPE) clearly verify the quantitative degree of metalation. The resulting stable macrocarbanion obtained by metalation with K/Na alloy was used to initiate living anionic polymerization of *tert*-butyl methacrylate (tBMA) yielding PIB-*b*-PtBMA block copolymers with nearly quantitative blocking efficiency. Hydrolysis of the ester groups by HCl in dioxane resulted in amphiphilic poly(isobutylene-*b*-methacrylic acid) block copolymers. Replacing K⁺ with Li⁺ by excess LiCl gave a PIB macroinitiator suitable for anionic polymerization of methyl methacrylate (MMA). A series of PMMA-*b*-PIB-*b*-PMMA block copolymers was successfully synthesized by telechelic PIB macroanions with high blocking efficiencies. Characterizations of these new thermoplastic elastomers were carried out by SEC, DSC, dynamic-mechanical, and stress-strain measurements.

Living polymerizations provide the most versatile synthetic routes for the preparation of a wide variety of well-defined polymer structures. Macromonomers

¹Current address: Central Research Institute for Chemistry of the Hungarian Academy of Sciences, H-1525 Budapest, Puskaszeri u. 59-67, P. O. Box 17, Hungary.

²Corresponding author.

and telechelic polymers are usually obtained by quantitative end-quenching of living chain ends and/or by further end-functionalization of end-quenched polymer chains. Sequential addition of different monomers yield block copolymers which are also of great scientific and commercial importance. Since specific living polymerization methods (e. g. living anionic and carbocationic polymerizations) are applicable only to a limited number of monomers, the combination of different living polymerization techniques is expected to lead to new and unique, otherwise unavailable polymer architectures.

In recent years, there have been significant developments in the field of living carbocationic polymerization (LCCP) of vinyl monomers, such as isobutylene (IB), styrene and its derivatives, and vinyl ethers, leading to a wide variety of functional polymers (for recent reviews see Refs. 1-4). Due to the attractive properties of polyisobutylene (PIB) available only by carbocationic polymerization, coupling this hydrophobic, thermally, oxidatively, and hydrolytically stable polymer with a low T_g to a variety of other chain segments is expected to result in new useful products. For instance, methacrylate-telechelic PIB (MA-PIB-MA) obtained by LCCP and subsequent chain end derivatization has been successfully used to synthesize novel amphiphilic networks by radical copolymerization of MA-PIB-MA with a variety of monomers, such as *N,N*-dimethylacrylamide and 2-trimethylsilyloxyethyl methacrylate, a protected 2-hydroxyethyl methacrylate (HEMA)^{1,5-7}.

Several attempts have also been made for obtaining block copolymers by utilization of end-functionalized PIBs as macroinitiators for living anionic polymerization in order to synthesize new useful thermoplastic elastomers (TPE). One attempt used isobutyrate-telechelic PIB which was prepared by the following reaction sequence: Living polymerization of isobutylene yielded *tert*-chlorine-telechelic PIB (Ref. 1 and references therein), then the *tert*-chlorine chain ends were quantitatively converted to isobutenyl endgroups by quantitative dehydrochlorination⁸ or alternatively, allyl-telechelic PIB was prepared by direct end-quenching of LCCP of isobutylene by allyltrimethylsilane⁹. Both olefin termini can be quantitatively converted to primary hydroxyl chain ends by hydroboration followed by oxidation^{9,10}. Reacting hydroxyl-telechelic PIB with isobutyrylchloride gave isobutyrate-telechelic PIB^{11,12}. Lithiation of these isobutyrate-telechelic PIBs with LDA^{11,12} was reported to lead to initiation of methyl methacrylate (MMA) polymerization for the synthesis of PMMA-*b*-PIB-*b*-PMMA block copolymers. The isobutyrate endgroups were also converted to silyl ketene acetal chain ends, which subsequently were used to initiate group transfer polymerization of MMA¹³.

In another approach¹⁴, lithiation of tolyl-telechelic PIB obtained by Friedel-Crafts alkylation of *tert*-chlorine-ended PIB¹⁵ and subsequent addition of 1,1-diphenylethylene (DPE) to the metalated chain ends were applied to initiate the polymerization of MMA. Living PMMA chains were also attached to PIB containing short endblocks of poly(*p*-vinylbenzylbromide)¹⁶. Although detailed characterization of the products is not available, this method is expected to yield PMMA branches at the PIB termini.

Metalated PIB obtained by one-pot dehydrochlorination-metalation of *tert*-chlorine-ended PIB by potassium-*t*-amylate/*n*BuLi and *t*BuOK/*n*BuLi mixtures was used to initiate the anionic polymerization of butadiene resulting PIB-polybutadiene block copolymers¹⁷.

All these methods have several disadvantages: multistep endgroup derivatizations are required for the synthesis of the telechelic PIB initiator precursor, and lithiation and thus the subsequent initiation of anionic polymerization is not quantitative or it requires extreme conditions. As a consequence of less than 100 % initiating efficiency these methods yielded mixtures of homopolymers and block copolymers. This is indicated by the fact that it was claimed that PMMA-*b*-PIB-*b*-PMMA was only obtained by selective extraction¹¹⁻¹⁴.

It has been recently found that one-pot end-quenching of LCCP with DPE, a non-homopolymerizable olefin in cationic polymerization, may yield either 1-methoxy-1,1-diphenylethyl (DPOMe)¹⁸ or 2,2-diphenylvinyl (DPV)^{19,20} chain ends depending on the conditions during quenching and workup.

The relatively stable, highly ionized cationic chain end formed by DPE addition was reacted with living PMMA chains carrying silyl ketene acetal endgroups obtained by group transfer polymerization resulting in PIB-*b*-PMMA block copolymer²¹. However, the major disadvantage of this method is its applicability only under very specific conditions and precise stoichiometry. In addition to this, the titanium compounds (most likely Ti(OR)_xCl_{4-x}) present in this system cleave the coupled blocks by forming PMMA with titanium enolate endgroups and thereby decrease the blocking efficiency.

Both the 2,2-diphenylvinyl and the 1-methoxy-1,1-diphenylethyl chain ends are potential endgroups for the anionic polymerization of a variety of monomers by metalation. Our earlier results indicate that quantitative metalation of the 2,2-diphenylvinyl endgroups with alkyllithium cannot be achieved, most likely because of steric hindrance²⁰. However, as described recently²², the ether cleavage of 1-methoxy-1,1-diphenyl-3,3,5,5-tetramethylhexane or electron transfer to 3,3,5,5-tetramethyl-1,1-diphenylhex-1-ene by K/Na alloy, Cs or Li led to quantitative metalation resulting in nearly quantitative initiation of the polymerization of methacrylic monomers. Both precursors led to identical (macro)initiators verified by ¹H NMR.²² These compounds can be considered as models of PIB chain ends formed by LCCP of IB and subsequent end-capping with DPE. The present study deals with the application of this method to the synthesis of different AB and ABA block copolymers by the combination of LCCP and living anionic polymerization.

Experimental Section

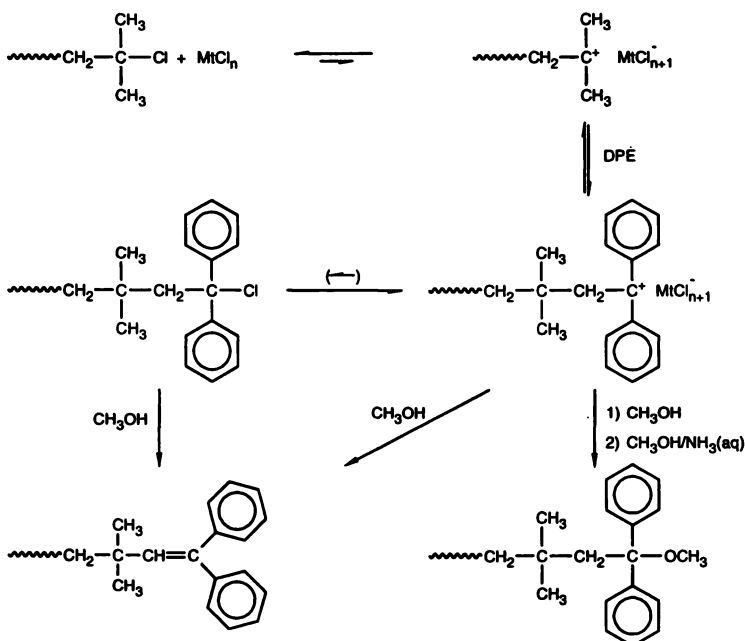
Experimental details can be found elsewhere.²²⁻²⁴

Results and Discussion

Effect of the reaction conditions on the end-capping with DPE. Two procedures were investigated for the synthesis of PIB macroinitiators by living carbocationic polymerization (LCCP) of isobutylene (IB) and for the subsequent endcapping with DPE. A two-step system²⁵ with sequential polarity change and addition of two different coinitiators, BCl₃ and TiCl₄, and a one-step polymerization in which only TiCl₄ was used as coinitiator. The reason for using the two-step system was based on earlier experience²⁵ according to which narrower molecular weight distributions (MWD) can be reached in the range 3000 ≤ M_n ≤ 8000 with this polymerization system than with that coinited by TiCl₄ alone.

The major processes occurring in the course of endcapping of living PIB with DPE are shown in scheme 1. Quenching the DPE-capped living polymers with methanol-ammonia lead to quantitative (> 98%, verified by ^1H NMR) formation of 1,1-diphenyl-1-methoxy (DPOMe) endgroups when only TiCl_4 was used. 2,2-Diphenylvinyl (DPV) chain ends were obtained quantitatively when only methanol was used as quenching agent and the quenched polymer solution was left for more than four hours before further purification. The formation of DPV chain ends is due to the acidic nature of the solution leading to elimination of methanol from the DPOMe termini formed initially. In some cases dissolution of the polymer in CHCl_3 containing traces of HCl provided quantitative elimination. When only BCl_3 was present as coinitiator less than quantitative capping was found²⁶ in $\text{CH}_2\text{Cl}_2/\text{n-hexane}$ 40:60 v/v solvent mixture since the DPE addition is an equilibrium reaction. The equilibrium constant for a system containing only BCl_3 is about 3 orders of magnitude smaller than that for the polymerization system with TiCl_4 coinitiator²⁶. However, in the two-step procedure, >96% capping efficiency was reached when the molar ratio of the two Lewis acids is 1:1 in $\text{CH}_2\text{Cl}_2/\text{n-hexane}$ (40:60 v/v) mixture.

Scheme 1. Functionalization of living PIB chain ends with DPE



Not only the choice of Lewis acid, solvents and quenching conditions are important but also the reaction temperature for obtaining precursors suitable for subsequent metalation.²⁶ In an experiment carried out in the usual way at -78 °C ($\text{CH}_2\text{Cl}_2/\text{n-hexane}$ and $\text{TiCl}_4/\text{N,N-dimethylacetamide}$), the polymerization system was allowed to warm up slowly, and samples were withdrawn at different temperatures. The yield of DPE-capped product is shown as a function of temperature in Figure 1.

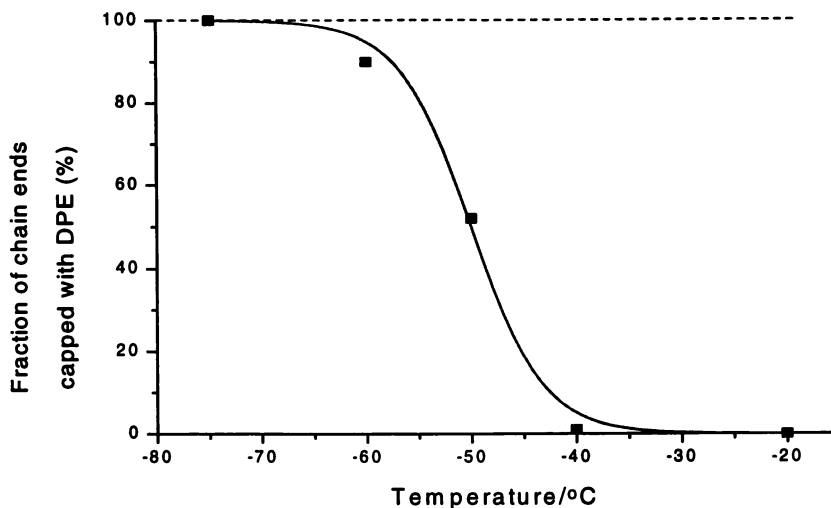


Fig. 1. Effect of temperature on the equilibrium addition of DPE to living PIB chain ends (solvent: 60:40 n-hexane/ CH_2Cl_2 , TiCl_4 , $n_{\text{DMA}} = n_{\text{initiator}} = n_{\text{DPE}}$).

While quantitative endcapping is observed at -78°C , the capping yield rapidly decreases with increasing temperature. ^1H NMR spectra show 90% DPE capping and 10% *tert*-chlorine endgroups at -60°C , and no DPE-capped PIB was found at and above -40°C .

In order to further investigate this phenomenon, DPOMe-ended PIB was prepared, purified, and then dissolved in CH_2Cl_2 /n-hexane solvent mixture (40/60 v/v), cooled to -78°C , and polymerization conditions were created by adding N,N-dimethylacetamide and TiCl_4 . This system was also allowed to warm up, and samples were withdrawn at different temperatures. Results identical to the experiment shown in Figure 1 were observed, indicating that retroaddition of DPE takes place from the DPOMe-ended PIB.

In conclusion, the polymerization temperature should be kept below -75°C in order to reach quantitative endcapping under the conditions used in this work (n-hexane: CH_2Cl_2 60:40, $[\text{I}] \approx 10^{-2}$ M, $[\text{DMA}] \approx 10^{-2}$ M, $[\text{TiCl}_4] \approx 10^{-1}$ M, and $[\text{DPE}] \approx 5 \cdot 10^{-2}$ M).

Metalation of diphenylmethoxy- and diphenylvinyl-ended PIB. As we reported recently²², metalation of model compounds of the corresponding PIB chain ends, i.e. 1-methoxy-1,1-diphenyl-3,3,5,5-tetramethylhexane and 1,1-diphenyl-3,3,5,5-tetramethylhex-1-ene, is quantitative with K/Na alloy, Cs, Na, and Li suspension. The resulting carbanions led to a living anionic polymerization of methacrylic monomers with $\approx 100\%$ initiating efficiency²². In order to prepare the desired block copolymers, it was of interest whether the quantitative metalation results obtained with the model compounds can be converted to the PIB macroprecursors within a broad range of molecular weights. Scheme 1 and 2 outline the chemical transformations in the course of endcapping of living PIB chains with DPE and the subsequent formation of the carbanionic macroinitiator upon metalation, respectively.

Scheme 2. Metalation of DPOMe- and DPV-ended PIB with alkali metals/alloys

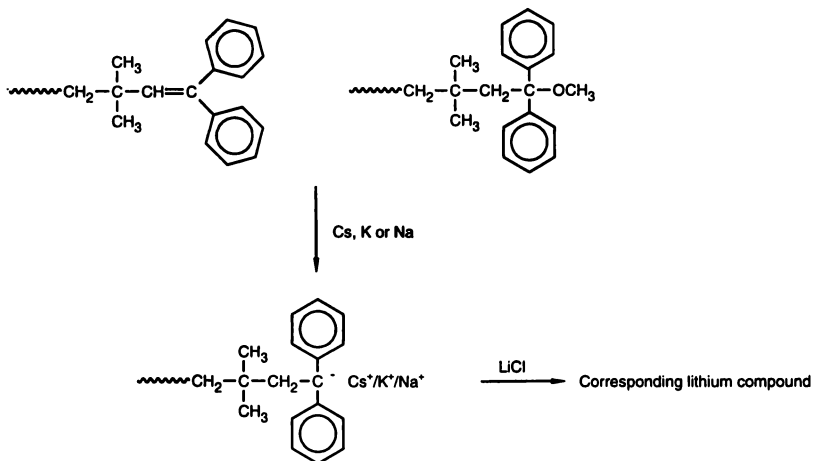


Figure 2 summarizes the time-conversion plots obtained by UV-visible spectroscopy for PIB samples with the degree of polymerization in the range of $2 \leq P_n \leq 570$. As shown in this figure, the molecular weight has no significant effect on the rate of metalation. Quantitative metalation of DPE-capped PIBs can be achieved within 60 minutes.

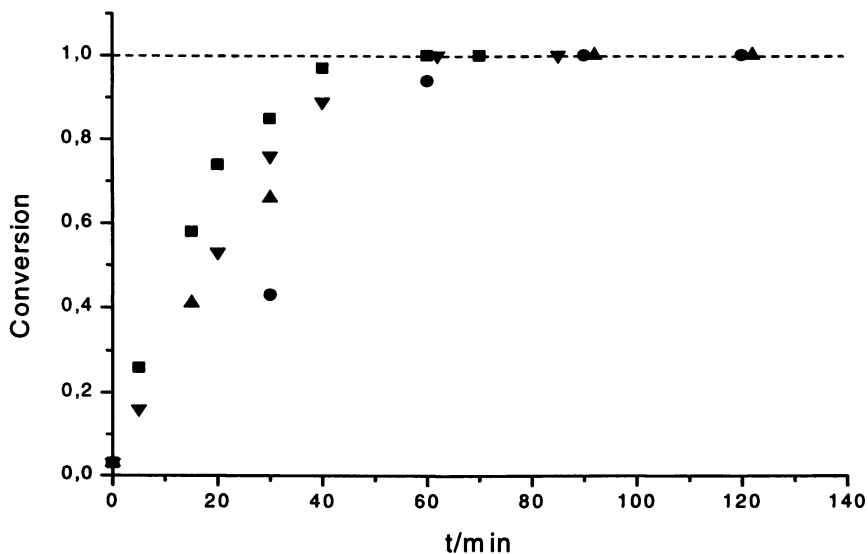


Fig. 2. Time-conversion plots for metalation of DPE-capped PIBs with K/Na alloy as followed by UV-VIS absorbance at $\lambda = 480$ nm, $M_n = 150$ (■), $M_n = 5000$ (●), $M_n = 17,500$ (▲), $M_n = 32,000$ (▼)

As it is known from literature²⁷, electron transfer to DPE with K/Na alloy at room temperature yields a radical anion which recombines leading to 1,1,4,4-tetra-phenyl butyl dianion which is a difunctional initiator. Therefore, coupling could also be expected when metalating DPV-ended PIB. However, the SEC eluograms of PIB with DPV endgroups before and after metalation are identical indicating the absence of coupling upon metalation. This confirms results obtained with the corresponding model compound²². The absence of coupling during metalation of DPV-ended PIB, can be explained by the steric hindrance caused by the two methyl groups adjacent to the radical carbon. The stability of the PIB-DPE⁻ K⁺ ion pair was also tested. It was found that the intensity of the UV-visible absorption at 480 nm did not change even after 10 days indicating the high stability of this macroinitiator in THF at room temperature.

The effect of non-quantitative endcapping on the metalation process was also investigated. A difunctional PIB sample having 85% DPV and 15% *tert*-chlorine chain ends was metalated with K/Na alloy as described (in ref. 23). After 60 min the reaction was quenched with methanol, and the resulting material was analyzed by SEC. Coupling occurs between the carbanion and the *tert*-chlorine containing endgroups. Since the precursor PIB is difunctional, multiple coupling occurs resulting in a multimodal MWD with peak maxima corresponding to multiples of the molecular weight of the precursor. There are two important consequences of these findings: The endcapping reaction with DPE should be quantitative during LCCP of IB, on one hand. The absence of coupling during metalation of the DPE-capped PIB is an indirect proof for quantitative endcapping, on the other hand. Since even relatively low amounts of coupling can be detected by SEC, this can be utilized for testing the yield of DPE capping for high molecular weight PIBs ($M_n > 10000$) when ¹H NMR or UV-VIS spectroscopies cannot be used for reliable endgroup analysis.

Synthesis and characterization of block copolymers. *Polyisobutylene-b-poly(tert-butyl methacrylate)* (PIB-*b*-PtBMA) block copolymers were synthesized by using the PIB-DPE⁻ K⁺ macroanion as initiator for the polymerization of tBMA.

First, an experiment was carried out for investigating the blocking efficiency. Therefore, the block lengths were chosen in a way that the peaks of the PIB precursor and the PIB-*b*-PtBMA block copolymer in the SEC eluogram are separated from each other. Figure 3 shows the SEC eluogram (UV signal at 260 nm) for such a block copolymer. It can be seen that only a small peak appears for the unreacted PIB. Since only the aromatic rings absorb at this wavelength, integration allows to estimate the blocking efficiency which is higher than 95%. The resulting block copolymer has narrow MWD with $M_w/M_n = 1.06$.

At the start of these series of blocking experiments the effect of the PIB endgroup structure in PIB was also investigated. To one reactor a DPOME-capped PIB was added, and to another a 50:50 mixture of DPOME- and DPV-capped PIB. After metalation with K/Na alloy tBMA was charged to both reactors. In both cases, nearly identical blocking efficiencies were obtained which proves that the metalation and the subsequent polymerization are not influenced by the ratio of the two chain ends. The independence of the metalation and anionic polymerization on the ratio of the diphenylvinyl and diphenylmethoxy endgroups is a very important finding. This means that it is not necessary at all to care about the chain end composition of the DPE-capped PIB in the course of its preparation by LCCP. Both the DPOME- and

DPV-capped PIB chains in a mixture yield the same macroanion (Scheme 2) and lead to the same block copolymer by anionic polymerization.

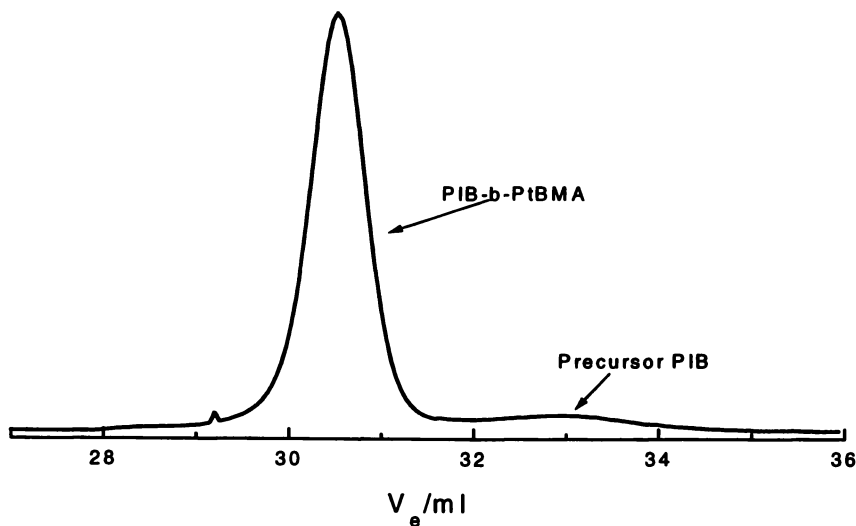
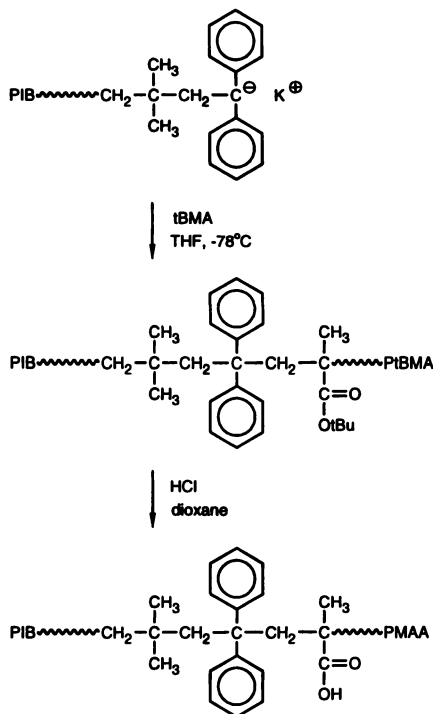


Fig. 3. SEC eluogram (UV signal at 260 nm) of PIB-*b*-PtBMA ($M_n \approx 32000$, $M_w/M_n \approx 1.05$) obtained from a PIB precursor with $M_n = 5800$

Scheme 3. Synthesis of amphiphilic PIB-*b*-PMAA block copolymer



Polyisobutylene-b-poly(methacrylic acid) (PIB-b-PMAA) was prepared by hydrolysis of the ester group under acidic conditions, using HCl(aq) in dioxane. After hydrolysis a new amphiphilic diblock copolymer is formed as shown in Scheme 3. The resulting amphiphilic block copolymers form a stable polymeric emulsions in dioxane.

Synthesis of *poly(methyl methacrylate)-b-polyisobutylene-b-poly(methyl methacrylate) (PMMA-b-PIB-b-PMMA)* triblock copolymers was also performed (see Table I). First, a series of DPE-capped telechelic PIBs were prepared by using a difunctional initiator (tBuDiCumCl) for LCCP of IB.

Table I. M_n of the PIB midsegment and the PMMA outer blocks, the blocking efficiency (f_{block}) and the polydispersity of the resulting block copolymer obtained by anionic polymerization of MMA using different difunctional DPOMe-PIB-DPOMe precursors in THF at $-78\text{ }^\circ\text{C}$ (gegenion: Li^\oplus).

sample no.	M_n PIB	M_n PMMA ^a	f_{block}^b	M_w/M_n^b
ABA1	6300	6400	> 0.95	1.13
TPE32	17,500	2200	> 0.95	1.10
TPE31	17,500	3200	> 0.95	1.09
TPE33	17,500	5800	> 0.95	1.11
TPE44	32,000	9000	> 0.95	1.13
TPE45	32,000	6900	> 0.95	1.13
TPE46	32,000	4500	> 0.95	1.12

^aPer block

^bCrude polymer - no extraction

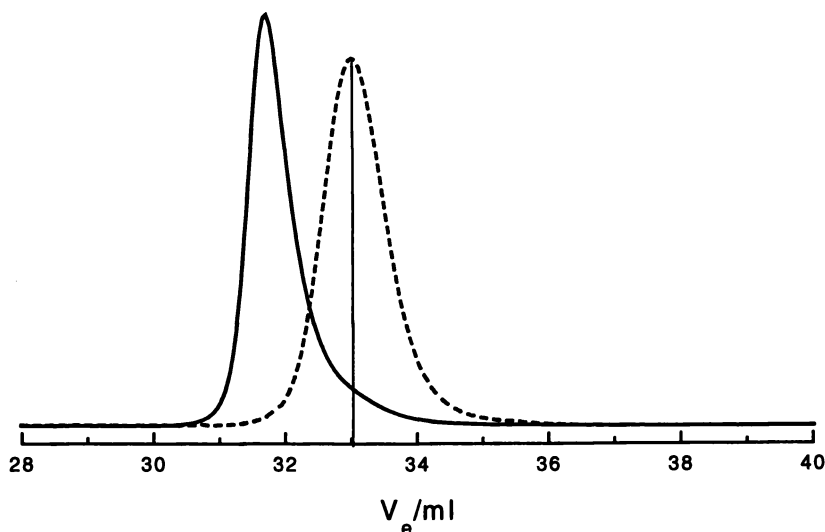


Fig. 4. SEC eluograms (RI signal) of a difunctional PIB precursor ($M_n = 6300$, $M_w/M_n = 1.12$) (---) and the corresponding triblock copolymer ABA1 (—) after anionic polymerization of MMA ($M_n = 18,000$, $M_w/M_n = 1.13$)

In an orienting experiment, the molecular weight of the difunctional PIB macroinitiator was relatively low compared to the outer PMMA segments in order to obtain sufficient separation by SEC between the PIB precursor and the expected triblock in order to check the efficiency of this new system. As shown in Figure 4, the resulting block copolymer has unimodal narrow MWD. The SEC eluograms in this figure also indicate high blocking efficiency. Indeed, extraction by hexane removed only 4% PIB and small amounts of block copolymer after 1 month. These results clearly verify nearly quantitative blocking efficiency and the formation of the desired PMMA-*b*-PIB-*b*-PMMA block copolymer.

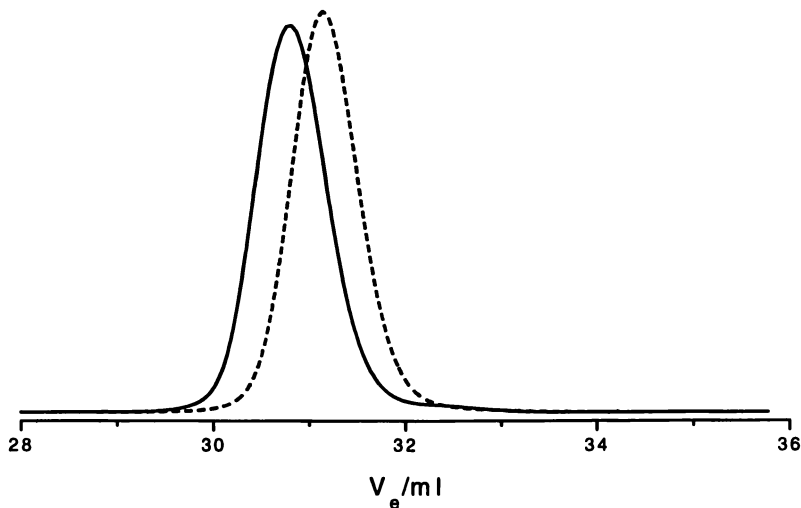


Fig. 5. SEC eluograms (RI signal) of a difunctional PIB precursor ($M_n = 17,500$) (---) and the corresponding PMMA-*b*-PIB-*b*-PMMA with $M_n(\text{PMMA}) = 3200$ (—)

Since thermoplastic elastomers usually have rubbery mid-segment of 60-70 wt-% and of higher molecular weight, difunctional PIB precursors with $M_n > 15,000$ were also prepared. The SEC eluograms of an example are shown in Figure 5. A uniform shift to higher molecular weights can be seen in this Figure after block formation. Since the eluograms of the PIB precursor with $M_n = 17,500$ and the ABA block copolymer having outer PMMA segments with $M_n = 3200$ overlap, it is difficult to use SEC for the verification of quantitative blocking efficiency in this range of block copolymer composition. However, the resulting triblock has unimodal and narrow MWD ($M_w/M_n = 1.10$) which is a good indication for controlled synthesis of the desired triblock copolymer.

A second PIB precursor with $M_n = 32,000$ was used for the synthesis of another series of triblock copolymers. However, solubility problems arose during the polymerization of MMA since the precursor precipitated in THF below $-55\text{ }^\circ\text{C}$. The polymerization of MMA with the high molecular weight PIB macroinitiator resulted in polymers with multimodal MWD due to uncontrolled polymerization of MMA at

-50 °C. In order to increase the solubility of PIB at -78 °C, anionic polymerizations of MMA were performed in a 70:30 THF/n-hexane mixture. PMMA-*b*-PIB-*b*-PMMA with unimodal MWD and low polydispersity ($M_w/M_n = 1.10$) indicating high blocking efficiency was obtained.

In experiments involving difunctional PIBs with $M_n > 15,000$ a temporary precipitation was observed right after the addition of MMA. The precipitate dissolves after about 10-15 min. The precipitation is most likely due to the aggregation of the lithiated chain ends surrounded by the non-polar PIB leading to the formation of a coordinative network which is redissolved after a certain length of the PMMA segments is reached.

Preliminary investigations were also carried out on the physical properties of the PMMA-*b*-PIB-*b*-PMMA block copolymers. A representative DSC curve is shown in Figure 6. As indicated in Figure 6 and in Table II the block copolymers have two glass transitions corresponding to microphase separation of the two segments.

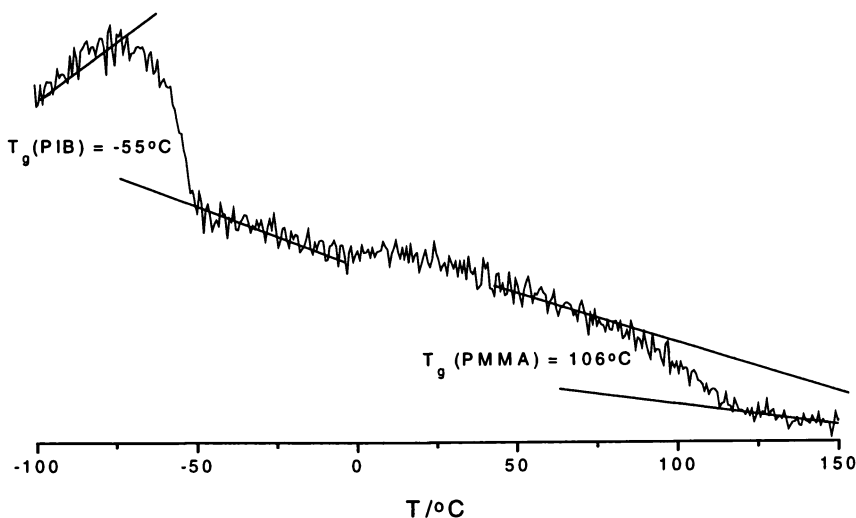


Fig. 6. DSC curve of PMMA-*b*-PIB-*b*-PMMA (TPE31) (see Table II) (2nd heating, 20°C/min)

Table II. Molecular weight of PMMA segments, composition, glass transition temperatures, tensile strength, and elongation at break of PMMA-*b*-PIB-*b*-PMMA block copolymers (precursor: difunctional PIB with $M_n = 17,500$)

Sample	M_n PMMA ^a	PMMA wt-%	T_g /°C PIB	T_g /°C PMMA	Ultimate tensile strength (MPa)	Elongation at break (%)
TPE32	2200	21	-55	94	1.7	150
TPE31	3200	27	-55	106	4.1	230
TPE33	5800	41	-56	110	8.1	310

^aPer block

Dynamic mechanical analysis also verifies the presence of the transitions in the vicinity of $-60\text{ }^{\circ}\text{C}$ and $110\text{ }^{\circ}\text{C}$ as displayed in Figure 7.

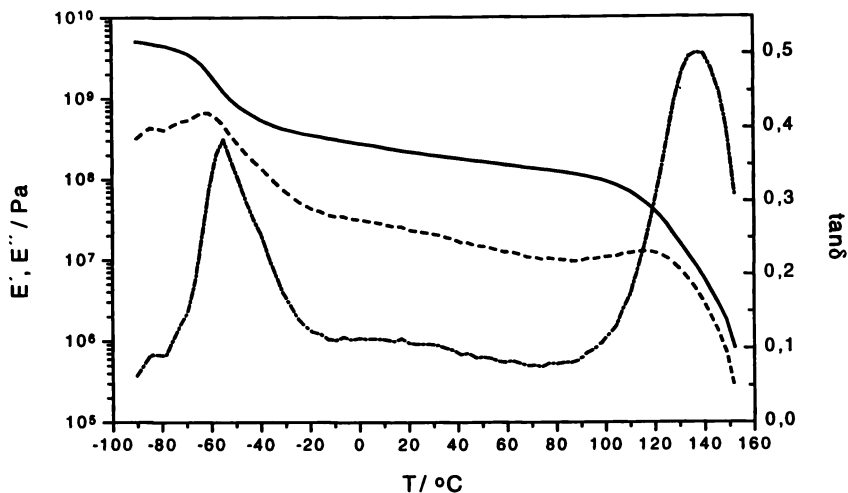


Fig. 7. Dynamic-mechanical analysis of TPE31 (see Table II); E' (—), E'' (---), $\tan\delta$ (-·-)

Stress-strain measurements were performed with solvent-cast films of three triblock copolymers having the same PIB precursor but different PMMA chain length (see Table II). A typical stress-strain curve is shown in Figure 8. The low tensile strength might be due to the sample/film preparation and/or the presence of a certain amount of PMMA-*b*-PIB diblock copolymer. Further mechanical studies and the synthesis of different thermoplastic elastomers are in progress.

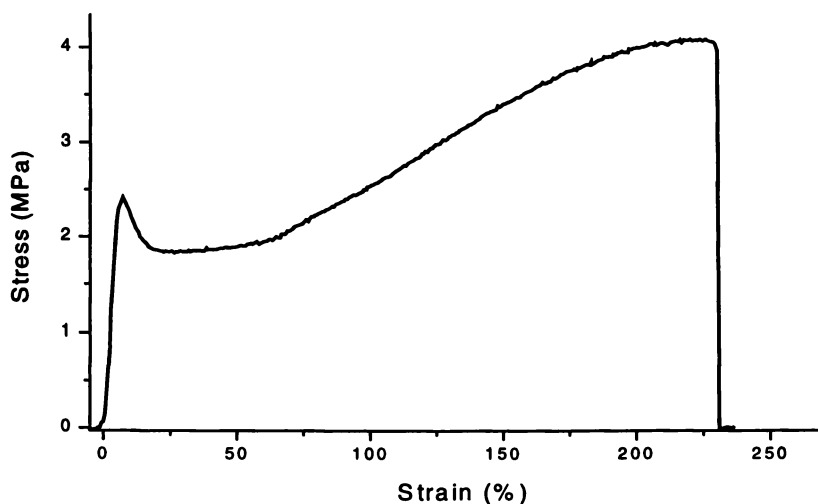


Fig. 8. Stress-strain curve of TPE31 (see Table II)

Conclusions

A new method for the synthesis of polyisobutylene-based block copolymers, involving living carbocationic polymerization of isobutylene and subsequent living anionic polymerization of methacrylic monomers has been demonstrated. Di- and triblock copolymers nearly free of PIB precursor and with narrow and unimodal MWD were synthesized under well-controlled conditions.

The PIB macroinitiators can also initiate living anionic polymerization of a wide variety of functional monomers, such as vinyl pyridine, N,N-dimethylacrylamide, and a variety of protected monomers, such as silylated 2-hydroxyethyl methacrylate. Polymerization studies with these monomers are in progress. The resulting products are potential new thermoplastic elastomers, dispersing agents, blending compounds, emulsifiers, non-ionic surfactants, biomaterials etc.

Acknowledgements. This work was supported by the *Deutsche Forschungsgemeinschaft* within the *Sonderforschungsbereich 262*. Support by the *Alexander von Humboldt Foundation* for B. Iván is gratefully acknowledged.

References

- Kennedy, J. P.; Iván B. "Designed Polymers by Carbocationic Macromolecular Engineering: Theory and Practice", Hanser Publishers, Munich, New York, 1992.
- Iván, B; Kennedy, J. P. *Ind. J. Technol.* **1993**, 31, 183.
- Iván, B. *Makromol. Chem., Macromol. Symp.* **1993**, 75, 181.
- Sawamoto, M. *Prog. Polym. Sci.* **1991**, 16, 111.
- Iván, B; Kennedy, J. P.; Mackey, P. W. *Polym. Prepr. (Am. Chem. Soc., Div. Polym. Chem.)* **1990**, 31(2), 215; *ibid.* **1990**, 31(2), 217.
- Iván, B; Kennedy, J. P.; Mackey, P.W. *ACS Symp. Ser.* **1991**, 469, 194 and 203.
- Iván, B; Kennedy, J. P.; Mackey, P. W. U. S. Patent 5,073,381 (Dec. 17, 1991).
- Kennedy, J. P.; Chang, V. S. C.; Smith, R. A.; Iván, B. *Polym. Bull.* **1979**, 1, 575.
- Iván, B; Kennedy, J. P. *J. Polym. Sci., Polym. Chem. Ed.* **1990**, 28, 89.
- Iván, B.; Kennedy, J. P.; Chang, V. S. C. *J. Polym. Sci., Polym. Chem. Ed.* **1980**, 18, 3177.
- Kitayama, T.; Nishiura, T.; Hatada, K. *Polym. Bull.* **1991**, 26, 513.
- Nishiura, T.; Kitayama, T.; Hatada, K. *Polym. Bull.* **1992**, 27, 615.
- Ruth, W. G.; Moore, C. G.; Brittain, W. J.; Si, J.; Kennedy, J. P. *Polym. Prepr. (Am. Chem. Soc., Div. Polym. Chem.)* **1993**, 34(1), 479.
- Kennedy, J. P.; Price, J. L.; Koshimura, K. *Macromolecules* **1991**, 24, 6567.
- Kennedy, J. P.; Hiza, M. *J. Polym. Sci., Polym. Chem. Ed.* **1983**, 21, 3573.
- Gyor, M.; Kitayama, K.; Fujimoto, N.; Nishiura, T.; Hatada, K. *Polym. Bull.* **1994**, 32, 155.
- Nemes, S.; Kennedy, J. P. *J. Macromol. Sci.-Chem.* **1991**, A28, 311.

18. Hadjikyriacou, S.; Fodor, Zs.; Faust, R. *J. Macromol. Sci.-Pure Appl. Chem.* **1995**, A32, 1137.
19. Feldthusen, J.; Iván, B.; Müller, A. H. E.; Kops, J. *Macromol. Reports* **1995**, A32, 639.
20. Feldthusen, J.; Iván, B.; Müller, A. H. E.; Kops, J. *Macromol. Symp.* **1996**, 107, 189.
21. Takacs, A.; Faust, R. *Macromolecules* **1995**, 28, 7266.
22. Feldthusen, J.; Iván, B.; Müller, A. H. E. *Macromolecules*, submitted.
23. Feldthusen, J.; Iván, B.; Müller, A. H. E. *Macromolecules*, submitted.
24. Everland, H.; Kops, J.; Nielsen, A.; Iván, B. *Polym. Bull.* **1993**, 31, 159.
25. Feldthusen, J.; Iván, B.; Müller, A. H. E.; Kops, J., *Macromol. Rapid Commun.*, **1997**, 18, 417.
26. Bae, Y. C.; Fodor, Zs.; Faust R. *Polym. Prepr. (Am. Chem. Soc., Div. Polym. Chem.)* **1996**, 37, 801.
27. Wang, H. C.; Levin, G.; Szwarc, M. *J. Am. Chem. Soc.* **1978**, 100, 6137.

Chapter 10

Synthesis and Characterization of α -Hydroxyl- ω -Methoxycarbonyl and α -Hydroxyl- ω -Carboxyl Asymmetric Telechelic Polyisobutylenes

Balint Koroskenyi and Rudolf Faust

Polymer Science Program, Chemistry Department, University of Massachusetts
at Lowell, One University Avenue, Lowell, MA 01854

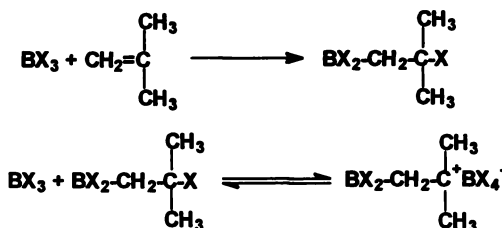
The convenient synthesis of α -hydroxyl- ω -methoxycarbonyl asymmetric telechelic PIBs has been achieved by the combination of two recently discovered techniques, haloboration-initiation and end capping with 1,1-diphenylethylene followed by end quenching with silyl ketene acetals, 1-methoxy-1-trimethylsiloxy-2-methyl-propene (MTSMP), 1-methoxy-1-trimethylsiloxy-propene (MTSP), and 1-methoxy-1-trimethylsiloxy-ethene (MTSE). Nearly quantitative chain end functionalization has been proved by ^1H NMR, quantitative ^{13}C NMR, and FT-IR spectroscopy. The methoxycarbonyl end arising by quenching with MTSMP could not be hydrolyzed under either basic or acidic conditions. These methods also failed to yield the acid when the corresponding diisobutylene derivative was used. The sterically less hindered esters, however, readily underwent hydrolysis resulting in the formation of α -hydroxyl- ω -carboxyl asymmetric telechelic PIBs.

Hydroxyl and carboxyl functional groups are very valuable in the chemistry of polymers due to the wide variety of reactions that can be carried out through these intermediates, such as transformations into other useful functional groups or block and graft copolymer synthesis. Thus, there have been many attempts to synthesize PIBs with such end groups, mostly by rather cumbersome methods [1-4]. Most of these methods involve the polymerization of isobutylene (IB) with a difunctional initiator, such as dicumyl chloride, followed by chain end functionalization resulting in symmetric telechelic PIBs with either hydroxyl or carboxyl end groups. The synthesis of asymmetric telechelic polymers is more difficult and usually carried out via a multi-step process. A most useful synthetic strategy would involve the living polymerization of IB by an initiator with a protected functional group or a precursor, and functionalization of the living chain end.

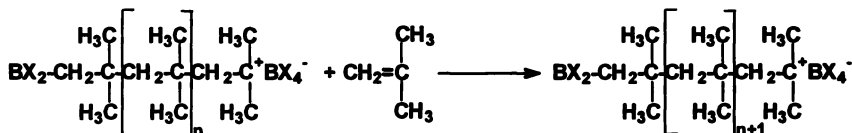
We recently reported that BX_3 ($\text{X}=\text{Cl}, \text{Br}$) alone can initiate the living polymerization of IB using polar solvents in the presence of a proton trap to prevent

initiation by protic impurities [5-7] (Scheme 1). The products are asymmetric telechelic polyisobutylenes (PIBs) with controlled molecular weight and narrow molecular weight distribution, carrying X_2B - head groups and *tert.*-halo end groups. Upon quenching with methanol, the X_2B - head groups are converted into alkylboronic esters. These materials are valuable intermediates to obtain asymmetric telechelic polymers carrying different functionalities that are difficult to obtain by conventional methods. One of the most important transformations of the head group to primary, HO- upon oxidation by alkaline hydrogen peroxide at room temperature, was shown to be rapid (<15 min) and quantitative [2] (Scheme 2).

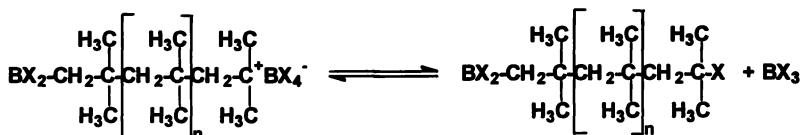
Initiation



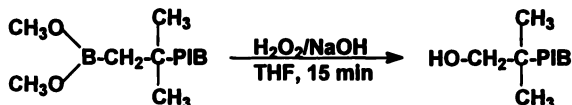
Propagation



Termination-reinitiation



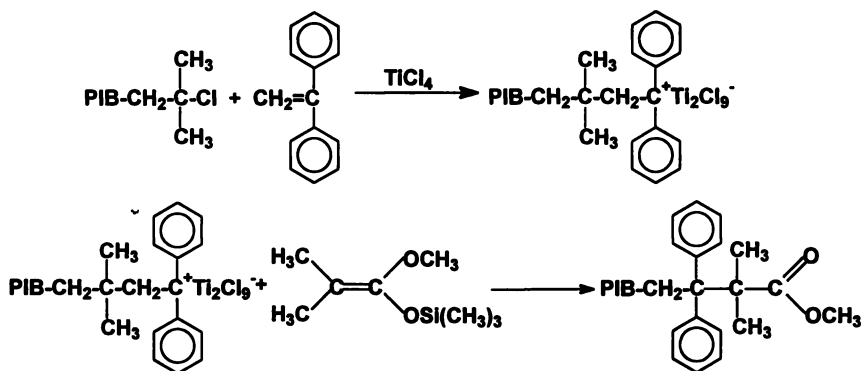
Scheme 1. Mechanism of haloboration-initiation.



Scheme 2. Oxidation of precursor alkylboronic ester.

In a series of recent publications, we also demonstrated synthetic applications of non-(homo)polymerizable monomers such as 1,1-diphenylethylene (DPE) and 1,1-ditolylethylene (DTE) in carbocationic macromolecular engineering [8-17]. These

processes involved the intermediate capping reaction of living PIB with DPE or DTE, in the course of quantitative end functionalization of PIB [8,9], coupling reaction of two homopolymers prepared by different mechanisms [10], and the clean synthesis of diblock [11-14] or triblock copolymers [15,16]. Capping of PIB with DPE and its derivatives has been shown to be an equilibrium reaction, shifted toward completion by increasing the Lewis acidity, solvent polarity, electron donating ability of *p*-substituents, and concentration of reactants such as DPE, Lewis acid, and chain end, and by decreasing the reaction temperature. In-situ functionalization of the living ends by a variety of nucleophiles was also realized using DPE capping followed by end quenching. Among these reactions, close to quantitative functionalization was observed with 1-methoxy-1-trimethylsiloxy-2-methyl propene giving rise to methoxycarbonyl functional PIB (Scheme 3).



Scheme 3. Capping and functionalization by end quenching with silyl ketene acetal.

Combination of the head and end group control provides a novel synthetic route for the synthesis of α -hydroxyl- ω -methoxycarbonyl asymmetric telechelic PIB {HOPIBC(R)(R')COOCH₃} (a condensation macromonomer). Hydrolysis of the methoxycarbonyl end group results in the formation of α -hydroxyl- ω -carboxyl asymmetric telechelic PIB {HOPIBC(R)(R')COOH}, while ester alcoholysis provides a method for polycondensation reactions of PIB. In the present publication we report the synthesis of these materials.

Experimental

Materials. IB (Matheson) was dried by passing the gas through in-line gas purifier columns packed with BaO/Drierite and condensed in the cold bath of the glove box prior to polymerization. Methylene chloride (DCM) was extracted three times with 10 w% NaOH solution, then with deionized water until neutral, and dried over anhydrous sodium sulfate. The dried DCM was refluxed for 24 hours and freshly distilled from CaH₂ under a nitrogen atmosphere. Hexane (Hex) was refluxed for 2 days with concentrated sulfuric acid followed by washing with deionized water, 10 w% NaOH solution, then with deionized water until neutral, dried over sodium sulfate, refluxed

for 24 hours, and freshly distilled from CaH_2 under a nitrogen atmosphere. 1,1-Diphenylethylene (DPE, 99%), BCl_3 (99.9%), di-*tert*-butylpyridine (DTBP, 99.1%), and titanium(IV) chloride (TiCl_4 , 99.9%) were used as received from Aldrich. MTSMF (United Chemical Technologies, Inc.) was also used as received. MTSP and MTSE were synthesized according to Ainsworth *et al.* [18]. 2-Chloro-2,4,4-trimethylpentane (TMPCl) was synthesized by hydrochlorination of 2,4,4-trimethyl-pentene-1 (TMPene, 99%, Aldrich, used as received) by passing hydrogen chloride through a 30 v% solution of TMPene in DCM at 0 °C overnight. The model compound, methyl 1,1,4,4,6,6-hexamethyl-2,2-diphenyl octanoate (MHMDPO) was synthesized similarly to the telechelic PIB. TMPCl was capped with DPE in DCM/Hex (60/40 v/v) at -80°C followed by end quenching with MTSMF. After quenching with prechilled methanol the product was purified by repeated extraction with methanol. Neopentyl alcohol (Aldrich, 99%) was used as received, carbon tetrachloride (Aldrich) was freshly distilled twice from phosphorus pentoxide.

Procedures. The polymerization of IB was carried out at -40 °C in DCM using the following concentrations: $[\text{BCl}_3]=0.103 \text{ M}$, $[\text{IB}]=0.938 \text{ M}$, $[\text{DTBP}]=0.003 \text{ M}$. After complete monomer conversion (14 h) DCM and Hex were added to obtain the DCM/Hex (60/40 v/v) solvent mixture and the desired concentrations for capping. The temperature was lowered to -80 °C, followed by the addition of TiCl_4 ($6.4 \times 10^{-2} \text{ M}$) and DPE ($8.0 \times 10^{-3} \text{ M}$) both from a stock solution in Hex. Large excess of silyl ketene acetal (silyl ketene acetal/PIB ~ 34) was used in the subsequent functionalization. After the desired reaction time, the reaction mixture was quenched with prechilled methanol. The polymers were purified by repeated precipitation from a Hex solution into methanol, followed by drying in vacuum.

For oxidation of the boronic ester or acid, 1 g of PIB was dissolved in 15 ml of THF, followed by the addition of 4 ml of 10 w% NaOH solution. The reaction was started by the addition of 1.02 ml of 30% hydrogen peroxide while maintaining the temperature below 50°C. The reaction mixture was stirred for 30 min, then 30 ml of Hex and 20 ml of saturated aqueous potassium carbonate were added. The mixture was washed with distilled water until the odor of THF could not be detected. The solution was dried over anhydrous sodium sulfate overnight, followed by evaporation of Hex on a rotavapor.

Hydrolysis was carried out according to the following procedure: 50 mg HOPIBC(R)(R')COOCH₃ was dissolved in 0.5 ml toluene (Aldrich, used as received), followed by the addition of a saturated solution of KOH in hexanol/water (98/2 v/v). The solution was heated under argon for the desired reaction time.

Characterizations. Molecular weights were measured using two Waters HPLC systems. One (MALLS) was equipped with a Model 510 HPLC pump, a Model 410 differential refractometer, Model 441 UV/Vis detector, on line multiangle laser light scattering detector (Minidawn, Wyatt technology inc.), Model 712 sample processor, and five ultrastryragel GPC columns connected in the following series: 500, 10^3 , 10^4 , 10^5 , and 100 Å. The other system (UC) was equipped with a Model 510 pump, a Model 486 tunable UV/Vis detector, a Model 250 dual refractometer/viscometer detector (Viscotek), a Model 712 sample processor, and five ultrastryragel columns connected in the same series as for the MALLS system. The flow rate of THF was 1.0

ml/min. For data acquisition and computing, the detector signals (RI, UV, and LS for MALLS, RI and viscosity for UC) were simultaneously recorded on a PC for the determination of absolute molecular weight and molecular weight distribution using the ASTRette software (MALLS), or the Viscotek software (UC), respectively. ^1H NMR and ^{13}C NMR spectra were recorded on Bruker 200, 250, and 500 MHz instruments using deuterated chloroform (Aldrich, 99.8%, used as received). FT-IR spectra were recorded on a Perkin Elmer 1760 X spectrometer in carbon tetrachloride using a 50 mm long path cell.

Results and Discussion

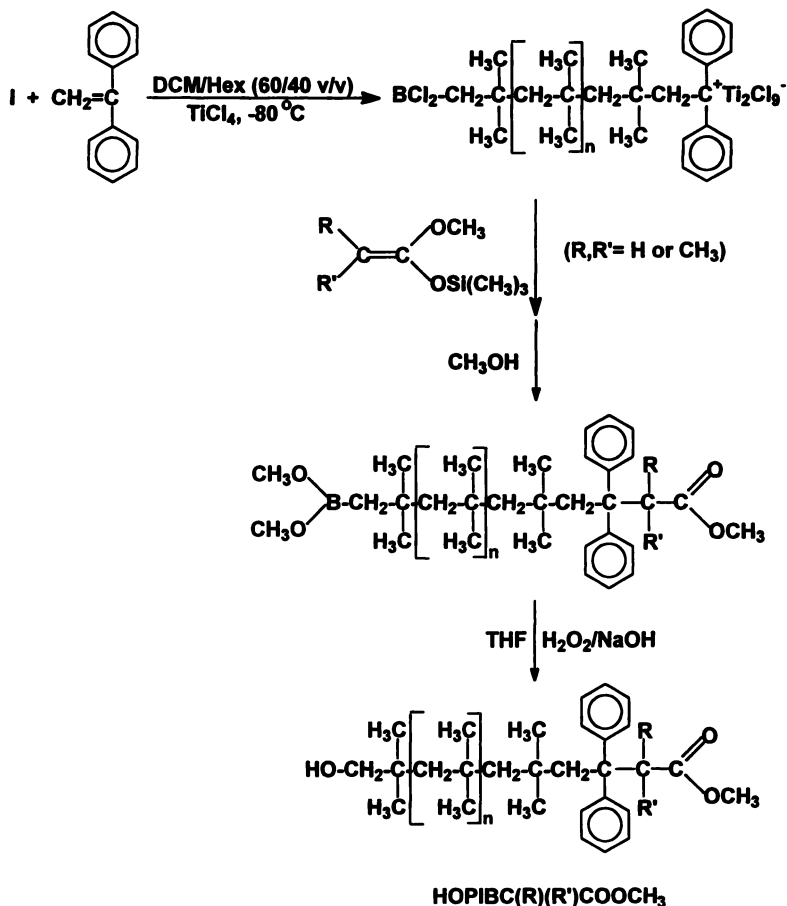
Synthesis of α -Hydroxyl- ω -Methoxycarbonyl Telechelic PIB. The synthesis of the asymmetric telechelic PIBs is based on the combination of two recently discovered techniques in cationic polymerization, haloboration-initiation and end capping followed by end quenching. In the first step, IB is polymerized in the absence of a separately added cationogen and in the presence of a proton trap according to Scheme 1 where $\text{X} = \text{Cl}$. Product I is a low molecular weight polymer ($M_n \sim 3000$) with relatively narrow molecular weight distribution ($M_w/M_n \sim 1.1-1.3$). This process results in the formation of alkyl boronic ester head group upon quenching with methanol, a precursor for hydroxyl functional group. The DPE capping, followed by functionalization with a silyl ketene acetal (Scheme 4) gives rise to a convenient synthesis of methoxycarbonyl functional PIB.

While BX_3 must be used for haloboration-initiation in order to obtain the precursor for the hydroxyl head group, capping was slow and incomplete using BCl_3 [17]. Complete capping was only achieved in conjunction with TiCl_4 . Thus after the complete polymerization of IB with BCl_3 at -40°C in DCM, Hex and DCM were added to reach the DCM/Hex = 60/40 v/v ratio and the desired concentrations followed by the addition of TiCl_4 and DPE at -80°C .

Unexpectedly, the capping efficiency was only 89%, most probably due to the high BCl_3 concentration (0.512M) used during IB polymerization. A two-step functionalization where PIB was first purified and the dried polymer redissolved at -80°C followed by the introduction of TiCl_4 and DPE, resulted in $\sim 90\%$ capping efficiency. The uncapped PIB was shown to carry primarily olefinic end, most probably due to elimination at room temperature. Thus, the one-step process described in the experimental section was followed. It has been shown that although the rate of polymerization is greatly influenced by $[\text{BCl}_3]$, the molecular weight (at identical monomer conversion) is unaffected [5]. Upon decreasing the concentration of BCl_3 to 0.103M, conversion of the monomer was complete in 14 hours and most importantly the subsequent complete capping and functionalization resulted in 100% ester functionality, as determined by ^1H NMR and ^{13}C NMR spectroscopy.

For the determination of the methoxycarbonyl chain end functionality, a model compound was synthesized under similar conditions to that of the telechelic polymer. TMPCl was capped with DPE, followed by end quenching with MTSMP . This model compound was used for the assignments of both the ^1H NMR and the ^{13}C NMR chemical shifts corresponding to the methoxycarbonyl chain end, as well as for calibration for IR measurements. The ^1H NMR spectrum of the model compound is shown with the assignments in Figure 1. The peaks corresponding to protons *c-i* are

expected to be present in the spectrum of HOIBC(CH₃)₂COOCH₃. The corresponding spectrum is shown in Figure 2. The protons of the hydroxyl head group are also present ($\delta_j=3.30$ ppm). The spectrum indicates virtually quantitative head and end group functionalities. The absence of the peaks corresponding to the possible byproducts (PIB-*t*-Cl: $\delta_{\text{CH}_2}=1.92$ ppm, $\delta_{\text{CH}_3}=1.66$ ppm; PIB-*exo* olefin: $\delta_{\text{CH}_2}=1.95$ ppm, $\delta_{\text{CH}_3}=4.61, 4.81$ ppm, $\delta_{\text{CH}_3}=1.82$ ppm; PIB-*endo* olefin: $\delta_{\text{CH}}=5.09$ ppm; PIB-DPE-OMe: $\delta_{\text{CH}_2}=2.45$ ppm, $\delta_{\text{CH}_3}=3.00$ ppm; PIB-DPE olefin: $\delta_{\text{CH}}=6.20$ ppm) also substantiates quantitative functionalization.



Scheme 4. Synthetic strategy for α -hydroxyl- ω -methoxycarbonyl asymmetric telechelic PIBs.

Quantitative ¹³C NMR spectra were also recorded on both the model compound and HOIBC(CH₃)₂COOCH₃. The spectra are shown in Figure 3 and Figure 4, respectively. The peaks corresponding to the methoxycarbonyl fragment are also present in the spectrum of the HOIBC(CH₃)₂COOCH₃ with close to quantitative

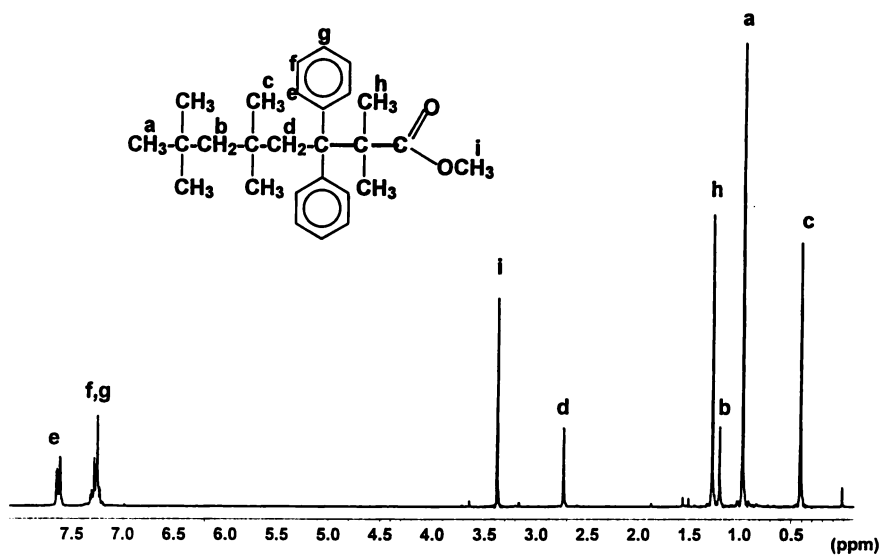


Figure 1. ^1H NMR spectrum of MHMDPO.

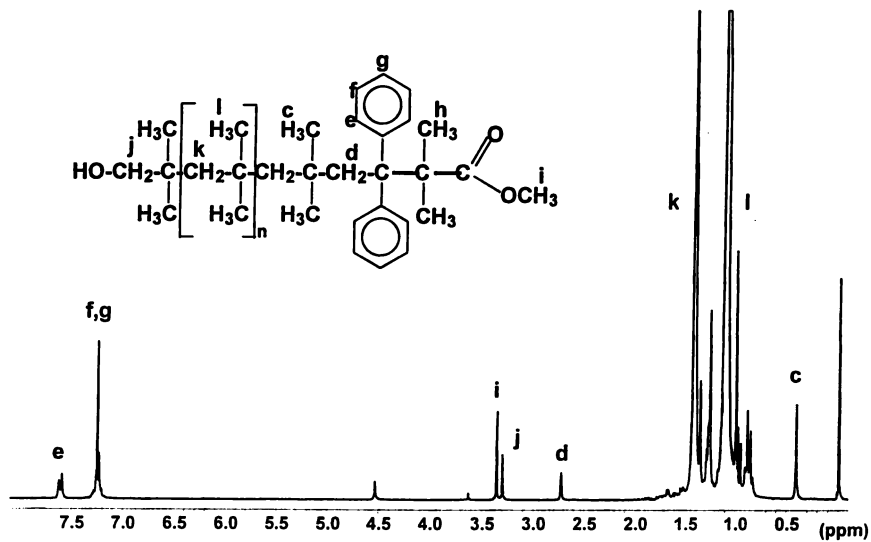


Figure 2. ^1H NMR spectrum of HOPIBC(CH₃)₂COOCH₃ after deuterium exchange.

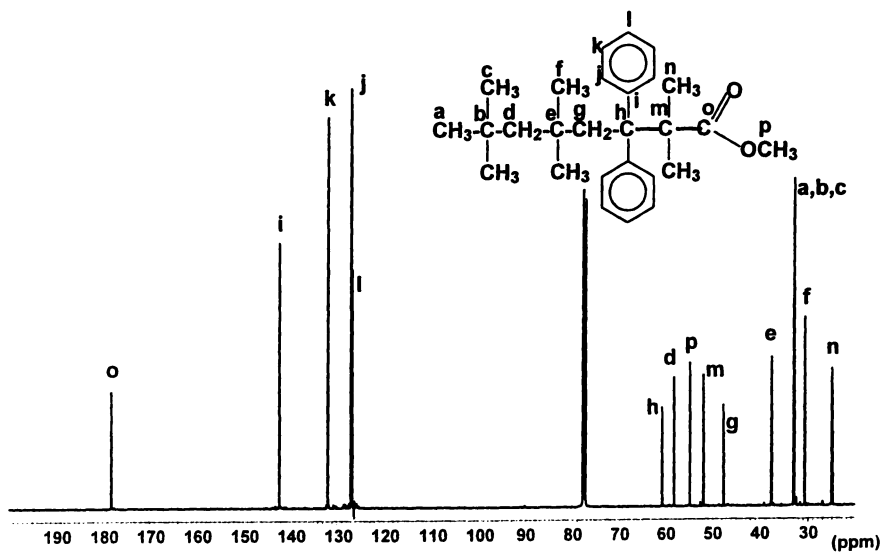


Figure 3. ^{13}C NMR spectrum of MHMDPO.

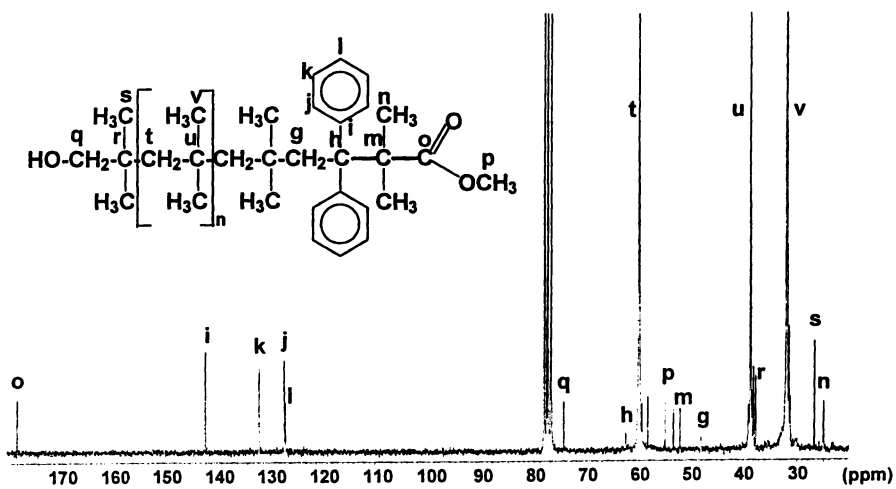


Figure 4. ^{13}C NMR spectrum of HOPIBC(CH₃)₂COOCH₃.

integration values. The spectrum was used to calculate the functionality of the chain ends based on the molecular weights obtained by size exclusion chromatography by two different methods (UC and MALLS) and the comparison of the integration values of the peaks corresponding to the chain ends to that of one of the main chain carbon atom. The averaged values for sample 3 in Table I gave 0.9 for the methoxycarbonyl and 1.2 for the hydroxyl functionality using the molecular weight determined by MALLS ($M_n=3400$). According to the molecular weight determined by UC ($M_n=2900$), these were 0.8 and 1.0, respectively. In addition, peaks corresponding to any expected byproducts [20] are clearly absent in the ^{13}C spectrum of the telechelic PIB.

Fourier transform infrared spectroscopy was also used to determine the chain end functionality. To determine the hydroxyl functionality, neopentyl alcohol was used to construct a calibration curve. The dissociated O-H stretching vibration appears at 3643 cm^{-1} , as shown in Figure 5. The calibration curve for the methoxycarbonyl end group was obtained with the MHMDPO model compound, which showed the C=O stretching vibration at the same wavenumber, 1720 cm^{-1} . The results are summarized in Table I.

Table I. Hydroxyl and methoxycarbonyl functionalities calculated by using infrared spectroscopy.

Sample	GPC	M_n	M_w/M_n	$F_n(\text{OH})$	$F_n(\text{COOMe})$
1	MALLS	4000	1.07	1.1	-
	UC	3200	1.17	0.9	-
2	MALLS	3700	1.08	1.3	1.3
	UC	2500	1.28	0.9	0.9
3	MALLS	3400	1.11	1.2	0.9
	UC	2900	1.16	1.0	0.8

Synthesis of α -Hydroxyl- ω -Carboxyl Asymmetric Telechelic PIBs. Hydrolysis of the ester should result in carboxyl functional PIB. Attempts to hydrolyze HOPIBC(CH₃)₂COOCH₃, however, remained unsuccessful, presumably due to the large steric hindrance of the carbonyl carbon atom. The steric hindrance due to the bulky substituents prevents S_N2 reactions on the carbonyl carbon, while the methoxy substituent does not facilitate S_N1 reactions. Branching in the α or β position next to the carbonyl carbon is known to largely decrease the reactivity of an ester toward S_N2 reactions, especially when the accessibility of the carbonyl carbon and the tetrahedral transition state are hindered by bulky groups, as well. In HOPIBC(CH₃)₂COOCH₃ both the α and the β carbons are branched with two phenyl rings in the β position. In addition, the bond between the two tertiary carbon atoms shows low thermal stability, thus only moderate temperatures could be applied. Decomposition of the chain end was observed above 80°C after an extended period of time. Attempts with acidic catalysis have been carried out using *p*-toluene sulfonic acid or hydrochloric acid in chloroform at temperatures varying from room temperature to 50°C . Hydrogen iodide was also used in toluene at room temperature and at 60°C . Basic catalysis have been attempted with KOH and NaOH solutions in water, methanol, isopropanol, and hexanol using solvents such as chloroform, THF, and toluene for the dissolution of the polymer. Such mild conditions have been reportedly used for the hydrolysis of

sterically hindered low molecular weight esters. Gassman *et al.* [21] reported successful hydrolysis of such sterically hindered esters as pivalate and mesitoate esters at ambient temperatures by using "anhydrous hydroxide". The above methods, however, failed to hydrolyze HOIBC(CH₃)₂COOCH₃, even when a phase transfer catalyst [22] was used. The hydrolysis of MHMDPO model compound has also been attempted. This low molecular weight material is soluble in polar solvents and the heterogeneity of the reaction is eliminated. However, MHMDPO also failed to undergo hydrolysis, which confirmed that steric hindrance is responsible for the low reactivity. In contrast to MHMDPO, methyl trimethyl acetate, which has a tertiary carbon with methyl substituents at the α position but neither bulky phenyl groups nor branched carbon at the β position, readily underwent complete hydrolysis in a 5M KOH solution in methanol at 60°C in 7 hrs.

In order to affect hydrolysis we decided to reduce the branching on the α carbon, thus decreasing the steric hindrance. Sterically less hindered derivatives can be synthesized by varying the substituents on the β -carbon of the silyl ketene acetal. We expected that the monomethyl and the unsubstituted derivatives (MTSP and MTSE, respectively) will result in methoxycarbonyl functional PIBs that would possess higher thermal stability and would undergo hydrolysis, as well as alcoholysis. The ease of hydrolysis and alcoholysis, as well as any nucleophilic substitution reaction is expected to increase with decreasing substitution in the α -position of the ester, in the order of HOIBC(CH₃)₂COOCH₃ < HOIBCH(CH₃)COOCH₃ < HOIBCH₂COOCH₃. These HOIBC(R)(R')COOCH₃ telechelic polymers have been synthesized similarly to the dimethyl derivative. No difference in the reactivity of the three different silyl ketene acetals have been observed, as nearly quantitative functionalization was observed with all three analogs under similar reaction conditions. The ¹H NMR spectra of the less hindered derivatives are shown in Figures 6 and 7. These telechelic PIBs readily underwent hydrolysis. They showed higher thermal stability; at 100°C they retained their functionalities for an extended period of time (over 48 hrs), although the chain ends slowly decomposed at 160°C. The telechelic PIBs were first dissolved in toluene and the catalyst (KOH) was added in hexanol. In this solvent system both the PIBs and the catalyst seemed to be soluble. As expected, the hydrolysis of HOIBCH₂COOCH₃ was faster than that of HOIBCH(CH₃)COOCH₃. While the latter hydrolyzed completely at 100°C in 6 hrs, hydrolysis was only 96% for HOIBCH(CH₃)COOCH₃. The hydrolysis was much slower at lower temperatures; HOIBCH(CH₃)COOCH₃ underwent only 80 % hydrolysis at 80°C during 10 hrs. The results are summarized in Table II. The regions of interest in the ¹H NMR spectra of the unsubstituted derivative are compared in

Table II. Results of hydrolysis of different derivatives

HOIB(R)(R')COOCH ₃		Temperature, °C	Time, hrs	% Hydrolysis
R	R'			
CH ₃	CH ₃	60	28	0
H	CH ₃	80	10	79
H	CH ₃	100	6	96
H	CH ₃	100	48	100
H	H	100	6	100

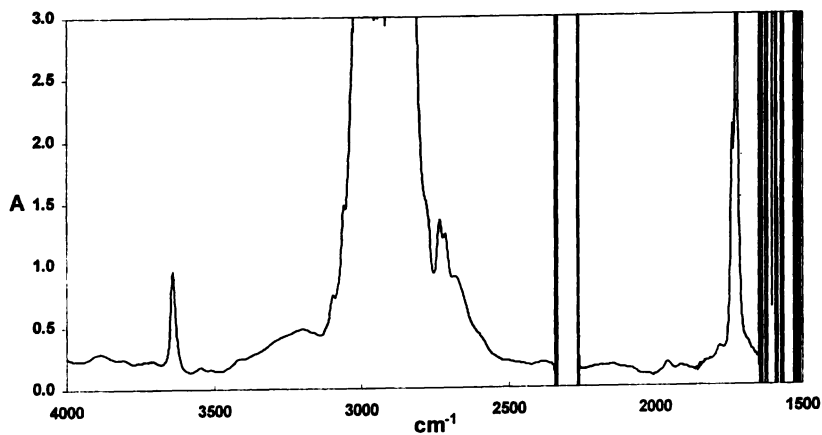


Figure 5. IR spectrum of HOPIBC(CH₃)₂COOCH₃.

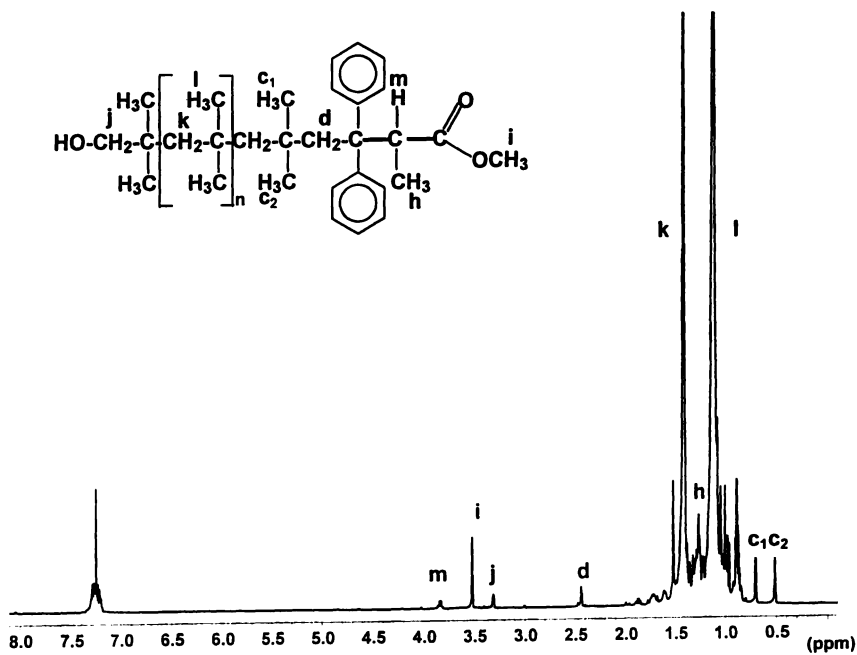


Figure 6. ¹H NMR spectrum of HOPIBC(CH₃)COOCH₃.

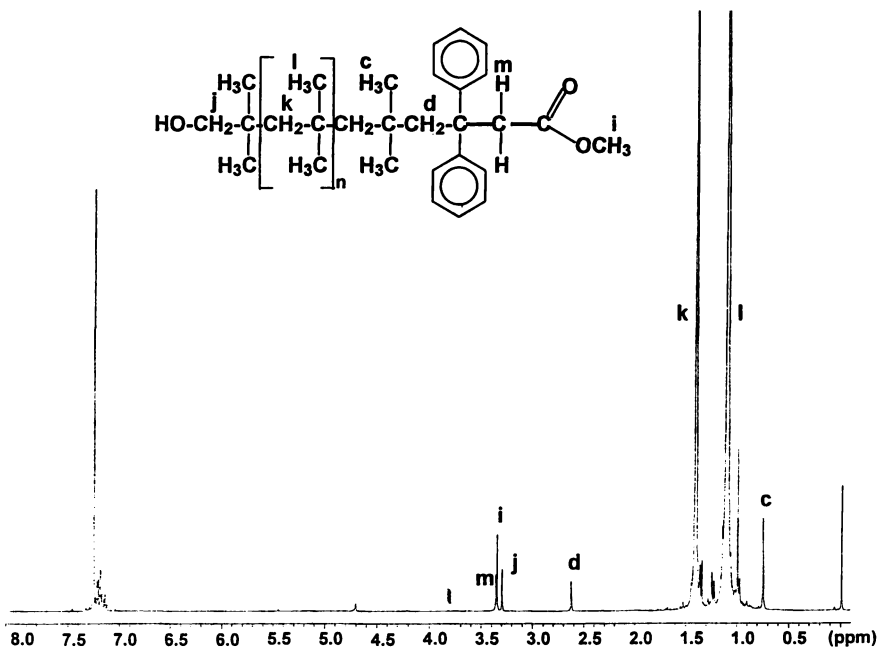


Figure 7. ¹H NMR spectrum of HOPIBCH₂COOCH₃.

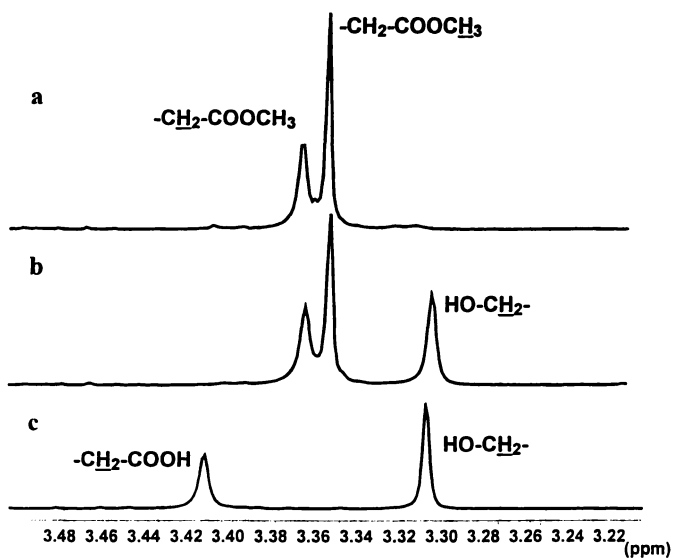


Figure 8. Development of functional groups followed by ¹H NMR. (a) α -boronic acid- ω -methoxycarbonyl PIB; (b) α -hydroxyl- ω -methoxycarbonyl PIB; (c) α -hydroxyl- ω -carboxyl PIB.

Figure 8 as the functional groups appear upon oxidation and hydrolysis. Oxidation of the boronic ester head group results in the appearance of the HO-CH₂- protons at 3.30 ppm. Hydrolysis shifts the protons on the α carbon (-CH₂COOCH₃ at 3.36 ppm and -CH₂COOH at 3.41 ppm) as the electronic environment changes. The most significant change, however, is the disappearance of the methoxy protons (-CH₂COOCH₃ at 3.34 ppm).

Conclusions

The facile synthesis of α -hydroxyl- ω -methoxycarbonyl asymmetric telechelic PIBs has been achieved by the combination of two recently discovered techniques, haloboration-initiation and end capping with 1,1-diphenylethylene followed by end quenching with silyl ketene acetals. The highly substituted methoxycarbonyl chain end in HOPIBC(CH₃)₂COOCH₃ has low thermal stability, with thermal decomposition occurring above 80 °C. Decreasing substitution increases the thermal stability; the analogs with lower substitution are stable at 100 °C, although they slowly decompose at 160 °C. While the methoxycarbonyl end group of the dimethyl derivative failed to undergo nucleophilic substitution reactions, the sterically less hindered derivatives readily underwent hydrolysis. Presumably, other nucleophilic substitution reactions, such as alcoholysis, can also be carried out on these materials. This is currently under investigation.

Acknowledgment

This material is based on research supported by the National Science Foundation (DMR-9502777).

Literature Cited

1. Nemes, S.; Peng, K. L.; Wilczek, L.; Kennedy, J. P. *Polym. Bull.* **1990**, *24*, 187.
2. Ivan, B.; Kennedy, J. P.; Chang, V. S. C. *J. Polym. Sci.: Polym. Chem. Ed.* **1980**, *18*, 3177.
3. Peters, E. N. *U.S. Patent* 4, 845,158, 1989.
4. Fehervari, A. F.; Faust, R.; Kennedy, J. P. *J. Macromol. Sci., Pure Appl. Chem.* **1990**, *A27(12)*, 1571.
5. Balogh, L.; Wang, L.; Faust, R. *Macromolecules* **1994**, *27*, 3453.
6. Wang, L.; Svirkin, J.; Faust, R. *ACS Polym. Mater. Sci. & Eng.* **1995**, *27*, 173.
7. Balogh, L.; Fodor, Z.; Kelen, T.; Faust, R. *Macromolecules* **1994**, *27*, 4648.
8. Fodor, Z.; Hadjikyriacou, S.; Li, D.; Faust, R. *Polym. Prepr. (Am. Chem. Soc., Div. Polym. Chem.)* **1994**, *35(2)*, 492.
9. Hadjikyriacou, S.; Fodor, Z.; Faust, R. *J. Macromol. Sci., Pure Appl. Chem.* **1995**, *A32(6)*, 1137.
10. Takacs, A.; Faust, R. *Macromolecules* **1995**, *28*, 7266.
11. Fodor, Z.; Faust, R. *J. Macromol. Sci., Pure Appl. Chem.* **1994**, *A31(12)*, 1985.
12. Li, D.; Faust, R. *Macromolecules* **1995**, *28*, 4893.
13. Hadjikyriacou, S.; Faust, R. *Macromolecules* **1995**, *28*, 7893.
14. Hadjikyriacou, S.; Faust, R. *Macromolecules* **1996**, *29*, 5261.

15. Fodor, Z.; Faust, R. *J. Macromol. Sci., Pure Appl. Chem.* **1995**, *A32(3)*, 575.
16. Li, D.; Faust, R. *Macromolecules* **1995**, *28*, 1383.
17. Bae, Y. C.; Fodor, Z.; Faust, R. *Polym. Prepr. (Am. Chem. Soc., Div. Polym. Chem.)* **1996**, *37(1)*, 801; *ACS Symp. Ser.* **1997**, *665*, 168.
18. Ainsworth, C.; Chen, F.; Kuo, Y. *J. Organometal. Chem.* **1972**, *46*, 59.
19. Si, J.; Kennedy, J. P. *J. Polym. Sci. Part A: Polym. Chem.* **1994**, *32*, 2011.
20. Nemes, S.; Si, J.; Kennedy, J. P. *Polym. Bull.* **1990**, *23*, 597.
21. Gassman, P. G.; Schenk, W. N. *J. Org. Chem.* **1977**, *42 (5)*, 918.
22. Loupy, A.; Pedoussaut, M.; Sansoulet, J. *J. Org. Chem.* **1986**, *51*, 740.

Organo Rare Earth Metal Initiated Living Polymerizations of Polar and Nonpolar Monomers

Hajime Yasuda, Eiji Ihara, Yuu Nitto, and Takamaro Kakehi,
Masakazu Morimoto, and Mitsufumi Nodono

Department of Applied Chemistry, Faculty of Engineering, Hiroshima University,
Higashi-Hiroshima 739, Japan

This article deals with the rare earth metal initiated living polymerization of polar and nonpolar monomers to give monodisperse high molecular weight polymers at high conversion. A typical example is seen in the polymerization of methyl methacrylate with $[\text{SmH}(\text{C}_5\text{Me}_5)_2]_2$ or $\text{LnMe}(\text{C}_5\text{Me}_5)_2$ (THF) ($\text{Ln}=\text{Sm}, \text{Y},$ and Lu), giving high molecular weight syndiotactic polymers ($M_n > 500,000$, syndiotacticity $> 95\%$) quantitatively at low temperature (-95°C). Synthesis of high molecular weight isotactic poly(MMA) with very low polydispersity was also achieved by the efficient catalytic action of $[(\text{SiMe}_3)_3\text{C}]_2\text{Yb}$. Living polymerizations of alkyl acrylates were successfully carried out by the excellent catalysis of $\text{LnMe}(\text{C}_5\text{Me}_5)_2(\text{THF})$ ($\text{Ln}=\text{Sm}$ and Y). By taking advantages of the living polymerization ability, we attempted the ABA triblock copolymerization of MMA/butyl acrylate/MMA to obtain rubber-like elastic polymers. Organo rare earth metal complexes such as $\text{LnOR}(\text{C}_5\text{R}_5)_2$ or $\text{LnR}(\text{C}_5\text{R}_5)_2$ ($\text{Ln} = \text{Sm}$ and Y , $\text{R} = \text{Me}$) conducted the living polymerizations of various lactones such as β -propiolactone, δ -valerolactone and ϵ -caprolactone, and also conducted the block copolymerizations of methyl methacrylate with various lactones.

C_1 symmetric bulky organolanthanide(III) complexes such as $\text{SiMe}_2[2(3),4-(\text{SiMe})_2\text{C}_5\text{H}_2]_2\text{LnCH}(\text{SiMe}_3)_2$ ($\text{Ln} = \text{La}, \text{Sm},$ and Y) show high catalytic activity for linear polymerization of ethylene. Organolanthanide(II) complexes such as *racemic* $\text{SiMe}_2[2-\text{SiMe}_3-4\text{-tBu-C}_5\text{H}_2]_2\text{Sm}(\text{THF})$ as well as C_1 symmetric $\text{SiMe}_2[2(3),4-(\text{SiMe}_3)_2\text{C}_5\text{H}_2]_2\text{Sm}(\text{THF})$ were found to show high catalytic activity for the polymerization of ethylene, giving $M_n > 10^6$ with $M_w/M_n = 1.6$. Utilizing the high polymerization activity of rare earth metal complexes towards both polar and nonpolar monomers, block copolymerizations of ethylene with polar monomers such as methyl methacrylate and lactones were realized for the first time.

Highly Stereospecific Living Polymerization of Alkyl Methacrylates

It is very significant to find ways which synthesize highly syndiotactic or isotactic polymers with $M_n > 500,000$ and $M_w/M_n < 1.05$. Although various living

polymerization systems have been reported, no type of anionic (1), cationic (2), Group Transfer(3), and metal carbene initiated polymerizations (4) has ever achieved this end. In this connection, it is remarkable that high molecular weight poly(MMA) having an unusually low polydispersity has been synthesized by the use of organolanthanide(III) complexes (Fig. 1)(5). The relevant complexes include lanthanide hydrides, bulky alkyl lanthanide, trialkylaluminum complexes of alkylaluminum, and simple alkyl complexes synthesized from $\text{LnCl}(\text{C}_5\text{Me}_5)_2$ (Fig. 2). Most of them have been isolated and well characterized by single X-ray analysis. The results from the polymerization of MMA with $[\text{SmH}(\text{C}_5\text{Me}_5)_2]_2$ initiator at different temperature are summarized in Table 1. The most striking is $M_w/M_n = 1.02-1.04$ for $M_n > 60 \times 10^3$. Remarkably, $\text{SmH}(\text{C}_5\text{Me}_5)_2$ complex gives high conversion (polymer yield) in a relatively short period, and allow the polymerization

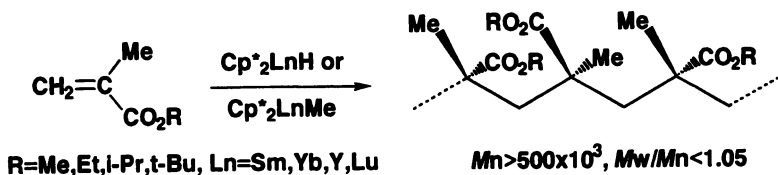


Fig. 1. Organolanthanide initiated polymerization of MMA

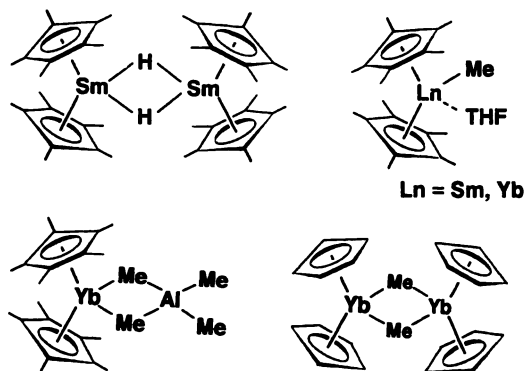


Figure 2. Typical initiator used for the living polymerization of methyl methacrylate

Table 1. Characterization of Monodisperse Poly(MMA) Synthesized by $[\text{SmH}(\text{C}_5\text{Me}_5)_2]_2$ Initiator

Polymerization temperature(°C)	MMA/initiator charged(mol/mol)	$M_n \times 10^3$	M_w/M_n	\bar{r} %	Conversion/% (reactn time)
40	500	55	1.03	77.3	99 (1 h)
0	500	58	1.02	82.4	99 (1 h)
0	1500	215	1.03	82.9	93 (2 h)
0	3000	563	1.04	82.3	98 (3 h)
-78	500	82	1.04	93.1	97 (18 h)
-95	1000	187	1.05	95.3	82 (60 h)

M_n and M_w/M_n were determined by GPC using standard poly(MMA) with M_w measured by light scattering. Solvent, toluene; solvent / $[M]_0 = 5$ (vol/vol)

to proceed over a wide range of reaction temperature from $-78\text{ }^{\circ}\text{C}$ to $60\text{ }^{\circ}\text{C}$. Furthermore, *syndiotacticity* exceeding 95% is attained when the polymerization temperature is lowered to $-95\text{ }^{\circ}\text{C}$ in toluene. The similar result was obtained in the reaction in THF.

Typical initiator systems reported so far for the synthesis of highly syndiotactic poly(MMA) are bulky alkyl lithium $\text{CH}_3(\text{CH}_2)_4\text{CPh}_2\text{Li}$ (6), Grignard reagent in THF (7), and some AlR_3 complexes (8). Although the $\text{CH}_3(\text{CH}_2)_4\text{CPh}_2\text{Li}$ initiator in THF reacted rapidly with MMA at $-78\text{ }^{\circ}\text{C}$, the M_n reached only 10,000 with $M_w/M_n = 1.18$, while it gave isotactic polymers in toluene. Isobutylmagnesium bromide and 4-vinylbenzylmagnesium bromide in THF at lower temperature also gave high syndiotacticity, but M_n remained as low as 14,000-18,000 and the yields were quite low. When $i\text{BuMgBr}$ or $t\text{BuMgBr}$ was used in toluene instead of THF, the resulting poly(MMA) had a high isotacticity of 96.7% with $M_n = 19,900$ and $M_w/M_n = 1.08$ (9). $\text{AlEt}_3 \cdot \text{PR}_3$ complexes gave high syndiotacticity, but not a high molecular weight.

Ketene silyl acetal/nucleophilic agent systems initiate the polymerization of alkyl methacrylates. These well-known Group Transfer systems yielded living polymers with atactic sequences at relatively high temperature (3). $\text{Me}_2\text{C}=\text{C}(\text{OMe})\text{OSiR}_3$ and $\text{R}_2\text{POSiMe}_3$ can be used as initiators, and Et_4CN is frequently used as catalyst. For example, the M_w/M_n of the resulting poly(MMA) was 1.06 for $M_n = 3800$, and 1.15 for $M_n = 6,300$. Thus, organolanthanide-initiated polymerization is superior in obtaining monodisperse high molecular weight poly(MMA).

These findings motivated us to isolate the 1:1 or 1:2 adduct of $[\text{SmH}(\text{C}_5\text{Me}_5)_2]_2$ with MMA in order to elucidate the initiation mechanism. After expending many efforts, we have obtained the desired 1:2 adduct as an air-sensitive orange crystal (mp $132\text{ }^{\circ}\text{C}$). The X ray analysis of the adduct indicates that one of the MMA unit is linked to the metal in an enolate form while at the other end the penultimate MMA unit is coordinated to the metal through its $\text{C}=\text{O}$ group. Thus 8 membered cyclic intermediate was formed (Fig. 3).

Although similar cyclic intermediates have been proposed by Bawn et al. and Cram and Copecky for the isotactic polymerization of MMA, no isolation of such active species has succeeded. On the basis of the X-ray structural data as well as the mode of polymerization, we have proposed a coordination anionic mechanism involving an 8-membered transition state for the present organolanthanide initiated polymerization of MMA. In the initiation step, the hydride attacks the CH_2 group of MMA, and a transient $\text{SmOC}(\text{OCH}_3)=\text{C}(\text{CH}_3)_2$ species should be formed. Then, the

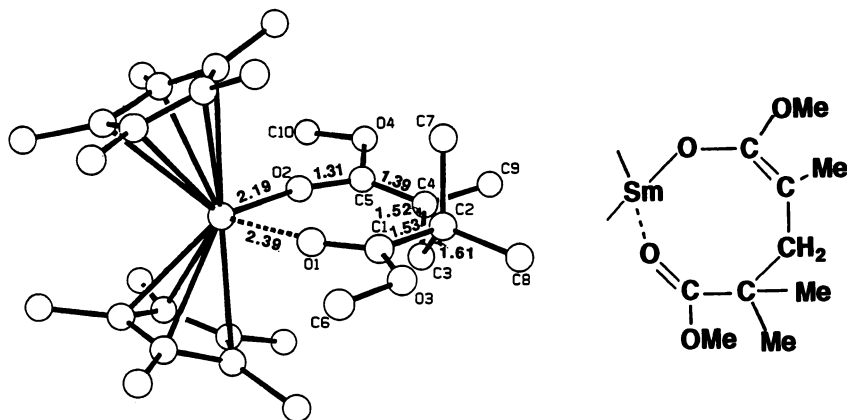


Fig. 3. X-ray analysis of $\text{Sm}(\text{C}_5\text{Me}_5)_2(\text{MMA})_2\text{H}$

incoming MMA molecule is supposed to participate in the 1,4-addition to produce an 8-membered cyclic intermediate. Further addition of MMA to the 1:2 addition compound liberates the coordinated ester group and the 8-membered cyclic intermediate is again generated. The intermolecular repulsion between C(7) and C(9) (or the polymer chain) should be the essential factor in determining the syndiotacticity.

Recently, *isotactic* polymerization of MMA has also been achieved ($mm = 94\%$, $M_n = 134 \times 10^3$, $M_w/M_n = 6.7$) by T. Marks using $\text{Me}_2\text{Si}(\text{C}_5\text{Me}_4)[\text{C}_5\text{H}_3-(1\text{S}), (2\text{S}), (5\text{R})\text{-neomenthyl}]\text{LaR}$ ($\text{R} = \text{CH}(\text{SiMe}_3)_2$ or $\text{N}(\text{SiMe}_3)_2$) (10), but $\text{Me}_2\text{Si}(\text{C}_5\text{Me}_4)[\text{C}_5\text{H}_3-(1\text{S}), (2\text{S}), (5\text{R})\text{-menthyl}]\text{LnR}$ ($\text{Ln} = \text{Lu}, \text{Sm}$; $\text{R} = \text{CH}(\text{SiMe}_3)_2$ or $\text{N}(\text{SiMe}_3)_2$) proceeded syndiotactic polymerization of MMA ($rr = 69\%$, $M_n = 177 \times 10^3$, $M_w/M_n = 15.7$). A possible explanation for this difference is that the menthyl complex produces a syndiotactic polymer via a cyclic 8-membered intermediate, while the neomenthyl complex produces an isotactic polymer via a nonlinear intermediate. Therefore, it was concluded that stereoregularity varies with subtle difference in steric bulkiness of the complexes. Actually, high molecular weight *isotactic* poly(MMA) ($mm = 97\%$, $M_n = 220,000$, $M_w/M_n = 1.1$) was first obtained quantitatively when the nonmetallocene system, $[(\text{Me}_2\text{Si})_3\text{C}]_2\text{Yb}$, was used as initiator (11). We propose here the initiation mechanism noted below for this isotactic polymerization of MMA (Fig. 4). The isotactic polymerization should proceed by the enantiomorphoric site control in toluene. However, syndiotactic polymer was obtained when THF was used ($rr = 87.0\%$, $M_n = 3.2 \times 10^4$, $M_w/M_n = 1.76$) presumably due to chain end control. More precise studies are now underway.

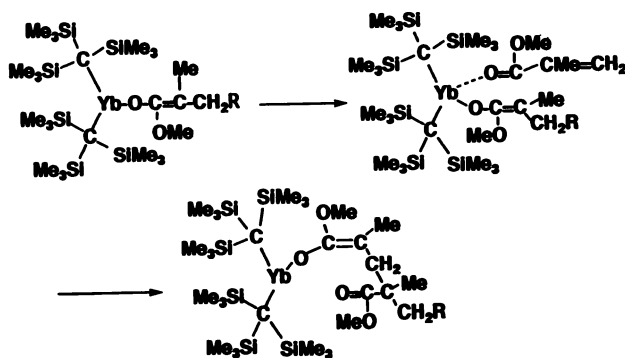


Fig. 4. Proposed mechanism for isotactic polymerization of MMA

Boffa and Novak found a divalent rare earth metal complex, $\text{Sm}(\text{C}_5\text{Me}_5)_2$, to be a good catalyst for polymerization of MMA (12). The initiation may start with the coupling of two coordinated MMA molecules to form $\text{Sm}(\text{III})$ species. The bis-allyl initiator, $\text{Sm}(\eta^3\text{-CH}_2\text{-CH-CH-})_2(\text{C}_5\text{Me}_5)_2$, was also effective for the living polymerization of MMA. In this case, MMA must add to both ends of the hexadiene group. In the polymerization of MMA initiated with methylaluminum tetraphenylporphyrine, sterically crowded Lewis acid such as $\text{MeAl}(\text{ortho-substituted phenolate})_2$ serves as a very effective accelerator without damaging the living character of polymerization (13). Thus, the polymer has very low polydispersity ($M_w/M_n = 1.09$) and sufficiently high molecular weight, $M_n = 25,500$ but the stereoregularity is very poor.

In general, Ziegler-Natta catalysts such as $\text{TiCl}_4/\text{MgCl}_2/\text{AlR}_3$ and Kaminsky catalysts such as $\text{Cp}_2\text{ZrCl}_2/(\text{AlMe}_2\text{-O})_n$ can not conduct the polymerization of polar monomers. However, a mixture of cationic species $\text{Cp}_2\text{ZrMe}(\text{THF})^+$ and Cp_2ZrMe_2 has been found to do so for MMA (14), allowing isotactic poly(MMA) ($mm = 90\%$,

$M_n = 120,000$, $M_w/M_n = 1.2-1.3$). Recently, Soga et al. (15) reported the syndio rich polymerization of MMA catalyzed by $Cp_2ZrMe_2/Ph_3CB(C_6F_5)_4/ZnEt_2$ and also the isotactic polymerization of MMA catalyzed by $rac-Et(ind)_2ZrMe_2/Ph_3CB(C_6F_5)_4/ZnEt_2$ ($mm = 96.5\%$, $M_n = 39.3 \times 10^4$, $M_w/M_n = 1.434$).

Living Polymerization of Alkyl Acrylates

In general, living polymerization of alkyl acrylates is difficult because the chain transfer or termination occurs preferentially, owing to a high sensitivity of the acidic α -proton to the nucleophilic attack. Exceptions are the living polymerization of a bulky acrylic ester catalyzed by the bulky alkyllithium/inorganic salt (LiCl) as well as the Group Transfer polymerization of ethyl acrylate with ZnI_2 as the catalyst. Porphyrinatoaluminum initiator systems also induced the living polymerization of t-

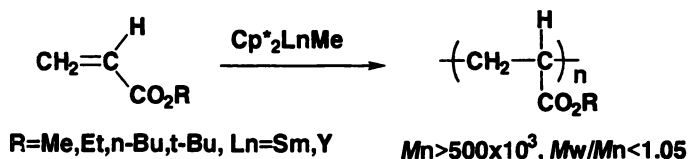


Fig. 5. Living polymerization of alkyl acrylates

butyl acrylate (16), but the upper limit of molecular weight was ca. 20,000. We have found the efficient initiating properties of $SmMe(C_5Me_5)_2(THF)$ and $YMe(C_5Me_5)_2(THF)$ for living polymerization of acrylic esters, i.e. methyl acrylate (MeA), ethyl acrylate (EtA), butyl acrylate (BuA), and t-butyl acrylate (tBuA), although the reactions were non-stereospecific (17). The initiator efficiency exceeded 85% except for tBuA. Thus, initiation occurs in a quantitative fashion. This reaction should proceed in a living manner, because the M_n of poly(BuA) initiated by

Table 2. Polymerization of Alkyl Acrylates Initiated by Organolanthanide Complexes

Initiator	Monomer	$M_n/10^3$	M_w/M_n	Tacticity/%			Conversion %
				rr	mr	mm	
$SmMe(C_5Me_5)_2(THF)$	MeA	48	1.04	30	50	20	99
	EtA	55	1.04	51	49		94
	BuA	70	1.05	28	53	19	94
	BuA	15	1.03	27	47	26	99

Polymerization conditions: 0 °C in toluene, initiator concentration 0.2 mol% of monomer

$SmMe(C_5Me_5)_2(THF)$ increased linearly in proportion to the conversion, while M_w/M_n remained unchanged (1.04-1.05), irrespective of the initiator concentration. In order to establish the characteristic nature of these initiation systems, the initiator concentration was decreased from 0.1 to 0.002 mol% and high molecular weight poly(EtA) of $M_n = 560,000$ with narrow molecular weight distribution ($M_w/M_n = 1.05$) was obtained.

ABA type triblock copolymerization of MMA/BuA/MMA should give rubber-like elastic polymers. The resulting copolymers should have two vitreous outer blocks, where the poly(MMA) moiety (hard segment) associates with the nodules, and the central soft poly(BuA) elastomeric block provides rubber elasticity. The first step polymerization of MMA gave M_n of 15,000 with $M_w/M_n = 1.04$ and then a

mixture of MMA and BuA was added to this growing end to result in the formation of desired ABA triblock copolymer (BuA polymerized more rapidly than MMA). Table 3 shows the typical mechanical properties of the ABA type copolymers thus obtained. It is seen that homo-poly(MMA) has large tensile modulus and large tensile strength, but is poor in elongation and shows very large compression set. In contrast, the

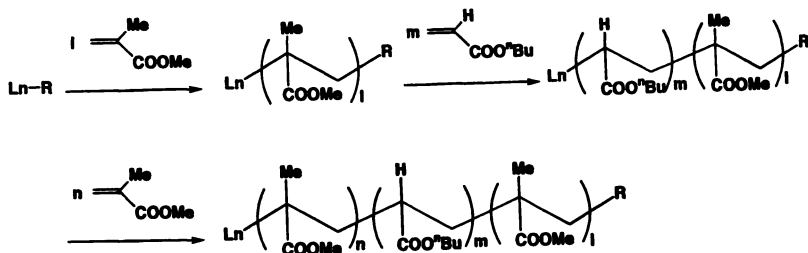


Fig. 6. ABA type block copolymerization of MMA/BuA/MMA

triblock copolymer (8:72:20) shows a large elongation (163%) and 58% compression set, indicating that this polymer is a thermoplastic elastomer. The triblock copolymer of MMA/EtA/EtMA in the ratio of 26:48:26 also showed large elongation and small compression set. Thus, elastic copolymers of alkyl methacrylate and alkyl acrylate were for the first time obtained by the living polymerization of organolanthanides.

Table 3. Mechanical Properties of Triblock Copolymers

Copolymer	Tensile modulus (MPa)	Tensile strength (MPa)	Elongation (%)	Izod impact strength (J/m)	Compression set/% (70 °C, 22 h)
poly(MMA)	610	80	21	18	100
poly(MMA/BuA/MMA) (20:47:33)	75	27	83	383 (N.B)	101
poly(MMA/BuA/MMA) (25:51:24)	46	22	8	390 (N. B)	103
poly(MMA/BuA/MMA) (8:72:20)	0.8	0.7	163	400 (N.B)	58
poly(MMA/BuA/MMA) (6:91:3)	0.2	0.1	246	410 (N.B)	97
poly(MMA/EtA/EtMA) (26:48:26)	119	22	276	34	62

N.B: not break

Block Copolymerization of Hydrophobic and Hydrophilic Acrylates

Trimethylsilyl methacrylate (TMSMA) was found to proceed the living polymerization with $\text{SmMe}(\text{C}_5\text{Me}_5)_2(\text{THF})$ to give high molecular weight syndiotactic polymer ($M_n = 56,000$, $\text{rr} = 92\%$) with very low polydispersity ($M_w/M_n = 1.09$). By utilizing this nature, we have performed the block copolymerization of TMSMA with MMA or butyl acrylate by the sequential addition of these monomers to obtain the adhesive materials upon hydrolysis with aq. HCl of the resulting polymer (18). The result was shown in Table 4. Thus, block copolymerization of TMSMA and MMA (or BuA) gave thermally stable adhesive materials composed of $[-\text{CH}_2\text{CMe}(\text{COOH})-]_m[-\text{CH}_2\text{CMe}(\text{COOMe})-]_n$ or $[-\text{CH}_2\text{CMe}(\text{COOH})-]_m[-\text{CH}_2\text{CH}(\text{CO}_2\text{Bu})-]_n$ (Fig. 7).

High thermostability may originate from their high syndiotactic sequence.

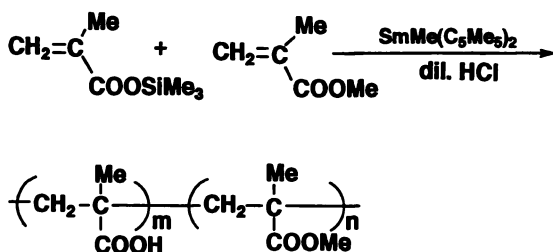


Fig. 7. Block copolymerization of MMA with TMSMA

Table 4. Block Copolymerization of TMSMA and MMA or BuA

Feed ratio ^a		M_n (calcd)	poly(TMSMA)		poly(TMSMA/MMA or BuA)		Yield/%
TMSMA	MMA	M_n	M_w/M_n	M_n	M_w/M_n		
67	124	23,000	8,900	1.13	28,100	1.17	99
TMSMA BuA							
30	42	10,100	52,00	1.11	10,500	1.16	98
67	93	22,500	81,00	1.10	22,600	1.26	99
30	304	43,700	51,00	1.11	77,300	1.15	98

^a mmol to the 1 mmol of initiator. Solvent, toluene; Polymerization of TMSMA 2 min, Polymerization temp. 0°C

Polymerization of Alkyl Isocyanates

Polyisocyanates have attracted much attention owing to their liquid crystalline properties, stiff-chain solution characteristics, and induced optical activities associated with the helical chain conformation. Patten and Novak discovered that such titanium complexes like $\text{TiCl}_3(\text{OCH}_2\text{CF}_3)$ and $\text{TiCl}_2(\text{C}_5\text{H}_5)(\text{OCH}_2\text{CF}_3)$ initiate the living polymerization of isocyanates, giving polymers with very narrow molecular weight distribution (19). When hexyl isocyanate was added to $\text{TiCl}_3(\text{OCH}_2\text{CF}_3)$ the polymerization took place at room temperature, with M_n increasing linearly with the



Fig. 8. Living polymerization of alkyl isocyanate

initial monomer-to-initiator mole ratio or the monomer conversion ($M_w/M_n = 1.1 - 1.3$). Recently, Fukuwatari et al. discovered that lanthanum isopropoxide initiates the polymerization of hexyl isocyanate at low temperature (-78 °C) to give high molecular weight polymers ($M_n > 10^6$) with rather narrow molecular weight distribution ($M_w/M_n = 2.08 - 3.16$) (20). Furthermore, butyl, isobutyl, octyl and m-tolyl isocyanates could be polymerized using lanthanum isopropoxide as the initiator. When the reaction temperature was raised to ambient temperature, only cyclic trimers were produced at high yields. More recently we have found that $\text{La}(\text{C}_5\text{Me}_5)_2[\text{CH}(\text{SiMe}_3)_2]_2$ also initiates the polymerization of butyl isocyanate and hexyl isocyanate in THF in 90% yields to give the polymer of $M_n = 59.4 \times 10^4$ with

$M_w/M_n = 1.57$ at -20°C , while $\text{Sm}[\text{C}_6\text{H}_3(\text{O}i\text{Pr})_2]_3$ gave poly(hexyl isocyanate) of $M_n = 74.6 \times 10^4$ with $M_w/M_n = 2.50$ at 25°C (21).

Living Polymerization of Lactones

$\text{AlEt}_3\text{-H}_2\text{O}$ or AlEt_3 -catalyzed polymerization of 3-methyl- β -propiolactone and ϵ -caprolactone has been reported (22,23), but this type of polymerizations generally gives a broad molecular weight distribution. We have explored the polymerization of various lactones including β -propiolactone (PL), 3-methyl- β -propiolactone (MePL), δ -valerolactone (VL) and ϵ -caprolactone (CL) initiated by single component organolanthanides, and found that VL and CL led to the living polymerization, yielding high polymers with $M_w/M_n = 1.05 - 1.10$ at quantitative yields (Table 5) (24). For ϵ -caprolactone, M_n obtained with the $\text{SmMe}(\text{C}_5\text{Me}_5)_2(\text{THF})$ or $[\text{SmH}(\text{C}_5\text{Me}_5)_2]_2$ system increased with increasing conversion, but M_w/M_n remained very narrow value, irrespective of the conversion. For β -propiolactone, the use of $\text{YOMe}(\text{C}_5\text{Me}_5)_2$ was more favorable. On the other hand, divalent organolanthanide complexes can initiate the polymerization of lactones, but the resulting polymers had rather broad molecular weight distributions and show bimodal pattern (25b). At the early stage of the polymerization of lactone with $\text{Y}(\text{OMe})(\text{C}_5\text{Me}_5)_2$, one mole of ϵ -caprolactone coordinates to the metal, as is the case for the reaction of YCl_3 with ϵ -caprolactone, giving the first six-coordinate mer complex, $\text{YCl}_3 \cdot (\epsilon\text{-caprolactone})_3$ in which each caprolactone molecule is coordinated as a monodentate ligand through its carbonyl oxygen (25a). The polymerization starts with the coordination of ϵ -caprolactone to form the 1:1 complex $\text{Y}(\text{OMe})(\text{C}_5\text{Me}_5)_2(\epsilon\text{-caprolactone})$, and in its propagation step the methoxide attacks the $\text{C}=\text{O}$ group to produce $\text{Y}[\text{O}(\text{CH}_2)_5\text{C}(\text{O})\text{R}](\text{C}_5\text{Me}_5)_2(\epsilon\text{-caprolactone})$. In the $\text{SmMe}(\text{C}_5\text{Me}_5)_2$ initiator system, the reaction is initiated by the attack of ϵ -caprolactone or δ -

Table 5. Living Polymerization of Lactones with Organolanthanide Complexes

Initiator	Monomer	$M_n/10^3$	M_w/M_n	Conversion/%
$\text{SmMe}(\text{C}_5\text{Me}_5)_2(\text{THF})$	VL	75.2	1.07	80.1 (7h)
	CL	109.4	1.09	92.0 (7h)
$[\text{SmH}(\text{C}_5\text{Me}_5)_2]_2$	VL	65.7	1.08	90.5 (7h)
	CL	71.1	1.19	28.7 (5h)
$[\text{YOMe}(\text{C}_5\text{H}_5)_2]_2$	CL	62.2	1.10	87.5 (5h)
	PL	60.5	2.12	94.5 (5h)

PL β -propiolactone, VL δ -valerolactone, CL ϵ -caprolactone. Polymerization, 0°C in toluene.

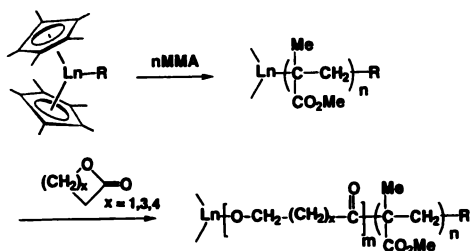


Fig. 9. Copolymerization of MMA with lactones

valerolactone to result in the formation of an acetal without ring opening. This process has been confirmed by ^{13}C NMR studies of the stoichiometric reaction products.

Anionic block copolymerizations of MMA with lactones proceeded smoothly by

the $\text{SmMe}(\text{C}_5\text{Me}_5)_2(\text{THF})$ initiator to give copolymers with low polydispersity, $M_w/M_n = 1.11 - 1.23$, when the monomers were added in this order. However, when the order of addition was reversed, no copolymerization took place, i.e. no addition of MMA to the polylactone active end occurred.

Stereospecific Polymerization of Olefins

Bulky organolanthanide(III) complexes such as $\text{LnH}(\text{C}_5\text{Me}_5)_2$ ($\text{Ln} = \text{La}, \text{Nd}$) were found to catalyze the polymerization of ethylene with high efficiency (26). These hydrides are, however, thermally unstable and cannot be isolated as crystals. Therefore, thermally more stable bulky *trivalent* organolanthanides were synthesized by introducing four trimethylsilyl groups into the Me_2Si bridged Cp ligand, as shown in Fig. 10 (27). The reaction of the dilithium salt of this ligand with anhydrous SmCl_3 produced a mixture of two stereo-isomeric complexes. The respective

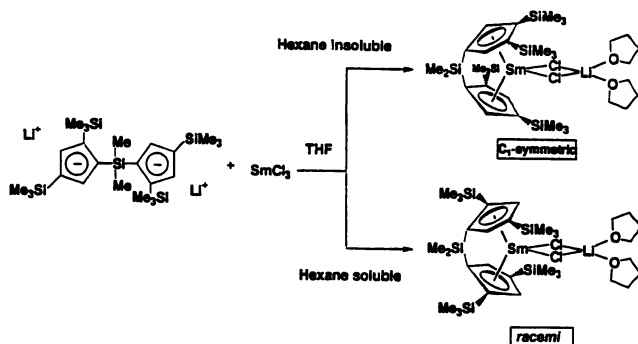


Fig. 10. Synthesis of organolanthanide(III) for polymerization of ethylene

isomers were isolated by utilizing their different solubilities in hexane, and their structures were determined by X-ray crystallography. Hexane soluble complex has a *racemic* structure in which two trimethylsilyl groups are located at the 2,4-positions of the Cp rings, while the hexane insoluble complex has a C_1 symmetric structure in which two trimethylsilyl groups are located at 2,4- and 2,3-positions of each Cp ring as was determined by X-ray analyses. Both were converted to alkyl derivatives when they were allowed to react with bis(trimethylsilyl)methyl lithium. The $\text{Cp}'\text{-Sm-Cp}'$ angle of the racemic-type precursor is 107° , which is about 15° smaller than that of non-bridged $\text{SmMe}(\text{C}_5\text{Me}_5)_2(\text{THF})$.

Meso type ligands were synthesized by forcing two trimethylsilyl groups to be located at the 4-position of the ligand with introduction of two bridges. Actually, the complexation of this ligand with YCl_3 yielded a *meso* type complex, and the structure of the complex was determined by X-ray analysis (Fig.11). The *meso* type alkyl complex was synthesized in a similar manner.

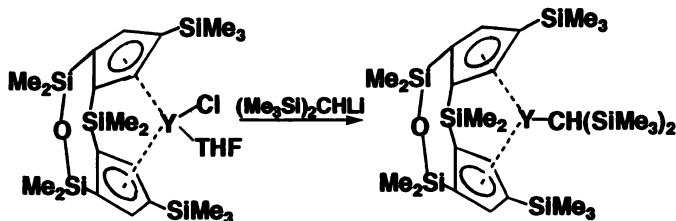


Fig. 11. Illustration of doubly bridged organoytterbium complex

Table 6. Ethylene Polymerization by Organolanthanide(III) Complexes

Initiator	$M_n/10^4$	M_w/M_n	Activity (g/mol·h)
$(C_5Me_5)_2SmCH(SiMe_3)_2$			no polymerization
$SiMe_2[2,4-(SiMe_3)_2C_5H_2]_2SmCH(SiMe_3)_2$ (<i>racemi</i>)			no polymerization
$SiMe_2(Me_2SiOSiMe_2)(4-SiMe_3-C_5H_2)YCH(SiMe_3)_2$ (<i>meso</i>)			no polymerization
$SiMe_2[2(3),4-(SiMe_3)_2C_5H_2]_2SmCH(SiMe_3)_2$ (C_1)	41.3	2.19	3.3×10^4
$SiMe_2[2(3),4-(SiMe_3)_2C_5H_2]_2YCH(SiMe_3)_2$ (C_1)	33.1	1.65	18.8×10^4

Initiator concentration, 0.2 mol%. Ethylene was introduced by bubbling at atmospheric pressure.

Table 6 summarizes the results of ethylene polymerization with these organolanthanide(III) complexes. Interestingly, only C_1 type complexes can initiate the polymerization, implying that the catalytic activity varies with the structure of the complex, catalysis is lacking for *meso*- and *racemic* organolanthanide(II) species due to the close packing. The X-ray structure of the C_1 symmetric complex shows that the $Cp'-Sm-Cp'$ angle is 108° , a very small dihedral angle. T. Marks reported that the polymerization of ethylene with $SmH(C_5Me_5)_2$ in the presence of $PhSiH_3$ formed PhH_2Si capped polyethylene ($M_n=9.8 \times 10^4$, $M_w/M_n=1.8$), and the copolymerization of ethylene with 1-hexene or styrene gave PhH_2Si capped copolymer (comonomer content 60 and 26mol%, respectively; $M_n=3.7 \times 10^3$, $M_w/M_n=2.9$ for ethylene-1-hexene copolymer, $M_n=3.3 \times 10^3$ for ethylene-styrene copolymer) (28).

Racemic, *meso*, and C_1 symmetric *divalent* organolanthanide complexes can be synthesized by allowing the dipotassium salt of the corresponding ligand to react

Table 7. Ethylene Polymerization by Divalent Samarium Complexes

Initiator	Time/min	$M_n/10^4$	M_w/M_n	Activity(g/mol. h)
$(C_5Me_5)_2Sm(THF)_2$	1	2.28	1.25	43
	3	2.46	2.28	41
<i>Racemi</i>	1	11.59	1.43	6
	3	35.63	1.60	14
<i>Meso</i>	5	1.94	3.29	14
	10	4.73	3.49	47
	15	100.8	1.60	1.6
C_1 Symmetry	30	> 100.0	1.64	1.1

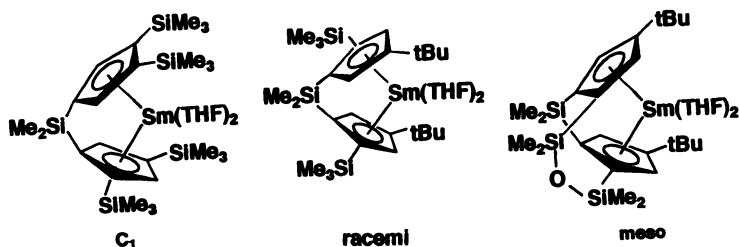


Fig. 12. Typical divalent organolanthanide complexes

with SmI_2 (29). Table 7 shows the results from the olefin polymerization with divalent samarium complexes. It is seen that the *meso* type complex has the highest activity for the polymerization of ethylene, but the molecular weights of the resulting polymers are the lowest. On the other hand, the *racemic* and C_1 symmetric complexes produce much higher molecular weight polyethylene but the activity is

rather low. Particularly, the very high molecular weight polyethylene ($M_n > 100 \times 10^4$) obtained with C_1 complex deserves attention. For the polymerization of α -olefins, only the *racemic* divalent complex showed good activity at 0 °C in toluene: poly(1-hexene) $M_n = 24,600$, $M_w/M_n = 1.85$; poly(1-pentene) $M_n = 18,700$, $M_w/M_n = 1.58$. Thus, we see that the reactivity of divalent organolanthanide complexes depends on their structure. The poly(1-alkene) obtained revealed highly isotactic structure (> 95%) when examined by ^{13}C NMR. The dihedral angles of $\text{Cp}'\text{-Ln-Cp}'$ of *racemic* and *meso* type divalent complexes were 117 and 116.7°, respectively; these values are much smaller than those of $\text{Sm}(\text{C}_5\text{Me}_5)_2(\text{THF})$ (136.7°) (32) and $\text{Sm}(\text{C}_5\text{Me}_5)_2$ (140.1°). Therefore, it can be concluded that the complexes having smaller $\text{Cp}'\text{-Ln-Cp}'$ angles are more active for the polymerization of ethylene and α -olefins. In the initiation step, an α -olefin inserts between two *racemic* lanthanide(II) species, but the insertion hardly occurs between two C_1 -symmetric lanthanide(II) complex due to steric reasons. On the other hand, *meso*-type lanthanide(II) should easily take place the β -elimination to result in lanthanide(III)-allyl complex. 1,5-Hexadiene was polymerized smoothly by the catalytic action of *rac*- $\text{Me}_2\text{Si}(2\text{-SiMe}_3\text{-4-tBu-C}_5\text{H}_2)_2\text{Sm}(\text{THF})_2$ to give poly(methylene-1,3-cyclopentane) at a ratio of *cis/trans* = 55/45.

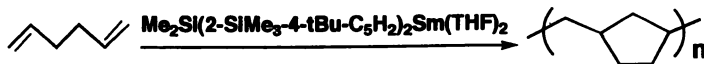


Fig. 13. Cyclic polymerization of 1,5-hexadiene

Polymerization of Styrene

Recent study showed that the single component initiator $[(\text{tBuCp})_2\text{LnCH}_3]_2$ ($\text{Ln} = \text{Pr}, \text{Nd}, \text{Gd}$) can initiate the polymerization of styrene at relatively high temperature, 70°C, with a conversion of 96% and the M_n of 3.3×10^4 for $[(\text{tBuCp})_2\text{NdCH}_3]_2$, though stereoregularity was very poor(30). Styrene polymerization was also performed successfully using the single component initiators, $[(\text{Me}_3\text{Si})_2\text{N}]_2\text{Sm}(\text{THF})_2$, $[(\text{Me}_3\text{Si})_2\text{CH}]_3\text{Sm}$, and $\text{La}(\text{C}_5\text{Me}_5)[\text{CH}(\text{SiMe}_3)_2]_2(\text{THF})$

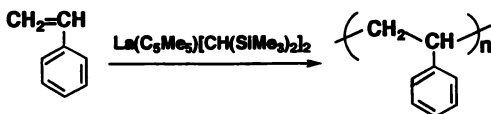


Fig. 14. Styrene polymerization by $\text{La}(\text{C}_5\text{Me}_5)[\text{CH}(\text{SiMe}_3)_2]_2$

at 50 °C in toluene without addition of any cocatalyst. The resulting polymers had $M_n = 1.5 - 1.8 \times 10^4$ and $M_w/M_n = 1.5 - 1.8$, and show atactic property (23). Thus no success has yet been achieved in synthesizing syndiotactic polystyrene with rare earth metal complexes, in contrast to the synthesis of highly syndiotactic polystyrene with $\text{TiCl}_3(\text{C}_5\text{Me}_5)/(\text{AlMe-O})_n$ (syndiotacticity > 95%) (31).

Block Copolymerization of Ethylene with Polar Monomers

Block copolymerization of ethylene or propylene with polar monomers is yet to be attained in polyolefin engineering. The success of this type of block copolymerization should give hydrophobic polymeric materials having remarkably high adhering, dyeing, and moisture adsorbing properties. The following is the first example of a well-controlled block copolymerization using the unique dual catalytic

function of $\text{LnR}(\text{C}_5\text{Me}_5)_2$ ($\text{Ln} = \text{Sm}, \text{Yb}, \text{and Lu}; \text{R} = \text{H}, \text{Me}$) complexes toward polar and nonpolar olefins (32). Block copolymerization was carried out by the homopolymerization of ethylene (17 - 20 mmol) with $\text{SmMe}(\text{C}_5\text{Me}_5)_2(\text{THF})$ or $[\text{SmH}(\text{C}_5\text{Me}_5)_2]_2(0.05 \text{ mmol})$ at 20 °C in toluene under atmospheric pressure,

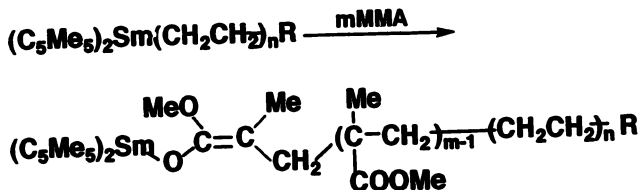


Fig. 15. Block copolymerizations of ethylene with MMA

followed by sequential addition of MMA (10 mmol) (Table 8). The initial step proceeded very rapidly, completed in 2 min, and gave a linear polymer of $M_n = \text{ca. } 10,100$ and $M_w/M_n = 1.42 - 1.44$. However, the second step was rather slow, with the reaction taking 2 h at 20 °C. The resulting polymer was soluble in 1,2-dichlorobenzene and 1,2,4-trichlorobenzene at 100 °C but insoluble in THF and CHCl_3 . This fact indicates quantitative conversion to the desired linear block copolymer. Repeated fractionation in hot THF did not change the molar ratio between the polyethylene and poly(MMA) blocks, though poly(MMA) blended with polyethylene can easily be extracted with THF. With the copolymerization, the elution maximum in GPC shifted to a higher molecular weight region, with its initial unimodal pattern unchanged. The relative molar ratio of the polyethylene and poly(MMA) blocks was controllable at will in the range of 100:1 to 100:103 if the M_n of the initial polyethylene was fixed to ca. 10,300. ^1H and ^{13}C NMR spectra for the copolymers as well as their IR absorption spectra were superimposable onto those of the physical mixtures of the respective homopolymers. The molar ratio of the poly(MMA) and polyethylene blocks, however, decreased as the M_n of the prepolymer increased, especially when it is exceeded ca. 12,000 at which value polyethylene began precipitating as fine colorless particles. It is noteworthy that smooth block copolymerization of ethyl acrylate or methyl acrylate to the growing polyethylene chain ($M_n = 6,600 - 24,800$) can be realized also by the sequential addition of these two monomers.

The above work was extended to the block copolymerization of ethylene with lactones. δ -Valerolactone and ϵ -caprolactone were incorporated to the growing polyethylene end at ambient temperature and the expected AB type copolymers (100:1 to 100:89) were obtained in high yield. Reversed addition of the monomers (first MMA or lactones and then ethylene) induced no block copolymerization at all, even in the presence of excess ethylene, and only homo-poly(MMA) and homo-poly(lactone) were produced. The treatment of the resulting block copoly(ethylene/MMA) (100:3, $M_n = 35,000$) and block copoly(ethylene/ ϵ -caprolactone) (100:11, $M_n = 12,000$) with dispersed dyes (Dianix AC-E) made them deeply dye with three primary colors, blue, red and yellow, though polyethylene itself was inert to these dyes. Hence, these copolymers can be said to have a very desirable chemical reactivity.

More recently, Yang et al. have examined a new approach in which a reactive functional group was introduced into polyolefins using methylenecyclopropane. Thus, ethylene (1.0 atm) was copolymerized with methylenecyclopropane (0.25 - 2.5 mL) using $[\text{LnH}(\text{C}_5\text{Me}_5)_2]_2$ ($\text{Ln} = \text{Sm}, \text{Lu}$) in toluene at 25 °C, and it was shown that 10-65 of exo-methylenes were incorporated per 1000 $-\text{CH}_2-$ units. The resulting polymer had a M_w of $66-92 \times 10^3$. Yet its M_w/M_n was larger than 4.0.

Table 8. Block Copolymerization of Ethylene with Polar Monomers

Polar monomer	Polyethylene block ^a		Polar polymer block ^b		Unit ratio
	$M_n/10^3$	M_w/M_n	$M_n/10^3$	M_w/M_n	
MMA	10.3	1.42	24.2	1.37	100:103
	26.9	1.39	12.8	1.37	100:13
	40.5	1.40	18.2	1.90	100:12
MeA	6.6	1.40	15.0	1.36	100:71
	24.5	2.01	3.0	1.66	100:4
EtA	10.1	1.44	30.8	2.74	100:85
	24.8	1.97	18.2	3.84	100:21
VL	10.1	1.44	7.4	1.45	100:20
	24.8	1.97	4.7	1.97	100:5
CL	6.6	1.40	23.9	1.76	100:89
	24.5q	2.01	6.9	2.01	100:7

a) Determined by GPC using standard polystyrene. b) Determined by ¹H NMR. Polymerization was carried out at 0 °C.

Acknowledgment

This work was partly supported by Grant-in-Aid for Scientific Research on Priority Areas (No. 283, "Innovative Synthetic Reactions") from Monbusho

References

- 1) a) Szwarc, M. *Adv. Polym. Sci.*, **1983**, *49*, 1 b) Nakahama, S.; Hirao, A. *Prog. Polym. Sci.*, **1990**, *13*, 299. c) Inoue, S. *Macromolecules*, **1988**, *21*, 1195.
- 2) a) Sawamoto, M.; Okamoto, O.; Higashimura, T. *Macromolecules*, **1987**, *20*, 2693. b) Kojima, K.; Sawamoto, M.; Higashimura, T. *Macromolecules*, **1988**, *21*, 1552.
- 3) a) Webster, O. W.; Hertler, W. R.; Sogah, D. Y.; Farnham, W. B.; RajanBabu, T. V. *J. Am. Chem. Soc.*, **1983**, *105*, 5706. b) Sogah, D. Y.; Hertler, W. R.; Webster, O. W.; Cohen, G. M. *Macromolecules*, **1987**, *20*, 1473.
- 4) a) Gillon, L. R.; Grubbs, R. H. *J. Am. Chem. Soc.*, **1986**, *108*, 733. b) Grubbs R. H.; Tumas, W. *Science*, **1989**, *243*, 907. c) Schrock, R. R.; Feldman, J.; Canizzo, L. F.; Grubbs, R. H. *Macromolecules*, **1989**, *20*, 1169. 5) a) Yasuda, H.; Yamamoto, H.; Yokota, K.; Miyake, S.; Nakamura, A. *J. Am. Chem. Soc.*, **1992**, *114*, 4908. b) Yasuda, H.; Yamamoto, H.; Takemoto, Y.; Yamashita, M.; Yokota, K.; Miyake, S.; Nakamura, A. *Makromol. Chem. Macromol. Symp.* **1993**, *67*, 187. c) Yasuda, H.; Yamamoto, H.; Yamashita, M.; Yokota, K.; Nakamura, A.; Miyake, S.; Kai, Y.; Kanehisa, N. *Macromolecules*, **1993**, *22*, 7134. d) Yasuda, H.; Tamai, H. *Prog. Polym. Sci.*, **1993**, *18*, 1097.
- 6) Cao, Z. K.; Okamoto, Y.; Hatada, K. *Kobunshi Ronbunshu*, **1986**, *43*, 857.
- 7) a) Joh, Y.; Kotake, Y. *Macromolecules*, **1976**, *3*, 337. b) Hatada, K.; Nakanishi, H.; Ute, K.; Kitayama, T. *Polym. J.*, **1986**, *18*, 581.
- 8) Abe, H.; Imai, K.; Matsumoto, M. *J. Polym. Sci.*, **1968**, *C23*, 469.
- 9) Nakano, N.; Ute, K.; Okamoto, Y.; Matsuura, Y.; Hatada, K. *Polym. J.*, **1989**, *21*, 935.
- 10) Yamamoto, Y.; Giardello, M. A.; Brard, L.; Marks, T. J. *J. Am. Chem. Soc.*, **1995**, *117*, 3726.
- 11) Hayakawa, T.; Ihara, E.; Yasuda, H. unpublished result.
- 12) Boffa, L. S.; Novak, B. M. *Macromolecules*, **1994**, *27*, 6993.

- 13) a) Kuroki, M.; Watanabe, T.; Aida, T.; Inoue, S. *J. Am. Chem. Soc.*, **1991**, *113*, 5903. b) Aida, T.; Inoue, S. *Acc. Chem. Res.*, **1996**, *29*, 39.
- 14) Collins, S.; Ward, D. G.; Suddaby, K. H. *Macromolecules*, **1994**, *27*, 7222.
- 15) a) Soga, K.; Deng, H.; Yano, T.; Shiono, T. *Macromolecules*, **1994**, *27*, 7938. b) Deng, H.; Shiono, T.; Soga, K. *Macromolecules*, **1995**, *28*, 3067.
- 16) Hosokawa, Y.; Kuroki, M.; Aida, T.; Inoue, S. *Macromolecules*, **1991**, *24*, 8243.
- 17) a) Ihara, E.; Morimoto, M.; Yasuda, H. *Proc. Japan Acad.*, **1996**, *71*, 126. b) Ihara, E.; Morimoto, M.; Yasuda, H. *Macromolecules*, **1995**, *28*, 7886. c) Suchoparek, M.; Spvacek, J. *Macromolecules*, **1993**, *26*, 102. d) Madruga, E. L.; Roman, J. S.; Rodriguez, M. J. *J. Polym. Sci., Polym. Chem. Ed.*, **1983**, *21*, 2739.
- 18) Kakehi, T.; Ihara, E.; Yasuda, H. unpublished results.
- 19) a) Patten, T. E.; Novak, B. M. *J. Am. Chem. Soc.*, **1991**, *113*, 5065. b) Patten T. E.; Novak, B. M. *Makromol. Chem. Macromol. Symp.*, **1993**, *67*, 203.
- 20) Fukuwatari, N.; Sugimoto, H.; Inoue, S. *Macromol. Rapid Commun.*, **1996**, *17*, 1.
- 21) Tanaka, K.; Ihara, E.; Yasuda, H. unpublished results.
- 22) Wang, J.; Nomura, R.; Endo, T. *J. Polym. Sci., Polym. Chem. Ed.*, **1995**, *33*, 2901.
- 23) a) Hofman, A.; Szymanski, R.; Slomkowski, S.; Penczek, S. *Makromol. Chem.*, **1980**, *185*, 655. b) Agostini, D. E.; Lado, J. B.; Sheeton, J. R. *J. Polym. Sci.*, **1971**, *A1*, 2775.
- 24) Yamashita, M.; Ihara, E.; Yasuda, H. *Macromolecules*, **1996**, *29*, 1798.
- 25) a) Evans, J. E.; Shreeve, J. L.; Doedens, R. J. *Inorg. Chem.*, **1993**, *32*, 245. b) Evans, J. E.; Katsumata, H. *Macromolecules*, **1994**, *27*, 2330.
- 26) Jeske, G.; Shock, L. E.; Swepstone, P. N.; Schumann, H.; Marks, T. J. *J. Am. Chem. Soc.*, **1985**, *107*, 8103.
- 27) a) Yasuda, H.; Ihara, E. *J. Synth. Org. Chem. Jpn.*, **1993**, *51*, 931. b) Yasuda, H.; Ihara, E.; Yoshioka, S.; Nodono, M.; Morimoto, M.; Yamashita, M. "Catalyst Design for Tailor-made Polyolefins", Kodansha-Elsevier, 1994, p. 237. c) Nodono, M.; Ihara, E.; Yasuda, H. unpublished result.
- 28) Fu, P.; Marks, T. J. *J. Am. Chem. Soc.*, **1995**, *117*, 10747.
- 29) Ihara, E.; Nodono, M.; Yasuda, H.; Kanehisa, N.; Kai, Y. *Macromol. Chem. Phys.*, **1996**, *197*, 1909.
- 30) Yang, M.; Chan, C.; Shen, Z. *Polym. J.*, **1990**, *22*, 919.
- 31) a) Ishihara, N.; Seimiya, T.; Kuramoto, M.; Uoi, M. *Macromolecules*, **1986**, *19*, 2464. b) Ishihara, N.; Kuramoto, M.; Uoi, M. *Macromolecules*, **1988**, *21*, 3356.
- 32) Yasuda, H.; Furo, M.; Yamamoto, H.; Nakamra, A.; Miyake, S.; Kibino, N. *Macromolecules*, **1992**, *25*, 5115.

Chapter 12

New Reactive Polyolefins Containing *p*-Methylstyrene; Ranging from Semicrystalline Thermoplastics to Amorphous Elastomers

H. L. Lu and T. C. Chung¹

Department of Materials Science and Engineering, The Pennsylvania State
University, University Park, PA 16802

This paper describes a new class of reactive polyolefins, containing reactive *p*-methylstyrene (*p*-MS) groups. The chemistry involves the copolymerization reactions between ethylene and *p*-MS and terpolymerization of ethylene *p*-MS and 1-octene in the presence of homogeneous metallocene catalyst systems. Three catalyst systems, i.e. Cp₂ZrCl₂/MAO (I), Et(Ind)₂ZrCl₂/MAO (II) and [C₅Me₄(SiMe₂Nt-Bu)]TiCl₂/MAO (III) were studied in the copolymerization reactions. *p*-MS-containing polyethylene copolymers with a broad range of compositions (from semi-crystalline thermoplastic, thermoplastic elastomer to completely amorphous elastomer) and narrow composition and molecular weight distribution were synthesized. Catalyst III was also studied in the terpolymerization of ethylene, 1-octene and *p*-MS to produce *p*-MS-containing polyolefin elastomers. A new class of polyolefin elastomers, containing reactive *p*-MS groups, with a broad composition and glass transition temperature (T_g) ranges, high molecular weight and narrow molecular weight and composition distributions were achieved.

Despite the commercial success of polyolefins, the lack of reactive groups in the polymer structure has limited some of their applications, particularly where adhesion, dyeability, or compatibility with other functional polymers is paramount. The functionalization of polyolefins has long been not only of industrial importance but also a scientific challenge. Unfortunately, both direct polymerization and post-modification processes toward the functionalization of polyolefins have suffered

¹Corresponding author.

from many undesirable side reactions [1,2] due to the catalyst poison [3] and the inert nature of polyolefins and therefore only achieved limited success.

Our functionalization approaches have been focusing on the reactive polyolefins. The approaches involve two steps, including the synthesis of reactive polyolefins via the copolymerization of α -olefin monomers with reactive monomers by Ziegler-Natta catalysts or metallocene catalysts and the subsequent functionalization reactions of the resulting reactive polyolefins. In our approaches, the concentration and distribution of functional groups in the polyolefins can be controlled by the copolymerization. The structures of the copolymers are designed in such a way that the "reactive" sites are pendant away from the polyolefin backbone. Accordingly, functional polyolefins with relatively well-defined composition and structure can be achieved, and undesirable side reactions, such as degradation of polymer backbone, can be completely avoided. The success of the approaches would mainly depend on the use of appropriate reactive monomers. The reactive monomer should fulfill the following requirements: i) the reactive monomer must be stable to Ziegler-Natta or metallocene catalysts, ii) it should be easily incorporated into polyolefin chain by copolymerization with α -olefin monomers, iii) it must possess a reactive site which should be chemically versatile for the further functionalization reactions under mild reaction condition. In addition, the reactive monomer should be commercially available or easy to synthesize and not too expensive.

Borane-containing α -olefinic monomers, which are completely stable to Ziegler-Natta catalysts and soluble in typical hydrocarbon solvents [4,5] have been copolymerized with α -olefins, such as propylene, 1-butene and 1-octene by using heterogeneous Ziegler-Natta catalysts, such as TiCl_3 , AA/ AlEt_2Cl [6,7]. Due to the chemical versatility of the borane moiety, the borane-containing polyolefins have served as reactive polymer intermediates for the preparation of functionalized polyolefins with various functional groups [8,9]. By adopting the new advanced metallocene technology, we have also extended our borane approach to the functionalization of polyethylene [10,11].

Recently, our reactive polyolefin approach has extended to another type of reactive comonomer, i.e. *p*-methylstyrene (*p*-MS) [12,13]. The major advantages of *p*-MS include i) polymerizability to Ziegler-Natta and metallocene catalysts, ii) chemical versatility of *p*-methyl group, iii) commercial availability and iv) cost effectiveness. The *p*-MS comonomer can be effectively incorporated into polyolefin, especially by using metallocene catalysts with constrained ligand geometry. The *p*-MS-containing polyolefins are very versatile, which can be efficiently and selectively converted into functionalized polyolefins with a variety of functional groups and polymeric initiators for "living" anionic graft-from reactions [14]. In our previous paper [13], we have shown that *p*-MS comonomer is superior to styrene and other methylstyrene derivatives in the copolymerization reactions with ethylene using metallocene catalysts. This paper reports the detailed results in the synthesis of poly(ethylene-co-*p*-MS) copolymers and poly(ethylene-ter-1-octene-ter-*p*-MS) terpolymers with a broad range of compositions and narrow molecular weight and com-

position distributions, which are very versatile and useful intermediates for the functionalization of polyolefins.

Synthesis of Poly(ethylene-co-p-MS) Copolymers

Three metallocene catalysts, Cp_2ZrCl_2 (I) $\text{Et}(\text{Ind})_2\text{ZrCl}_2$ (II) and $[\text{C}_5\text{Me}_4(\text{SiMe}_2\text{NtBu})]\text{TiCl}_2$ (III) along with MAO cocatalyst were used to synthesize poly(ethylene-co-p-MS) copolymers. The chemical compositions of the resulting copolymers were analyzed by ^1H NMR measurements. Figure 1 shows ^1H NMR spectra of the copolymers with different p-MS concentrations. In addition to the major peak at 1.35 ppm, corresponding to methylene protons CH_2 in both ethylene and p-MS units, there are three other minor peaks around 2.35, 2.50 and 7.0-7.1 ppm, corresponding to benzylic protons of p-methyl group $-\text{CH}_3$, benzylic protons in backbone $-\text{CH}-$ and aromatic protons in p-MS units, respectively. The integrated peak areas at 1.35 and 7.0-7.1 ppm were used to estimate p-MS concentration in the copolymers. The conversion of p-MS comonomer was calculated from the p-MS concentration in the copolymer, copolymer yield and comonomer concentration in the feed. The results are summarized in Table 1.

The Effect of Catalysts. Overall, the copolymerization activity and the incorporation of p-MS in the copolymers follow the order of $[(\text{C}_5\text{Me}_4\text{SiMe}_2\text{N}(\text{t-Bu}))\text{TiCl}_2$ (III) > $\text{Et}(\text{Ind})_2\text{ZrCl}_2$ (II) > Cp_2ZrCl_2 (I). By comparing p365 and p360, p368 and p362 in Table 1, one can clearly see that, catalyst II gives higher copolymerization activity and much higher p-MS incorporation than catalyst I at the same conditions. Comparison between p386 and p377 clearly shows that catalyst III is much more efficient than catalyst II in terms of activity, p-MS incorporation and conversion under the same conditions.

The big performance differences among the catalysts must be attributed to the structure difference of the catalysts. catalyst I is the simplest zirconocene catalyst, the active site is sandwiched between two Cp rings, with Cp-Zr-Cp angle of 180° . In catalyst II, ethylene bridge induces the constrained ligand geometry by pulling the two indenyl groups together, which gives a Cp-Zr-Cp angle of 125.8° [15]. On the other hand, in catalyst III, the titanium is asymmetrically bound to the Cp ring, due to the covalent attachment of the amide through the silicon bridging group. The silicon bridge is pulled out of the plane of the Cp ring while the nitrogen atom of the amide ligand is pulled down from a normal position due to the covalent attachment to silicon bridge and titanium. The unique structure gives a highly constrained ligand geometry with a Cp-Ti-N angle of 107.6° [16]. Therefore, the spatial opening of the catalytic sites must increase in the order $\text{I} < \text{II} < \text{III}$. According to the structure/property relationship of the metallocene catalysts, the more opening of the active site, the higher the activity of copolymerization and the stronger the ability to incorporate the higher α -olefins or other bulky monomers like p-MS.

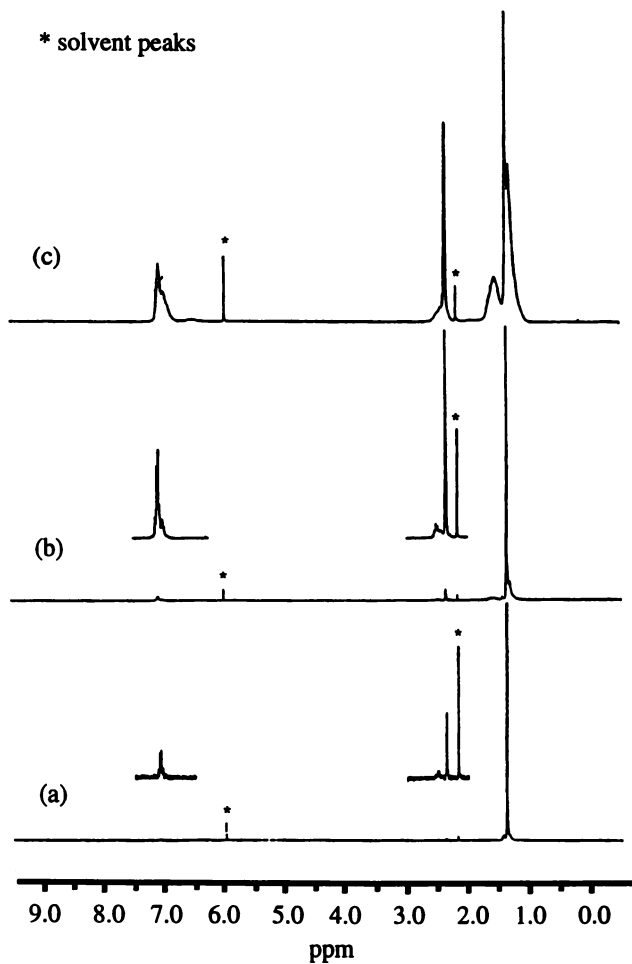


Figure 1. ^1H NMR spectra of poly(ethylene-co-p-MS) copolymers containing (a) 1.08, (b) 5.40 and (c) 18.96 mol% of p-MS.

Table 1. A summary of the copolymerization reactions^{b)} between ethylene and p-MS

Run No.	Catalyst ^{a)}	Ethylene	p-MS	Solvent	Temp.	Yield	Catalyst Ac-tivity	p-MS in Co-polymer	Conversion of p-MS %
	μmol	psi ^{c)}	mol/l		$^{\circ}\text{C}$	g	kg P/mol M.h	mol %	%
p381	I/17	45	0.175	Hexane	50	17.2	1011.8	1.32	44.4
p363	I/17	45	0.678	Hexane	50	24.2	1423.5	2.20	26.2
p365	I/17	45	0.678	Toluene	50	8.44	496.5	1.84	7.72
p368	I/17	45	1.36	Toluene	50	8.31	488.8	2.88	5.75
p356	II/17	45	0.085	Hexane	50	6.5	382.4	1.83	47.2
p372	II/17	45	0.508	Hexane	50	19.8	1164.7	3.94	48.7
p358	II/17	45	0.678	Hexane	50	21.9	1288.2	5.16	51.1
p361	II/17	45	1.36	Hexane	50	18.9	1111.8	7.20	29.0
p371	II/17	45	2.03	Hexane	50	20.8	1223.5	8.94	25.4
p386	II/17	45	0.456	Hexane	30	5.90	590.0	3.24	13.6
p357	II/17	45	0.085	Toluene	50	5.70	335.3	1.30	29.9
p392	II/17	45	0.456	Toluene	50	8.63	507.6	3.85	23.2
p360	II/17	45	0.678	Toluene	50	15.1	888.2	4.76	32.8
p362	II/17	45	1.36	Toluene	50	19.5	1147.1	6.36	27.0
p375	II/17	45	2.03	Toluene	50	19.4	1141.2	8.49	22.8
p270	III/10	45	0	Toluene	30	4.40	440.0	-	-
p377	III/10	45	0.447	Hexane	30	12.0	1200.0	13.5	90.3
p378	III/10	45	0.912	Hexane	30	15.5	1550.0	22.6	81.3
p267	III/10	45	0.447	Toluene	30	13.0	1300.0	10.9	83.8
p379	III/10	45	0.912	Toluene	30	17.4	1740.0	21.6	86.9
p380	III/10	45	1.82	Toluene	30	24.2	2420.0	32.8	75.8
p383	III/10	10	1.82	Hexane	30	15.9	1590.0	40.0	54.6

a) I: $\text{Cp}_2\text{ZrCl}_2/\text{MAO}$, II: $\text{Et}(\text{Ind})_2\text{ZrCl}_2/\text{MAO}$, III: $[(\text{C}_3\text{Me}_5)_2\text{SiMe}_2\text{N}(\text{t-Bu})]\text{TiCl}_2/\text{MAO}$.b) Polymerization conditions: Al/Zr , $\text{Al}/\text{Ti} = 1500$; solvent: 100 ml; reaction time: 1 hour.c) 45 psi ethylene ~ 0.309 mol/l in toluene, 0.424 mol/l in hexane at 50 $^{\circ}\text{C}$; ~ 0.398 mol/l in toluene, 0.523 mol/l in hexane at 30 $^{\circ}\text{C}$; 10 psi ethylene ~ 0.116 mol/l in hexane at 30 $^{\circ}\text{C}$.

To examine the homogeneity of the copolymers produced by different catalysts, two copolymers with 1.08 mol % and 1.01 mol % of p-MS produced by catalyst III and II, respectively, at 40 °C in toluene for 15 minutes, were analyzed by DSC. The DSC curves are shown in Figure 2. As it can be seen that catalyst III produces a copolymer with a lower melting point (T_m) (118.88 °C) and a smaller heat of fusion (ΔH_f) (81.99 J/g) (curve a) than that of the copolymer produced by catalyst II ($T_m = 123.06$ °C, $\Delta H_f = 98.58$ J/g) (curve b). This suggests that p-MS in the copolymer produced by catalyst III distributes more uniformly than that by catalyst II.

The effect of p-MS concentration in the monomer feed. From the results in Table 1, one can see that in each catalyst system p-MS concentrations in the copolymers increase with the increase of p-MS concentration in the monomer feed. For catalyst I and II, the maximum copolymer compositions are limited to 3 and 9 mol % of p-MS, respectively, even at very high p-MS concentration in the monomer feed. Indeed, at high concentration of p-MS, considerable amounts of p-MS homopolymer were also produced during the copolymerization reactions. On the other hand, in the case of catalyst III, p-MS concentrations in the copolymers almost proportionally increased with the increase of p-MS in the feed. A poly(ethylene-co-p-MS) containing as high as 40 mol % of p-MS was obtained in run p383, which is close to the ideal 50 mol %, as will be discussed later the consecutive insertion of p-MS in all three catalyst systems is unlikely.

Overall, the presence of p-MS greatly enhances the polymerization reaction and the catalyst activity systematically increases with the increase of p-MS content. Similar enhancements were also observed in the ethylene copolymerization reactions with borane and 1,4-hexadiene monomers as described in our previous study [10,11]. This could be either a physical phenomenon relative to the improvement of monomer diffusion in the lower crystalline copolymer structures or chemical phenomenon relative to the improved modification of active sites by comonomers or the combination of both phenomena. It is very interesting to note that, in the case of catalyst III, the catalyst activity attains a value of more than 2.4×10^6 g of copolymer/mole of Ti per hour in run p380 even with as high as 32.8 mol % of p-MS in the copolymer, which is about 6 times the value for the ethylene homopolymerization in run p270 under similar reaction conditions. This is completely different from the results obtained in the case of ethylene copolymerization with styrene using the same catalyst by other group, where the activity was observed to drop very rapidly with the increase of styrene concentration, particularly at the high styrene concentrations [17].

The Effect of Solvents. Both toluene and hexane were used as solvents in the copolymerization reactions. Normally, toluene is the solvent for metallocene catalytic polymerization of olefins, since both catalyst and MAO are soluble in toluene. Hexane and other aliphatic hydrocarbon solvents are typical solvents for Ziegler-Natta catalytic polymerization. They are poor solvents for MAO. The original idea of using hexane as solvent for copolymerization of ethylene and p-MS was to improve the morphology of the copolymer in order to facilitate the filtration and purifi-

cation procedures. In toluene, the copolymer produced was very fine powder and the light slurry solution was difficult to handle, especially, in large scale reactions. In addition to obtaining better morphology of the polymers, it was very unexpected that hexane also offered higher polymerization activity and enhanced the incorporation of p-MS into polyethylene. This effect was particularly significant with catalysts I and II, and in the relatively low p-MS concentration range, as shown in Table 1. All comparative reaction pairs (i.e. p363/p365, p356/p357, p358/p360), carried out under similar reaction conditions, consistently show higher activity and p-MS incorporation in hexane solution than in toluene solution. When relatively high p-MS concentrations are used, the solvent effect seems to level off. As in p361/p362 and p371/375, although hexane still gives better results than toluene, the difference is less significant. It is very interesting to note that a very small solvent effect was observed for catalyst III in the comparative run pairs p377/p267 and p378/p379.

To further explore the advantages of using hexane as solvents, two poly(ethylene-co-p-MS) copolymers with similar p-MS concentrations (1.36 and 1.30 mol %) obtained in hexane and in toluene using catalyst II/MAO at 50 °C, respectively, were analyzed by DSC and GPC. Figure 3 shows the DSC curves of both copolymers. The copolymer obtained in hexane has significant lower T_m (121.2 °C) and crystallinity ($\Delta H_f = 100.2$ J/g) than that obtained in toluene ($T_m = 125.6$ °C, $\Delta H_f = 112.8$ J/g), which indicates that the former copolymer is more homogeneous than the later one. GPC results show that molecular weights and molecular weight distributions of the both copolymers are almost identical

Overall, hexane gives higher activity and better incorporation of p-MS than toluene. The copolymers produced in hexane have similar molecular weight and molecular distribution, but more uniform composition distribution than that produced in toluene. Since toluene is more toxic and more difficult to remove from the polymer than hexane, replacing toluene with hexane could be very significant for the commercialization. In ethylene/p-MS system, we have demonstrated that the replacement is not only feasible but also greatly advantageous. The reasons behind this solvent effect are not very clear.

Reactivity Ratios. The best way to investigate the copolymerization reaction is to determine the reactivity ratio of the comonomers. To obtain meaningful results, a series of experiments were carried out by varying monomer feed ratio at low monomer conversion. The reactivity ratios between ethylene ($r_1 = k_{11}/k_{12}$) and p-MS ($r_2 = k_{22}/k_{21}$) are estimated by Kelen-Tüdös method [18]. In general, a good fit of the experimental results in the straight line was observed in each case. Figure 4 shows two η vs. ξ plots with the least squares best fit lines for catalyst III at 20 and 60 °C, respectively. The calculated values of r_1 and r_2 for both catalysts III and II at different temperature are summarized in Table 2.

In catalyst III cases, high r_1 ($r_1 = 19.6$ and 20 for 20 and 60 °C, respectively) and low r_2 ($r_2 = 0.04$ and 0.017 for 20 and 60 °C, respectively) indicate the strong tendency of ethylene consecutive insertion and very low possibility in continuous p-

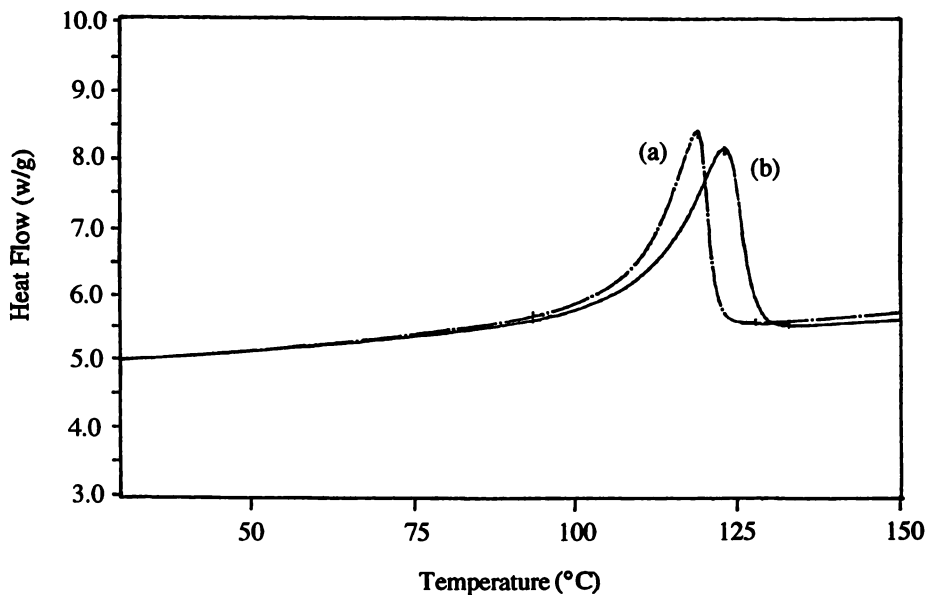


Figure 2. DSC curves of poly(ethylene-co-p-MS) copolymers containing 1.0 mol% of p-MS produced by (a) $[C_5Me_4SiMe_2N(t-Bu)]TiCl_2/MAO$ and (b) $Et(Ind)_2ZrCl_2/MAO$ catalysts.

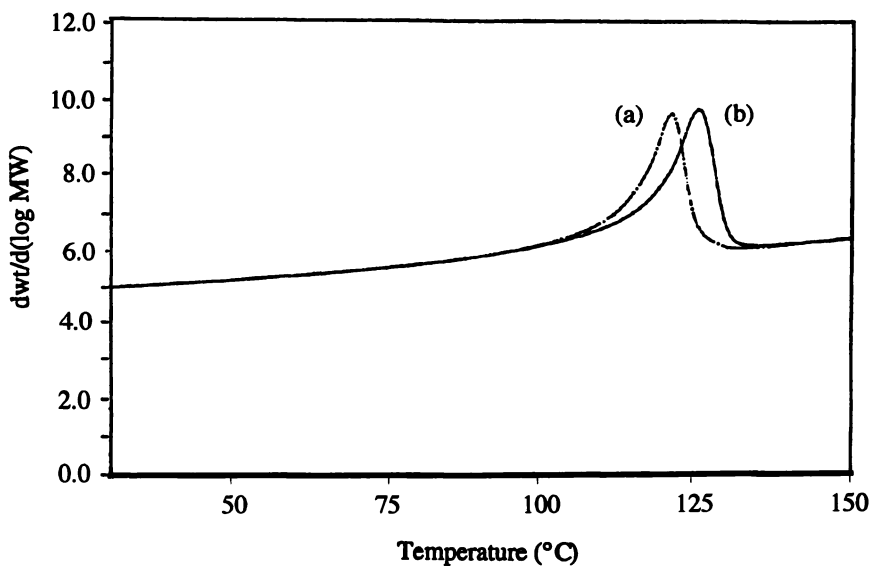


Figure 3. DSC curves of poly(ethylene-co-p-MS) copolymers containing about 1.30 mol% of p-MS by $Et(Ind)_2ZrCl_2/MAO$ catalyst in (a) hexane and (b) toluene.

MS insertion. The values of $r_1 \times r_2$ are less than but near to unity in both temperatures, which suggests the nearly ideal random copolymerization reactions and very small probability to find two adjacent p-MS units in the polymer chain. In other words, the p-MS units shall be homogeneously distributed in the polymer chain. In catalyst II cases, the copolymerization reactions exhibit even higher r_1 ($r_1 > 60$), very strongly favorable for ethylene incorporation, and almost no possibility of p-MS consecutive insertion ($r_2 \sim 0$). The less opened active site in $\text{Et}(\text{Ind})_2\text{ZrCl}_2$ catalyst may sterically prohibit p-MS consecutive insertion.

Table 2. A summary of reactivity ratios in the copolymerization reactions between ethylene (r_1) and p-MS (r_2)

Catalyst	Reaction Temp., °C	r_1	r_2	$r_1 \times r_2$
III/MAO	20	19.6	0.039	0.77
III/MAO	60	20.0	0.017	0.33
II/MAO	20	89.0	~ 0	-
II/MAO	40	72.0	~ 0	-
II/MAO	60	64.1	~ 0	-

Relationship Between Molecular Structure and Composition of Poly(ethylene-co-p-MS) Copolymers. From above discussion, we have shown that poly(ethylene-co-p-MS) copolymers with a wide range of compositions can be achieved by varying the p-MS monomer concentration in the feed. To fully understand the properties of this new class of materials, it is very important to know the correlation between the copolymer compositions and their molecular structures. In this section, we focus on the effect of p-MS concentration on molecular weight, molecular weight distribution, melting point (T_m), crystallinity and glass transition temperature (T_g) of the copolymer. A series of copolymers with various p-MS concentrations were analyzed by GPC and DSC.

Table 3 summarizes the molecular weight and molecular weight distribution results of three sets of poly(ethylene-co-p-MS) copolymers with various p-MS contents. The polymers in set A were produced by catalyst III at 40 °C in toluene for 15 minutes, the copolymers in set B were produced by catalyst II at 60 °C in hexane for 15 minutes, and the copolymers in set C were produced using catalyst II at 50 °C in hexane for 60 minutes. In each set, the polymerization conditions were the same except the different p-MS monomer concentrations in the feed.

By comparing results within set A, one can see that, the weight average molecular weight (M_w) only slightly decreases with the increase of p-MS concentration, the number average molecular weight (M_n) seems to be even less sensitive to the change of p-MS concentration, and even at as high as 18.96 mol % of p-MS concentration, the copolymer still has very good molecular weights ($M_w = 160,988$, $M_n = 95,588$). This is a very unique feature of p-MS comonomer compared to other α -

olefins. Usually, the incorporation of high α -olefins or dienes, such as 1,4-hexadiene, significantly reduces polyethylene molecular weight due to the higher termination rate mainly caused by β -hydrogen elimination reaction. It is believed that the insertion of p-MS into the bond between active site and propagating polymer chain is predominantly secondary. Therefore, the β -H is always the hydrogen on methylene (CH_2) unit, which is too stable to be readily eliminated. It is very interesting to note that the polydispersities ($\text{PD} = M_w/M_n$) of all copolymers with various p-MS concentration produced by catalyst III are close to 2, indicating that the copolymerization reaction follows single-site mechanism and p-MS units are homogeneously distributed along the whole polymer chain.

Table 3. The effect of p-MS concentration on molecular weight of the copolymers

Set no.	Polymer no.	catalyst	p-MS content (mol %)	M_w (g/mol)	M_n (g/mol)	M_w/M_n
A	PE	III	0	260,622	91,216	2.86
	P410	III	1.08	210,856	105,187	2.00
	P419	III	2.11	208,448	102,995	2.02
	P418	III	5.40	195,705	89,822	2.18
	P417	III	9.82	181,602	89,588	2.03
	P416	III	18.96	160,988	95,588	1.68
B	P459	II	1.29	138,516	45,209	3.06
	P458	II	2.32	89,857	35,790	2.51
	P359	II	1.36	76,288	20,936	3.64
C	P371	II	8.94	34,215	14,985	2.28

Another unique phenomenon is that the molecular weight distribution of the copolymer actually slightly narrows down with the increase of p-MS concentration as revealed in Figure 5, which shows normalized GPC curves of (a) PE and three poly(ethylene-co-p-MS) copolymers with (b) 1.08, (c) 9.82 and (d) 18.96 mol % of p-MS, respectively. Polymer P416 (curve d) gives narrowest molecular weight distribution with $\text{PD} = 1.68$, while polyethylene homopolymer gives broadest peak with $\text{PD} = 2.86$. The improved diffusibility of the monomers due to the reduced crystallinity, which is caused by the incorporation of p-MS, may help to provide the ideal polymerization condition. Indeed, P416 is completely soluble in toluene and formed homogeneous solution during the copolymerization, while PE is completely insoluble in toluene and formed heterogeneous suspension during the polymerization. For the copolymers produced by catalyst II (set B and set C in Table 3), the reduction of the molecular weight due to the increase of p-MS content is more significant compared to that by catalyst III (set A in Table 3), which may due to relatively low reactivity of p-MS in the presence of catalyst II. In both sets B and C, the molecular weight distribution also narrows down with the increasing p-MS concentration.

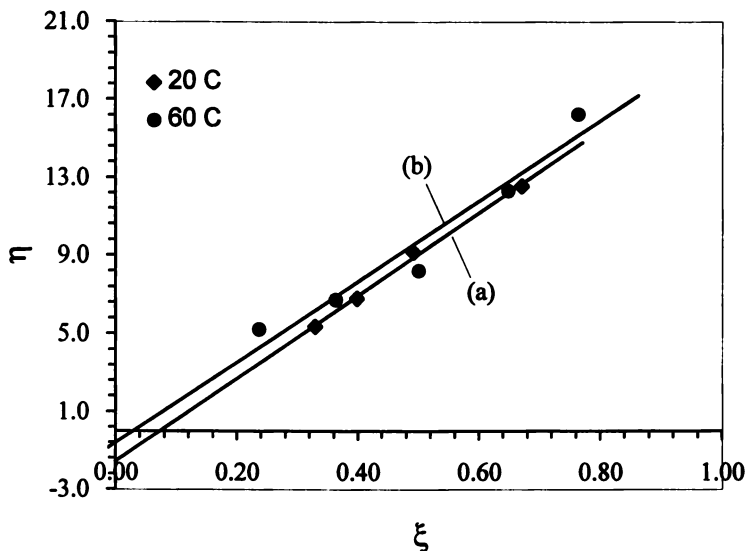


Figure 4. Kelen-Tudos plots for copolymerization of ethylene and p-MS using $[C_5Me_4SiMe_2N(t-Bu)]TiCl_2/MAO$ catalyst at (a) 20 °C and (b) 60 °C.

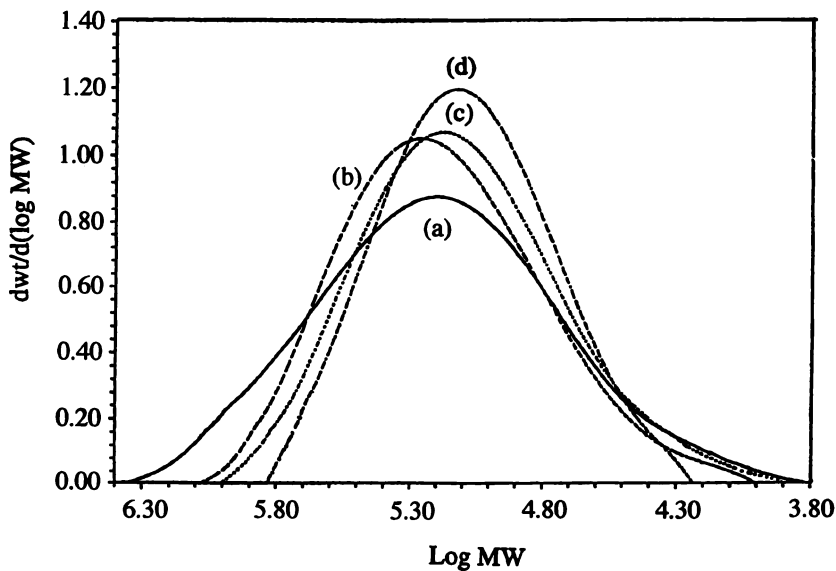


Figure 5. GPC curves of (a) PE and three poly(ethylene-co-p-MS) copolymers produced by $[C_5Me_4SiMe_2N(t-Bu)]TiCl_2/MAO$ catalyst, containing (b) 1.08, (c) 9.80 and (d) 18.98 mol% of p-MS.

Thermal analysis is a very convenient way to study the molecular structure of the copolymer, as the shape of the thermal transitions and the changes of the transition temperatures, such as T_m and T_g , and crystallinity reflect the homogeneity of the copolymer composition. Figure 6 shows DSC curves of PE homopolymers and a series poly(ethylene-co-p-MS) copolymers with various compositions produced by catalyst III. Each copolymer with less than 10 mol % of p-MS shows a sharp single melting peak. The T_m and crystallinity drop dramatically due to the presence of p-MS (even small amount) in the copolymer. The T_m and crystallinity of the copolymer are strongly dependent on the density of comonomer, the higher the density the lower the T_m and crystallinity. When p-MS concentration is increased to about 10 mol %, the melting peak almost completely disappears. As revealed in Figure 6 (f), the copolymer with 18.96 mol % becomes completely amorphous and shows no melting peak.

The systematic decrease of T_m and uniform reduction of crystallinity imply the homogeneous reduction of PE consecutive sequences, in other words, the p-MS units are homogeneously distributed in the PE chain. It is interesting to note that the T_m peak (ranging 80–45 °C shown in Figure 6 (e) of the copolymer containing 9.82 mol % of p-MS covers the similar T_m range (45–55 °C) of paraffin wax. This poly(ethylene-co-p-methylstyrene) copolymer is consisted of an average 20–22 consecutive methylene units, which is right in the molecular weight range of solid paraffin wax.

The effective removal of crystallinity by the incorporation of p-MS provides the opportunity to obtain elastic properties in polyethylene copolymers. The copolymer containing 18.96 mol % of p-MS is actually an elastomer with a T_g of -5.7 °C. Further increase of p-MS concentration provides the copolymers with higher T_g and the copolymers become glassy at room temperature. Figure 7 shows DSC curves of poly(ethylene-co-p-methylstyrene) copolymers with (a) 18.98, (b) 32.8 and (c) 40 mole % p-MS, respectively. The T_g increases from -5.7 °C to 30.9 °C and to 38.8 °C. The single T_g with sharp thermal transition in each case is indicative of homogeneous copolymer structure even at as high as 40 mol % of p-MS concentration.

Synthesis of Poly(ethylene-*ter*-1-octene-*ter*-p-MS) Terpolymers

As discussed above that the completely amorphous poly(ethylene-co-p-MS) copolymers can be achieved by incorporating high concentration of p-MS using $[(C_5Me_4)SiMe_2N(t-Bu)]TiCl_2/MAO$ catalyst. However, it is difficult to synthesize a good elastomer by copolymerization of ethylene and p-MS due to the high T_g of poly(p-MS). To achieve a good elastic polymer with a lower T_g , the system requires an appropriate third monomer. This lead us to investigate the terpolymerization of ethylene, 1-octene and p-MS, as poly(1-octene) provides the lowest T_g among the polyolefin families.

Since catalyst III has excellent ability to incorporate high α -olefin and styrene

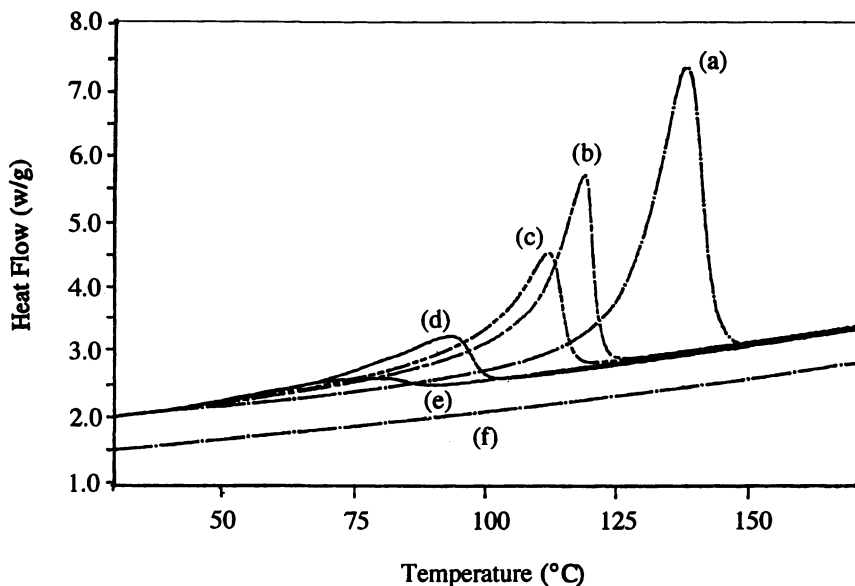


Figure 6. DSC curves of (a) PE and five poly(ethylene-co-p-MS) copolymers containing (b) 1.08, (c) 2.11, (d) 5.40, (e) 9.82 and (f) 18.96 mol% of p-MS, obtained by $[C_5Me_4SiMe_2N(t-Bu)]TiCl_2/MAO$ catalyst.

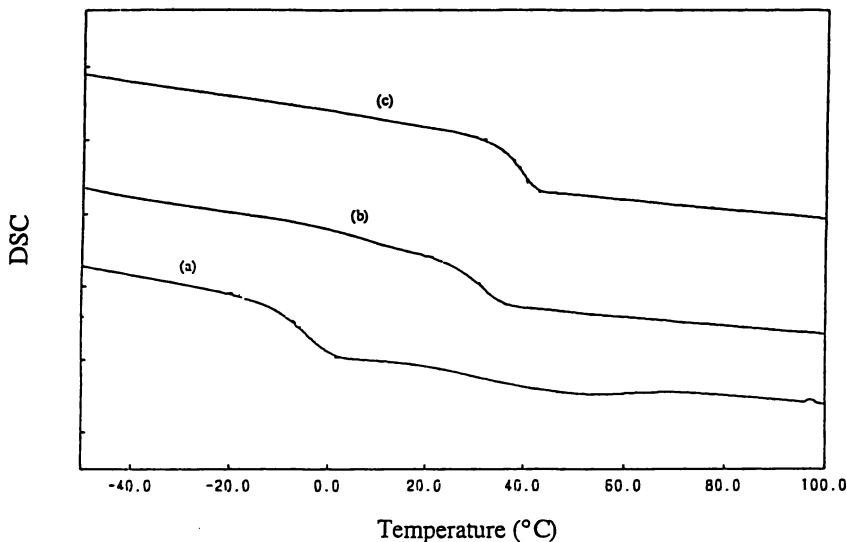


Figure 7. DSC curves of amorphous poly(ethylene-co-p-MS) copolymers containing (a) 18.96, (b) 32.8, (c) 40.0 mol% of p-MS, obtained by $[C_5Me_4SiMe_2N(t-Bu)]TiCl_2/MAO$ catalyst.

derivatives, it was chosen for the terpolymerization. Various monomer compositions in the feed were used to monitor the composition and consequently T_g , as well as molecular weight of the terpolymer. The chemical composition of the terpolymer was estimated by ^1H NMR. Figure 8 compares ^1H NMR spectra of an ethylene/1-octene/p-MS terpolymer (a), an ethylene/1-octene copolymer (b) and an ethylene/p-MS copolymer (c). Besides the solvent peak at 5.99 ppm, four major peaks 0.8-0.9, 1.0-1.6, 2.3-2.6 and 6.9-7.1 ppm are corresponding to the protons of CH_3 group in 1-octene unit, CH_2 groups in ethylene, 1-octene and p-MS units, p- CH_3 group and CH group in p-MS unit and aromatic protons in p-MS unit, respectively. The integrated peak areas around 0.8-0.9, 1.0-1.6 and 6.9-7.1 ppm were used to estimate the composition of the terpolymer.

The terpolymers were also subject to DSC and GPC measurements to determine the T_g , molecular weight and molecular weight distribution, respectively. The results are summarized in Table 4. The increase of ethylene concentration in the monomer feed increases the yield and molecular weight of the terpolymer, as shown in run p470 and p471. Runs p472/p473/p477 and runs p476/p475/p478 compare the influence of 1-octene concentration on the composition and the properties of the terpolymer, respectively. It is revealed that the T_g and molecular weight of the terpolymer increase with the decrease of 1-octene concentration. By comparing runs p471/p472/476, p473/p478 and p475/p474, where the concentrations of ethylene and 1-octene are identical and p-MS concentration varies, one can see that with the increase of p-MS concentration T_g of the terpolymer consistently increases, while molecular weight of the terpolymer very slightly decreases.

To estimate the relative reactivity of ethylene, 1-octene and p-MS, the identical concentration for the three monomers was used as shown in run p478. The molar ratio of $[\text{ethylene}]/[\text{1-octene}]/[\text{p-MS}]$ in the terpolymer is $73.3/18.5/8.12 = 9/2.3/1$, which clearly indicates that the reactivity of the monomer in the terpolymerization follows the order of ethylene > 1-octene > p-MS. Therefore, one could empirically control the composition of the terpolymer by varying the composition of the monomer in the feed.

In general, the molecular weight of the terpolymer is not very sensitive to the polymer composition and maintains sufficiently high ($M_w \sim 200,000$ g/mol) over a wide composition range. Narrow molecular weight distribution is observed for each sample. The polydispersities (PD) of all samples in Table 4 are close to 2, indicating that the terpolymerization also follows the single-site mechanism and the monomers are uniformly distributed in the terpolymer.

Figure 9 shows DSC curves of the terpolymers with different compositions. A single sharp T_g transition is observed in each curve, which further demonstrates that the monomers are randomly distributed in the terpolymers. The T_g of the terpolymer can be readily controlled by varying the composition of the terpolymer. It is very interesting to note that the samples from runs p477 and p478 with 19.8 and 26.6 mol % of total 1-octene and p-MS concentration, respectively, also have a very weak melting peaks at 47.1 and 5.1 $^\circ\text{C}$, respectively. Some small crystalline phases

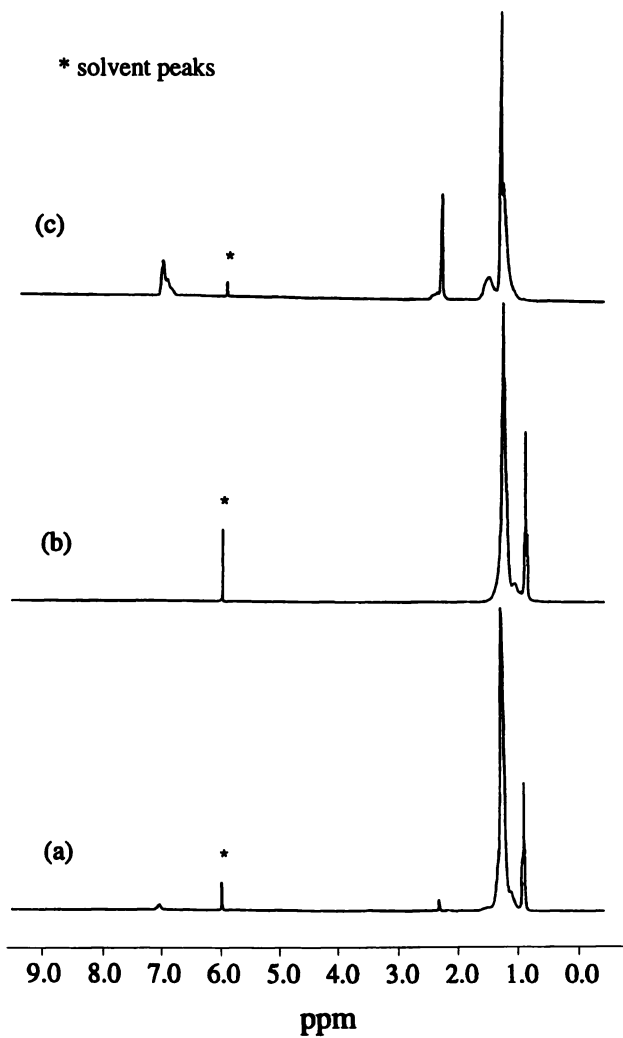


Figure 8. ^1H NMR spectra of (a) poly(ethylene-ter-1-octene-ter-p-MS), (b) poly(ethylene-co-1-octene) and (c) poly(ethylene-co-p-MS).

Table 4. A summary of terpolymerization^{a)} of ethylene, 1-octene and p-MS by using $[(C_2Me_5)_2SiMe_2N(t-Bu)TiCl_2/MAO]$ catalyst

Run	Monomer concn. In the feed, mol/L		Yield	Copolymer composition			T _g	M _w	M _n	PD
	E ^{b)}	1-Oct		p-MS	mol %					
No.			g	[E]	[O]	[p-MS]	°C	g/mol	g/mol	
p470	0.20	0.80	0.10	7.26	54.2	43.0	2.74	173,989	74,703	2.33
p471	0.40	0.80	0.10	10.07	61.1	36.0	2.92	219,752	96,802	2.27
p472	0.40	0.80	0.20	9.78	60.3	36.3	4.43	182,185	77,497	2.35
p473	0.40	0.40	0.20	8.15	59.6	34.0	6.37	208,920	86,812	2.41
p477	0.40	0.20	0.20	6.44	80.2	14.1	5.69	227,461	91,490	2.49
p476	0.40	0.80	0.40	9.01	63.4	29.3	7.26	202,085	96,035	2.10
p475	0.40	0.60	0.40	9.14	67.2	24.7	8.09	205,124	93,763	2.19
p478	0.40	0.40	0.40	7.94	73.3	18.5	8.12	246,300	122,306	2.01
p474	0.40	0.60	0.15	9.02	64.7	31.3	3.96	224,476	102,617	2.19
p396 ^{b)}	0.523	0.383	0.912	5.60	64.0	18.1	17.7	106,954	55,825	1.92

a) polymerization conditions: 100 ml of toluene, [Ti] = 2.5×10^{-6} mol, [MAO]/[Ti] = 3000, 50 °C, 30 minutes;

b) solvent: 100 ml of hexane, 30 °C, [Ti] = 2.5×10^{-5} mol, [MAO]/[Ti] = 2000, ethylene pressure: 45 psi;

c) solubility of ethylene: 0.249 mol/l for 29 psi in hexane at 60 °C, 0.20 M for 2 bar, 0.40 M for 4 bar in toluene at 50 °C, 0.523 M for 45 psi in hexane at 30 °C.

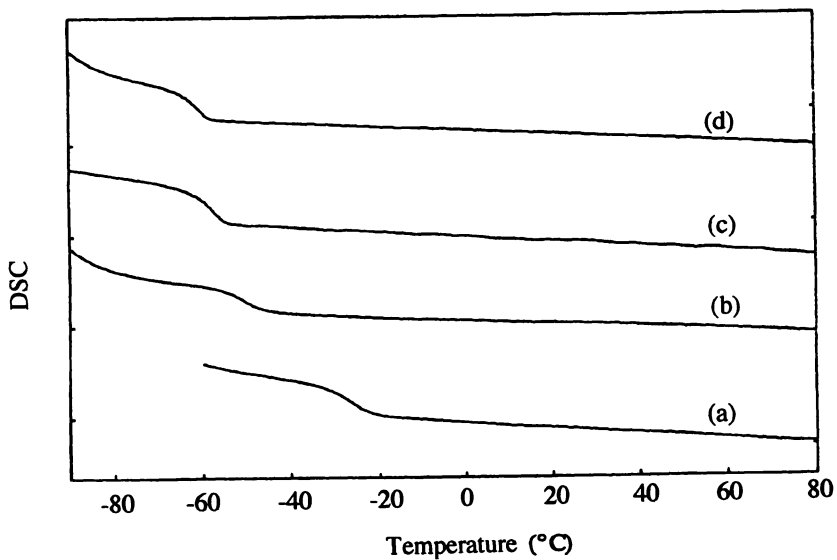


Figure 9. DSC curves poly(ethylene-ter-1-octene-ter-p-MS) terpolymers with different compositions. (a) [E] = 64.0, [O] = 18.1, [p-MS] = 17.7 mol%; (b) [E] = 40.0, [O] = 54.5, [p-MS] = 5.55 mol%; (c) [E] = 61.1, [O] = 36.0, [p-MS] = 2.92 mol%; and (d) [E] = 41.4, [O] = 58.6, [p-MS] = 0 mol%.

still exist in the terpolymer in these composition range. On one hand, more than 30 mol % of the total concentration of 1-octene and p-MS may be necessary to completely eliminate the crystallization of ethylene sequences. On the other hand, the existence of some small crystalline phases may be very desirable, as they may greatly enhance the physical properties of the elastomers, i.e. the terpolymers may behave as thermoplastic elastomers.

It is also interesting to note that, p-MS in the terpolymer not only provides a versatile reactive site for the further reactions, such as functionalization and cross-linking reaction, but also improves environmental stability and the morphology of the elastomer.

Conclusion

A new class of random poly(ethylene-co-p-methylstyrene) copolymers, with a wide range of compositions and narrow molecular weight and composition distributions, have been extensively developed by using metallocene catalysts with a constrained ligand geometry. The combination of spatially opened catalytic site and cationic coordination mechanism in the metallocene catalysts provides a very favorable reaction condition for the p-MS comonomer to be readily and randomly incorporated into PE chain. In addition, terpolymerization of ethylene, 1-octene and p-MS provides a new class of polyolefin elastomers with a controllably wide range of T_g, relatively high molecular weight and narrow molecular weight and composition distributions. In turn, the copolymers and terpolymers containing p-MS units are very useful reactive intermediates in the preparation of functional polyolefins.

Acknowledgments. Authors would like to thank the Polymer Program of the National Science Foundation for financial support.

Literature Cited

1. Jois, Y. H. R.; Harrison, J. B. *J. Macromol. Sci.: Rev. Macromol. Chem. Phys.* **1996**, C36(3), 433.
2. Naqvi, M. K.; Choudhary, M. S. *J. Macromol. Sci.: Rev. Macromol. Chem. Phys.* **1996**, C36(3), 601.
3. Boor, J., Jr. *Ziegler-Natta Catalysts and Polymerizations*, Academic Press: New York, 1979.
4. Chung, T. C. *Macromolecules* **1988**, 21, 865.
5. Ramakrishnan, S.; Berluche, E.; Chung, T. C. *Macromolecules* **1990**, 23, 378.
6. Chung, T. C.; Rhubright, D. *Macromolecules*, **1991**, 24, 970.
7. Chung, T. C.; Rhubright, D.; Jiang, G. J. *Macromolecules* **1993**, 26, 3467.

8. Chung, T. C.; Jiang, G. J. *Macromolecules* **1992**, *26*, 1993.
9. Chung, T. C.; Rhubright, D. *Macromolecules* **1994**, *27*, 1313.
10. Chung, T. C.; Lu, H. L.; Li, C. L. *Macromolecules* **1994**, *27*, 7533.
11. Chung, T. C.; Lu, H. L.; Li, C. L. *Polymer International* **1995**, *37*, 197.
12. Chung, T. C.; Lu, H. L. *U.S. Pat.* 5,543,484, **1996**.
13. Chung, T. C.; Lu, H. L. *J. Polym. Sci., Polym. Chem. Ed.* **1997**, *35*, 575.
14. Chung, T. C.; Lu, H. L.; Ding, R. D. *Macromolecules* **1997**, *30*, 1272.
15. Ewen, J. A.; Jones, R. L.; Razavi, A.; Ferrara, J. *J. Am. Chem. Soc.* **1988** *110*, 6255.
16. Stevens, J. C. *Stud. Surf. Sci. Catal.* **1994**, *89*, 277.
17. Sernetz, F. G.; Mulhaupt, R.; Waymouth, R. M. *Macromol. Chem. Phys.* **1996**, *197*, 1071.
18. Kelen, T.; Tudos, T. *React. Kinet. Catal. Lett.* **1974**, *1*, 487.

Chapter 13

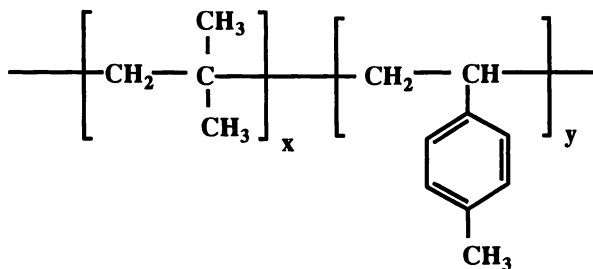
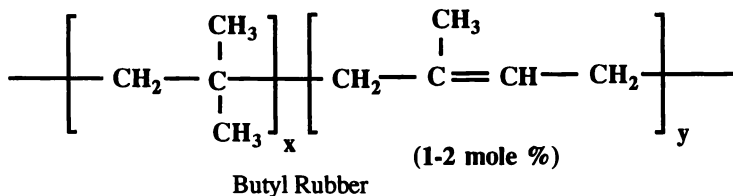
A Novel Reactive Functionalization of Polyolefin Elastomers: Direct Functionalization of Poly(isobutylene-*co-p*-methylstyrene) by a Friedel-Crafts Acylation Reaction

Abhimanyu O. Patil

Corporate Research Laboratory, Exxon Research and Engineering Company,
Route 22 East, Clinton Township, Annandale, NJ 08801

Copolymers of isobutylene and *p*-methylstyrene [poly (IB-PMS)] represent a new type of elastomer with a saturated hydrocarbon backbone. This polymer has many desirable properties such as good environmental and aging resistance. However, these polymers have low reactivity and are incompatible with most other polymeric materials. We have developed a new method of directly modifying poly (IB-PMS) copolymer by the electrophilic substitution reaction of aromatic rings of the copolymer using Friedel-Crafts acylation chemistry. This paper deals primarily with synthesis and characterization of functionalized poly (IB-PMS) copolymers using succinic anhydride as an acylating agent and a Lewis acid, aluminum chloride, as a catalyst. This ring functionalization approach enables selective functionalization of the aromatic ring of *p*-methylstyrene in the copolymer. This is a general approach that can be extended to other catalysts or acylating agents to generate different functionalized polymers.

Butyl rubber consists mostly of isobutylene (95-98%) and about 2-5% isoprene units.¹ The isoprene unit is halogenated by either chlorine or bromine to obtain the corresponding halobutyl rubbers. Despite the superior elastomeric properties of halobutyl, the elastomer can easily undergo dehydrohalogenation leading to crosslinking, and the isoprene unsaturation is subject to ozone cracking. To remedy these problems and to improve the halobutyl properties, a new class of elastomer poly(isobutylene-*co-p*-methylstyrene) [poly (IB-PMS)] was developed.² Unlike butyl rubber, it contains no double bonds and therefore cannot be crosslinked unless otherwise functionalized. The chemical structures of butyl rubber and poly (IB-PMS) copolymers are shown below.



Poly (IB-PMS) is a copolymer of isobutylene and *p*-methylstyrene with a saturated hydrocarbon backbone. The pairing of these two monomers produces an ideal copolymer that can readily be prepared by commercial low-temperature carbocationic polymerization in the presence of a Lewis acid catalyst.³ The copolymer consists mostly of poly(isobutylene) backbone [isobutylene (IB): 97.7 mole %] and a very small number of *p*-methylstyrene (PMS) units (2.3 mole %). The introduction of functional groups to a few *p*-methylstyrene units can broaden the applicability of this material while preserving the desired mechanical properties of the initial material. The copolymer is brominated selectively at the *p*-methyl position of the aromatic unit, yielding a product free of unsaturation but stable to dehydrohalogenation.^{3,4} The brominated poly (IB-PMS) can be converted to other desirable polar functional groups. Several derivatives of poly (IB-PMS) copolymers have been developed over the years.⁵ The nucleophilic displacement of benzylic bromide allows synthesis of new derivatives that include cationic and anionic ionomers, hydroxyl and carboxylic derivatives, and esters such as dithiocarbamates, acetate, acrylate and cinnamate. Similarly, poly (IB-PMS) copolymer can also be functionalized through metallation chemistry using a superbases and oxidation chemistry. Both of these methods allow functionalization at the methyl group of *p*-methylstyrene units.⁵

Friedel-Crafts acylation is a well-known reaction.⁶ For example, one can react benzene with succinic anhydride using a Lewis acid, aluminum chloride, to synthesize β -ketocarboxylic acid.⁷ Chemical modification of polystyrene-based resins has also been studied, because the aromatic rings can be readily modified through electrophilic aromatic substitution or other reactions.⁸ Although these reactions have been widely used in the preparation of crosslinked ion-exchange resins or polymer-supported catalysts and reagents, they need to be carefully considered if they are to be used for linear polymers where a well-defined structure is needed. In such derivatization reactions, side reactions, crosslinking, and/or degradation of the polymer chains are usually difficult to avoid. Our challenge is to introduce functional groups selectively and efficiently on a linear, high-molecular-weight polymer that contains very low levels of reactive PMS units.

This paper deals with a novel approach of functionalizing poly (IB-PMS) copolymers using the Friedel-Crafts acylation reaction. Poly (IB-PMS) copolymer was reacted with an acylating agent, succinic anhydride, using aluminum chloride as a Lewis acid. The reaction involves the aluminum chloride-catalyzed substitution of an acyl group on the aromatic ring.

Experimental Section

Dr. H. C. Wang of Exxon Chemical Company provided the copolymers of poly(isobutylene-*p*-methylstyrene), [poly (IB-PMS)] designated XP-50. These copolymers had been prepared by carbocationic polymerization of isobutylene (IB) and *p*-methylstyrene (PMS) at various ratios to give a saturated copolymer backbone chain with randomly distributed pendant PMS units. The synthesis of the copolymer has been reported.⁴ The composition and molecular weight of the copolymer can be varied depending on the reaction conditions. Usually the composition is maintained at 2-5 mole % PMS, with a number average molecular weight ranging from 5,000 to a half a million.

The copolymer of *p*-methylstyrene and isobutylene utilized for this derivatization and characterization were contained 15.0 wt % *p*-methylstyrene. It had a number average molecular weight (M_n) of 149,600, a weight average molecular weight (M_w) of 377,500 with polydispersity of 2.52. Reagent grade chemicals were used as received unless otherwise stated.

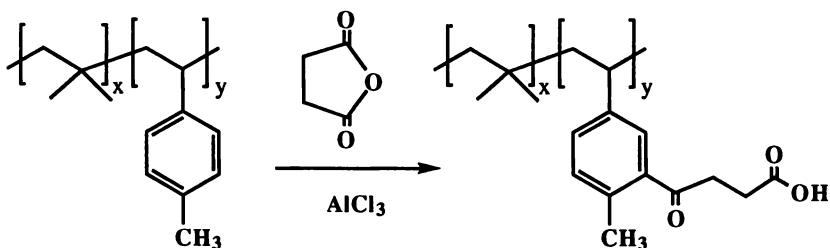
In the experiment, 5.00 g (0.00635 mole PMS) of copolymer was dissolved in 50 ml dichloromethane (Aldrich, anhydrous 99.8%) in a three-neck flask equipped with condenser, nitrogen bubbler, and a dropping funnel. Then 0.64 g (1 mole equivalent with respect to PMS) of succinic anhydride (Aldrich) was added, and the solution was stirred for 1 hour at room temperature under nitrogen. 1.70 g (2 mole equivalent with respect to PMS) of $AlCl_3$ (Aldrich) was then added and the mixture was stirred at room temperature. The colorless viscous solution turned into a red-brown gel in 5 minutes. The product polymer was isolated by adding the reaction mixture to a acetone, to precipitate the product. The functionalized polymer was purified by dissolving in THF/methanol mixture and reprecipitating with excess acetone. The product was dried under vacuum.

Further characterization of the product required that it be soluble in solvents like THF and chloroform. Therefore, the acid-functionalized polymer was converted to an ester-functionalized polymer using ethanol/sulfuric acid. The general procedure is given below.

The acid functionalized copolymer (1.00 g) was dissolved in 25 ml of toluene in a three neck, 100ml flask equipped with condenser, nitrogen bubbler, and a dropping funnel. 25 ml of ethyl alcohol was added, followed by 1 ml of concentrated sulfuric acid. The solution was heated in an oil bath at 85°C for six hours under nitrogen. The product was isolated by adding the reaction mixture to 200 ml of water. The product was washed with water three times, then with acetone, then was dried under vacuum. The ester-functionalized polymer was completely soluble in solvents such as THF, chloroform, and toluene.

Results and Discussion

The functionalization reaction of the poly (IB-PMS) copolymer involves the aluminum chloride catalyzed substitution of an acyl group on the aromatic ring. Unlike alkylation reactions, acylation reactions tend to give monosubstituted products. The reaction scheme for acid functionalization of the copolymer is shown below.



The infrared spectrum of the product was similar to that for the starting polymer with additional peaks due to carboxylic acid and ketone carbonyl functional groups. Figure 1 shows the infrared spectra of the starting poly (IB-PMS) copolymer (bottom spectrum), the β -ketocarboxylic acid-functionalized poly (IB-PMS) copolymer (middle spectrum). The infrared spectrum of the product showed a broad peak at $3500\text{--}3100\text{ cm}^{-1}$ due to a carboxylic acid group and two characteristic carbonyl peaks, a sharp peak at 1690 cm^{-1} and a broad peak at 1610 cm^{-1} . The β -ketocarboxylic acid functionalized poly (IB-PMS) polymer (5 wt % functionalized polymer) was insoluble in THF but was soluble in THF/methanol (95:5) solution. This solubility behavior was similar to that of mildly associated polymers.

To determine whether this association is due to carboxylic acids or whether it also involves the aluminum salt of carboxylic acid, the acid-functionalized polymer was evaluated using X-ray photoelectron spectroscopy (XPS). Figure 2 shows that there is no metal aluminum. Thus the association is most likely due to dimerization of carboxylic acids, as is commonly seen in smaller organic molecules. The XPS spectrum also shows the incorporation of oxygen functionality into the copolymer by the acylation reaction. The reaction scheme is as follows:

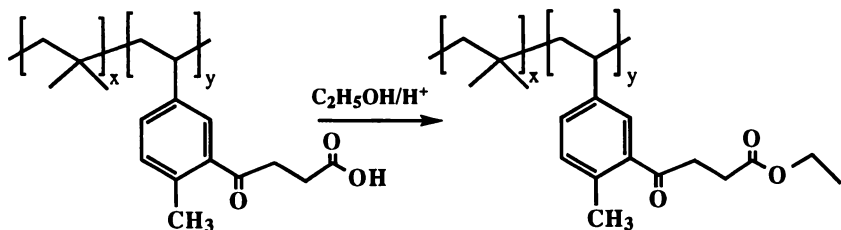


Figure 1 shows the infrared spectra of the β -ketocarboxylic acid-functionalized poly (IB-PMS) copolymer (middle spectrum) and the ester-functionalized poly (IB-PMS) copolymer (top spectrum). The infrared spectrum of the ester product shows the disappearance of a broad peak at $3500\text{--}3100\text{ cm}^{-1}$ due to the carboxylic acid group and the appearance of new characteristic ester peaks at 1738 cm^{-1} and 1718 cm^{-1} , in addition to the carbonyl peak at 1610 cm^{-1} (Figure 1). This suggests complete conversion of the acid-functionalized polymer to the ester-functionalized polymer.

Figure 3 shows the ^{13}C NMR spectra of the starting poly (IB-PMS) copolymer (bottom spectrum) and the ester-functionalized poly (IB-PMS) copolymer (top spectrum). The ^{13}C NMR spectrum of the product resembled that of the starting polymer, with additional peaks in the carbonyl region and a peak at 14 ppm due to a methyl group. Figure 4 shows the ^{13}C NMR spectra of expanded aromatic and carbonyl regions of the starting poly (IB-PMS) copolymer (bottom spectrum) and the

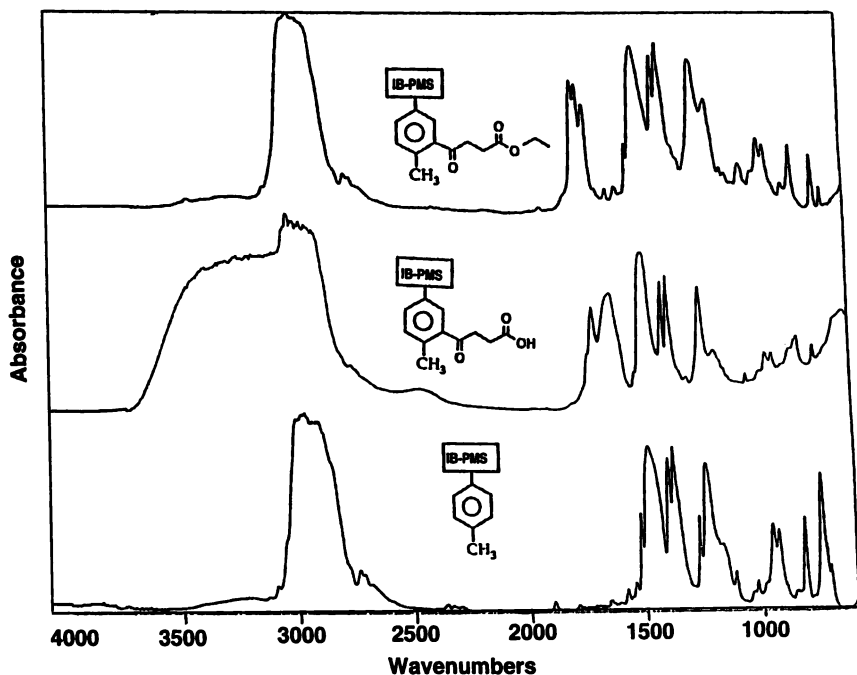


Figure 1. a) FTIR spectrum of starting poly (IB-PMS) copolymer (bottom spectrum), b) FTIR spectrum of acid functionalized poly (IB-PMS) copolymer (middle spectrum), c) FTIR spectrum of ester functionalized poly (IB-PMS) copolymer (top spectrum).

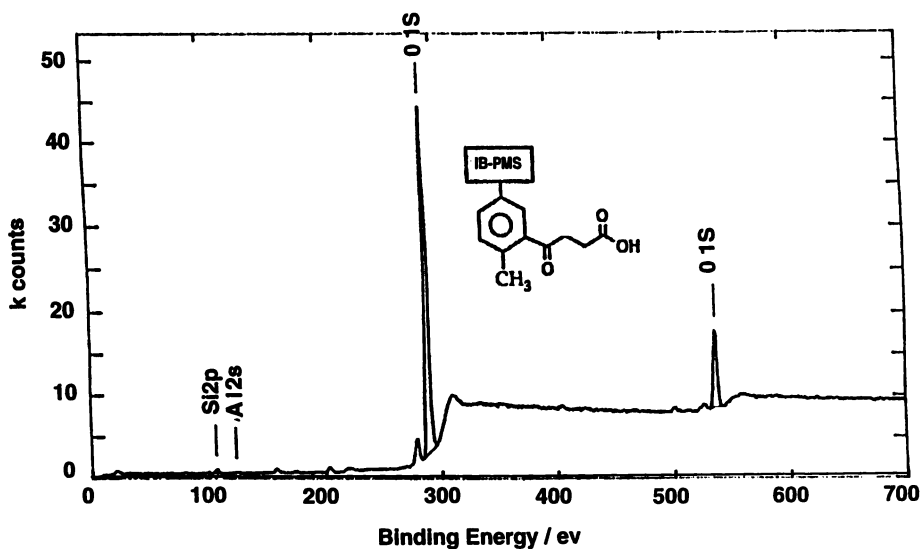


Figure 2. XPS survey scan of acid functionalized poly (IB-PMS) copolymer.

ester functionalized poly (IB-PMS) copolymer (top spectrum). The product ester shows carbonyl peaks at 173 ppm and 202 ppm due to ester and ketone carbonyl, respectively. The changes due to functionalization in the aromatic region are also clearly seen in the product. Integration of the carbonyl region and the aromatic region can be used to calculate the proportion of the aromatic rings that were functionalized with ester groups. In this reaction, approximately one third number of the rings have been derivatized with ester groups.

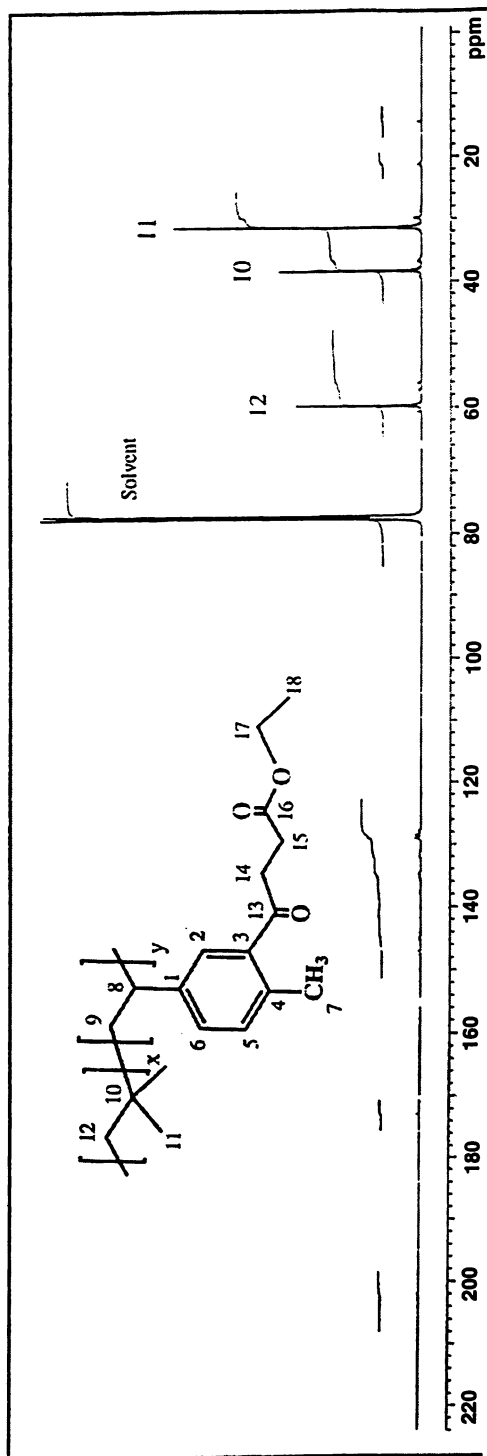
Figure 5 shows the ^{13}C NMR spectra of the expanded aliphatic methyl region of the starting poly (IB-PMS) copolymer (bottom spectrum) and the ester-functionalized poly (IB-PMS) copolymer (top spectrum). The starting poly (IB-PMS) copolymer shows only one methyl absorption peak at 21.2 ppm, while the product ester-functionalized poly (IB-PMS) copolymer shows methyl peaks at 21.2 and 20.9 ppm as well as 14.4 ppm; due to the two kinds of methyl groups. The integration of the 20.9 ppm absorption peak is the same as 14.4 ppm absorption peak, suggesting that both of these peaks are due to methyl groups on the substituted aromatic rings. The peak at 21.2 ppm could be due to a methyl group on the unsubstituted aromatic ring of the functionalized polymer. Thus, relative integration of just the methyl peaks at 21.2 and 20.9 ppm can be used to calculate the extent of ester functionalized aromatic rings. In this reaction, approximately one third of the rings have been substituted with ester groups; this agrees with the results from integration of the aromatic and carbonyl peaks.

These spectroscopic data are useful in characterizing derivatization of the copolymer, but they do not give information about the effect of molecular weight change of the copolymer as a result of functionalization. Molecular weights and molecular weight distributions were measured by gel permeation chromatography (GPC) relative to polystyrene standards. Figure 6 shows GPC analysis in THF solution of the starting poly (IB-PMS) copolymer and the ester-functionalized poly (IB-PMS) copolymer using both refractive index (RI) and ultraviolet (UV) detectors. The GPCs indicates a molecular weight breakdown of the ester-functionalized copolymer (RI detector). The GPCs also indicates a uniform distribution of *p*-methylstyrene over the entire molecular weight range in both the starting poly (IB-PMS) copolymer and the ester-functionalized poly (IB-PMS) copolymer (RI and UV detector).

The intensity of the GPC peak of the ester functionalized poly (IB-PMS) copolymer is much higher than that of the starting poly (IB-PMS) copolymer. To understand this result, the UV-visible spectra of the starting poly (IB-PMS) copolymer and the ester-functionalized poly (IB-PMS) copolymer were recorded in hexane solutions (Figure 7). The UV-visible spectra of the product had almost 20-fold larger absorption at wavelength 254 nm (UV detector position) than the starting polymer (Figure 7). This explains the greater intensity of the GPC peak of the ester functionalized poly (IB-PMS) copolymer compared to that of the starting poly (IB-PMS) copolymer.

Summary

We have shown that we can introduce functional groups selectively and efficiently on a linear, high-molecular-weight poly (IB-PMS) copolymer containing a very low level of reactive aromatic groups of PMS monomer. The functionalization occurs by an electrophilic substitution reaction of aromatic rings of the copolymer using Friedel-Crafts acylation chemistry. In the copolymer, the functionalized *p*-methylstyrene unit was quite uniformly distributed over the entire molecular weight range. This ring functionalization approach enables selective functionalization of the aromatic ring of *p*-methylstyrene in the copolymer and is a general approach that can be extended to other catalysts or acylating agents to generate different functionalized polymers.



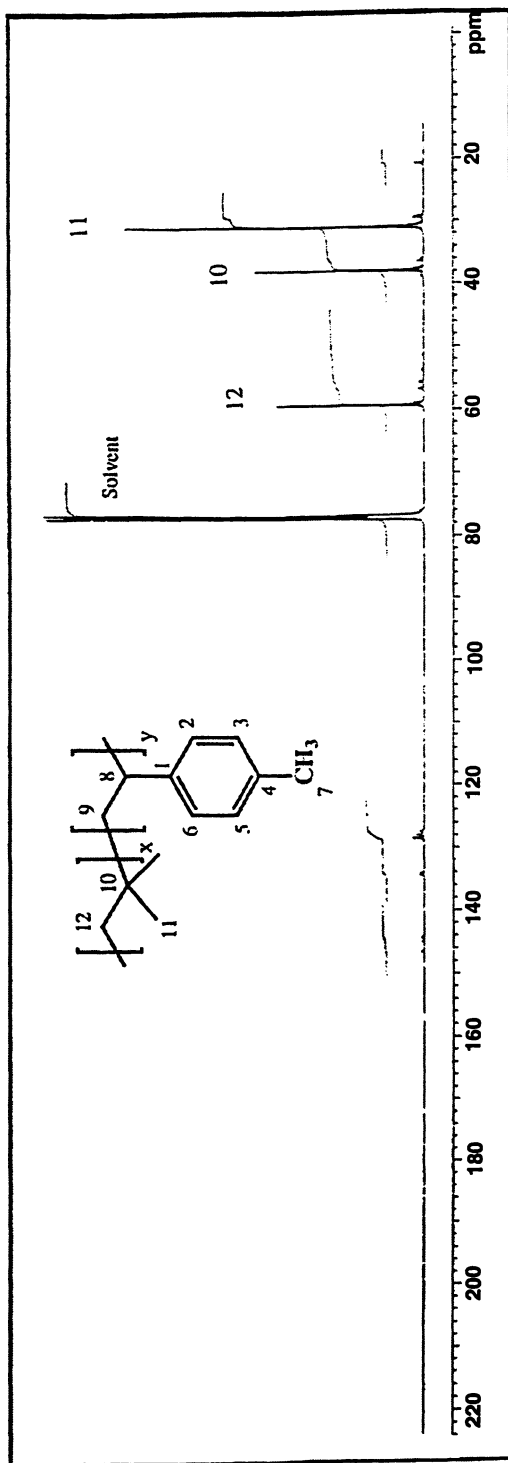
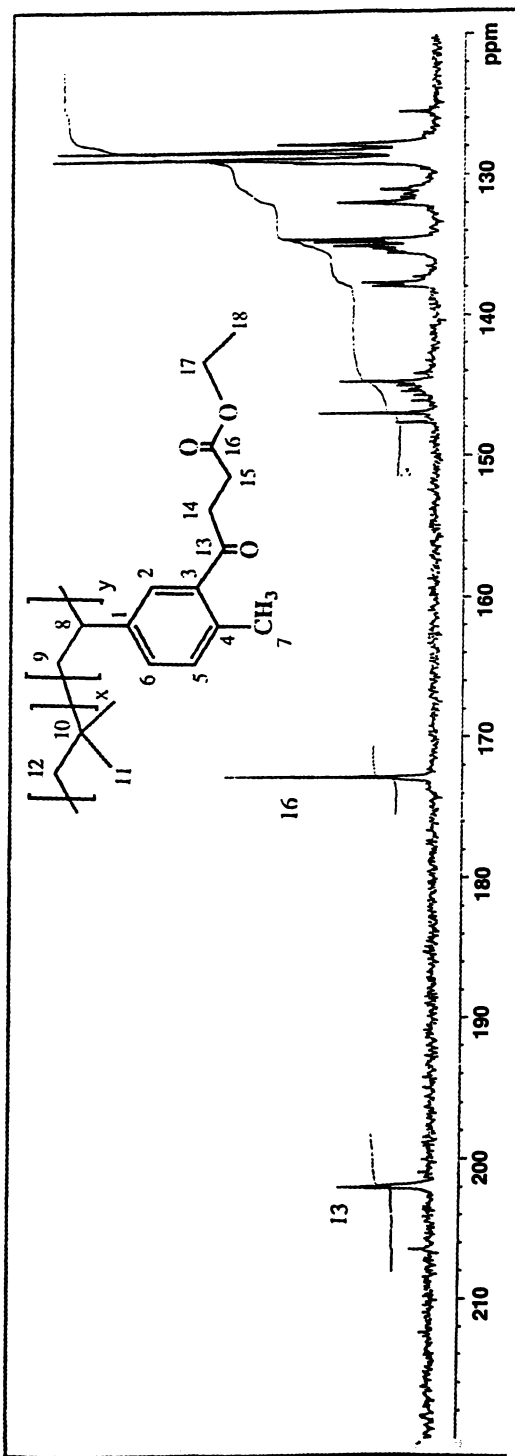


Figure 3. ^{13}C NMR (CDCl_3) spectra of starting poly (IB-PMS) copolymer (bottom spectrum) and ester functionalized poly (IB-PMS) copolymer (top spectrum).



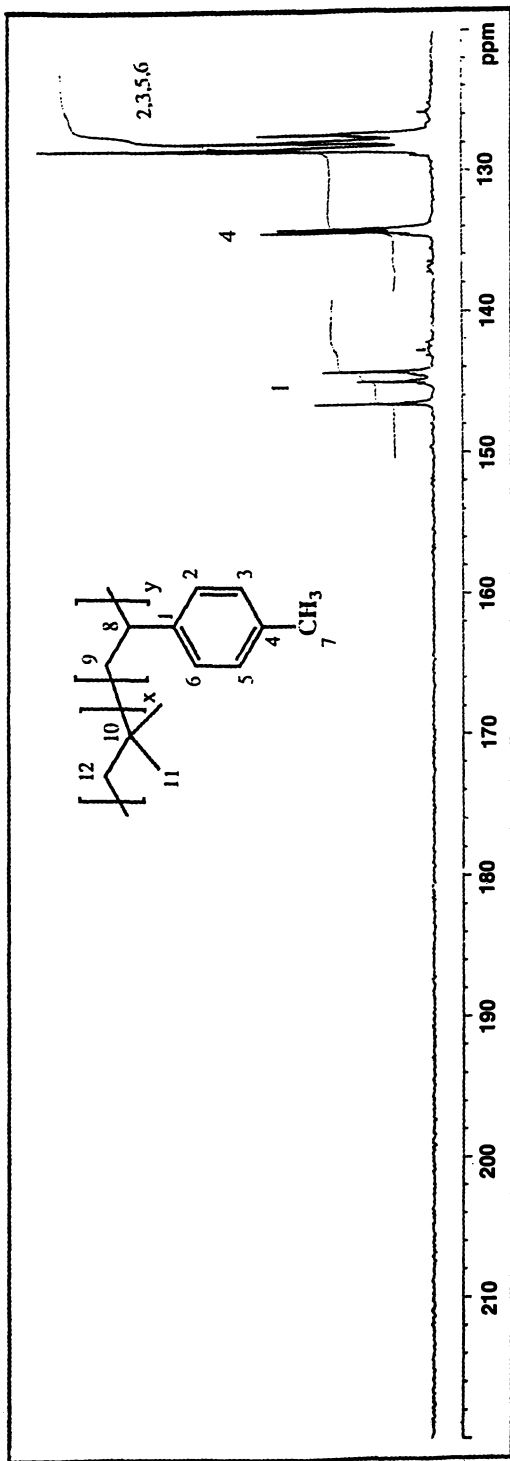
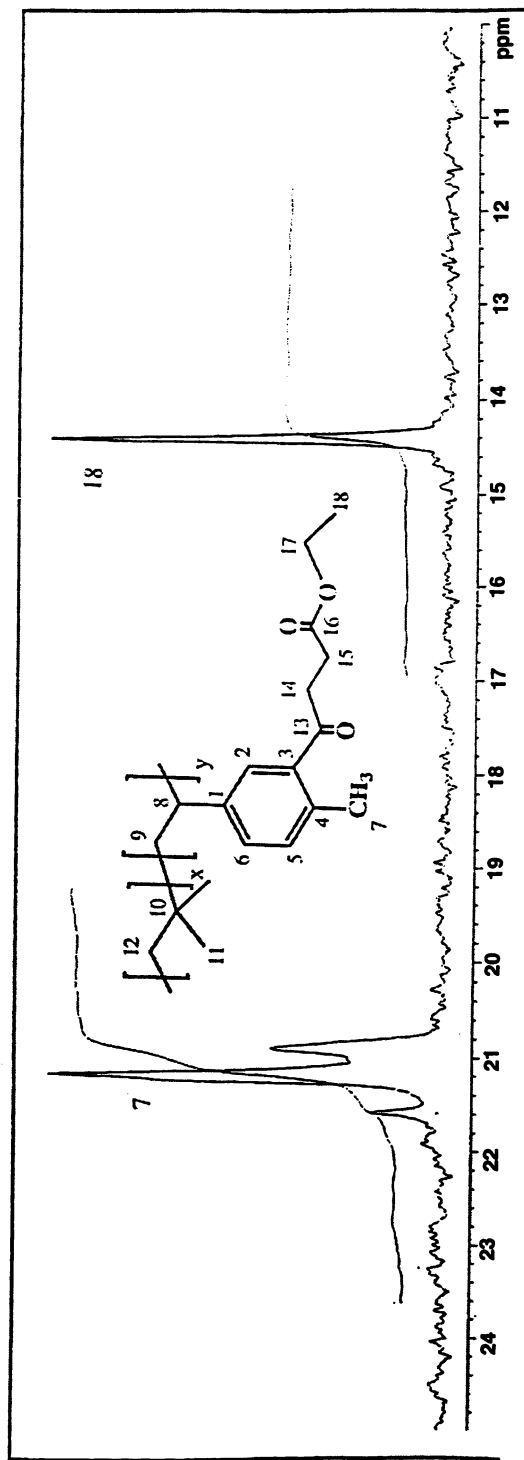


Figure 4. ^{13}C NMR (CDCl_3) spectra of starting poly (IB-PMS) copolymer (bottom spectrum) and ester functionalized poly (IB-PMS) copolymer (top spectrum) showing aromatic region of the spectra.



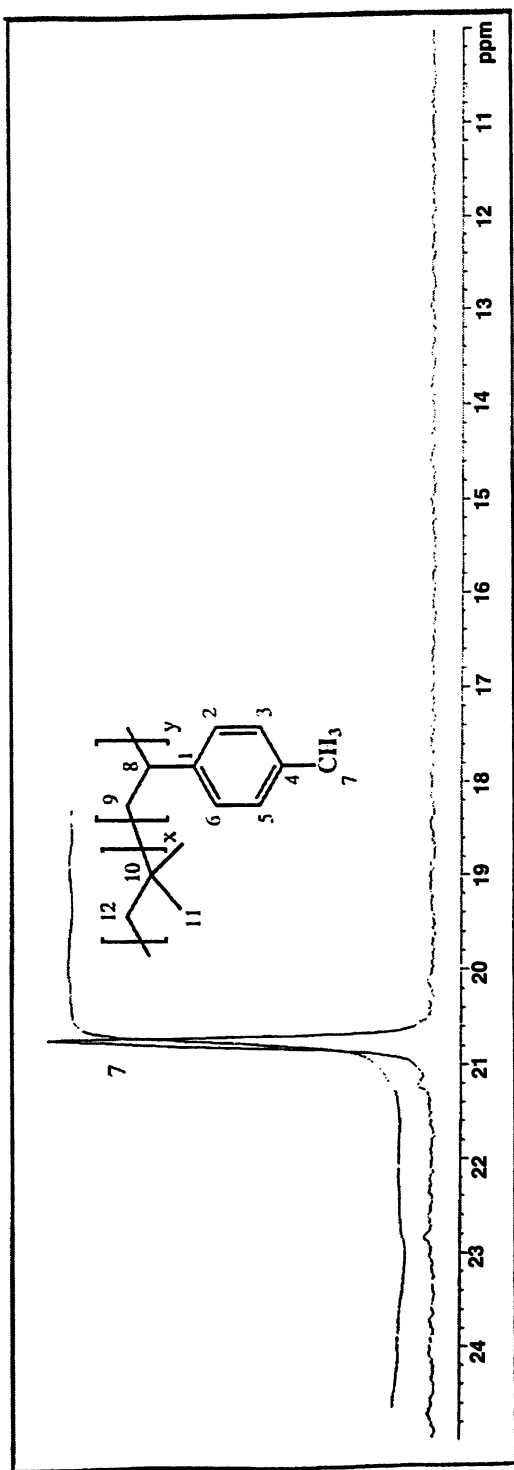


Figure 5. ^{13}C NMR (CDCl_3) spectra of starting poly (IB-PMS) copolymer (bottom spectrum) and ester functionalized poly (IB-PMS) copolymer (top spectrum) showing only methyl carbons.

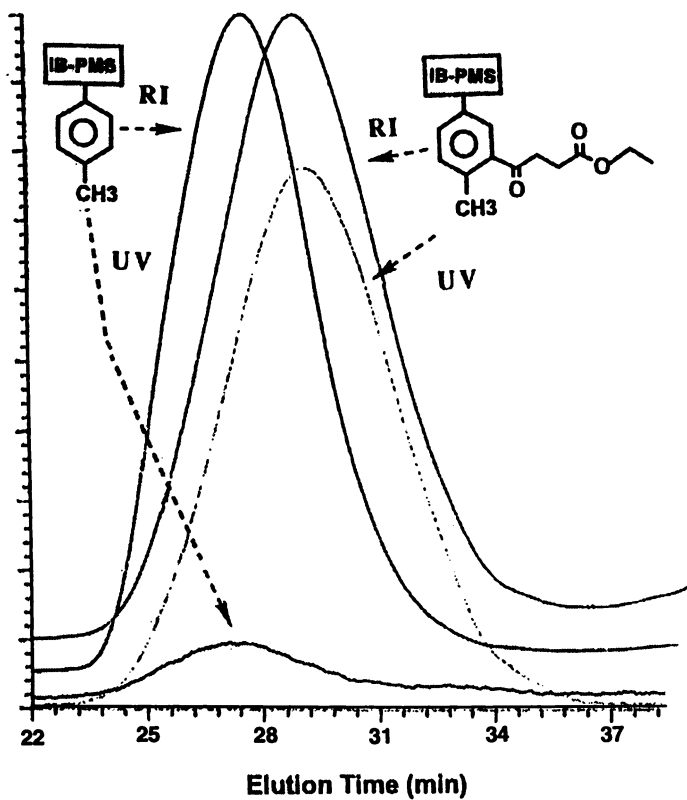


Figure 6. GPC chromatograms of the starting poly (IB-PMS) copolymer and ester functionalized poly (IB-PMS) copolymer using both RI and UV detectors.

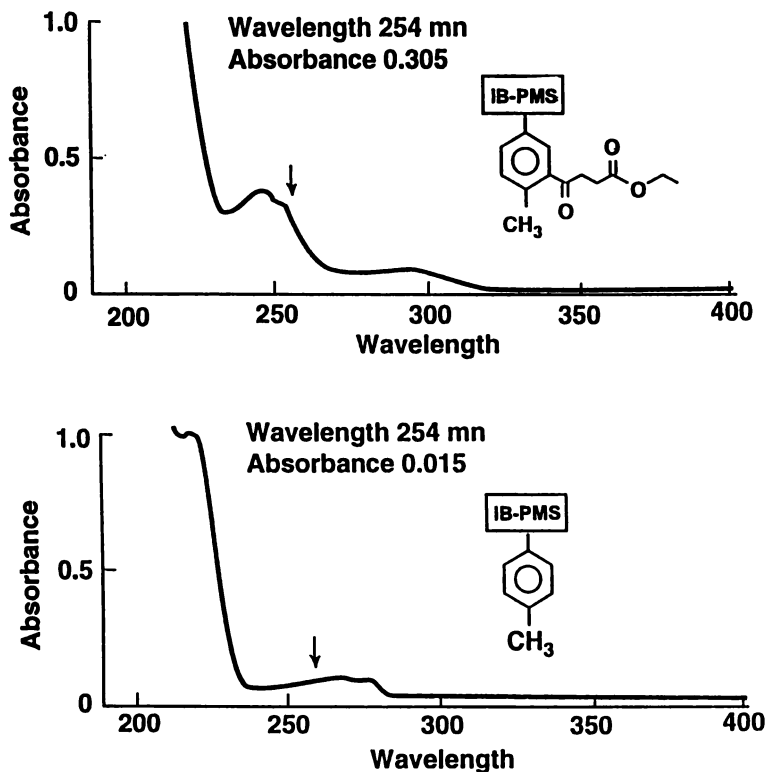


Figure 7. UV-visible absorption spectra of starting poly (IB-PMS) copolymer (bottom spectrum) and ester functionalized poly (IB-PMS) copolymer (top spectrum) in hexane solvent.

Acknowledgment

I would like to thank Greg Springstun for experimental help and Dr. Hsien Wang of Baytown Polymer Center for poly (IB-PMS) samples. I would also like to thank Debbie Sysyn for NMR spectra.

Literature Cited

1. Kresge, E.; Wang, H. C. *Kirk-Othmer Encyclopedia of Chemical Technology*, 4th ed., Vol. 8. Wiley, New York, 1993, p.934.]
2. Wang, H. C.; Powers, K. W. paper no. 85, presented at a meeting of the Rubber Division, American Chemical Society, Toronto, Canada, May 21-24, 1991.
3. Wang, H. C.; Powers, K. W. *Elastomerics*, Jan. & Feb., 1992.
4. Powers, K. W.; Wang, H. C.; Chung, T. C.; Dias, A. J.; Olkusz, J. A. *U.S. Patent*, 5,162,445, 1992.
5. Merrill, N. A.; Powers, K. W.; Wang, H. C. *Polym. Prepr. (Am. Chem. Soc., Div. Polym. Chem.)* **1992**, 32, 968. Haque, S. A.; Powers, K. W.; Wang, H. C.; Frechet, J. M. J.; Steinke, J. H. G. *Polym. Mater. Sci. Eng.* **1997**, 76, 87.
Arjunan, P.; Wang, H. C.; Olkusz, J. A. *Polym. Mater. Sci. Eng.* **1997**, 76, 310.
6. Olah, G. A. in *Friedel-Crafts and Related Reactions*, Vols. I-IV, Wiley, New York, 1963-1964, Olah, G. A. in *Friedel-Crafts Chemistry*, Wiley, New York, 1973 .
7. Grummitt, O.; Becker, E. I.; Miesse, C. in "Organic Synthesis" Collective Volume 3, p. 109.
8. Frechet, J. M. J.; Darling, G. D.; Itsuno, S.; Lu, P. Z.; Meftahi, M. V.; Rolls, W. A. *Pure Appl. Chem.* **1988**, 60, 353. Hodge, P.; Sherrington, D. C. Eds., *Polymer-Supported Reactions in Organic Synthesis*, Wiley, New York, 1980.
9. Kresge, E. N.; Schatz, R. H.; Wang, H. C. *Encyclopedia of Polymer Science and Engineering*, 2nd ed.; Wiley: New York, vol. 8, p 423, 1987.

Chapter 14

New Options via Chemical Modifications of Polyolefins: Part 1. Synthesis and Properties of Novel Phosphonium Ionomers From Poly(Isobutylene-co-4- Bromomethylstyrene)

P. Arjunan¹, H-C. Wang¹, and J. A. Olkusz²

¹Exxon Chemical Company, 5200 Bayway Drive, Baytown, TX 77520

²Exxon Chemical Company, 1900 E. Linden Avenue, Linden, NJ 07036

A new ionomer, - poly[Isobutylene-co-(4-methylstyrenyl, triphenyl phosphonium tetraphenyl borate)] was synthesized by reacting the Exxpro elastomer, - poly[Isobutylene-co-(4-bromomethylstyrene)] with triphenyl phosphine and sodium tetraphenyl borate in tetrahydrofuran as solvent. This phosphonium ionomer had interesting mechanical properties that were in the range of typical thermoplastic elastomers : tensile strength = 1200 to 1600 psi and elongation at break = 275 - 652%. The thermomechanical behavior of these ionomers indicated the presence of strong ionic interactions which resulted in higher glass transition temperature and retention of modulus up to 70° C. A ten fold increase in melt viscosity of these ionomers with reference to the starting material indicated the presence of their strong ionic associations. The mechanical, thermal, and rheological properties of the above ionomers were controlled by their molecular structure characteristics such as the molecular weight, ion content, and type of the counter ion. These novel phosphonium ionomers could be useful as impact modifiers, tire-tread components, adhesives, polymer-bound catalysts, biocides, and flame retardants.

Chemical modification of polyolefins is a broad and rapidly growing field of science. Such modification, often times, is done to introduce either subtle or gross changes that enhance the attributes of the original polymer. For example, introduction of ionic interactions in polymers provides a means of controlling polymer structure and properties. As would be expected, ion-containing polymers, otherwise known as "ionomers", display properties which are dramatically different from those of the parent polymer. Therefore, a broad spectrum of material properties may be created by varying the ion content, type of counter ion, and extent of neutralization.

The Exxon Chemical Company, USA has developed a new elastomer, Exxpro via chemical modification of its precursor, XP50 - a copolymer of isobutylene and 4-

methylstyrene. Using free radical bromination, the 4-methylstyrene moiety in the above precursor was selectively brominated to form 4-bromomethylstyrene derivative. This highly reactive and versatile benzyl bromide moiety was exploited as a precursor for many types of functional groups as well as for the synthesis of graft copolymers.(1) This paper describes our work on a novel ionomer, - poly [Isobutylene-co-(4-methyl styrenyl, triphenyl phosphonium tetraphenyl borate)] that was derived by a simple chemical modification of its precursor - the Exxpro elastomer.(2)

Background

Although much of early work on ionomers had focused on non-elastomeric materials, attention has recently been shifted to elastomeric ionomers as potential thermoplastic elastomers(TPE), i.e. elastomers which flow at high temperatures yet retain their network structure at ambient temperatures. For a material to function as a useful elastomer, the polymer chains must be interconnected in a three-dimensional network. Classically, such crosslinked elastomers cannot flow readily. However, if an elastomer is physically crosslinked via strong ionic bonds, this may lead to a potential TPE. The ionic bonds form physical crosslinks between the polymer chains and thus promote good elastomeric character, yet at higher temperatures they become sufficiently labile to allow the material to flow and be processed as a TPE.

The pioneering work on elastomeric ionomers was done by Brown who first neutralized carboxylated elastomers with metal oxides resulting in ionically crosslinked elastomers - the first ionomers.(3) Using polystyrene, Lundberg and Makowski(4) also demonstrated that sulfonated polymers exhibited much stronger ionic association than the corresponding carboxylate material. Exxon patents in the mid-1970's(5-7) on sulfonated EPDM materials revitalized the efforts to probe the potential of elastomeric ionomers. Elastomeric ionomers based on polypentenamers were studied by MacKnight and coworkers.(8) Another class of elastomeric ionomers consisted of the segmented polyurethanes.(9)

There is, however, limited information on ionomers containing quaternary phosphonium salts. Poly(tributylvinylphosphonium bromide) was reported to be an effective flame retardant for thermoplastic products.(10) The salts of monomeric phosphonium cations with polyacrylate anions were reported to be useful for preparing nonflammable and heat resistant polymers.(11) Synthesis of water-soluble polyelectrolytes by quaternizing copolymers containing chloromethyl styrene with a phosphine were also reported.(12,13) Polymers containing phosphonium salts were developed for applications such as liquid toner for electrostatic images(14), dry electrographic developers(15), polymer-bound catalysts(16), and ion-exchange resins(17). However, work on elastomeric ionomers containing quaternary phosphonium salts is nonexistent to date.

Experimental

Materials. The commercial grade Exxpro elastomer, BrXP50 (Exxon Chemical Co., Baytown, TX), triphenyl phosphine(Aldrich F. Wt. 262.29, M.P.: 79-81° C), sodium tetraphenyl borate(Aldrich, 99.5+ %), tetrahydrofuran(Baker, reagent grade), methanol and isopropanol(Baker, reagent grade) were purchased and were used as such.

Methods. ^1H NMR spectra were obtained using a Varian XL 400 NMR spectrometer; the FTIR spectra were recorded using a Mattson Sirius 100 spectrometer; the rheological data were collected using Rheometrics System IV instrument; the DMTA data were obtained using a Polymer Labs instrument; DSC data (T_g and TGA) were gathered by using a Perkin Elmer instrument; the mechanical properties (tensile strength, % elongation and modulus) were measured using a Monsanto Tensometer 10; the Shore Hardness (ASTM D2240) measurements were made using a Durometer Shore instrument.

Synthesis of Poly[Isobutylene-co-(4-Methylstyrenyl, Triphenyl Phosphonium Tetraphenyl Borate)]

General Procedure. A 1 liter, 3-neck, jacketed resin kettle (equipped with a thermometer, a mechanical stirrer and a condenser with N₂ bubbler outlet) was charged with the Exxpro elastomer and the solvent tetrahydrofuran. The above mixture was stirred under N₂ and was heated to 55° C (Lauder water circulating heating bath) to dissolve the polymer completely. The triphenyl phosphine was added with continuous stirring and the reaction was continued under the same conditions for another 24 hr, after which a solution of sodium tetraphenyl borate in tetrahydrofuran was added slowly. The reaction mixture was then kept under the same conditions for an additional 24 hr and was allowed to cool to ambient temperature. The mixture was poured into 750 ml IEC polypropylene screw cap centrifuge bottles and was centrifuged in an IEC Centra 8 model centrifuge equipped with an IEC 216 four place rotor for 7 minutes at 3400 rpm. The clear solution was decanted off and was coagulated with two volumes of 1:1 mixture of methanol and isopropanol. The coagulant was again kneaded into a fresh two volumes portion of the above alcohol mixture, was filtered off (150 mesh stainless steel screen), and was dried under vacuum (-32°Hg) at 80° C for 48 hr.

The stoichiometric amounts of reactants were dependent upon the bromine content of the starting material, Exxpro elastomer, and typical examples (based on 50 g Exxpro elastomer) are listed below.

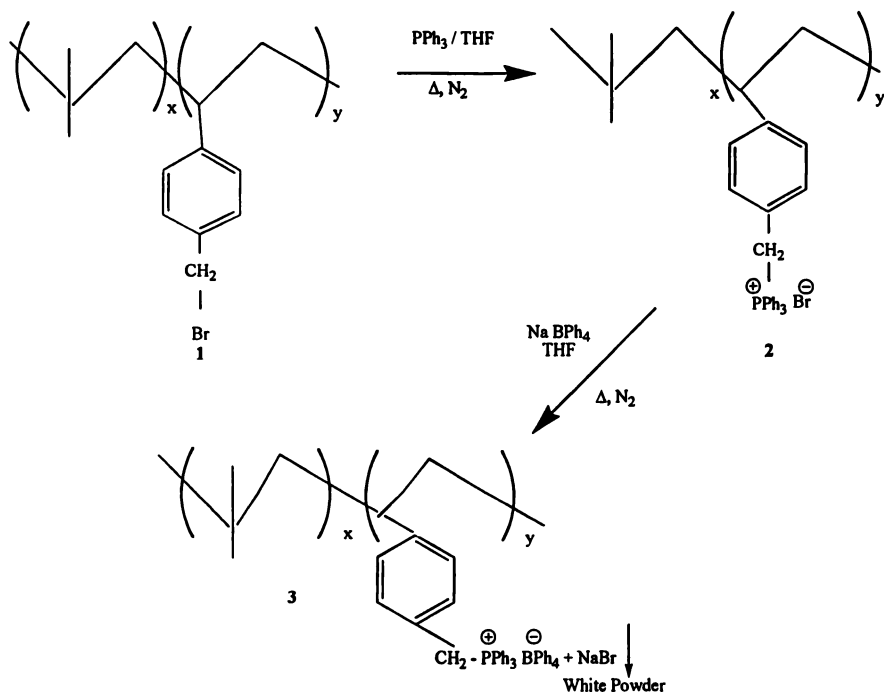
Exxpro elastomer	Pφ ₃	NaBφ ₄	THF
M _n = 60 K (BrPMS = 1.3 mol % Br = 10.5 mmol)	2.75 g (10.5 mmol)	3.59 g (10.5 mmol)	500 ml
M _n = 100 K (BrPMS = 1.3 mol % Br = 10.5 mmol)	2.75 g (10.5 mmol)	3.59 g (10.5 mmol)	500 ml
M _n = 280 K (BrPMS = 3.5 mol % Br = 28 mmol)	7.34 g (28 mmol)	9.58g (28 mmol)	750 ml
M _n = 280 K (BrPMS = 3.5 mol % Br = 28 mmol)	3.67 g (14 mmol)	4.79 g (14 mmol)	750 ml

Results and Discussion

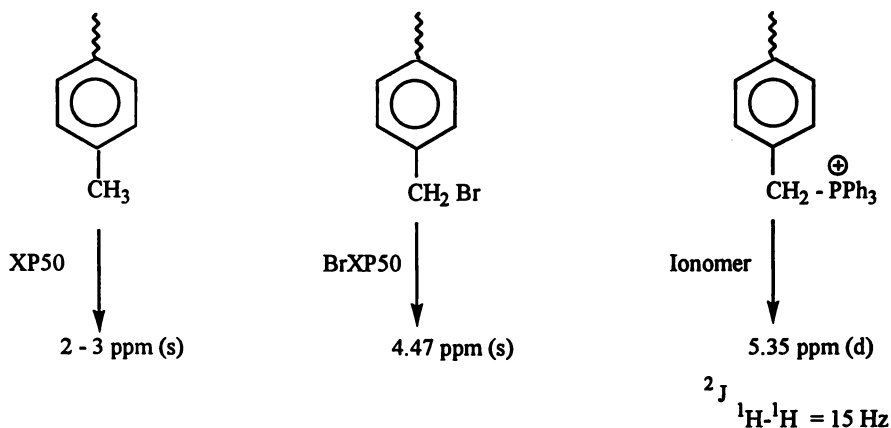
Synthesis. Polymers containing the vinyl-benzyl phosphonium unit can be made by either direct synthesis of the monomers and subsequent polymerization or phosphonation of chloromethyl styrene containing polymers. The latter is preferred due to the difficulty of obtaining the vinyl benzyl phosphonium monomer in good yield and purity without spontaneous polymerization. In either case, synthesis of elastomers containing quaternary phosphonium salts have not been reported to date.

The conversion of the E_xpro elastomer into an ionomer, - the quaternary phosphonium salt (tetraphenyl borate) was accomplished by using a one-pot reaction that involved a two-step reaction sequence (Scheme 1). Tetrahydrofuran was the preferred solvent to carry out the above sequence of reactions in the same pot without isolating the intermediate. The above synthesis involved a nucleophilic displacement of 'Br' from the benzylic carbon of BrPMS by triphenylphosphine. Analogous reactions involving simple organic compounds such as benzyl bromide or other active halogenated hydrocarbons were well known and served as precursors for the so called Wittig reaction.⁽¹⁸⁾

Scheme 1



Characterization. The conversion of Exxpro elastomer to its phosphonium tetraphenyl borate ionomer was followed by analyzing the ^1H NMR and FTIR spectral data. The benzylic protons in Expro elastomer had an unique signal at 4.47 ppm (Figure 1). Formation of phosphonium ionomer from Exxpro elastomer involved the nucleophilic displacement of "Br" by $\text{P}\phi_3$ and created phosphonium ion, vicinal to the benzylic protons. Due to the proximity of the phosphonium ion, the signal for benzylic protons was shifted downfield from that of the starting material, Exxpro elastomer. The benzylic protons of the ionomer were found to have a doublet signal at 5.35 ppm (Figure 2). This doublet was due to the geminal proton (CH_2) coupling, $^2J_{\text{H-H}} = 15$ Hz. The ionomer formation was almost quantitative as there was no signal at 4.47 ppm in ^1H NMR spectrum of the ionomer.



Analysis of FTIR spectra of the ionomer (Figures 3 and 4) was also informative about the structure. It was reported previously that IR absorption bands at 1893 cm^{-1} and 1905 cm^{-1} were characteristics of 4-methylstyrene (of XP50) and 4-bromomethyl styrene (of Exxpro elastomer, Figure 5). Such absorption bands were not found in the FTIR spectra of the above ionomers. However, new absorption peaks, characteristics of the quaternary phosphonium salts, at 1580 , 1100 , 100 , & $670\text{-}730 \text{ cm}^{-1}$ were observed. The presence of both phosphorous and boron in the above ionomers was also confirmed in terms of the elemental analysis data, collected from the inductively coupled plasma/atomic emission spectroscopy (ICP/AES) technique. These results were in good agreement with the expected conversion of the respective phosphonium salts.

Properties

Mechanical Behavior. The ionomers, - poly[Isobutylene-co-(4-methyl styrenyl, triphenyl phosphonium bromide or tetraphenyl borate)] were found to be different in physical appearance (hard and strong) and tougher than the starting material, the Exxpro elastomer. The mechanical properties of these quaternary phosphonium

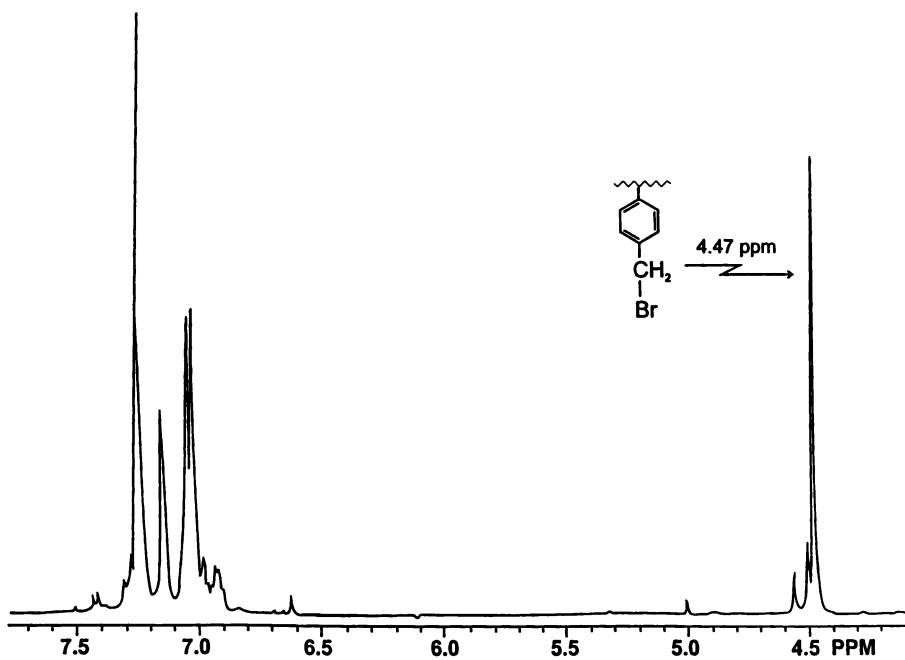


Figure 1. ^1H NMR Data, Expro Elastomer.

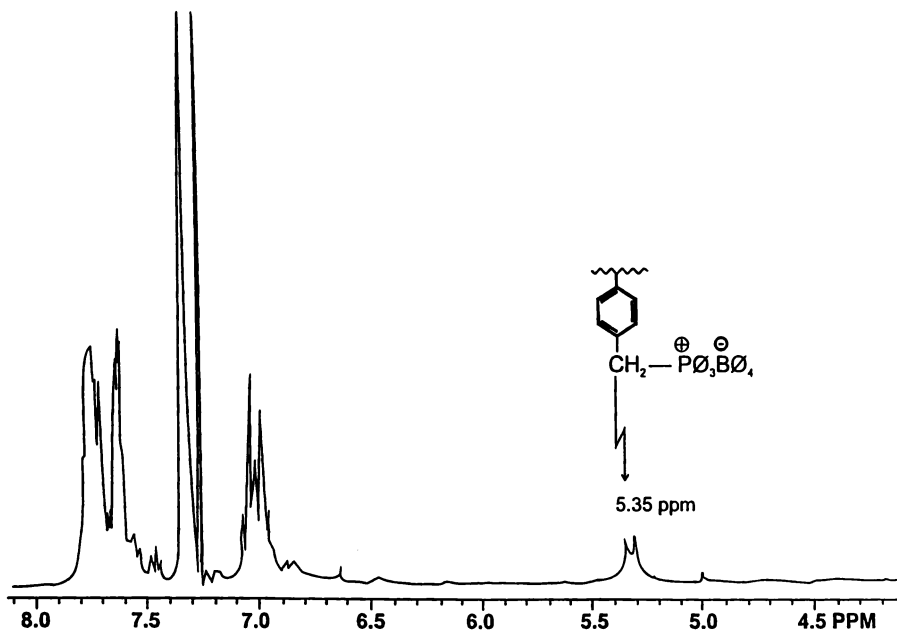


Figure 2. ^1H NMR Data, Poly[Isobutylene-co-(4-methylstyrenyl, triphenyl phosphonium tetraphenyl borate)]

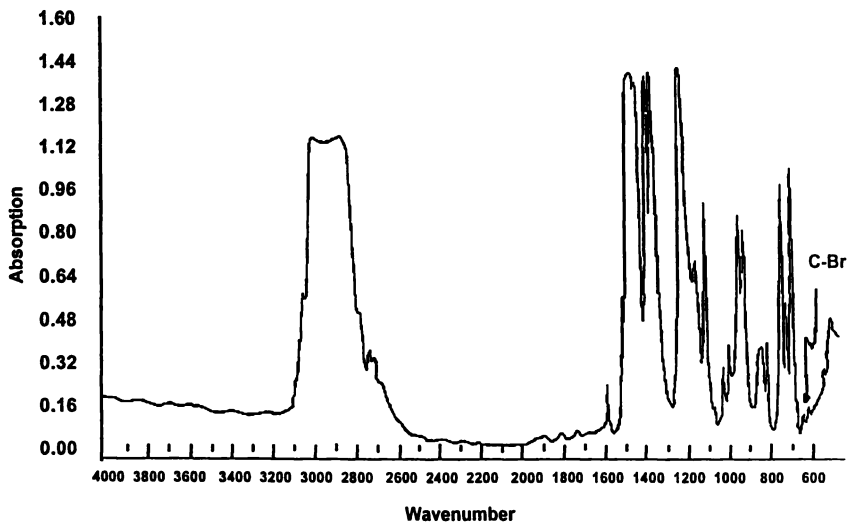


Figure 3. FTIR Data, Exxpro Elastomer.

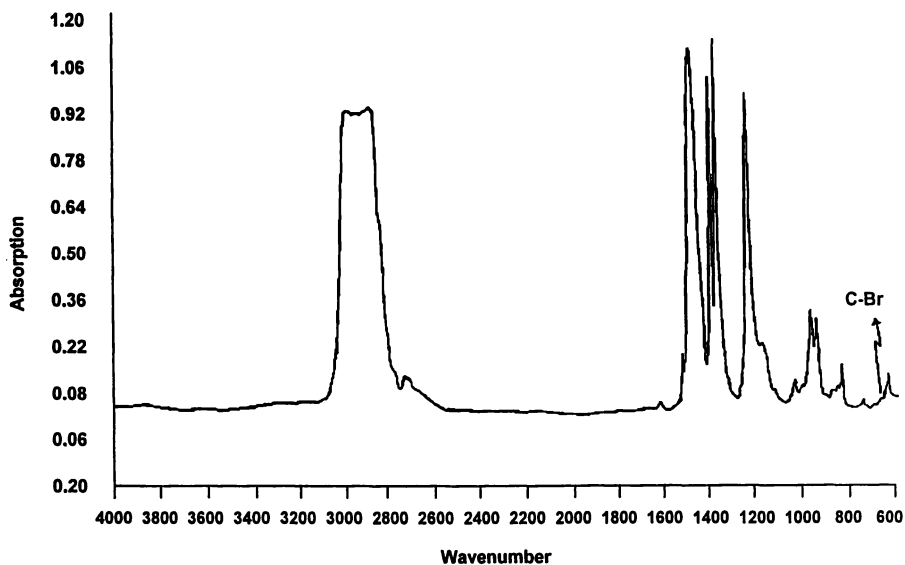


Figure 4. FTIR Data, Poly[Isobutylene-co-(4-methylstyrenyl, triphenyl phosphonium tetraphenyl borate)]

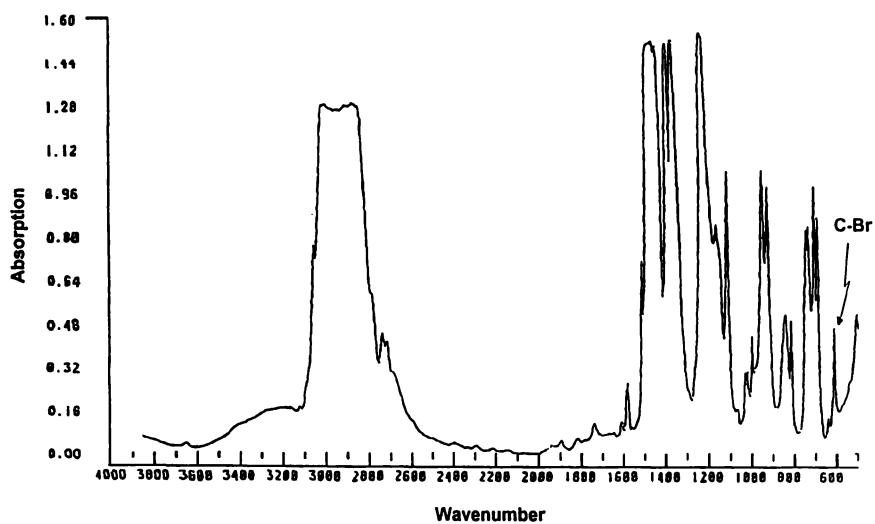


Figure 5. FTIR Data, Poly[Isobutylene-co-(4-methylstyrenyl, triphenyl phosphonium tetraphenyl borate)]

ionomers and some other commercial TPEs (fully compounded materials that had typically 20-25% rubber) are listed in Table I. Incorporation of the phosphonium salts in the 'Exxpro elastomer' backbone improved significantly the tensile properties, i.e. tensile strength has increased to almost 10^3 fold; also the tensile properties (tensile strength, % elongation at break, modulus) of these ionomers were in the range of typical ionic elastomer compounds.(19)

Thermomechanical Behavior. The starting material, Exxpro elastomer had a T_g at -62°C (DMTA) and flowed readily above its T_g with no signs of significant intermolecular attraction. However, incorporation of the phosphonium groups in the 'Expro elastomer' backbone brought out two significant changes in the thermomechanical behavior: 1) The T_g of the Exxpro elastomer was shifted to higher temperatures, $= -37$ to -27°C , 2). A strong rubbery plateau was observed (Figure 6) which persisted up to about 70°C . These observations implied that strong ionic associations were present in the phosphonium salts of Expro elastomer. Also, it seemed that an optimum concentration of phosphonium ions was needed to form the ionic clusters which led to the strong rubbery plateau. The ionomers from low molecular weight Expro elastomer ($M_n = 60$ and 100K) did not exhibit strong rubbery plateau in the DMTA study. As expected, the rubbery plateau region for the high molecular weight ($M_n = 280\text{K}$) phosphonium ionomer was extended to relatively high temperature, 70°C . However, the ionic associations were not permanent and their strength was dependent upon temperature. There were two opposing forces acting on the ionic crosslinks. First, the forces arising from the entropically driven molecular motions pull the chains away from the ionic aggregates. The opposing force was to coulombic force of attraction between oppositely charged ions. These forces lead the ionic crosslinking of different molecules unless intramolecular cyclization occurs. However, the coulombic forces of attraction were a weak function of temperature and decreased in strength with increasing temperature. Thus, above a certain temperature these ionic crosslinks could be sufficiently weakened to allow the polymer to flow readily.

Rheological Properties. Incorporation of ions into a polymer invariably causes an increase in the melt viscosity of the polymer. This is mainly due to the strong association between the ionic segments (which lead to the so called 'cluster' formation in some cases!) which can best be described as time - dependent crosslinks. Such crosslinks are regarded as extra entanglements or as decreasing the segmental mobility which can be described by free volume considerations.

Several authors who studied the rheological properties of ionomers reported a typical but unusual increase in the melt viscosity of ionomers. Canter(5) reported higher viscosity of sulfonated butyl rubber, i.e. almost three times that of the parent rubber at 90% neutralization. A significant difference between the rheological behavior of sulfonated and carboxylated polystyrenes was observed by Lundberg and coworkers.(20) At the level of 2 mole % sodium salt, the sulfonate was 100 times greater in viscosity than the carboxylate, the difference becoming greater with increased acid content. A dramatic increase in the viscosity (20 fold) of the ethylene-methacrylic acid ionomers (sodium salt, 2 mole %) was reported by Longworth and coworkers.(21)

Table I. Properties of Phosphonium Ionomers Vs. Commercial TPEs

Polymer	Tensile Strength psi	Elongation at break (%)	Hardness Shore A	Modulus 100% 300%
Exxpro™ (60 K Mn, 1.3 mol.% BR)	<1	0	-	-
Exxpro™ P Ø ₃ B Ø ₄ (60 K Mn, 1.3 mol. % Br) ⊕ ⊖	1,583	652	0	162 235
Exxpro™ (100 K Mn, 1.3 mol. % Br)	3	2,000	-	19 17
Exxpro™ P Ø ₃ B Ø ₄ (100 K Mn, 1.3 mol. % Br) ⊕ ⊖	1,217	1,215	50	170 284
Exxpro™ (280 K Mn, 3.5 mol. % Br.)	19	2,100	-	38 46
Exxpro™ P Ø ₃ B Ø ₄ (280 K Mn, 3.5 mol. % Br) ⊕ ⊖	1,532	275	90	1,047 -
Kraton G 2705	1,200	700	55	- 350
Santoprene (EPDM/PP, DVA)	1,200	475	72	470 -

We observed similar rheological behavior of the above quaternary phosphonium ionomers. As shown in Figures 7-10, the viscosity of the above ionomers were 10 fold higher than the starting materials, Exxpro elastomer. This increase in viscosity of these ionomers was due to the powerful intermolecular attraction between the ionic species, which might exist as "clusters". These clusters could act as "ionic crosslinks" which caused the significant increase in viscosity of the ionomers. The intermolecular attraction via ionic association of these ionomers was dependent upon temperature and shear force. As we discussed earlier, the rubbery plateau region(Figure 6) dropped off with increasing temperatures, $> 70^{\circ}\text{C}$ due to the temperature dependence of these so called "ionic crosslinks". The viscosity of these ionomers ($M_n = 60$ and 100 K) was high at temperatures $< 100^{\circ}\text{C}$ and began to drop off at higher temperatures. Interestingly, the temperature at which the viscosity dropped off sharply depended upon the molecular weight of these ionomers. As shown in Figure 11, the viscosity of the lower molecular weight ($M_n = 60\text{ K}$) ionomer dropped off sharply at the temperature range of $125\text{-}130^{\circ}\text{C}$, while that of the higher molecular weight ($M_n = 100\text{ K}$) ionomer occurred at somewhat higher temperature range, $230\text{-}35^{\circ}\text{C}$. The high viscosity of these ionomers at lower temperatures was due to the ionic associations which became weak at higher temperatures when the ionomers started flowing readily just like the parent polymer, Exxpro elastomer. Similar rheological behavior was exhibited by other TPEs such as Kraton D and G(unpublished data from Exxon Chemical Company Reports), as shown in Figure 11.

As the shear stress was increased, the viscosity of an ionomer decreased in common with high molecular weight polymers. There was a dramatic increase in the low shear rate viscosity, but the effect was much less at higher shear rates. This suggested that there was a breakdown in some flow unit in the ionomer at high shear rate when it behaved like the parent polymer, Exxpro elastomer. Similar results were reported by other workers.(22-23)

Applications

Most ionomer applications exploit several characteristics which can be attributed to ionic aggregation or cluster formation, or interaction of polar groups with ionic aggregates. Changes in physical properties caused by ionic aggregation in elastomeric systems or in polymer melts are readily detected. Therefore, the marked enhancement in elastomeric green strength is a general characteristic of ionomer-based systems. The ionic aggregation is also apparent in enhanced melt viscosity, which can be utilized in heat sealing. It also provides a particular processing advantage during extrusion operation. Other properties generally attributable to ionic aggregation include toughness and outstanding abrasion resistance, as well as oil resistance in packaging applications.

The interactions of various polar agents with the ionic groups and the ensuing property changes are unique to ionomer systems. This plasticization process is also important in membrane applications. A different application of ionic cluster plasticization involves the interaction of metal stearates to induce softening transitions. The plasticization process is required to achieve the processability of TPEs based on this technology.

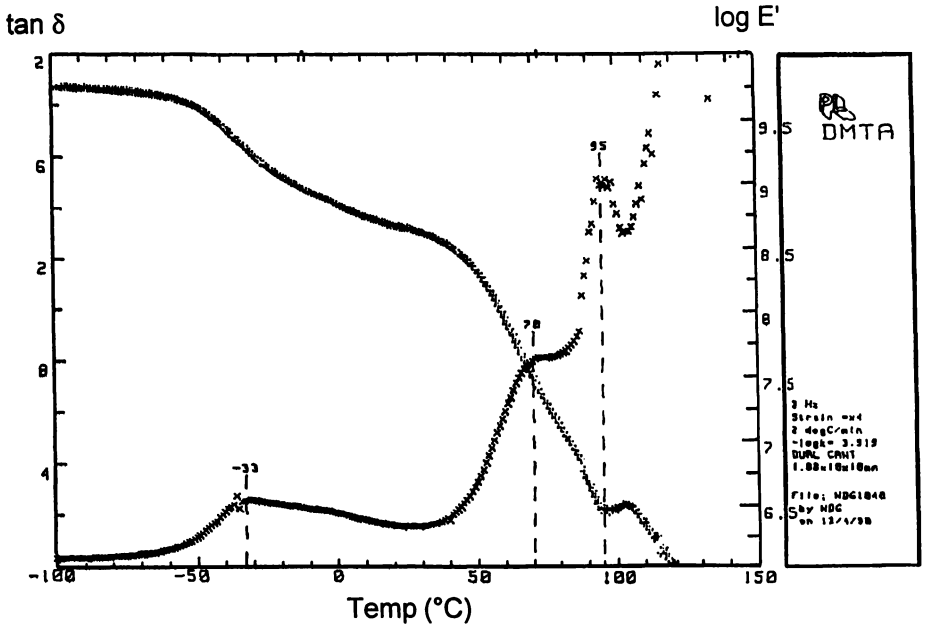


Figure 6. DMTA Data, Poly[Isobutylene-co-(4-methylstyrenyl, triphenyl phosphonium tetraphenyl borate)]

TEMP SWP @40-160C, @10C INT

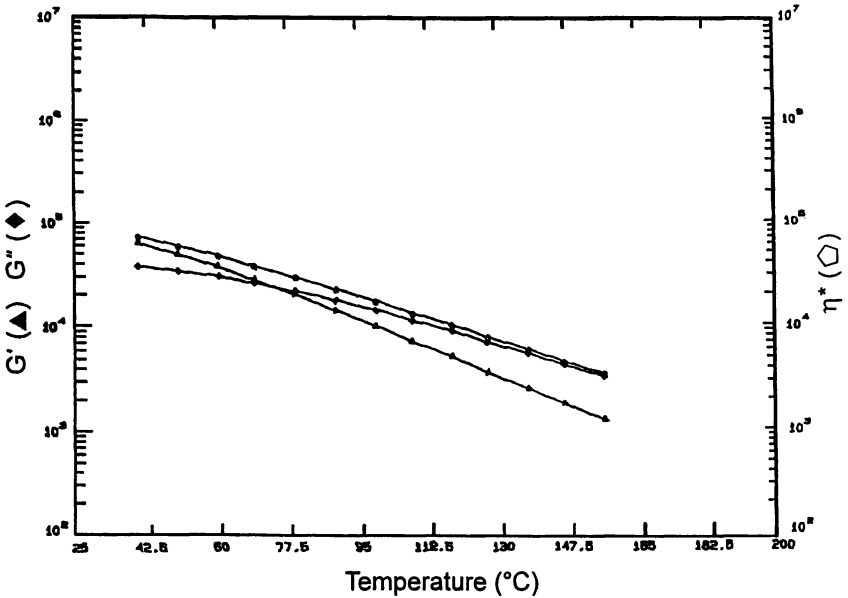


Figure 7. Viscosity Data, Exxpro Elastomer, $M_n = 100$ K.

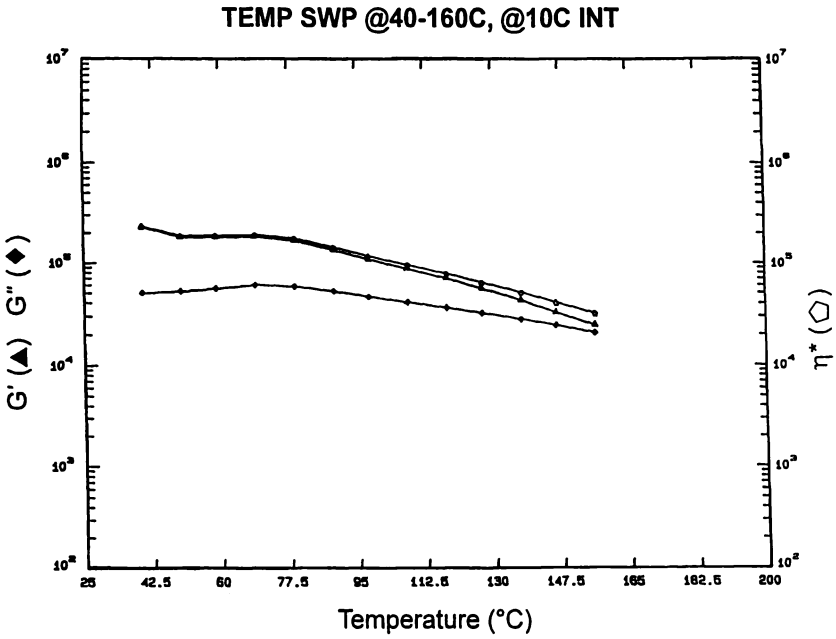


Figure 8. Viscosity Data, Poly[Isobutylene-co-(4-methylstyrenyl, triphenyl phosphonium tetraphenyl borate)

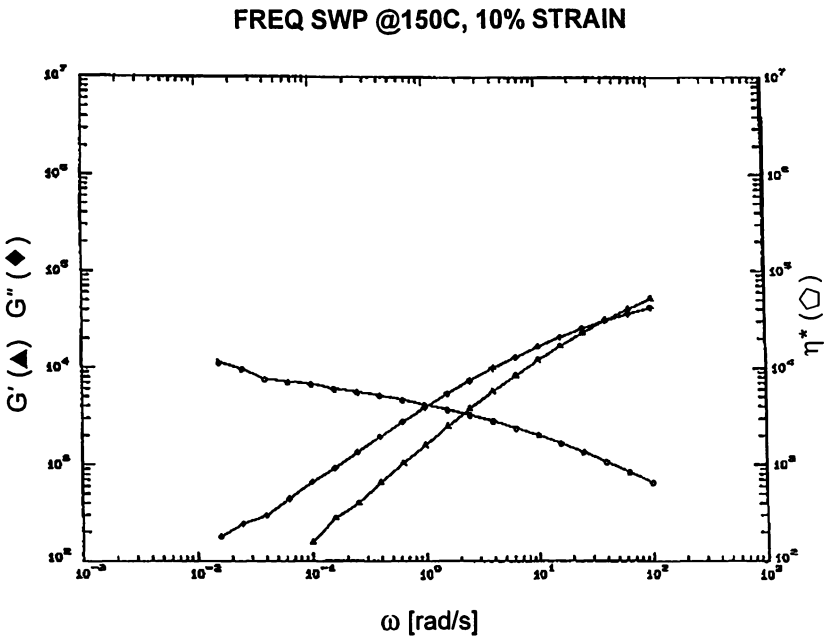


Figure 9. Viscosity Data, Exxpro Elastomer, $M_n = 100$ K.

FREQ SWP @150C, 10% STRAIN

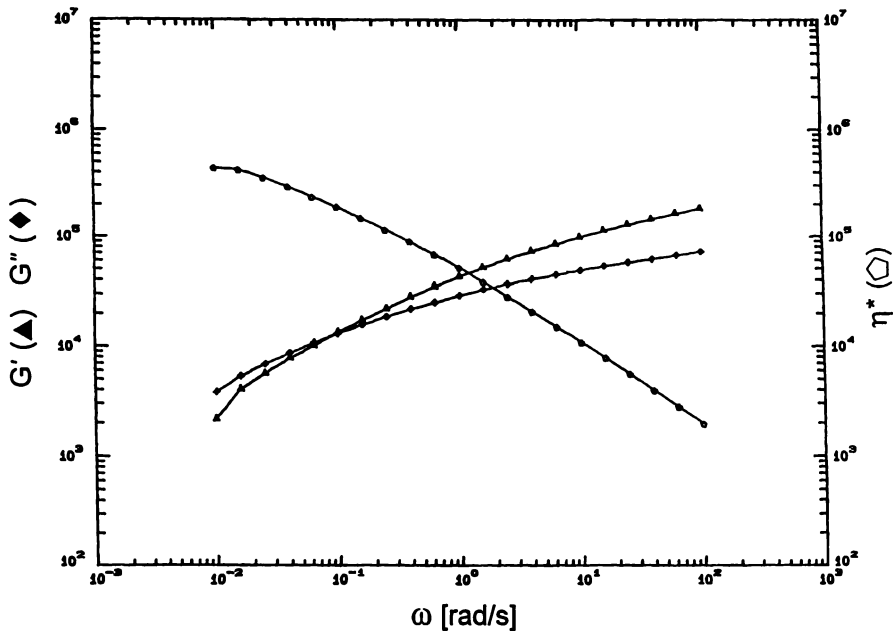


Figure 10. Viscosity Data, Poly[Isobutylene-co-(4-methylstyrenyl triphenyl phosphonium tetraphenyl borate)]

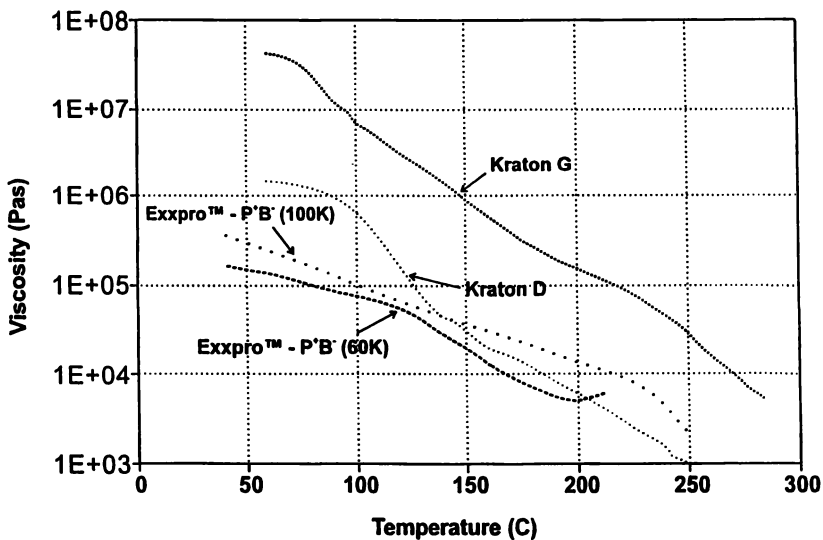


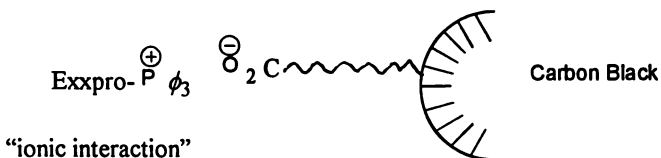
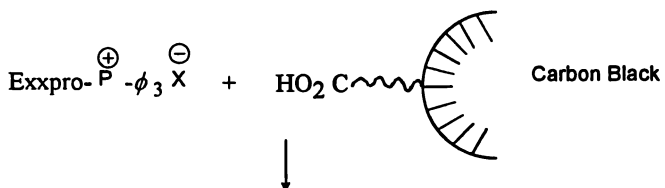
Figure 11. Viscosity Vs. Temperature Data Of Ionomers.

Modification of Engineering Resins: Specific interaction of the phosphonium ionomer from Exxpro elastomer with selected engineering resins such as Polycarbonates(PC), Polyesters(PET), Polyacrylates(PAE), Polyamides(PA), Polyphenylene Oxide(PPO), and Acetals(PAc) can be utilized to compatibilize, impact modify or nucleate the above resin in blends with similar polymers. Typical examples are:

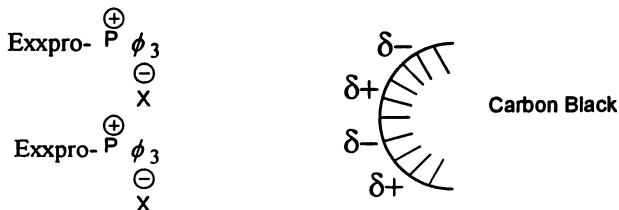
Polymer Modification	Expected Property Improvement
PC/Exxpro- $\oplus\ominus$ P X	Impact strength, notch sensitivity, solvent resistance, flame retardance
PA/Exxpro- $\oplus\ominus$ P X	Impact strength, dimensional stability, processability, and flame retardance
PET/Exxpro- $\oplus\ominus$ P X	Impact strength, dimensional stability, nucleation, processability, and flame retardance
PAc/Exxpro- $\oplus\ominus$ P X	Impact strength, processability, moisture sensitivity, and flame retardance
PC/PA/Exxpro- $\oplus\ominus$ P X	Impact strength, compatibility, notch sensitivity, processability, solvent resistance, and flame retardance, etc.
PC/PET/Exxpro- $\oplus\ominus$ P X	Impact strength, solvent resistance, processability, and flame retardance
PPO/Exxpro- $\oplus\ominus$ P X	Impact strength, processability, and flame retardance
PPO/PA/Exxpro- $\oplus\ominus$ P X	Impact strength, compatibility, processability, and flame retardance
Polyolefins/PPO/Exxpro- $\oplus\ominus$ P X	Impact strength processability, compatibility, HDT, and flame retardance
Polyolefins/PA/Exxpro- $\oplus\ominus$ P X	Impact strength, processability, dimensional stability, HDT, flame retardance, and compatibility
Polyolefins/PC/Exxpro- $\oplus\ominus$ P X	Impact strength, HDT, flame retardance, solvent resistance, compatibility, and surface appearance
Polyolefins/PET/Exxpro- $\oplus\ominus$ P X	Impact strength, processability(nucleation and moldability), HDT, and flame retardance

Note: HDT = Heat Distortion Temperature

Tire-Tread Formulations. The isobutylene polymers are notorious for their poor affinity toward carbon black relative to other elastomers that are rich in unsaturation. Yet reinforcement with carbon black is critical to use in these polymers in tire treads where a certain degree of abrasion resistance is required. It is expected that the Exxpro-phosphonium ionomers can interact with the carbon black (both regular and oxidized forms) surface and thereby localize them within the PIB phase as shown:



or



“dipole-dipole interaction”

Rubber Blends For Automotive Applications. The ionomers from Exxpro elastomer can be blended with other elastomers such as Neoprene(CR), Nitrile(NBR), and Acrylics(VAMAC) for selected automotive applications, e.g., hoses, air springs, and belts.

Polymer-bound Catalysts: Various quaternary phosphonium salts are known to be excellent catalysts for trans-esterification and condensation polymerizations, e.g. melt polymerization of polycarbonates and polyesters. The ionomers from Exxpro elastomer can be used in those applications with added advantages such as solubility in the melt, ease of recovery and thermal stability.

Flame Retardants. Due to the presence of phosphorous and ‘phosphonium borates/bromides’ in the backbone of these ionomers, they are expected to be flame retardant materials.

Biocides. Quaternary phosphonium salts are known to be biocides and can be useful in various applications based on this attribute (e.g., purification of beer in the brewing industry). The ionomer has an added advantage in that it can be recovered easily and be regenerated for repeated applications.

Adhesives. Due to the presence of the ionic groups on the backbone, the phosphonium ionomer from Exxpro elastomer is expected to have polar surface which can be utilized in various adhesive applications.

Other Applications. The phosphonium ionomer from the Exxpro elastomer can be formulated into a wide variety of compounds of interest in applications such as calendered sheet, garden hose, footwear, membranes and packaging materials.

Conclusion

A simple chemical modification of the Exxpro elastomer, poly[Isobutylene-co-(4-bromomethylstyrene)] with triphenyl phosphine and sodium tetraphenyl borate produced a new ionomer, - poly[Isobutylene-co-(4-methylstyrenyl, triphenyl phosphonium tetraphenyl borate)]. The structure of this phosphonium ionomer was identified by using various analytical methods, ^1H NMR, FTIR, DSC, DMTA and elemental analysis. The physical and mechanical properties of the above ionomer were investigated. This phosphonium ionomer had interesting mechanical properties that were in the range of typical ionic thermoplastic elastomers: tensile strength = 1200 to 1600 psi and elongation at break = 275 - 652%. The thermomechanical behavior of these ionomers indicated the presence of strong ionic interactions which resulted in a higher glass transition temperature and retention of modulus up to 70° C. A ten fold increase in melt viscosity of these ionomers with reference to the starting material indicated the presence of their strong ionic associations. The mechanical, thermal, and rheological properties of the above ionomers were controlled by their molecular structure characteristics such as the molecular weight, ion content, and type of the counter ion. Based on the physical and mechanical properties, these novel phosphonium ionomers could be useful in various applications such as impact modifiers/compatibilizers for polyblends, tire-tread components, adhesives, polymer-bound catalysts, biocides, flame retardants, membranes, and others.

Acknowledgment

The financial support for this work by the Exxon Chemical Company, USA - Polymer Group: Butyl Technology and Polymer Science Department is greatly appreciated. The authors would like to thank D.M. Cheng, C.B. Frederick, and C.L. Kiley for obtaining the spectroscopic data (^1H NMR, FTIR); W.D. Gallagher for collecting DMTA data; W.R. Gerald, M. Monahan and K. Wissbrun for providing rheological data; A. Anastasio for measuring mechanical properties of micro tensile samples and K. Powers for providing the Exxpro elastomer samples.

Literature Cited

1. Powers, K.W. et. al. *U.S. Patent*, 1992, 5,162,445.
2. Arjunan, P. et. al. *ACS PMSE Preprint*, 1997, Vol. 76.; pp 310-311.
3. Brown, H.P., *U.S. Patent*, 1953, 2,626,248.
4. Lundberg, R.D.; Makowski, H.S. *Ions in Polymers, Adv. Chem Serv.* 187, Ed. Eisenberg, A. 1980, Ch. 2
5. Canter, N.H. *U.S. Patent*, 1974, 3,642,728.
6. Farrel, C.P.O. et. al. *U.S. Patent*, 1974, 3,836,511.
7. Makowski, H.S. et. al. *U.S. Patent*, 1975, 3,870,841.
8. Sanui, K. et. al. *J. Polym. Sci., Polym. Phys. Edn.* 1975, Vol. 12.; pp. 1965.
9. Dietreirich, D. et. al. *Angew Chem. Int. Edn.* 1970, Vol. 9.; pp. 40.
10. Gillham, et. al. *U.S. Patent*, 1969, 3,431,324.
11. Garner, A.Y. *U.S. Patent*, 1962, 3,065,272.
12. Sexsmith, D.R. *U.S. Patent*, 1965, 3,168,502.
13. Sexsmith, D.R. *U.S. Patent*, 1962, 3,068,214.
14. Uytterhoven, H.J. et. al. *U.S. Patent*, 1985, 4,525,446.
15. Anderson, J.H. et. al. *U.S. Patent*, 1989, 4,837,392.
16. Bauld, N.L. et. al. *U.S. Patent*, 1985, 4,503,195.
17. Rakshys, J.W. et. al. *U.S. Patent*, 1977, 4,043,943.
18. March, J. *Advanced Organic Chemistry*; 3rd Edn., John Wiley and Sons, 1985, pp. 845-854.
19. MacKnight, W.J. et. al. *Thermoplastic Elastomers - A Comprehensive Review*; Ed. Legge, N.R., et. al. Hanser Publishers; 1987, Chapter 10B, pp. 265.
20. Lundberg, R.D. et. al. *ACS Polymer Reprints*, 1978, Vol. 19.; pp. 287.
21. Longworth, R. In *Ionic Polymers*; Ed. Holliday, L.; John-Wiley and Sons, 1975, Chap. 2.
22. Rees, R.H. et. al. *ACS Polymer Reprints*, 1967, Vol. 6.; pp. 287.
23. Sakamoto, K. *J. Polym. Sci.*, 1967, Vol. A2.; pp. 277.

Chapter 15

Multifunctional Supramolecular Materials

Gregory N. Tew¹ and S. I. Stupp^{2,3}

¹Department of Chemistry and Beckman Institute for Advanced Science and Technology and ²Department of Materials Science and Engineering and Materials Research Laboratory, University of Illinois, Urbana, IL 61801

The ability to create regularly shaped nanoscale objects which serve as the building blocks of supramolecular materials is an extremely important goal in materials science. Herein, we report on a general class of supramolecular materials created by self organizing triblock molecules that form nanostructures lacking a center of inversion. The supramolecular materials formed by these molecules have been characterized by a number of techniques including, transmission electron microscopy, second harmonic generation, small angle X-ray scattering, and photoluminescence. These supramolecular units organize spontaneously into films thousands of layers thick. Interestingly, second harmonic generation measurements demonstrate the stacking of nanostructures in the films is polar. The hierarchical organization of these objects could offer materials with defined nanopores, chemically and topographically defined surfaces, large arrays of quantum dots, as well as other interesting properties such as second order nonlinear optical response, piezoelectricity, pyroelectricity and strong luminescence.

A skill not yet mastered in synthetic chemistry is the preparation of designed supramolecular nanostructures with great diversity in shape and functionality. The potential of this unachieved goal in molecular materials science is enormous because it will deliver nanoscale synthetic units analogous to folded proteins as the constituents of materials. Such units could combine shape invariance and sectorial chemical structure for self organization into designer networks, solids with defined nanopores, 2D and 3D superlattices of the nanostructures, surfaces that are not only defined chemically but topographically, and uniquely packed assemblies. The units would essentially offer a new form of coordination chemistry connecting nanostructures rather than ions and small molecules. With conventional synthetic chemistry it is not currently possible to create these nanostructures as covalent chemical compounds. Thus, we must look to self assembly of small molecules to achieve formation of well defined units one might describe as supramolecular polymers since the targeted size is that of folded proteins and polymers in solution. Most previous work in supramolecular chemistry, pioneered by Lehn and co-workers (*1*), has targeted small aggregates of molecules (*2,3*), 1D chains of irregular

³Corresponding author.

length (l), the appendage of side chains to polydisperse linear polymers (4,5), and small dendrimers (l). The understanding of thermodynamic rules that mediate formation of supramolecular nanostructures with molar mass exceeding 100 kilodaltons, and the development of the necessary molecular toolbox remain important goals for science. In this work we present some of our efforts in this area, and describe a family of self assembling molecules which form supramolecular materials composed of highly regular nanostructures. The initial discovery of the molecular systems of interest here was reported elsewhere (7).

Mushroom Shaped Nanostructures From Triblock Molecules

The construction of a miniature triblock copolymer system was inspired by traditional block copolymers. The initial triblock molecule synthesized consists of short blocks of styrene, isoprene, and aromatic biphenyl units, producing a molecular construction that is described as a rodcoil since two of its blocks are conformationally flexible and the third has stiff, rod-like character. Formation of the oligostyrene and oligoisoprene block copolymer employed living anionic polymerization based on seminal work by Szwarc (8). Using *n*-butyl lithium to initiate the sequential polymerization of styrene and isoprene, resulted in an oligo(styrene-co-isoprene) molecular backbone with an average degree of polymerization equal to 9 for both styrene and isoprene. The reaction is quenched with CO₂ gas followed by HCl_{aq}/THF to afford a carboxylated diblock coil. This carboxyl terminus serves as a connection site for the third block of the copolymer which is composed of a perfectly monodispersed sequence of biphenyl units. Gel permeation chromatography measured the polydispersity of the diblock oligo(styrene-co-isoprene) coil to be in the range of 1.06 to 1.10. Sequential attachment of biphenyl units controls the rod length resulting in **1** which has three biphenyl units in the rod block (see Figure 1). This construction leads to a collection of molecules in which polydispersity is only associated with the diblock oligo(styrene-co-isoprene) coil, while the rod block is composed of perfectly monodisperse molecular species.

Transmission electron microscopy (TEM) studies of these rodcoil molecules show they self organize into well-defined, nanoaggregates when cast from solution. The micrograph in Figure 2 was obtained without any staining compounds and the contrast observed is due to both phase and diffraction contrast based on wide angle electron diffraction. Figure 2 clearly shows the nanoaggregates are similar in size and shape. Calculations suggest these aggregates are composed of approximately 100 molecules. Jean-Marie Lehn defined supramolecular chemistry as "the next step in increasing complexity beyond the molecule towards the supermolecule and organized polymolecular systems, held together by non-covalent interactions" (1). Based on this definition, we refer to these nanoaggregates as supramolecular units because they are well-defined collections of individual molecules. Until now the preparation of well-defined supramolecular units with molar masses near the range of hundreds of kDa had not been achieved.

Small angle X-ray scattering (SAXS) measurements indicate the supramolecular units of **1** stack into layers with a *d*-spacing of 74 Å. The fully extended length of **1** is 94 Å, therefore monolayer formation was suspected (9). The fully extended length for several molecules, including **1**, are given in Figure 1. In order to further investigate monolayer formation from this system, a series of ultramicrotomy experiments were performed. TEM micrographs of ultramicrotomed samples revealed the formation of large domains of oriented stripes, up to 1 μm in thickness and 1 cm² in area (see Figure 3). The dark bands are interpreted as being composed of the rigid rod blocks, while the light bands contain the flexible coil-like segments. In agreement with the SAXS investigations, this TEM micrograph indicates **1** forms monolayers in the solid state. In addition, not only are monolayers formed but other

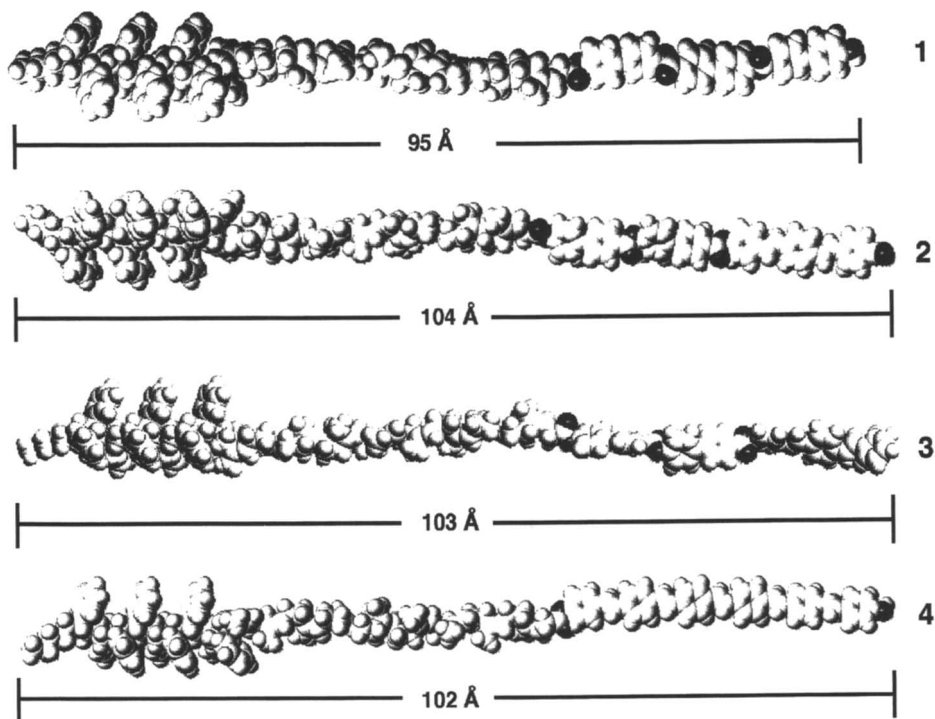


Figure 1. Molecular graphics of several triblock rodcoil molecules along with the fully extended molecular length.

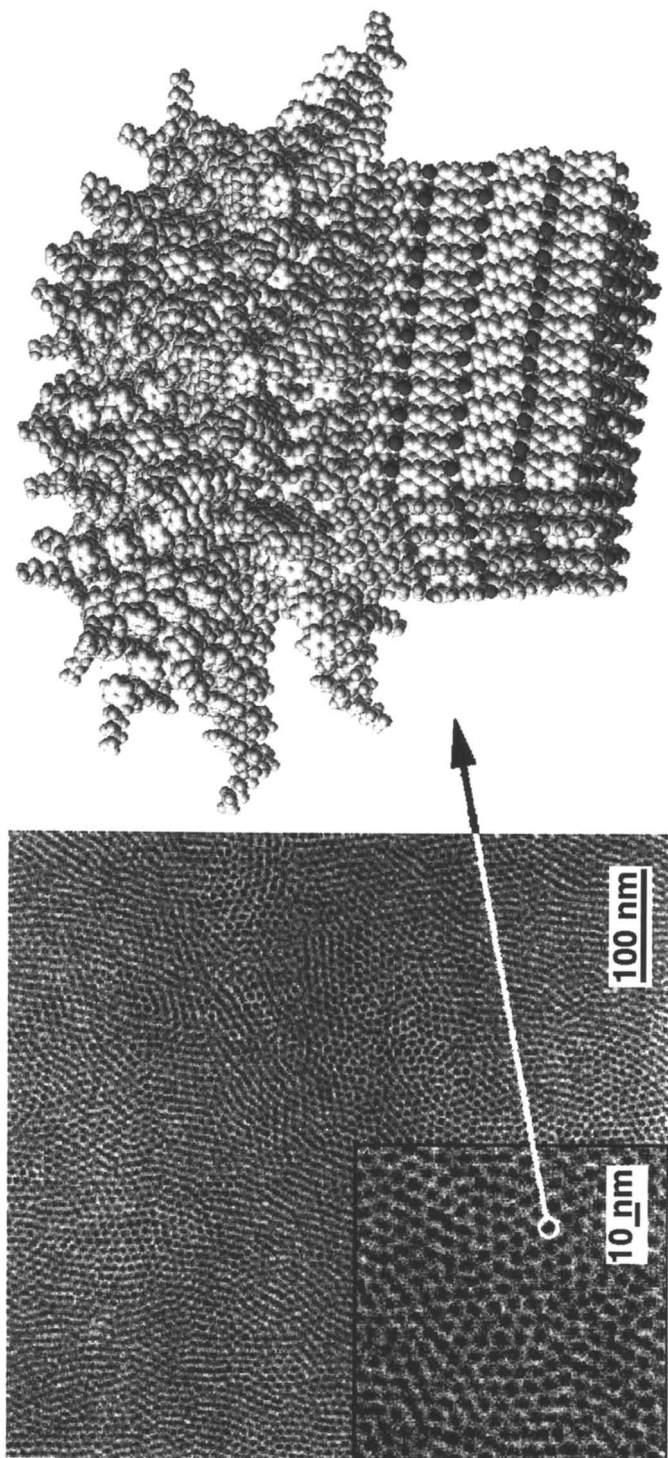


Figure 2. Transmission electron micrograph of rodcoil 1 showing the formation of supramolecular units and the molecular graphics representation of the mushroom-shaped nanostructure that is formed.

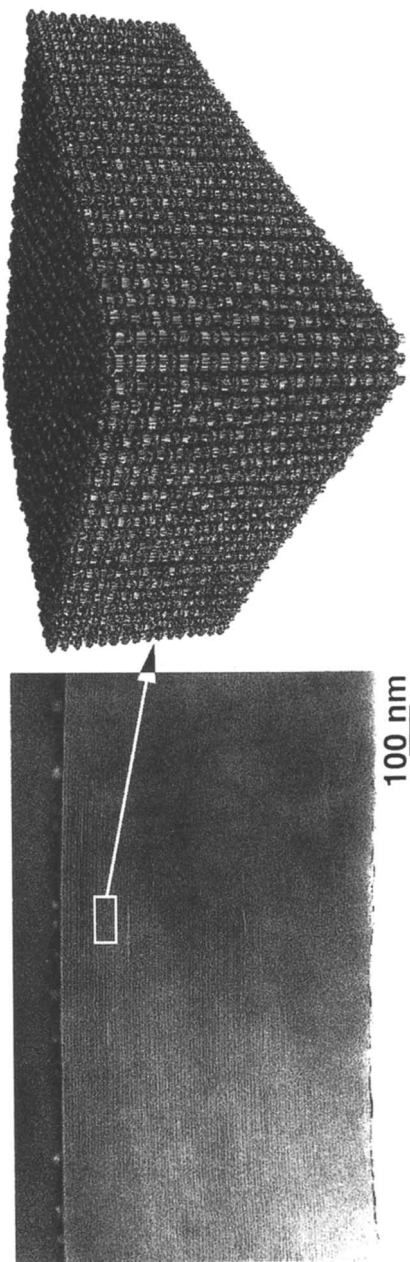


Figure 3. Transmission electron micrograph of an ultramicrotomed sample of **1** showing the formation of layers and the corresponding schematic representation of polar stacked mushroom nanostructures.

micrographs suggest the stripes are composed of individual supramolecular units which are believed to be mushroom shaped objects.

Further investigations into the film structure included receding water contact angle measurements. When films were cast onto water, the air side always revealed highly hydrophobic surfaces with receding water contact angles of $\sim 98^\circ$. If these films are inverted, they expose a more hydrophilic surface with receding water contact angles in the range of $\sim 27\text{--}40^\circ$. The dissimilar surface properties observed suggested the formation of polar order within the films. Polar films as envisioned in Figure 3 should exhibit dissimilar surface properties resulting in films where one surface is sticky and hydrophilic (phenol terminus) and the other surface is slippery and hydrophobic (methyl terminus). Water contact angle measurements demonstrate the ability of the films to express their polar driven dissimilar surface properties, thus creating tape-like materials. The formation of polar order has implications for many important properties in materials technology including piezoelectricity, materials coupling in composites, the formation of protective coatings, and second order nonlinear optical activity. To confirm the polar nature of these films, second-order nonlinear optical activity experiments were performed. The films as envisioned in Figure 3 would not possess a center of inversion, and would result in the generation of a second harmonic (SHG) signal from the material. Indeed, SHG measurements on films of **1** confirmed the polar nature of this material. The properties associated with the supramolecular film suggest this system is capable of integrating a number of important materials properties.

Luminescent Supramolecular Objects

After the discovery of well defined supramolecular units which organized into polar materials, we began integrating functionality into the molecular backbone of the triblock rodcoil motif to create novel supramolecular materials. The triblock structure possesses multiple sites to design functionality into the system. Initially, a stilbene or phenylene vinylene segment was integrated into the rod portion of the triblock molecule to create luminescent supramolecular objects. For our system, phenylene vinylene represents an ideal choice because it is known to be a robust material with interesting electronic properties and the all *trans* conformation possesses the rod-like character necessary to retain the triblock rodcoil structure.

The same sequence of carboxylated oligo(styrene-co-isoprene) was used to begin the synthesis of these triblock rodcoil molecules. Two biphenyl segments were attached followed by a phenylene vinylene segment, to produce the appropriate rod to coil volume fraction within the triblock structure. The phenylene vinylene rod blocks were prepared by Horner-Emmons olefination chemistry which affords high yields of the *E*-isomer (10). The rodcoil molecules, **2** and **3**, in Figure 1 are similar in chemical structure except **2** contains a cyano terminus while **3** possesses a hydrogen terminus. The detailed syntheses of these luminescent rodcoil molecules will be reported elsewhere (11). In addition, we have prepared rodcoil molecules, **4**, which contain an all phenylene vinylene rod segment (see Figure 1).

Molecules **2**, **3**, and **4** were characterized by polarized optical microscopy and SAXS. The triblock structure **2** flows above 130°C and becomes isotropic at 290°C , just before the isoprene units in the diblock coil crosslink (resulting in a new texture). The clearing point of **3** is approximately 40°C lower than **2** such that a completely isotropic phase is observed before the isoprenes crosslink resulting in a new texture ($\sim 300^\circ\text{C}$). Rodcoil molecules **4** are liquid crystalline as well but do not undergo isotropization even up to 350°C . The extremely high isotropization temperature of **4** is not surprising considering phenylene vinylene is much more rigid than biphenyl units. SAXS investigations suggest these molecules form films composed of monolayer structures of the type required for polar order. When films of these

molecules are annealed at 140 °C for 8 h, SAXS patterns for **2** show (001) and (002) reflections corresponding to d-spacings of 78 Å and 39 Å, while **3** and **4** show one reflection at 76 Å and 85 Å, respectively. The photoluminescence spectra of dilute solutions of **2** and **3** show emissions at 450 nm and 420, respectively, nm when excited with 331 nm light. In addition, these materials exhibit photoluminescence as solid state films. The properties of these supramolecular materials are currently under investigation in our laboratory, but these initial studies demonstrate the ability to integrate properties within the supramolecular units via rodcoil functionality.

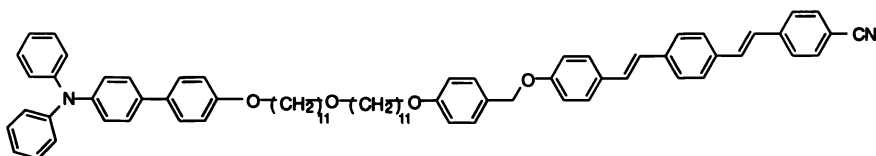
Mechanism for Supramolecular Unit Formation

The inspiration for this work originated partly in the challenge of confining molecular layers into nanoscale objects and the potential novel properties these objects could possess once packed to form macroscopic materials. The triblock rodcoil molecule was designed to frustrate the formation of infinite layers by incorporating steric, repulsive forces in the same molecular backbone as the mesogenic segment capable of parallel packing. The repulsive and attractive forces are physically separated within the molecule with the major steric factors found in the coil block and the majority of attractive forces found in the rod block. The oligo(styrene-co-isoprene) diblock coil contains extensive chemical aperiodicity; the styrene block is an atactic sequence of meso and racemic diads and the isoprene block is composed of mostly 1,4 and 3,4 additions but does contain some 1,2 repeat units. The chemical diversity found in the triblock molecules is believed to be essential to the novel and interesting structures they form. The oligo(styrene-co-isoprene) segment would have a random coil-type conformation in solution, presenting a sharp contrast to the very rigid rod segment. The rod block is composed of chemically identical species in which the tendency for π - π stacking drives the system to aggregate. However, the presence of the coil limits the crystallization of the rod blocks causing the formation of nanoscale objects. Crystallization of the rod block, requires the chemically diverse coil to be excluded from the crystalline phase. Furthermore, as crystallization of rod block occurs, the styrene blocks will experience increasingly strong hard-core repulsive forces further limiting the aggregate size. Most likely, it is this balance between attractive forces in the rod segments and repulsive forces in the coil segments which leads to the formation of well-defined supramolecular units. However, the entropic penalties associated with formation of finite aggregates in the system need to be considered. In addition to the usual entropic costs associated with molecular aggregation (i.e. translational), the stretching of the flexible isoprene units could reduce entropy further (12,13). This further reduction of entropy would increase the energy costs associated with the formation of large aggregates.

Triblock Structures Containing Electron and Hole Accepting Blocks

Research efforts directed toward creating and understanding electronic and photonic properties of organic materials continues to be important (14,15). The triblock rodcoil motif, we have discovered provides an excellent platform to design, synthesize, and investigate novel materials properties. One effort in our group to prepare electronically active nanostructures has focused on systems containing hole accepting groups on one end of the triblock molecule and electron accepting groups on the other end. These materials have many potentially interesting properties including the formation of photoluminescent and electroluminescent nanostructures. In addition, the creation of electroactive nanostructures could lead to devices like variable frequency light emitting diodes, large arrays of quantum dots, data storage systems, and if polar in nature, pyroelectricity and ferroelectricity. Our initial design of these systems employ phenylene vinylene as the electron accepting species while

triphenyl amine derivatives are introduced as potential hole accepting blocks at the opposite end of the molecule. The two electroactive blocks are connected by a long chain alkyl ether. One can envision this molecule as a triblock structure composed of a triphenyl amine block, a flexible alkyl block, and a rigid phenylene vinylene block. We have been able to prepare molecule **5** and the details of its synthesis will be reported later. Interestingly however, preliminary characterization of its physical structure indicates **5** self organizes into a liquid crystalline substance over a fairly broad temperature range (exceeding 100 °C). This assembly-philic behavior is clearly important in meeting our supramolecular objectives.



Conclusions

We have discovered the spontaneous formation of highly regular nanoscale supramolecular units from triblock molecules resulting in macroscopically organized material. Interestingly, three dimensional polar stacking of the supramolecular units is observed and as a result materials are obtained from these systems with properties such as second harmonic generation and chemically dissimilar surfaces. Novel analogous triblock molecules have been reported with the goal of integrating other properties into the supramolecular materials.

Acknowledgments

Supported by grants from the Army Research Office (DAAH04-96-1-0450), the Department of Energy (DEFG02-91ER45439), the National Science Foundation (DMR 93-12601), and the Office of Naval Research (N00014-96-1-0515). The authors also acknowledge the Visualization Laboratory of the Beckman Institute for Advanced Science and Technology and the Materials Chemistry Laboratory, both at the University of Illinois at Urbana-Champaign.

Literature Cited

- (1) Lehn, J. M. *Supramolecular Chemistry*; VCH Press: New York, 1995.
- (2) Mathias, J. P.; Simanek, E. E.; Whitesides, G. M. *J. Amer. Chem. Soc.* **1994**, *116*, 4326.
- (3) Seto, C. T.; Mathias, J. P.; Whitesides, G. M. *J. Amer. Chem. Soc.* **1993**, *115*, 1321.
- (4) Kumar, U.; Kato, T.; Frechet, J. M. J. *J. Amer. Chem. Soc.* **1992**, *114*, 6630.
- (5) Kato, T.; Frechet, J. M. J. *J. Amer. Chem. Soc.* **1989**, *111*, 8533.
- (6) Zimmerman, S. C.; Zeng, F.; Reichert, D. E. C.; Kolotuchin, S. V. *Science* **1996**, *271*, 1095.
- (7) Stupp, S. I.; LeBonheur, V.; Walker, K.; Li, L. S.; Huggins, K. E.; Keser, M.; Amstutz, A. *Science* **1997**, *276*, 384.
- (8) Swzarc, M. *Carbanions, Living Polymers, and Electron Transfer Processes*; Wiley: New York, 1968.

- (9) The fully extended lengths are measured in the molecular graphics program SYBYL.
- (10) Wadsworth, W. *Organic Reactions*, 1977; Vol. 25, 73.
- (11) Tew, G. N.; Stupp, S. I. , submitted for publication.
- (12) Radzilowski, L. H.; Carragher, B. O.; Stupp, S. I. *Macromolecules* **1997**, *30*, 2110.
- (13) Radzilowski, L. H.; Stupp, S. I. *Macromolecules* **1994**, *27*, 7747.
- (14) Sheats, J. R.; Antoniadis, H.; Hueschen, M.; Leonard, W.; Miller, J.; Moon, R.; Roitman, D.; Stocking, A. *Science* **1996**, *273*, 884.
- (15) *Conjugated Conducting Polymers*; Keiss H. G.; Ed; Springer-Verlag: Berlin, 1992.

Well-Defined Smectic C* Side Chain Liquid Crystalline Polymers

Wen-Yue Zheng, Thomas Epps, David Wall, and Paula Hammond¹

Department of Chemical Engineering, Massachusetts Institute of Technology, Room 66-553, Cambridge, MA 02139

Introduction

Ferroelectric liquid crystals and liquid crystalline polymers have been a primary focus in the area of liquid crystal display and optical storage materials, due to the bistable electro-optical properties and fast switching speeds of these materials. The presence of the chiral group on the mesogen in layered smectic C* mesophases can induce desired ferroelectric behavior¹. For this reason, a number of studies of side chain liquid crystalline polymers functionalized with chiral smectic C* mesogens have been undertaken in the past few years. Most of these studies have characterized fairly polydisperse functionalized side chain liquid crystalline polysiloxanes and polymethacrylates formed by the polymer-analogous substitution of the mesogenic group onto a pre-existing polymer backbone. Polymer analogous substitution usually results in less than 100% substitution of the polymer backbone, particularly in cases where the substitution is limited by solubility or steric factors². Free radical polymerization may be used with a substituted liquid crystalline monomer to form fully substituted chains, but the resulting polymers are very polydisperse. In these cases, the molecular structure of the polymers cannot be precisely controlled. To achieve a true understanding of the nature and structure-property relations in these mesogenic polymers, we must be able to achieve well defined polymer structures.

Recently, researchers have found successful routes to the formation of highly monodisperse liquid crystalline polymers with well defined structures via direct polymerization of the mesogens³⁻⁷. In particular, anionic polymerization is very attractive and allows synthesis of liquid crystalline polymers with well-defined structures, high stereoregularity, and a uniform chain length. In addition, living anionic polymerization is

¹Corresponding author.

an effective and straightforward approach towards well-defined block copolymers containing side chain liquid crystalline segments^{3,7,8}.

It is known that increased polydispersity can result in the suppression or disappearance of mesophases which appear in monodisperse samples⁹. It was also reported that main chain tacticity has had great impact on liquid crystallinity^{10,11}. The degree of LC substitution may have a similar effect on LC mesophase behavior and thermal stability. The influences of factors such as polydispersity, tacticity and mesogen spacer on the appearance or stabilization of liquid crystalline phase types can be critical to the design of LC polymers for a number of applications. For example, a short nematic range above the smectic C* or smectic A phase is considered desirable because it can be used to align the LC at much lower viscosities. We are currently investigating homo- and block copolymers synthesized using direct anionic polymerization of a methacrylate mesogen. In this paper, a series of methacrylate monomers with biphenyl benzoate mesogen and varied spacers have been synthesized, and their corresponding polymers were polymerized by both anionic and free-radical techniques in this study. We seek to understand the effects of polydispersity and conformational structure on LC mesophase behavior, and the nature and stability of the smectic C* phase, by comparing polymers from anionic and free-radical polymerizations.

Experimental Section

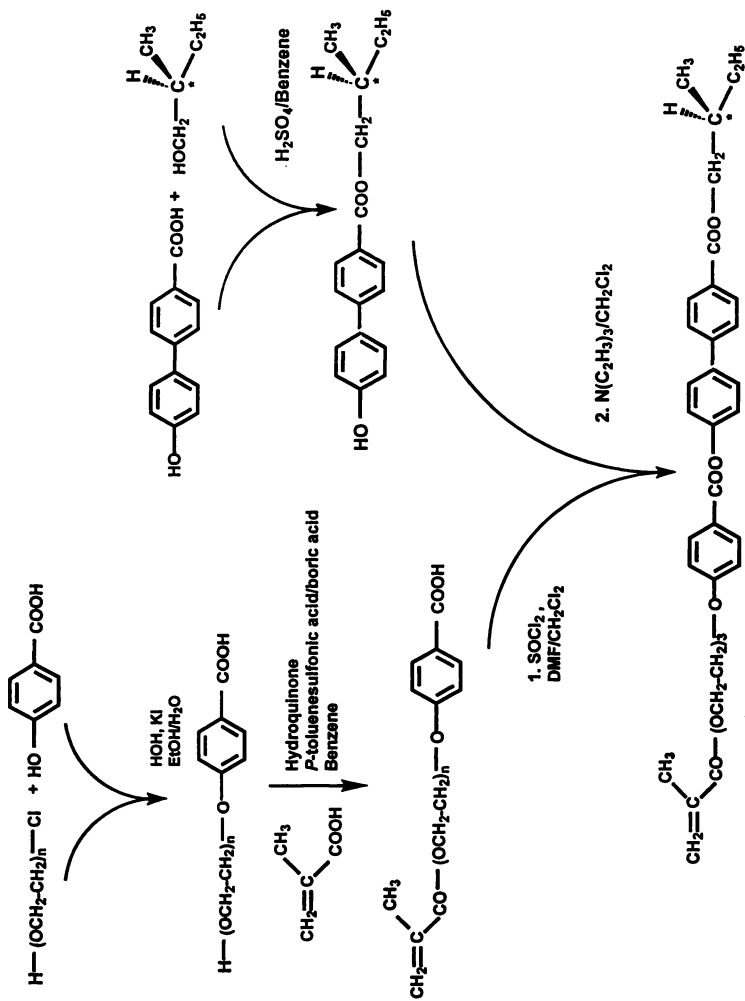
Materials

Anionic initiator, *sec*-Butyllithium 1.3 M solution in cyclohexane (Aldrich) was used as obtained. Free-radical initiator, 1,1'-Azobis(cyclohexane carbonitrile)(ACHN, Aldrich) was purified by recrystallization in methanol. 1,1'-Diphenylethylene (DPE, Aldrich) was purified by two consecutive distillations over CaH₂ and *n*-butyl-lithium. The solvent, tetrahydrofuran (THF, Aldrich) used in anionic polymerization was dried by distillation over sodium wire in the presence of benzoquinone until a blue color developed and remained, and by consecutive vacuum distillations over LiAlH₄ and *n*-butyllithium. Toluene used for free-radical polymerization was purified by distillation over CaH₂ in a vacuum apparatus. All other chemicals used in monomer synthesis were used as purchased.

Monomer Synthesis

Methacrylate monomers consisting of 4-(S)-2-methyl-1-butyl 4'-[[[(4-hydroxy benzyl-4'-yl)carbonyl]oxy]-1,1'-biphenyl-4-carboxylate as rigid core, alkyl group (HBPB and DBPB) and oligo(ethylene oxide) group (2EOBPB and 3EOBPB) as spacers were synthesized according to the previous report, as shown in Scheme 1.⁸ All monomers were carefully purified by column chromatography, using ethyl acetate/hexane as eluent, and by recrystallization in ethanol, and extensively dried under high

Scheme 1



4-(S)-2-Methyl-1-butyl [[[4-[6-(methacryloyloxy) alkyl-1-oxy] biphenyl-4'-y]] carbonyl] oxy] benzoate
 $[\alpha]_{25\text{D}} = 1.54 - 1.70$

vacuum. The monomer 3EOBPB required purification twice with column chromatography, followed by freeze-drying in benzene solution for 24 h.

Polymerization

Anionic polymerizations were carried out in a VAC MC-10-M glovebox in dry nitrogen atmosphere at $-40\text{ }^{\circ}\text{C}$ as shown in Scheme 1. All glass apparatus, syringes and needles were flame dried and then dried in a high temperature oven for 2 days prior to use. In the polymerization of the methacrylate homopolymers, a small amount of *sec*-butyllithium was initially added to dry THF solvent to eliminate any protonic impurities; the THF was in a round bottom flask equipped with a magnetic stirrer and an oil bath cooled by a Neslab CC-100 II Immersion Cooler. A calculated amount of 1,1'-diphenylethyene and *sec*-butyllithium was charged into the system with a microsyringe. A deep red color immediately formed, indicating the formation of 3-methyl-1,1'-diphenylpentyllithium initiator complex. A predetermined amount of methacrylate monomer in THF was introduced into the reaction flask. The color of the reaction gradually turned slightly green, indicating the formation of methacrylate carbanions. After 2-3 h, the polymerization was terminated with 1 ml of degassed methanol, and the reaction solution was precipitated in a large volume of methanol, filtered and purified by reprecipitation from THF solution into methanol.

The free-radical polymerizations of the monomers were carried out in test tubes. In the glovebox, each methacrylate monomer (10 wt%) and the initiator ACHN (1 part initiator:10 parts monomer) was dissolved in toluene and loaded into a test tube. Then the tubes were moved out of the glovebox and were gradually heated under nitrogen purge to $120\text{ }^{\circ}\text{C}$ to initiate the reaction in a hot oil bath. The polymerization system remained above $80\text{ }^{\circ}\text{C}$ for 8 hrs. Each polymer was then precipitated in a large volume of methanol, filtered and purified by reprecipitation from THF solution into methanol.

Characterization

A Nicolet Magna 550 Fourier Transform Infrared Spectrometer (FTIR) and a Bruker MW 250 MHz proton NMR were used to verify the chemical structure of all monomers and polymers. Optical activity of the compounds was measured at $25\text{ }^{\circ}\text{C}$ on a Perkin-Elmer Polarimeter in chloroform. A Waters Gel Permeation Chromatograph with 440 UV absorption detector and R401 differential refractometer was used to determine the molecular weights of the polymers; tetrahydrofuran was used as the mobile phase at 1.0 mL/min, and the Waters polystyrene gel columns were calibrated with monodisperse polystyrene standards. Polarizing optical microscopy was used to identify liquid crystalline phases using a Leitz optical microscope with a CCD camera attachment

and a Mettler FP-82 hot stage and controller. A Perkin-Elmer DSC-7 (Differential Scanning Calorimeter) with a cooling accessory was used to determine the thermal transitions in the monomers and polymers. X-ray diffraction measurements were performed with nickel-filtered Cu K α radiation with a Rigaku diffractometer.

Results and Discussion

Monomers

The monomers reported in this paper have the same chiral mesogen and methacrylate group; however, different spacer groups were incorporated into the mesogen, including hexylene (HBPB), decamethylene (DBPB), two ethyleneoxy (2EOBPB) and three ethyleneoxy (3EOBPB) groups, to examine the effects of spacer type and length on liquid crystalline transitions. The synthetic routes and structural characterization of these monomers have been reported in our previous papers⁸.

Table 1 summarizes the thermal transitions and corresponding enthalpy changes of the monomers. All thermotropic transitions were characterized using DSC and optical microscopy. The LC phases of these monomers were confirmed by X-ray diffraction measurements, and the corresponding *d*- spacings of smectic layers in the monomers are also listed in Table 1. The representative DSC thermograms of the monomer HBPB and 3EOBPB are presented in Figure 1. When heated at a rate of 10 °C/min, the HBPB monomer shows a huge melting endothermic transition at 75 °C to the smectic C* phase, a transition from smectic C* to smectic A at 129 °C, a small transition from smectic A to Cholesteric phase at 138 °C and a final isotropic transition at 170 °C. On the cooling scan, the phase transitions are reversed, with the exception of the crystallization transition, which is highly supercooled, and does not appear in the DSC scan. The mesophase identification was made by direct optical microscopic observation. Optical micrographs of the HBPB monomer exhibited a mosaic texture for the crystalline phase at room temperature, a Schlieren texture for Smectic C* phase in the range of 76-127 °C, focal conic fan texture for smectic A phase near 130 °C and Cholesteric texture above 130 °C until 170 °C. The phase transitions for DBPB monomer were lowered by the increase of the alkyl spacer length as shown in Table 1. It should also be noted that sufficiently long alkyl chains tend to crystallize as indicated by melting endotherms at 16 °C. The 2EOBPB monomer shows the same phase sequence as HBPB and DBPB, Cryst \rightarrow S_{C*} \rightarrow S_A \rightarrow Ch \rightarrow I, and with lower thermal transitions due to the flexible 2 ethyleneoxide moiety. In the case of 3EOBPB, the more flexible

Table I. Mesogen Monomers and Their Thermal Behaviors

Monomers	Phase Transitions ($^{\circ}\text{C}$) and ΔH (J/g)	Smectic d-spacing, (\AA)
HBPB	^(H) K 75 (64.2) S_{C}^* 129 (2.2) S_{A} 138 (0.76) Ch 170 (0.72) I ^(C) I 153 (-0.52) Ch 133 (-0.49) S_{A} 125 (-0.74) S_{C}^* 27 (-4.86) K	21.4
DBPB	^(H) K' 16(3.5) K 47(37.8) S_{C}^* 93(0.55) S_{A} 116(4.6) I ^(C) I 113(-4.48) S_{C}^* 15(-16.8) K -8(-7.2) K_{s}	27.8
2EOBPB	^(H) K 43(28.0) S_{C}^* 68(0.73) S_{A} 90(1.30) Ch 102(0.52) I ^(C) I 96(-0.53) Ch 83(-1.25) S_{A} 62(1.13) S_{C}^* < -20 K	22.8
3EOBPB	^(H) S_{C}^* 41(0.68) S_{A} 52(0.69) Ch 65(0.46) I ^(C) I 59(-0.39) Ch 45(-0.78) S_{A} 34(-0.78) S_{C}^* < -40 K	30.0

* determined by DSC and Optical Microscope with hot-stage run by a rate of $10^{\circ}\text{C}/\text{min}$; (H), heating and (C), cooling. K': melting transition which may be corresponding to crystal formed by alkyl spacer.

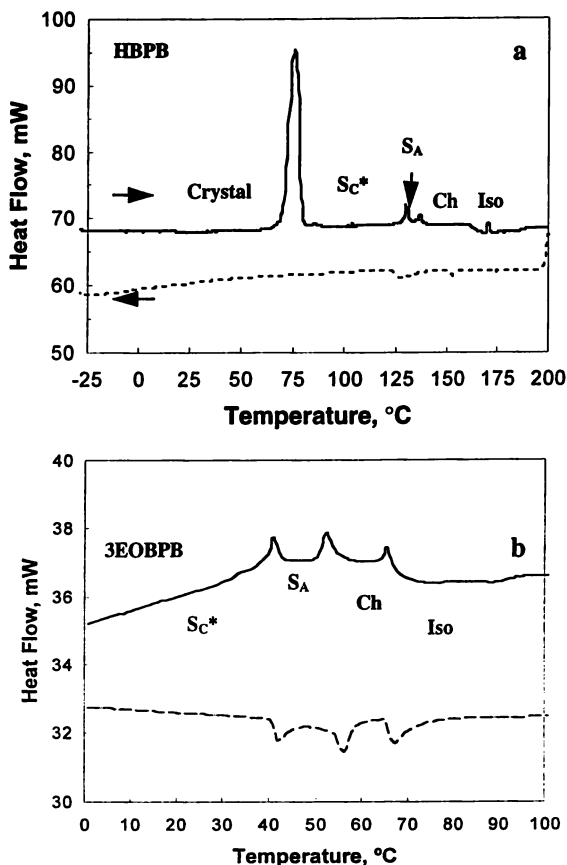


Figure 1. DSC thermograms of mesogen monomers in a heating and cooling cycle by $10^{\circ}\text{C}/\text{min}$. HBPB (a) and 3EOBPB (b).

spacer results in a much lower smectic C* temperature range of -40 to 40 °C as presented in Figure 1b; the crystalline melting point was not observed within the range of the DSC. The X-ray patterns of HBPB, DBPB and 2EOBPB monomers show many sharp reflections representing well ordered crystalline smectic phase. The X-ray pattern of 3EOBPB measured at room temperature features three sharp reflections at small angle associated with smectic layer structure and a diffuse reflection at wide angle. These diffraction characteristics are in agreement with that of the liquid like smectic C* phase of this monomer.

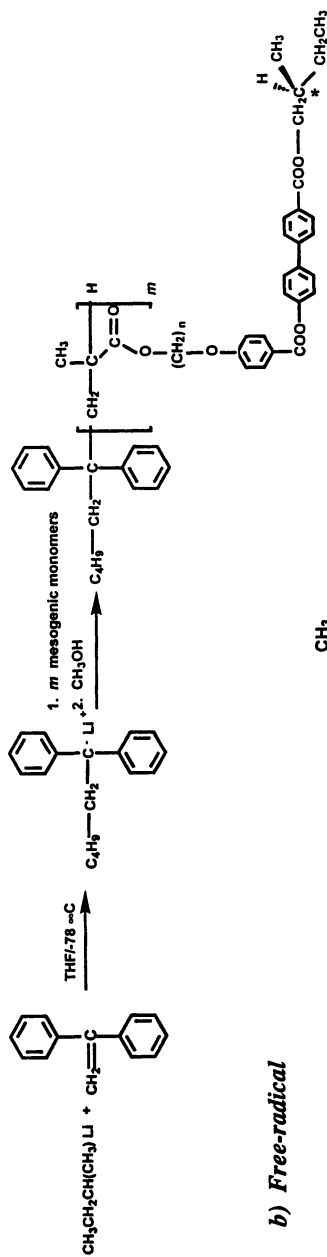
Monomers with similar mesogenic moieties have been reported in the literature¹². In general, these monomers exhibit completely different mesomorphic behavior from previously reported vinyl mesogens, although the only difference is the methacrylate functional group.

Polymerization

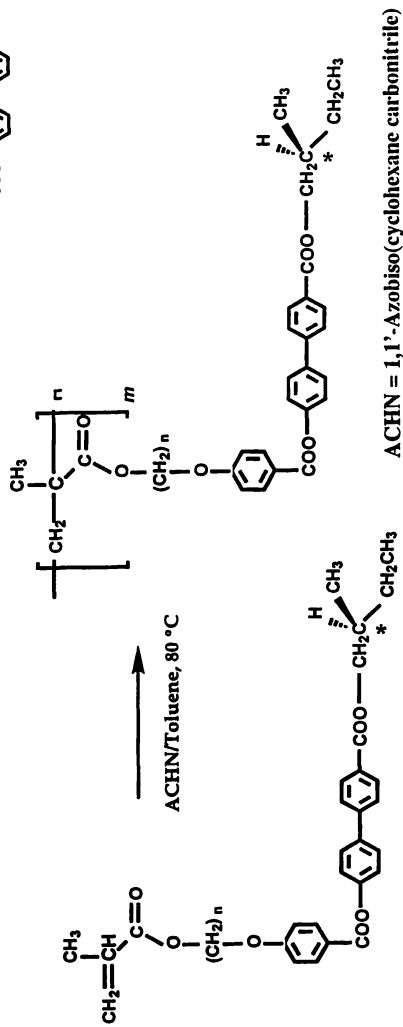
The methacrylate monomers were polymerized using both anionic and free-radical polymerization. The synthesis and structure of the polymethacrylate liquid crystalline polymers with alkyl and oligo(ethyleneoxide) spacers are shown in Scheme 2 (a) and (b) for anionic and free radical routes respectively. Anionic polymerization of all methacrylate monomers was performed by using a calculated amount of 1,1-diphenyl-(3-methyl)-pentyllithium initiator formed from diphenylethylene and *sec*-butyl lithium in THF; this initiator produces a carbanion which propagates without attacking the ester side groups of the monomer.³ It is generally known that anionic polymerization of methacrylates in THF leads to highly syndiotactic polymer^{3,11}. Higher molecular weights can be obtained in the presence of LiCl additive as reported in another publication, due to improved solubility and disassociation of propagating ionic chain ends on growing polymer chains. The molecular weights of the anionic polymers have unimodal and narrow distributions with Mw/Mn ratios ranging from 1.10 to 1.13 as summarized in Table 2, as measured by GPC with THF as the eluent. Free radical polymerization of the methacrylate monomers was initiated by 1,1'-azobis(cyclohexane carbonitrile) above 80 °C. The molecular weights of the resulting polymers were controlled to approximately equal to that of corresponding anionic polymers. Compared to the anionic polymers, the free-radical polymers have high polydispersities (Mw/Mn) ranging from 2.60 to 3.20 although they all exhibited unimodal GPC curves.

Scheme 2

a) Anionic



b) Free-radical



ACHN = 1,1'-Azobis(cyclohexane carbonitrile)

Table 2. Phase Behaviors, Molecular Weights and Smectic d-spacing of the polymers

Case	Polymerization n Type	Mn, kg/mol	Mw/Mn	Phase Behaviors, °C*	Sm. d-spacing (Å)
PHBPPB	Anionic	7.1	1.10	^(H) G _{LC} 35 S _C * 120 S _D 137 S _A 157 Ch 170 I ^(C) I 153 Ch 132 S _A 125 S _C * 27 G _{LC}	37.8
PHBPPB	Free-radical	7.2	2.60	^(H) G _{LC} 24 S _C * 143 S _A 220 I ^(C) I 205 S _A 140 S _C * ~10 G _{LC}	28.8
PDBPB	Anionic	8.3	1.10	^(H) G _{LC} 18 S _C * 128 S _A 140 Ch 146 I ^(C) I 138 S _A 116 S _C * 12 G _{LC}	43.7
PDBPB	Free-radical	12.0	3.20	^(H) G _{LC} -4 S _C * 103 S _A 189 I ^(C) I 181 S _A 103 S _C * -20 G _{LC}	34.9
P2EOBPPB	Anionic	7.8	1.11	^(H) G _{LC} 46 S _C * 83 S _A 140 Ch 157 I ^(C) I 147 ND S _C * ~40 G _{LC}	41.1
P3EOBPPB	Anionic	5.3	1.13	^(H) G _{LC} 13 S _C * 96 S _D 103 S _A 178 I ^(C) I 173 S _A 96 S _C * ND G _{LC}	44.0

* determined by DSC and Optical Microscope with a hot-stage run by a rate of 20 °C/min; ND, not determined;
Mn*, measured by GPC with PS standards in THF.

Anionic Polymers

The role of spacer flexibility has been verified with regard to its effects on the formation of mesophase and the thermostability of the mesophase.¹³ An understanding of these effects can be crucial when designing specific monomers and their polymers to have a desired temperature range of a targeted mesophase. Table 2 also includes glass transition, liquid crystalline phase transitions and *d*-spacings of smectic layer structures measured at room temperature for each polymer. Mesophase transition temperatures were determined by combining the results of differential scanning calorimetry (DSC) and the results of polarized optical microscopy. In the case of PHBPB and PDBPB, liquid crystalline behavior was also confirmed with temperature controlled wide angle X-ray diffraction. Figures 2 and 3 show representative DSC heating and cooling curves for anionic PHBPB and P3EOBPB. The heating curve of PHBPB indicates a glass transition at 35 °C, two broad transitions from S_C^* to S_A at 137 °C and from S_A to Ch at 157 °C, and final isotropization near 170 °C. The cooling curve shows a reversed isotropization transition and relatively weak smectic transitions. As shown in Figure 2, the polymer exhibits fine Schlieren texture for S_C^* phase, batonnet texture for S_A phase, and a cholesteric phase at high temperature. It is difficult to observe the cholesteric texture during the cooling run, probably due to supercooling effects. It is interesting to note that PHBPB lost birefringence between 120 °C to 135 °C under polarized light in the optical microscope. It is postulated that this dark phase is a form of a smectic D phase, which has rarely been found in side chain polymeric liquid crystals. This phase sequence was confirmed by X-ray diffraction measurements conducted at elevated temperatures, which have been reported in our previous paper¹⁴. The abrupt increase of *d*-spacing of the WAXD reflection at small angles clearly indicated a transition from the tilted Smectic C* to a vertical smectic A layer arrangement. The disappearance of the small angle reflection at high temperature distinguishes the smectic and cholesteric (twisted nematic) phases. A comparison between the layer *d*-spacing (38 Å) and the fully extended length of side chain mesogens (29 Å) suggests that the polymer has an interdigitated bilayer structure. A WAXD pattern of anionic PHBPB measured at room temperature is shown in Figure 5.

There are also visible differences in the mesophase behavior of the anionically polymerized PHBPB and PDBPB polymers. It appears that the range of the smectic C* phase is broader in polymers with a decyl spacer due to the increased flexibility of the alkyl group and the lowering of the glass transition temperature to 18 °C. The anionic PDBPB polymer also exhibits lower LC phase transitions: 128 °C, 140 °C and 146 °C for

Sc*→Sa, Sa→Ch, and Ch→I respectively. The smectic D phase is observed in the hexyl series but not in the decyl analogs. This observation suggests that the increased flexibility provided by the longer alkyl group destabilizes the higher temperature smectic phases, while stabilizing the smectic C*. Optical micrographs of the PDBPB polymer exhibit a fine broken focal conic fan texture for S_C* phase, and focal conic fan textures for the S_A phase and cholesteric texture.

The polymers containing ethylene oxide spacer groups exhibited considerably narrow smectic C* mesophase ranges and broader smectic A phases. The two ethyleneoxide spacers in polymer P2EOBPB raise the glass transition to 46 °C but lower the other phase transitions compared to PHBPB. P2EOBPB exhibits the same phase sequence

G→S_C*→S_A→Ch→I as PHBPB and PDBPB. It is interesting to note that main chain mobility is not greatly improved by the EO spacer; the glass transition temperature of the P2EOBPB polymer is actually higher than that of the hexyl spacer, despite the fact that each spacer contains the equivalent number of C-C or C-O linkages. Only minor changes in a very fine LC texture were observed under the polarized optical microscope during mesophase transitions in P2EOBPB.

Polymer P3EOBPB, which has the longest spacer group in this polymer series with three ethyleneoxide spacers, has a phase sequence without a cholesteric phase though the 3EOBPB monomer displays classic cholesteric texture above 50 °C. Its phase sequence, G→S_C*→S_A→I, as observed with DSC and optical micrographs, is shown in Figure 3. This polymer has a relatively low glass transition at 13 °C, so that the polymer is in the S_C* phase at room temperature, transitions to the S_A phase at 96 °C and clears out above 105 °C. P3EOBPB exhibits a loss of birefringence between 96 and 103 °C which may be due to a smectic D phase, as is observed in PHBPB. Optical microscopy observations revealed barely detectable changes in a fine texture from the smectic C* and smectic A phases, with features that were obscure and difficult to distinguish even after annealing the polymer for long period times as shown in Figure 3. Apparently, the presence of the ethylene oxide spacers lowers the thermal stability of the smectic C* phase, while further stabilizing the smectic A phase. These results indicate an opposite effect when contrasted with the effect of increasing alkyl spacer length, which ultimately stabilizes smectic C* over smectic A. Also contrary to expectation, the increased ethylene oxide spacer length appears to increase, rather than decrease, the isotropization temperature. For all of the anionic polymers examined, an increase in spacer length did increase smectic layer thicknesses, as revealed by the X-ray d-spacing values in Table 2.

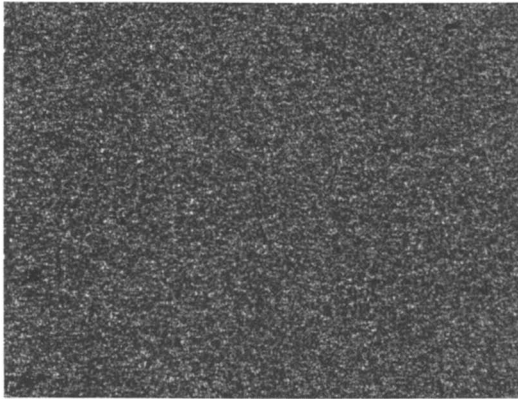
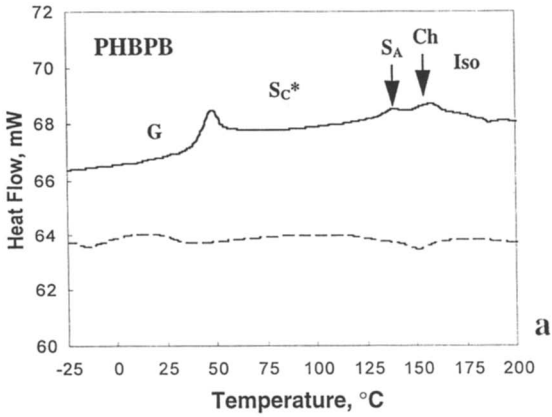
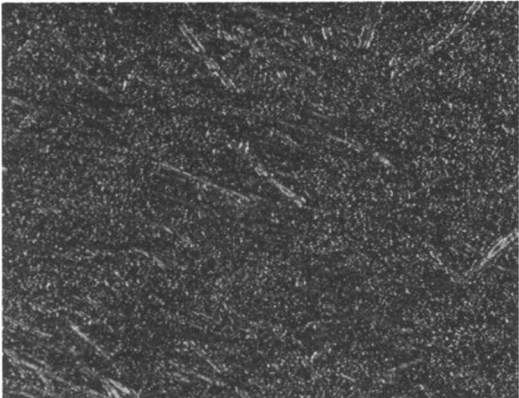
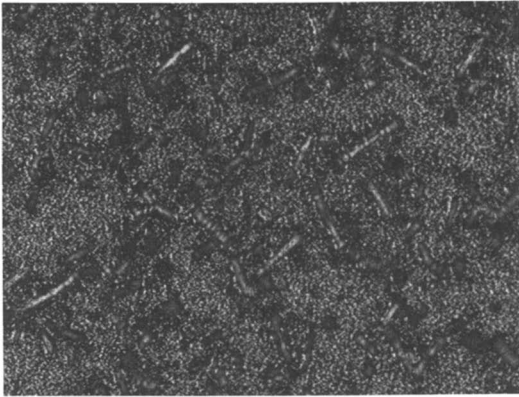


Figure 2. DSC thermograms of anionic PHBPB polymer in a heating and cooling cycle by 20 °C/min; arrows indicate phase transitions (a); Optical micrographs of this polymer taken during heating process on a hot-stage by 10 °C/min. 25 °C (b), 153 °C (c) and 166 °C (d). (280x)



c



d

Figure 2. *Continued.*

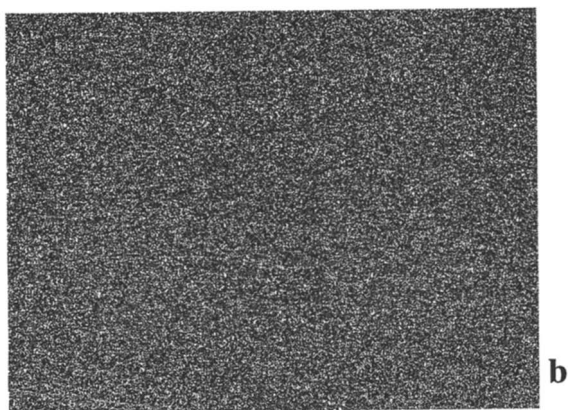
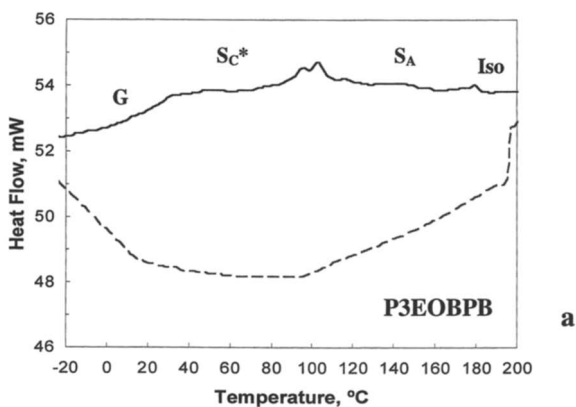
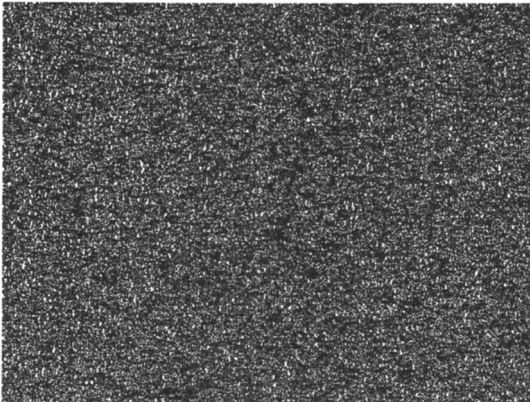


Figure 3. DSC thermograms of anionic P3EOBPB polymer in a heating and cooling cycle by 20 °C/min (a); Optical micrographs of this polymer taken during heating process on a hot-stage by 10 °C/min. 50 °C (b) and 110 °C (c). (280x)



c

Figure 3. *Continued.*

Free-radical Polymers

Notable differences were observed between the anionically and free radically polymerized polymers. The glass transition temperatures of the free radically polymerized polymers are much lower for both PHBPB and PDBPB. The T_g of free-radically polymerized PHBPB and PDBPB are 24 and -4 °C respectively, as opposed 35 °C and 18 °C. This effect is probably due to differences in the tacticity of the methacrylate backbone. Anionically polymerized methacrylates in polar media are generally highly syndiotactic, but free radically polymerized backbones are highly heterotactic, resulting in a more flexible substituted backbone. It was reported that the anionic polymerization of methacrylates bearing bulky side groups in polar solvents leads to 75-95% syndiotacticity, whereas free-radical polymerization yields only 40-60% syndiotacticity^{3,11}. The tacticity in this particular polymer series is very difficult to analyze with ¹H NMR due to interference from methyl and ethyl groups near the chiral center. Unfortunately, this interference made it very difficult to ascertain and compare the stereoregularity of the anionic and free radical polymers. However, based on the known literature for methacrylate polymerization as cited above, we believe that the anionic polymers synthesized in THF medium should have higher stereoregularity than the free-radical polymers.

The effects of molecular weight distribution on liquid crystallinity were emphasized by Shibaev et al.⁹ It was reported that the side chain liquid crystalline polyacrylic polymers (fractionated and unfractionated samples) with close M_w 's but different polydispersities exhibited essentially different mesophases and phase transition temperatures. In this study, the difference in the polydispersities of the two PHBPB polymers is also notable; the anionic polymer has a M_w/M_n of 1.1, versus 2.6 for the free radically polymerized polymer. As seen in the Figure 4, the resulting liquid crystal mesophases exhibited by the anionic polymer are more diverse than those of the polydisperse sample. A cholesteric phase exists in the anionic sample which does not appear in the free-radically polymerized counterpart, and a smectic D, or nonbirefringent dark phase is also present between the smectic A and smectic C phase only in the anionic polymer. On the other hand, the polydisperse free radically polymerized PHBPB exhibits a much broader temperature range for the smectic C* phase, and a more thermally stable smectic A phase, resulting in an isotropization temperature that is 50°C higher than the anionically polymerized polymer. The fine Schlieren texture in S_C^* phase and the well-defined focal conic fan texture for S_A phase in the optical micrographs of Figure 4 suggest fewer grains and defects in the texture, due to the increased mobility of the mesophase and perhaps assisted by a more

effective decoupling of mesogen orientation from the main chain. DSC indicates much broader, less pronounced LC phases for the free radically polymerized polymer, as well. Temperature controlled X-ray diffraction of the free-radical PHBPB confirmed the liquid crystalline behavior and smectic C* phase identified by DSC and optical microscopy. The X-ray results demonstrate a similar relationship between the smectic layer *d*-spacings and elevated temperatures as illustrated in Figure 5. The *d*-spacing of smectic C* layer (29 Å), compared to the calculated extended length of the side group (30 Å) indicates that the polymer chains are organized in a tilted monolayer structure rather than the interdigitated bilayer structure deduced for anionic PHBPB, though they show similar classic smectic diffraction patterns as seen in Figure 5. The monolayer structure is a probable result of the more flexible, and therefore more accommodating, backbone of the free-radical polymer with high proportion of atactic repeat units.

A similar effect was determined for anionic and free-radical PDBPB polymers with molecular weight distribution 1.1 and 3.20. The free radical polymer showed a lower glass transition at -4 °C, a S_C* to S_A transition at 103 °C, and a higher isotropic transition at 189 °C (more thermally stable smectic A phase) than the anionic polymer. The cholesteric phase was found absent in the free-radical polymer. The *d*-spacing of the 1st order and 2nd order smectic C* layer reflection are 35 Å and 17.4 Å. These diffraction results, when compared to the 34 Å calculated length of the side group, suggest that this polymer has a tilted monolayer smectic C* structure. It has been found that liquid crystal transitions increase rapidly with molecular weight before levelling off above a critical M_n. The thermal properties of LC polymers with molecular weights higher than 7000 were not found to be greatly affected by molecular weight in our block copolymer study¹⁵. Therefore, the contribution of molecular weight to phase transition temperature may be small for these materials.

Conclusions

A new series of liquid crystalline smectic C* polymers has been successfully synthesized using anionic polymerizations of optically active mesogenic methacrylate monomers containing alkyl and oligoethylene oxide spacers. In using anionic polymerization techniques, we have been able to achieve well defined, 100% substituted, monodisperse liquid crystalline polymer. We have directly compared the properties of polymers with alkyl versus oligoethyleneoxide spacer groups. Variations in spacer type and length reveal that the smectic C* is stabilized by longer spacers, in general, and

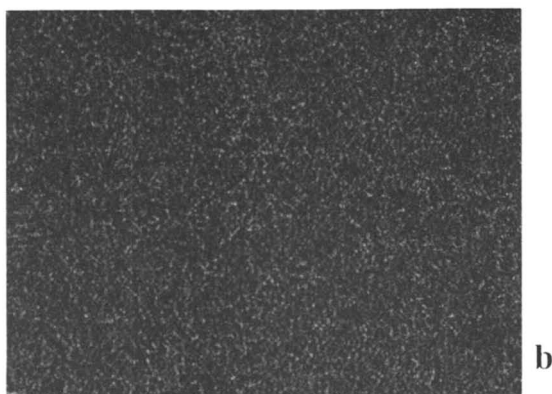
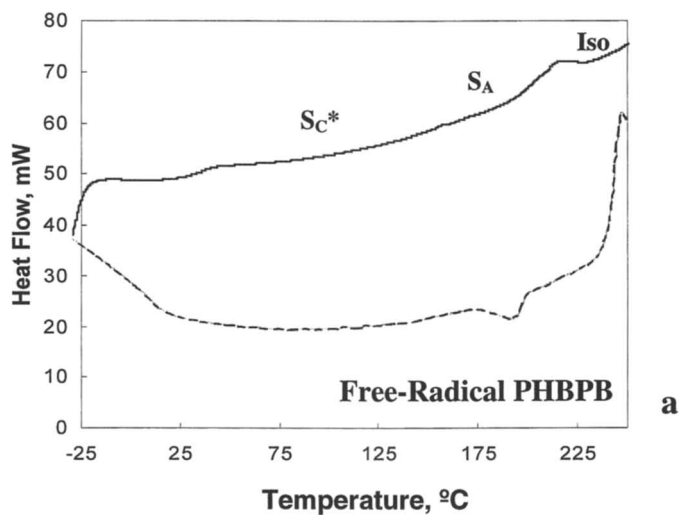


Figure 4. DSC thermograms of free-radical PHBPB polymer in a heating and cooling cycle by 20 °C/min (a); Optical micrographs of this polymer taken during heating process on a hot-stage by 10 °C/min. 75 °C (b) and 185 °C (c). (280 \times)

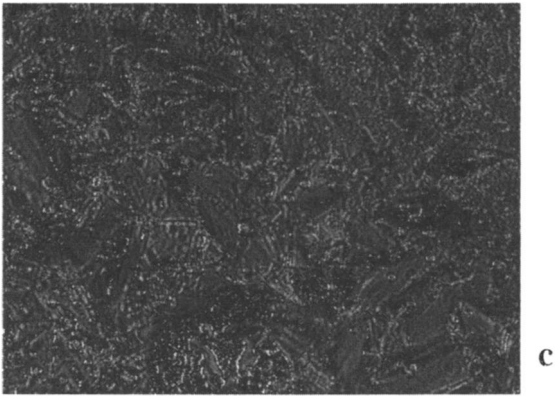


Figure 4. *Continued.*

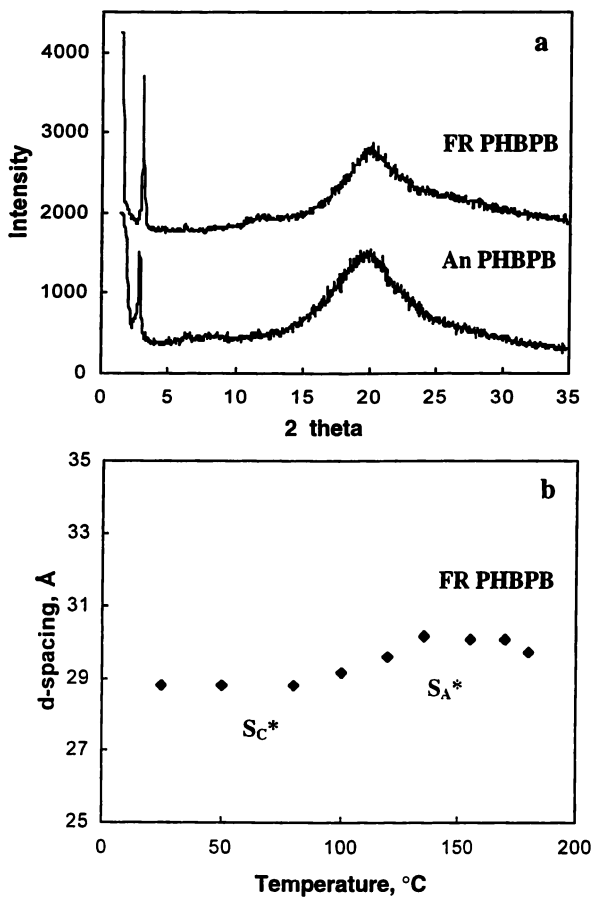


Figure 5. Wide angle X-ray diffraction of the polymers from anionic polymerization and free-radical polymerization (a); d-spacing of smectic layer structures as a function of temperature (b).

References

- 1) Kozlovsky, M.V.; Beresnev, L.A. *Phase Transitions* **1992**, *40*, 129-169.
- 2) Goodby, J.W.; Blinc, R.; Clark, N.A.; Lagerwall, S.T.; Osipov, M.A.; Pikin, S.A.; Sakurai, T.; Yoshino, K.; Zeks, B. *Ferroelectric Liquid Crystals: Principles, Properties, and Applications*; Goodby, J.W.; Blinc, R.; Clark, N.A.; Lagerwall, S.T.; Osipov, M.A.; Pikin, S.A.; Sakurai, T.; Yoshino, K.; Zeks, B., Ed.; Gordon and Breach Science: Philadelphia, 1991.
- 3) Bohnert, R.; Finkelmann, H. *Macromol. Chem. Phys.* **1994**, *195*, 689-700.
- 4) Percec, V.; Tomazos, D. *Macromolecules* **1989**, *22*, 2062-2069.
- 5) Laus, M.; Bignozzi, M.C.; Fagnani, M.; Angeloni, A.S. *Macromolecules* **1996**, *29*, 5111-5118.
- 6) Omenat, A.; Hikmet, R.A.M.; Lub, J.; van der Sluis, P. *Macromolecules* **1996**, *29*, 6730-6736.
- 7) Yamada, M.; Iguchi, T.; Hirao, A.; Nakahama, S.; Watanabe, J. *Macromolecules* **1995**, *28*, 50-58.
- 8) Zheng, W.Y.; Hammond, P.T. *Macromol. Rapid Commun.* **1996**, *17*, 813-824.
- 9) Shibaev, V.P.; Freidzon, Ya.S.; Kostromin, S.G. *Molecular Architecture and Structure of Thermotropic Liquid Crystal Polymers with Mesogenic Side Groups*; Shibaev, V.P.; Freidzon, Ya.S.; Kostromin, S.G., Ed.; Springer-Verlag: New York, 1994, pp 77-120.
- 10) Hahn, B.; Wendorf, J.H.; Portugal, M.; Ringsdorf, H. *Colloid Polym. Sci.* **1981**, *259*, 875.
- 11) Nakano, T.; Hasegawa, T.; Okamoto, Y. *Macromolecules* **1993**, *26*, 5494-5502.
- 12) Hsuie, G-H; Chen, J-H. *Macromolecules* **1995**, *28*, 4366-4376.
- 13) Zentel, R. *Liquid Crystalline Polymers*; Zentel, R., Ed.; Steinkopff Darmstadt: Springer, New York, 1994, pp 103-141.
- 14) Zheng, W.Y.; Hammond, P.T. in *MRS proceedings*, "Liquid Crystals for Advanced Technologies", Ed. Bunning, Chen, Hawthorne, Kajiyama, Koide: San Francisco, 1996.
- 15) Zheng, W. Y.; Hammond, P. *Macromolecules*, *accepted* **1997**.

Chapter 17

Design of Assemblies of Functionalized Nanoscopic Gridlike Coordination Arrays

Ulrich S. Schubert^{1,3}, Jean-Marie Lehn¹, Jörg Hassmann², Catherine Y. Hahn²,
Nikolaus Hallschmid², and Paul Müller²

¹Laboratoire de Chimie Supramoléculaire, Institut Le Bel, Université Louis Pasteur,
4 Rue Blaise Pascal, 67000 Strasbourg, France

²Physikalisches Institut III, Universität Erlangen-Nürnberg, 91058 Erlangen,
Germany

The controlled arrangement of metal ions into specific arrays and patterns is one of the major goals in modern metallo-supramolecular chemistry. Such two- or three- dimensional superstructures, formed by programmed self-assembly from mixtures of organic ligands and metal ions, potentially may display new magnetic, photochemical or redox properties. As a result, they can be used as building blocks for novel functional supramolecular assemblies. A recent investigation into synthesis and properties of tetranuclear [2 x 2]-grid complexes using 4,6-bis(6-(2,2'-bipyridyl))pyrimidine and its derivatives as ligands and metal ions such as cobalt(II) or zinc(II) has been extended to include peripherally functionalized analogues. These ligands and grids open avenues towards polymolecular assemblies and supramolecular polymers with novel material properties. The hydroxy-functionalized coordination arrays were found to form extended molecular assemblies, as visualized by microscopic techniques.

The design and synthesis of highly ordered materials is one main aim in polymer, supramolecular and material science (1,2). Such architectures, e.g. on surfaces or in thin films, could provide new mechanical, thermal, electrochemical, photochemical or magnetic properties. In particular systems containing metal ions are of special interest. Several approaches lead to such materials:

E.g., in polymer chemistry phase separation of block copolymers or the formation of defined micelles is being used (3-10).

Alternatively, materials scientists develop more and more precise methods for the microstructuring of surfaces or films (11-14).

³Current address: Lehrstuhl für Makromolekulare Chemie, Technische Universität München, Lichtenbergstrasse 4, 85747, Garching, Germany.

A very promising approach comes from supramolecular chemistry (1). Recent work in this field has demonstrated that information stored in molecular components can be read out by non-covalent interactions to assemble the final architectures using hydrogen-bonding (15-18), metal-ligand (19-21) and cation (22) interactions. A number of described systems contain infinite lattices or exist only in the solid state (23,24). Further development requires to construct novel components which may assemble novel architectures presenting desired properties.

One interesting procedure used molecular building blocks with repeating subunits, with the capability to complex metal ions in a defined and predicted arrangement. In particular, multimetallic complexes of precise $[m \times n]$ nuclearity and two-dimensional geometry as models for information storage were developed. Their basic geometries may be termed *racks* $[n]R$, *ladders* $[2n]L$, and *grids* $[m \times n]G$ (Figure 1), where the nuclearity of the R, L, and G species is given by $[n]$, $[2n]$, and $[m \times n]$, in sequence of increasing complexity. The ligand components are oriented more or less orthogonal to each other (1,25).

The metal ions serve as connecting centers of the structures and provide additional electrochemical, photochemical, and reactional properties. Main points in the design of such coordination arrays are the choice of the ligands and metal ions. Transition metal ions with octahedral coordination geometry are expected to cover a wider range of elements and properties compared to tetrahedral metal ions used in ladder- (26) and grid-type (27) complexes. As basic tridentate complexing unit, the well-known terpyridine was chosen, due to its stable complexes with transition metal ions (28) and to its interesting oxidative and reductive behavior (29-31). To promote metal-metal interaction (32) and to enforce the alignment of the metal centers, a small metal-to-metal distance is required in the coordination arrays. This is the case for ligands consisting of fused terpyridine subunits containing bridging pyrimidine groups (1,25).

Two-dimensional grid-like structures are of particular interest, as their architectures may serve as a basis for the construction of information storage devices (33). By addressing the metal ions photo- or electrochemically, it might be possible to inscribe into the arrays patterns which could be read out non-destructively (1). Such ion dots would still be of smaller size than quantum dots (34), and they would form spontaneously by self-assembly, not requiring microfabrication.

A recent investigation of this class of coordination arrays concerned the synthesis, structure and properties of stable tetranuclear cobalt(II) complexes of the ligand 4,6-bis(6-(2,2'-bipyridyl))pyrimidine and its derivatives, which have a grid-type structure ($[2 \times 2]$ -Grid) (35,36). Studies of the electronic, magnetic, and structural properties of these molecules on surfaces, as crystals, and in solution demonstrated interesting properties of these units (37,38).

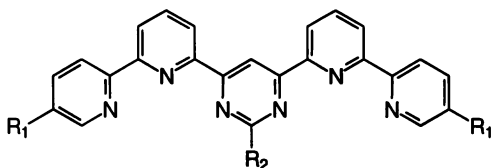
Besides the design and synthesis of such „isolated“ grid units, one major point in the design of new materials is the ordered and stable arrangement of grids on surfaces or into thin films. For this purpose, functionalized ligands and grids are required. New directed synthetic strategies allow the preparation of functionalized ligands and functionalized $[n \times n]$ -grids (Schubert, U. S.; Lehn, J.-M., to be published.). This opens new ways towards molecular assemblies and supramolecular polymers with novel material properties (39).

We describe here the design and synthesis of functionalized ligands and their complexation into functionalized grid-like coordination arrays, as well as some first results on the formation of Langmuir-Blodgett (LB) films.

A second important focus of our work is the development of suitable analytical methods for the solid state and in solution. The physical characterization of metallo-supramolecular systems has mainly relied on crystal structure determination. Studies have also been performed on surface layers (40-42). The classical analytical methods (like FAB mass spectrometry) or most polymer methods (like light scattering, vapor pressure osmometry or membrane osmometry) can not be used. In solution, ESI mass spectrometry (43-45) and NMR (27,46) have been successfully applied. We have explored whether MALDI-TOF mass spectrometry in the solid state (Schubert, U. S.; Lehn, J.-M.; Weidl, C. H.; Spickermann, J.; Goix, L.; Räder, J.; Müllen, K., unpublished data.) and sedimentation equilibrium analysis in the analytical ultracentrifuge for solutions may be employed. Grid-like cobalt coordination arrays ($[2 \times 2]$ Co(II)-Grid) were used as model systems in the analytical ultracentrifuge (47).

Ligand Synthesis

The synthesis of fused terpyridine ligands was recently described (35). The oligo-tridentate ligands **1** - **3** based on alternating pyridines and pyrimidines were obtained by Stille type carbon-carbon bond forming reactions using organotin intermediates.



1: $R_1 = R_2 = H$

2: $R_1 = H, R_2 = CH_3$

3: $R_1 = CH_3, R_2 = H$

Initially, variations were made on the 5-position of the terminal pyridine ($R_1 = H$ or CH_3) and on the 2-position of the central pyrimidine ring ($R_2 = H$ or CH_3).

In order to further incorporate these ligands into polymers or larger assemblies, we developed a way to functionalize the R_1 -positions using radical bromination reactions of the terminal methyl groups resulting in a *bis*functionalized ligand (35). Due to the rather low yields and difficult separation procedures, we decided to search for an alternative synthetic approach using an already functionalized starting material. The commercially available 6-chloro-nicotinic acid seems to be the best starting material for such an approach (Figure 2). It can easily be converted in a multi-step procedure to a versatile precursor for the ligand synthesis.

An overall yield of 60% can be obtained with only one purification step at the end of the reaction sequence. The corresponding functionalized oligo-tridentate ligands **16** and **17** were synthesized by Stille type carbon-carbon bond forming reactions using organotin intermediates similar to the previous reported reactions (35) as shown in Figure 3. The yields were in all reactions slightly lower than in the reported

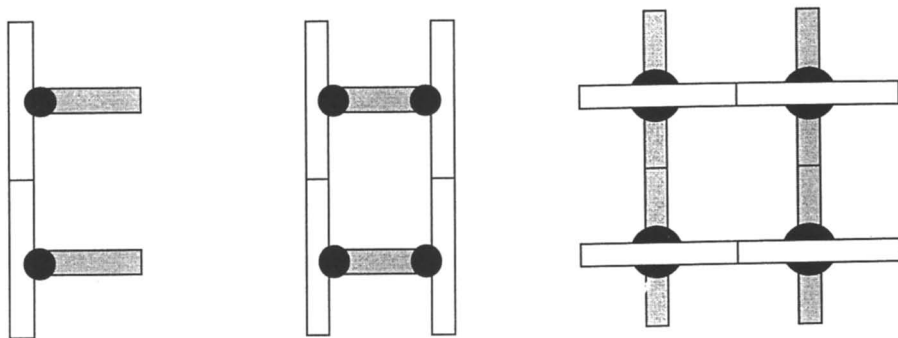


Figure 1. Schematic representation of inorganic architectures of coordination arrays of rack (left), ladder (center), and grid (right) type (1,25).

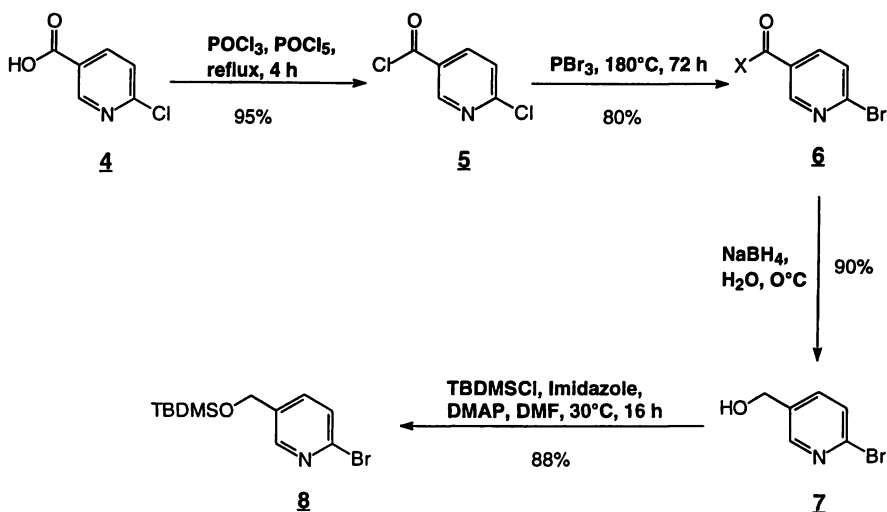


Figure 2. Synthesis of the functionalized bromo-pyridine building block, starting from the commercially available 6-chloro-nicotinic acid. The reactions can be performed on a multigram scale with one workup in the final step (TBDMS = *t*-butyl-dimethylsilyl).

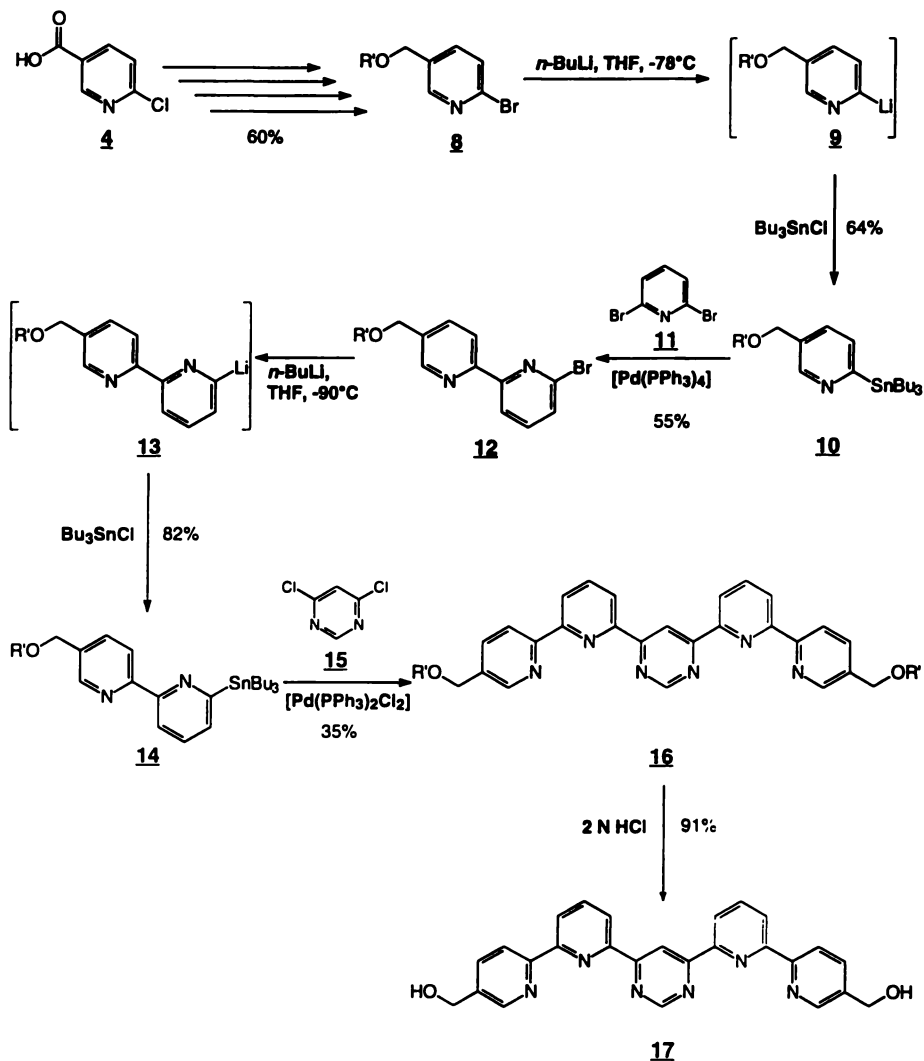


Figure 3. Synthesis of the functionalized ligands **16** and **17** using Stille type carbon-carbon bond forming reactions via organotin intermediates ($\text{R}' = \text{TBDMS} = \text{tbutyl-dimethylsilyl}$).

procedures for the unfunctionalized ligands (Schubert, U. S.; Lehn, J.-M., to be published.).

The diol **17** represents a versatile building block for the subsequent incorporation into polymers or for the combination with other structural units. It can also be used for the preparation of extended two-dimensional assemblies of grids based on hydrogen bonding interactions.

Preparation and Structure of the Complexes

The reaction of equimolar quantities of the ligand 4,6-bis(6-(2,2'-bipyrid-yl))-pyrimidine **1** (or the methyl substituted analogs **2**, **3**) and Co(II)acetate in refluxing MeOH has been shown to lead exclusively to the formation of tetranuclear complexes $[M_4(L)_4]^{8+}$, $G_1 - G_3$ ($L = \mathbf{1} - \mathbf{3}$ respectively) as shown in Figure 4 (36,37). Furthermore, metal salts like Ni(II)acetate, Zn(II)acetate and Cu(II)acetate could also be used for the preparation of these complexes (Hanan, G. S.; Volkmer, D.; Schubert, U. S.; Romero-Salguero, F.; Lehn, J.-M.; Baum, G.; Fenske, D. to be published.). The crystalline complexes were characterized using ESI mass spectrometry, UV and IR spectroscopy, elemental analysis and NMR spectroscopy.

The functionalized ligands **16** and **17** were reacted in the same way with Co(II)acetate in refluxing MeOH. Again the exclusive formation of one complex could be observed. The results of MALDI-TOF mass spectrometry clearly show the existence of tetranuclear complexes G_4 and G_5 $[M_4(L)_4]^{8+}$ ($L = \mathbf{16}, \mathbf{17}$).

The structure of these complexes in solution was investigated using sedimentation equilibrium analysis in the analytical ultracentrifuge. The grid-like cobalt coordination array G_3 (based on the ligand **3**) was used as model systems. The results showed the existence of the grid also in solution. However, a more complex association behavior could be observed in some cases, depending on the history of the sample and on the salt concentration in this solution (47). Extended studies are in progress (48).

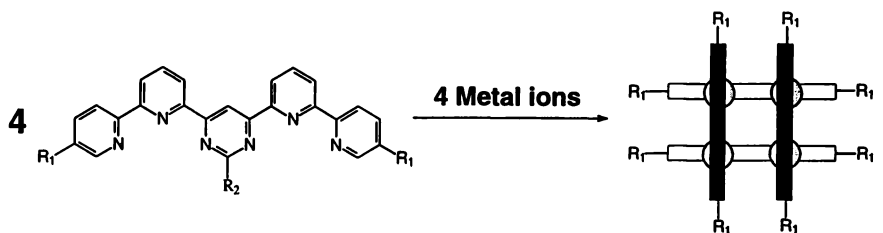
The grid-type architecture of the complexes was confirmed by the determination of the crystal structure of the Co(II) compound $[Co_4(\mathbf{2})_4](SbF_6)_8$ (Figure 5) (36). The metal ions are in a distorted octahedral coordination environment.

It can be assumed that the corresponding functionalized grids have the same basic structure in view of the similar behavior in UV spectroscopy, the MALDI-TOF mass spectrometry and the preliminary results of sedimentation equilibrium analysis in the analytical ultracentrifuge (48).

Physical-Chemical Properties

The grids showed interesting redox properties indicating electronic interactions between the metal centers (36).

Magnetic measurements (SQUID) on several crystals of the $[2 \times 2]$ -Co(II) grid G_2 display an antiferromagnetic transition at a Néel temperature of approximately 7 K. The intermolecular center to center distance in the crystal is 2 nm. The same behavior was seen in a $2.85 \cdot 10^{-3}$ M solution (intermolecular distance of 18 nm). A powdered sample of mononuclear $[Co(\text{terpyridine})_2]^{2+}$ shows no transition down to a



with

R₁ = H, CH₃, CH₂OH, CH₂OTBDMS

R₂ = H, CH₃,

Metal ions = Co(II), Ni(II), Zn(II), Cu(II)

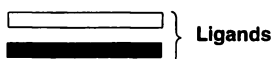
G₁: R₁ = H, R₂ = H

G₂: R₁ = H, R₂ = CH₃

G₃: R₁ = CH₃, R₂ = H

G₄: R₁ = CH₂OTBDMS, R₂ = H

G₅: R₁ = CH₂OH, R₂ = H



Counter ions are not drawn

Figure 4. Schematic presentation of the complex formation. The reactions were performed in refluxing MeOH (for the Co(II)acetate) or in water/methanol mixtures, see (36,37).

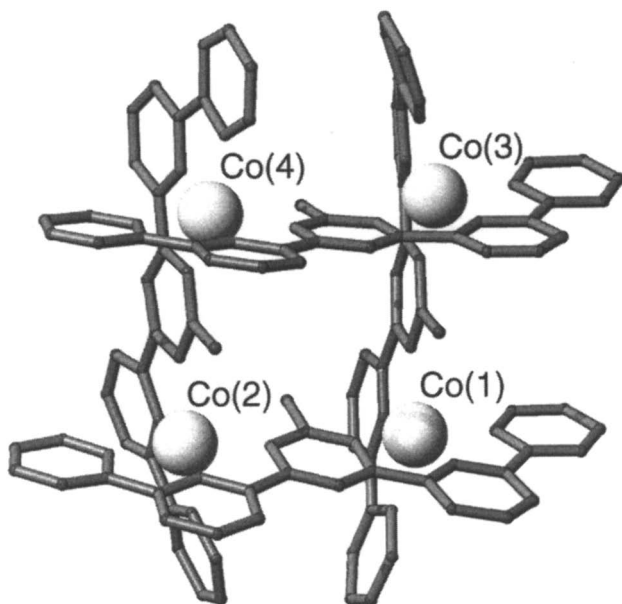


Figure 5. Structure of the $[\text{Co}_4(\mathbf{2})_4]^{8+}$ cation (wireframe model) showing the grid-like arrangement of the four ligands and the four metal ions (36).

temperature of 2 K, which suggests that grids form antiferromagnetic domains, containing one grid molecule (38).

Ordered structures of electrochemically deposited [2 x 2]-grids on gold(111) surfaces (room temperature, nitrobenzene solution) were visualized *in situ* by scanning tunneling microscopy (STM) (37, Hahn, C. Y.; Hassmann, J.; Müller, P.; Hanan, G. S.; Volkmer, D.; Schubert, U. S.; Lehn, J.-M., to be published.).

The electrochemical, surface and magnetic studies of the complexes indicate that coordination arrays of grid-type may be suitable building blocks for the construction of molecular information storage devices. One possibility would be to include single grids into highly ordered monolayers or thin polymer films and address individual grids by altering their redox state with the tip of a scanning tunneling microscope. Another strategy could form molecular magnetic domains. Such investigations are being pursued using higher ranking racks, ladders and grids and other transition metal ions (49) as well as in polymer films (39).

Formation of Langmuir-Blodgett Films

The Langmuir-Blodgett(LB) technique allows the preparation of thin films with a defined number of monolayers. This is of special importance for the development of molecular electronic devices based on ordered superstructures of the grids with an exactly defined film thickness.

The studies presented here are of particular interest, because they were performed on complex, non-amphiphilic systems with a defined molecular structure. Pressure-area isotherms on an ultrapure water subphase are useful particularly for the study of the structural properties of supramolecular thin films. The isotherms of Co-[2x2] grids with PF₆ counterions and different end groups attached to the R₁ positions of each ligand are shown in Figure 6.

For the non-functionalized grid G₁ as well as for the -CH₃ (G₃) and -CH₂OTBDMS (G₄) derivatized grids, the mean molecular areas (MMAs) of the phase transitions correspond very well to the grid geometries. The underivatized G₁ and methyl-derivatized G₂ grids reveal continuous phase transitions. The first phase transition occurs at a MMA, which corresponds to the area of the grids flat on the subphase. The grids are then compressed and lifted to an orientation perpendicular to the water surface. At MMAs smaller than the area of the grid in perpendicular orientation, a clear collapse is visible, the film leaves its two-dimensional geometry. Solely due to the molecular geometry, the grids reveal a behavior similar to classic amphiphilic molecules such as fatty acids. In the case of the -CH₂OTBDMS grid G₄, intermediate phases are visible which are attributed to the mobility of the large endgroups. The isotherm implies that first the end groups are lifted from the subphase, before the grids themselves move to a position perpendicular to the subphase.

The situation changes in the case of the CH₂OH-derivatized grid G₅. Due to their hydroxy end groups, the grids may form a two-dimensional hydrogen-bonding network. The first phase transition occurs at smaller areas than expected from the grid size. This indicates, that already there, the grids have left their two-dimensional order. This agrees with tapping-mode AFM observations (Figure 7).

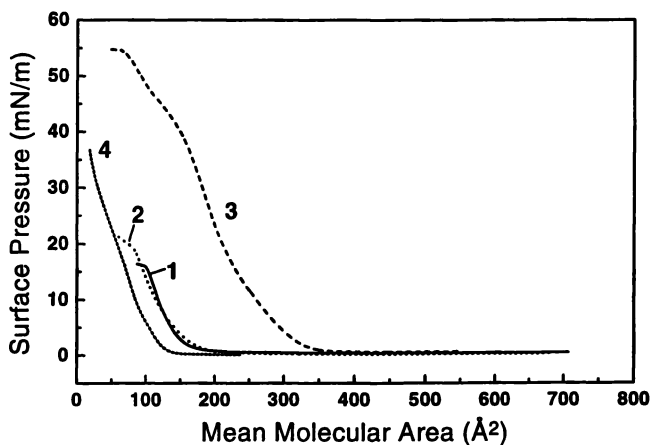


Figure 6. Isotherms of Co-[2×2] grids with different ligand end groups on a water subphase ($T = 20^{\circ}\text{C}$): (1) G_1 ($R_1 = \text{H}$); (2) G_3 ($R_1 = \text{CH}_3$); (3) G_4 ($R_1 = \text{CH}_2\text{OTBDMS}$); (4) G_5 ($R_1 = \text{CH}_2\text{OH}$).

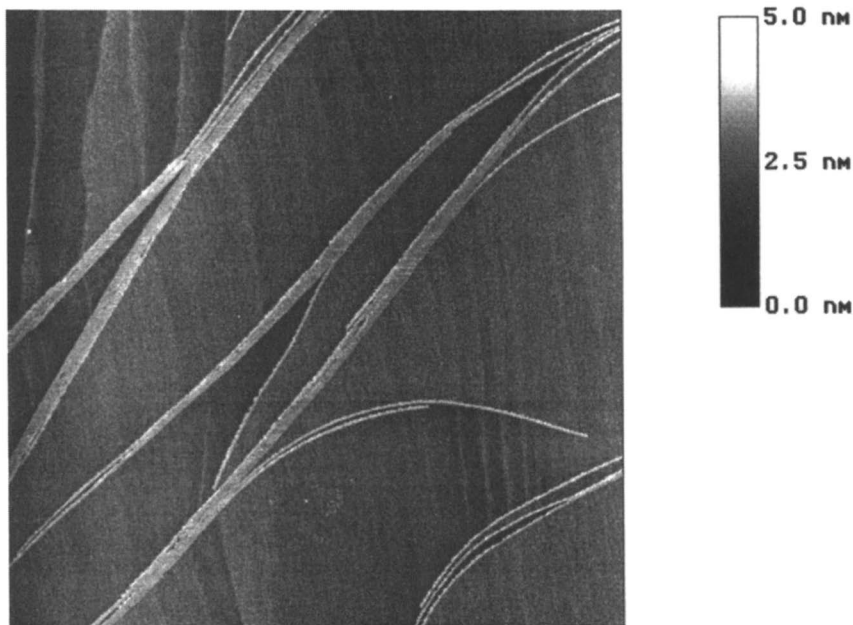


Figure 7. Tapping-mode AFM image of one monolayer of $-\text{CH}_2\text{OH}$ derivatized grid G_5 prepared by the LB-technique. Surface pressure at transfer 1.5 mN/m , scan size $5 \times 5 \mu\text{m}^2$ (liquid-expanded phase).

Nevertheless, there is a phase transition from the gas- to the liquid-expanded and solid phase. A collapse of the isotherms could never be observed. This is a further indication for the formation of a polymer-like hydrogen bonding network.

In conclusion, the analysis of the two-dimensional phase transitions of the supramolecular thin films can be an important means to understand the structural properties of polymolecular assemblies as well as of the components themselves. The AFM image of 1 monolayer of CH₂OH-derivatized grid G₅ reveals rod-like faults. Their typical width is 30 nm. The structure of the rods varies significantly with surface pressure and film thickness. One very important aim now is the preparation and visualization of superstructures of grids by the LB method. This would lead to ordered superlattices suitable for electronic functionalization (Hassmann, J.; Hallschmid, N.; Hahn, C. Y.; Müller, P.; Schubert, U. S.; Lehn, J.-M., work in progress.).

Conclusion

Studies of the electronic, magnetic, and structural properties of the supramolecular cobalt coordination arrays described here on surfaces, as crystals, and in solution demonstrate the interesting properties of these units and their potential utility as molecular device components in a futuristic information processing molecular electronics technology. The hydroxy-terminated [2 x 2] grid-type coordination array was found to form extended molecular assemblies, as visualized by microscopic techniques. Such functionalized ligands and grids provide new approaches towards ordered molecular assemblies and supramolecular polymers with novel material properties (Figure 8).

Acknowledgments

We thank the Fonds der Chemischen Industrie for a postdoctoral fellowship (U.S.S.) and the Bayerische Forschungsförderung via the FORSUPRA consortium for partial financial support.

Literature Cited

1. Lehn, J.-M. *Supramolecular Chemistry - Concepts and Perspectives*; VCH: Weinheim, Germany, 1995.
2. Lehn, J.-M. *Macromol. Chem., Macromol. Symp.* **1993**, *69*, 1.
3. Golden, J. H.; DeSalvo, F. J.; Fréchet, J. M. J.; Silcox, J.; Thomas, M.; Elman, J. *Science* **1996**, *273*, 782.
4. Stupp, S. I.; Son, S.; Lin, H. C.; Li, L. S. *Science*, **1993**, *259*, 59.
5. Stupp, S. I.; LeBonheur, V.; Walker, K.; Li, L. S.; Huggins, K. E.; Keser, M.; Amstutz, A. *Science* **1997**, *276*, 384.
6. Spatz, J. P.; Roescher, A.; Möller, M. *Adv. Mater.* **1996**, *8*, 337.
7. Spatz, J. P.; Mößmer, S.; Möller, M. *Chem. Eur. J.* **1996**, *2*, 1552.
8. Spatz, J. P.; Mößmer, S.; Möller, M. *Angew. Chem.* **1996**, *108*, 1673; *Angew. Chem., Int. Ed. Engl.* **1996**, *35*, 1510.

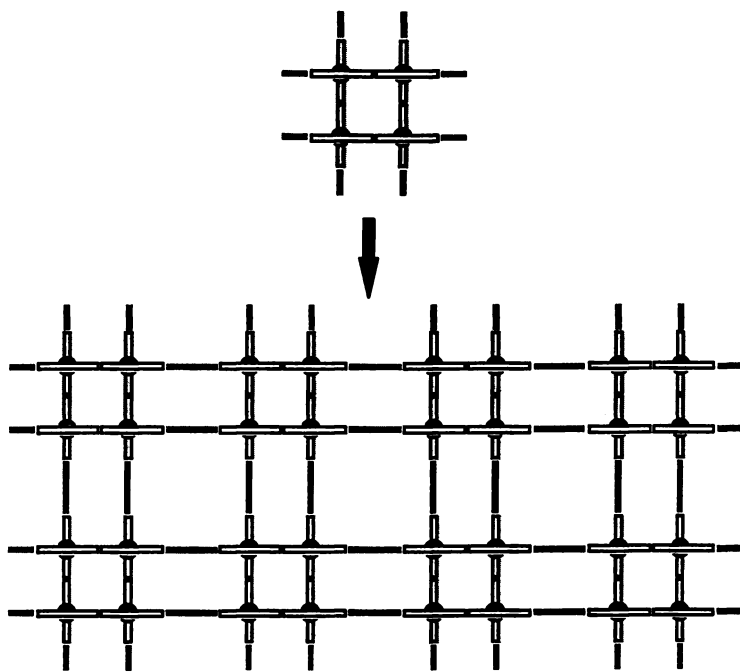


Figure 8. Schematic drawing of a potential arrangement of grids into two-dimensional layers using non-covalent or covalent polymerization.

9. Antonietti, M.; Henke, S.; Thünemann, A. *Adv. Mater.* **1996**, *8*, 41.
10. Antonietti, M.; Göltner, C. *Angew. Chem.* **1997**, *109*, 944; *Angew. Chem., Int. Ed. Engl.* **1997**, *36*, 910.
11. Xia, Y.; McClelland, J. J.; Gupta, R.; Qin, D.; Yhao, X.-M.; Sohn, L. L.; Celotta, R. J.; Whitesides, G. M. *Adv. Mater.* **1997**, *9*, 147.
12. Xia, Y.; Kim, E.; Mrksich, M.; Whitesides, G. M. *Chem. Mater.* **1996**, *8*, 601.
13. Qin, D.; Xia, Y.; Whitesides, G. M. *Adv. Mater.* **1997**, *9*, 407.
14. Renak, M. L.; Bazan, G. C.; Roitman, D. *Adv. Mater.* **1997**, *9*, 392.
15. Lawrence, D. S.; Jiang, T.; Levett, M. *Chem. Rev.* **1995**, 2229.
16. Zimmerman, S. C.; Zeng, F.; Reichert, D. E. C.; Kolotuchin, S. V. *Science* **1996**, *271*, 1095.
17. Kotera, M.; Lehn, J.-M.; Vigneron, J.-P. *J. Chem. Soc., Chem. Comm.* **1994**, 197.
18. Grotzfeld, R. M.; Branda, N.; Rebek J. J. *Science* **1996**, *271*, 487.
19. Lehn, J.-M.; Rigault, A.; Siegel, J.; Harrowfield, J.; Chevrier, B.; Moras, D. *Proc. Natl. Acad. Sci. USA* **1987**, *84*, 2565.
20. Baxter, P. N. W.; Lehn, J.-M. *Angew. Chem.* **1993**, *105*, 92; *Angew. Chem., Int. Ed. Engl.*, **1993**, *32*, 69.
21. Constable, E. C. *Prog. Inorg. Chem.* **1994**, *42*, 67.
22. Dougherty, D. A. *Science* **1996**, *271*, 163.
23. Abrahams, B. F.; Hardie, M. J.; Hoskins, B. F.; Robson, R.; Williams G. A. *J. Am. Chem. Soc.* **1992**, *114*, 10641.
24. Constable, E. C.; Edwards, A. J.; Phillips, D.; Raithby, P. R. *Supramol. Chem.* **1995**, *5*, 93.
25. Hanan, G. S.; Arana, C. R.; Lehn, J.-M.; Fenske, D. *Angew. Chem.* **1995**, 107, 1191; *Angew. Chem., Int. Ed. Engl.* **1995**, *34*, 1122.
26. Baxter, P.; Hanan, G. S.; Lehn, J.-M. *J. Chem. Soc., Chem. Comm.* **1996**, 2019.
27. Baxter, P.; Lehn, J.-M.; Fischer, J.; Youinou, M.-T. *Angew. Chem.* **1994**, 106, 2432; *Angew. Chem., Int. Ed. Engl.* **1994**, *33*, 2284.
28. Morgan, G.; Burstall, F. H. *J. Chem. Soc.* **1937**, 1649.
29. McWhinnie, W. R.; Miller, J. D. *Adv. Inorg. Chem. Radiochem.* **1969**, *12*, 135.
30. Constable, E. C. *Adv. Inorg. Chem. Radiochem.* **1986**, *30*, 69.
31. Kirchoff, J. R.; McMillin, D. R.; Marnot, P. A.; Sauvage, J.-P. *J. Am. Chem. Soc.* **1985**, *107*, 1138.
32. Steel, P. J. *Coord. Chem. Rev.* **1990**, *106*, 227.
33. Friedman, J. R.; Sarachik, M. P.; Tejada, J.; Ziolo, R. *Phys. Rev. Lett.* **1992**, *64*, 849.
34. Ashoori, R.C. *Nature* **1996**, 379, 413.
35. Hanan, G. S.; Schubert, U. S.; Volkmer, D.; Riviere, E.; Lehn, J.-M.; Kyritsakas, N.; Fischer, J. *Can. J. Chem.* **1997**, *75*, 169.
36. Hanan, G. S.; Volkmer, D.; Schubert, U. S.; Lehn, J.-M.; Baum, G.; Fenske, D. *Angew. Chem.*, **1997**, *109*, 1929; *Angew. Chem., Int. Ed. Engl.* **1997**, *36*, 1842.
37. Hanan, G. S.; Schubert, U. S.; Volkmer, D.; Lehn, J.-M.; Hassmann, J.; Hahn, C. Y.; Waldmann, O.; Müller, P.; Baum, G.; Fenske, D. In *9th International*

Symposium on Molecular Recognition and Inclusion, Colman, A. ed., Kluwer Academic Press: Dordrecht, in press.

38. Waldmann, O.; Hassmann, J.; Müller, P.; Hanan, G. S.; Volkmer, D.; Schubert, U. S.; Lehn, J.-M. *Phys. Rev. Lett.* **1997**, *78*, 3390.
39. Schubert, U. S.; Weidl, C. H.; Eigner, M. K.; Hochwimmer, G.; Eschbaumer, C.; Lehn, J.-M., work in progress.
40. Cohen, S. R.; Weissbuch, I.; Popovitz-Biro, R.; Majewski, J.; Mauder, H. P.; Lavi, R.; Leiserowitz, L.; Lahav, M. *Israel J. Chem.* **1996**, *36*, 97.
41. Stevens, F.; Dyer, D. J.; Walba, D. M. *Angew. Chem.* **1996**, *108*, 955; *Angew. Chem., Int. Ed. Engl.* **1996**, *35*, 900.
42. Cyr, D. M.; Venkataraman, B.; Flynn, G. W. *Chem. Mater.* **1996**, *8*, 1600.
43. Leize, E.; Van Dorsselaer, A.; Krämer, R.; Lehn, J.-M. *J. Chem. Soc., Chem. Commun.* **1993**, 990.
44. Marquis-Rigault, F.; Dupont-Gervais, A.; Van Dorsselaer, A.; Lehn, J.-M. *Chem. Eur. J.* **1996**, *2*, 1395.
45. Przybylsky, M.; Glocker, M. O. *Angew. Chem.* **1996**, *108*, 878; *Angew. Chem., Int. Ed. Engl.* **1996**, *35*, 806.
46. Hanan, G. S.; Arana, C. R.; Lehn, J.-M.; Baum, G.; Fenske, D. *Chem. Eur. J.* **1996**, *2*, 1292.
47. Schubert, D.; van den Broek, J. A.; Sell, B.; Durchschlag, H.; Mächtle, W.; Schubert, U. S.; Lehn, J.-M. *Prog. Colloid Polym. Sci.*, **1997**, in press.
48. Schubert, D.; van den Broek, J. A.; Sell, B.; Durchschlag, H.; Mächtle, W.; Lehn, J.-M.; Weidl, C. H.; Schubert, U. S., to be published.
49. Hanan, G. S. *Ph.D. thesis*, Université Louis Pasteur, Strasbourg, 1995; Bassani, D.; Baxter, P. N. W.; Rojo, J.; Romero-Salguero, F.; Lehn, J.-M., work in progress.

Chapter 18

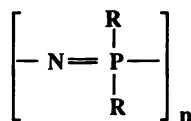
Functional Polyphosphazenes

Harry R. Allcock

Department of Chemistry, The Pennsylvania State University,
University Park, PA 16802

The early development of polyphosphazene science and technology focused on the preparation of polymers that are unreactive. However, the expansion of this field is being driven by the need for functional polymers that bear -OH, -COOH, SO₃H, -NH₂, and numerous other reactive units in the side group structure. This article reviews the methods that are being developed to accomplish this at both the molecular level and at surfaces.

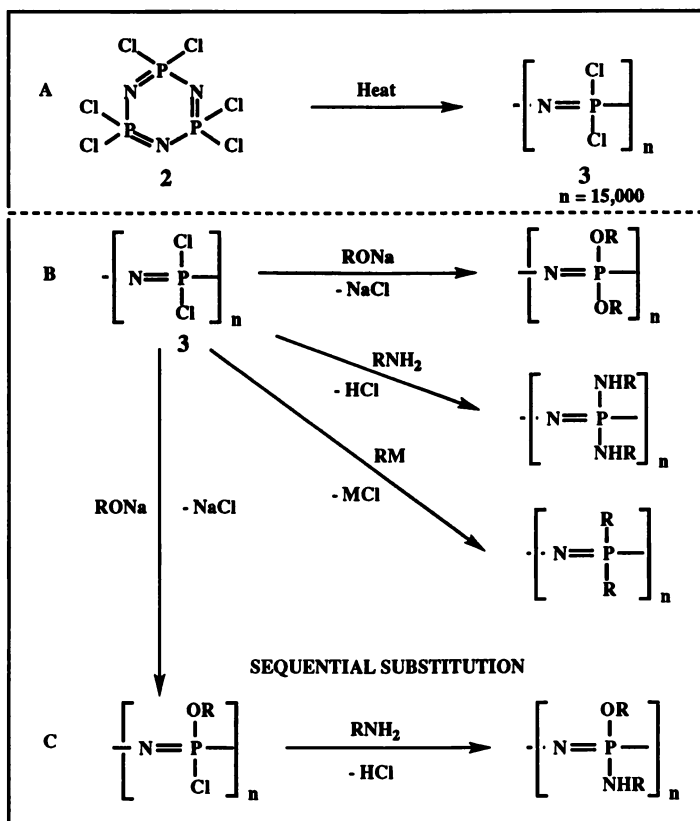
Polyphosphazenes are synthetic macromolecules with a backbone of alternating phosphorus and nitrogen atoms and with two organic, inorganic, or organometallic side groups linked to each phosphorus (1).



1

The first stable examples were reported by Allcock and Kugel in 1965 and, since that time, the polyphosphazenes have grown into a very large platform of polymers, with several hundred different examples synthesized and characterized (1-10). This broad diversity arises because a large number of different side groups can be linked to the backbone by macromolecular substitution reactions. The most widely used synthetic approach makes use of poly(dichlorophosphazene) (3) as a reactive polymeric intermediate (Scheme I) (11-15), but poly(difluorophosphazene), (NPF₂)_n, behaves in a similar way (16-18). Poly(dichlorophosphazene) (3) is normally prepared by the thermal polymerization of the cyclic trimer (2) or by various condensation procedures, including the recently discovered "living" polymerization of the phosphoranimine, Me₃SiN=PCl₃ (19-22).

Scheme I

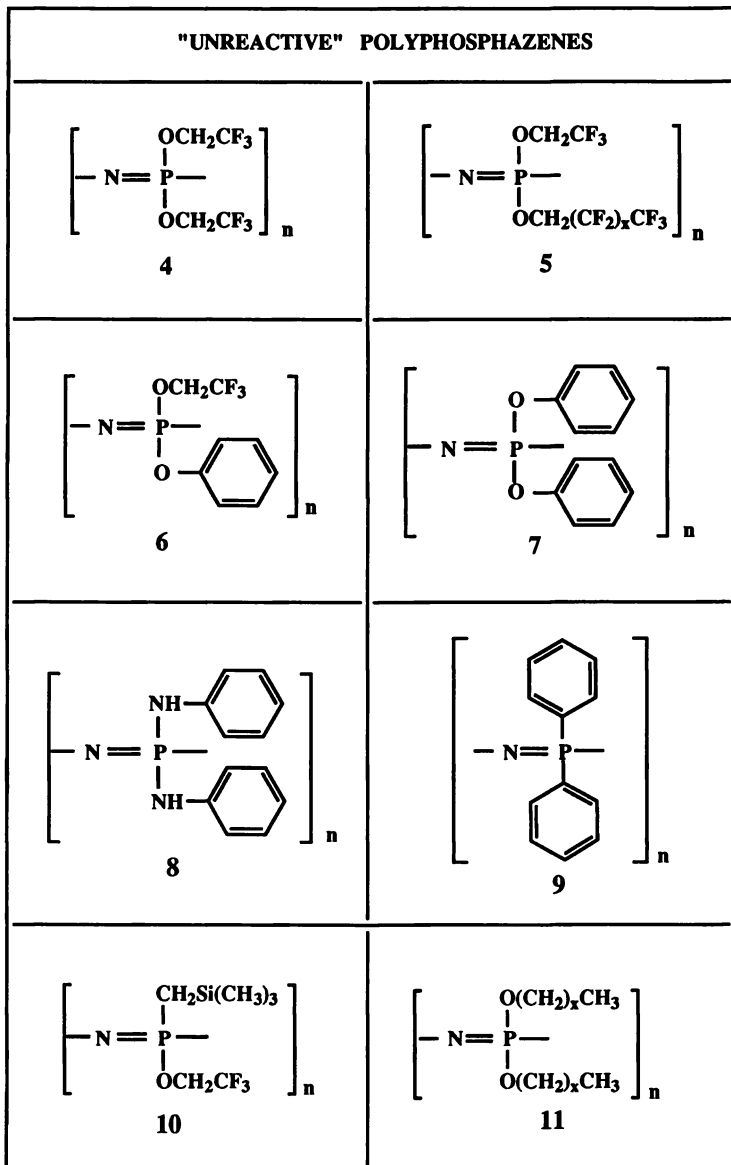


It is the high reactivity of the phosphorus-chlorine bonds in **3** that allows the chlorine atoms to be replaced by reactions with reagents such as alkoxides, aryloxides, amines, or other nucleophiles. Because the average chain length in **3** corresponds to approximately 15,000 repeating units, this means that roughly 30,000 halogen atoms per molecule are replaced in these reactions. Thus, in many ways, poly(dichlorophosphazene) is the ultimate functional polymer.

The broad molecular diversity in these polymers is also a consequence of the ease of introduction of two or more different types of side groups into each macromolecule. This is accomplished by simultaneous or sequential halogen replacement by different nucleophiles (Scheme I). Depending on the reagents used and the reaction conditions, the different side groups may be distributed along the chain randomly (**23**, **24**) or in some ordered sequence. The polymer properties depend critically on the types of side groups present and on their distribution. For example, although the backbone is inherently flexible, the overall flexibility and T_g depend on the size and polarity of the side groups. The T_g values of known polymers range from -100°C to $+180^\circ\text{C}$. Flexible aliphatic side groups generate low T_g 's and elastomeric character. Aryloxy or fluorinated aliphatic side groups can give rise to crystalline materials. Two or more different aryloxy or fluoroalkoxy side units distributed randomly along the same chain

prevent crystallization because of the lack of molecular symmetry, and such species have been developed as high performance non-burning elastomers (5, 6) (23,-26).

Chart 1



This combination of macromolecular substitution and access to mixed-substituent polymers underlies the extraordinary versatility of the polyphosphazene platform. By mid-1997 more than 3000 publications and patents had appeared on this subject, and

applications had been developed in fields as diverse as elastomer technology (23, 25, 26), vaccine adjuvants (27), dental materials (28), and solid battery electrolytes (29-38)

The development of polyphosphazenes has proceeded through two stages. Most of the organic-substituted polymers prepared and studied initially were designed specifically to be *non*-functional; in other words, to be as unreactive as possible. Examples include the species shown in Chart 1. However, in recent years the emphasis has turned to the design and development of synthesis routes to polyphosphazenes with organo-functional side groups. Much of the interest in functional polyphosphazenes is driven by attempts to incorporate them into applications-oriented materials such as in composites, solid battery electrolytes, biomedical materials, electro-optical glasses, and polymeric liquid crystals. In this context, "functionality" is defined as a site that is capable of undergoing a chemical reaction, including coordination with metal ions. In our program, we have introduced functional groups into polyphosphazenes at two levels - first at the level of individual macromolecules, and second at polymer surfaces. In this article the main emphasis will be on reactions carried out in solution at the molecular level, with only a brief review of the surface science.

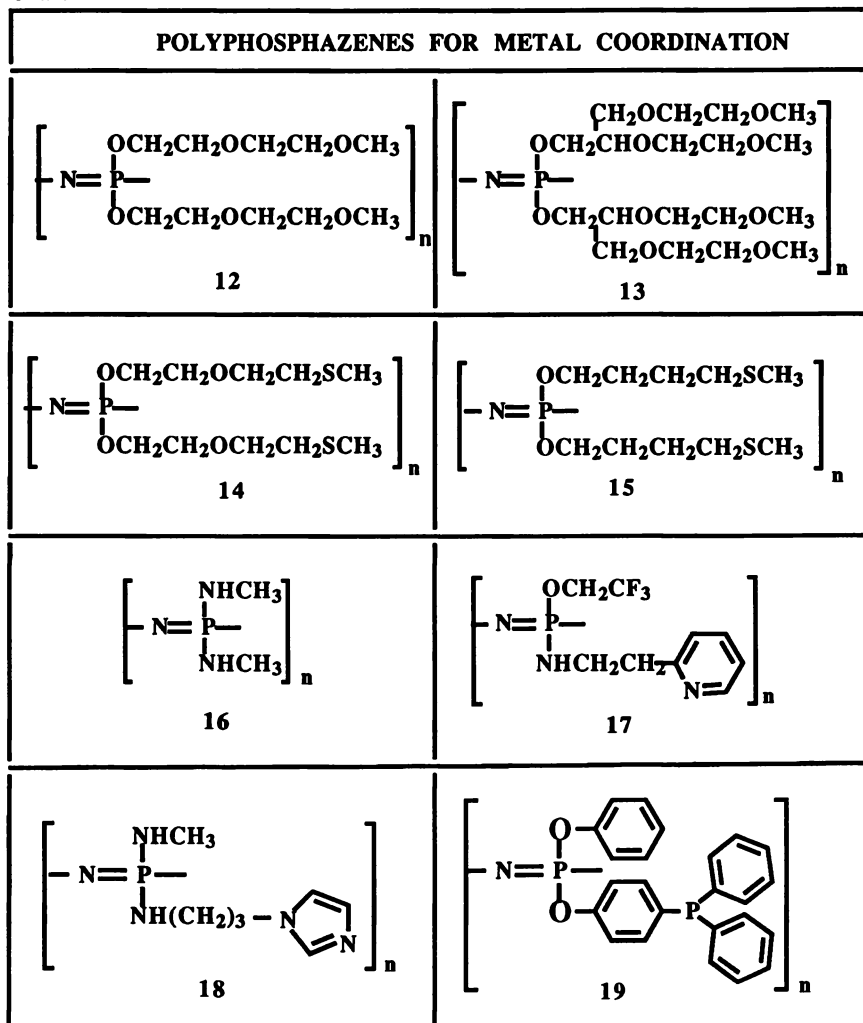
Functionalization at the Molecular Level

Three methods have been developed to introduce functionality at the macromolecular level. These are: (a) by the use of organic side groups that have "soft" functionality, (b) by the reactions of "unreactive" polyphosphazenes with aggressive reagents, and (c) via protection-deprotection reactions. These will be considered in turn.

"Soft" Functionality: Coordination Sites. The incorporation of coordination sites for cations into the side group structure of a polyphosphazene has been studied in detail. The polymers shown in Chart 2 are examples. The broadest emphasis so far has been placed on polymers with alkoxy ether side groups. These macromolecules are important because they serve as solid polymeric solvents for salts such as lithium triflate or perchlorate. The side group oxygen atoms coordinate to lithium, assist solubilization of the salt, and bring about ion-pair separation. This, in turn, facilitates ion transport and electrical conductivity. The first phosphazene example to demonstrate this phenomenon was poly[bis(methoxyethoxyethoxy)phosphazene] ("MEEP") (12). Thin films of this polymer containing lithium or silver triflate conduct an electric current with conductivities at 25°C in the range of 10^{-5} ohms⁻¹ cm⁻¹ (29-33). This is two to three orders of magnitude higher than can be obtained for the "standard" in this field, which is lithium triflate dissolved in poly(ethylene oxide). More recent work has demonstrated the utility of polyphosphazenes with longer chain alkyl ether side groups and branched side chain counterparts (34-38). For example, branched alkyl ether side groups ("podands") stiffen the polymer (presumably by side chain entanglement) without impeding ion transport. These polymers are under active development as thin film polymeric electrolytes in lightweight rechargeable lithium batteries.

Nitrogen coordination sites, in the form of pyridine- or imidazole-bearing side chains (17, 18), can also be introduced into the polymer at the initial macromolecular substitution stage. For example, the reaction of $C_5H_4N-CH_2CH_2NH_2$ and $NaOCH_2CF_3$ with poly(dichlorophosphazene) yields polymers of the type shown in 17 (39). These reactions are not so straightforward as those that involve the introduction of alkyl ether side chains. The pyridine nitrogen atom is sufficiently basic that it can

Chart 2



react with phosphorus-chlorine bonds, and careful control over the reaction conditions is needed to avoid side reactions. Nevertheless, these polymers are effective coordination donors for a variety of transition metal species (39)

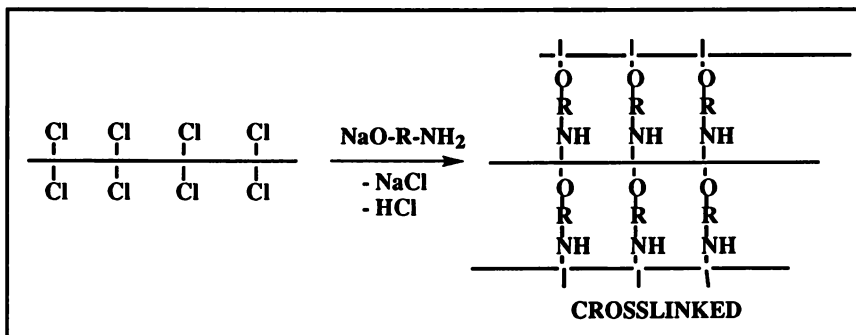
The imidazole-bearing polymer shown as 18 functions as a carrier molecule for heme and heme-like molecules in experimental oxygen-carrier polymers (40, 41).

Avoiding the Difunctional Reagent Problem. A need exists for polyphosphazenes with side groups that bear reactive sites such as -OH, -NH₂, -COOH, -SO₃H groups, etc. These sites are required for the coupling of biological, catalytic, or photonic units to the polymer, for enhancing compatibility with other

polymers, to improve adhesion, for generating solubility in specific solvents, to change the surface character, for grafting to other polymers, or for crosslinking.

The most obvious synthesis route to such polymers is the use of a difunctional reagent in the macromolecular substitution step. However, this method cannot be employed. For example, the reaction of poly(dichlorophosphazene) with $\text{NaOCH}_2\text{CH}_2\text{NH}_2$ leads to crosslinking of the chains (Scheme II). Even a small amount of crosslinking in the initial stages of a macromolecular substitution will result in precipitation of the polymer, and this will prevent further halogen replacement. Avoidance of this complication requires the use of two alternative strategies.

Scheme II



First, it may be possible to introduce a functional site by reactions carried out on the side groups of an "unreactive" poly(organophosphazene). For example, aryloxy side groups may be sulfonated or nitrated, and alkyl units on an aromatic ring may be oxidized to carboxylic acid functions. For this approach to be successful the reaction must be restricted to the side group system only and must not involve cleavage of the inorganic backbone or cleavage of the organic side groups from phosphorus. This procedure can be utilized at two different levels. It may be carried out at the level of individual molecules, in which case all the polymer molecules in the reaction mixture will be modified. Alternatively, the reaction may be restricted to the surface of a solid polymer. This last method may be advantageous if, for example, the bulk properties of the polymer are appropriate for a particular application, but the adhesion behavior or the biomedical compatibility needs to be improved. In general, surface reactions of this type are easier to control than functionalizations carried out in solution at the molecular level.

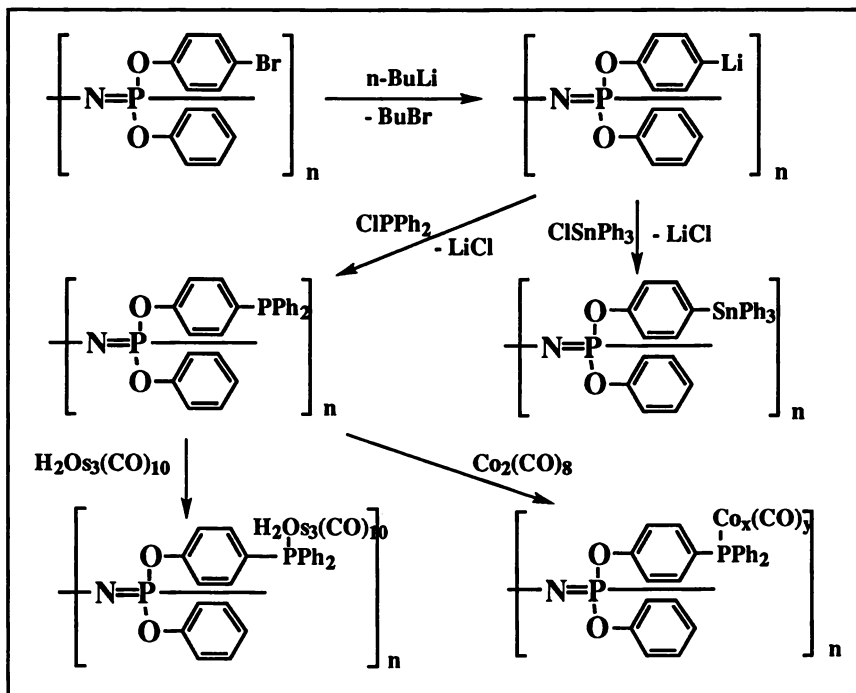
The second main method to avoid crosslinking during macromolecular substitution is to use a protection-deprotection protocol for one of the reactive sites in a difunctional reagent. Several examples will be given to illustrate this approach.

Functionalization of "Unreactive" Poly(organophosphazenes)

Lithiation Reactions. One of the earliest reactions of this type made use of metal-halogen exchange reactions carried out on poly[bis(p-bromophenoxy)phosphazene]. Polyphosphazenes that bear p-bromophenoxy side groups are normally unreactive. However, they can be lithiated, as shown in Scheme III, and the lithio derivatives react with a wide variety of electrophiles that range from chlorophosphines (19) to organometallic halides (42-45). This provides an access route to polymer-bound transition metal catalysts and other metallated or silylated polymers.

Wisian-Neilson, Neilson, and coworkers have applied the lithiation route to another class of polyphosphazenes - those with methyl side groups (46-51) For

Scheme III



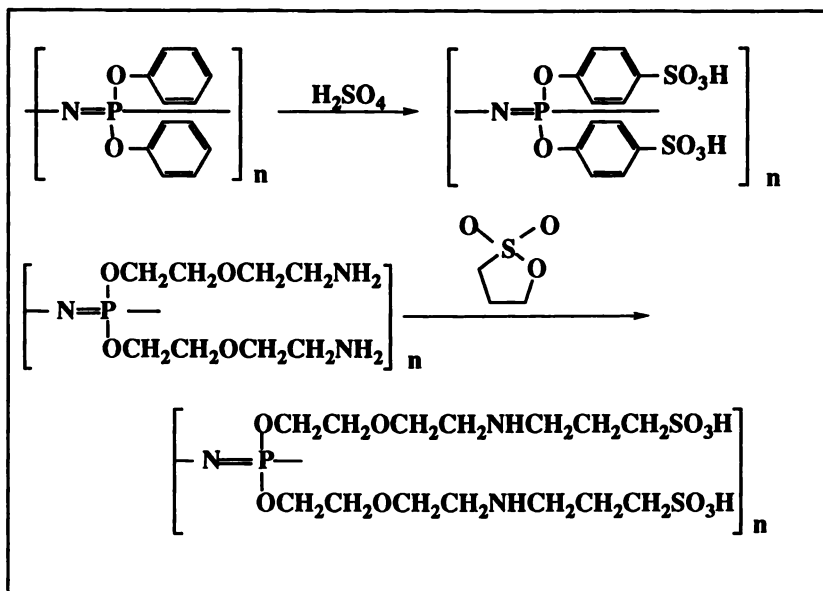
example, the methyl groups in poly(methylphenylphosphazene) undergo metal-hydrogen exchange in the presence of butyllithium, and the lithiated polymer can then react with electrophiles such as chlorophosphines or chlorosilanes.

Sulfonation of Aromatic Side Groups. A wide variety of aryloxyphosphazene polymers such as **7** can be sulfonated by treatment with strong sulfuric acid or sulfur trioxide (Scheme IV) (52-54). These reactions must be conducted with considerable care to maximize the degree of sulfonation while, at the same time, minimizing acidic cleavage of the polymer backbone. Levels of sulfonation approaching one sulfonic acid group for every aryloxy unit have been achieved. The introduction of sulfonic acid groups converts a hydrophobic, water-insoluble polymer to a water-soluble polyelectrolyte.

Sulfonation Via the Use of Sultones. Direct sulfonation is generally not possible when aliphatic side chains are present. However, sulfonated aliphatic side chains can be produced via the reactions of polyphosphazenes that bear aliphatic amino side groups with sultones (55) (Scheme IV). The pendent terminal amino units must be introduced by a protection-deprotection route (see later).

Other Direct Functionalization Reactions. In addition to the above processes, other direct functionalization reactions at the molecular level include the addition of organosilicon hydrides to allyl groups at the terminus of aryloxy side groups (56), the free-radical grafting of epoxy-, organosilyl-, or pyridine-bearing vinyl compounds to *p*-methylphenoxy side units (57), the quaternization of pendent tertiary amino groups, and

Scheme IV

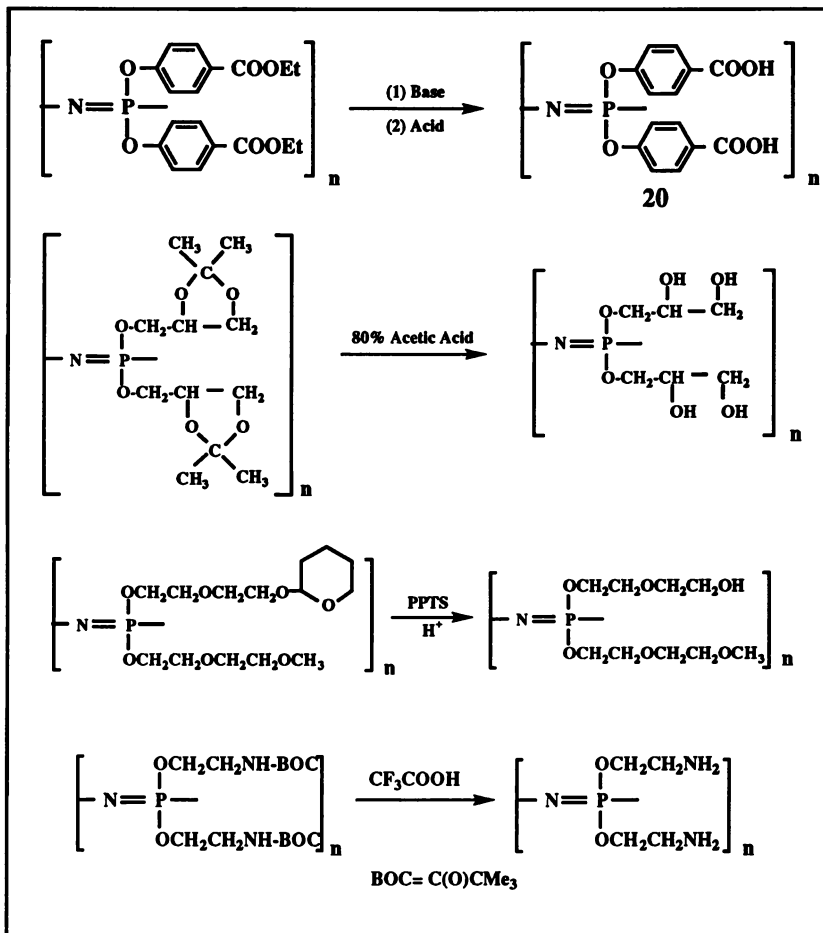


gamma-ray- or UV-induced coupling reactions at side group aliphatic carbon-hydrogen bonds. Thermal crosslinking reactions via the addition reactions of pendent allyl groups, and photocrosslinking through pendent cinnamate and chalcone groups are also known. In addition, borazine, metallocarborane, and steroidal side groups have also been studied as functional units in the polyphosphazene system.

Protection-Deprotection Approaches

Use of Esters as Protecting Groups for Carboxylic Acids. The introduction of carboxylic acid groups into the side chains of polyphosphazenes opens up many opportunities for using these polymers in medicine, in composites, and as water-soluble materials. However, for the reasons discussed above, carboxylic acid units cannot be introduced at the initial macromolecular substitution stage. An early approach to solving this problem involved the reaction of lithioaryloxyphosphazenes with carbon dioxide (42-45). A more recent approach, which is more suited for larger-scale reactions, is to first introduce side groups that bear ester functions, followed by hydrolytic deprotection of these to carboxylic acid groups. Scheme V illustrates the first application of this protocol to polyphosphazenes (58). The product polymer (20) (known as "PCPP") is insoluble in water, but is soluble as its sodium salt. It can, however, be precipitated from aqueous solution by the addition of calcium ions. This procedure has been developed as a process for the microencapsulation of biologically active species for use in tissue engineering and biotechnology (59-63). PCPP is also currently undergoing human clinical trials as a vaccine adjuvant (64-66). The same polymer has been studied as the polymeric reinforcing agent in composites with calcium hydroxyapatite, with the polyphosphazene being chemically linked to the mineral component via calcium crosslink sites (67, 68). Recent work has also shown that the carboxylic acid groups in PCPP provide a valuable means for the incorporation of the flame-retardant polyphosphazene into polyurethanes (69).

Scheme V



The ester protection technique has also been used in the preparation of amino acid derivatives of polyphosphazenes (70, 71). For example, ethyl glycinate reacts with poly(dichlorophosphazene) to link the amino function to the phosphorus atoms of the backbone. Subsequent exposure of the protected polymer to water in a biological environment leads to hydrolysis of the ester function and breakdown of the polymer to ethanol, glycine, phosphate, and ammonia. This has been used both for the controlled delivery of drugs and for stimulating the regrowth of bone in tissue engineering experiments (72).

Protection and Deprotection of Pendent Hydroxyl Groups. The presence of hydroxyl groups in the side chains of polyphosphazenes is required for a variety of purposes, including the preparation of water-soluble or bioerodible polymers, and for the introduction of sites for the linkage of biologically active or electro-optical units to the polymer. Two typical approaches are shown in Scheme V.

In the first, a tetrahydropyranyl ether group is used to protect one of the hydroxyl groups of diethylene glycol (73). After the side chain has been linked to the polyphosphazene backbone, the pendent hydroxyl function is deprotected with the use of PPTS. The hydroxyl-bearing polymer was used as an immobilization substrate for a cadmium sulfide precursor for possible uses in electro-optical applications. A second approach, which has been used to protect all but one of the hydroxyl groups in glycerol and glucose prior to coupling to the phosphazene backbone, involves the use of an acetal moiety, which protects two hydroxyl groups per side chain (74, 75). Treatment of the polymer with acid then deprotects the hydroxyl units. Both the glyceryl and glucosyl polyphosphazenes are soluble in water and will hydrolyze slowly at body pH. Both polymers are of interest for tissue engineering and drug delivery applications.

Protection and Deprotection of Pendent Amino Groups. Scheme V illustrates a method used recently for the preparation of polyphosphazenes with pendent alkylamino groups (76). 2-Aminoethanol was first amino-protected by reaction with di-*t*-butyl dicarbonate to yield a "BOC" unit. The alcohol function was then converted to the alkoxide salt by treatment with sodium hydride, and this reagent was used for halogen replacement with poly(dichlorophosphazene). Subsequent deprotection of the amino unit then took place following exposure of the polymer to acid.

These protection-deprotection sequences are well-developed for small-molecule compounds (77). The difference here is that up to 30,000 deprotection reactions must be performed on each molecule. In these macromolecular processes the objective is to generate the functional site without subjecting the polymer to conditions that might bring about skeletal cleavage. However, the use of deprotection conditions, such as exposure of the polymer to acids in aqueous media, carries the risk of skeletal cleavage if the reaction conditions are not optimized. In practice, some decrease in polymer chain length can often be detected, but the polymeric intermediates have such high molecular weights that, for example, an average of two or three skeletal cleavage reactions per molecule still allows high molecular weight products to be isolated.

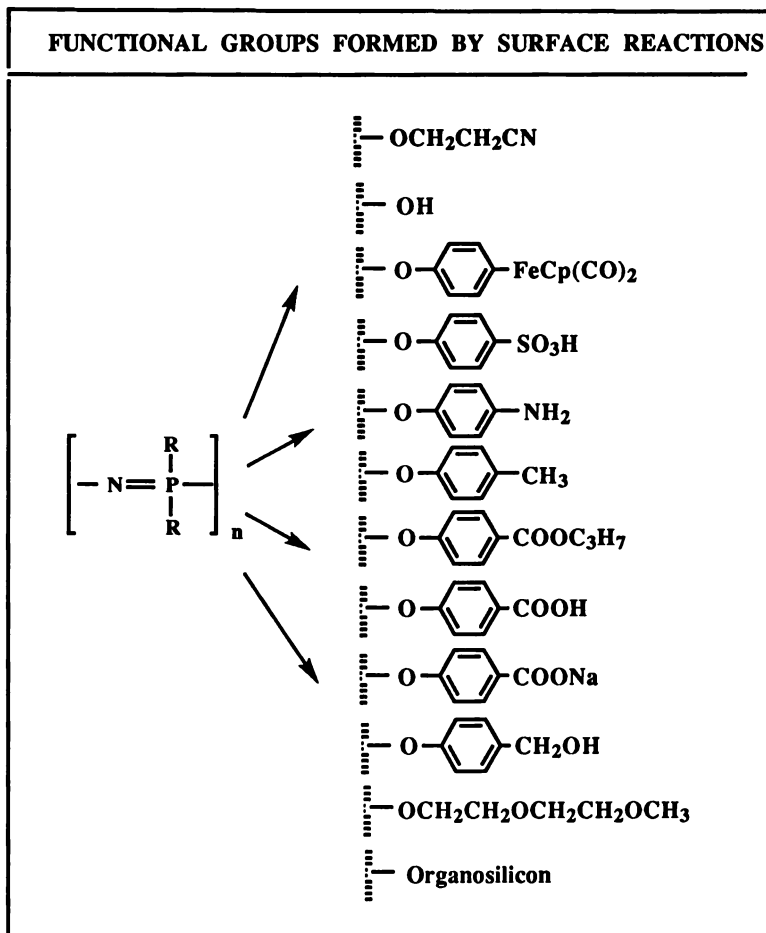
Surface Reactions

Many polymers exist that have valuable bulk properties but possess surface characteristics that are inappropriate for specific uses. An example is a polymer targeted for biomedical applications that should have bulk properties that resist the ingress of water but have a hydrophilic surface to favor overgrowth by endothelial cells. A similar combination of properties might be required for the preparation of adhesive laminates. Reactions that take place only at the surface of a solid polymer provide an access route to property combinations of this kind. Polyphosphazenes are particularly appropriate for surface chemistry since the side groups introduced initially (by the halogen replacement technique) can be chosen to optimize the eventual reactivity or lack of reactivity of the surface regions. Moreover, the ability to introduce two or more different types of side groups (for example, one which reacts during surface functionalization and one which does not) allows the density of reactive sites on the surface to be controlled. Ideally, surface reactions should be such that they take place rapidly at moderate temperatures, and without penetration into the bulk material when a film, fiber, or molded object is immersed in the reaction medium.

Virtually all the reactions described for molecular level functionalization are, in principle, applicable to surface functionalization as well, and additional alternatives also become possible. In our program we have been able to do this using a wide variety of reagents to generate hydroxyl, arylamino, arylcarboxylate, sulfonic acid, epoxide, and allyl-units at the polymer surfaces, and to use these functional sites to control hydrophobicity or hydrophilicity or to link metals, enzymes, or other biologically active species to the surface regions (78-89). Inherent in this work has been the

characterization of these surfaces to monitor the depth and concentrations of active sites and study the degree to which specific groups either remain at the surface after they have been formed or are buried by molecular motions.

Scheme VI



Summary of Surface Reactions. Scheme VI lists some of the functional units that have been introduced into polyphosphazenes by surface reactions. Sulfonic acid moieties were introduced by the surface sulfonation of aryloxyphosphazene polymers (83). Carboxylic acid sites were produced either by the oxidation of the methyl groups of *p*-methylphenoxy side chains (84), or by the hydrolysis of aryloxy carboxylic acid ester groups (88). The same ester functions were surface reduced to methylenehydroxy units (88). Organosilicon hydrides have been coupled to surface allyl functionalities through hydrosilylation reactions (87). Surface *p*-bromophenoxy side groups have been lithiated and reacted with organometallic iodides to give, for example, FeCp(CO)₂ covalently bound to the surface regions (89). Surface trifluoroethoxy groups in 4 were

converted to hydroxyl units by basic hydrolysis (80). One of the earliest demonstrations of the utility of polyphosphazene surface chemistry was the surface nitration of poly[bis(phenoxy)phosphazene] followed by reduction of the nitro groups to amino units, and the use of these to bind enzymes such as trypsin or glucose 6-phosphate dehydrogenase through glutaric dialdehyde coupling (79). The surface immobilized enzymes were then used in demonstration continuous flow reactors.

Advantages of Polyphosphazenes for the Development of Functional Polymers

Functional polymers in general have many uses in surface science, biomedicine, biotechnology, controlled drug delivery, separations science, human tissue engineering, membrane science, electrode modification, and in the study of adhesion. Why then are functional polyphosphazenes of special interest in view of the hundreds of more traditional polymers that already exist? The answer lies in the extraordinary combinations of properties that can be generated through the introduction of different organic or organometallic side groups. This is a consequence of the polarity and high reactivity of the P-Cl or P-F bonds in the starting polymer, and of the architecture of the polyphosphazene chain, in which side groups exist on every *other* skeletal atom, thus reducing the steric shielding constraints that exist for most organic backbone polymers. Thus, many more *starting points* for functionalization exist for polyphosphazenes than for almost any other polymer system. The inorganic backbone in polyphosphazenes confers some additional advantages such as resistance to gamma-rays and high intensity ultraviolet light. Provided chemical attack on the backbone can be avoided by the use of mild functionalization conditions, bulky hydrophobic side groups, or protection-deprotection reactions, almost no limit seems to exist to the range of functional sites that can be built into these molecules. Although most of the applications for polyphosphazenes that have been developed in the past have been based on the low reactivity of specific polymers, it seems clear that future developments will be concentrated increasingly on the functional derivatives.

Acknowledgments

I am grateful to many coworkers, including those listed in the references, for their contributions to this topic. Different aspects of this research were supported at various times by the U.S. Army Research Office, Office of Naval Research, Department of Energy, E.P.R.I., National Science Foundation, and the Federal Aviation Administration.

Literature Cited

1. Allcock, H. R. *Heteroatom Ring Systems and Polymers*, Academic Press: New York, 1967.
2. Allcock, H. R. *Phosphorus-Nitrogen Compounds. Cyclic, Linear, and High Polymeric Systems*, Academic Press: New York, 1972.
3. Allcock, H. R. Chapter in *Hydrophilic Polymers* (J. E. Glass, ed.) ACS. Symp. Ser. 1996, 248, 3.
4. Allcock, H. R. *Chemistry of Materials Review* 1994, 6, 1476.
5. Allcock, H. R.; Klingenberg, E. H. *Macromolecules* 1995, 28, 4351.
6. Ibim, S. M.; Ambrosio, A.; Larrier, D.; Allcock, H. R.; Laurencin, C. T. *J. Control. Release* 1996, 40, 31.
7. Allcock, H. R.; Ambrosio, A. M. A. *Biomaterials* 1996, 17, 2295.
8. Allcock, H. R. *Annals of the New York Academy of Sciences* (in press).
9. Allcock, H. R.; Napierala, M. E.; Olmeijer, D. L.; Cameron, C. G.;

- Kuharcik, S. E.; Reed, C. S.; O'Connor, S. J. M. *Proc. Intern. Conf. on Solid Polym. Electrolytes, Uppsala, Sweden* (in press).
10. Olshavsky, M.A.; Allcock, H. R. *Macromolecules* (in press).
 11. Allcock, H. R.; Kugel, R. L. *J. Am. Chem. Soc.* **1965**, *87*, 4216.
 12. Allcock, H. R.; Kugel, R. L.; Valan, K. J. *Inorg. Chem.* **1966**, *5*, 1709.
 13. Allcock, H. R.; Kugel, R. L. *Inorg. Chem.* **1966**, *5*, 1716.
 14. Allcock, H. R.; Mack, D.P. *J. Chem. Soc., Chem. Commun.* **1970**, *11*, 685.
 15. Allcock, H. R.; Cook, W. J.; Mack, D. P. *Inorg. Chem.* **1972**, *11*, 2584.
 16. Allcock, H. R.; Kugel, R. L.; Stroh, E. H. *Inorg. Chem.* **1972**, *11*, 1120.
 17. Allcock, H. R.; Patterson, D. B.; Evans, T. L. *Macromolecules* **1979**, *12*, 172.
 18. Allcock, H. R.; Evans, T. L. *Inorg. Chem.* **1979**, *18*, 2342.
 19. Honeyman, C. H.; Manners, I.; Morrissey, C. T.; Allcock, H. R. *J. Am. Chem. Soc.* **1995**, *117*, 7035.
 20. Allcock, H. R.; Nelson, J. M.; Reeves, S. D. *Macromolecules* (submitted).
 21. Allcock, H. R.; Reeves, S. D.; Nelson, J. M.; Crane, C. A.; Manners, I. *Macromolecules* **1997**, *30*, 2213.
 22. Nelson, J. M.; Allcock, H. R.; Manners, I. *Macromolecules* **1997**, *30*, 3191.
 23. Rose, S. H. *J. Polym. Sci. B.* **1968**, *6*, 837.
 24. Allcock, H. R.; Kim, Y.-B. *Macromolecules* **1994**, *27*, 3933.
 25. Singler, R. E.; Schneider, N. S.; Hagnauer, G. L. *Polym. Eng. Sci.* **1975**, *15*, 321.
 26. Tate, D. P. *J. Polym. Sci., Polym. Symp.* **1974**, *48*, 33.
 27. Andrianov, A. K.; Payne, L. G. in *Microparticulate Systems for the Delivery of Proteins and Vaccines* (S. Cohen and H. Bernstein, eds.) Marcel Dekker: New York, **1996**, 127.
 28. (a) Gettleman, L.; Vargo, J. M.; Gebert, P. H.; Farris, C. L.; LeBoeuf, R. J., Jr.; Rawls, H. R. *Adv. Biomed. Polymers* (C. G. Gebelein, eds.) **1987**, *55*; (b) Gettleman, L.; Farris, C. L.; Rawls, H. R.; LeBoeuf, R. J., Jr. U.S. Patent 4,432,730 (1984)..
 29. Blonsky, P. M.; Shriver, D. F.; Austin, P. E.; Allcock, H. R. *J. Am. Chem. Soc.* **1984**, *106*, 6854.
 30. Allcock, H. R.; Austin, P. E.; Neenan, T. X.; Sisko, J. T.; Blonsky, P. M. Shriver, D. F. *Macromolecules* **1986**, *19*, 1508.
 31. Blonsky, P. M.; Shriver, D. F.; Austin, P. E.; Allcock, H. R. *Polym. Mater. Sci. Eng.* **1985**, *53*, 118.
 32. Blonsky, P. M.; Shriver, D. F.; Austin, P. E.; Allcock, H. R. *Solid State Ionics* **1986**, *18 & 19*, 254.
 33. Bennett, J. L.; Dembek, A. A.; Allcock, H. R.; Heyen, B. J.; Shriver, D. F. *Chemistry of Materials* **1989**, *1*, 14.
 34. Allcock, H. R.; Napierala, M. E.; Cameron, C. G.; O'Connor, S. J. M. *Macromolecules* **1996**, *29*, 1951.
 35. Allcock, H. R.; Kuharcik, S. E.; Reed, C. S.; Napierala, M. E. *Macromolecules* **1996**, *29*, 3384.
 36. Allcock, H. R.; O'Connor, S. J. M.; Olmeijer, D. L.; Napierala, M. E.; Cameron, C. G. *Macromolecules* **1996**, *23*, 7544.
 37. Allcock, H. R.; Napierala, M. E.; Olmeijer, D. L.; Cameron, C. G.; Kuharcik, S. E.; Reed, C. S.; O'Connor, S. J. M. *Proc. Int. Conf. on Solid Polym. Electrolytes, Uppsala, Sweden* (in press).
 38. Allcock, H. R.; Ravikiran, R.; O'Connor, S. J. M. *Macromolecules* **1997**, *30*, 3184.
 39. Diefenbach, U.; Allcock, H. R. *Inorg. Chem.* **1994**, *33*, 4562.
 40. Allcock, H. R.; Bissell, Greigger, P. P.; Gardner, J. E.; Schmutz, J. L. *J. Am. Chem. Soc.* **1979**, *101*, 606.

41. Allcock, H. R.; Neenan, T. X.; Boso, B. *Inorg. Chem.* **1985**, *24*, 2656.
42. Allcock, H. R.; Evans, T. L.; Fuller, T. L. *Inorg. Chem.* **1980**, *19*, 1026.
43. Allcock, H. R.; Fuller, T. J.; Evans, T. L. *Macromolecules* **1980**, *13* 1325.
44. Allcock, H. R.; Lavin, K. D.; Tollefson, N. M.; Evans, T. L. *Organometallics* **1983**, *2*, 267.
45. Dubois, R. A.; Garrou, P. E.; Lavin, K. D.; Allcock, H. R. *Organometallics* **1984**, *3*, 649.
46. Wisian-Neilson, P.; Ford, R. R.; Neilson, R. H.; Roy, A. K. *Macromolecules* **1986**, *19(7)*, 2089.
47. Roy, A. K.; Neilson, R. H.; Wisian-Neilson, P. *Organometallics* **1987**, *6(2)*, 378.
48. Wettermark, U. G.; Wisian-Neilson, P.; Scheide, G. M.; Neilson, R. H. *Organometallics* **1987**, *6(5)*, 959.
49. Wisian-Neilson, P.; Ford, R. R. *Organometallics* **1987**, *6(10)*, 2258.
50. Wisian-Neilson, P.; Islam, M. S.; Ganapathiappan, S.; Scott, D. L.; Rughuveer, K. S.; Ford, R. R. *Macromolecules* **1989**, *22(11)*, 4382.
51. Wisian-Neilson, P.; Islam, M. S. *Macromolecules* **1989**, *22(4)*, 2026.
52. Montoneri, E.; Gleria, M.; Ricca, G.; Pappalardo, G. C. *J. Macromol. Sci. Chem.* **A26**, **1989**, *4*, 645.
53. Montoneri, E.; Gleria, M.; Ricca, G.; Pappalardo, G. C. *Makromol. Chem.* **1989**, *190(1)*, 191.
54. Allcock, H. R.; Fitzpatrick, R. J. *Chemistry of Materials* **1991**, *3*, 1120.
55. Allcock, H. R.; Klingenberg, E. H.; Welker, M. F. *Macromolecules* **1993**, *26*, 5512.
56. Allcock, H. R.; Smith, D. E. *Chemistry of Materials* **1995**, *7*, 1469.
57. Allcock, H. R.; Evans, T. L.; Fuller, T. L. *Inorg. Chem.* **1980**, *19*, 1026.
58. Allcock, H. R.; Kwon, S. *Macromolecules* **1989**, *22*, 75.
59. Cohen, S.; Bano, M. C.; Visscher, K. B.; Chow, M.; Allcock, H. R.; Langer, R. *J. Am. Chem. Soc.* **1990**, *112*, 832.
60. Bano, M. C.; Cohen, S.; Visscher, K. B.; Allcock, H. R.; Langer, R. *Biotechnology* **1991**, *9*, 468.
61. Cohen, S.; Bano, M. C.; Cima, L. G.; Allcock, H. R.; Vacanti, J. P.; Vacanti, C. A.; Langer, R. *Clinical Materials* **1993**, *13*, 3.
62. Andrianov, A.; Cohen, S.; Langer, R.; Visscher, K. B.; Allcock, H. R. *J. Control. Release* **1993**, *27*, 69.
63. Cohen, S.; Allcock, H. R.; Langer, R. *Minutes* (Editions de Sante, France) **1993**, 36.
64. Payne, L. G.; Jenkins, S. A.; Andrianov, A.; Roberts, B. E. in *Vaccine Design: The Subunit and Adjuvant Approach* (M. F. Powell and M. J. Newman, eds.) Plenum Press: New York, **1995**, 473.
65. Andrianov, A. J.; Sargent, J. R.; Sule, S. S.; LeGolvan, M. P.; Payne, L. G. *Am. Chem. Soc. Polym. Sci. Eng.* **1997**, *76*, 367.
66. Andrianov, A. K.; LeGolvan, M. P.; Sule, S. S.; Payne, L. G. *Amer. Chem. Soc. Polym. Sci. Eng.* **1997**, *76*, 369.
67. TenHuisen, K. S.; Brown, P. W.; Reed, C. S.; Allcock, H. R. *J. Mater. Sci. Mater. Med.* **1996**, *7*, 673.
68. Reed, C. S.; TenHuisen, K. S.; Brown, P. W.; Allcock, H. R. *Chemistry of Materials* **1996**, *8*, 440.
69. Reed, C. A.; Taylor, J. P.; Guigley, K. S.; Kully, K. S.; Bernheim, K. A.; Coleman, M. M.; Allcock, H. R. *J. Polym. Sci. & Eng.* (submitted)
70. Allcock, H. R.; Fuller, T. J.; Mack, D. P.; Matsumura, K.; Smeltz, K. M. *Macromolecules* **1977**, *10*, 824.
71. Allcock, H. R.; Pucher, S. R.; Scopelianos, A. G. *Macromolecules* **1994**, *27*, 1071.

72. Laurencin, C. T.; El-Amin, S. F.; Ibim, S. E.; Willoughby, D. A.; Attawia, M.; Ambrosio, A.; Allcock, H. R. *J. Biomed. Mater. Res.* **1996**, *30*, 133.
73. Olshavsky, M. A.; Allcock, H. R. *Chemistry of Materials* **1997**, *9*, 1367.
74. Allcock, H. R.; Scopelianos, A. G. *Macromolecules* **1983**, *16*, 715.
75. Allcock, H. R.; Kwon, S. *Macromolecules* **1988**, *21*, 1980.
76. Allcock, H. R.; Klingenberg, E. H.; Welker, M. F. *Macromolecules* **1993**, *26*, 5512.
77. Greene, T. W.; Wuts, P. G. M. *Protective Groups in Organic Synthesis*, 2nd ed., Wiley-Interscience: New York, **1991**.
78. Allcock, H. R.; Hymer, W. C.; Austin, P. E. *Macromolecules* **1983**, *16*, 1401.
79. Allcock, H. R.; Kwon, S. *Macromolecules* **1986**, *19*, 1502.
80. Allcock, H. R.; Rutt, J. S.; Fitzpatrick, R. J. *Chemistry of Materials* **1991**, *3*, 442.
81. Allcock, H. R.; Fitzpatrick, R. J. *Chemistry of Materials* **1991**, *3*, 450.
82. Allcock, H. R.; Pucher, S. R.; Fitzpatrick, R. J. *Biomaterials* **1992**, *13*, 857.
83. Allcock, H. R.; Fitzpatrick, R. J. *Chemistry of Materials* **1991**, *3*, 1120.
84. Allcock, H. R.; Fitzpatrick, R. J.; Salvati, L. *Chemistry of Materials* **1992**, *4*, 769.
85. Allcock, H. R.; Fitzpatrick, R. J.; Visscher, K. B. *Chemistry of Materials* **1992**, *4*, 775.
86. Allcock, H. R.; Nelson, C. J.; Coggio, W. D. *Chemistry of Materials* **1994**, *6*, 516.
87. Allcock, H. R.; Smith, D. E. *Chemistry of Materials* **1995**, *7*, 1469.
88. Allcock, H. R.; Morrissey, C. T.; Way, W. K.; Winograd, N. *Chemistry of Materials* **1996**, *8*, 2730.
89. Allcock, H. R.; Silverberg, E. N.; Nelson, C. J.; Coggio, W. D. *Chemistry of Materials* **1993**, *5*, 1307.

Synthesis of Biodegradable Copolymers with Pendant Hydrophilic Functional Groups

S. Jin and K. E. Gonsalves¹

Department of Chemistry and Polymer Program at the Institute of Materials Science, U-136, University of Connecticut, Storrs, CT 06269

Copolymers with hydrophilic groups pendant on the backbone of two biodegradable polymers polylactide and poly(ϵ -caprolactone) were synthesized and characterized. Poly(lactic acid-*co*-serine) with 2% and 6% of free hydroxy groups were synthesized by ring opening polymerization reactions. The ϵ -caprolactone copolymers with phosphonic acid (P(O)(OH)₂), phosphoester (P(O)(OMe)₂) and carboxylic acid (COOH) functional groups were synthesized by using free radical polymerizations of 2-methylene-1,3-dioxepane (MDO) and three vinyl monomers: vinylphosphonic acid, dimethylvinylphosphonate and acrylic acid, respectively. These copolymers were characterized by FT-IR, ¹H and ¹³C NMR spectra. The thermal properties, molecular weights, and solubility behavior of the above copolymers are also discussed.

Aliphatic polyesters are one of the most widely utilized classes of biodegradable polymers in medicine (1-2). Among these, polylactide and poly(ϵ -caprolactone) polymers are few degradable polymers used clinically. The introduction of functional groups in polylactide for the modification of its properties have been investigated. Barrera et al synthesized a copolymer poly(lactic acid-*co*-lysine) containing lysine residues (3-4). The free amino group in the lysine residue was used to chemically attach a biologically active peptide GRGDY (3). Other biodegradable copolymers with functional groups, such as carboxylic acid, have also been synthesized (5-9). We synthesized a copolymer poly(lactic acid-*co*-serine) with different amounts of free hydroxy functional groups. The latter were reacted with diisocyanate ended poly(ethylene glycol) to give low T_g and less crystalline copolymers.

The free radical polymerizations of cyclic ketene acetals have recently evoked a lot of interest (10-13). The poly(ϵ -caprolactone) (PCL) can be synthesized by free radical ring opening polymerization (10). The copolymerization of its monomer, 2-methylene-1,3-dioxepane (MDO), with some vinyl monomers resulted in an aliphatic ester backbone, as well as the pendant functional groups from the vinyl monomers (10). By free radical polymerization of MDO and the vinyl monomers: vinylphosphonic acid (VPA), dimethylvinylphosphonate (VPE) and acrylic acid (AA), we synthesized a series of biodegradable copolymers including PCL

¹Corresponding author.

backbones and pendant hydrophilic functional groups: phosphoric acid, dimethylphosphonate and carboxylic acid groups, respectively. These copolymers have both hydrophobic ester backbones and hydrophilic side groups. The presence of ionic groups on the surface of the polymers is very important for the preparation of organic polymer-inorganic composite materials (14-18).

Experimental

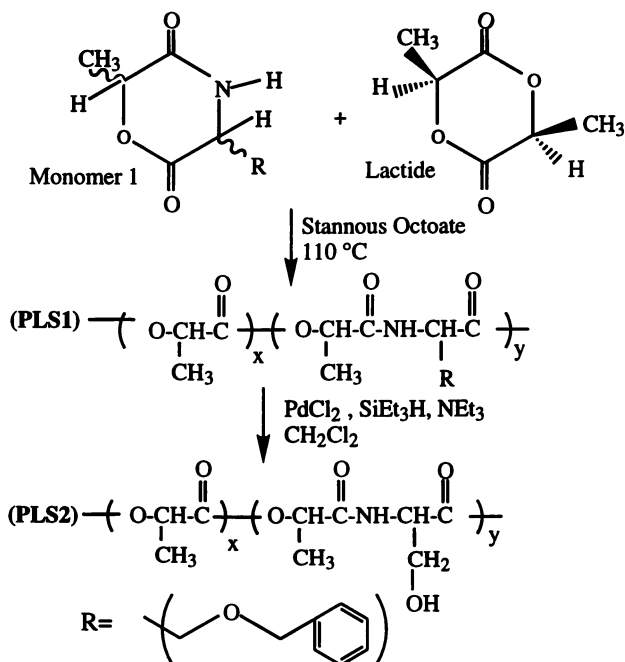
Synthesis of Poly(lactide Copolymers. The synthesis of monomer Monomer 1 and the copolymers poly(lactide-co-serine) (PLS1) were similar to the method by Barrera *et al.* (3). The ring opening polymerization of Monomer 1 and lactide is shown in Scheme 1. Different feed ratios of Monomer 1 to lactide (6 mol% and 20 mol%, respectively) were used. The copolymers were deprotected to give copolymers PLS2 with free hydroxy groups (3). The copolymers PLS2 were reacted with diisocyanate terminated poly(ethylene glycol) (DIPEG) to give grafted copolymer PLSPEG(a) and crosslinked copolymer PLSPEG(b), depending on the percentage of the free hydroxy groups in PLS2, as depicted in Scheme 2.

Synthesis of Poly(ϵ -caprolactone) Copolymers. The synthesis of the monomer 2-methylene-1,3-dioxepane (MDO) was similar to that by Bailey *et al.* (10). The purity of MDO was examined by GC-MS and found to be 99.99% pure. Homopolymers, polyester P(MDO), poly(vinylphosphonic acid) (P(VPA)), poly(dimethylvinylphosphonate) (P(VPE)) and copolymers, poly(ϵ -caprolactone-co-vinylphosphonic acid) (P(MDOVPA)), poly(ϵ -caprolactone-co-dimethylvinyl phosphonate) (P(MDOVPE)) and poly(ϵ -caprolactone-co-acrylic acid) (P(MDOAA)), were synthesized following Scheme 3 by using AIBN as the initiator. Pressure tubes were heated at 300 °C overnight and then were transferred into a glove box. All the chemicals were added in the glove box. The comonomer molar feed ratio used in all the polymerization reactions was 1:1. The reaction mixture was heated in an oil bath at 50 °C and was stirred for different time periods. After the reactions, the tubes were removed from the oil bath, and different solvents were added into the mixtures to dissolve or disperse the polymers. Since the solubility of each copolymer was different, the purification technique for each copolymer had to be varied. P(MDOVPA) swelled in water, and the hydrogel formed was filtered, followed by washing with water and CHCl₃. P(MDOVPE) was dissolved in CHCl₃, and was precipitated in hexane. P(MDOAA) was dispersed in CHCl₃ and filtered. After drying, it was immersed in water and then filtered. The copolymer samples were dried in a vacuum oven overnight. For each copolymer, the copolymerization time and yield are listed in Table 1.

Table 1 Poly(ϵ -caprolactone) copolymers and their composition and thermal properties

Copolymer	Polymerization Time (h)	Yield (%)	Ester mol %	T _g (°C)	M _w	M _n
P(MDOVPA)	48	78	19	74	-	-
P(MDOVPE)	48	72	33	9	146,000	43,000
P(MDOAA)	24	51	47	10	-	-

- Molecular weight not measured



Scheme 1 Synthesis of Functionalized Poly(lactide) Copolymers

Results and Discussion

Poly(lactide) Copolymers. After deprotecting, 2 mol% and 6 mol% of serine with free hydroxy groups were incorporated into the poly(lactide) for 6 mol% and 20 mol% feed ratios, respectively. These copolymers PLS2 were functionalized polyesteramide copolymers with high molecular weights (M_w s of PLS2 are 88,000 and 45,000, respectively, relative to polystyrene). The addition of the serine unit into the lactide has been established by analyzing the ^1H NMR spectrum of the unprotected copolymers PLS1. Analysis of the ^1H NMR spectrum of PLS1 [6 mol% feed ratio, Figure 1(a)] showed an aromatic peak around 7.3 ppm. After deprotecting, the integration of the aromatic peak decreased [Figure 1(b)]. The presence of the free hydroxy groups in the copolymers was proved by reaction with DIPEG. Grafted or crosslinked copolymers [PLSPEG(a) or PLSPEG(b)] were formed, and the formation of the urethane was identified by analyzing the IR spectra. The new peaks in the IR spectra [Figure 2(d) and (e) for PLSPEG(a) and PLSPEG(b), respectively] were due to the urethane. Due to the addition of the flexible poly(ethylene oxide) chain, the glass transition temperature (T_g) of the polymer PLSPEG (4 $^{\circ}\text{C}$) was much lower than that of poly(lactide) (64 $^{\circ}\text{C}$) and also the copolymer (60 $^{\circ}\text{C}$). The addition of the flexible chain into poly(lactide) is a means of increasing the amorphous property of poly(lactide).

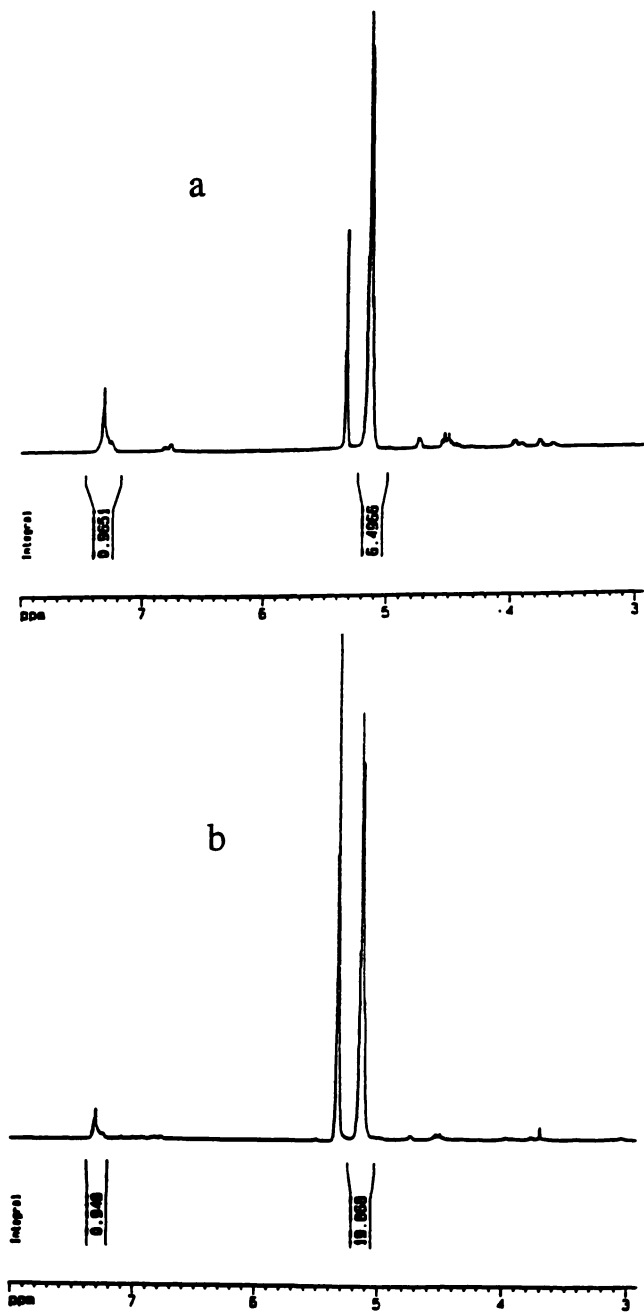


Figure 1 ^1H NMR spectra (CDCl_3) of polylactide copolymers with 6 mol% feed ratio (a) PLS1, and (b) PLS2.

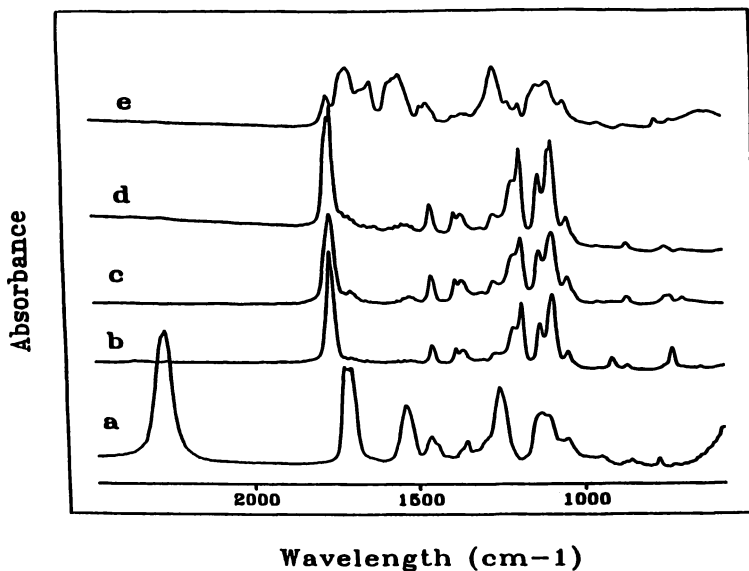


Figure 2 FT-IR spectra of the polymers (a) DIPEG, (b) PLS1, (c) PLS2, (d) PLSPEG(i), and (e) PLSPEG(ii).

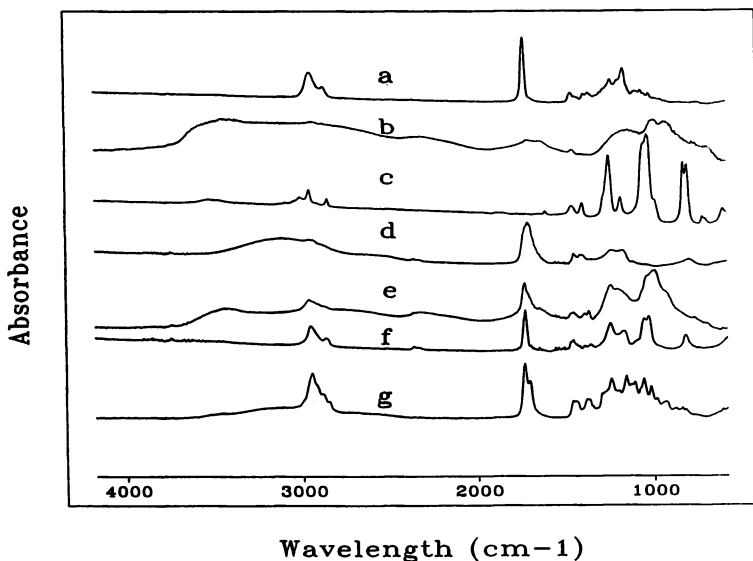


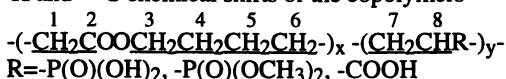
Figure 3 FT-IR spectra of ϵ -Caprolactone copolymers (a) P(MDO), (b) P(VPA), (c) P(VPE), (d) P(AA), (e) P(MDOVPA), (f) P(MDOVPE), and (g) P(MDOAA).

respectively, as measured in our laboratory. T_g of VPA homopolymer was not obtained due to its degradation before reaching the glass transition temperature.).

The molecular weight of the copolymer P(MDOVPE) was measured by using GPC (Table 1). The molecular weight of this copolymer was high, but the molecular weight distribution was broad, probably because of the poor mixing during bulk polymerization. The other two copolymers were not soluble in any solvents or mixture of solvents. Molecular weight of these copolymers were not measured.

Solubility. The solubility of the copolymers varied with different pendant functional groups on the backbones, and is listed in Table 3. All the copolymers had both hydrophilic (pendant functional groups) and hydrophobic (ester and vinylene) parts. P(MDOVPA) had a very hydrophilic phosphonic acid group. The polymer was not soluble in any solvents that were tried. It swelled in water and formed a hydrogel with very high swelling ratio (276%). Hydrogels are usually crosslinked either chemically or physically to maintain the three-dimensional network (20). The hydrogel formation in this case was probably caused by physical crosslinking, resulting from the strong intramolecular and intermolecular hydrogen bonding between the phosphonic acid $P(O)(OH)_2$ and the ester $-CO$ in the backbone. The physical crosslinking was not broken in the presence of water, although there are some interactions between water and the phosphonic acid groups (21-22). P(MDOVPE) had very good solubility in all the solvents that were tried because of the presence of the hydrophilic $-P(O)(OMe)_2$ pendant groups. P(MDOAAA) swelled in less polar solvents such as $CHCl_3$ but not in polar solvents such as water, probably because of the breaking of the hydrogen bonding in the presence of water (21-22).

Table 2 1H and ^{13}C chemical shifts of the copolymers



Copolymer	1H position or ^{13}C position								
	1	2	3	4	5	6	7	8	H or C in R
P(MDOVPA)									
1H	2.2	-	4.0	1.5-----1.7			1.9-----3.6	5-8	
^{13}C	29.3	170.6 173.7	60.4 63.5	28.6	24.6	27.0	20.9	171.5	-
P(MDOVPE)									
1H	2.3	-	4.0	1.6	1.4	1.6	1.2--2.8		3.8
^{13}C	34.2	171.9 173.6	64.2 65.0	26.0	24.7	25.6	25--34		52.8
P(MDOAAA)									
1H	2.3	-	4.0	1.6	1.3	1.6	1.2-3.0		-
^{13}C	34.3	171.2 172.1	64.0 64.7	25.7	24.8	25.4	21-30	36-41	175.0

Table 3 Solubility of Poly(ϵ -caprolatone) copolymers

Copolymer	Solvent					
	CHCl ₃	MeOH	DMSO	m-Cresol	H ₂ O	CH ₃ COOH
P(MDOVPA)	-	o	o	o	o	-
P(MDOVPE)	+	+	+	+	+	+
P(MDOAA)	o	o	o	o	-	o

+ soluble - not soluble o swelling

Conclusion

A series of polyester copolymers with hydrophilic functional groups were successfully synthesized and characterized. These polymers have biodegradable polyester in the polymer backbone as well as pendant hydrophilic functional groups. Also, the properties of the copolymers can be modified by changing the feed ratio of the comonomers. The copolymers have the potential of biodegradability. The presence of these functional groups will be used for making biodegradable polymer-inorganic hybrid materials.

Literature Cited

1. *Polymeric Materials*; Dumitriu, S., Ed.; Marcel Dekker, Inc., New York, **1993**.
2. *Biodegradable Polymers as Drug Delivery Systems*; Chasin, M.; Langer, R., Eds.; Marcel Dekker, Inc., New York, **1990**.
3. Barrera, D. A.; Zylstra, E. P.; Lansbury, T.; Langer, R. *J. Am. Chem. Soc.* **1993**, 115, pp 11010.
4. Hrkach, J. S.; Ou, J.; Lotan, N.; Langer, R. *Macromolecules* **1995**, 28, pp 4736.
5. In't Veld, P. J. A.; Dijkstra, P. J.; Feijen, J. *Makromol. Chem.* **1992**, 193, pp 2713.
6. Arndt, S. C.; Lentz, R. W. *Makromol. Chem. Macromol. Symp.* **1986**, 6, pp 285.
7. Caron, A.; Braud, C.; Bunel, C.; Vert, M. *Polymer* **1990**, 31, pp 1797.
8. Gelbin, M. E.; Kohn, J. *J. Am. Chem. Soc.* **1992**, 114, pp 3962.
9. Fieter, J.; Borgne, A. L.; Spassky, N. *Polym. Bull.* **1990**, 24, pp 348.
10. Bailey, W. J.; Wu, S. R.; Ni, Z. *J. Polym. Sci., Polym. Chem. Ed.* **1982**, 20, pp 3021.
11. Pan, C. Y.; Wang, Y. *J. Polym. Sci., Polym. Chem. Ed.* **1988**, 26, pp 2737.
12. Bailey, W. J.; Cho, J. L.; Feng, P. Z.; Issari, B.; Kuruganti, V.; Zhou, L. *J. Macromol. Sci.-Chem.* **1989**, A25 (5-7), pp 781.
13. Bailey, W. J.; Wu, S. R.; Ni, Z. *Makromol. Chem.* **1982**, 183, pp 1913.
14. Zhang, S.; Gonsalves, K. E. *Mater. Sci. Eng.* **1995**, C3, pp 117.
15. Rawls, H. R.; Martels, T.; Arends, J. *J. Coll. And Inter. Sci.* **1982**, 87, pp 339.

16. Kallitsis, K.; Kautsoukos, P. G. *Langumir* **1991**, 7, pp 1882.
17. *Polymers of Biological and Biomedical Significance*; Shalaby, S. W.; Ikada, Y.; Langer, R.; Willams, J., Eds. ACS Symposium Series 540, **1994**, Chapter 10.
18. Mucalo, M. R.; Yokogawa, Y.; Toriyama, M.; Suzuki, T.; Kawamoto, Y.; Nagata, F.; Nishizawa *J. Mater. Sci., Mater. in Med.* **1995**, 6, pp 597& 658.
19. Zhu, P. C.; Pittman, C. U. Jr. *J. Polym. Sci.: Part A: Polym. Chem.* **1996**, 34, pp 73.
20. *Hydrogels and Biodegradable Polymers for Bioapplications*; Ottenbrite, R. M.; Huang, S. J.; Park, K., Eds. ACS Symposium 627, ACS, **1996**, Chapter 1.
21. Jeffrey, G. A.; Saenger, W. *Hydrogen Bonding in Biological Structures*, Springer-Berlin Heidelberg, **1991**, Chapter 8
22. Jeffrey, G. A., *An Introduction to Hydrogen Bonding* Oxford University Press, New York, **1997**, Chapt. 4.

Chapter 20

Photoinitiated Ring-Opening Polymerization of Epoxidized Polyisoprene

C. Decker and T. Hoang Ngoc

Laboratoire de Photochimie Générale (URA-CNRS n°431), Ecole Nationale Supérieure de Chimie, Université de Haute-Alsace 3, rue Werner, 68200 Mulhouse, France

Epoxy-functionalized polyisoprene has been cross-linked by UV-irradiation in the presence of a cationic photoinitiator. The reaction kinetics has been monitored by IR spectroscopy and shown to proceed extensively within less than 1 s upon intense illumination. From the conversion dependence of the insolubilization process, it was concluded that both inter- and intramolecular propagation reactions occur during the polymerization of the epoxy ring. Blends of epoxidized polyisoprene and difunctional vinyl ether or acrylate monomers were shown to undergo a fast and extensive cross-linking polymerization, with formation of interpenetrating polymer networks. The kinetic chain length was evaluated from quantum yield measurements and found to be on the order of 1000 epoxy groups polymerized per initiating proton.

Light-induced polymerization of functionalized oligomers or polymers is one of the most efficient methods for generating rapidly tridimensional polymer networks^{1,2}. A few second exposure to intense UV radiation in the presence of an adequate photoinitiator is usually sufficient to obtain a tightly cross-linked and totally insoluble polymer. This process, called UV-curing, is currently applied to a large variety of polymers bearing functional groups which undergo either radical polymerization (acrylate, maleate) or cationic polymerization (epoxy, vinyl ether). Polymer networks with tailor-made properties have thus been synthesized by acting on the chemical structure of the polymer chain (polyurethane, polyester, polyphenoxy, silicones), as well as on the nature and number of the functional groups. Recently, the UV-curing technology has been successfully applied to the vulcanization at ambient temperature

of rubber-based materials, previously functionalized by epoxy³⁻⁶ or acrylate^{7,8} groups. In this article, we report the cross-linking of epoxidized polyisoprene (EPI) by photoinitiated cationic polymerization of the in-chain epoxy rings. In some experiments, difunctional monomers have been blended to the epoxidized rubber in order to accelerate the curing process and to generate interpenetrating polymer networks. Both the kinetics of these ultrafast reactions and the properties of the photocured polymers have been examined, in consideration of the potential applications of these organic materials in various industrial sectors, in particular as coatings, adhesives and photoresists.

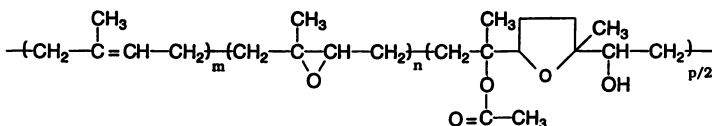
Experimental

Materials. The epoxidation of liquid natural rubber ($M_w = 8000$) was carried out by mixing a chloroform solution of the polymer and an acetic acid solution of peracetic acid at 5°C for 6 h, according to the method of Burfield⁹. The epoxidized liquid natural rubber (ELNR) was recovered by precipitation in methanol and dried under vacuum at 50°C. The epoxy content was measured by IR spectroscopy to be 8.1 mol kg⁻¹, which indicates that 70% of the isoprene double bonds have been transformed, i.e. 75 epoxy rings per EPI chain. Samples with lower epoxy content (40%, 50% or 60%) were obtained by shortening the reaction time. Photocross-linking experiments were also performed on two other EPI samples : (i) an epoxidized natural rubber (ENR-55) in which 55% of the isoprene units have been epoxidized, and (ii) an epoxidized cyclized rubber (ECR) in which 80% of the isoprene units have been cyclized and all of the remaining double bonds have been epoxidized.

In some experiments, a difunctional monomer, hexanediol diacrylate (HDDA from UCB) or divinyl ether of triethyleneglycol (DVE-3 from ISP), was mixed to EPI in various weight ratios. The epoxidized polymer was blended at 40°C to the monomer containing the photoinitiator. A hexafluorophosphate triarylsulfonium (TAS) salt was used as cationic photoinitiator (Cyracure UVI-6990 from Union Carbide), typically at a weight concentration of 3%. It proved to be well soluble in EPI, at TAS concentrations up to 5%, because of both the low molecular weight and the high epoxy content of the polymer. For acrylate-based formulations, an acyl phosphine oxide (Lucirin TPO from BASF) was used, in addition, as radical photoinitiator. The chemical formulas of the various compounds used in this study are given in Figure 1.

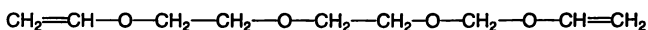
Irradiation. The liquid formulation was applied with a calibrated bar onto either a KBr crystal for infrared analysis, or a glass plate for hardness and gel fraction measurements. 10 to 20 μm thick films were exposed to the radiation of a 80 W/inch medium pressure mercury lamp, in the presence of air, at a passing speed of 60 m/min, which corresponds to a 0.1 s exposure at each pass. The incident light intensity (I_0) at the sample position was measured by radiometry (International Light IL-390) and

Functional polymer : Epoxidized polyisoprene (EPI)

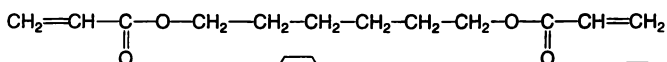


EPI	m	n	p	[Epoxy] mol/kg
ELNR 40	60	40	-	5.4
ELNR 50	50	50	-	6.5
ELNR 60	25	60	15	7.1
ELNR 70	14	70	16	8.1
ENR 55	30	55	15	6.5

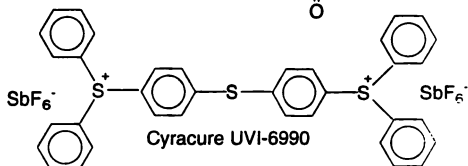
Difunctional monomers : Divinyl ether of triethylene glycol (DVE-3)



Hexanediol diacrylate



Cationic photoinitiator



Radical photoinitiator

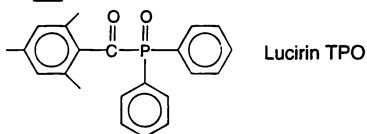


Fig. 1 Chemical formulas of products used.

found to be on the order of 500 mW cm^{-2} . Some photocuring experiments have also been performed by simply exposing the sample outdoor to sunlight.

Analysis. The kinetics of the light-induced cross-linking of EPI-based coatings was studied by infrared spectroscopy, by following the decrease upon UV exposure of the absorption bands characteristic of the related functional groups : epoxy ring at 877 cm^{-1} , vinyl ether and acrylate double bonds at 1628 and 812 cm^{-1} , respectively. The degree of conversion (x) was calculated from the equation :

$$x = 1 - \frac{(A_\lambda)_t - (A_\lambda)_{BG}}{(A_\lambda)_0 - (A_\lambda)_{BG}}$$

where $(A_\lambda)_0$ and $(A_\lambda)_t$ are the sample absorbances at the considered IR wavelength before and after UV exposure, respectively, and $(A_\lambda)_{BG}$ the absorbance of the background. The gel fraction of the UV cured polymer was determined by soaking the sample in toluene for 2 days at room temperature. The insoluble polymer was recovered by filtration and dried at 40°C to a constant weight. The degree of swelling (DS), which is inversely related to the cross-link density, was determined from the weight ratio of the swollen polymer to the dry polymer : $DS = (P_{\text{swollen}} / P_{\text{dry}}) - 1$. The hardness of the irradiated coating was evaluated by measuring the damping time of the oscillations from 12 to 4° of a pendulum placed onto the sample (Persoz hardness). Persoz values typically range from 50 s for soft elastomers to 300 s for hard polymer materials.

Photocross-linking of Epoxidized Polyisoprene.

The ring-opening polymerization of the EPI epoxy groups was followed by IR spectroscopy and shown to proceed rapidly upon UV exposure. The photoinitiated chain reaction can be formally written as follows :

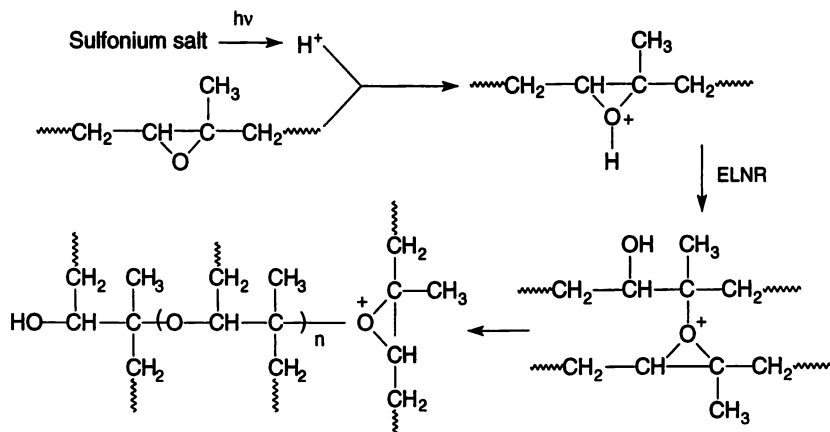
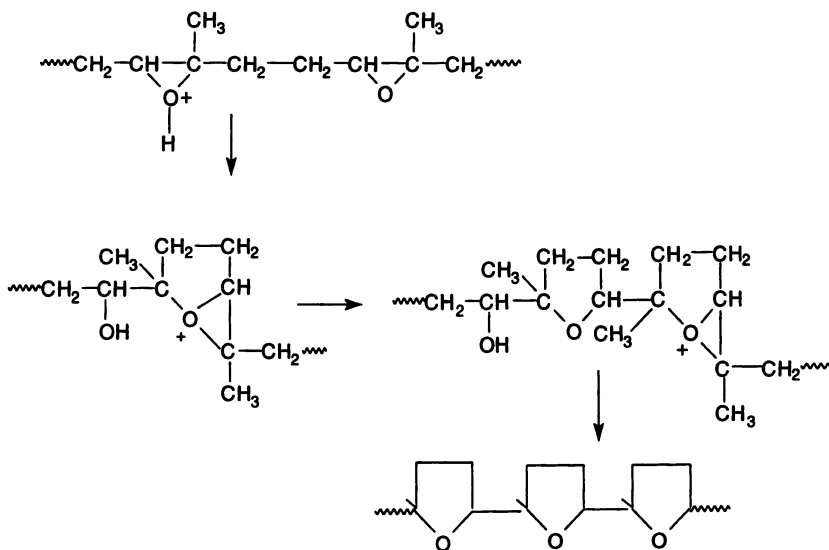


Figure 2 shows the conversion *versus* time profiles obtained for the four ELNR samples examined. For ELNR-70, a 0.4 s irradiation proved to be sufficient to polymerize half of the oxirane groups. From the initial slope of the conversion *versus* time curve, the initial rate of polymerization was evaluated to be on the order of $18 \text{ mol kg}^{-1} \text{ s}^{-1}$. The marked slowing down observed after 30% conversion was attributed to both molecular mobility restrictions brought upon by gelation of the irradiated sample and a rapid drop of the initiation rate due to the photolysis of the onium salt (Fig.2). Therefore, the photo-cured polymer emerging from the UV-oven contains a significant amount of unreacted epoxy groups (1.6 mol kg^{-1}). However, the cationic ring-opening polymerization was found to continue to proceed slowly in the dark, so that the irradiated sample was essentially free of residual epoxy groups after two days of storage at ambient temperature.

It can be seen in Figure 2 that different conversion *versus* time profiles have been obtained for the four ELNR samples epoxidized at various levels (40 to 70%). If the rate of polymerization were proportional to the concentration of epoxy groups, one should get a single curve for the four samples. Actually the rate of polymerization shows an accelerated profile with the epoxy initial content, instead of the expected linear variation (Fig.3). This result can be accounted for by considering that the polymerization reaction is involving, not only epoxy groups of different ELNR chains, but also neighboring epoxy groups located on the same polymer chain. Such an intramolecular process is expected to become increasingly important as the number of epoxy groups per chain is growing. It will lead to the formation of tetrahydrofuran structures on the polymer chain, according to the following scheme :



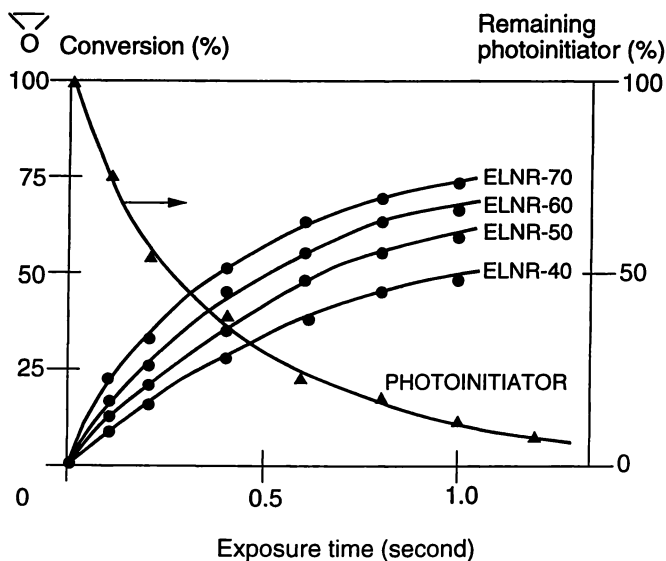


Fig.2 Influence of the epoxy content on the photoinitiated cationic polymerization of epoxidized liquid natural rubber (ELNR). (●) Photolysis of the photoinitiator (▲) : [TAS] = 3 wt %.

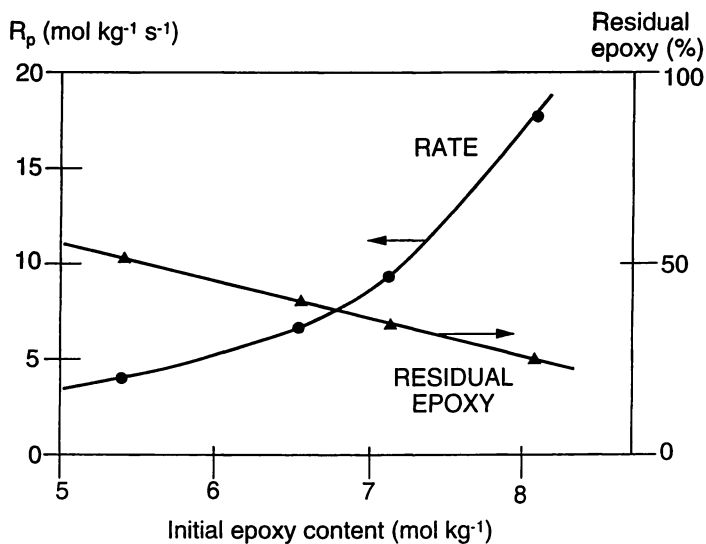


Fig.3 Dependence of the rate of polymerization (●) on the initial epoxy content of ELNR. (▲) : residual epoxy content in a 1 s UV-exposed ELNR sample.

THF structures have indeed been characterized by ^{13}C -NMR spectroscopy in epoxidized polyisoprene exposed to UV radiation in the presence of a sulfonium photoinitiator ⁵.

The polymerization of epoxy groups located on different EPI chains leads to the formation of a tridimensional polymer network and therefore to insolubilization. The gelation kinetics is very similar to that of the conversion (Fig.4). The UV-cured polymer has a strong elastomeric character, as shown by the low value of the Persoz hardness (80 s after a 2 s exposure). As expected, the cross-link density of the network increases with the exposure time, as shown by the sharp drop of the swelling ratio which levels off after 1 s. The relatively large value reached ($\text{DS} = 5$) indicates the formation of a loose polymer network, i.e., a poorly efficient intermolecular cross-linking process. This conclusion could already have been drawn from the fact that insolubilization of EPI required the polymerization of more than 80% of the epoxy groups, as shown by the gel fraction *versus* conversion curve of Figure 5. Because, theoretically, only a few interchain ether linkages need to be formed to get an insoluble material, this high value of the conversion (60 epoxy rings polymerized per EPI chain) indicates that most of the epoxy groups do polymerize by an intramolecular process with formation of primary cycles which do not affect the polymer solubility.

Photocross-linking of epoxidized polyisoprene - vinyl ether blends

When divinylether of triethyleneglycol (DVE-3) was added to ELNR-70, in a 1 to 2 weight ratio, the photoinitiated cationic polymerization of the epoxy groups was found to proceed substantially faster and more extensively than in the neat EPI, as shown in Figure 6. After a 0.4 s exposure, as many as 95% of the epoxy groups had already polymerized, with formation of a tack-free film, compared to less than 50% for the vinyl ether-free sample. The rate increase was found to be directly related to the added amount of DVE-3 (Fig.6). The accelerating effect of DVE-3 was attributed to the decrease of the formulation viscosity which will favor the propagation of the cationic polymerization, as already shown in the UV-curing of cycloaliphatic epoxides and vinyl ether functionalized resins ¹⁰. Similar results have been obtained with an epoxidized natural rubber (ENR-55) containing 20% by weight of divinyl ether of diethyleneglycol, which acts as a reactive plasticizer ¹¹.

The viscosity factor was also taken as responsible for the observed slowing down of the polymerization of DVE-3 when ELNR-70 was added to this monomer (Fig.7). For instance, a five fold decrease of the rate of polymerization of the vinyl ether double bond was noticed in the highly viscous 1 to 10 blend by weight of DVE-3 and ELNR-70. Despite the faster cure, insolubilization of the irradiated sample was not taking place more rapidly when DVE-3 was added to EPI (Fig.8), which means that a certain level of insolubilization requires a higher degree of conversion of the epoxy

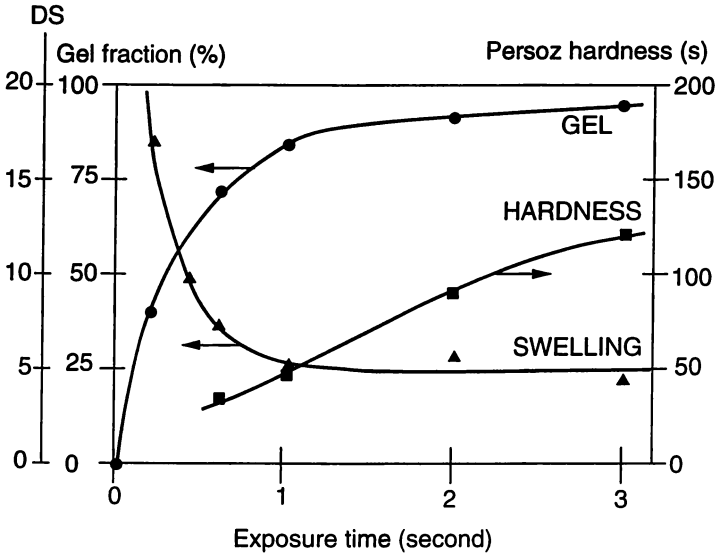


Fig.4 Influence of the exposure time on the insolubilization (●), the swelling (▲) and the hardening (■) of ELNR-70.

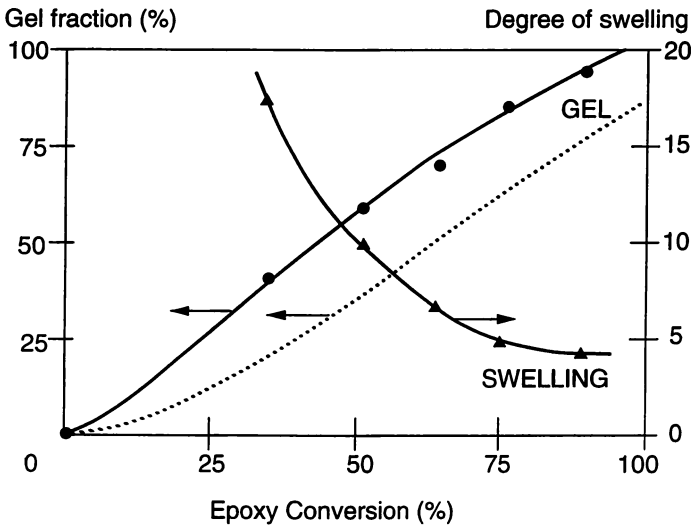


Fig.5 Dependence of the insolubilization (●) and the swelling (▲) on the epoxy conversion in UV-cured ELNR-70. ----- : Blend of DVE-3 and ELNR-70 in a 1 to 2 weight ratio.

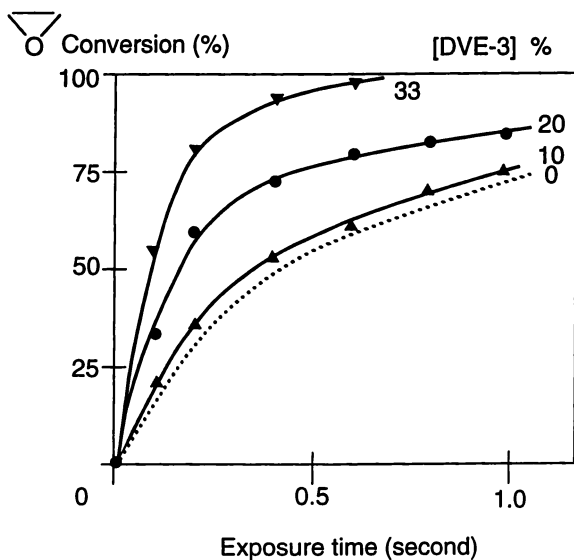


Fig.6 Influence of the DVE-3 concentration on the polymerization of the epoxy group, upon UV irradiation of DVE-3/ELNR-70 blends. [DVE-3] = 10% (\blacktriangle), 20% (\bullet) and 33% (\blacktriangledown).----- : neat ELNR-70.

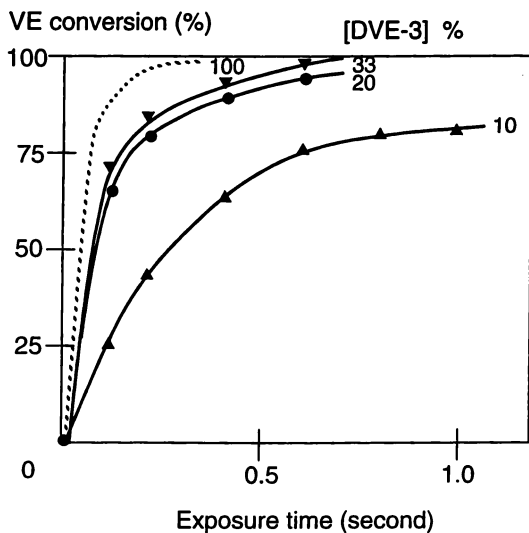


Fig.7 Influence of the DVE-3 concentration on the polymerization of the vinyl ether group, upon UV irradiation of DVE-3/ELNR-70 blends. [DVE-3] = 10% (\blacktriangle), 20% (\bullet) and 33% (\blacktriangledown).----- : neat ELNR-70.

group to be reached for the blend than for the neat EPI, as shown in Figure 5. This result suggests that the presence of DVE-3 is favoring the intramolecular polymerization of the epoxy group, probably because the added monomer is separating the EPI molecules from one another. On the other hand, the UV-cured polymer was found to be at least as cross-linked when DVE-3 was present, based on the swelling ratio : 4.0 for the DVE-3/ELNR-70 blend in a 1 to 4 weight ratio, compared to 4.8 for the neat ELNR-70. This trend, which became more pronounced as the DVE-3 content was increased (DS = 2.5 for a 1/1 blend), as shown in Figure 8, can be attributed to the additional contribution of the difunctional vinyl ether monomer to the building up of the polymer network.

In systems undergoing cross-linking polymerization, it is usually not possible to evaluate the kinetic chain length because of the formation of a polymer of infinite molecular weight. One of the distinct advantages of photoinitiation is to make this quantity accessible through quantum yield measurements. The kinetic data reported in Figures 6 and 7 have been used to evaluate the polymerization quantum yield, Φ_p , i.e. the number of epoxy or vinyl ether functions polymerized per photon absorbed by the irradiated sample. Φ_p was calculated from the equation :

$$\Phi_p = \frac{[M]_t \text{ mol l}^{-1} \times l \text{ cm}}{10^3 \times t \text{ s} \times f \times I_0 \text{ E s}^{-1} \text{ cm}^{-2}}$$

where $[M]_t$ is the amount of functional groups polymerized after UV exposure during time t at a light intensity I_0 , f being the fraction of incident light absorbed by the sample of thickness l . In the early stage of reaction (up to 40% conversion), the polymerization quantum yield was calculated to be 750 mol E⁻¹ for the epoxy group and 620 mol E⁻¹ for the vinyl ether. By taking an average value of 0.7 for the initiation quantum yield of the triarylsulfonium salt, the kinetic chain length of both polymerization reactions was found to be on the order of 10³ mol per cation. The fact that the EPI epoxy groups polymerize as effectively as the very reactive vinyl ether double bonds argues in favor of an intramolecular process, which is propagating rapidly along the epoxidized polyisoprene chain.

Although EPI and DVE-3 exhibit very similar polymerization profiles, copolymerization is not likely to occur in such epoxide-vinyl ether blends, as demonstrated recently by Crivello¹². The UV-cured polymer, which consists essentially of two interpenetrating polymer networks, combines the excellent adhesion of the epoxides and rubbers with the physical properties of vinyl ether polymers. The Persoz hardness of the UV-cured DVE-3/EPI blend was markedly larger than that of the UV-cured EPI. For the DVE-3/ELNR-70 blend in a 1 to 2 weight ratio, it was found to reach a value of nearly 300 s after a 1 s exposure (Fig.9), while the film remained highly flexible. Therefore, the UV-curing of EPI/DVE-3 blends appears as a promising method to produce rapidly protective coatings showing a good resistance to both scratching and abrasion.

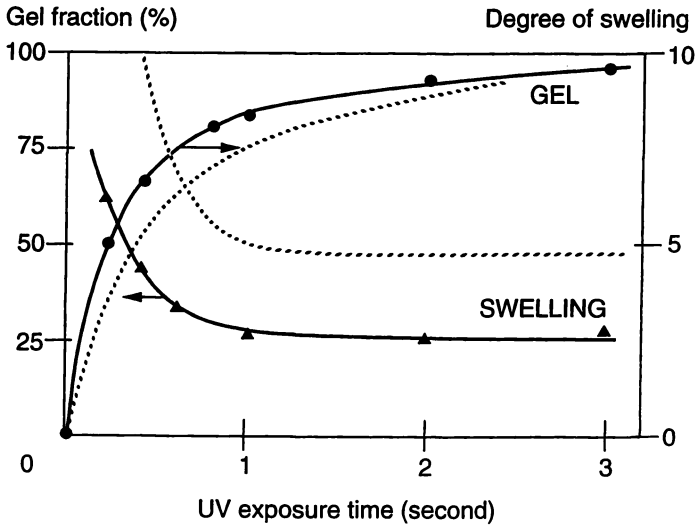


Fig.8 Insolubilization (●) and swelling (▲) profiles in photocuring of a ELNR-70/DVE-3 blend (1/1 ratio). ---- neat ELNR-70.

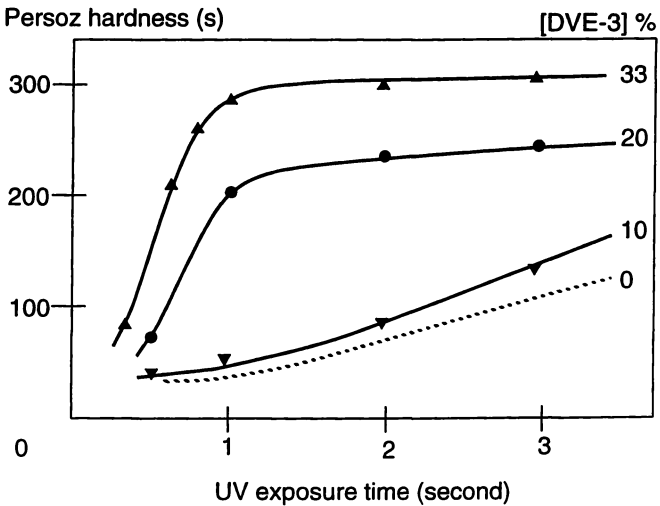
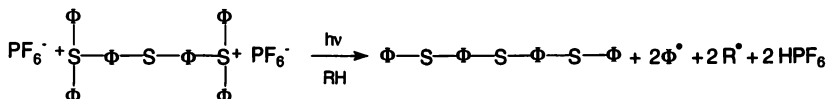


Fig.9 Influence of the DVE-3 concentration on the hardening of epoxidized polyisoprene (ELNR-70). [DVE-3] = 10% (▲), 20% (●) and 33% (▼). ---- : neat ELNR-70.

Some photocuring experiments of EPI have been performed by using epoxidized soybean oil (ESO) as reactive diluent instead of DVE-3. The polymerization of the two types of epoxy groups was followed by IR spectroscopy through their distinct absorbances at 840 cm^{-1} for ESO and at 870 cm^{-1} for ELNR. It can be seen on Figure 10 that the ring-opening polymerization of both epoxy groups is proceeding effectively upon UV-irradiation in the presence of a TAS photoinitiator. Here, copolymerization is most likely to occur with formation of a single polymer network containing as cross-link chains both the soybean oil and the polyisoprene. The interest of this UV-curable resin is that it is made of environment friendly natural compounds which can be produced in large quantities at a low cost. The low-modulus polymer obtained has a strong elastomeric character, which makes it well suited for applications as quick-setting adhesives or to produce impact resistant glass laminates ¹³.

Photocross-linking of epoxidized polyisoprene-acrylate blends

A similar study has been performed on EPI blends in which the vinyl ether was replaced by an acrylate monomer (HDDA) to produce, by different mechanisms, two interpenetrating polymer networks. With the onium salt as sole photoinitiator, the cationic polymerization of the EPI epoxy groups occurred as fast in the formulation containing 20% of HDDA by weight as in the EPI/DVE-3 blend, to reach nearly 100% conversion within 0.6 s (Fig.11). The polymerization quantum yield was found to be similar to that measured in the EPI/vinyl ether blend : $\Phi_p \sim 650\text{ mol E}^{-1}$. By contrast, the acrylate double bonds were found to polymerize at a much slower pace, most probably because of the low reactivity of the free radicals generated by the cationic-type photoinitiator.



The polymerization rate of both functional groups was markedly increase when the HDDA content was risen from 20 to 60% (Fig.11), as expected from the resulting increase in the molecular mobility. The addition of a phosphine oxide radical-type photoinitiator (2 wt % of TPO) leads to a drastic increase of the acrylate polymerization rate (75% conversion after 0.1 s), as shown in Figure 12 for an equimolar blend of ELNR-70 and HDDA exposed to UV-radiation. The early formation of the acrylate polymer network will reduce the molecular mobility of the reactive species and is therefore responsible for the observed decrease of both the rate of polymerization and the final conversion of the epoxy groups. A most remarkable feature of this

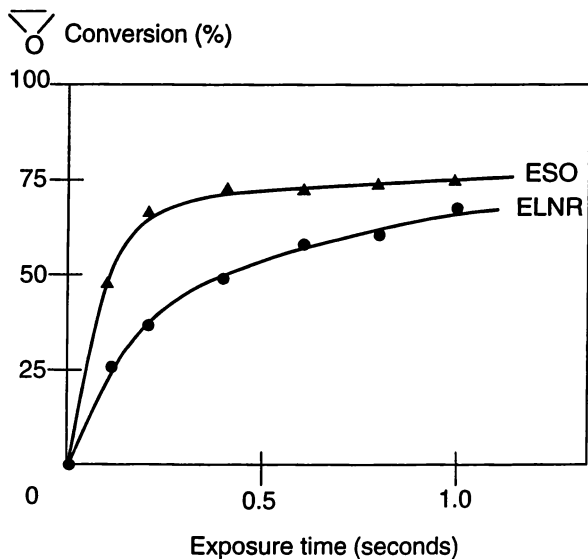


Fig. 10 Photocuring of a 1/1 blend of ELNR-70 and epoxidized soybean oil (ESO). Conversion of the epoxy ring of ELNR (●) and of ESO (▲).

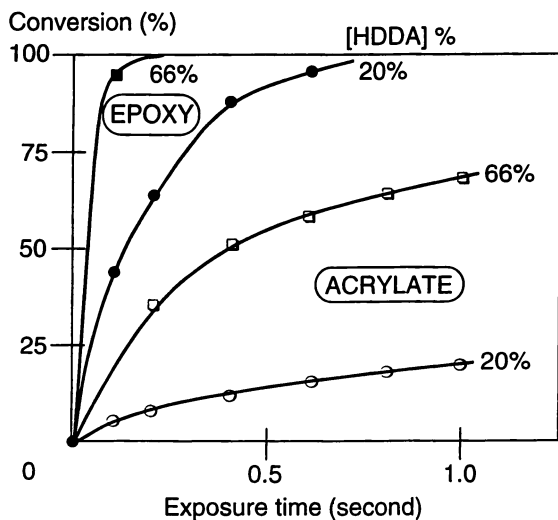


Fig.11 Photocuring of blends of ELNR-70 and hexanedioldiacrylate (HDDA). Photoinitiator : [TAS] = 3 wt %. Epoxy conversion (●,■), acrylate conversion (○,□) for 20% HDDA (●,○) and 66% HDDA (■,□).

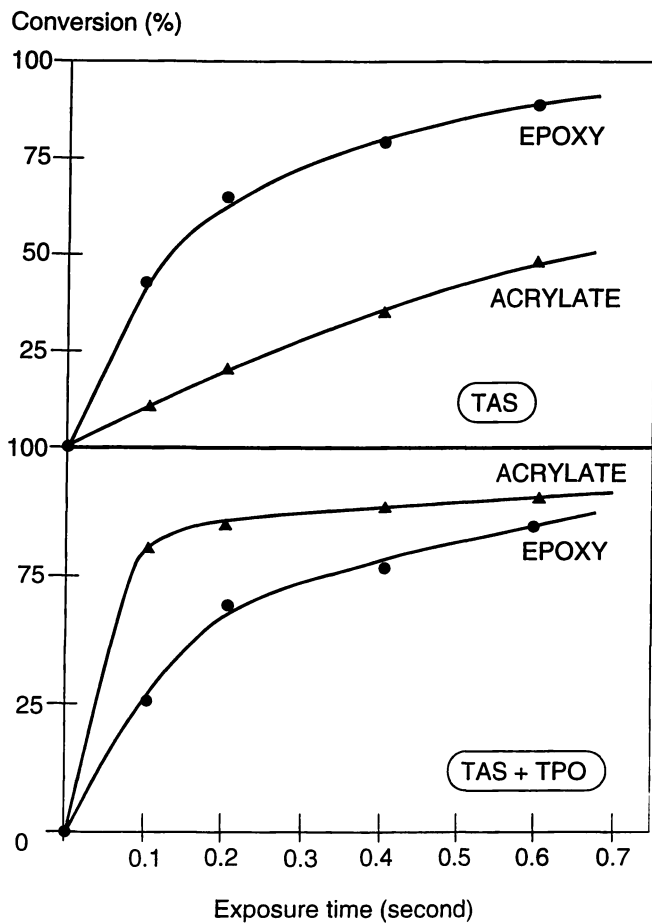


Fig.12 Influence of the photoinitiator on the UV-curing of an EPI-acrylate blend. HDDA/ELNR-70 = 1/1 by weight. (●) epoxy conversion, (■) acrylate conversion. Top : [TAS] = 3 wt %, bottom : [TAS] = 3 wt % and [TPO] = 2 wt %.

photocurable system containing two types of photoinitiators is that the IPN can be generated in a two step process¹⁴: a first exposure at 365 nm where TPO absorbs will induce the radical polymerization of the acrylate monomer, whereas a second exposure at 300 nm will induce the cationic polymerization of the epoxidized polyisoprene. Such two-step UV-curable photoresists are much valuable for some specific applications, in particular in laser imaging and in holography to create superimposed 3D images in a single film.

When both cationic and radical photoinitiators were introduced in the formulation, a 0.6 s UV exposure proved to be sufficient to transform the liquid resin into a solid and insoluble polymer, as shown in Figure 13. At that stage of the reaction, the cross-linked polymer, which contains about 20% of unreacted epoxy and acrylate groups, is still soft (Persoz hardness = 60 s) and exhibits a strong elastomeric character. It will continue to harden upon further UV exposure, up to relatively high values of the Persoz hardness (320 s). By acting on the irradiation time, it is therefore possible to modulate the viscoelastic properties of the IPN, depending on the considered application (soft adhesives or hard coatings). It should be mentioned that, even the extensively UV-cured polymer film remains flexible and shows a good adhesion on various substrates, because of the rubber moiety of the IPN. The cross-link density of the insoluble polymer formed was found to be significantly higher than that of the UV-cured EPI, as shown by the twice lower value of the swelling ratio (Fig.13). This is due to the additional formation of the acrylate polymer network, which contributes also to the hardening of the UV-cured material.

Similar results have been obtained by UV irradiation of a solid epoxidized natural rubber (ENR) or an epoxidized cyclized rubber (ECR) in the presence of a triarylsulfonium salt ([TAS] = 3 wt %) and a diacrylate monomer ([HDDA] = 20 wt %), as shown in Figure 14. The ring-opening polymerization of the epoxy group was found to develop slower and less extensively in the high-modulus ECR, with formation of a hard material (Persoz ~ 300 s), than in the low modulus ENR, which gives a relatively soft cross-linked elastomer (Persoz ~ 150 s). Here again, the addition of a radical photoinitiator (Lucirin TPO) proved to be very effective in accelerating the polymerization of the acrylate double bonds to produce a tightly cross-linked polymer.

Conclusion

The photoinitiated cationic polymerization of liquid epoxidized polyisoprene is an efficient method to generate rapidly crosslinked elastomers. In the presence of a triarylsulfonium salt, the reaction develops readily upon UV exposure, with formation of both inter and intramolecular ether linkages. The formulation reactivity can be substantially enhanced by the addition of a difunctional vinyl ether or acrylate monomer, which acts as a reactive diluent and leads to the formation of an

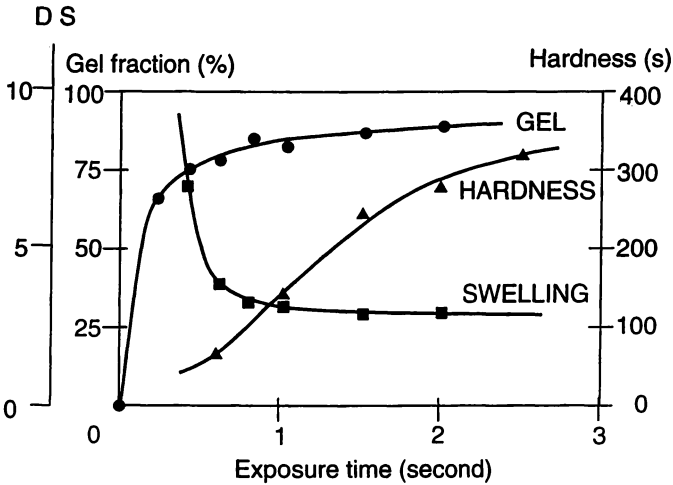


Fig.13 Insolubilization (●), swelling(■) and hardness(▲) profiles in UV-curing of an equimolar HDDA/ELNR-70 blend. [TAS] = 3 wt % ; [Lucirin TPO] = 2 wt %.

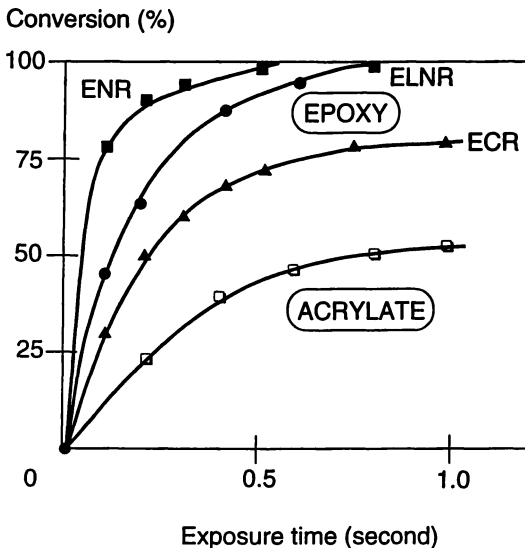


Fig.14 UV-curing of various blends of EPI with HDDDA (20 wt %). Photoinitiator : [TAS] = 3 wt % ; ENR : epoxidized natural rubber ; ECR : epoxidized cyclized rubber. Epoxy conversion (■,●,▲) ; acrylate conversion in ENR/HDDA mixture (□).

interpenetrating polymer network. The UV-cured polymers show remarkable mechanical properties, in particular a great flexibility and hardness, which make these polymer materials very resistant to impact, abrasion and scratching, and therefore well suited for coating applications.

One of the authors (T.H N) wishes to thank the CNRS for a research fellowship.

References

1. C. Decker, *Polymeric Materials Encyclopedia*, J.C. Salomone ed. CRC Press, New York, Vol 7, 1996, p.5181
2. C. Decker, *Prog.Polym.Sci.* **21**, 593 (1996)
3. J.E. Puskas, G. Kaszas and J.P. Kennedy, *J. Macromol.Sci.Chem.* **A28**, 65 (1991).
4. J.V. Crivello and B. Yang, *J. Macromol.Sci.Chem.* **A31**, 517 (1994).
5. C. Decker, H. Le Xuan and T. Nguyen Thi Viet, *J.Polym.Sci., Polym.Chem. Ed.*, **33**, 2759 (1995).
6. F. Cazaux, X. Coqueret, B. Lignot, C. Loucheux, J.J. Flat, S. Leraoux, C. Verge, *J.Coat.Techn.* **66(838)**, 27 (1994)
7. H. Le Xuan and C. Decker, *J.Polym.Sci., Polym.Chem.Ed.*, **31**, 769 (1993)
8. C. Decker, T. Nguyen Thi Viet and H. Le Xuan, *Europ.Polym.J.* **32**, 559 (1996).
9. D.R. Burfield, K.L. Lim and K.S. Law, *J.Appl.Polym.Sci.*, **29**, 1661 (1984).
10. C. Decker, F. Morel, *Polym.Mater.Sci.Eng.* **76**, 70 (1997).
11. C. Decker, H. Le Xuan, T. Nguyen Thi Viet, *Europ.Polym.J.*, **32**, 1319 (1996)
12. J.A. Dougherty and J.V. Crivello, *Polym.Mater.Sci.Eng.* **72**, 410 (1995).
13. C. Decker, K. Moussa, *J.Appl.Polym.Sci.* **55**, 359 (1995).
14. C. Decker, H. Le Xuan, T. Nguyen Thi Viet, *J.Polym.Sci., Polym.Chem.Ed.*, **34**, 1771 (1996).

Chapter 21

Synthesis of Cyclic Carbonate Functional Polymers

Dean C. Webster and Allen L. Crain

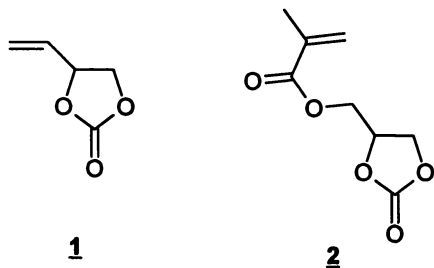
Research Laboratories, Eastman Chemical Company, P.O. Box 1972,
Kingsport, TN 37662-5150

Polymers with pendant cyclic carbonate functionality were synthesized via the free radical copolymerization of vinyl ethylene carbonate (4-ethenyl-1,3-dioxolane-2-one, VEC) with other unsaturated monomers. Both solution and emulsion free radical processes were used. In solution copolymerizations, it was found that VEC copolymerizes completely with vinyl ester monomers over a wide compositional range. Conversions of monomer to polymer are quantitative with complete incorporation of VEC into the copolymers. Cyclic carbonate functional latex polymers were prepared by the emulsion copolymerization of VEC with vinyl acetate and butyl acrylate. VEC incorporation was quantitative and did not affect the stability of the latex. When copolymerized with acrylic monomers, however, VEC is not completely incorporated into the copolymer. Sufficient levels can be incorporated to provide adequate cyclic carbonate functionality for subsequent reaction and crosslinking. The unincorporated VEC can be removed using a thin film evaporator. The T_g of VEC copolymers can be modeled over the compositional range studied using either linear or Fox models with extrapolated values of the T_g of VEC homopolymer.

Cyclic carbonate functional polymers have been explored on a limited basis over a number of years. The cyclic carbonate group is an attractive functional group due to its reactivity with primary amines at ambient or slightly elevated temperatures to form crosslinked networks [1]. Cyclic carbonate functional polymers will also react with carboxylic acid functional polymers [2] at higher temperatures to form crosslinked coatings.

Cyclic carbonate functional polymers have been prepared using several different routes. Bisphenol-A epoxy resins have been transformed into cyclic

carbonate functional resins by reaction of the oxirane with CO_2 [3,4,5]. Similarly, trimethylolpropane triglycidyl ether has been converted to the corresponding trifunctional cyclic carbonate by reaction with CO_2 [6]. A more usual route has been through the copolymerization of an unsaturated cyclic carbonate functional monomer. A number of investigators have reported on the copolymerization of the methacrylic ester of glycidyl carbonate, **2** [2,7,8]. This monomer is readily copolymerized with other acrylic monomers.



Limited information exists in the literature, however, on the homo- or copolymerization of vinyl ethylene carbonate, **1** (VEC or 4-ethenyl-1,3-dioxolane-2-one) for the preparation of cyclic carbonate functional polymers. A few comments regarding polymerization of VEC are given in an early patent [9]. In the only reported study of the copolymerization behavior of VEC, Asahara, Seno, and Imai described the copolymerization of VEC with vinyl acetate, styrene, and maleic anhydride and determined reactivity ratios [10]. Their results indicated that VEC would copolymerize well with vinyl acetate, but in copolymerizations with styrene, little VEC could be incorporated into the copolymer. VEC appeared to copolymerize with maleic anhydride, however the compositions of the copolymers was not reported. Our goal was to further explore the use of VEC in the synthesis of cyclic carbonate functional polymers.

Experimental

Materials. VEC was prepared by the catalyzed addition of CO_2 to 3,4-epoxy-1-butene using conditions typical of that used industrially [11], then purified by vacuum distillation. Other raw materials were used as received without any additional purification. Mixed xylenes, vinyl acetate (VA), butyl acrylate (BA), butyl methacrylate (BMA), methyl methacrylate (MMA), styrene (St), and *t*-butyl hydroperoxide were obtained from Aldrich Chemical Company. Lupersol 575 (*t*-amyl peroxy (2-ethylhexanoate)) was supplied by Elf Atochem. Vazo 67 (2,2'-azobis(2-methylbutyronitrile)) was obtained from DuPont Chemical Company. Vinyl pivalate (NEO5), vinyl 2-ethylhexanoate (V2EH), Tergitol NP-40 (non-ionic surfactant) and QP-300 (hydroxy ethyl cellulose) were obtained from Union Carbide Corporation. Aerosol OT-75 (surfactant) was obtained from Cytec. Sodium formaldehyde sulfoxylate was obtained from Henkel Corporation. Ethyl 3-ethoxy propionate (EEP), propylene glycol monomethyl ether (PM) and PM acetate (PM Ac) are Eastman Chemical Company products.

Solution Polymerization. Solution copolymers were prepared using either a 500 ml or 1000 ml two-piece glass resin kettle equipped with a mechanical stirrer, nitrogen inlet, thermocouple, and condenser. Temperature was maintained using a heating mantle and a Jack-O-Matic (I²R) controlled by a Camile TG process control system. In a typical procedure to prepare a vinyl acetate/VEC copolymer, 140 g of propylene glycol monomethyl ether (PM) was charged to the reactor and heated with stirring to the polymerization temperature. Then, 10.7 g Lupersol 575, 78 g VEC, and 182 g vinyl acetate were mixed in a separate container. When the solvent reached the polymerization temperature, the monomer mixture was fed using a metering pump at a rate of 1.5 g/min. The monomer addition was complete in three hours. One hour after completion of the addition, 0.5 g Lupersol 575 was added, and the reaction was held for an additional one hour and then cooled.

Emulsion Polymerization. Emulsion polymerizations were carried out in a one-liter two-piece resin kettle equipped with a mechanical stirrer, heating mantle, nitrogen inlet, thermocouple and condenser. Temperature was controlled as described above and the monomer, initiator and reducer feed rates were also controlled by the Camile TG process control system. To 280 g deionized water was added 24 g of a 5% aqueous solution of QP-300, 0.45 g of Aerosol OT-75, 19.4 g Tergitol NP-40, and 1.2 g sodium carbonate. With stirring the mixture was heated to 65°C. In a separate container, 400 g of monomers (vinyl acetate, butyl acrylate, and VEC) and 1.7 g of Aerosol OT-75 were mixed. 40 g of the monomer mixture was added to the reactor. Feed 2 was prepared consisting of 1.03 g of a 70% aqueous solution of t-butyl hydroperoxide and 38.97 g water. Feed 3 was also prepared consisting of 0.70 g of sodium formaldehyde sulfoxylate and 39.30 g water. After 10 minutes, four solutions consisting of: (1) 0.25 g of a 1% aqueous solution of FeSO₄·7H₂O and 2.0 g water; (2) 0.25 g of a 1% aqueous solution of ETDA and 2.0 g water; (3) 0.51 g of a 70% aqueous solution of t-butyl hydroperoxide and 4.89 g water; and (4) 0.35 g sodium formaldehyde sulfoxylate and 5.0 g water were added to the reactor. After 10 minutes the monomer mixture was added to the reactor at a rate of 1.71 g/min (total feed time 210 minutes). After 30 minutes Feeds 2 and 3 were started at a rate of 0.190 g/min (total feed time 210 minutes). Thirty minutes after completion of the feeds, solutions consisting of (1) 0.26 g of a 70% aqueous solution of t-butyl hydroperoxide and 1.74 g water and (2) 0.15 g of sodium formaldehyde sulfoxylate and 1.85 g water were added. This addition was repeated after thirty minutes. After an additional 30 minute hold, the reaction mixture was cooled and filtered.

VEC Hydrolysis. 0.2 M NaOAc and 0.2 M HOAc solutions were mixed to yield a buffer solution with pH of 4.03. 75 ml of this solution was placed in a 100 ml 3-necked flask equipped with a magnetic stirrer, condenser, heating mantle and thermometer. 1.5 ml of VEC was added to the solution. The solution was heated at 80°C for four hours with stirring then cooled to room temperature and analyzed for 3-butene-1,2-diol by gas chromatography.

Characterization of Solution Polymers. Resin percent solids was determined by weighing approximately 1 gram of resin solution into an aluminum weighing pan, covering with additional solvent, then determining weight retention after heating in an oven for 1 hour at 150°C. Percent conversion is calculated as the ratio of the measured solids to theoretical solids. Unreacted monomer content was determined by gas chromatography and data (e.g., Table I) reported as a percent of theoretical polymer solids. FTIR spectroscopy was conducted using a Midac Prospect-IR. A solution of the polymer was cast on a sodium chloride crystal and the solvent (and any unreacted monomers) removed by force drying in an oven at 150-160°C. For differential scanning calorimetry (DSC), 1-3 grams of resin solution was placed in an aluminum pan and placed in an oven at 160°C for 1-2 hours. Analysis was run using a TA Instruments Model 2200 DSC at a rate of 20°C/min. Reported T_g values are the midpoint of the inflection. Gel Permeation Chromatography was done using a PL-Gel Mixed B and 100 Å columns (Polymer Laboratories) in N-methyl pyrrolidinone solvent at 1 ml/min. Average molecular weights are reported relative to polystyrene standards.

Characterization of Latex Polymers. Percent solids was determined using a CEM Labwave 9000 microwave solids analyzer. Viscosity was determined using a Brookfield Digital Viscometer Model DV II using a #3 LV spindle at 30 rpm. Minimum film-formation temperature was determined using a Rhopoint MFFT Bar 90 from Paul N. Gardner, Inc. Particle size was determined using a Brookhaven Instruments Corporation BI-90 Particle Sizer. Samples for DSC were prepared by drawing down a sample of latex onto release paper and allowing to air dry for one week. Unreacted monomers were determined using Gas Chromatography.

Results and Discussion

Solution Copolymerizations. Our primary objective in this preliminary study was to gain a qualitative understanding of the copolymerization behavior of VEC with various types of unsaturated monomers. Particularly, we wanted to determine if VEC could be incorporated into a variety of polymer types of interest to the coatings industry. Since VEC is used to provide cyclic carbonate functionality for subsequent reaction or crosslinking, limited amounts of VEC are used in the copolymerizations. A semi-batch process was used in the copolymerization experiments to approach starved-feed conditions. Starved-feed conditions can result in copolymers with more uniform composition since the conversion is kept high in the reactor. While there are a large number of variables to consider, we elected to focus on monomer composition, polymerization temperature, and initiator level.

The initial experiments consisted of screening various monomer combinations to determine if VEC could be successfully copolymerized. Table I lists a number of these initial experiments with typical methacrylate and acrylate monomers as well as styrene. Copolymerizations carried out in the presence of styrene resulted in low conversions with essentially none of the VEC charged being incorporated into the polymer (A, B, C). There was a slight increase in conversion

Table I. Copolymerization of VEC with (Meth)acrylate Monomers.

Sample	Monomers	Ratio	Wt. % Initiator	Temp. (°C)	Unreacted VEC, GC	Percent Conv.
A	VEC/BMA/St	25/50/25	2	80	25.2	64.9
B	VEC/BMA/St	25/50/25	2	100	24.0	73.7
C	VEC/St/BA	25/50/25	2	100	23.8	67.8
D	VEC/MMA/BA	25/50/25	2	100	16.8	83.8
E	VEC/MMA/BA	25/50/25	2	120	15.0	83.1
F	VEC/BA/MMA	25/50/25	2	100	13.8	85.8
G	VEC/BA/MMA	25/50/25	4	100	11.5	88.3
H	VEC/BA	25/75	4	100	8.0	93.0

Reaction conditions: Solvent: mixed xylenes; Monomer addition time: 3 hours; Initiator: 2,2'-Azobis(2-methylbutyronitrile) (Vazo 67); Theoretical solids: 60%.

noted with a polymerization temperature increase from 80° to 100°C; thus 100°C was used for the rest of the experiments.

When styrene is eliminated from the monomer mix, there is an increase in conversion from 67 percent to 84 percent (D vs. C) with a corresponding decrease in the amount of unreacted VEC. Increasing the temperature from 100° to 120°C did not have a significant effect. Increasing the amount of butyl acrylate monomer relative to MMA improved the conversion (F), as did increasing the level of initiator (G). One of the better results we have been able to attain thus far is the copolymer with butyl acrylate (H), however, there is still some unreacted VEC present in the copolymer.

The copolymerizations in Table I were all conducted using 2,2'-azobis(2-methylbutyronitrile) as the initiator. All of the polymer solutions, while clear, had a bright yellow color. When the copolymerizations were conducted using t-amyl peroxy (2-ethylhexanoate), the polymer solutions were clear and colorless. Thus, we continued using the t-amyl peroxy (2-ethylhexanoate) for the rest of the solution copolymerizations.

In order to more systematically understand the effects of VEC copolymerization with butyl acrylate, a series of copolymers was prepared. Table II lists the compositions and characteristics of these copolymers. Complete incorporation of VEC into the copolymers was not achieved under these conditions (Figure 1). The unreacted monomers consisted predominately of VEC; only a trace of unreacted butyl acrylate was detected. The amount of VEC actually incorporated into the copolymer can be determined by subtraction either using the unreacted monomer data or the conversion data. If the amount of VEC incorporated into the copolymer is compared to what was charged to the reaction, level of incorporation is relatively constant at 60-65%. This is illustrated in Figure 2.

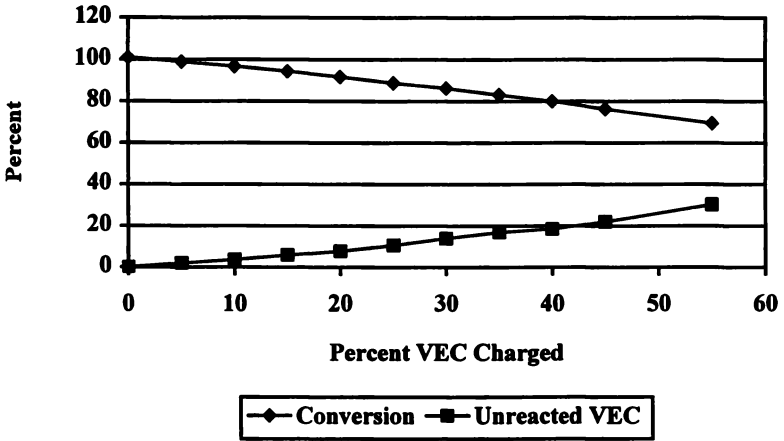


Figure 1. VEC/Butyl Acrylate Copolymers. Effect of VEC content on conversion and unreacted VEC levels.

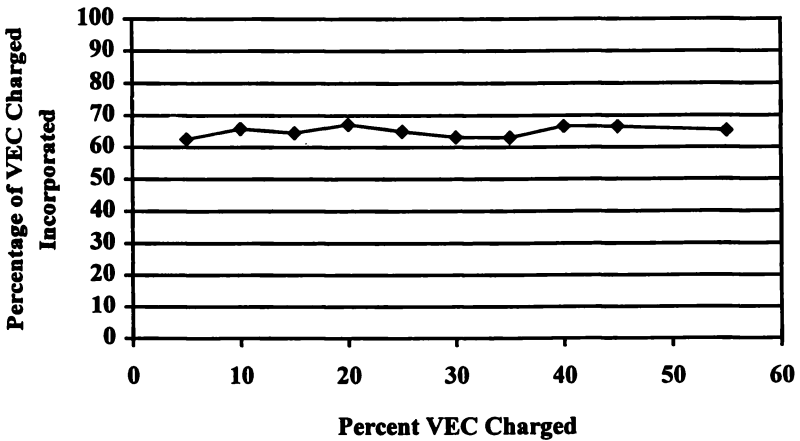


Figure 2. VEC/Butyl Acrylate Copolymers. Effect of VEC charged on percent VEC incorporated into the copolymer.

Table II. VEC/Butyl Acrylate Copolymers

Sample	% VEC	% BA	% Solids	% Conv.	T _g (°C)	% Unreacted VEC	GPC Mn	GPC Mw
A	0	100	65.64	100.98	-51.6	0.00	3780	7840
B	5	95	64.23	98.81	-46.4	1.95	3970	7390
C	10	90	62.90	96.77	-42.1	3.71	3240	7370
D	15	85	60.70	94.40	-39.1	5.97	3040	6570
E	20	80	59.58	91.66	-29.5	7.72	2620	5890
F	25	75	57.71	88.78	-26.3	10.60	2790	5920
G	30	70	56.10	86.31	-22.0	13.85	2690	5580
H	35	65	54.01	83.09	-16.6	16.88	2530	5060
I	40	60	51.98	79.97	-13.9	18.51	2490	4790
J	45	55	49.60	76.31	-11.2	21.89	2380	4520
K	55	45	45.14	69.45	-3.3	30.31	2150	3850

Conditions: Solvent: mixed xylenes; Theoretical solids: 65%; Temperature: 100°C; Monomer addition time: 3 hours; Initiator: t-amyl peroxy (2-ethylhexanoate)

There appears to be a slight decrease in the molecular weight as a function of VEC level (Figure 3). It is important to recognize that this molecular weight decrease could be an artifact of the GPC method: either due to changes in the hydrodynamic volume or refractive index of the copolymers as a function of composition. However, if this is a real decrease in molecular weight as a function of VEC content, a number of possibilities can be speculated. One possible cause for this effect is that VEC may more readily undergo termination by disproportionation than can butyl acrylate due to its allylic proton. Also, the allylic proton on VEC could be abstracted, reducing the molecular weight via chain transfer. Additional analysis of the microstructure of the copolymer is required to determine if these mechanisms are operating. We are also planning copolymerization experiments of VEC and butyl acrylate which will be more amenable to the determination of reactivity ratios.

The glass transition temperature also increases systematically as the level of VEC increases. The T_g data will be discussed more fully in a later section.

To form crosslinked coatings, the polymer must be free of unreacted functional monomer that would act as a chain terminator in the crosslinking reaction. The unreacted VEC could be easily removed from the acrylic copolymer by passing the resin solution through a wiped film still under vacuum, then redissolving the polymer in solvent. GC analysis indicated that the unreacted VEC had been totally removed.

Table III lists the initial solution copolymerization experiments conducted using vinyl ester monomers. Since our main objective is the synthesis of polymers for durable coatings, these experiments were conducted using more hindered vinyl monomers which are reported to have better durability than vinyl acetate.

Table III. Copolymerization of VEC with Vinyl Ester Monomers.

Sample	Monomers	Ratio	Percent Initiator	Solvent	Temp. (°C)	% Conv.
A	VEC/V2EH/NEO5	20/40/40	4	Xylene	100	88.9
B	VEC/V2EH/NEO5	20/40/40	4	EEP	100	101.7
C	VEC/V2EH/NEO5	20/40/40	4	PM Ac	100	99.5
D	VEC/V2EH/NEO5	20/40/40	4	PM	100	99.7
E	VEC/VA/NEO5	10/45/45	4	PM	80	100.6
F	VEC/VA/NEO5	30/35/35	4	PM	80	101.2
G	VEC/VA/NEO5	17.5/20/62.5	2	PM	80	101.0

Conditions: Theoretical solids: 65%; Addition time: 5 hours; Initiator: t-amyl peroxy (2-ethylhexanoate)

The first set of experiments indicates the importance of using the appropriate solvent for the copolymerizations. Sample A (Table III) was conducted using similar conditions used for the acrylic copolymerizations. While there were no signs of insolubility of the polymer in the solvent, only low conversion was achieved. Using a more polar solvent such as ethyl 3-ethoxy propionate (EEP) (B), propylene glycol monomethyl ether (PM) (D) and its acetate (PM Acetate) (C) resulted in essentially complete conversion of monomer to polymer. (Copolymerizations using PM and EEP solvents generally indicate higher conversion than theoretical, indicating that these solvents are becoming incorporated into the polymer via a chain transfer process.) The remainder of the copolymerizations listed in the table demonstrate some of the compositional variation that we explored.

A series of copolymers of VEC with vinyl acetate was prepared to study the copolymerization with vinyl esters more systematically. Table IV contains the results from those copolymerizations. As in the initial experiments, complete conversion of the monomers was achieved, with complete incorporation of VEC into the

Table IV. VEC/Vinyl Acetate Copolymers

Sample	% VEC	% VA	% Solids	% Conv.	Tg (°C)	GPC Mn	GPC Mw
A	0	100	64.52	99.68	20.6	5150	7400
B	5	95	65.19	100.29	26.5	3900	6300
C	10	90	66.43	102.20	29.2	3250	5700
D	15	85	65.13	100.20	32.7	2950	5100
E	20	80	65.30	100.46	34.0	2800	4900
F	25	75	65.73	101.10	41.6	2750	4900
G	30	70	66.08	101.66	41.5	2650	4700
H	35	65	66.02	101.60	46.0	2700	4900
I	40	60	-Hazy-		57.0		

Conditions: Theoretical solids: 65%; Solvent: PM; Initiator: t-amyl peroxy 2-ethyl hexanoate; Temperature: 80°C

copolymers. Unreacted monomer levels were less than 0.1 percent and not listed in the table. Also, as before, many of the conversions are greater than theoretical possibly indicating incorporation of solvent due to chain transfer. The copolymer solution with 40% VEC was hazy due to insolubility in the PM solvent and was not analyzed. This solution could be cleared by adding dimethyl formamide or N-methyl pyrrolidinone.

The Tgs of the copolymers increase systematically as the level of VEC increases. As in the case of copolymers with butyl acrylate the molecular weights also decreases with increasing levels of VEC. However, unlike with the butyl acrylate copolymers, the molecular weight appears to be reaching a limiting value as the VEC content increases (Figure 4). Again, more detailed analysis of the copolymers are required to fully understand these effects.

FT-IR spectra of typical VEC-butyl acrylate and VEC-vinyl acetate copolymers are shown in Figure 5. The cyclic carbonate carbonyl absorbance can be clearly seen at 1800 cm^{-1} . This peak is useful for determining cyclic carbonate content of the copolymer. Since this absorbance is well-resolved, it can also be used to follow reactions of the cyclic carbonate group.

Emulsion Copolymerizations. Due to the good copolymerizability of VEC with vinyl ester monomers, it seemed likely that VEC could be incorporated into a vinyl acetate/butyl acrylate latex. First, it was important to determine if VEC is prone to hydrolysis in the acidic medium used for vinyl acetate emulsion polymerization. As a check, a single experiment was carried out using an acetic acid-sodium acetate buffer at $\text{pH}=4$ and heating for 4 hours at 80°C . In this experiment, 6.1% of the VEC was hydrolyzed to the 3-butene-1,2-diol. Since VEC is only soluble in water up to 3.3 %, it is expected that most of the VEC will be in the oil phase during the emulsion polymerization and that only a small amount will be hydrolyzed.

A series of latex copolymers were prepared using a typical emulsion polymerization recipe and procedure; only the monomer composition was varied. The control composition (80/20 vinyl acetate/butyl acrylate) is similar to that used for interior latex paint. Table V lists the compositions and properties of the latexes. Percent solids, pH, and particle size are similar for all the latexes. Viscosity varies somewhat, but is within limits for this type of latex. The only unreacted monomer detected was the vinyl acetate. Thus, the incorporation of VEC into the emulsion polymerization via the monomer mixture did not affect the latex synthesis. The Tg and minimum film formation temperature (MFFT) of the latexes increase with increasing VEC content, which is expected based on the previous results.

Stability testing was conducted at 50°C for 10 and 30 days. The pH of the latexes was adjusted to 7.0 using triethylamine, then, the pH and viscosity measured after oven aging. The data is listed in Table VI. The pH data indicates no difference among the samples (Figure 6). There are some differences in the change of viscosity (Figure 7), however, these results do not indicate a problem of latex stability as a result of VEC incorporation.

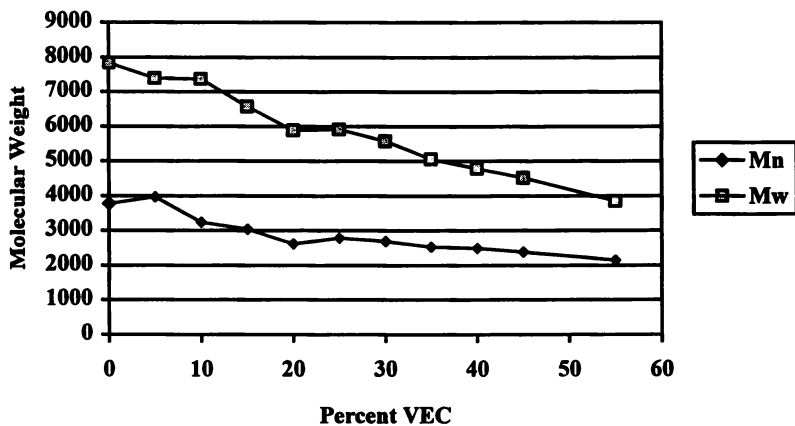


Figure 3. VEC/Butyl acrylate copolymers. Effect of VEC content on average molecular weights.

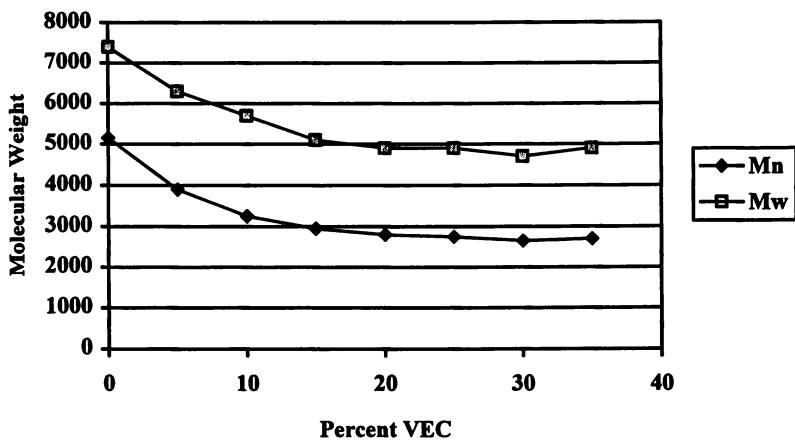


Figure 4. VEC/Vinyl acetate copolymers. Effect of composition on average molecular weights.

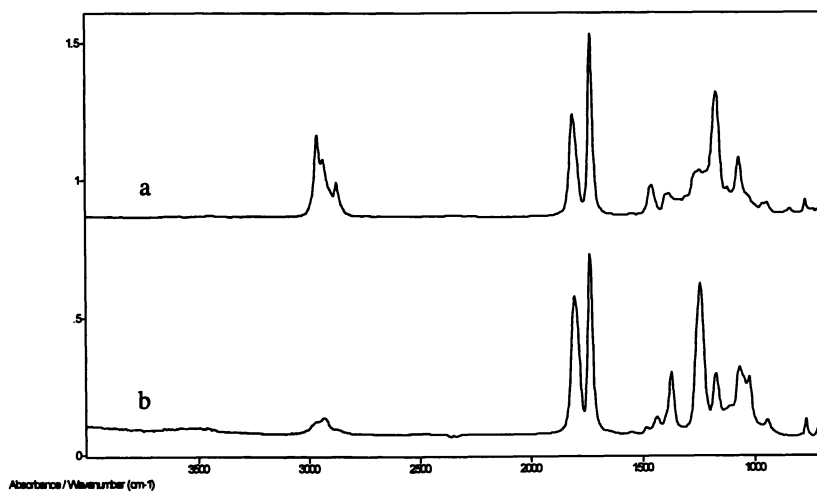


Figure 5. FT-IR spectra of a VEC/butyl acrylate copolymer (a) and a VEC/vinyl acetate copolymer (b).

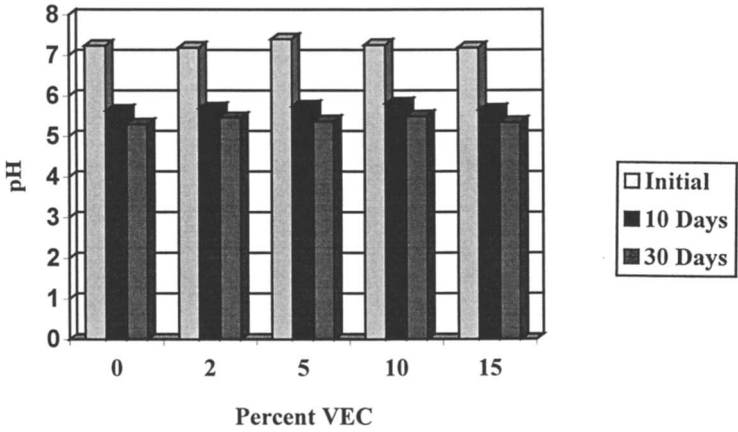


Figure 6. Effect of aging of latex samples at 50°C on pH.

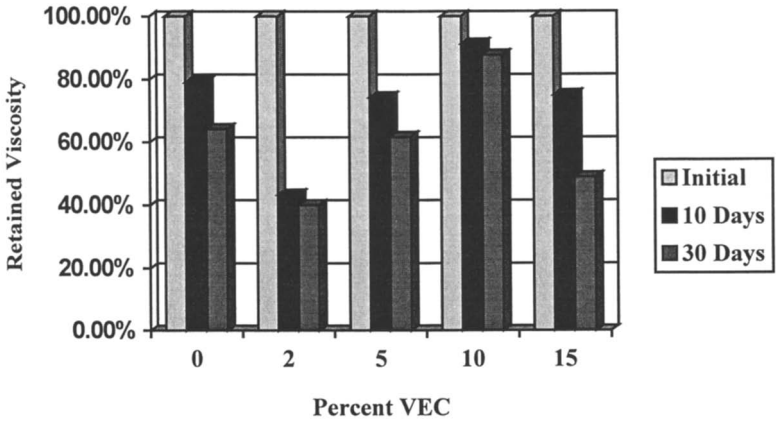


Figure 7. Effect of aging of latex samples at 50°C on viscosity.

Table V. Properties of VEC-containing Latex Resins.

<i>Composition</i>	A	B	C	D	E
%VEC	0	2	5	10	15
%Vinyl Acetate	80	78	75	70	65
%Butyl Acrylate	20	20	20	20	20
<i>Properties</i>					
%Solids	50.2	50.4	50.0	50.2	50.0
PH	5.3	5.2	5.3	5.3	5.2
Visc, cps	1304	792	1048	1244	1776
Mean dia, nm	377	318	401	410	368
PD	0.15	0.10	0.20	0.22	0.19
Tg, °C	19.9	21.1	25.8	30.7	34.0
MFFT, visual	8.8	11.5	11.7	15.7	17.5
MFFT, resistance	17.3	22.0	19.3	~24	>25
<i>Unreacted Monomers (ppm)</i>					
VEC	--	ND	ND	ND	ND
Vinyl acetate	960	831	671	573	1237
Butyl Acrylate	ND	ND	ND	ND	ND

ND = none detected

Analysis of Copolymer Tg Data. The Tg data of the copolymers can be fit to appropriate models to determine the values of the homopolymer glass transition temperatures of the individual monomers. Since the Tg of butyl acrylate and vinyl acetate are well known, we hoped to use this analysis to determine the Tg of a VEC homopolymer. We chose a linear model (also known as the Gibbs-DeMarzio theory):

$$T_g = W_A T_{gA} + W_B T_{gB}$$

where W_A and W_B are the weight fractions of monomers A and B and T_{gA} and T_{gB} are the respective Tgs of the individual homopolymers. We also fit the data to the Fox Equation:

$$\frac{1}{T_g} = \frac{W_A}{T_{gA}} + \frac{W_B}{T_{gB}}$$

where W_A , W_B , T_{gA} , and T_{gB} are defined as above. The composition of the butyl acrylate copolymers was corrected using the GC analysis of unreacted VEC.

In all cases the data fit the models equally well. The data is summarized in Table VII. The plots of the data and the line of fit are in Figures 8 through 13. In the case of the solution copolymers, the extrapolated Tg values for butyl acrylate and vinyl acetate agree reasonably well with typical literature values of -54°C and 32°C , respectively [12]. However, there is a wide variation in the values determined for

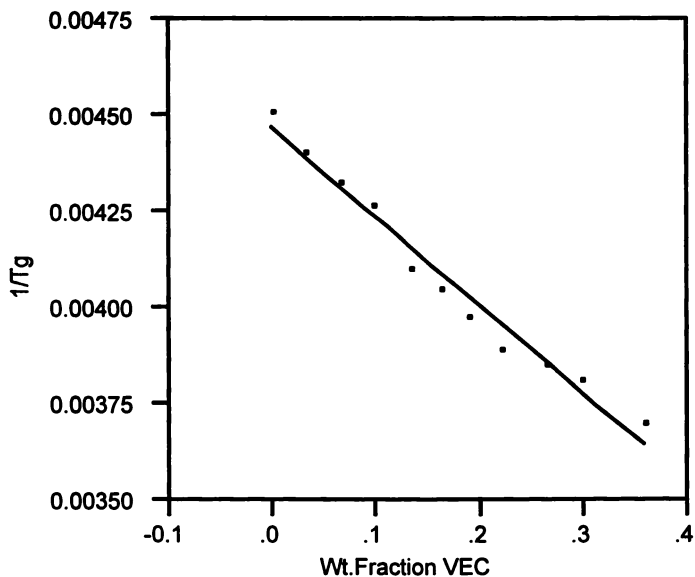


Figure 8. VEC/Butyl acrylate copolymers. Fit of T_g data to the Fox equation.

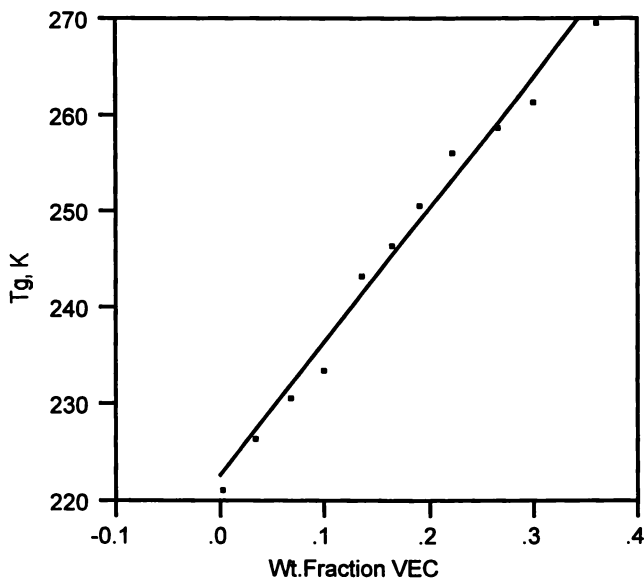


Figure 9. VEC/Butyl acrylate copolymers. Fit of T_g data to linear model.

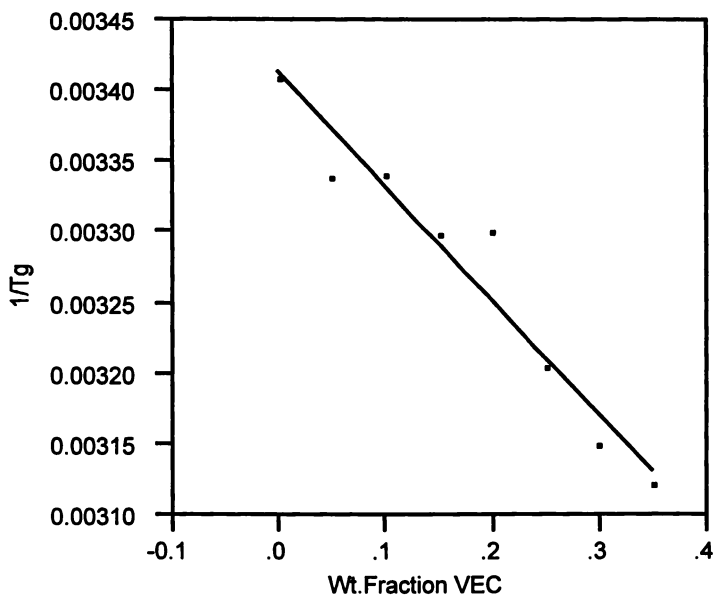


Figure 10. VEC/Vinyl acetate copolymers. Fit of T_g data to Fox equation.

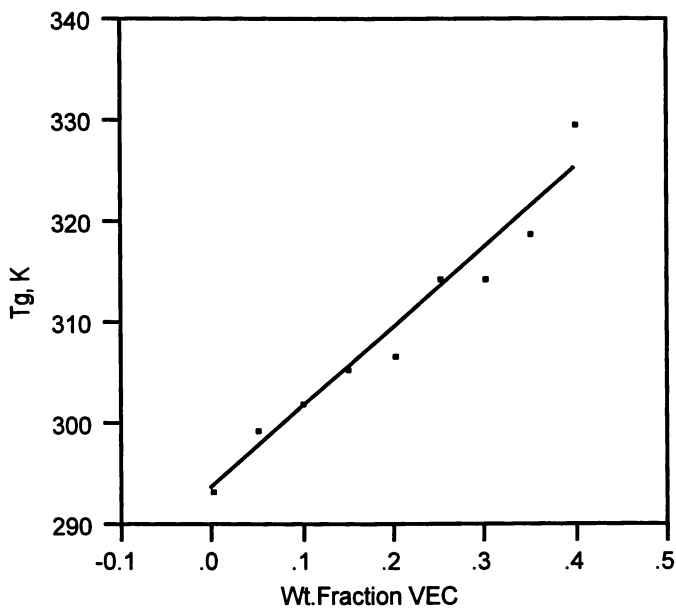


Figure 11. VEC/Vinyl acetate copolymers. Fit of T_g data to linear model.

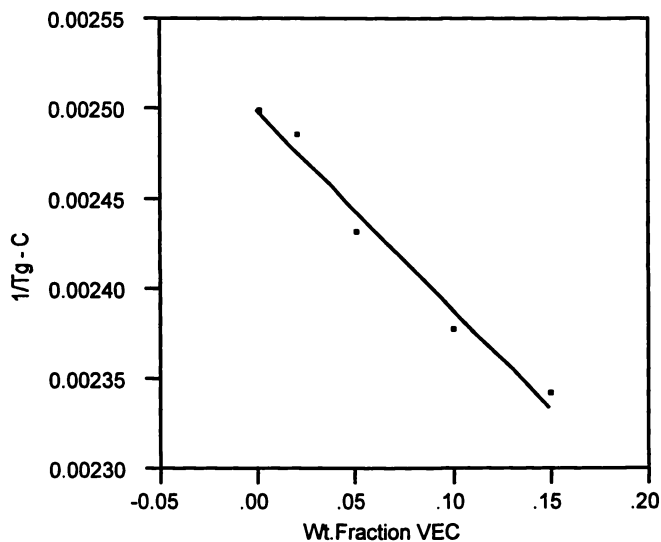


Figure 12. VEC latex resins. Fit of T_g data to Fox equation.

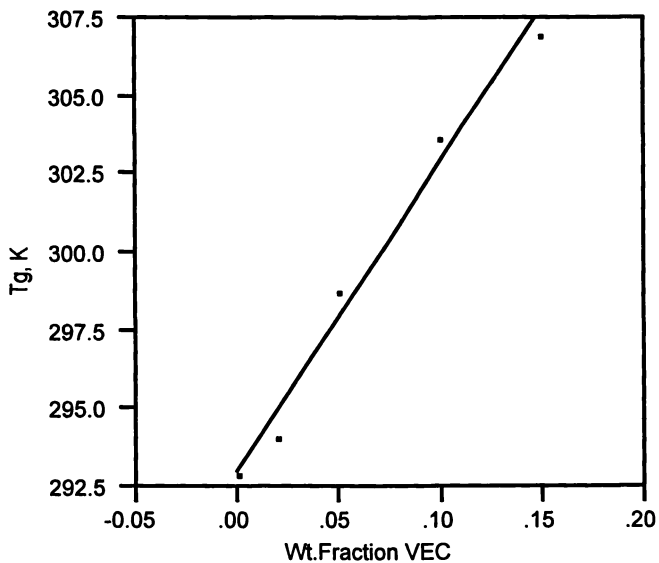


Figure 13. VEC latex resins. Fit of T_g data by linear model.

Table VI. Stability Testing of Latexes at 50°C.

	A	B	C	D	E
pH – 10 days					
Initial	7.24	7.19	7.40	7.26	7.19
Final	5.64	5.70	5.75	5.82	5.66
% Retained	77.9	79.3	77.7	80.2	78.7
pH – 30 days					
Initial	7.05	7.10	7.11	7.22	7.15
Final	5.30	5.42	5.38	5.50	5.35
% Retained	75.2	76.3	75.7	76.2	74.8
Viscosity (cps) – 10 days					
Initial	1208	600	940	1144	1328
Final	948	256	700	1036	992
% Retained	78.5	42.7	74.5	90.6	75.0
Viscosity (cps) – 30 days					
Initial	1160	664	848	1100	1216
Final	772	236	580	996	652
% Retained	66.6	35.5	68.4	90.5	53.6

VEC. Asahara, Seno, and Imai report a “softening point” for poly(VEC) at 150°C. Our extrapolated values all fall around their reported value.

In the latex systems, the T_g of poly(butyl acrylate) was fixed at -54°C and the butyl acrylate content fixed at 20 percent. The fit of the data is good for both models, however, the calculated T_g for poly(vinyl acetate) using the Fox model is closer to literature values. The calculated T_g for poly(VEC) is much higher than that calculated for the solution polymers.

The variation in the extrapolated values for the T_g of poly(VEC) is primarily due to the fact that we have conducted experiments only in the lower compositional range of VEC (<50 %). There are numerous examples in the literature of copolymer systems that have linear T_g -composition relationships in a lower composition range, but deviate significantly at higher compositions [13,14,15]. Additional experiments

Table VII. Analysis of VEC Copolymer T_g Data.

Comonomer	Model	r^2	$T_{g_i} (^\circ\text{C})$	$T_{g_{VEC}} (^\circ\text{C})$
Butyl Acrylate	Linear	0.983	-50.2	86.6
Butyl Acrylate	Fox	0.971	-49.3	185.7
Vinyl Acetate	Linear	0.952	20.7	99.9
Vinyl Acetate	Fox	0.961	21.1	114.6
Vinyl Acetate – Latex	Linear	0.981	93.3	191.5
Vinyl Acetate -- Latex	Fox	0.978	47.0	218.4

at higher VEC contents are required, as well as studies of the sequence distribution of VEC in the copolymers to completely understand the Tg-composition relationship in VEC copolymers. However, within the range we have studied, it is possible to select a model and a Tg value for VEC homopolymer and calculate the Tg of the copolymer.

Conclusions

VEC copolymerizes well with vinyl ester monomers over a range of compositions. To a more limited extent, VEC can also be incorporated into acrylic copolymers, however, we have not achieved quantitative incorporation. In the presence of styrene, essentially no VEC is incorporated into the copolymer. VEC can also be easily incorporated into a vinyl acetate/butyl acrylate latex, yielding a latex polymer containing cyclic carbonate functionality. The Tg of the copolymers can be modeled using extrapolated values for the Tg of a VEC homopolymer.

Acknowledgements. We would like to thank Shawn Dougherty and Gabe DeTomasso for helpful discussions, and Robert Chen for supplying the latex recipe used in this work. We would also like to thank Eastman Chemical Company for permission to publish this work.

Literature Cited

1. Burgel, T.; Fedtke, M. *Polym. Bull.*, **1991**, *27*, 171-177.
2. Iwamura, G.; Kinoshita, H.; Kometani, A. U. S. Pat. No. 5,374,699 1994.
3. Rokicki, G.; Lewandowski, M. *Angew. Makromol. Chem.*, **1987**, *148*, 53-66.
4. Burgel, T.; Fedtke, M. *Polym. Bull.*, **1993**, *30*, 61-68.
5. Burgel, T.; Fedtke, M.; Franzke, M. *Polym. Bull.*, **1993**, *30*, 155-162.
6. December, T. S.; Harris, P. J. EP 0,661,355 1995.
7. Feng, J. C.; Hill, S. U.S. Pat. No. 2,967,173 1961.
8. Wendler, K.; Fedtke, M.; Pabst, S. *Angew. Makromol. Chem.*, **1993**, *213*, 65-72.
9. Pritchard, W. W. U.S. Pat. No. 2,511,942 1950.
10. Asahara, T.; Seno, M.; Imai, T. *Seisan Kenkyu*, **1973**, *25(7)*, 297-299.
11. For example, Weissrnel, K.; Arpe, H.-J. *Industrial Organic Chemistry: Important Raw Materials and Intermediates*; Verlag Chemie: New York, NY, 1978, pp.143-144.
12. Brandrup J.; Immergut, E. H. *Polymer Handbook, Third Edition*; Wiley: New York, NY, 1986.
13. Tonelli, A. E. *Macromolecules*, **1974**, *7*, 632-634.
14. Johnston, N.W. *J. Macromol. Sci.—Rev. Macromol.Chem.*, **1976**, *C14(2)*, 215-250.
15. Bailey, D.B.; Henrichs, P.M. *J. Polym. Sci.: Polym. Chem. Ed.*, **1978**, *16*, 3185-3199.

Chapter 22

Functionalized Polydiacetylenes with Polar, Hydrogen Bonding and Metal-Containing Groups

I. H. Jenkins, W. E. Lindsell, C. Murray, P. N. Preston, and T. A. J. Woodman

Department of Chemistry, Heriot-Watt University, Riccarton, Edinburgh, EH14 4AS, United Kingdom

New polydiacetylenes (PDAs) have been synthesized either by UV or γ -irradiation of diacetylenes or by 'polymer analogous' reactions of suitable precursors. PDAs with platinum moieties coordinated to the backbone have been synthesized and characterized by reference to novel, metallated oligomeric enynes. Metal-containing groups (e.g. Ru, Mo, Ni, Cu) have also been attached to PDAs through suitably functionalized side-chains, e.g. phosphinyl, (dialkyl)amino and bipyridyl groups. New diacetylenes incorporating the bases of DNA (adenine, thymine, cytosine) have been synthesized but in general do not polymerize by γ -irradiation. Nevertheless, thymine- and cytosine-containing PDAs have been characterized. The nonlinear optical properties of selected functionalized PDAs have been studied by the z-scan technique.

Certain diacetylenes (**1**; R = e.g. aryl, functionalized alkyl) undergo a solid state (topochemical) polymerization induced by heat, UV or gamma radiation to give polydiacetylenes (PDAs) (**2**);^{1,2} the process only occurs if the molecules are properly aligned, with a critical repeat distance near 5.0Å and an orientation angle *ca.* 45° relative to the translation axis. PDAs are highly coloured, often red or purple insoluble materials, but many, including polymers resulting from diacetylenes with urethane,³ sulfonate,⁴ or carboxylic acid ester^{5,6} side-chains, are soluble in common organic solvents. An interesting feature of some PDAs is their property of chromism⁷ which can be manifested in bulk samples as thermo- and photo-chromism; soluble PDAs can also show thermochromic effects in solution, and a related solvatochromism is observed on variation of the solvent to non-solvent ratio. An intriguing feature of PDAs containing carboxylic acid groups [**2**; R = (CH₂)_nCO₂H; n = e.g. 2, 3, 8] is the effect of pH changes on absorption spectra {acids (**2**) are yellow

in alkaline solution but red in acid}.⁸ The origin of such dichromism probably relates to a change in effective conjugation length⁹ and, for certain PDAs, an aggregation phenomenon.^{4b}



There have been recent significant advances in connection with the manner in which chromic effects in PDAs can be harnessed for potential applications in biosensor technology. Charych, Bednarsky *et al.* recognised that a chromic effect in certain PDAs can arise from the influence on the backbone chromophore of subtle conformational effects within a Langmuir-Blodgett bilayer assembly containing a receptor binding ligand (sialic acid analogue) specific to viral hemagglutinin.¹⁰ Exposure of the assembly to influenza virus elicits a colour change from blue to red. A more convenient colorimetric procedure for this assay has subsequently been devised using PDA liposomes derived from diacetylenes.¹¹ More recently, paramagnetic PDA liposomes have been characterised, and applications of such materials for magnetic resonance imaging can be anticipated.¹²

PDAs are also promising candidates for incorporation into optical devices on account of their large third order susceptibilities ($\chi^3 \sim 10^9 - 10^{10}$ esu).^{13,14} The ultrafast non-resonant refractive nonlinearities of PDAs are amongst the largest of any materials, and the resonant nonlinearities (orders of magnitude larger) have time-scales of the order of picoseconds, which closely match the likely shortest practical pulse durations of optical communication and processing systems. The figures-of-merit for all-optical mechanisms (switching, directional-coupling) in PDAs continue to offer the prospect that usable devices could be fabricated. Most optical measurements have been carried out on thin solid films, but soluble PDAs (see above) also show significant χ^3 values in solution.¹⁵

Objectives and Technological Relevance of the Programme

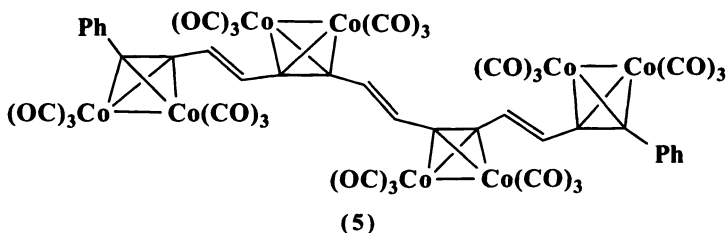
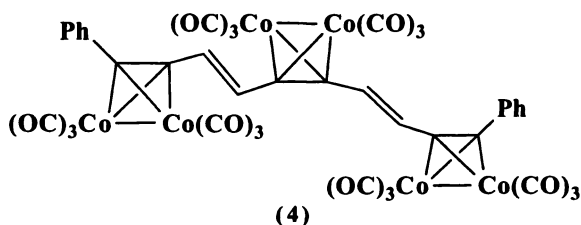
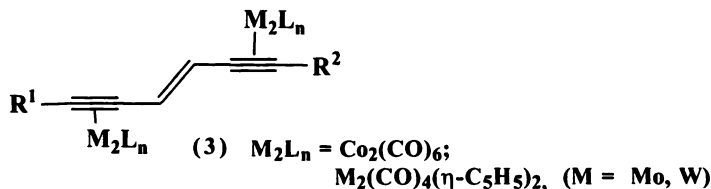
The extended conjugation of the PDA backbone is undoubtedly responsible for the extraordinary optical nonlinearity observed in such materials. In our programme we have attempted to modify the 'effective conjugation length' in PDAs in two ways. First, we have modified the unsaturated enyne polymer backbone by metallation, and characterized the ensuing materials by reference to model organometallics prepared from oligomeric conjugated enynes. Secondly, in the light of studies by Patel⁹ and ourselves,⁸ we have considered whether the unusual properties of PDA carboxylic acids might be manifested in related ionomeric materials. The following groups of PDAs have featured in our studies:

- (a) Metallated PDAs involving η -bonding of metals to alkyne moieties of the polymer backbone.
- (b) PDAs with ligating groups, e.g. diphenylphosphinyl, dialkylamino and 2,2'-bipyridyl, incorporated into the side-chains, and metallated species derived therefrom.
- (c) PDAs with side-chains incorporating ammonium, phosphonium and zwitterionic groups.

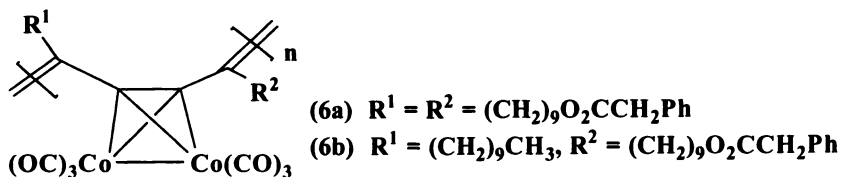
- (d) PDAs containing appropriate specific pairwise combinations of DNA bases, the combinations being chosen so that H-bonded interactions can occur between separate PDAs or in assemblies of monomers prior to polymerisation. Interactions of such functionalized PDAs with other compatible substrates are also of interest.

Synthetic Studies

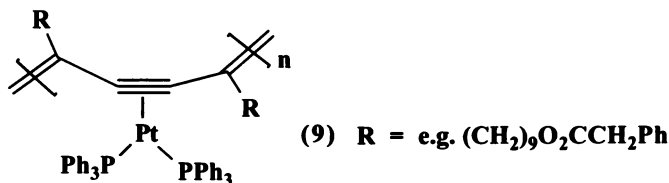
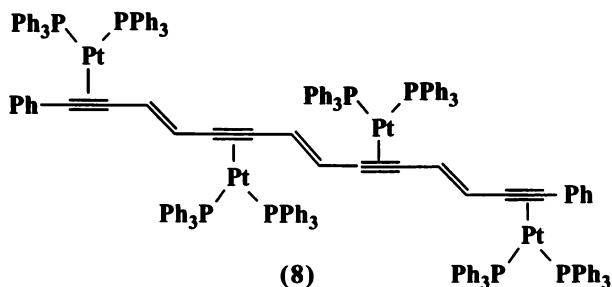
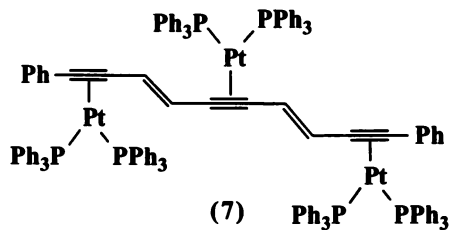
Metallated PDAs and Model Compounds. We have already reported metallated 'model' enynes (e.g. 3 - 5) related to PDAs.¹⁶



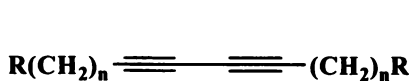
The above organometallic complexes have been used to aid spectroscopic characterization of novel metallated PDAs (e.g. 6)¹⁷.



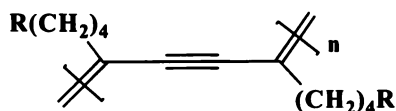
More recently we have prepared analogous platinum containing enynes (e.g. 7, 8) and achieved up to 35% metallation of the alkyne component of the PDA backbone in reactions with $[Pt(\eta^2-C_2H_4)(PPh_3)_2]$ (see 9).¹⁸



Metallated Materials derived from PDAs with Phosphine-, Amine- and Bipyridyl-terminated Side-chains. We prepared bis(diphenylphosphinyldiynes (10a - c) but found that they do not polymerize under the influence of γ - or UV-irradiation, and form PDAs in only very low conversions by thermal treatment.⁷



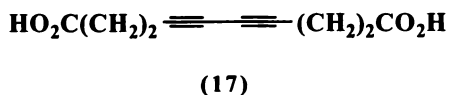
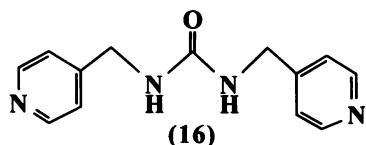
- (10) a R = PPh_2 , n = 2
 b R = PPh_2 , n = 3
 c R = PPh_2 , n = 4
 d R = $\text{PPh}_2\{\text{Mo}(\text{CO})_5\}$, n = 4



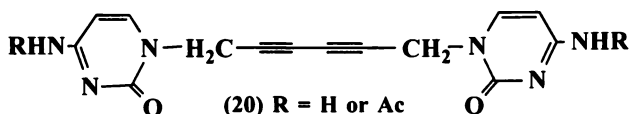
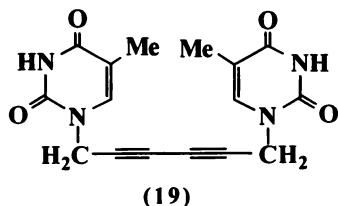
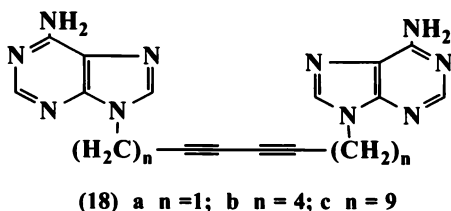
- (11) a R = PPh_2
 b R = OTs
 c R = $\text{PPh}_2\text{Mo}(\text{CO})_5$ or PPh_2
 d R = NEt_2

Accordingly, the phosphinated PDA (11a) was prepared using a method related to that of Kiji *et al.*,¹⁹ by reaction of the PDA tosylate (11b, PTS-12) with diphenylphosphinyllithium or -potassium.²⁰ A model, metallated diyne (10d) has recently been prepared from (10c) and $[\text{Mo}(\text{CO})_5(\text{THF})]$, and a 'polymer analogous' reaction has generated the partially metallated PDA (11c); e.g. $^{31}\text{P}\{^1\text{H}\}$ NMR (CDCl_3): (10d) 28.7 ppm; (11c) 28.4 ppm; IR $\nu(\text{CO})$ (CHCl_3): (10d) 2071, 1986, 1945 cm^{-1} ; (11c) 2072, 1983, 1944 cm^{-1} (+ weaker bands from some bis(phosphine)tetracarbonyl molybdenum sites).

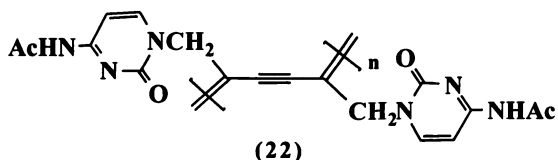
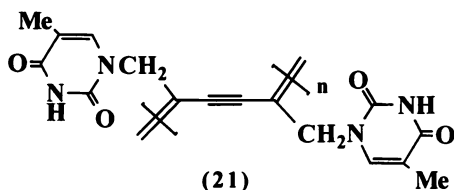
bonds. For example, layered diacetylene structures with the necessary topochemistry for polymerization have been prepared through the host/guest approach (see 16 and 17).²¹



In our programme, we are synthesizing diacetylenes with side-chains containing the base components of DNA [adenine (A), thymine (T), guanine (G) and cytosine (C)]. We anticipate that diacetylenes or ensuing PDAs can be mixed so that interactions between compatible base pairs (A-T, G-C) can occur either prior to polymerization or in solutions of the polymers; interactions in the latter medium could generate supramolecular assemblies of PDAs. It is also our intention to generate novel ionomeric PDAs through alkylation of such PDAs with heteroaromatic substituents.



In preliminary studies, we have prepared adenine (18), thymine (19) and cytosine (20) derivatives in the 1,3-diyne series. PDA (21) was prepared by γ -irradiation of (19), although no success has been achieved in attempts to polymerize (18b, c) using this method. Also, the PDA (22) has been produced by UV-irradiation of (20, R = Ac).



Optical Studies

The metallated PDA (**6a**) and the 'metal-free' polymer have previously been investigated¹⁷ using picosecond-resolution fluorescence lifetime studies and a picosecond characterization of the two photon absorption coefficient, β ; the latter has been related to the imaginary part of the macroscopic third order susceptibility $Im(\chi^3)$ and the absorptive nonlinearity increases proportionally with increasing metallation.

The nonlinear optical properties in solution of selected functionalized PDAs, described herein, have also been evaluated by means of the z-scan technique. Off resonance studies (at 705 nm) show that nonlinear refraction is only comparable to that of the solvent for these dilute solutions, but that nonlinear absorption, characterized by β values, varies significantly, with the nature of the side-chains.²⁰ It can be inferred that if bulk films of these PDAs possess suitable nonresonant nonlinear refractive properties for optical devices, modification of side-chain structure can reduce the magnitude of undesirable two photon absorption.

Table I. Two photon absorption coefficients (β) and nonlinear refractive coefficients (n_2) for PDA solutions from z-scan measurements at 532 nm (near resonance).

PDA [=RC-C≡C-CR=] _n Substituent R	Solvent	Conc ^a	α_{532}^b cm ⁻¹	β cm GW ⁻¹	n_2 10 ⁻¹⁵ cm ² W ⁻¹	T ^c
(CH ₂) ₄ O ₂ CNHCH ₂ CO ₂ Bu (poly-4-BCMU)	CHCl ₃	1.4	4.8	1.4	-200	0.4
(CH ₂) ₄ NEt ₂ (11d)	CHCl ₃	0.7	1.5	0.33	-60	0.3
(CH ₂) ₄ NMe(Et) ₂ ⁺ I ⁻ (15a)	H ₂ O	2.5	1.8	1.0	-180	0.3
(CH ₂) ₄ NEt ₂ /Ni(II) ^d (12a)	H ₂ O	1.0	1.8	0.85	-35	1.3
(CH ₂) ₄ NEt ₂ /Ni(II) ^e (12a)	H ₂ O	0.96	~0.7	0.25	-11	1.2
(CH ₂) ₄ NEt ₂ /Cu(II) ^d (12b)	H ₂ O	1.1	2.3	1.1	-40	1.5
(CH ₂) ₄ NEt ₂ /Cu(II) ^e (12b)	H ₂ O	1.02	~0.8	0.4	-13	1.6
(CH ₂) ₉ O ₂ CCH ₂ Ph	PhMe	0.29	1.8	0.57	-16	1.9
(CH ₂) ₉ O ₂ CCH ₂ Ph / Co ₂ (CO) ₆ (45%) (6a)	PhMe	0.29	5.0	2.0	-1.7	63

a Molar concentration x 10² - based on monomer unit;

b linear absorption coefficient;

c T = $\beta\lambda/|n_2|$, figure of merit for all optical switching {T < 3 required for a nonlinear Fabry-Perot etalon and T < 0.5 required for a nonlinear directional coupler};

d Metal:Nitrogen ratio 1:1;

e Metal:Nitrogen ratio 1:2.

Near resonant z-scan studies provide both nonlinear refractive coefficients, n_2 , and two photon absorption coefficients, β . Results for a selection of PDAs in solution at 532 nm are given in Table I. Diethylamino-PDA (11d) and the related quaternized polymer (15a) show comparable magnitudes of nonlinear absorption and refraction to those of poly-4-BCMU, with figures of merit, T , which satisfy the requirement for nonlinear optical switching devices. The metal-containing PDAs (12) and (6a), with metals coordinated to amine ligands in the side-chain or η -bonded to the polymer backbone, respectively, show an increase in two photon absorption but a decrease in n_2 on metallation.

At 532 nm, dilute solutions of potassium salts of urethane carboxylic acid PDAs, $\{[RC-C\equiv C-CR]_n\}$, $R = (CH_2)_mO_2CNHCH_2CO_2\cdot K^+$, $m = 3, 4$ show resonant optical nonlinearities dominated by a saturable absorption effect, with $Im(\chi^3)$ coefficients of $\sim 2 \times 10^{-18} \text{ m}^2\text{V}^{-2}$. The excited state lifetime of the salt ($m = 3$) was determined as 1.2 ps from an excite-probe experiment at 595 nm, confirming a rapid response time for these PDAs.

Acknowledgements

We acknowledge the support of the Engineering and Physical Sciences Research Council, UK (Research Fellowship to IHJ/CM and Postgraduate Studentship to TAJW). We also thank Dr. C. Wang and Professor B.S. Wherrett (Department of Physics, Heriot-Watt University) for optical measurements.

References

1. Wegner, G. *Z. Naturforsch., Teil B*, **1969**, *24*, 824; *Macromol. Chem.*, **1972**, *154*, 35.
2. See e.g.: *Polydiacetylenes*; Bloor, D., Chance, R. R., Eds.; Martinus Nijhoff: Dordrecht, The Netherlands, 1985.
3. Patel, G. N.; Chance, R. R.; Witt, J.D. *J. Polym. Sci., Polym. Lett. Ed.*, **1978**, *16*, 607; Patel, G. N.; Walsh, E. K. *J. Polym. Sci., Polym. Lett. Ed.*, **1979**, *17*, 203.
4. (a) Wenz, G.; Wegner, G. *Makromol. Chem. Rapid Commun.*, **1982**, *3*, 231; (b) Wenz, G.; Müller, M. A.; Schmidt, M.; Wegner, G. *Macromolecules*, **1984**, *17*, 837.
5. Plachetta, C.; Rau, N. O.; Hauck A.; Schulz, R. C. *Makromol. Chem. Rapid Commun.*, **1982**, *3*, 249; Plachetta, C.; Schulz, R. C. *Makromol. Chem. Rapid Commun.*, **1982**, *3*, 815; Plachetta, C.; Rau, N. O.; Schulz, R. C. *Mol. Cryst. Liq. Cryst.*, **1983**, *96*, 141.
6. (a) Tieke, B. *Macromol. Chem.*, **1984**, *185*, 1455; (b) Tieke, B.; Weiss, K. *Colloid Polym. Sci.*, **1985**, *263*, 576.
7. Lindsell, W. E.; Preston, P. N.; Tomb, P. J. *Polym. Int.*, **1994**, *33*, 87; and references cited therein.
8. See: Agh-Atabay, N. M.; Lindsell, W. E.; Preston, P. N.; Tomb, P. J. *Polym. Int.* **1993**, *31*, 367; and references cited therein.
9. Patel, G. N.; Preziosi, A. F.; Bhattacharjee, H. R. *J. Polym. Sci. Polym. Symp.*, **1984**, *71*, 247.
10. Charych, D. H.; Nagy, J. O.; Spevak, W.; Bednarski, M. D. *Science*, **1993**, *261*, 585.
11. Reichert, A.; Nagy, J. O.; Spevak, W.; Charych, D. *J. Am. Chem. Soc.*, **1995**, *117*, 829. See also: Charych, D., *et al.* *Chem. Biol.*, **1996**, *3*, 113, and *Adv. Mater.*, **1995**, *7*, 85.
12. Storrs, R. W.; Tropper, F. D.; Li, H. Y.; Song, C. K.; Kuniyoshi, J. K.; Sipkins, D. A.; Li, K. C. P.; Bednarski, M. D. *J. Am. Chem. Soc.*, **1995**, *117*, 7301.

13. See e.g.: *Nonlinear Optical and Electroactive Polymers*; Prasad, P. N., Ulrich, D. R., Eds.; Plenum Press: New York, 1988. *Nonlinear Optical Effects in Organic Polymers*; Messier, J., Kajzar, F., Prasad, P., Ulrich, D., Eds.; Kluwer Academic Publishers: Dordrecht, The Netherlands, 1989. *Non Linear Optical Properties of Organic Molecules and Crystals*; Chemla, D. S., Zyss, J., Eds.; Academic Press: Orlando, FL, 1987, Vol. 2.
14. See: Pender, W. A.; Boyle, A. J.; Lambkin, P.; Blau, W. J.; Mazaheri, K.; Westland, D. J.; Skarda, V.; Sparpaglione, M. *Appl. Phys. Lett.*, **1995**, *66*, 786; and references cited therein.
15. See e.g.: Dorsinville, R.; Yang, L.; Alfano, R. R.; Tubino, R.; Destri, S. *Solid State Commun.*, **1988**, *68*, 875.
16. Lindsell, W. E.; Preston, P. N.; Tomb, P. J. *J. Organomet. Chem.*, **1992**, *439*, 201.
17. Agh-Atabay, N. M.; Lindsell, W. E.; Preston, P. N.; Tomb, P. J.; Lloyd, A. D.; Rangel-Rojo, R.; Spruce, G.; Wherrett, B. S. *J. Mater. Chem.*, **1992**, *2*, 1241.
18. Lindsell, W. E.; Preston, P. N.; Wells, D. K., unpublished results.
19. See: Kiji, J.; Inaba, M. *Angew. Macromol. Chem.*, **1997**, *65*, 237; and references cited therein.
20. Jenkins, I. H.; Kar, A. K.; Lindsell, W. E.; Murray, C.; Preston, P. N.; Wang, C.; Wherrett, B. S. *Macromolecules*, **1996**, *29*, 6365.
21. Kane, J. J.; Liao, R. F.; Lauher, J. W.; Fowler, F. W. *J. Am. Chem. Soc.*, **1995**, *117*, 12003.

Author Index

- Allcock, Harry R., 261
Arjunan, P., 199
Cho, Jae Cheol, 85
Chung, T. C., 163
Coca, Simion, 16
Coessens, Veerle, 16
Crain, Allen L., 303
Datta, S., 38
Decker, C., 286
Epps, Thomas, 227
Faust, Rudolf, 135
Feldthusen, Jesper, 121
Gaynor, Scott, 16
Georges, Michael K., 28
Gonsalves, K. E., 276
Hadjichristidis, Nikos, 96
Hahn, Catherine Y., 248
Hallschmid, Nikolaus, 248
Hamer, Gordon K., 28
Hammond, Paula, 227
Han, Kwansoo, 71
Hassmann, Jörg, 248
Ihara, Eiji, 149
Iván, Bela, 121
Jang, Sung H., 71
Jasieczek, Christina, 16
Jenkins, I. H., 321
Jin, S., 276
Jo, Won Ho, 85
Kakehi, Takamaro, 149
Kim, Jungahn, 85
Kim, Keon Hyeong, 85
Kim, Kwang Ung, 85
Koroskenyi, Balint, 135
Lee, Youngjoon, 71
Lehn, Jean-Marie, 248
Lindsell, W. E., 321
Lu, H. L., 163
Lukose, Pushpamma, 28
MacLeod, Paula J., 28
Matyjaszewski, Krzysztof, 16
Morimoto, Masakazu, 149
Müller, Axel H. E., 121
Müller, Paul, 248
Murray, C., 321
Nakagawa, Yoshiki, 16
Ngoc, T. Hoang, 286
Nitto, Yuu, 149
Nodono, Mitsufumi, 149
Olkusz, J. A., 199
Patil, Abhimanyu O., 1, 184
Pispas, Stergios, 96
Pitsikalis, Marinos, 96
Preston, P. N., 321
Qiu, Jian, 16
Quirk, Roderic P., 71, 85
Rix, Brad, 71
Schubert, Ulrich S., 248
Schulz, D. N., 1, 38
Schwindeman, James A., 58
Stupp, S. I., 218
Sutton, Douglas E., 58
Tew, Gregory N., 218
Wall, David, 227
Wang, H-C., 199
Waymouth, R. M., 38
Webster, Dean C., 303
Woodman, T. A. J., 321
Xia, Jianhui, 16
Yang, Huimin, 71
Yasuda, Hajime, 149
Zheng, Wen-Yue, 227

Subject Index

A

α,ω -difunctional polymers

applications, 58

use of protected functionalized initiator for synthesis, 58–59

Acrylates, substituted, synthesis using atom transfer radical polymerization, 17, 19*t*

Acrylonitrile–styrene, synthesis using stable free radical polymerization, 34–36

Aliphatic polyesters, use in medicine, 276

Alkyl acrylates, organo rare earth metal initiated living polymerization, 153–154

Alkyl isocyanates, organo rare earth metal initiated living polymerization, 155–156

Alkyl methacrylates, organo rare earth metal initiated living polymerization, 149–153

Alkyl lithium initiators, use in anionic polymerization of hydroxyl-functionalized polymers, 71–82

Amino group carrying macromonomer, anionic polymerization using diphenylethylene derivative, 85–94

Amino-protected vinyl ether monomers, use in cationic polymerization, 41, 49

Amorphous elastomers, synthesis, 163–180

Anionic polymerization

hydroxyl-functionalized polymers using protected functionalized alkyl lithium and isoprenyllithium initiators

easy removal of protected functional group after polymerization completion, 82

experimental materials, 74, 78

experimental procedure characterization, 75

polymerizations and deprotection, 74–75

functionalized alkyl lithium initiators, 72–73

initiator criteria, 73–74

initiator efficiency

diene polymerization, 79, 80*r*

styrene polymerization, 75, 77–79, 81*f*

initiator solubility, 75, 76*f*

initiator structures, 75, 78

previous studies, 71–72

rate of initiation relative to that of propagation

diene polymerization, 79, 81*f*

styrene polymerization, 79

stable protected functional group with respect to conditions, 79, 82

macromonomer-carrying amino group using diphenylethylene derivative characterization

crossover reaction kinetics, 88–89, 91*f*

¹H-NMR spectra, 89–90, 92–94

size exclusion chromatograms, 90, 93*f*

UV-visible absorption spectra, 88, 90*f*

experimental materials, 86

experimental procedure

characterization, 86

synthesis, 86

synthesis, 86–88

synthesis of functional copolymers in combination with anionic polymerizations, 121–132

use

protected functionalized initiators, 58–69

protecting groups, 39–47

well-defined smectic C* side chain

liquid-crystalline polymers, 227–246

Applications

- atom transfer radical polymerization, 27
- functional polymers, 10–11
- poly{isobutylene-*co*-[(4-methylstyrenyl)(triphenyl phosphonium tetraphenyl borate)]}, 209, 213–215
- protecting group usage in polymerization, 53
- Approaches, studies, 218–328
- Assembly design, *See also* Functionalized nanoscopic gridlike coordination array assembly design
- Asymmetric telechelic polyisobutylenes, synthesis and characterization, 135–147
- Atom transfer radical polymerization
 - advantages, 16
 - applications, 27
 - functional initiators, 20–24
 - functionalization approach, 17, 18*f*
 - hyperbranched polymers, 25–26
 - mechanism, 16–17
 - polymers with side functional groups, 17, 19–20
 - synthesis of functional polymers, 7, 36
 - transformation of halogen chain ends, 21, 24–25
- B
- Benzyl protecting groups, use in metathesis polymerization, 52–53
- Biodegradable copolymers with pendant hydrophilic functional group synthesis
 - poly(ϵ -caprolactone) copolymers
 - comonomer composition, 279
 - copolymer structure and sequence distribution, 280, 282–284
 - experimental procedure, 277, 280
 - solubility, 283
 - polylactide copolymers
 - experimental procedure, 277–279
 - ¹H-NMR spectra, 278, 281*f*
 - IR spectra, 278, 282*f*
 - previous studies, 276–277
- 4,6-Bis[6-(2,2'-bipyridyl)]pyrimidine, use in design of functionalized nanoscopic gridlike coordination array assembly, 248–258
- 1-{4-[*N,N*-Bis(trimethylsilyl)amino]-phenyl}-1-phenylethylene
 - synthesis, 86–87, 88*f*
 - use in anionic polymerization of macromonomer-carrying amino group, 86–87, 88*f*
- Borane-containing polyolefins, use as intermediates for functionalized polyolefins, 164
- Butadiene
 - anionic polymerization, 71–82
 - synthesis, 59–60
- Butyl rubber
 - chemical structure, 184–185
 - composition, 184
- ω -*tert*-Butyldimethylsilyl chloride, use in anionic polymerizations, 62
- tert*-Butyldimethylsilyl-protected initiator, use in anionic polymerization, 40–43
- tert*-Butyldimethylsilyl-protected monomer use, anionic polymerization, 39–40, 46–47*t*
- ω -(*tert*-Butyldimethylsilyloxy)-1-alkyllithiums, use in anionic polymerizations, 58–69
- 3-(*tert*-Butyldimethylsilyloxy)-1-chloropropane, synthesis, 68–69
- 6-(*tert*-Butyldimethylsilyloxy)-1-hexyllithium, use in anionic polymerizations, 60–61
- 3-(*tert*-Butyldimethylsilyloxy)-1-propyllithium, synthesis, 69
- cationic polymerization, 41, 49
- Butyllithiums, use as initiators for anionic polymerizations, 60–61
- BX₃, initiation of living polymerization of isobutylene, 135–136

- C
- C¹ symmetric bulky organolanthanide complexes, initiation of living polymerization of polar and nonpolar monomers, 149–161
 - Carbocationic polymerization, synthesis of functional copolymers in combination with anionic polymerizations, 121–132
 - Carbonate functional polymer synthesis, *See* Cyclic carbonate functional polymer synthesis
 - Cationic polymerization
 - synthesis of functional polymers, 4–6
 - use of protecting groups, 41, 48–49, 51*t*
 - Characterization, poly{isobutylene-*co*-[(4-methylstyrenyl)triphenyl phosphonium tetraphenyl borate]}, 203–206
 - Chemical functional groups, role in properties of functional polymers, 1
 - Chemical modification
 - factors affecting reactivity of functional group, 9–10
 - polyolefins, 199–215
 - 4-Chloro-1-butanol, use in anionic polymerizations, 61–63
 - Cobalt(II), use in design of functionalized nanoscopic gridlike coordination array assembly, 248–258
 - Complexity, synthesis of functional polymers, 11–12
 - Conducting polymers, applications, 11
 - Coordination array assembly design, *See* Functionalized nanoscopic gridlike coordination array assembly design
 - Coordination polymerization, synthesis of functional polymers, 8–9
 - Copolymers, random, synthesis using stable free radical polymerization, 28–36
 - Copolymers with pendant hydrophilic functional group synthesis, *See* Biodegradable copolymers with pendant hydrophilic functional group synthesis
 - Cost, synthesis of functional polymers, 11–12
 - Cyclic carbonate functional polymer synthesis
 - advantages, 303
 - copolymer thermal glass transition temperature analysis, 315–320
 - emulsion copolymerizations
 - latex compositions and properties, 311, 315*t*
 - procedure, 311
 - stability testing, 311, 314*f*, 319*t*
 - experimental materials, 304
 - experimental procedure
 - characterization
 - latex polymers, 306
 - solution polymers, 306, 307*t*
 - emulsion polymerization, 305
 - solution polymerization, 305
 - vinyl ethylene carbonate hydrolysis, 305
 - solution copolymerizations
 - 4-ethenyl-1,3-dioxolan-2-one incorporation, 307–309
 - Fourier-transform IR spectra, 311, 313*f*
 - glass transition temperatures, 311, 312*f*
 - initial experiments, 306–307
 - initial solution copolymerization experiments, 309–311
 - molecular weight vs. 4-ethenyl-1,3-dioxolan-2-one level, 309, 312*f*
 - structure, 304
 - synthetic methods, 303–304
 - Cytosine-containing polydiacetylenes, synthesis, 325–326
- D
- Design, functionalized nanoscopic gridlike coordination array assemblies, 248–258
 - Diacetylenes

- solid-state polymerization, 321
 structure, 321–322
- Diblock copolymers
 characterization, 99
 synthesis, 99
- Diene, anionic polymerization, 71–82
- Dimethylamine end groups, synthesis
 and properties of functional polymers,
 96–118
- [3-(Dimethylamino)propyl]lithium, use
 as initiator in functional polymer
 synthesis, 96–118
- Diphenylethylene derivative, use in
 anionic polymerization of
 macromonomer-carrying amino group,
 85–94
- Direct functionalization of
 poly(isobutylene-*co-p*-methylstyrene)
 by Friedel-Crafts acylation reaction
¹³C-NMR spectra, 187, 189–195
 experimental materials, 186
 experimental procedure, 186
 gel permeation spectroscopy, 189
 IR spectra, 187, 188f
 reaction, 186–187
 UV-visible spectra, 189, 197f
 X-ray photoelectron spectroscopy, 187,
 188f
- Direct polymerization
 cationic polymerization for functional
 polymer synthesis, 4–6
 coordination polymerization for
 functional polymer synthesis, 8–9
 free radical polymerization for
 functional polymer synthesis, 6–8
 studies, 16–180
- DNA-containing polydiacetylenes,
 synthesis, 325–326
- E**
- Elastomers, synthesis, 163–180
- End-functionalized polymers
 advantages, 96
 synthetic methods, 96
- Epoxidized polyisoprene
 photo-cross-linking, 289–292, 293f
See also Photoinitiated ring opening
 polymerization of epoxidized
 polyisoprene
- Epoxidized polyisoprene-acrylate
 blends, photo-cross-linking, 297–300,
 301f
- Epoxidized polyisoprene-vinyl ether
 blends, photo-cross-linking, 292, 294–
 297, 298f
- 4-Ethenyl-1,3-dioxolan-2-one, use in
 synthesis of cyclic carbonate
 functional polymers, 303–320
- Ethylene, organo rare earth metal
 initiated living polymerization, 159–
 161
- Ethylene-1,2-bis(η^5 -4,5,6,7-tetrahydro-
 1-indenyl) catalysts, use in
 metallocene polymerization, 51–52
- F**
- Fox equation, description, 315
- Free radical polymerization, synthesis of
 functional polymers, 6–8
- Friedel-Crafts acylation
 examples, 185
 direct functionalization of
 poly(isobutylene-*co-p*-
 methylstyrene), 184–197
- Functional copolymers using
 combination of living carbocationic
 and anionic polymerizations
 experimental procedure, 123
 metallation of diphenylmethoxy- and
 diphenylvinyl-ended
 polyisobutylene, 125–127
 previous studies, 121–123
 reaction condition effect on end
 capping with 1,1-diphenylethylene,
 123–125
 synthesis and characterization of block
 copolymers, 127–132
- Functional initiators, use in atom transfer
 radical polymerization, 20–24
- Functional polymer(s)

- applications, 10–11
- chemical modification, 9–10
- definition, 38
- linear backbone, 1
- role of chemical functional groups on properties, 1
- synthesis
 - atom transfer radical polymerization, 16–27
 - cost and complexity, 11–12
 - direct polymerization
 - cationic polymerization, 4–6
 - coordination polymerization, 8–9
 - free radical polymerization, 6–8
 - problems, 38
 - stable free radical polymerization, 28–36
 - three-dimensional polymer backbones, 1–2
- Functional polymer synthesis, *See* Cyclic carbonate functional polymer synthesis
- Functional polyphosphazenes
 - advantages, 272
 - functionalization methods
 - protection–deprotection approaches
 - esters as protecting groups, 268–269
 - pendant amino group protection–deprotection, 269–270
 - pendant hydroxyl group protection–deprotection, 269–270
 - soft functionality
 - coordination sites, 264–265
 - difunctional reagent problem
 - avoidance, 265–266
 - unreactive poly(organophosphazenes)
 - lithiation reactions, 266–267
 - other reactions, 267–268
 - sulfonation
 - aromatic side groups, 267–268
 - via use of sultones, 267
- surface reactions
 - advantages, 270
 - functional groups formed, 271–272
 - reactions, 270–271
- Functionalized initiators for anionic polymerizations, *See* Protected functionalized initiators for anionic polymerizations
- Functionalized monomers,
 - polymerization by atom transfer radical polymerization, 19–20
- Functionalized nanoscopic gridlike coordination array assembly design approaches, 248–249
 - grid arrangement, 257f, 258
 - Langmuir–Blodgett film formation, 255–257
 - ligand synthesis, 250–253
 - physical–chemical properties, 253, 255
 - structure, 253, 254f
 - synthesis, 253, 254f
- Functionalized polydiacetylenes with polar, hydrogen bonding, and metal-containing groups
 - experimental objectives, 322
 - optics, 327–328
 - polydiacetylene types, 322–323
 - previous studies, 322
 - synthesis
 - metallated materials with phosphine-, amine- and bipyridyl-terminated side chains, 324–325
 - metallated polydiacetylenes, 323–324
 - polydiacetylenes with ammonium, phosphonium, and zwitterionic side chain substituents, 325
 - polydiacetylenes with side chains incorporating the base components of DNA, 325–326
- Functionalized polymers with dimethylamine and sulfozwitterionic end groups
 - diblock copolymers
 - characterization, 99
 - synthesis, 99
 - dilute solution and bulk properties
 - homopolymers, 106–108, 109f
 - ω -functionalized copolymers of styrene and isoprene, 108, 110–115

- star-shaped polybutadienes with end functional groups, 114, 116–118
 - [3-(dimethylamino)propyl]lithium as initiator, 96–97
 - functionalized three arm star polybutadienes
 - characterization, 102, 104*t*
 - synthesis, 101–102, 103*f*
 - homopolymers
 - characterization, 97–99
 - synthesis, 97
 - postpolymerization reaction, 104–106
 - triblock copolymers
 - characterization, 99
 - synthesis, 99
 - Functionalized polyolefins, *See* Polyolefins containing *p*-methylstyrene
 - Functionalized three arm star polybutadienes
 - characterization, 102, 104*t*
 - synthesis, 101–102, 103*f*
- G**
- Gibbs–DeMarzio theory, equation, 315
 - Grid(s), description, 249, 251*f*
 - Gridlike coordination array assembly
 - design, *See* Functionalized nanoscopic gridlike coordination array assembly design
 - Group VI or VII metathesis catalysts, use in metathesis polymerization, 52
- H**
- ω -Halo alcohols, use in anionic polymerizations, 61–68
 - Haloboration–initiation and end capping, synthesis and characterization of α -hydroxyl- ω -methoxycarbonyl and α -hydroxyl- ω -carboxyl asymmetric telechelic polyisobutylenes, 135–147
 - Halogen chain ends, transformation using atom transfer radical polymerization, 21, 24–25
 - Highly ordered materials
 - importance, 248
 - synthetic approaches, 248
 - Homopolymers
 - characterization, 97–99
 - dilute solution and bulk properties, 106–108, 109*f*
 - synthesis, 97
 - Hydrogen bonding groups, attachment to functionalized polydiacetylenes, 321–328
 - Hydrophilic functional groups, synthesis of biodegradable copolymers, 276–284
 - Hydrophobic and hydrophilic acrylates, organo rare earth metal initiated living polymerization, 154–155
 - α -Hydroxyl- ω -carboxyl asymmetric telechelic polyisobutylenes
 - characterization, 139–143, 145*f*
 - synthesis, 139–140
 - Hydroxyl-functionalized polymers, anionic polymerization using protected functionalized alkylolithium and isoprenyllithium initiators, 71–82
 - α -Hydroxyl- ω -(methoxycarbonyl) and α -hydroxyl- ω -carboxyl asymmetric telechelic polyisobutylenes
 - ω -carbonylpolyisobutylenes
 - characterization, 144–147
 - synthesis, 143–144
 - experimental materials, 137–138
 - experimental procedure
 - characterization, 138–139
 - procedures, 138
 - future work, 147
 - ω -(methoxycarbonyl)polyisobutylenes
 - characterization, 139–147
 - synthesis, 139–140, 143–144
 - previous studies, 135–137
 - Hydroxyl-protected vinyl ether monomers, use in cationic polymerization, 41, 49
 - Hyperbranched polymers, atom transfer radical polymerization, 25–26

- I
- Initiators
- anionic polymerizations, *See* Protected functionalized initiators for anionic polymerizations
 - hydrocarbon solutions, use in anionic polymerizations, 66–68
- Isoprene, anionic polymerization, 71–82
- Isoprene–styrene, synthesis using stable free radical polymerization, 30–34
- Isoprenyllithium initiators, use in anionic polymerization of hydroxyl-functionalized polymers, 71–82
- L
- Lactones, organo rare earth metal initiated living polymerization, 156–157
- Ladders, description, 249, 251f
- Langmuir–Blodgett films, formation, 255–257
- Light-induced polymerization of functionalized oligomers and polymers, generation of rapidly tridimensional polymer networks, 286
- Liquid-crystalline polymers
- applications, 11
 - See also* Well-defined smectic C* side chain liquid-crystalline polymers
- 2-(6-Lithio-*n*-hexyloxy)tetrahydropyran, synthesis, 59
- Living anionic polymerization, applications, 71
- Living polymerizations, advantages of combination of techniques, 121–122
- $\text{LnMe}(\text{C}_5\text{Me}_5)_2$, initiation of living polymerization of polar and nonpolar monomers, 149–161
- $\text{LnMe}(\text{C}_5\text{Me}_5)_2$ (tetrahydrofuran), initiation of living polymerization of polar and nonpolar monomers, 149–161
- $\text{LnOR}(\text{C}_5\text{R}_5)_2$, initiation of living polymerization of polar and nonpolar monomers, 149–161
- $\text{LnR}(\text{C}_5\text{R}_5)_2$, initiation of living polymerization of polar and nonpolar monomers, 149–161
- Luminescent supramolecular objects, synthesis, 223
- M
- Macromonomer
- definition, 85
 - importance of molecular weight choice, 85
 - synthetic techniques, 85
- Macromonomer-carrying amino group, anionic polymerization using diphenylethylene derivative, 85–94
- Mechanical behavior, poly{isobutylene-*co*-[(4-methylstyrenyl)triphenyl phosphonium tetraphenyl borate]}, 203, 207, 208f
- Metal-containing groups, attachment to functionalized polydiacetylenes, 321–328
- Metal-containing polymers, applications, 10
- Metal ions, use in design of functionalized nanoscopic gridlike coordination array assembly, 248–258
- Metallocene catalyst systems, role in synthesis of polyolefins containing *p*-methylstyrene, 163–180
- Metallocene polymerization
- synthesis of functional polymers, 8
 - use of protecting groups, 51–52
- Metathesis polymerization
- synthesis of functional polymers, 8
 - use of protecting groups, 52–53
- 1-Methoxy-1-(trimethylsiloxy)ethene, synthesis and characterization of α -hydroxyl- ω -(methoxycarbonyl) and α -hydroxyl- ω -carboxyl asymmetric telechelic polyisobutylenes, 135–147

- 1-Methoxy-1-(trimethylsiloxy)-2-methylpropene, synthesis and characterization of α -hydroxyl- ω -(methoxycarbonyl) and α -hydroxyl- ω -carboxyl asymmetric telechelic polyisobutylenes, 135–147
- 1-Methoxy-1-(trimethylsiloxy)propene, synthesis and characterization of α -hydroxyl- ω -(methoxycarbonyl) and α -hydroxyl- ω -carboxyl asymmetric telechelic polyisobutylenes, 135–147
- p*-Methylstyrene comonomer, advantages for functionalized polyolefins, 164
- p*-Methylstyrene-containing polyolefins, synthesis, 163–180
- Monoamine oxidase activated Zr metallocene catalysts, use in Ziegler–Natta polymerization, 52
- Multifunctional supramolecular materials
- luminescent supramolecular objects characterization, 223–224
 - synthesis, 223
 - mechanism, 224
- mushroom-shaped nanostructures from triblock molecules
- molecular graphics of triblock molecules, 219, 220*f*
 - receding water contact angle measurements, 223
 - second harmonic generation measurements, 223
 - synthesis, 219
 - transmission electron micrographs, 219, 221–223
- triblock structures containing electron and hole-accepting blocks
- properties, 224
 - synthesis, 224–225
- Mushroom-shaped nanostructures from triblock molecules, synthesis, 219

N

- Nanosopic gridlike coordination array assembly design, *See* Functionalized nanoscopic gridlike coordination array assembly design
- Nonhomopolymerizable monomers, synthetic applications in carbocationic macromolecular engineering, 136–137
- Nonpolar monomers, organo rare earth metal initiated living polymerization, 149–161
- Number-average molecular weight, calculation, 73

O

- ω -functionalized block copolymers of styrene and isoprene, 108, 110–115
- Olefins, organo rare earth metal initiated living polymerization, 157–159
- Optically active mesogenic methacrylate monomers containing alkyl and oligoethylene oxide spacers, synthesis, 27–246
- Organo rare earth metal initiated living polymerization of polar and nonpolar monomers
- alkyl acrylates, 153–154
 - alkyl isocyanates, 155–156
 - alkyl methacrylates, 149–153
 - ethylene, 159–161
 - hydrophobic and hydrophilic acrylates, 154–155
 - lactones, 156–157
 - olefins, 157–159
 - styrene, 159
- Organoborane catalysts, use in metathesis polymerization, 53
- Organoborane-mediated synthesis, Ziegler–Natta polymers, 51
- Organolanthanide complexes, initiation of living polymerization of polar and nonpolar monomers, 149–161

- P
- Pendant hydrophilic functional groups, synthesis of biodegradable copolymers, 276–284
 - Phosphonium ionomers, synthesis and properties, 199–215
 - Photoinitiated ring opening polymerization of epoxidized polyisoprene
 - experimental materials, 287, 288*f*
 - experimental procedure analysis, 289
 - irradiation, 287–289
 - photo-cross-linking epoxidized polyisoprene, 289–292, 293*f*
 - epoxidized polyisoprene–acrylate blends, 297–300, 301*f*
 - epoxidized polyisoprene–vinyl ether blends, 292, 294–297, 298*f*
 - previous studies, 286–287
 - Photosensitive polymers, applications, 10–11
 - Polar groups, attachment to functionalized polydiacetylenes, 321–328
 - Polar monomers, organo rare earth metal initiated living polymerization, 149–161
 - Poly(ϵ -caprolactone) copolymers
 - characterization, 279–284
 - synthesis, 177, 180
 - Polydiacetylenes
 - applications, 322
 - properties, 321–322
 - See also* Functionalized polydiacetylenes with polar, hydrogen bonding, and metal-containing groups
 - structure, 321–322
 - Polydienes, chemical modification, 9–10
 - Poly(ethylene-*co-p*-methylstyrene)
 - copolymer synthesis catalyst effect, 165, 168, 170*f*
 - copolymerization reactions, 165, 167*t*
 - ¹H-NMR spectra, 165, 166*f*
 - p*-methylstyrene concentration effect, 168
 - molecular structure–composition relationship, 171–174, 175*f*
 - reactivity ratios, 169, 171, 173*f*
 - solvent effect, 168–169, 170*f*
 - Poly(ethylene-*ter*-1-octene-*ter-p*-methylstyrene) terpolymer synthesis
 - ¹H-NMR spectra, 174, 176, 177*f*
 - molecular structure–composition relationship, 176, 179–180
 - reactivity ratios, 176
 - terpolymerization reactions, 176, 178*t*
 - Polyisobutylene(s)
 - synthesis and characterization, 135–147
 - use in block copolymer synthesis, 122–123
 - Polyisobutylene-based block copolymers, synthesis using combination of living carbocationic and anionic polymerizations, 121–132
 - Poly{isobutylene-*co*-[(4-bromomethyl)-styrene]}, modification, 199–215
 - Poly(isobutylene-*co-p*-methylstyrene)
 - advantages, 184
 - chemical structure, 184–185
 - composition, 185
 - direct functionalization by Friedel-Crafts acylation reaction, 184–197
 - Poly{isobutylene-*co*-[(4-methylstyrenyl)-triphenyl phosphonium tetraphenyl borate]}
 - applications, 209, 213–215
 - characterization
 - ¹H-NMR spectra, 203, 204*f*
 - Fourier-transform IR spectra, 203, 205–206*f*
 - experimental materials, 200
 - experimental procedure, 201
 - previous studies, 200
 - properties
 - mechanical behavior, 203, 207, 208*t*
 - rheological properties, 207, 209–212
 - thermomechanical behavior, 207, 210*f*

- synthesis
 general procedure, 201
 reactions, 202
- Polyisobutylene-*b*-poly(*tert*-butyl methacrylate) block copolymers, synthesis and characterization, 127–128
- Polyisobutylene-*b*-poly(methacrylic acid), synthesis and characterization, 128–129
- Polyisoprene, photo-cross-linking, 289–292, 293*f*
- Polyisoprene-acrylate blends, photo-cross-linking, 297–300, 301*f*
- Polyisoprene-vinyl ether blends, photo-cross-linking, 292, 294–297, 298*f*
- Poly lactide copolymers
 characterization, 278, 281–282*f*
 synthesis, 277–279
- Polymer(s)
 hydroxyl functionalized, anionic polymerization using protected functionalized alkyl lithium and isoprenyllithium initiators, 71–82
 hyperbranched, *See* Hyperbranched polymers
See also Functional polymers
- Polymer-supported catalysts, applications, 10
- Polymer(s) with side functional groups, atom transfer radical polymerization, 17, 19–20
- Polymerization, use of protecting groups, 38–53
- Poly[methyl methacrylate-*b*-polyisobutylene-*b*-poly(methyl methacrylate)], synthesis and characterization, 129–132
- Polyolefins
 chemical modification, 9–10, 199–215
 functionalization approaches, 164
 importance of functionalization, 163–164
- Polyolefins containing *p*-methylstyrene
 poly(ethylene-*co-p*-methylstyrene) copolymer synthesis, 165, 167–175
 poly(ethylene-*ter-1*-octene-*ter-p*-methylstyrene) terpolymer synthesis, 174, 176–180
- Polyphosphazenes
 applications, 263–264
 functional, *See* Functional polyphosphazenes
 functionalization, 264–272
 importance of side groups, 262–263
 synthetic approaches, 261–262
 unreactive examples, 263–264
- Polystyrenes, substituted, polymerization by atom transfer radical polymerization, 17, 19*t*
- Postpolymerization, studies, 184–215
- Properties
 poly{isobutylene-*co*-[(4-methylstyrenyl)triphenyl phosphonium tetraphenyl borate]}, 203, 207–210
 role of chemical functional groups, 1
- Protected functional cationic coinitiators, use in cationic polymerization, 41, 48–49
- Protected functional initiators, use in anionic polymerization, 39–43
- Protected functionalized alkyl lithium and isoprenyllithium initiators, anionic polymerization of hydroxyl-functionalized polymers, 71–82
- Protected functionalized initiators for anionic polymerizations
 butyllithiums, 60–61
 experimental procedure, 68–69
 ω -halo alcohols, 61–68
 initiators in hydrocarbon solutions, 66–68
 previous studies, 59–60
- Protected monomers, use in anionic polymerization, 39–41, 46–47*t*
- Protected terminating agents, use in cationic polymerization, 41, 48–49, 50*t*
- Protecting group usage in polymerization

- advantages, 53
 - anionic polymerization, 39–47
 - applications, 53
 - cationic polymerization, 41, 48–49, 50r
 - metallocene polymerization, 51–52
 - metathesis polymerization, 52–53
 - Ziegler–Natta polymerization, 49–51
 - Protection–deprotection, functional polyphosphazenes, 268–270
- R**
- Racks, description, 249, 251f
 - Radical polymerizations, importance, 16
 - Random copolymers, synthesis using stable free radical polymerization, 28–36
 - Rapidly tridimensional polymer networks, generation, 286
 - Rheological properties, poly[isobutylene-*co*-(4-methylstyrenyl, triphenyl phosphonium tetraphenyl borate)], 207, 209–212
 - Ring opening metathesis polymerization, use of silyl protecting group, 52
 - Ring opening polymerization of epoxidized polyisoprene, *See* Photoinitiated ring opening polymerization of epoxidized polyisoprene
 - Ruthenium catalysts, use in metathesis polymerization, 53
- S**
- Self-assemblies, formation, 1
 - Semicrystalline thermoplastics, synthesis, 163–180
 - Side chain liquid-crystalline polymers, *See* Well-defined smectic C* side chain liquid-crystalline polymers
 - Silyl groups, use in Ziegler–Natta polymerization, 50–51
 - Silyl ketene acetals, synthesis and characterization of α -hydroxyl- ω -(methoxycarbonyl) and α -hydroxyl- ω -carboxyl asymmetric telechelic polyisobutylenes, 135–147
 - [(SiMe₃)₃C]₂Yb, initiation of living polymerization of polar and nonpolar monomers, 149–161
 - SiMe₂[2-SiMe₃-4-tBu-C₅H₂]₂Sm-(tetrahydrofuran), initiation of living polymerization of polar and nonpolar monomers, 149–161
 - SiMe₂[2(3),4-(SiMe₂)₂C₅H₂]₂LnCH-(SiMe₃)₂, initiation of living polymerization of polar and nonpolar monomers, 149–161
 - SiMe₂[2(3),4-(SiMe₃)₂C₅H₂]₂Sm-(tetrahydrofuran), initiation of living polymerization of polar and nonpolar monomers, 149–161
 - Smectic C* side chain liquid-crystalline polymers, *See* Well-defined smectic C* side chain liquid-crystalline polymers
 - [SmH(C₅Me₅)₂]₂, initiation of living polymerization of polar and nonpolar monomers, 149–161
 - Soft functionality, functional polyphosphazenes, 264–266
 - Stable free radical polymerization random copolymers
 - advantages, 28
 - description, 28
 - experimental materials, 29
 - experimental procedure analysis, 29–30
 - polymerization reactions, 30
 - propagation reactions, 28–29
 - styrene–acrylonitrile, 34–36
 - styrene–isoprene, 30–34
 - synthesis of functional polymers, 7
 - Star-shaped polybutadienes with end functional groups, dilute solution and bulk properties, 114, 116–118
 - Structures, studies, 218–328
 - Styrene
 - anionic polymerization, 71–82

- organo rare earth metal initiated living polymerization, 159
- Styrene–acrylonitrile, synthesis using stable free radical polymerization, 34–36
- Styrene–isoprene, synthesis using stable free radical polymerization, 30–34
- Substituted acrylates, polymerization by atom transfer radical polymerization, 17, 19*t*
- Substituted polystyrenes, polymerization by atom transfer radical polymerization, 17, 19*t*
- Sulfozwitterionic end groups, synthesis and properties of functional properties, 96–118
- Supramolecular materials, *See* Multifunctional supramolecular materials
- Supramolecular nanostructures with great diversity in shape and functionality, preparation problems, 218–219
- Surface reactions, functional polyphosphazenes, 270–272
- Synthesis
- amorphous elastomers, 163–180
 - biodegradable copolymers with pendant hydrophilic functional group, 276–284
 - 1-[4-[*N,N*-bis(trimethylsilyl)amino]-phenyl]-1-phenylethylene, 86–87, 88*f*
 - cyclic carbonate functional polymers, 303–320
 - functional polymers, 2–12
 - functionalized polydiacetylenes with polar, hydrogen bonding, and metal-containing groups, 321–328
 - α -hydroxyl- ω -carboxyl asymmetric telechelic polyisobutylenes, 139–140
 - α -hydroxyl- ω -(methoxycarbonyl) asymmetric telechelic polyisobutylenes, 143–144
 - multifunctional supramolecular materials, 218–225
 - poly(ethylene-*co-p*-methylstyrene) copolymer, 174, 176–180
 - poly(ethylene-*ter-1*-octene-*ter-p*-methylstyrene terpolymer, 174, 176–180
 - poly{isobutylene-*co*-[(4-methylstyrenyl)triphenyl phosphonium tetraphenyl borate]}, 201–202
 - semicrystalline thermoplastics, 163–180
 - use of atom transfer radical polymerization, 16–27
- T
- Telechelic polyisobutylenes, synthesis and characterization, 135–147
- Terminating agents, use in anionic polymerization, 39–41, 44–45
- Thermomechanical behavior, poly{isobutylene-*co*-[(4-methylstyrenyl)triphenyl phosphonium tetraphenyl borate]}, 207, 210*f*
- Thermoplastics, synthesis, 163–180
- Thymine-containing polydiacetylenes, synthesis, 325–326
- Transformation of halogen chain ends, atom transfer radical polymerization, 21, 24–25
- Triblock copolymers
- characterization, 99
 - synthesis, 99
- Triblock structures containing electron and hole-accepting blocks, synthesis, 224–225
- Trimethylsilyl-protected monomer use
- anionic polymerization, 39–40, 46–47*t*
 - cationic polymerization, 41, 49
- U
- Unreactive poly(organophosphazenes), functional polyphosphazenes, 266–268

UV curing, applications, 286–287
UV irradiation, photoinitiated ring
opening polymerization of epoxidized
polyisoprene, 286–301

V

Vinyl ethylene carbonate, use in
synthesis of cyclic carbonate
functional polymers, 303–320
Viscosity, poly{isobutylene-*co*-[(4-
methylstyrenyl)triphenyl
phosphonium tetraphenyl borate]},
209, 210–212*f*

W

Well-defined smectic C* side chain
liquid-crystalline polymers
anionic polymers
liquid-crystalline behavior, 236, 238–
241*f*
role of spacer flexibility, 236–237
experimental materials, 228

experimental procedure
characterization, 230–231
monomer synthesis, 228–230
polymerization, 230
free radical polymers
glass transition temperatures, 242
molecular weight distribution vs.
liquid crystallinity, 242–246
influencing factors, 228
monomers
structure, 231
thermotropic transitions, 231–232
polymerization, 233–235
previous studies, 227–228

Z

Ziegler–Natta polymerization
synthesis of functional polymers, 8
use of protecting groups, 49–51
Zinc(II), use in design of functionalized
nanoscopic gridlike coordination array
assembly, 248–258